ภาคผนวก

โครงการการพัฒนาศักยภาพการวิจัยเชิงสถาบันของภาควิชาพืชศาสตร์
และทรัพยากรการเกษตร คณะเกษตรศาสตร์ มหาวิทยาลัยขอนแก่น
เลขที่สัญญา IRG5780003

ศาสตราจารย์สนั่น จอกลอย และคณะ
ภาควิชาพืชศาสตร์และทรัพยากรการเกษตรศาสตร์
คณะเกษตรศาสตร์ มหาวิทยาลัยขอนแก่น

สนับสนุนโดยสำนักงานกองทุนสนับสนุนการวิจัย
และมหาวิทยาลัยขอนแก่น

Ultrasonics Sonochemistry 37 (2017) 83–93

Contents lists available at ScienceDirect

Ultrasonics Sonochemistry

journal homepage: www.elsevier.com/locate/ultson

Fe_3O_4/hydroxyapatite/graphene quantum dots as a novel nano-sorbent for preconcentration of copper residue in Thai food ingredients: Optimization of ultrasound-assisted magnetic solid phase extraction

Phitchan Sricharoen [a], Nunticha Limchoowong [a], Yonrapach Areerob [a], Prawit Nuengmatcha [a,b], Suchila Techawongstien [c], Saksit Chanthai [a,*]

[a] Materials Chemistry Research Center, Department of Chemistry and Center of Excellence for Innovation in Chemistry, Faculty of Science, Khon Kaen University, Khon Kaen 40002, Thailand
[b] Department of Chemistry, Faculty of Science and Technology, Nakhon Si Thammarat Rajabhat University, Nakhon Si Thammarat 80280, Thailand
[c] Department of Plant Science and Agricultural Resources, Faculty of Agriculture, Khon Kaen University, Khon Kaen 40002, Thailand

ARTICLE INFO

Article history:
Received 16 October 2016
Received in revised form 28 December 2016
Accepted 28 December 2016
Available online 31 December 2016

Keywords:
Ultrasound-assisted extraction
Magnetic solid-phase extraction
Copper
Hydroxyapatite
Graphene quantum dots
Nanocomposite

ABSTRACT

Fe_3O_4/hydroxyapatite/graphene quantum dots (Fe_3O_4/HAP/GQDs) nanocomposite was synthesized and used as a novel magnetic adsorbent. This nanocomposite was characterized using scanning electron microscopy, transmission electron microscopy, Fourier transform infrared spectroscopy, X-ray diffraction, energy dispersive X-ray spectroscopy, and magnetization property. The Fe_3O_4/HAP/GQDs was applied to pre-concentrate copper residues in Thai food ingredients (so-called "Tom Yum Kung") prior to determination by inductively coupled plasma-atomic emission spectrometry. Based on ultrasound-assisted extraction optimization, various parameters affecting the magnetic solid-phase extraction, such as solution pH, amount of magnetic nanoparticles, adsorption and desorption time, and type of elution solvent and its concentration were evaluated. Under optimal conditions, the linear range was 0.05–1500 ng mL^{-1} ($R^2 > 0.999$), limit of detection was 0.58 ng mL^{-1}, and limit of quantification was 1.94 ng mL^{-1}. The precision, expressed as the relative standard deviation of the calibration curve slope ($n = 5$), for intra-day and inter-day analyses was 0.87% and 4.47%, respectively. The recovery study of Cu for real samples was ranged between 83.5% and 104.8%. This approach gave the enrichment factor of 39.2, which guarantees trace analysis of Cu residues. Therefore, Fe_3O_4/HAP/GQDs can be a potential and suitable candidate for the pre-concentration and separation of Cu from food samples. It can easily be reused after treatment with deionized water.

1. Introduction

The well known "Tom Yum Kung" is a traditional Thai soup that is generally cooked with giant shrimp (Fig. S1). It is one of the most famous and popular dishes not only in Thailand but also worldwide in Thai restaurants, which have made it well known among foreigners who have experimented with Thai foods. This soup is characterized by its distinct hot and sour flavors with fragrant herbs generously used. To enhance its flavoring appeal, savory complements of various Thai herbs such as chili pepper, tomato, shallot, lemon grass, kaffir lime leaves, galangal, coriander, leek, stinkweed, and lime are combined. The soup is not only delicious but also nutritious. The different herbs and spices used have several health benefits, as they possess antioxidant, antimicrobial, antibacterial antidiabetic, and anticancer properties [1,2].

At a global level, environmental pollution due to heavy metals has become a major concern. Metals are natural occurring chemical compounds. They can be present at various levels in the environment, e.g. soil, water and atmosphere. Metals can also occur as residues in food because of their presence in the environment, as a result of human activities such as farming, industry or car exhausts or from contamination during food processing and storage. People can be exposed to these metals from the environment or by ingesting contaminated food or water. Their accumulation in the body can lead to harmful effects over time, depending on the dose and toxicity. Among the heavy metals, copper is an essential micronutrient that is indispensable for life as it is involved in various biological processes [3]. It plays a central role in human

* Corresponding author at: 123 Mittraphab Road, M. 16, T. Ni-Muang, A. Muang, Khon Kaen University, Department of Chemistry, Faculty of Science, Khon Kean 40002, Thailand.
E-mail address: sakcha2@kku.ac.th (S. Chanthai).

http://dx.doi.org/10.1016/j.ultsonch.2016.12.037
1350-4177/

metabolism. Most of the copper in the body is tightly bound with different metalloproteins. Furthermore, many copper enzymes have been characterized to have a variety of cellular and extracellular activities, including those in immune reactions, neural function, bone metabolism, hematopoietic system, antioxidant function, and energy production [4]. Moreover, copper deficiency can possibly increase the incident risk of coronary heart diseases [5]. However, copper is one of the most harmful pollutants in the environment as it is highly toxic and non-degradable; it also has a high bioaccumulation rate [6]. High intake of copper in the blood system may generate reactive oxygen species and damage the DNA, lipids and protein as well as affect the kidney, pancreas, and liver [7]. In addition, it causes liver damage in infants [8]. Furthermore, patients suffering from Wilson's disease must carefully control their copper intake through water and food [9]. With the increasing use of new food production technologies, the possibility of food contamination with various environmental pollutants, particularly heavy metals, has also increased [10]. Therefore, the internationally accepted maximum level of copper is set at 30 mg kg^{-1} to safeguard public health [7]. It is thus extremely essential to analyze and measure copper in food samples. Modern instrumental techniques, such as flame [11–13] and/or graphite furnace atomic absorption spectrometry [14], inductively coupled plasma-optical emission spectrometry [15,16], inductively coupled plasma-mass spectrometry [17], electrochemical method [18], and X-ray absorption spectrometry [19], have been used to accurately and precisely determine heavy metal ions at trace levels in food, water, and environmental samples.

Ultrasound-assisted extraction (UAE) is another popular technique that has several advantages (e.g., expeditious, inexpensive, and environmental friendly) over other conventional techniques [20–22]. It has been increasingly used for the primary extraction of target compounds from complex matrices. UAE is widely used for analytical sample preparations because it requires much lower extraction solvent volume, reduces extraction time, enhances the extraction efficiency through disruption of cell walls, reduces particle size, and enhances mass transfer of the cell contents as a result of cavitation [23–26]. This technique has been proven to be a very useful tool in intensifying the mass transfer process and breaking the affinity between adsorbate and adsorbent [27].

To remove the interference or sample matrix and increase the analyte concentration, pre-concentration techniques such as ionic liquid extraction [28], ion exchange [29,30], liquid–liquid extraction [31,32], cloud point extraction [33,34], co-precipitation [35], and solid-phase extraction (SPE) [36–41] have been used. SPE has several major advantages including operation simplicity, minimum eluent volume, shorter extraction time, high pre-concentration factor and reduction of disposal cost [42,43]. In addition, the availability of a wide variety of sorbent materials primarily affects the extraction efficiency. Therefore, SPE has become a well-established sample preparation method to extract and pre-concentrate the desired components. Currently, the application of iron oxide (such as Fe_3O_4)-based nanomaterials or magnetic nanoparticles (NPs) in SPE (MSPE) simplifies sample pre-treatment and overcomes some limitations of conventional SPE [44]. The sorbent does not need to be packed into the cartridge and the phase separation can be easily realized by applying an external magnetic field. NPs possess large surface area, high adsorption capacity, and rapid adsorption rate. Therefore, to extract analytes from the large volumes of samples, low amounts of sorbent and short equilibrium time are required [45]. In recent years, this novel solid material has become increasingly important owing to its special properties. One of its special properties is that most of the atoms are on the surface of the NPs. The surface atoms are unsaturated, and therefore, they can bind with other atoms that feature high chemical reactivity. Subsequently, the NPs can adsorb metal ions with a great adsorption speed [46]. Among various NPs, hydroxyapatite (HAP) and graphene quantum dots (GQDs) are of particular interest due to their wide applications. HAP ($Ca_{10}(PO_4)_6(OH)_2$), the main inorganic calcium phosphate mineral component of human bones and teeth, has been used extensively for medical and dental applications [47]. It shows excellent potential in heavy metals treatment because of their high specific surface area, abundant hydroxyl groups, low water solubility, high stability under reducing and oxidizing conditions, good dispersibility, low cost, environmental friendly and simple synthesis method with calcium hydroxide or nitrate as precursors. The reports on the use of hydroxyapatite for the capture of several heavy metals, such as Cr, Cu, Pb, Cd, Zn, Co, V, Ni and Sb [48]. GQDs are graphene sheets with lateral size smaller than 100 nm in single, double and multiple layers, and diameters spanning the range 3–20 nm mainly. These materials possess special properties including low toxicity, high biocompatibility, high fluorescent activity, robust chemical inertness and excellent photostability. The presence of oxygen-containing (carbonyl, epoxy, hydroxyl, carboxyl) functional groups at the edge of GQDs. GODs had great interaction ability toward metal ion such as Hg^{2+}, Fe^{2+}, Cu^{2+}, Ni^{2+}, Mn^{2+} and Co^{2+} [49]. It can be assumed that using these types of adsorbent decorated magnetite Fe_3O_4 NPs in MSPE with ultrasound as agitator can improve the adsorption performance of copper and reduce the analysis time through the rapid isolation of MNPs with a strong magnet from large volumes of the sample solution. Ultrasonic technique was also applied for ions determination because of improving the mass transfer in the adsorption and desorption processes [13,40].

In this regard, the preparation, characterization, and application of Fe_3O_4/HAP/GQDs magnetic nanocomposite as a novel adsorbent for an ultrasound-assisted magnetic solid-phase extraction (UA-MSPE) have been described. Fe_3O_4/HAP/GQDs was synthesized with a simple co-precipitation method. The resultant nanocomposite was characterized by Fourier transform infrared (FT-IR) spectra, X-ray diffraction (XRD), scanning electron microscopy (SEM), transmission electron microscopy (TEM), energy dispersive X-ray spectrometry (EDX), and vibrating sample magnetometry (VSM) techniques. Subsequently, the as-prepared nanocomposite was used for the pre-concentration and determination of copper in Thai food ingredients using inductively coupled plasma-atomic emission spectrometry (ICP-AES). The green approach, i.e., UAE, was used as an efficient sample pre-treatment method, followed by UA-MSPE and ICP-AES.

2. Materials and methods

2.1. Chemicals and reagents

All the chemicals and reagents were of analytical grade. Copper (II) chloride, calcium nitrate tetrahydrate, sodium phosphate monobasic monohydrate, sodium phosphate dibasic anhydrous, and sodium acetate were purchased from Sigma-Aldrich (USA). Citric acid was purchased from Carlo Erba (Italy). Sodium hydroxide, paraffin oil, ammonium hydroxide, ferric chloride hexahydrate and iron(II) sulphate heptahydrate were obtained from QRec™ (New Zealand). Acetic acid, phosphoric acid, hydrochloric acid, and sulfuric acid were purchased from UNILAB (Australia). A Millipore water purification system (Molsheim, France) was used to produce deionized water with a resistivity of 18.2 MΩ cm.

2.2. Plant materials

Fresh samples of chili pepper, tomato, shallot, lemon grass, kaffir lime leaves, galangal, coriander, leek, stinkweed, and lime were

purchased from a fresh market in Khon Kaen, Thailand. Only the edible parts of each sample were used for the analyses. Any rotten or damaged parts were eliminated for the real food simulation for human consumption. The fresh samples were weighed, cut into small portions, and completely dried in an oven at 70 °C. The dried samples were ground in a household grinder and sieved through a 100 mesh. All the samples were analyzed as soon as they arrived at the laboratory. Alternatively, they were stored in plastic bottles and kept in a desiccator until analysis. Fig. S1 summarizes some fruit and vegetable samples that were used in this study.

2.3. Apparatus

The FT-IR spectrum was recorded using an IR spectrometer (Tensor 27, Bruker Optics, Germany) with KBr pellet. The transmission infrared spectra of all the samples exhibited broad peaks in a range of 400–4000 cm^{-1} at a resolution of 4 cm^{-1}. Surface morphological images and EDX spectra were recorded using a HITACHI S–3000N scanning electron microscope (SEM, Hitachi Co. Ltd., Japan). The XRD patterns were recorded with monochromatic Cu Kα radiation (λ = 0.15406 nm), a 2θ range of 10–80°, and a speed of 4 min^{-1} using an Empyrean (PANalytical, Netherlands). JEM–2010 (JEOL, USA) was used to obtain TEM images. The magnetic property was characterized using VSM (Lake Shore VSM 7403, USA) at 300 K. Both UAE and UAMSPE were performed in an ultrasonic bath (Sonorex Digitec DT 510 H, Bandelin, Germany) at internal tank dimensions of 300 × 240 × 150 mm, a frequency of 35 kHz, a maximum power of 640 W and heater 20–80 °C, thermostatically adjustable, with LED-display for target value and actual value of temperature. UB–10 Ultra Basic pH meter (Denver Instrument, USA) was used to measure the pH of the solution. The copper content in the sample extract was measured by Perkin–Elmer OPTIMA 2100 DV ICP-AES (Wellesley, Massachusetts, USA), associated with a standard ICP torch, axially viewed plasma system, and peristaltic pump. The operational system was controlled using the PE Winlab software. Table S1 describes the instruments and operating conditions for ICP-AES.

2.4. Preparation of Fe_3O_4/HAP/GQDs NPs

The protocol for GQDs preparation was slightly modified by pyrolysis of citric acid [50]. In brief, 0.2 g of citric acid was placed in a 100 mL round bottom flask and heated at 200 °C on a paraffin oil bath for 5 min. This transformed the white powder of citric acid to a dark yellow viscous liquid. This resulting liquid was added dropwise to 20 mL NaOH solution (0.25 M) while vigorously stirring at room temperature. After constantly stirring the obtained GQDs aqueous solution for 30 min, it was stored at 4 °C in an amber bottle. Scheme 1(a) illustrates the preparation procedure of the Fe_3O_4/HAP/GQDs NP. First, 100 mL of the aqueous solution containing $FeCl_3{\cdot}6H_2O$ (5 g) and $FeSO_4{\cdot}7H_2O$ (2.5 g) was added into a 500 mL three-necked flask (Fe^{3+}/Fe^{2+} molar ratio = 2) [51]. Subsequently, 28% NH_4OH solution (20 mL) was slowly and simultaneously dropped into the solution to obtain the colloidal solution by heating at 80 °C for 30 min on a paraffin oil bath with vigorous stirring in N_2 atmosphere. The solution was then mixed with 10 mL $Ca(NO_3)_2{\cdot}4H_2O$ solution (0.835 mol L^{-1}) and 10 mL NH_4OH (28% w/v) to control pH approximately at 11. Further, 10 mL H_3PO_4 (0.5 mol L^{-1}) was added drop by drop (Ca/P molar ratio was approximately 1.67) [52]. After incubation at 80 °C for 30 min, the mixture was mixed with GQDs (20 mL) and stirred at 80 °C for 30 min. Consequently, the resultant ultrafine magnetic particles were cooled to room temperature and aged for 2 h without stirring. The obtained precipitate was separated by a magnet, repeatedly washed with deionized water till neutrality, dried in the drying oven at 90 °C, and grinded with a mortar. The as-prepared products of Fe_3O_4/HAP/GQDs were obtained prior to use as a magnetic solid-phase adsorbent.

2.5. UAE

Under optimum conditions, copper in the food samples was extracted by UAE prior to determination. The dried sample powder (approximately 0.1 g) was accurately weighed into a 30 mL PTFE bottle with a screw cap. It was extracted under ultrasonication for 5 min using 10 mL of 1 M HCl as the extraction solvent. Subsequently, the extract was transferred into a 15 mL plastic centrifuge tube and centrifuged at 5000 rpm for 5 min. The aqueous supernatant was subjected to Cu analysis using ICP-AES. Scheme S1(a) shows the experimental procedure of UAE. The Cu concentration in the real sample was expressed as microgram per gram dry weight (μg g^{-1} DW) and calculated according to the following Eq. (1):

$$Copper\ (\mu g\ g^{-1}) = (C \times V)/(1000 \times W) \quad (1)$$

where C, V, and W are the content of Cu(II) obtained from the linear calibration graph (μg), the volume of the extraction solvent (mL), and the sample weight (g), respectively.

2.6. UA-MSPE

To study the optimum conditions for Cu(II), adsorption and desorption experiments were performed using Fe_3O_4/HAP/GQDs as SPE under the ultrasonication. The PTFE bottle with the screw cap containing 20 mg adsorbent in 10 mL model solution (50 μg L^{-1} Cu(II)), which was buffered at pH 5 with sodium acetate buffer solution, was placed on an ultrasonic bath at room temperature (30 ± 1 °C) and sonicated for 10 min. Subsequently, the adsorbent with the adsorbed Cu(II) was separated from the solution using an external magnetic field (magnet) and the supernatant was discarded. For elution, 1 M HNO_3 (5 mL) was added into the bottle and further sonicated for 5 min to desorb the Cu(II) from the adsorbent. With the aid of the magnet, the magnetic NPs were then deposited at the bottom of the PTFE bottle and its aqueous part was taken. The initial and final Cu(II) concentrations were determined using ICP-AES. The magnetic particles could be reused after a cleaning process with 5 mL re-extraction solution (1 M HNO_3) and 10 mL deionized water. Scheme S1(b) illustrates the route steps for MSPE of the target Cu(II) using the as-prepared Fe_3O_4/HAP/GQDs nanocomposite.

The residual concentration of Cu(II) in the aqueous solution was measured using ICP-AES. The equilibrium adsorption capacity (q_e, μg g^{-1}) of the magnetic adsorbent was calculated using Eq. (2) [53]:

$$q_e = (C_0 - C_e) \times V/m \quad (2)$$

where q_e is the equilibrium adsorption capacity (μg g^{-1}), V is the initial sample volume (mL), m is the mass of adsorbent (g), and C_0 and C_e are initial and residual concentrations after equilibrium of Cu(II) (μg mL^{-1}), respectively. The residual concentrations were calculated using the calibration of the instrument. The relative percentage recovery was calculated using Eq. (3) [54]:

$$Recovery\ (\%) = [(C_{found} - C_{real})/C_{added}] \times 100 \quad (3)$$

where C_{found}, C_{real}, and C_{added} are the Cu(II) concentration after an addition of the known amount of Cu(II) standard in the real sample, the Cu(II) concentration in the real sample, and the concentration of the known amount of Cu(II) standard that was spiked in the real sample, respectively.

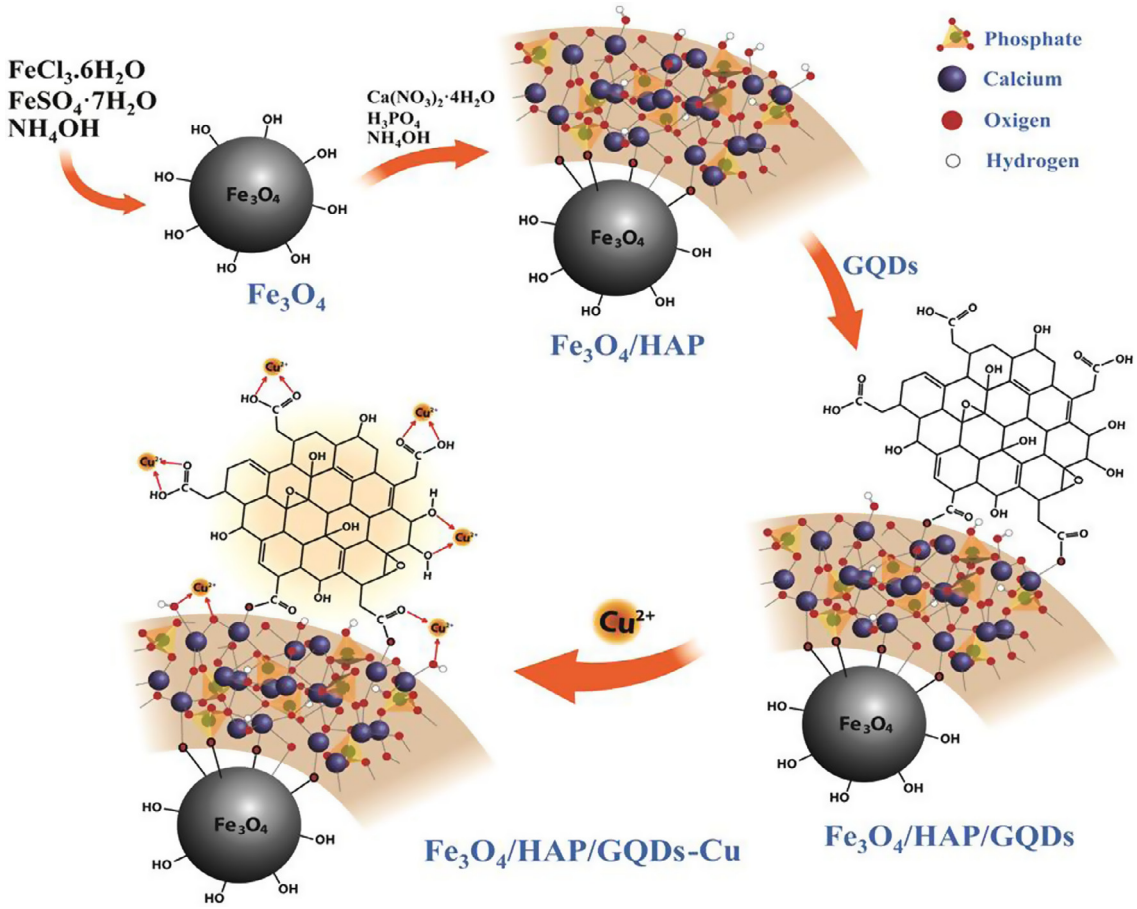

Scheme 1. The synthesis of the Fe_3O_4/HAP/GQDs nanocomposite (a) and its adsorption mechanism of copper (b).

3. Results and discussion

3.1. Characterization of Fe_3O_4/HAP/GQDs

Fig. 1 shows the TEM and SEM images of Fe_3O_4, Fe_3O_4/HAP and Fe_3O_4/HAP/GQDs. The particle size of the materials was analyzed using ImageJ software, and expressed as mean ± standard deviation (SD). Uniform and consistent spherical shapes were obtained with a mean diameter of approximately 8.4 ± 3.2 nm (Fe_3O_4), 10.6 ± 3.9 nm (Fe_3O_4/HAP), and 15.8 ± 4.4 nm (Fe_3O_4/HAP/GQDs). They were aggregated with many NPs, resulting in a rough surface.

Furthermore, to evaluate the relative quantity of the main elements of the Fe_3O_4/HAP/GQDs composite including Fe, O, Ca, P, and C, EDX measurements were conducted to confirm their elemental compositions (Fig. 1). The contents of Fe and O in the synthesized Fe_3O_4 were 71% and 29% weight, respectively. According to the EDX spectra, Fe (63.49%), O (32.12%), Ca (2.74%), and P (1.65) were present in Fe_3O_4/HAP and Fe (55.78%), O (32.14%), Ca (2.36%), P (1.43%), and C (8.29%) were in Fe_3O_4/HAP/GQDs. This demonstrated the successful deposition of Fe_3O_4/HAP/GQDs composite. The Ca:P ratios estimated from the EDX were 1.66 and 1.65 for Fe_3O_4/HAP and Fe_3O_4/HAP/GQDs, respectively, which are close to the stoichiometric ratio (1.67) that exists in the natural HAP [55,56]. This indicated that the HAP composite was successfully prepared with the proposed process.

The FT-IR spectra of Fe_3O_4, Fe_3O_4/HAP, and Fe_3O_4/HAP/GQDs were measured to get insights into the hyperfine chemical structure (Fig. 2). The peak of stretching vibrations at 587 cm^{-1} for Fe–O suggests the presence of iron oxide (Fe_3O_4) deposition [57]. The bands around 3445 cm^{-1} and 1631 cm^{-1} are due to O–H vibration of adsorption water. The IR spectrum of Fe_3O_4/HAP showed new absorption peaks at 1047 cm^{-1}, associated with the stretching modes of the P–O bonds of HAP. Therefore, HAP has a PO_4^{3-} group [58]. The pH of the medium solution using 28% (v/v) NH_4OH for the synthesis of Fe_3O_4/HAP was maintained. Excess NH_4OH was removed from the suspension with repeated washing with deionized water. However, it could be the residual base left in the Fe_3O_4/HAP powder. IR analysis showed a small broad peak at 1454 cm^{-1}, which is the characteristic peak of NH_4^+ group. However, this interference band in the IR spectrum of Fe_3O_4/HAP/GQDs was significantly reduced as trace. The appearance of the C–O (alkoxy) stretch band at 1100 cm^{-1} and C=O stretching vibration peak at 1626 cm^{-1} provides a strong evidence of GQDs and the formation of the Fe_3O_4/HAP/GQDs composite.

Fig. 3 shows the XRD patterns of (a) Fe_3O_4, (b) Fe_3O_4/HAP, and (c) Fe_3O_4/HAP/GQDs, which have been normalized based on the peak intensity of the (3 1 1) diffraction. Six peaks were located at 2θ = 30.1°, 35.5°, 43.1°, 53.5°, 57.0°, and 62.6°, which were accordingly indexed to the (2 2 0), (3 1 1), (4 0 0), (4 2 2), (5 1 1), and (4 4 0) diffractions of Fe_3O_4 (JCPDS No. 75–0033), respectively (Fig. 3(a)). Pure Fe_3O_4 with a face-centered cubic structure was confirmed [59,60]. In addition, the XRD patterns of the Fe_3O_4/HAP (Fig. 3(b)) and Fe_3O_4/HAP/GQDs (Fig. 3(c)) NPs demonstrated that the intensity of diffraction peak at 30.1°, 35.5°, 53.5°, 57.0°, and 62.6° decreased and some peak disappeared (43.1°) due to the effect of both HAP and GQDs that obstructed the crystal plane of Fe_3O_4. Therefore, the XRD results confirmed the existence of

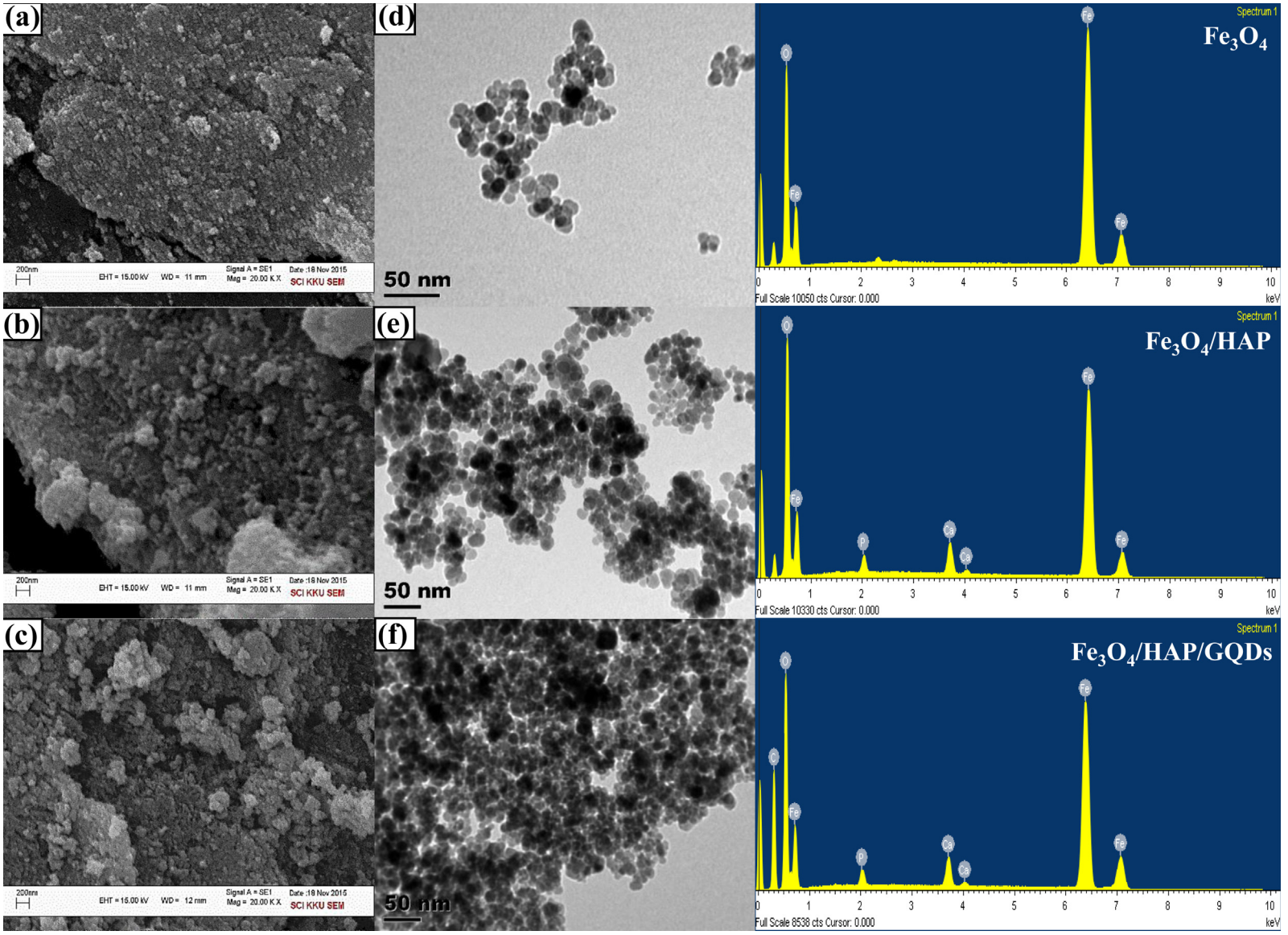

Fig. 1. SEM (a–c) and TEM (d–f) images of Fe_3O_4 (a, d), Fe_3O_4/HAP (b, e), and Fe_3O_4/HAP/GQDs (c, f) and their EDX spectra.

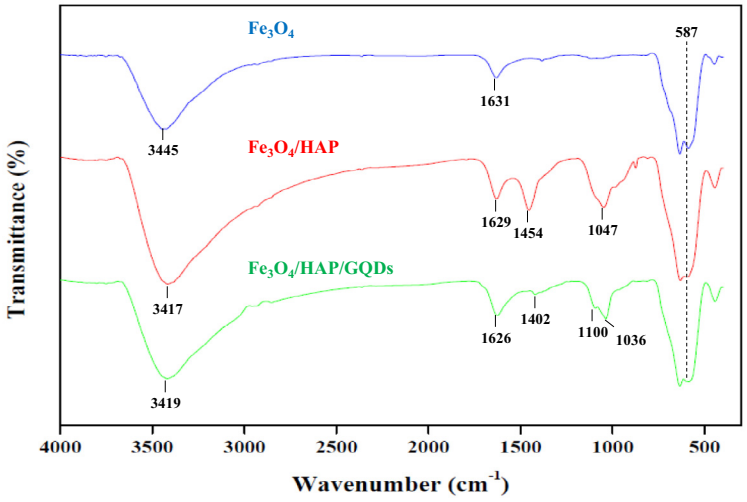

Fig. 2. FT-IR spectra of Fe_3O_4, Fe_3O_4/HAP, and Fe_3O_4/HAP/GQDs.

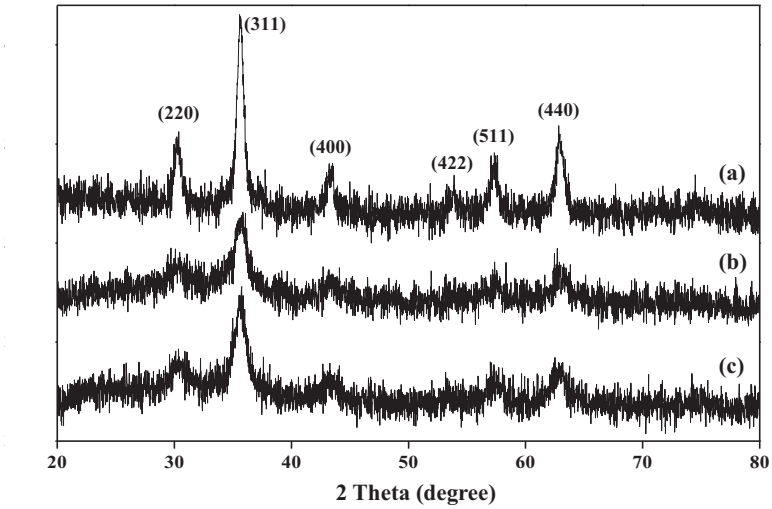

Fig. 3. XRD patterns of (a) Fe_3O_4, (b) Fe_3O_4/HAP, and (c) Fe_3O_4/HAP/GQDs.

both HAP and GQDs composites on Fe_3O_4 spinel without damaging most of its crystal structure.

The saturation magnetization values measured using VSM at room temperature were 69.5 emu g^{-1}, 47.6 emu g^{-1}, and 37.5 emu g^{-1} for Fe_3O_4, Fe_3O_4/HAP, and Fe_3O_4/HAP/GQDs, respectively (Fig. 4). Although the saturation magnetization of Fe_3O_4/HAP and Fe_3O_4/HAP/GQDs slightly decreased, which may be associated with a group of HAP and GQDs and grafted onto the surface of the free Fe_3O_4, complete magnetic separation can be achieved in 30 s by placing a magnet near the vessel containing the aqueous dispersion of Fe_3O_4/HAP/GQDs NPs. In the absence of an external magnetic field, a dark homogeneous dispersion exists. When an external magnetic field was applied, the black particles were attracted to the wall of vial and the dispersion became clear and transparent. Therefore, magnetic Fe_3O_4/HAP/GQDs can be used for a rapid Cu^{2+} ion magnetic separation.

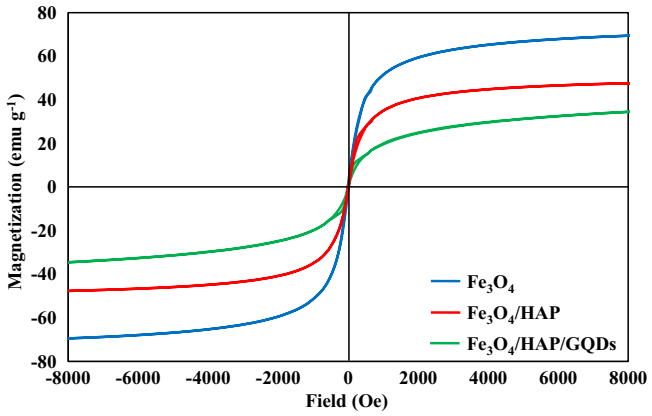

Fig. 4. Magnetization curves of the Fe_3O_4, Fe_3O_4/HAP, and Fe_3O_4/HAP/GQDs nanoadsorbent.

3.2. Optimization of the UAE procedure

The influence of the sample particle size, acid, concentration and volume of the extraction solution, sonication time, sample mass, and the ultrasonic power has been well studied on the extraction procedure. The nature and concentration of the extraction solution and sonication time are the most significant factor and are often evaluated during the UAE of inorganic species [61]. Therefore, to optimize the ultrasound extraction conditions, the extraction solvent, its concentration, and sonication time were

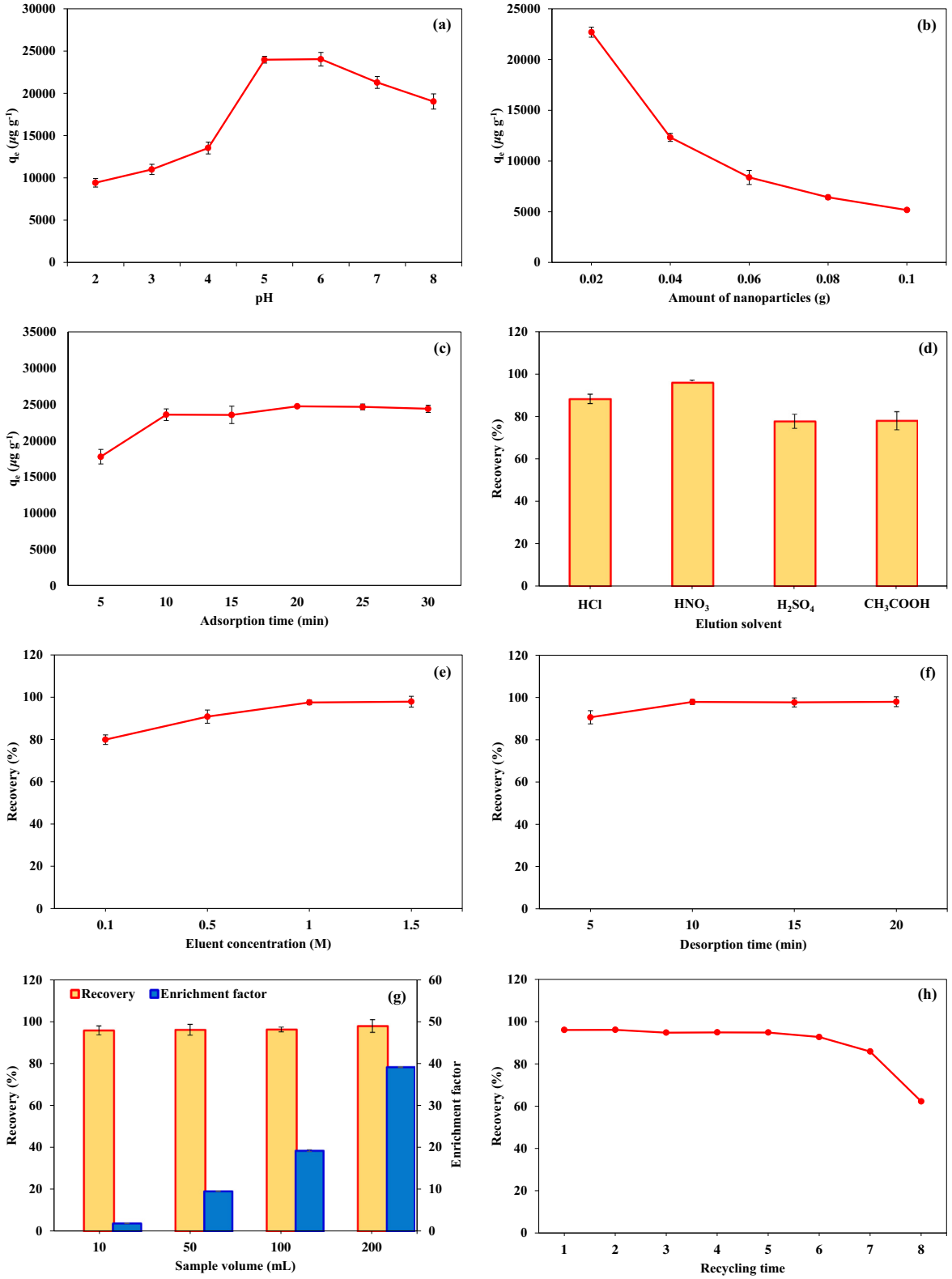

Fig. 5. UA-MSPE of (a) pH, (b) amount of MNPs, (c) adsorption time (d) type of elution solvent, (e) concentration of elution solvent, (f) desorption time, and (g) sample volume and EF and (h) performance of the magnetic nanosorbents in terms of reusability.

varied, whereas the sample mass (0.1 g), solvent volume (10 mL), and ultrasonic power (35 kHz) were constant. All experiments were carried out at room temperature at various conditions and performed in triplicates with real chili pepper as a model sample. It can be concluded from the results shown in Supporting information and Fig. S2 and to understand how the UAE works, it is better to study the extraction mechanism in detail (see Supporting information and Scheme S1(a)) [62–66].

3.3. Optimization of UA-MSPE procedure

3.3.1. Effect of pH

The pH of an aqueous solution is a very critical parameter that affects the adsorption process due to the functional groups of both the adsorbed molecules and adsorbent particles. At the active sites of the adsorbent, hydrogen ions (H^+) in the solution are directly involved in the adsorption process. Thus, we evaluated the influence of an initial pH on the adsorption efficiency in terms of the equilibrium adsorption capacity (q_e, $\mu g\ g^{-1}$). The effect of pH on adsorption was evaluated over a pH range of 2–8 using 10 mL water sample containing 50 $\mu g\ mL^{-1}$ of Cu^{2+} and 0.02 g magnetic NPs (MNPs) over 15 min of adsorption time. Fig. 5(a) clearly shows that the adsorption of Cu^{2+} increased with an increasing pH. At pH 2, the extent of Cu^{2+} adsorption was 9425 $\mu g\ g^{-1}$. The adsorption capacity of Cu^{2+} was lower at lower solution pH due to the competition between H^+ and Cu^{2+} ions anchored at the adsorption sites. The equilibrium adsorption capacity increased from pH 2 to 5, reaching its maximum value at pH 5 (23980 $\mu g\ g^{-1}$). Subsequently, the adsorption capacity declined as the pH of the solution increased further due to the precipitation of $Cu(OH)_2$ formed between Cu^{2+} and OH^-. The high q_e of Cu^{2+} was possibly attributed to the anionic behavior of the adsorbent at pH 5 because the Fe_3O_4/HAP/GQDs-based adsorbent has numerous hydroxyl and carboxyl groups acting as an anion even at a marginally acidic pH (i.e., pH 5). The adsorption mechanism of Cu^{2+} on the Fe_3O_4/HAP/GQDs could be attributed to the strong chelating tendency containing hydroxyl and carboxyl groups with Cu^{2+} and the electrostatic interactions of the NPs surface (Scheme 1(b)). When the sample solution is alkaline at pH > 8, Cu^{2+} majorly precipitates; therefore, the q_e at a pH > 8 was not studied due to the precipitation of $Cu(OH)_2$ in the solution. In conclusion, a sample pH of 5 was selected to guarantee the quantitative adsorption of Cu^{2+} for further experiments.

3.3.2. Mnps

The MNP mass is also a crucial factor that needs to be considered during the extraction process. It is beneficial from an economical point of view to conduct an adsorbent dosage assessment as it can provide information about which effective adsorbent to use and the ability of Cu(II) to be adsorbed with a minimum dosage. The adsorption study was performed using 0.02–0.1 g Fe_3O_4/HAP/GQDs to evaluate their equilibrium adsorption capacity. The other conditions were as follows: 10 mL water sample containing 50 $\mu g\ mL^{-1}$ Cu(II), pH 5, and 15-min adsorption time. According to Fig. 5(b), 0.02 g of MNPs was sufficient for the adsorption of Cu(II), and an additional amount of the sorbents caused a decrease in the equilibrium adsorption capacity. Higher amounts of NPs did not possibly disperse and adsorb effectively in the same adsorption time. A decrease in the surface area available to Cu(II) resulted from an overlapping or aggregation of the adsorption sites that decrease the adsorption efficiency [67]. Therefore, 0.02 g MNPs was the minimum concentration required to ensure complete adsorption of Cu(II).

3.3.3. Adsorption time

The effect of adsorption time on the equilibrium adsorption capacity of MNPs for Cu(II) was evaluated. For an optimization study, the effect of adsorption time in the range of 5–30 min was investigated. The q_e increased continuously with the increasing time from 5 to 10 min, following which it remained constant till 30 min (Fig. 5(c)). The short diffusion routes within the nanosorbents led to a highly rapid adsorption process; therefore, the equilibrium between the sample solution and adsorbent surface could also be reached within a shorter contact time. Therefore, an adsorption time of approximately 10 min was used for further studies.

3.3.4. Type of elution acid

The adsorption of Cu(II) was negligible at pH < 5; thus, an acidic medium was favorable for its desorption. The effect of type of acid eluent on the recovery of Cu(II) was investigated. A few acids (HCl, HNO_3, H_2SO_4, and CH_3COOH; 1 M; 5 mL) were examined as the eluent for the desorption of Cu(II) retained by the restricted access of the Fe_3O_4/HAP/GQDs. The highest recovery of Cu(II) was obtained with HNO_3 (Fig. 5(d)); therefore, HNO_3 was selected as the suitable eluting agent.

3.3.5. Concentration of elution acid

In general, dilute HNO_3 is widely used in sample preparation using UAE for metal ion determination [68]; hence, different concentrations of HNO_3 (0.1, 0.5, 1, and 1.5 M) were further investigated in detail and expressed as percent recovery of Cu(II). The recovery of Cu(II) increased with the increasing HNO_3 concentration up to 1 M, and then, it remained constant (Fig. 5(e)). Therefore, 5 mL of 1 M HNO_3 was chosen as the eluting acid.

3.3.6. Desorption time

The effect of desorption time on the ultrasonic extraction of the Cu(II) by MSPE was also studied in the range 5–20 min. The recovery of Cu(II) was highest at 10 min (Fig. 5(f)). The nanosorbents have small size and high surface area; hence, the desorption equilibrium could be attained with shorter times, and no significant change in its recovery was observed after 10 min. Therefore, the optimal desorption time for Cu(II) recovery was set at approximately 10 min for all subsequent experiments.

3.3.7. Effect of sample volume and enrichment factor (EF)

For this green approach, the UA-MSPE was used as a simple and fast step. In addition, the easy clean-up provided a high EF that guaranteed trace detections. The volume of the sample and elution acid could affect the EF. The sample volume was studied in the range of 10–200 mL, but it is advisable to set the maximum volume of the eluting acid at 5 mL because of the limitation of ICP-AES, which requires an injection volume of >3 mL. The EF was calculated using Eq. (4) [69]:

$$EF = C_{ext}/C_{ini} \quad (4)$$

where C_{ext} and C_{ini} are the analyte concentration in the extraction phase and initial analyte concentration in the aqueous phase, respectively. All the sample volumes used had no effect on the Cu (II) extraction recoveries (>95%) under the UA-MSPE procedure (Fig. 5(g)). Therefore, this extraction step could be performed with the abovementioned sample volumes. However, the EF increased with the increase in the sample volume up to 200 mL (EF = 1.9–39.2). Larger sample volumes were not considered due to difficulty and inconvenience in the sample preparation. Therefore, for real sample analysis, 200 mL sample extract that provided the highest EF was considered.

3.4. Effect of competing ions

The adsorption of target species on a sorbent can be influenced by the presence of other ions in the solutions that may compete for the binding sites. The efficiency of the proposed nano-sorbent to Cu (II) ion was performed in the presence of diverse metal ions of As(III), Cd(II), Cr(III), Fe(III), Hg(II), Mn(II), Ni(II), Pb(II), Sn(II) and Zn(II). In this experiment, 10 mL of solution containing 50 $\mu g\ L^{-1}$ Cu(II) as well as each interfering ion at two concentration levels (50 and 250 $ng\ mL^{-1}$) was analyzed according to the recommended extraction procedure. Table S3 reveals that the recoveries

were >95% in most cases, the investigated ions did not interfere with the adsorption of Cu(II) ion under this optimum condition. Therefore, it was confirmed that Fe_3O_4/HAP/GQDs had the capability of adsorbing Cu (II) ion in the presence of other metals and still maintained good recoveries.

3.5. Analytical performance evaluation

Table S2 lists the characteristic calibration data. To construct the calibration curve, a series of working solutions containing Cu (II) at six concentration levels of 1, 5, 10, 20, 40, and 60 μg L^{-1} were used. Linearity was in the range of 0.05–1500 μg L^{-1} with a regression coefficient of 0.9994. The limits of detection (LOD) and quantification (LOQ), defined as $3 \times SD_c/m$ and $10 \times SD_c/m$ (where SD_c is the SD of low Cu concentration and m is the slope of the calibration curve), were 0.015 and 0.049 μg L^{-1}, respectively. The precision, expressed as percent relative SD (%RSD) using the slope of the calibration graph in terms of repeatability (data from five independent standard preparations, intra-day%RSD) and reproducibility (work performed during five consecutive days, inter-day% RSD), was 0.87% and 4.47%, respectively. Therefore, the proposed method has high sensitivity and precision. The EF is defined as the ratio between Cu(II) concentration after extraction and its initial concentration in the standard solution. The EF of this method was 39.2, which ensured trace determination of Cu(II) residues in food samples.

Table 1 compares the analytical characteristics of the proposed method with those of the other reported methods. The proposed method provides superior performance compared to other reports in terms of linearity, LOD, LOQ, and EF. In addition, this method is robust as it requires less adsorbent, and is also cost effective and simple. It also offers high sensitivity and rapid pre-concentration with satisfied recovery.

3.6. Reusability of the nanosorbent

One of the significant factors considered while assessing the performance of the sorption materials is reusability of the magnetic nanosorbent. Thus, the sorption–desorption cycles were repeated eight times using the same sorbent. The magnetic nanosorbent was stable during the operation process for seven reusable times without loss of significant sorption capacity. High recovery was >85%, which then decreased to 62.3% (Fig. 5(h)). Therefore, the studied metal ion was reusable at least seven times.

3.7. Analysis of real samples

To demonstrate the applicability and reliability of the proposed method (both UAE and UA-MSPE), it was successfully applied to eleven samples of Thai food, i.e., ingredients of "Tom Yum Kung," including ten types of herbs (chili pepper, tomato, shallot, lemon grass, kaffir lime leaves, galangal, coriander, leek, stinkweed, and lime). The results presented in Table 2 confirmed that the Cu contents were found in all samples for UAE method and ranged from 10.95 ± 0.34 to 29.38 ± 1.38 μg g^{-1} DW. The chili pepper (1) sample had the highest Cu(II) concentration, whereas leek had the lowest. After the UAE method, all the samples were diluted to 200 mL with 0.1 M acetate buffer (pH 5) to reduce the concentration of Cu(II)

Table 1
Comparison of the present method with other sorbent-based methods for the determination of copper.

SPE material	Technique	Concentration range (ng mL^{-1})	Recovery (%)	LOD (ng mL^{-1})	LOQ (ng mL^{-1})	EF	References
APDC-AC[a]	UV–Vis	2–800	91.6–106	0.019	–	5	[70]
MWCNTs-D_2EHPA-TOPO[b]	FAAS	50–3000	97.4–99.6	50	–	25	[71]
ZrO_2/B_2O_3	FAAS	11–5000	–	3.3	11	10	[72]
Amidoamidoxime silica	FAAS	4–91	95–101	0.009	–	20	[73]
Cu-LIX-CNT-A[c]	FAAS	100–500	–	0.004	–	18.3	[74]
Nanometer-sized Al_2O_3	ICP-MS	1–100	95.9	0.045	–	5	[75]
Fe_3O_4@SiOH	ICP-AES	2–50	89.1–120	0.54	–	10	[76]
Fe_3O_4/HAP/GQDs[d]	ICP-AES	0.05–1500	83.5–104.84	0.015	0.049	39.2	This work

[a] Ammonium pyrrolidine dithiocarbamate impregnated activated carbon.
[b] Multiwalled carbon nanotubes impregnated with di-(2-ethyl hexyl phosphoric acid) and tri-*n*-octyl phosphine oxide.
[c] Carbon nanotubes impregnated with Cu(II)-LIX 622® complex.
[d] Fe_3O_4/hydroxyapatite/graphene quantum dots.

Table 2
The copper contents found in various Thai food ingredients.

Sample	Scientific name	UAE[a]		UA-MSPE[b]		
		Cu (μg g^{-1} DW)	Recovery (%)	Cu (μg g^{-1} DW)	Recovery (%)	EF[c]
Chili pepper (1)	*Capsicum chinense*	29.38 ± 1.38	96.21 ± 2.04	29.01 ± 0.77	94.21 ± 5.11	37.7
Chili pepper (2)	*Capsicum annuum*	22.26 ± 1.03	92.14 ± 3.06	20.96 ± 0.25	91.12 ± 4.10	36.4
Tomato	*Solanum lycopersicum*	17.62 ± 0.76	92.57 ± 2.37	17.04 ± 0.36	83.5 ± 1.53	33.3
Shallot	*Allium cepa var. aggregatum*	11.68 ± 0.34	94.10 ± 2.99	10.71 ± 0.25	99.73 ± 5.97	39.9
Lemon grass	*Cymbopogon Citratus*	11.07 ± 0.17	95.92 ± 1.97	10.43 ± 0.31	92.58 ± 8.45	37.0
Kaffir lime leaves	*Citrus hystrix*	11.06 ± 0.04	93.57 ± 1.18	10.22 ± 0.57	95.10 ± 4.67	38.0
Galangal	*Alpinia galanga*	11.85 ± 0.28	98.59 ± 6.54	11.36 ± 0.11	100.56 ± 5.48	40.2
Coriander	*Coriandrum sativum*	14.09 ± 0.43	93.66 ± 8.02	12.96 ± 0.60	90.17 ± 7.77	36.1
Leek	*Allium ampeloprasum*	10.95 ± 0.34	105.88 ± 4.78	10.48 ± 0.22	104.84 ± 5.95	41.9
Stinkweed	*Datura stramonium*	15.53 ± 0.26	95.21 ± 0.61	15.05 ± 0.69	96.73 ± 4.75	38.7
Lime	*Citrus aurantifolia*	11.55 ± 0.54	93.92 ± 5.43	10.67 ± 0.66	96.52 ± 5.96	38.6

Data are represented as mean ± SD of the determination in triplicate.
[a] Ultrasound assisted extraction.
[b] Ultrasound assisted magnetic solid-phase extraction.
[c] Enrichment factor (n = 3).

and the matrix effect prior to analysis under the optimal conditions using the UA-MSPE method. Cu(II) concentrations using ICP-AES followed by UA-MSPE ranged from 10.22 ± 0.57 to 29.01 ± 0.77 μg g^{-1} DW. In addition, the accuracy of the method was verified by calculating the recovery study in the real samples to complement the evaluation of the proposed method and to check matrix effects. Each sample was spiked with 100 μg L^{-1} of the Cu(II) standard solution and subjected to the optimized extraction procedure. The recoveries are expressed as the mean value of three independent determinations. The recovery ranged from 92.14 ± 3.06 to 105.88 ± 4.78% for UAE and 83.5 ± 1.53 to 104.84 ± 5.95% for UA-MSPE, indicating that both the extraction methods were free of the matrix interferences. The methods provide acceptable recovery, demonstrating that they are a relatively better choice for Cu(II) determination in the real samples. Moreover, the pre-concentration performance in terms of the EF from the UA-MSPE was also obtained. The remarkable EF values ranging from 33.3 to 41.9 indicated a good outcome of this approach.

4. Conclusion

A new reusable robust Fe_3O_4/HAP/GQDs NPs can be prepared by rapid, simple, and inexpensive synthetic method. The Fe_3O_4/HAP/GQDs NPs has a number of advantages, such as high surface area, easy elution of analytes and complete regeneration of adsorbent using deionized water treatment. The magnetic separation greatly improved the separation rate while avoiding the time-consuming column passing or filtration operation. Both UAE and UA-MSPE operation are convenient, effective, and rapid for the extraction of Cu^{2+} in different food samples prior to ICP-AES analysis. In addition, good recoveries, precision and high enrichment factor were obtained. Based on the obtained results, it is anticipated that the proposed method has a great analytical potential for pre-concentration of other trace metal residues in complicated food samples.

Conflicts of interest

The authors have declared no conflict of interest.

Acknowledgements

The authors thank the Higher Education Research Promotion and National Research University Project of Thailand, Office of the Higher Education Commission, through the Food and Functional Food Research Cluster of Khon Kaen University, Materials Chemistry Research Center, Department of Chemistry, Center of Excellence for Innovation in Chemistry (PERCH-CIC), Thailand for financial support of this study.

Appendix A. Supplementary data

Supplementary data associated with this article can be found, in the online version, at http://dx.doi.org/10.1016/j.ultsonch.2016.12.037.

References

[1] S. Siripongvutikorn, P. Thummaratwasik, Y.-W. Huang, Antimicrobial and antioxidation effects of Thai seasoning, Tom-Yum, LWT – Food Sci. Technol. 38 (2005) 347–352.
[2] M. Nakornriab, D. Puangpronpitag, Antioxidant activities and total phenolic contents of thai curry pastes, Int. J. Appl. Chem. 7 (2011) 43–52.
[3] C. Karadaş, D. Kara, Dispersive liquid–liquid microextraction based on solidification of floating organic drop for preconcentration and determination of trace amounts of copper by flame atomic absorption spectrometry, Food Chem. 220 (2017) 242–248.
[4] M.R. Moghadam, S.M.P. Jahromi, A. Darehkordi, Simultaneous spectrophotometric determination of copper, cobalt, nickel and iron in foodstuffs and vegetables with a new bis thiosemicarbazone ligand using chemometric approaches, Food Chem. 192 (2016) 424–431.
[5] C. Bo, Z. Ping, A new determining method of copper(II) ions at ng ml^{-1} levels based on quenching of the water-soluble nanocrystals fluorescence, Anal. Bioanal. Chem. 381 (2005) 986–992.
[6] Y. Yu, J.G. Shapter, R. Popelka-Filcoff, J.W. Bennett, A.V. Ellis, Copper removal using bio-inspired polydopamine coated natural zeolites, J. Hazard. Mater. 273 (2014) 174–182.
[7] H. Gupta, P.R. Gogate, Intensified removal of copper from waste water using activated watermelon based biosorbent in the presence of ultrasound, Ultrason. Sonochem. 30 (2016) 113–122.
[8] C. Boonmee, T. Noipa, T. Tuntulani, W. Ngeontae, Cysteamine capped CdS quantum dots as a fluorescence sensor for the determination of copper ion exploiting fluorescence enhancement and long-wave spectral shifts, Spectrochim. Acta Part A Mol. Biomol. Spectrosc. 169 (2016) 161–168.
[9] M.I.S. Veríssimo, J.A.B.P. Oliveira, M.T.S.R. Gomes, The evaluation of copper contamination of food cooked in copper pans using a piezoelectric quartz crystal resonator, Sens. Actuators, B 111–112 (2005) 587–591.
[10] Y. Shahbazi, F. Ahmadi, F. Fakhari, Voltammetric determination of Pb, Cd, Zn, Cu and Se in milk and dairy products collected from Iran: an emphasis on permissible limits and risk assessment of exposure to heavy metals, Food Chem. 192 (2016) 1060–1067.
[11] M. Chiha, O. Hamdaoui, F. Ahmedchekkat, C. Pétrier, Study on ultrasonically assisted emulsification and recovery of copper(II) from wastewater using an emulsion liquid membrane process, Ultrason. Sonochem. 17 (2010) 318–325.
[12] M. Khajeh, Multivariate optimization of microwave-assisted extraction of zinc and copper from soybean, J. Food Sci. Technol. 51 (2014) 2576–2583.
[13] R. Zare-Dorabei, S.M. Ferdowsi, A. Barzin, A. Tadjarodi, Highly efficient simultaneous ultrasonic-assisted adsorption of Pb(II), Cd(II), Ni(II) and Cu (II) ions from aqueous solutions by graphene oxide modified with 2,2′-dipyridylamine: central composite design optimization, Ultrason. Sonochem. 32 (2016) 265–276.
[14] N. Bilandžić, M. Dokić, M. Sedak, Metal content determination in four fish species from the Adriatic Sea, Food Chem. 124 (2011) 1005–1010.
[15] C.E. Banks, A.H. Wylie, R.G. Compton, Ultrasonically induced phthalocyanine degradation: decolouration vs. metal release, Ultrason. Sonochem. 11 (2004) 327–331.
[16] R. Kaş, Ö. Birer, Sonochemical shape control of copper hydroxysulfates, Ultrason. Sonochem. 19 (2012) 692–700.
[17] H.M. Jajda, K.G. Patel, S.R. Patel, V.H. Solanki, K.N. Patel, S. Singh, Comparative efficacy of two standard methods for determination of iron and zinc in fruits, pulses and cereals, J. Food Sci. Technol. 52 (2015) 1096–1102.
[18] P.R. Oliveira, A.C. Lamy-Mendes, E.I.P. Rezende, A.S. Mangrich, L.H. Marcolino Junior, M.F. Bergamini, Electrochemical determination of copper ions in spirit drinks using carbon paste electrode modified with biochar, Food Chem. 171 (2015) 426–431.
[19] M.J. Ceko, J.B. Aitken, H.H. Harris, Speciation of copper in a range of food types by X-ray absorption spectroscopy, Food Chem. 164 (2014) 50–54.
[20] S. Dashamiri, M. Ghaedi, K. Dashtian, M.R. Rahimi, A. Goudarzi, R. Jannesar, Ultrasonic enhancement of the simultaneous removal of quaternary toxic organic dyes by CuO nanoparticles loaded on activated carbon: central composite design, kinetic and isotherm study, Ultrason. Sonochem. 31 (2016) 546–557.
[21] F. Chemat, N. Rombaut, A.-G. Sicaire, A. Meullemiestre, A.-S. Fabiano-Tixier, M. Abert-Vian, Ultrasound assisted extraction of food and natural products. Mechanisms, techniques, combinations, protocols and applications. A review, Ultrason. Sonochem. 34 (2017) 540–560.
[22] P. Sricharoen, N. Lamaiphan, P. Patthawaro, N. Limchoowong, S. Techawongstien, S. Chanthai, Phytochemicals in *Capsicum oleoresin* from different varieties of hot chilli peppers with their antidiabetic and antioxidant activities due to some phenolic compounds, Ultrason. Sonochem. (2017), http://dx.doi.org/10.1016/j.ultsonch.2016.08.018.
[23] Z. Lianfu, L. Zelong, Optimization and comparison of ultrasound/microwave assisted extraction (UMAE) and ultrasonic assisted extraction (UAE) of lycopene from tomatoes, Ultrason. Sonochem. 15 (2008) 731–737.
[24] Q.-H. Chen, M.-L. Fu, J. Liu, H.-F. Zhang, G.-Q. He, H. Ruan, Optimization of ultrasonic-assisted extraction (UAE) of betulin from white birch bark using response surface methodology, Ultrason. Sonochem. 16 (2009) 599–604.
[25] G. Pan, G. Yu, C. Zhu, J. Qiao, Optimization of ultrasound-assisted extraction (UAE) of flavonoids compounds (FC) from hawthorn seed (HS), Ultrason. Sonochem. 19 (2012) 486–490.
[26] M. Kolaei, K. Dashtian, Z. Rafiee, M. Ghaedi, Ultrasonic-assisted magnetic solid phase extraction of morphine in urine samples by new imprinted polymer-supported on MWCNT-Fe_3O_4-NPs: central composite design optimization, Ultrason. Sonochem. 33 (2016) 240–248.
[27] F.N. Azad, M. Ghaedi, K. Dashtian, M. Montazerozohori, S. Hajati, E. Alipanahpour, Preparation and characterization of MWCNTs functionalized by N-(3-nitrobenzylidene)-N[prime or minute]-trimethoxysilylpropyl-ethane-1,2-diamine for the removal of aluminum(iii) ions via complexation with eriochrome cyanine R: spectrophotometric detection and optimization, RSC Adv. 5 (2015) 61060–61069.
[28] S.M. Álvarez, N.E. Llamas, A.G. Lista, M.B. Álvarez, C.E. Domini, Ionic liquid mediated extraction, assisted by ultrasound energy, of available/mobilizable metals from sediment samples, Ultrason. Sonochem. 34 (2017) 239–245.

[29] T. Sardohan, E. Kir, A. Gulec, Y. Cengeloglu, Removal of Cr(III) and Cr(VI) through the plasma modified and unmodified ion-exchange membranes, Sep. Purif. Technol. 74 (2010) 14–20.

[30] G. Dugo, T.M. Pellicanò, L.L. Pera, V.L. Turco, A. Tamborrino, M.L. Clodoveo, Determination of inorganic anions in commercial seed oils and in virgin olive oils produced from de-stoned olives and traditional extraction methods, using suppressed ion exchange chromatography (IEC), Food Chem. 102 (2007) 599–605.

[31] X. Jia, Y. Han, X. Liu, T. Duan, H. Chen, Dispersive liquid–liquid microextraction combined with flow injection inductively coupled plasma mass spectrometry for simultaneous determination of cadmium, lead and bismuth in water samples, Microchim. Acta 171 (2010) 49–56.

[32] A.B. Tabrizi, Development of a dispersive liquid–liquid microextraction method for iron speciation and determination in different water samples, J. Hazard. Mater. 183 (2010) 688–693.

[33] G. Xiang, S. Wen, X. Wu, X. Jiang, L. He, Y. Liu, Selective cloud point extraction for the determination of cadmium in food samples by flame atomic absorption spectrometry, Food Chem. 132 (2012) 532–536.

[34] A. Shokrollahi, M. Shamsipur, F. Jalali, H. Nomani, Cloud point extraction preconcentration and flame atomic absorption spectrometric determination of low levels of zinc in water and blood serum samples, Cent. Eur. J. Chem. 7 (4) (2009) 938–944.

[35] B. Feist, B. Mikula, Preconcentration of some metal ions with lanthanum-8-hydroxyquinoline co-precipitation system, Food Chem. 147 (2014) 225–229.

[36] S. de La Rochebrochard, E. Naffrechoux, P. Drogui, G. Mercier, J.-F. Blais, Low frequency ultrasound-assisted leaching of sewage sludge for toxic metal removal, dewatering and fertilizing properties preservation, Ultrason. Sonochem. 20 (2013) 109–117.

[37] E.A. Dil, M. Ghaedi, A. Asfaram, S. Hajati, F. Mehrabi, A. Goudarzi, Preparation of nanomaterials for the ultrasound-enhanced removal of Pb^{2+} ions and malachite green dye: chemometric optimization and modeling, Ultrason. Sonochem. 34 (2017) 677–691.

[38] H. Ciftci, Solid phase extraction method for the determination of cobaltin water samples on Duolite XAD-761 resin using 4-(2-pyridylazo) resorcinol by FAAS, Curr. Anal. Chem. 6 (2010) 154–160.

[39] B.K. Saikia, A.C. Dalmora, R. Choudhury, T. Das, S.R. Taffarel, L.F.O. Silva, Effective removal of sulfur components from Brazilian power-coals by ultrasonication (40 kHz) in presence of H_2O_2, Ultrason. Sonochem. 32 (2016) 147–157.

[40] A. Tadjarodi, S. Moazen Ferdowsi, R. Zare-Dorabei, A. Barzin, Highly efficient ultrasonic-assisted removal of Hg(II) ions on graphene oxide modified with 2-pyridinecarboxaldehyde thiosemicarbazone: adsorption isotherms and kinetics studies, Ultrason. Sonochem. 33 (2016) 118–128.

[41] N. Pourreza, J. Zolgharnein, A.R. Kiasat, T. Dastyar, Silica gel–polyethylene glycol as a new adsorbent for solid phase extraction of cobalt and nickel and determination by flame atomic absorption spectrometry, Talanta 81 (2010) 773–777.

[42] N.A. Al-Dhabi, K. Ponmurugan, P. Maran Jeganathan, Development and validation of ultrasound-assisted solid-liquid extraction of phenolic compounds from waste spent coffee grounds, Ultrason. Sonochem. 34 (2017) 206–213.

[43] A. Asfaram, M. Ghaedi, A. Goudarzi, Optimization of ultrasound-assisted dispersive solid-phase microextraction based on nanoparticles followed by spectrophotometry for the simultaneous determination of dyes using experimental design, Ultrason. Sonochem. 32 (2016) 407–417.

[44] X. Jiang, K. Huang, D. Deng, H. Xia, X. Hou, C. Zheng, Nanomaterials in analytical atomic spectrometry, TrAC, Trends Anal. Chem. 39 (2012) 38–59.

[45] Q. Liu, J. Shi, T. Wang, F. Guo, L. Liu, G. Jiang, Hemimicelles/admicelles supported on magnetic graphene sheets for enhanced magnetic solid-phase extraction, J. Chromatogr. A 1257 (2012) 1–8.

[46] Y. Zhai, X. Chang, Y. Cui, N. Lian, S. Lai, H. Zhen, Q. He, Selective determination of trace mercury (II) after preconcentration with 4-(2-pyridylazo)-resorcinol-modified nanometer-sized SiO_2 particles from sample solutions, Microchim. Acta 154 (2006) 253–259.

[47] Z. Zou, K. Lin, L. Chen, J. Chang, Ultrafast synthesis and characterization of carbonated hydroxyapatite nanopowders via sonochemistry-assisted microwave process, Ultrason. Sonochem. 19 (2012) 1174–1179.

[48] S. Saber-Samandari, S. Saber-Samandari, M. Gazi, Cellulose-graft-polyacrylamide/hydroxyapatite composite hydrogel with possible application in removal of Cu (II) ions, React. Funct. Polym. 73 (2013) 1523–1530.

[49] S. Benítez-Martínez, M. Valcárcel, Graphene quantum dots in analytical science, TrAC, Trends Anal. Chem. 72 (2015) 93–113.

[50] S. Benítez-Martínez, M. Valcárcel, Fluorescent determination of graphene quantum dots in water samples, Anal. Chim. Acta 896 (2015) 78–84.

[51] T. Harifi, M. Montazer, A robust super-paramagnetic TiO_2:Fe_3O_4: Ag nanocomposite with enhanced photo and bio activities on polyester fabric via one step sonosynthesis, Ultrason. Sonochem. 27 (2015) 543–551.

[52] R.K. Brundavanam, Z.-T. Jiang, P. Chapman, X.-T. Le, N. Mondinos, D. Fawcett, G.E.J. Poinern, Effect of dilute gelatine on the ultrasonic thermally assisted synthesis of nano hydroxyapatite, Ultrason. Sonochem. 18 (2011) 697–703.

[53] E.A. Dil, M. Ghaedi, A. Asfaram, The performance of nanorods material as adsorbent for removal of azo dyes and heavy metal ions: Application of ultrasound wave, optimization and modeling, Ultrason. Sonochem. 34 (2017) 792–802.

[54] P. Sricharoen, N. Limchoowong, S. Techawongstien, S. Chanthai, A novel extraction method for β-carotene and other carotenoids in fruit juices using air-assisted, low-density solvent-based liquid-liquid microextraction and solidified floating organic droplets, Food Chem. 203 (2016) 386–393.

[55] A.O. Lobo, M.A.F. Corat, S.C. Ramos, J.T. Matsushima, A.E.C. Granato, C. Pacheco-Soares, E.J. Corat, Fast preparation of hydroxyapatite/superhydrophilic vertically aligned multiwalled carbon nanotube composites for bioactive application, Langmuir 26 (2010) 18308–18314.

[56] W. Kim, F. Saito, Sonochemical synthesis of hydroxyapatite from H_3PO_4 solution with $Ca(OH)_2$, Ultrason. Sonochem. 8 (2001) 85–88.

[57] X. Tian, W. Wang, N. Tian, C. Zhou, C. Yang, S. Komarneni, Cr(VI) reduction and immobilization by novel carbonaceous modified magnetic Fe_3O_4/halloysite nanohybrid, J. Hazard. Mater. 309 (2016) 151–156.

[58] A. Singh, Hydroxyapatite, a biomaterial: its chemical synthesis, characterization and study of biocompatibility prepared from shell of garden snail, *Helix aspersa*, Bull. Mater. Sci. 35 (2012) 1031–1038.

[59] C. Ding, W. Cheng, Y. Sun, X. Wang, Novel fungus-Fe_3O_4 bio-nanocomposites as high performance adsorbents for the removal of radionuclides, J. Hazard. Mater. 295 (2015) 127–137.

[60] Y. Zhao, J. Li, L. Zhao, S. Zhang, Y. Huang, X. Wu, X. Wang, Synthesis of amidoxime-functionalized Fe_3O_4@SiO_2 core–shell magnetic microspheres for highly efficient sorption of U(VI), Chem. Eng. J. 235 (2014) 275–283.

[61] I. Lavilla, P. Vilas, J. Millos, C. Bendicho, Development of an ultrasound-assisted extraction method for biomonitoring of vanadium and nickel in the coastal environment under the influence of the *Prestige* fuel spill (North east Atlantic Ocean), Anal. Chim. Acta 577 (2006) 119–125.

[62] C.E.R. de Paula, L.F.S. Caldas, D.M. Brum, R.J. Cassella, Development of a focused ultrasound-assisted extraction method for the determination of trace concentrations of Cr and Mn in pharmaceutical formulations by ETAAS, J. Pharm. Biomed. Anal. 74 (2013) 284–290.

[63] A.-G. Sicaire, M.A. Vian, F. Fine, P. Carré, S. Tostain, F. Chemat, Ultrasound induced green solvent extraction of oil from oleaginous seeds, Ultrason. Sonochem. 31 (2016) 319–329.

[64] R. Vardanega, D.T. Santos, M.A. De Almeida, Intensification of bioactive compounds extraction from medicinal plants using ultrasonic irradiation, Pharmacogn. Rev. 8 (2014) 88–95.

[65] I.A. Saleh, M. Vinatoru, T.J. Mason, N.S. Abdel-Azim, E.A. Aboutabl, F.M. Hammouda, A possible general mechanism for ultrasound-assisted extraction (UAE) suggested from the results of UAE of chlorogenic acid from *Cynara scolymus* L. (artichoke) leaves, Ultrason. Sonochem. 31 (2016) 330–336.

[66] M. Vinatoru, An overview of the ultrasonically assisted extraction of bioactive principles from herbs, Ultrason. Sonochem. 8 (2001) 303–313.

[67] E. Akar, A. Altinişik, Y. Seki, Using of activated carbon produced from spent tea leaves for the removal of malachite green from aqueous solution, Ecol. Eng. 52 (2013) 19–27.

[68] V.C.D. Peronico, J.L. Raposo Jr., Ultrasound-assisted extraction for the determination of Cu, Mn, Ca, and Mg in alternative oilseed crops using flame atomic absorption spectrometry, Food Chem. 196 (2016) 1287–1292.

[69] S. Mukdasai, C. Thomas, S. Srijaranai, Two-step microextraction combined with high performance liquid chromatographic analysis of pyrethroids in water and vegetable samples, Talanta 120 (2014) 289–296.

[70] P. Daorattanachai, F. Unob, A. Imyim, Multi-element preconcentration of heavy metal ions from aqueous solution by APDC impregnated activated carbon, Talanta 67 (2005) 59–64.

[71] S. Vellaichamy, K. Palanivelu, Preconcentration and separation of copper, nickel and zinc in aqueous samples by flame atomic absorption spectrometry after column solid-phase extraction onto MWCNTs impregnated with D2EHPA-TOPO mixture, J. Hazard. Mater. 185 (2011) 1131–1139.

[72] Ö. Yalçınkaya, O.M. Kalfa, A.R. Türker, Chelating agent free-solid phase extraction (CAF-SPE) of Co(II), Cu(II) and Cd(II) by new nano hybrid material (ZrO_2/B_2O_3), J. Hazard. Mater. 195 (2011) 332–339.

[73] W. Ngeontae, W. Aeungmaitrepirom, T. Tuntulani, A. Imyim, Highly selective preconcentration of Cu(II) from seawater and water samples using amidoamidoxime silica, Talanta 78 (2009) 1004–1010.

[74] A. Tobiasz, S. Walas, A. Soto Hernández, H. Mrowiec, Application of multiwall carbon nanotubes impregnated with 5-dodecylsalicylaldoxime for on-line copper preconcentration and determination in water samples by flame atomic absorption spectrometry, Talanta 96 (2012) 89–95.

[75] J. Yin, Z. Jiang, G. Chang, B. Hu, Simultaneous on-line preconcentration and determination of trace metals in environmental samples by flow injection combined with inductively coupled plasma mass spectrometry using a nanometer-sized alumina packed micro-column, Anal. Chim. Acta 540 (2005) 333–339.

[76] C. Cui, B. Hu, B. Chen, M. He, Ionic liquid-based magnetic solid phase extraction coupled with inductively coupled plasma-optical emission spectrometry for the determination of Cu, Cd, and Zn in biological samples, J. Anal. At. Spectrom. 28 (2013) 1110–1117.

Ultrasonics Sonochemistry 38 (2017) 629–639

Contents lists available at ScienceDirect

Ultrasonics Sonochemistry

journal homepage: www.elsevier.com/locate/ultson

Phytochemicals in *Capsicum* oleoresin from different varieties of hot chilli peppers with their antidiabetic and antioxidant activities due to some phenolic compounds

Phitchan Sricharoen [a], Nattida Lamaiphan [a], Pongpisoot Patthawaro [a], Nunticha Limchoowong [a], Suchila Techawongstien [b], Saksit Chanthai [a,*]

[a] Materials Chemistry Research Center, Department of Chemistry and Center of Excellence for Innovation in Chemistry, Faculty of Science, Khon Kaen University, Khon Kaen 40002, Thailand
[b] Department of Plant Science and Agricultural Resources, Faculty of Agriculture, Khon Kaen University, Khon Kaen 40002, Thailand

ARTICLE INFO

Article history:
Received 17 April 2016
Received in revised form 11 August 2016
Accepted 11 August 2016
Available online 12 August 2016

Keywords:
Phytochemicals
Antidiabetic
Antioxidants
Phenolics
Chilli pepper
Ultrasound assisted extraction

ABSTRACT

Due to its wide use in nutritional therapy, a capsicum oleoresin extraction from hot chilli pepper was optimized using ultrasound assisted extraction. Under optimal conditions, a 0.1 g sample in 10 mL of a 20% water in methanol solution was extracted at 50 °C for 20 min to remove phytochemicals consisting of oleoresin, phenolics, carotenoids, flavonoids, capsaicinoids (pungency level), reducing sugars. Antioxidant and antidiabetic activities of the crude extracts from 14 chilli pepper varieties were examined. The antioxidant and antidiabetic activities of some phenolic compounds were also tested individually. The results showed that these chilli pepper samples are a rich source of phytochemicals with antioxidant and antidiabetic activities. High antioxidant activity of the extracts was evaluated using the 2,2-diphenyl-1-picrylhydrazyl, N,N-dimethyl-p-phenylenediamine dihydrochloride, 2,2′-azino-bis(3-ethylbenzothiazolin-6-sulfonic acid) and ferric ion reducing antioxidant power assays. The crude extracts had a lower level of sugars induced by the inhibitory effect of α-amylase activity. Thus, their enzymatic inhibitory effect might have resulted from a synergism among the phytochemicals concerned. Therefore, a diet with this type of food may have beneficial health effects.

1. Introduction

Chilli or chilli pepper (the genus *Capsicum*) is consumed worldwide with a continually increasing demand for fresh fruits and/or in products such as pastes, powders and oleoresin. Their popularity is derived from a combination of their characteristics such as color, taste and pungency [1–3]. It is a well-known and important economic crop in Thailand. Their cultivars are generally found in tropical and sub-tropical regions and require a warm humid climate. Chilli peppers can be grown in any variety of soils. They are just an indispensable condiment of every Thai household. It is consumed daily either as a single ingredient or as a food supplement. They are even reputed to have medicinal properties. Today, even though synthetic drugs are readily available and highly effective in curing various diseases, there are people who still prefer using traditional folk medicines because they have fewer harmful side effects. There is a wide diversity of compounds, especially secondary metabolites, found and isolated from plants. Some studies have shown that these compounds have therapeutic benefits including anticancer, antibacterial, analgesic, anti-inflammatory, antitumor, and antiviral properties to a greater or lesser extent [4,5]. More recently, a number of biological properties and potential health benefits of consuming chilli peppers have been investigated, e.g., antioxidants (free radical scavengers) [6], anti-inflammatory [7], anti-arthritic [8], anti-neoplastic [9], anticancer [10] and antifungal properties [11]. Additionally, chilli extracts also used in biochemical pest repellants and pesticides [8]. Their common phytochemical compounds include flavonoids, carotenoids, phenolics, vitamins, saponins and cyanogenic glycosides, stilbenes, tannins, nitrogenous compounds (alkaloids, amines, betalains), terpenoids and other endogenous metabolites [4,12]. This makes them extremely important pharmacological and medicinal agents, in addition to their traditional uses. Capsaicin is the main active component of chilli peppers, followed by dihydrocapsaicin, nordihydrocapsaicin, homodihydrocapsaicin, and homocapsaicin,

* Corresponding author at: 123 Mittraphab Road, M. 16, T. Ni-Muang, A. Muang, Khon Kaen University, Department of Chemistry, Faculty of Science, Khon Kean 40002, Thailand.
E-mail address: sakcha2@kku.ac.th (S. Chanthai).

http://dx.doi.org/10.1016/j.ultsonch.2016.08.018
1350-4177/

among others. Together, these are called capsaicinoids [13,14] and are responsible for the pungency of chilli pepper (the capsicum fruits) and their products [15,16]. Pungency is often expressed in Scoville Heat Units (SHUs) [17]. The interest in carotenoids from a nutritional standpoint has greatly increased recently because of their purported health benefits [18–20] including the ability to act as a provitamin A. Flavonoids are bioactive compounds found in plants. Previous studies indicated that consumption of food containing these compounds may reduce the incidence of cancer and cardiovascular diseases [21,22]. The protective effects of fruits and vegetables may be attributed to their antioxidants. These antioxidants may help to relieve oxidative stress, i.e., preventing free radicals from damaging biomolecules such as proteins, DNA, and lipids. Through additive and synergistic effects, the complex mixture of phytochemicals in vegetables and fruits may provide better protection than a single phytochemical [23–25]. Various techniques have been employed for the extraction of phytochemicals from plants, such as maceration [26], magnetic stirring [27], enzymatic extraction [28,29], ultrasound-assisted extraction (UAE) [15,30], Soxhlet extraction [31], supercritical fluid extraction [32], pressurized liquid extraction [33], microwave-assisted extraction [34–36] and pressurized hot water extraction [37]. Ultrasonic techniques are widely used in analytical chemistry to facilitate various steps some analytical process, particularly sample preparation. They are expeditious, inexpensive, and efficient alternatives to traditional extraction techniques. UAE may enhance extraction efficiency through disruption of cell walls, particle-size reduction, and enhanced mass transfer of the cell contents as a result of cavitation [38–41].

In the past, it was reported that consumption of spices such as chilli peppers may have positive effects on health. Therefore, the aim of the present study was to evaluate the antioxidant and antidiabetic activities of 20% water in methanol extracts of three species (14 samples) of the chilli peppers containing phytochemicals (oleoresin, capsaicinoids, phenolics, carotenoids, flavonoids, and reducing sugars) using four comparative assays (DPPH, DMPD, ABTS, and FRAP) for antioxidant activity and a 3,5-dinitrosalicylic acid (DNS) method for antidiabetic activity. Additionally, a comprehensive comparative study of DPPH free radical scavenging activity, total phenolics content and α-amylase inhibition of sixteen phenolic compounds was done. It may give a better understanding of which species have the greatest potential to benefit human health.

2. Materials and methods

2.1. Chemicals and reagents

All chemicals and reagents used were of analytical reagent grade. Folin-Ciocalteu reagent was acquired from Merck (USA). Aluminum chloride hexahydrate, sodium phosphate monobasic monohydrate, sodium phosphate diabasic anhydrous, 3,5-dinitrosalicylic acid, potato starch, acarbose, α-amylase from *Aspergillus oryzae*, 2,2-diphenyl-1-picrylhydrazyl (DPPH), N,N-dimethyl-p-phenylenediamine dihydrochloride (DMPD), 2,2′-azinobis(3-ethylbenzothiazolin-6-sulfonic acid (ABTS) and 2,4,6-tri(2-pyridyl)-s-triazine (TPTZ) were purchased from Sigma-Aldrich (USA). Sodium carbonate and sodium nitrite were purchased from Carlo Erba (Italy). Methanol, ethanol, acetonitrile, sodium hydroxide sodium acetate, acetic acid, ferric chloride hexahydrate and potassium persulfate were obtained from QRec™ (New Zealand). Tetrahydrofuran was purchased from UNILAB (Australia). Sodium potassium tartrate tetrahydrate was acquired from Ajax Finechem, (Australia). Maltose monohydrate was obtained from Acros Organics (USA). Deionized water with a resistivity of 18.2 MΩ cm produced using a Millipore water purification system (Molsheim, France) was used throughout.

2.2. Plant materials

Fourteen varieties of chilli pepper (*Capsicum annuum*, *Capsicum chinense*, and *Capsicum frutescens*) used in this study were collected from local breeding cultivars. Their common Thai names are PBC932, Shima Sakon Nakhon, Ratchaburi, Homkhao, Habanero White, Habanero Orange, Som, Thapthim Mo Dindaeng, Akkhani Phirot, Phet Mo Dindaeng, Phirot, Yot Son Khem 80, Huai Si Thon Kanlapaphruek and Mokho 2. All samples were cultivated in the experimental plots of the Department of Plant Science and Agricultural Resources, Faculty of Agriculture, Khon Kaen University. These samples were dried in an oven at 60 °C for 48 h. They were ground in a kitchen grinder (Philips, Indonesia) to pass a 100 mesh sieve and analyzed upon arrival at our laboratory. Otherwise, they were stored in plastic bottles and kept in a desiccator until analysis. Fig. 1 shows the chilli pepper varieties used in this study (the plant species are summarized in Table 4).

2.3. Apparatus

Ultrasound assisted extraction was done in an ultrasonic bath (Sonorex Digitec DT 510 H, Bandelin, Germany) at a frequency of 35 kHz and a maximum power of 640 W. Chromatographic analysis was performed with a HPLC (LC-20A, Shimadzu, Japan) that included an LC-20AD HPLC pump (Shimadzu, Japan), a Rheodyne injector with sample loop of 25 μL and a photodiode array detector (SPD-M20A, Shimadzu, Japan). Empower software was used for data acquisition. The separations were done using a Vertisep AQS C18 column (250 × 4.6 mm I.D., with 5 μm particle size). All absorbance measurements were performed using a UV–Visible spectrophotometer (Agilent Technologies Cary 60, Germany) with 750 μL quartz cuvettes (Fisher Scientific, USA) having a 10 mm optical path length.

2.4. Extraction procedure

Under the optimal conditions, an ultrasound assisted extraction (UAE) of chilli pepper samples was done prior to phytochemical determination and biological activity measurement. The dried powder of chilli pepper (0.1 g) was accurately weighed and placed in 20 mL amber glass bottle. It was extracted for 20 min in 10 mL of a water-methanol solvent (20:80%v/v). The temperature was maintained at 50 °C. Then, the extract was transferred into a 15 mL plastic centrifuge tube and centrifuged at 5000 rpm for 5 min to remove solid material. The liquid solutions were poured into brown screw capped bottles and stored at −20 °C until further use. Assays were done in triplicate throughout the study.

2.5. Capsicum oleoresin content

Capsicum oleoresin was extracted by UAE using the same conditions as described in Section 2.4. All the extracts were pooled and then evaporated to dryness. Dry weights of the extracted residue were noted. The oleoresin content was determined and expressed as g/100 g DW [42].

2.6. Determination of total phenolics

Total phenolic contents of the chilli pepper extracts were determined with a slight modification of [43,44] using Folin-Ciocalteu reagent and catechin standard compounds. The sample extract (100 μL) was mixed with 500 μL of 10% Folin-Ciocalteu reagent. After 3 min, 400 μL of 7.5% Na_2CO_3 was added to the mixture. This

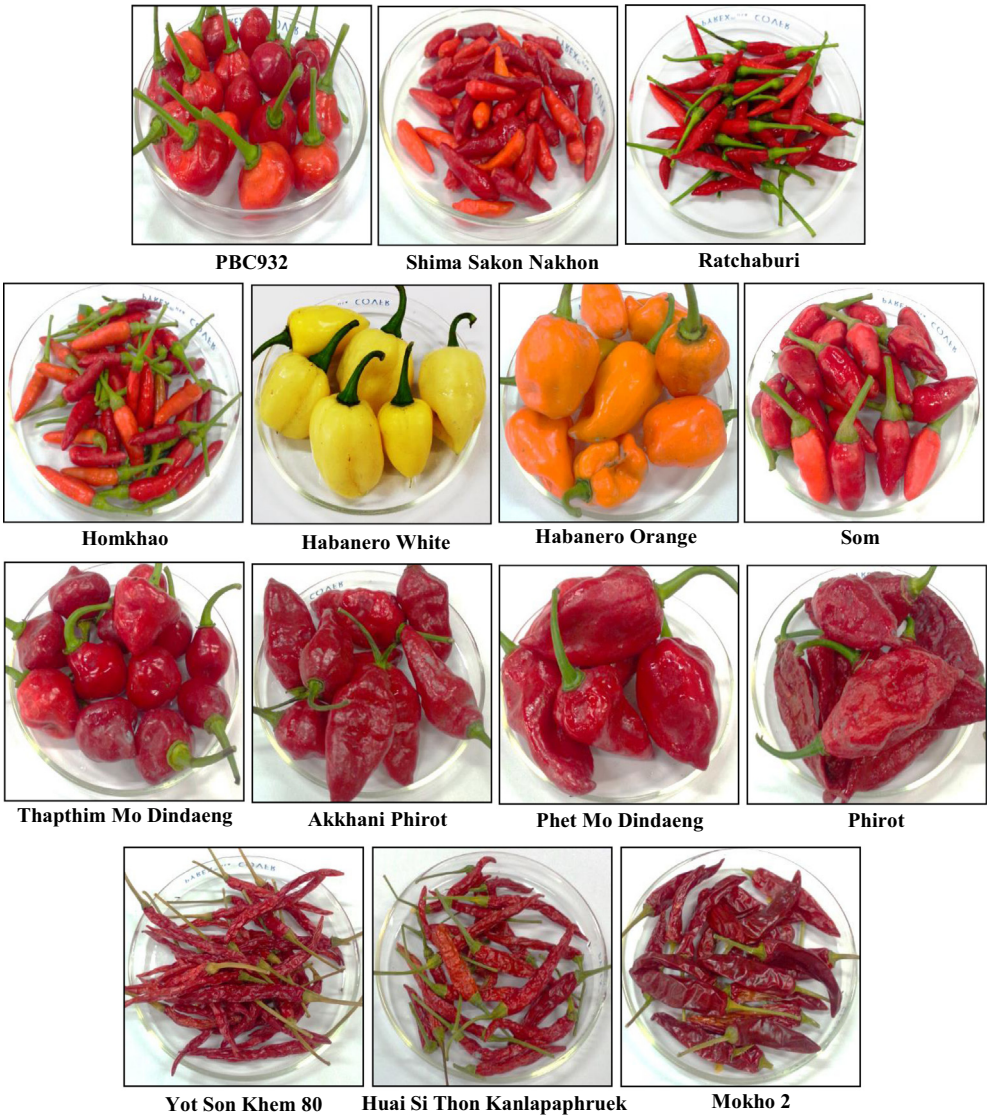

Fig. 1. Images showing the typical shapes and colors of 14 different varieties of chilli peppers.

solution was allowed to stand under dark conditions for 30 min at room temperature. The absorbance was measured spectrophotometrically at 765 nm against a blank solution. This procedure was repeated for all standard solutions of catechin. The total phenolics content is expressed as mg of catechin equivalent per gram of dry weight (mg CE/kg DW).

2.7. Determination of carotenoids

The total carotenoid content was determined by measuring the absorption of the extracts at 460 nm using UV–Visible spectrophotometry. β-Carotene was used as a standard. The total carotenoid contents were determined in triplicate and expressed as β-carotene equivalents in milligram per kilogram of dry weight (mg βCE/kg DW) [45].

2.8. Determination of flavonoids

The flavonoid content was measured using a previously reported colorimetric assay [46]. A 0.5 mL aliquot of the extracts or standard solutions of catechin, 2.8 mL of DI water and 0.2 mL of 5% (w/v) sodium nitrite were added into test tubes. After 5 min, 0.5 mL of 10% (w/v) $AlCl_3{\cdot}6H_2O$ was added. After incubation for 6 min at ambient temperature, 1 mL of 1 M NaOH was added to the reaction mixture. The absorbance was read at 510 nm against the blank solution. Total flavonoid contents in each sample were estimated using a catechin standard curve. The flavonoid content was expressed as mg catechin equivalents per gram of dry weight (mg CE/kg DW).

2.9. Determination of capsaicin and dihydrocapsaicin and its pungency level

Capsaicinoid content in the crude extracts was evaluated using RP-HPLC-PDA with a Vertisep AQS C_{18} column at ambient temperature. The injection volume was 20 μL for all standards and samples. A mixture of water:acetonitrile (30:70, v/v) was used as the mobile phase in an isocratic elution with flow rate of 1 mL min^{-1}. The elution time of the analytes was 10 min and detection was done at 280 nm. Quantitative data were obtained from integration of the HPLC peak areas for three injections of each sample using commercial capsaicin and dihydrocapsaicin as external standards. A stock solution of capsaicin and dihydrocapsaicin was prepared in methanol at a concentration of 10 μg mL^{-1} and stored at 20 °C.

The standard working solutions were prepared by appropriate dilution of the stock standard solution with methanol to the required concentrations. The pungency level of each of the chilli pepper variety used in this work is based on these two capsaicinoids tested in terms of Scoville Heat Units (SHU) [17].

2.10. Determination of reducing sugar

Total reducing sugars were determined using a 3,5-dinitrosalicylic acid (DNS) method [47]. For this application, 100 μL a standard solution or sample extract, 1400 μL of water and 500 μL of DNS reagent were used. It was prepared by mixing a sodium potassium tartrate solution (12.0 g of sodium potassium tartrate tetrahydrate in 8.0 ml of 2 M NaOH, heat at 50–70 °C), 96 mM 3,5-dinitrosalicylic acid solution (0.4381 g in 20 mL DI water, heated to 50–70 °C directly on a heating/stir plate with constant stirring) and 12 mL of DI water) were added to a test tube, and the mixture was vortexed and immersed in a boiling water bath for 5 min. After cooling in an ice bath, 3 mL of DI water was added and the absorbance of sample was recorded at 540 nm against a reagent blank. Linear regression was done using a maltose standard solution. The DNS solution was stored in an amber bottle at room temperature and was found to be stable for 6 months.

2.11. Bioassay for α-amylase inhibition

An α-amylase inhibition assay was performed with slight modification of [48]. Briefly, a starch solution (1% w/v) was obtained by stirring 1 g of potato starch in 100 mL of 20 mM sodium phosphate buffer (0.1324 g of $NaH_2PO_4{\cdot}H_2O$ and 0.2788 g of Na_2HPO_4) with 6.7 mM sodium chloride (0.039 g) at pH 6.9. An α-amylase solution (EC 3.2.1.1) was prepared by mixing 0.0253 g of α-amylase in 100 mL of cold DI water (1 unit/mL). Then, 100 μL of control, standard or sample was added to 900 μL an α-amylase solution and then incubated at 37 °C for 10 min. After that, 500 μL of the starch solution was added and incubated at 37 °C for 10 min. Then, 500 μL of DNS reagent was mixed added to the mixture and boiled in a water bath for 5 min. After cooling in an ice bath, 3 mL of DI water was added and the absorbance was measured at 540 nm against a reagent blank. The generation of maltose was quantified by the reduction of 3,5-dinitrosalicylic acid to 3-amino-5-nitrosalicylic acid, which is detectable at 540 nm. In the presence of α-amylase inhibitors, less maltose was produced and absorbance decreased. The results were expressed as milligrams of acarbose equivalent per gram dry weight (mg ACE/g DW). Percentage of inhibition determined using the following equation:

$$\%\ \text{Inhibition} = [(A_c - (A_{s1} - A_{s0}))/A_c] \times 100 \quad (1)$$

where A_c is the absorbance of control reaction which contains all reagents except the standard or the sample, A_{s1} is the absorbance in the presence of a standard or sample with enzyme and a starch solution and A_{s0} is the absorbance in the presence of a standard or sample with neither enzyme nor starch solution.

2.12. DPPH free radical scavenging activity assay

Radical scavenging activity of the sample extract was measured using the slightly modified procedure of [49,50]. Stable DPPH radicals in methanol or ethanol are dark purple in color. The compounds, against hydrogen atoms or electron donating ability, are measured by the bleaching of the purple colored DPPH solution. The final concentration of DPPH in ethanol was 0.1 mM with a 900 μL reaction volume, and 100 μL of various concentrations of standard (catechin) or sample extract were added. These solutions were vortexed and then incubated for 30 min in the dark at room temperature. Then, they were spectrophotometrically analyzed at 517 nm against a blank sample. The percentage of an inhibition of the DPPH was determined and plotted as a function of concentration of a gallic acid used as the reference. The final DPPH values were determined using a regression of catechin concentration and the percentage of DPPH inhibition. The results were expressed as milligrams of catechin equivalent per kilogram dry weight (mg CE/kg DW). The percentage of an inhibition of DPPH free radicals was determined using the following equation:

$$\%\ \text{Inhibition} = [(A_c - A_s)/A_c] \times 100 \quad (2)$$

where A_c is the absorbance of the control reaction containing all reagents except the standard or a sample and A_s is the absorbance in the presence of the standard or a sample.

2.13. DMPD radical scavenging activity assay

The method is based on the use of the radical $DMPD^+$ (purple color) generated by a reaction of Fe (III) in an acidic medium with DMPD. The antioxidant components have the ability to transfer a hydrogen atom to the colored radical $DMPD^+$ turning it into a colorless $DMPD^+$. The $DMPD^+$ radical has an absorbance peak at 505 nm [51]. Radical $DMPD^+$ was generated by mixing 1 mL of 100 mM DMPD, 100 mL of 0.1 M acetate buffer at pH 5.25 and 0.4 mL of 0.05 M $FeCl_3$. The standard antioxidant or the chilli pepper extract (100 μL) and 900 μL of the $DMPD^{\cdot+}$ solution was incubated at 29 °C for 10 min with continuous stirring. The absorbance at 505 nm was measured. The percentage inhibition was determined by:

$$\%\ \text{Inhibition} = [1 - A_s/A_c] \times 100 \quad (3)$$

where A_c is the absorbance of uninhibited radical cations and A_s is the absorbance measured after 10 min incubation followed by the addition of an antioxidant sample.

2.14. ABTS radical cation decolorization assay

Radical cation scavenging capacity of the chilli pepper extract using a reference standard was examined against $ABTS^{\cdot+}$ [25,52]. $ABTS^+$ was produced by a reaction of 7.4 mM of ABTS in water with 2.6 mM $K_2S_2O_8$, incubated in the dark at room temperature for 12–16 h. Before use, the $ABTS^+$ solution was diluted with methanol to produce an absorption between 0.7 and 0.9 a.u. at 734 nm. Briefly, 100 μL of the standard or the antioxidant extract was mixed with 900 μL of the $ABTS^+$ solution and incubated at room temperature in the dark. The absorbance at 734 nm was read after 30 min, and the percentage inhibition of ABTS was determined in the same manner as described for the DPPH and DMPD assays. Catechin was used to develop a standard curve. The free radical scavenging activity was expressed as mg CE/kg DW. All determinations were performed in triplicate.

2.15. Ferric ion reducing antioxidant power (FRAP) assay

The ferric ion reducing antioxidant power (FRAP) assay was used to evaluate the antioxidant capacity of the different varieties of chilli pepper extracts. This method was done with slight modifications [53]. The FRAP method measures the ability of antioxidants to reduce a ferric–tripyridyl-triazine (Fe^{3+}-TPTZ) complex to the blue colored ferrous form, which absorbs light at 593 nm. The ferric-TPTZ reagent was prepared by mixing 300 mM acetate buffer at pH 3.6, 10 mM TPTZ in 40 mM HCl and 20 mM $FeCl_3$ in a ratio of 10:1:1 (v/v/v). Fresh FRAP reagent was prepared before each experiment. Briefly, 100 μL of various concentrations of the reference standard or the sample extract were mixed with 900 μL of the FRAP reagent and incubated at 37°C for the duration

of the reaction. Absorbance was measured at 593 nm after 30 min. The increasing absorbance of the reaction mixture indicates an increase in reduction capacity. Catechin was used to prepare the standard curve. The antioxidant activities of the chilli pepper extracts were expressed as mg CE/kg DW.

2.16. Comparative study on antioxidant and antidiabetic activity of some phenolic compounds

For comparison of some phenolic compounds using DPPH free radical scavenging activity, both the total phenolics value and its α-amylase inhibitory effect were determined. The phenolic compounds included caffeic acid, capsaicin, catechin, catechol, dihydrocapsaicin, ferulic acid, gallic acid, guaiacol, *m*-cresol, *o*-coumaric acid, *o*-cresol, *p*-coumaric acid, *p*-cresol, quercetin, syringol and vanillin. Their activities were compared with those of the crude chilli pepper extracts. The reaction of each standard solution at a variety of concentrations was measured in the manner as described above (see Sections 2.6,2.11 and 2.12).

3. Results and discussion

3.1. Optimization of the extraction parameters and extraction mechanism

The following parameters were studied to optimize the ultrasonic extraction conditions: sample amount, type of extraction solvent, ratio of binary solvent, extraction temperature and extraction time. For the entire optimization study, the solvent volume and ultrasonic power were held constant at 10 mL and a frequency of 35 kHz, respectively. Each experiment was performed in triplicate with "Akkhani Phirot" chilli pepper sample. All the detailed optimizations and the extraction mechanism [54–57] are presented in the Supporting Information 1 (Figs. S1 and S2).

3.2. Capsicum oleoresin, phenolics, carotenoid and flavonoid contents

A phytochemical study of the chilli pepper extracts was done including some plant pigments and phenolic compounds shown in Table 1. The results showed comparative data for capsicum oleoresin, total phenolic, carotenoid and flavonoid contents of each chilli pepper variety. The capsicum oleoresin in these samples ranged from 19.23 ± 0.31 to 45.13 ± 2.23 g/100 g DW. Habanero White had the highest amount of capsicum oleoresin, while Ratchaburi had the lowest one. Total phenolic contents showed a wide variation from 6,392 ± 385 (Phirot) to 12,115 ± 141 (Phet Mo Dindaeng) mg CE/kg DW. This is in agreement with a previous report [58], which highlighted the importance of the plant genotype (species and variety within species) in the total phenolics content. The Phirot extract showed the highest carotenoid content (350.12 ± 15.99 mg βCE/kg DW) and Homkhao extract gave the lowest (99.47 ± 2.01 mg βCE/kg DW). Additionally, flavonoid contents found in 14 varieties of chilli peppers ranged from 6,541 ± 490 mg CE/kg DW (Yot Son Khem 80) to 23,110 ± 2797 mg CE/kg DW (Phirot).

3.3. Capsaicin, dihydrocapsaicin, total capsaicinoids and pungency level

Using UAE to produce chilli pepper extracts, quantitative determination was done of capsaicin and dihydrocapsaicin by RP-HPLC-PDA. These are the two main capsaicinoids in chilli peppers, by RP-HPLC-PDA, and this analysis allowed identification of their chemical structures. A mixture of water–methanol (20:80,%v/v) was chosen as the extraction solvent because of its lower toxicity and high extraction efficiency. The standard solutions used for the calibration curve were injected at regular time intervals between sample injections to confirm the retention time. The chromatograms shown in Fig. 2(a) and (b) correspond to the standard capsaicinoids and the sample extracts, respectively. It was found that capsaicin and dihydrocapsaicin were eluted at retention times of 5.70 and 6.87 min, respectively. The analytical characteristics were validated under the optimized conditions in terms of linearity, limit of detection, limit of quantification, and precision to estimate the efficiency and feasibility of the separation method. The results obtained are shown in Table 2. Linearity was observed over the range of 50-10,000 ng mL^{-1} for both capsaicinoids. The linear regression equations were: $y = 12{,}907x - 241.26$ and $y = 8248x + 146.47$ with regression coefficients of 0.9997 and 0.9995 for capsaicin and dihydrocapsaicin, respectively. The limits of detection (LOD) were 24 and 30 ng mL^{-1} for capsaicin and dihydrocapsaicin, respectively, while their limits of quantification (LOQ) were found to be 81 and 100 ng mL^{-1}. The precision was expressed as relative standard deviations (RSDs%). Their intra-day %RSDs ($n = 5$) were 2.68 and 1.11 at 100 and 500 ng mL^{-1} spiked concentrations for capsaicin and 2.36 and 1.44 at 100 and 500 ng mL^{-1} spiked concentrations for dihydrocapsaicin. The inter-day %RSDs ($n = 5$) were 3.99 and 2.71 at 100 and 500 ng mL^{-1} spiked concentrations for capsaicin and 3.77 and 2.42 at 100 and 500 ng mL^{-1} spiked concentrations for dihydrocapsaicin. This indicated an acceptable repeatability of the method. A comparison of the proposed extraction method with other published reports for the extraction and

Table 1
The contents of capsicum oleoresin, total phenolics, carotenoids and flavonoids found in 14 varieties of hot chilli peppers.

Sample	Oleoresin (g/100 g DW)	Total phenolics (mg CE/kg DW)[a]	Carotenoids (mg βCE/kg DW)[b]	Flavonoids (mg CE/kg DW)[a]
PBC932	28.20 ± 4.91	8517 ± 423	204.30 ± 4.47	9117 ± 617
Shima Sakon Nakhon	20.67 ± 0.96	11,189 ± 129	143.27 ± 3.59	7433 ± 992
Ratchaburi	19.23 ± 0.31	6691 ± 322	126.99 ± 6.47	7944 ± 325
Homkhao	24.60 ± 2.72	11,116 ± 140	99.47 ± 2.01	7903 ± 932
Habanero White	45.13 ± 2.23	7315 ± 218	209.01 ± 5.82	7333 ± 287
Habanero Orange	34.90 ± 4.86	7109 ± 353	282.80 ± 4.99	13,660 ± 507
Som	27.40 ± 1.56	6479 ± 98	201.87 ± 4.27	7056 ± 965
Thapthim Mo Dindaeng	40.47 ± 5.54	7156 ± 108	273.76 ± 4.24	14,331 ± 1023
Akkhani Phirot	33.63 ± 6.87	7974 ± 178	338.29 ± 2.70	12,784 ± 387
Phet Mo Dindaeng	43.50 ± 1.77	12,115 ± 141	262.22 ± 7.82	14,139 ± 889
Phirot	41.27 ± 5.50	6392 ± 385	350.12 ± 15.99	23,110 ± 2797
Yot Son Khem 80	28.03 ± 4.21	10,999 ± 125	207.26 ± 11.70	6541 ± 490
Huai Si Thon Kanlapaphruek	28.93 ± 2.39	11,571 ± 143	199.32 ± 6.60	20,576 ± 1325
Mokho 2	35.93 ± 2.57	9211 ± 476	213.87 ± 8.28	9593 ± 743

All data are represented as mean ± SD for triplicate determinations.
[a] Milligrams of catechin equivalent per kilogram of dry weight.
[b] Milligrams of β-carotene equivalent per kilogram of dry weight.

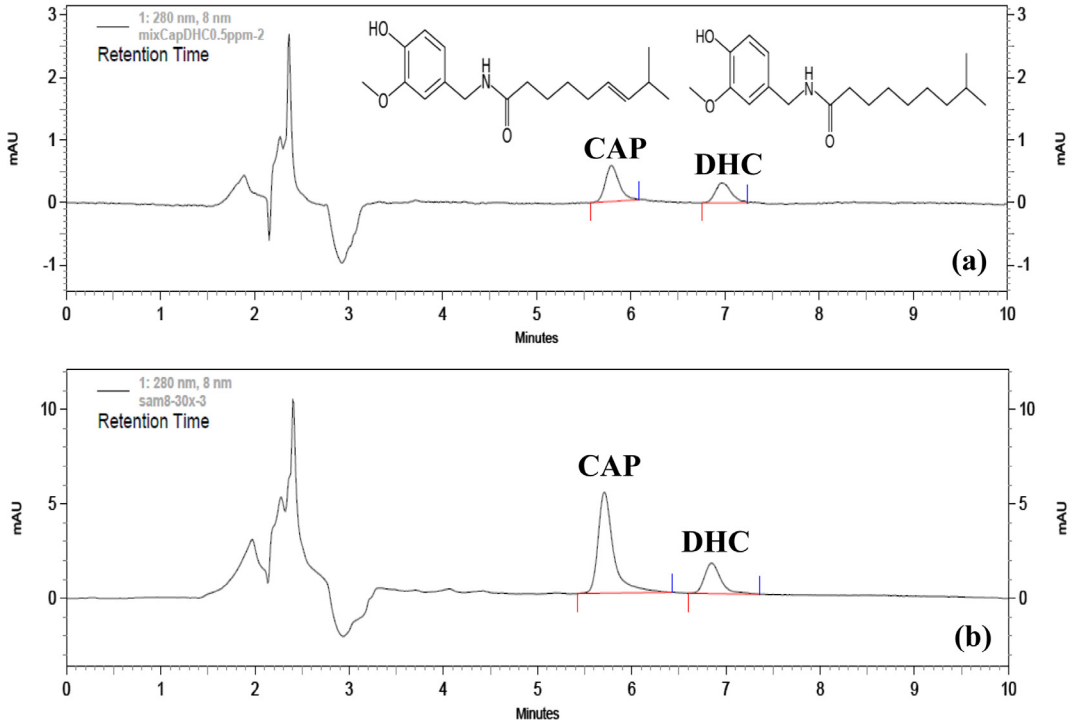

Fig. 2. HPLC chromatograms obtained from (a) capsaicin and dihydrocapsaicin standards, each 0.5 mg L^{-1} and (b) chilli pepper extract.

Table 2
Analytical features of merit for UAE-HPLC for determination of capsaicinoids.

Analytical feature	Analytical data	
	Capsaicin	Dihydrocapsaicin
Linear range (ng mL^{-1})	50–10,000	50–10,000
Linear equation	y = 12,907x − 241.26	y = 8248x + 146.47
Coefficient of regression (R^2)	0.9997	0.9995
Limit of detection (ng mL^{-1}, n = 12)	24	30
Limit of quantification (ng mL^{-1}, n = 12)	81	100
Relative standard deviations (RSDs,%) for		
Intra-day analysis (n = 5)	2.68[a], 1.11[b]	2.36[a], 1.44[b]
Inter-day analysis (n = 5)	3.99[a], 2.71[b]	3.77[a], 2.42[b]

RSDs (%) were calculated at each concentration of 100[a] and 500[b] ng mL^{-1} (n = 5).

determination of capsaicinoids is also compiled. The present method has better analytical features than others, especially for shorter extraction time to achieve high recovery when compared with those using rotisserie shaker (1 h) or hand shake (15 min) [59], rotary shaker (24 h) [60], and magnetic stirring extraction (2 h) [61]. Therefore, the main advantage of the extraction method is such superior extraction time with satisfactory analytical features of merit comparing with other sample preparations.

The UAE method was applied to determine the contents of capsaicin and dihydrocapsaicin of fourteen chilli pepper samples and their corresponding pungency levels. The capsaicinoids contents were determined and are presented in Table 3. The results confirmed that the capsaicinoids were found in all samples and the concentrations ranged from 614 to 25,976 mg kg^{-1} for capsaicin and 609 to 22,130 mg kg^{-1} for dihydrocapsaicin. Phirot had the highest level of total capsaicinoids (48,106 mg kg^{-1}), which was comparable with that of the other thirteen samples, which ranged from 1222 to 23,440 mg kg^{-1}. Mokho 2 had the lowest level (1222 mg kg^{-1}). The amount of capsaicinoids in a given variety can vary depending on the light intensity and temperature at which the plant is grown, the age of the fruit, and the position of the fruit on the plant. The first organoleptic test developed to measure the pungency level was the Scoville test [17]. Capsaicinoid content can be converted to Scoville heat units (SHU) by multiplying the capsaicinoid concentration in parts per million (ppm) by the coefficient of the heat value for each compound which is 9.3 for nordihydrocapsaicin (NDHC), 9.2 for nonivamide (PAVA) and 16.1 for both capsaicin (CAP) and dihydrocapsaicin (DHC) [37], as depicted in Eq. (4):

$$\mathrm{SHU} = 16.1 \times [\mathrm{CAP(ppm)} + \mathrm{DHC(ppm)}] \quad (4)$$

There are five levels of the pungency classified using SHU: non-pungent (0700 SHU), mildly pungent (700–3000 SHU), moderately pungent (3000–25,000 SHU), highly pungent (25,000–70,000 SHU) and very highly pungent (>80,000 SHU) [62]. The highest pungency was observed with Phirot (774,506 SHU), while Mokho 2 (19,681 SHU) had the lowest. Moreover, the accuracy of the method was verified by calculating the recovery studies in the real samples to evaluate the matrix effect. Each sample was spiked with 0.5 mg mL^{-1} of each capsaicin and dihydrocapsaicin solution. Then, the relative percentage recoveries were calculated as follows:

$$\%\ \mathrm{Recovery} = [(C_{found} - C_{real})/C_{added}] \times 100 \quad (5)$$

where C_{found}, C_{real}, and C_{added} are the concentration of the analyte after addition of the known amount of standard in a real sample, the concentration of the analyte in a real sample, and the concentration of the known amount of standard spiked in a real sample, respectively.

The results shown in Table 3 indicated that the recoveries of the proposed method expressed as the mean percentage (n = 3) were in the ranges of 62.2–92.4% and 52.4–94.8% for capsaicin and dihydrocapsaicin, respectively. This demonstrates that the method provides acceptable recovery for determination of capsaicinoids in these chilli pepper samples and implies that the matrix effect has a negligible impact on the efficiency of the analytical method.

Table 3
The content (mg) of capsaicinoids per kilogram of dried sample analyzed, recovery (%) and pungency level.

Sample	Capsaicin[a,b]		Dihydrocapsaicin[a,b]		Total capsaicinoids[b]	SHU[c]	Pungency level
	mg kg^{-1}	Recovery%	mg kg^{-1}	Recovery%	mg kg^{-1}		
PBC932	7364 ± 306	62.2	5805 ± 157	70.1	13,169	212,022	Very highly pungent
Shima Sakon Nakhon	3445 ± 81	81.4	1735 ± 73	52.4	5180	83,401	Very highly pungent
Ratchaburi	3238 ± 90	78.1	1414 ± 51	86.8	4652	74,898	Highly pungent
Homkhao	2240 ± 14	65.8	942 ± 38	94.4	3181	51,222	Highly pungent
Habanero White	4523 ± 123	62.8	811 ± 37	90.2	5334	85,879	Very highly pungent
Habanero Orange	11,042 ± 109	92.4	9332 ± 156	84.1	20,374	328,015	Very highly pungent
Som	1461 ± 44	67.6	916 ± 22	72.4	2377	38,271	Highly pungent
Thapthim Mo Dindaeng	13,626 ± 467	89.2	6986 ± 116	76.0	20,612	331,855	Very highly pungent
Akkhani Phirot	12,593 ± 282	86.2	6978 ± 237	92.7	19,571	315,098	Very highly pungent
Phet Mo Dindaeng	15,003 ± 151	90.4	8437 ± 158	62.7	23,440	377,383	Very highly pungent
Phirot	25,976 ± 272	88.6	22,130 ± 55	94.8	48,106	774,506	Very highly pungent
Yot Son Khem 80	1826 ± 58	70.1	1009 ± 37	56.5	2834	45,634	Highly pungent
Huai Si Thon Kanlapaphruek	1644 ± 32	77.4	1089 ± 48	68.7	2733	44,001	Highly pungent
Mokho 2	614 ± 28	76.7	609 ± 13	59.5	1222	19,681	Moderately pungent

[a] Value in mg kg^{-1} ± SD on dry weight basis.
[b] Mean of three independent measurements (n = 3).
[c] SHU: Scoville heat unit (1 mg kg^{-1} = 16.1 SHU).

Table 4
Plant species, reducing sugars and antidiabetic activities of the chilli peppers examined in this study.

Sample	Plant species	Reducing sugars[a] (mg maltose/g DW)	Antidiabetic activity	
			Inhibition[a] ± SD (%)	α-amylase activity[a] (mg ACE/g DW)[b]
PBC932	*C. chinense*	172.12 ± 12.58	40.61 ± 1.34	111.97 ± 4.64
Shima Sakon Nakhon	*C. frutescens* + *C. chinense*	67.63 ± 9.85	28.58 ± 1.16	70.46 ± 4.01
Ratchaburi	*C. frutescens*	72.07 ± 6.44	29.57 ± 2.05	73.87 ± 7.07
Homkhao	*C. chinense*	44.90 ± 3.30	38.33 ± 2.73	104.11 ± 9.42
Habanero White	*C. chinense*	163.59 ± 4.90	44.82 ± 4.45	126.47 ± 15.34
Habanero Orange	*C. chinense*	226.06 ± 9.86	50.76 ± 1.46	146.98 ± 5.02
Som	*C. chinense*	86.26 ± 5.28	43.66 ± 0.91	122.47 ± 3.15
Thapthim Mo Dindaeng	*C. chinense*	132.78 ± 1.41	32.39 ± 4.88	83.60 ± 16.83
Akkhani Phirot	*C. chinense*	93.69 ± 5.00	49.52 ± 3.32	142.70 ± 11.45
Phet Mo Dindaeng	*C. chinense*	113.54 ± 8.50	34.11 ± 3.98	89.54 ± 13.73
Phirot	*C. chinense*	69.60 ± 3.64	27.01 ± 1.22	65.04 ± 4.22
Yot Son Khem 80	*C. annuum*	60.40 ± 3.51	27.69 ± 1.55	67.38 ± 5.34
Huai Si Thon Kanlapaphruek	*C. annuum*	63.99 ± 5.35	26.61 ± 2.15	63.65 ± 7.41
Mokho 2	*C. annuum*	90.51 ± 5.56	20.61 ± 2.23	42.98 ± 7.69

[a] Measured in triplicate (n = 3) ± standard deviation (SD).
[b] Milligrams of acarbose equivalent per gram of dry weight.

3.4. Reducing sugar and antidiabetic activity

Determination of reducing sugar in the chilli pepper extracts by a dinitrosalicylic acid (DNS) method was done [63]. For this method, DNS reacts with a free carbonyl group of the sugar under an alkaline condition, forming 3-amino-5-nitrosalicylate, an aromatic compound with maximum absorption at 540 nm. The optical absorbance is directly proportional to the amount of reducing sugar. The reducing sugars with a potential aldehyde or keto group include glucose, galactose, lactose, fructose, arabinose and maltose [64]. In chilli peppers, the reducing sugar levels ranged from 60.40 ± 3.51–226.06 ± 9.86 mg maltose/g DW. Habanero Orange possessed the highest amount of reducing sugars (226.06 ± 9.86 mg maltose/g DW), whereas Yot Son Khem 80 had the lowest (60.40 ± 3.51 mg maltose/g DW). Furthermore, levels of reducing sugars are known to increase during the ripening of chilli peppers (Table 4) [64]. α-Amylase is responsible for the breakdown of starch to more simple sugars like maltose. Thus, the inhibition of this enzyme can delay the carbohydrate digestion and reduce the rate of glucose absorption [65]. The antidiabetic effect was assessed against α-amylase inhibitory activity using specific optimizations. In the subsequent experiments, α-amylase concentration, inhibition time and digestion time were preliminarily optimized. Then the optimal conditions were applied to the chilli pepper extracts. The α-amylase concentration and inhibition time, which are considered influential factors, were investigated in detail (Supporting Information 2, Fig. S3(a) and (b)). The α-amylase inhibitory activity (expressed in percent) of the chilli pepper extracts was investigated. All samples significantly inhibited α-amylase activity in the range of 20.61 ± 2.23% (for Mokho 2) and 50.76 ± 1.46% (for Habanero Orange). The α-amylase inhibitory activities of less than 50% were found for all concentrations tested of the extraction solvent, thus, its IC_{50} value could not be determined. However, the α-amylase inhibitory activity (expressed in mg ACE/g DW) of these samples was found to be in the range of 42.98 ± 7.69 mg ACE/g DW (for Mokho 2) to 146.98 ± 5.02 mg ACE/g DW (for Habanero Orange) (Table 4).

3.5. Antioxidant activity

Alternative common standards for the test methods, different calibration standards and different ways of expressing concentrations (dry weight, DW; fresh weight, FW; molar or mass unit) were applied to compare the results reported in the literature. Generally, having applicable standard for all methods enables us to obtain a set of simple and comparable results. Therefore, the calibration data of catechin were used for the evaluation of antioxidant activity of the 14 varieties of chilli peppers, expressed as mg CE/kg DW.

Table 5
Antioxidant activities of the chilli pepper extracts determined using four different assays.

Sample	DPPH	DMPD	ABTS	FRAP
PBC932	3623 ± 179	1250 ± 59	10,152 ± 300	7824 ± 276
Shima Sakon Nakhon	5197 ± 42	1787 ± 14	13,214 ± 118	10,911 ± 88
Ratchaburi	3088 ± 156	1045 ± 52	8587 ± 138	6601 ± 229
Homkhao	4975 ± 92	1587 ± 30	14,022 ± 258	10,402 ± 194
Habanero White	3214 ± 146	1088 ± 48	9515 ± 210	6814 ± 108
Habanero Orange	3093 ± 48	998 ± 16	8612 ± 133	6587 ± 100
Som	2450 ± 117	852 ± 39	6912 ± 228	5214 ± 146
Thapthim Mo Dindaeng	3169 ± 126	1101 ± 42	8864 ± 254	6432 ± 166
Akkhani Phirot	3449 ± 151	1214 ± 50	9641 ± 212	7211 ± 118
Phet Mo Dindaeng	6071 ± 75	2114 ± 25	17,057 ± 210	12,741 ± 158
Phirot	2304 ± 186	763 ± 62	6511 ± 320	5024 ± 191
Yot Son Khem 80	4782 ± 100	1424 ± 33	13,378 ± 281	12,141 ± 111
Huai Si Thon Kanlapaphruek	5418 ± 72	1812 ± 24	15,102 ± 201	11,000 ± 151
Mokho 2	3730 ± 43	1287 ± 14	10,488 ± 120	7211 ± 90

DPPH, DMPD, ABTS, and FRAP were expressed as milligrams of catechin equivalent per kilogram of dry weight (mg CE/kg DW).
Data are given as mean ± SD (n = 3).

These results are presented in Table 5, listing the antioxidant activity measurements of each chilli pepper extract evaluated by DPPH, DMPD, ABTS and FRAP assays. Different samples showed various profiles of their antioxidant activity. Using the DPPH assay, Phet Mo Dindaeng gave the highest antioxidant activity (6071 ± 75 mg CE/kg DW), while Phirot had the lowest (2304 ± 186 mg CE/kg DW). Phet Mo Dindaeng also showed the highest antioxidant activity determined by DMPD (2114 ± 25 mg CE/kg DW), ABTS (17,057 ± 210 mg CE/kg DW) and FRAP (1274 ± 158 mg CE/kg DW) assays. Phirot gave the lowest values as assayed with DMPD (763 ± 62 mg CE/kg DW), ABTS (646,511 ± 320 mg CE/kg DW) and FRAP (5024 ± 191 mg CE/kg DW).

3.6. Antioxidant activity, phenolics power and α-amylase inhibition of standard compounds

Sixteen relevant phenolic standards were used. These included caffeic acid, capsaicin, dihydrocapsaicin, catechin, catechol, ferulic acid, gallic acid, guaiacol, m-cresol, o-coumaric acid, o-cresol, p-coumaric acid, p-cresol, quercetin, syringol and vanillin. They were comparatively evaluated, ranking their antioxidant power (by DPPH), total phenolic power (by Folin-Ciocalteu) and antidiabetic power (by α-amylase inhibitory assay). First, the results of DPPH and α-amylase inhibitory assays were reported as the concentration providing 50% radical scavenging (IC_{50}), while that of Folin-Ciocalteu assay was reported the concentration of a total phenolics having an absorbance equal to 0.5 a.u. ($C_{A0.5}$). Lower IC_{50} and $C_{A0.5}$ values correspond to larger scavenging activities. The DPPH radical scavenging activities of these reference compounds were comparatively evaluated as shown in Table 6. Gallic acid exhibited the highest radical scavenging activity, 0.90 ± 0.04 μg mL^{-1}, compared with other phenolics, and o-coumaric acid had the lowest activity of 2,007.62 ± 58.41 μg mL^{-1}. The total phenolic activity was ranked as follows: caffeic acid > quercetin > catechol > o-cresol > catechin > m-cresol > o-coumaric acid > p-cresol > gallic acid > guaiacol > p-coumaric acid > ferulic acid > vanillin > syringol > capsaicin > dihydrocapsaicin (Table 7). The scavenging activity of the antidiabetic power was also evaluated (Table 8). With the α-amylase inhibitory assay, only caffeic acid (IC_{50} = 144.58 ± 1.11 μg mL^{-1}), catechin (IC_{50} = 133.71 ± 1.45 μg mL^{-1}), ferulic acid (IC_{50} = 152.92 ± 0.54 μg mL^{-1}) and quercetin (IC_{50} = 176.80 ± 0.44 μg mL^{-1}) were observed to exhibit ways inhibitory activities with an increasing concentration, which was comparable with that of 16 phenolic standards. The compounds like these four standards can inhibit enzymes, causing a delay in carbohydrate digestion, thereby reducing the rate of glucose absorption. However, the enzymatic inhibition of the four phenolics was lower than that of acarbose (the positive control, IC_{50} = 27.91 ± 0.2 μg mL^{-1}). Therefore, these reference standards can be used for directing *in vitro* antioxidant activity, total phenolics and antidiabetic activity of the chilli pepper crude extracts depending on screening method used and the selection of suitable and generally applicable standards for the methods used. The linearity and regression equation of their calibration curves allowed quantification of antioxidant activity, total phenolics and antidiabetic activity using the standards listed in Tables 6–8.

3.7. Correlation analysis

Table S1 shows the correlations among different evaluated parameters. In this study, linear correlations among each of the antioxidant assays were found with their correlation coefficients (r) of 0.9858 for DPPH *vs* DMPD, 0.9931 for DPPH *vs* ABTS, 0.9716 for DPPH *vs* FRAP, 0.9751 for DMPD *vs* ABTS, 0.9278 for DMPD *vs* FRAP and 0.9666 for ABTS *vs* FRAP. It is indicated that when all 14 varieties of these chilli peppers were comparatively analyzed using statistical methodology, the correlation coefficients among their antioxidant activities based on DPPH, DMPD, ABTS, and FRAP assays were high and statistically significant. Also, the high correlation between the DPPH, DMPD, ABTS and FRAP assays is indicative of interchangeability of the four methods in evaluating the antioxidant activity of the chilli pepper extracts. The total phenolic content represents most, but not all of the antioxidant compounds in the extracts. So, there is a clear relationship between antioxidant activity and the total phenolic content. The correlations between the DPPH, DMPD, ABTS and FRAP assays were compared with their TP resulting in correlation coefficients of 0.9800, 0.9515, 0.9721 and 0.9642 for DPPH, DMPD, ABTS and FRAP, respectively. This result indicates that when the phenolic contents of all 14 chilli pepper varieties were statistically analyzed, there was a positive and highly significant trend, indicating that total phenolics are mainly responsible for the antioxidant activity of these chilli peppers. However, TP did not correlate with TC, TF, CAP, DHC, SHU, RS, α-AIA. The SHU values positively correlated with CAP (0.9924) and DHC (0.9985), which is related with their pungency or hotness.

4. Conclusions

This study was aimed to extract capsicum oleoresin using ultrasound assisted extraction. In general, the ultrasonic waves have proved to be effective in obtaining extracts from chilli pepper, and it can be an alternative technique to conventional extraction methods. It is a simple, effective method and can be applied to other chemicals. The maximum amount of capsaicinoid extraction was found using 20% water in methanol solvent which was quantified by high performance liquid chromatography. Details of a nutritional study of chilli peppers with respect to their antidiabetic, antioxidant and phytochemical contents were also presented. The crude extract showed potent antioxidant activity and antidiabetic activity. In addition, the study gives the profiles of bioactive components such as phenolics, carotenoids, flavonoids and reducing sugars. Most importantly, the widespread use of this method can be recommended as an alternative green extraction methodology to monitor the phytochemicals in various samples with good recovery. Therefore, the potential benefits of chilli pepper consumption to human health are suggested based upon the functional properties of phytochemicals and their biological activities.

Table 6
Calibration data of phenolic standards analyzed by DPPH assay.

Standard	Regression equation ($n = 3$)	Calibration (μg mL^{-1})	R^2	IC_{50}[a] ± SD (μg mL^{-1})
Caffeic acid	y = 1.4461x − 1.5834	2–7	0.9955	3.56 ± 0.19
Capsaicin	y = 0.785x + 38.606	10–60	0.9964	14.51 ± 0.57
Catechin	y = 18.3131x − 2.8232	0.5–6.0	0.9995	3.33 ± 0.15
Catechol	y = 18.3131x − 2.8232	0.06–0.4	0.9995	0.29 ± 0.01
Dihydrocapsaicin	y = 0.6921x + 38.087	10–60	0.9918	17.21 ± 0.25
Ferulic acid	y = 0.8036x − 9.7586	2–10	0.9962	7.46 ± 0.26
Gallic acid	y = 46.044x + 8.6987	0.1–2.0	0.9952	0.90 ± 0.04
Guaiacol	y = 29.723x + 3.0569	0.1–2.0	0.9964	1.58 ± 0.02
m-Cresol	y = 0.0318x + 8.8568	50–2000	0.9956	1,294.46 ± 41.77
o-Coumaric acid	y = 0.0016x + 17.222	500–3000	0.9964	2,007.62 ± 58.41
o-Cresol	y = 0.1639x + 21.362	10–400	0.9956	174.65 ± 4.44
p-Coumaric acid	y = 0.0018x + 30.288	500–2500	0.9951	1,087.66 ± 20.52
p-Cresol	y = 0.3983x + 20.366	10–100	0.9986	74.39 ± 1.68
Quercetin	y = 1.4022x + 15.097	0.5–6.0	0.9953	2.49 ± 0.23
Syringol	y = 26.664x + 2.9758	0.1–3.0	0.9961	1.79 ± 0.09
Vanillin	y = 0.0444x + 36.909	200–1000	0.9918	294.56 ± 5.41

[a] Measured in triplicate ($n = 3$) ± standard deviation (SD).

Table 7
Calibration data of phenolic standards analyzed by Folin-Ciocalteu assay.

Standard	Regression equation ($n = 3$)	Calibration (μg mL^{-1})	R^2	$C_{A0.5}$[a] ± SD (μg mL^{-1})
Caffeic acid	y = 0.2819x − 0.1898	1.5–3.5	0.9958	2.45 ± 0.04
Capsaicin	y = 0.024x + 0.0079	5–40	0.9955	20.54 ± 1.01
Catechin	y = 0.1877x − 0.2220	2–5	0.9956	3.77 ± 0.08
Catechol	y = 0.1703x + 0.0495	0.5–6	0.9954	2.64 ± 0.06
Dihydrocapsaicin	y = 0.0139x + 0.1553	5–35	0.9960	24.88 ± 1.27
Ferulic acid	y = 0.0819x − 0.0221	2–10	0.9950	6.37 ± 0.07
Gallic acid	y = 0.1298x − 0.0882	2–7	0.9997	4.53 ± 0.10
Guaiacol	y = 0.0961x − 0.0051	2–8	0.9905	5.25 ± 0.06
m-Cresol	y = 0.0113x + 0.0848	1–8	0.9940	3.80 ± 0.20
o-Coumaric acid	y = 0.1366x − 0.0181	2–7	0.9990	3.80 ± 0.08
o-Cresol	y = 0.0127x + 0.0687	2–8	0.9910	3.44 ± 0.10
p-Coumaric acid	y = 0.0927x − 0.0121	1–7	0.9940	5.45 ± 0.35
p-Cresol	y = 0.1157x − 0.0175	1–8	0.9922	4.47 ± 0.03
Quercetin	y = 0.2817x − 0.0788	1–3	0.9964	2.60 ± 0.05
Syringol	y = 0.0445x + 0.0783	4–16	0.9961	9.45 ± 0.09
Vanillin	y = 0.0427x + 0.1540	4–16	0.9927	8.07 ± 0.07

[a] Measured in triplicate ($n = 3$) ± standard deviation (SD).

Table 8
Calibration data of phenolic standards analyzed by α-amylase inhibitory assay.

standard	Regression equation ($n = 3$)	Calibration (μg mL^{-1})	R^2	IC_{50}[a] ± SD (μg mL^{-1})
Acarbose	y = 1.4494x + 8.1557	2–60	0.9949	27.91 ± 0.2
Caffeic acid	y = 0.8300x − 70.0194	100–200	0.9910	144.58 ± 1.11
Capsaicin	–	–	–	N.I. (200)
Catechin	y = 0.5611x − 25.0596	100–200	0.9984	133.71 ± 1.45
Catechol	–	–	–	N.I. (200)
Dihydrocapsaicin	–	–	–	N.I. (200)
Ferulic acid	y = 0.8056x − 69.0464	120–200	0.9847	152.92 ± 0.54
Gallic acid	–	–	–	N.I. (200)
Guaiacol	–	–	–	N.I. (200)
m-Cresol	–	–	–	N.I. (200)
o-Coumaric acid	–	–	–	N.I. (200)
o-Cresol	–	–	–	N.I. (200)
p-Coumaric acid	–	–	–	N.I. (200)
p-Cresol	–	–	–	N.I. (200)
Quercetin	y = 0.8780x − 105.2333	120–200	0.9877	176.80 ± 0.44
Syringol	–	–	–	N.I. (200)
Vanillin	–	–	–	N.I. (200)

[a] Measured in triplicate ($n = 3$) ± standard deviation (SD), N.I.: not inhibited; that is no significant inhibition above the maximum possible concentration given in parentheses.

Conflicts of interest

The authors have declared no conflict of interest.

Acknowledgements

The authors thank the Higher Education Research Promotion and National Research University Project of Thailand, Office of the Higher Education Commission, through the Food and Functional Food Research Cluster of Khon Kaen University, Materials Chemistry Research Center, Department of Chemistry, Center of Excellence for Innovation in Chemistry (PERCH-CIC), Thailand for financial support of this study.

Appendix A. Supplementary data

Supplementary data associated with this article can be found, in the online version, at http://dx.doi.org/10.1016/j.ultsonch.2016.08.018.

References

[1] Y. Wahyuni, A.-R. Ballester, E. Sudarmonowati, R.J. Bino, A.G. Bovy, Secondary metabolites of *Capsicum* species and their importance in the human diet, J. Nat. Prod. 76 (2013) 783–793.
[2] D. Giuffrida, P. Dugo, G. Torre, C. Bignardi, A. Cavazza, C. Corradini, G. Dugo, Evaluation of carotenoid and capsaicinoid contents in powder of red chili peppers during one year of storage, Food Res. Int. 65 (2014) 163–170.
[3] P. Santos, A.C. Aguiar, G.F. Barbero, C.A. Rezende, J. Martínez, Supercritical carbon dioxide extraction of capsaicinoids from malagueta pepper (*Capsicum frutescens* L.) assisted by ultrasound, Ultrason. Sonochem. 22 (2015) 78–88.
[4] Y. Cai, Q. Luo, M. Sun, H. Corke, Antioxidant activity and phenolic compounds of 112 traditional Chinese medicinal plants associated with anticancer, Life Sci. 74 (2004) 2157–2184.
[5] G. Miliauskas, P.R. Venskutonis, T.A. van Beek, Screening of radical scavenging activity of some medicinal and aromatic plant extracts, Food Chem. 85 (2004) 231–237.
[6] K.K. Reddy, T. Ravinder, R.B.N. Prasad, S. Kanjilal, Evaluation of the antioxidant activity of capsiate analogues in polar, nonpolar, and micellar media, J. Agric. Food Chem. 59 (2011) 564–569.
[7] H.M. Tag, O.E. Kelany, H.M. Tantawy, A.A. Fahmy, Potential anti-inflammatory effect of lemon and hot pepper extracts on adjuvant-induced arthritis in mice, J. Basic Appl. Zool. 67 (2014) 149–157.
[8] M.S. Chinn, R.R. Sharma-Shivappa, J.L. Cotter, Solvent extraction and quantification of capsaicinoids from *Capsicum chinense*, Food Bioprod. Process. 89 (2011) 340–345.
[9] G.F. Barbero, J.M.G. Molinillo, R.M. Varela, M. Palma, F.A. Macías, C.G. Barroso, Application of Hansch's model to capsaicinoids and capsinoids: a study using the quantitative structure-activity relationship. A novel method for the synthesis of capsinoids, J. Agric. Food Chem. 58 (2010) 3342–3349.
[10] M.K. Meghvansi, S. Siddiqui, M.H. Khan, V.K. Gupta, M.G. Vairale, H.K. Gogoi, L. Singh, Naga chilli: a potential source of capsaicinoids with broad-spectrum ethnopharmacological applications, J. Ethnopharmacol. 132 (2010) 1–14.
[11] T. Singh, C. Chittenden, In-vitro antifungal activity of chilli extracts in combination with *Lactobacillus casei* against common sapstain fungi, Int. Biodeterior. Biodegrad. 62 (2008) 364–367.
[12] E. Iqbal, K.A. Salim, L.B.L. Lim, Phytochemical screening, total phenolics and antioxidant activities of bark and leaf extracts of *Goniothalamus velutinus* (Airy Shaw) from Brunei Darussalam, J. King Saud Univ. Sci. 27 (2015) 224–232.
[13] C.B. Davis, C.E. Markey, M.A. Busch, K.W. Busch, Determination of capsaicinoids in Habanero peppers by chemometric analysis of UV spectral data, J. Agric. Food Chem. 55 (2007) 5925–5933.
[14] E. Mueller-Seitz, C. Hiepler, M. Petz, Chili pepper fruits: content and pattern of capsaicinoids in single fruits of different ages, J. Agric. Food Chem. 56 (2008) 12114–12121.
[15] S. Boonkird, C. Phisalaphong, M. Phisalaphong, Ultrasound-assisted extraction of capsaicinoids from *Capsicum frutescens* on a lab- and pilot-plant scale, Ultrason. Sonochem. 15 (2008) 1075–1079.
[16] D.J. Schneider, I. Seuß-Baum, E. Schlich, Relationship between pungency and food components – a comparison of chemical and sensory evaluations, Food Qual. Prefer. 38 (2014) 98–106.
[17] W.L. Scoville, Note on capsicums, J. Am. Pharm. Assoc. 1 (1912) 453–454.
[18] G. Aruna, V. Baskaran, Comparative study on the levels of carotenoids lutein, zeaxanthin and β-carotene in Indian spices of nutritional and medicinal importance, Food Chem. 123 (2010) 404–409.
[19] E. Murillo, D. Giuffrida, D. Menchaca, P. Dugo, G. Torre, A.J. Meléndez-Martinez, L. Mondello, Native carotenoids composition of some tropical fruits, Food Chem. 140 (2013) 825–836.
[20] H.G. Daood, G. Palotás, G. Palotás, G. Somogyi, Z. Pék, L. Helyes, Carotenoid and antioxidant content of ground paprika from indoor-cultivated traditional varieties and new hybrids of spice red peppers, Food Res. Int. 65 (2014) 231–237.
[21] I.S.L. Lee, M.C. Boyce, M.C. Breadmore, Extraction and on-line concentration of flavonoids in *Brassica oleracea* by capillary electrophoresis using large volume sample stacking, Food Chem. 133 (2012) 205–211.
[22] H. Bae, G.K. Jayaprakasha, J. Jifon, B.S. Patil, Extraction efficiency and validation of an HPLC method for flavonoid analysis in peppers, Food Chem. 130 (2012) 751–758.
[23] J. Nilsson, R. Stegmark, B. Åkesson, Total antioxidant capacity in different pea (*Pisum sativum*) varieties after blanching and freezing, Food Chem. 86 (2004) 501–507.
[24] T. Stangeland, S.F. Remberg, K.A. Lye, Total antioxidant activity in 35 Ugandan fruits and vegetables, Food Chem. 113 (2009) 85–91.
[25] P. Sricharoen, S. Techawongstein, S. Chanthai, A high correlation indicating for an evaluation of antioxidant activity and total phenolics content of various chilli varieties, J. Food Sci. Technol. 52 (2015) 8077–8085.
[26] P. Kirschbaum-Titze, C. Hiepler, E. Mueller-Seitz, M. Petz, Pungency in paprika (*Capsicum annuum*). 1. Decrease of capsaicinoid content following cellular disruption, J. Agric. Food Chem. 50 (2002) 1260–1263.
[27] M. Contreras-Padilla, E.M. Yahia, Changes in capsaicinoids during development, maturation, and senescence of Chile peppers and relation with peroxidase activity, J. Agric. Food Chem. 46 (1998) 2075–2079.
[28] R.I. Santamaría, M.D. Reyes-Duarte, E. Bárzana, D. Fernando, F.M. Gama, M. Mota, A. López-Munguía, Selective enzyme-mediated extraction of capsaicinoids and carotenoids from chili guajillo puya (*Capsicum annuum* L.) using ethanol as solvent, J. Agric. Food Chem. 48 (2000) 3063–3067.
[29] J. Jiao, Y.-J. Fu, Y.-G. Zu, M. Luo, W. Wang, L. Zhang, J. Li, Enzyme-assisted microwave hydro-distillation essential oil from *Fructus forsythia*, chemical constituents, and its antimicrobial and antioxidant activities, Food Chem. 134 (2012) 235–243.
[30] M. Sganzerla, J.P. Coutinho, A.M.T. de Melo, H.T. Godoy, Fast method for capsaicinoids analysis from *Capsicum chinense* fruits, Food Res. Int. 64 (2014) 718–725.
[31] F. Korel, N. Bağdatlioğlu, M.Ö. Balaban, Y. Hişil, Ground red peppers: Capsaicinoids content, scoville scores, and discrimination by an electronic nose, J. Agric. Food Chem. 50 (2002) 3257–3261.
[32] A.C. de Aguiar, P. dos Santos, J.P. Coutinho, G.F. Barbero, H.T. Godoy, J. Martínez, Supercritical fluid extraction and low pressure extraction of Biquinho pepper (*Capsicum chinense*), LWT – Food Sci. Technol. 59 (2014) 1239–1246.
[33] G.F. Barbero, M. Palma, C.G. Barroso, Pressurized liquid extraction of capsaicinoids from peppers, J. Agric. Food Chem. 54 (2006) 3231–3236.
[34] Y. Pan, C. He, H. Wang, X. Ji, K. Wang, P. Liu, Antioxidant activity of microwave-assisted extract of *Buddleia officinalis* and its major active component, Food Chem. 121 (2010) 497–502.
[35] F. Dahmoune, B. Nayak, K. Moussi, H. Remini, K. Madani, Optimization of microwave-assisted extraction of polyphenols from *Myrtus communis* L. leaves, Food Chem. 166 (2015) 585–595.
[36] B. Nayak, F. Dahmoune, K. Moussi, H. Remini, S. Dairi, O. Aoun, M. Khodir, Comparison of microwave, ultrasound and accelerated-assisted solvent extraction for recovery of polyphenols from *Citrus sinensis* peels, Food Chem. 187 (2015) 507–516.
[37] T. Bajer, P. Bajerová, D. Kremr, A. Eisner, K. Ventura, Central composite design of pressurised hot water extraction process for extracting capsaicinoids from chili peppers, J. Food Compos. Anal. 40 (2015) 32–38.
[38] Z. Lianfu, L. Zelong, Optimization and comparison of ultrasound/microwave assisted extraction (UMAE) and ultrasonic assisted extraction (UAE) of lycopene from tomatoes, Ultrason. Sonochem. 15 (2008) 731–737.
[39] Q.-H. Chen, M.-L. Fu, J. Liu, H.-F. Zhang, G.-Q. He, H. Ruan, Optimization of ultrasonic-assisted extraction (UAE) of betulin from white birch bark using response surface methodology, Ultrason. Sonochem. 16 (2009) 599–604.
[40] G. Pan, G. Yu, C. Zhu, J. Qiao, Optimization of ultrasound-assisted extraction (UAE) of flavonoids compounds (FC) from hawthorn seed (HS), Ultrason. Sonochem. 19 (2012) 486–490.
[41] Y.-G. Xia, B.-Y. Yang, J. Liang, D. Wang, Q. Yang, H.-X. Kuang, Optimization of simultaneous ultrasonic-assisted extraction of water-soluble and fat-soluble characteristic constituents from *Forsythiae Fructus* using response surface methodology and high-performance liquid chromatography, Pharmacogn. Mag. 10 (2014) 292–303.
[42] R.K. Dubey, V. Singh, G. Upadhyay, A.K. Pandey, D. Prakash, Assessment of phytochemical composition and antioxidant potential in some indigenous chilli genotypes from North East India, Food Chem. 188 (2015) 119–125.
[43] S. Maqsood, I. Omer, A.K. Eldin, Quality attributes, moisture sorption isotherm, phenolic content and antioxidative activities of tomato (*Lycopersicon esculentum* L.) as influenced by method of drying, J. Food Sci. Technol. 52 (2015) 7059–7069.
[44] A. Kawee-ai, A. Srisuwun, N. Tantiwa, W. Nontaman, P. Boonchuay, A. Kuntiya, T. Chaiyaso, P. Seesuriyachan, Eco-friendly processing in enzymatic xylooligosaccharides production from corncob: Influence of pretreatment with sonocatalytic–synergistic Fenton reaction and its antioxidant potentials, Ultrason. Sonochem. 31 (2016) 184–192.
[45] P. Sricharoen, N. Limchoowong, S. Techawongstien, S. Chanthai, A novel extraction method for β-carotene and other carotenoids in fruit juices using

air-assisted, low-density solvent-based liquid-liquid microextraction and solidified floating organic droplets, Food Chem. 203 (2016) 386–393.
[46] K.M. Yoo, C.H. Lee, H. Lee, B. Moon, C.Y. Lee, Relative antioxidant and cytoprotective activities of common herbs, Food Chem. 106 (2008) 929–936.
[47] G.L. Miller, Use of dinitrosalicylic acid reagent for determination of reducing sugar, Anal. Chem. 31 (1959) 426–428.
[48] R. Tundis, M.R. Loizzo, G.A. Statti, P.J. Houghton, A. Miljkovic-Brake, F. Menichini, *In vitro* hypoglycemic and antimicrobial activities of *Senecio leucanthemifolius* Poiret, Nat. Prod. Res. 21 (2007) 396–400.
[49] A. Golmohamadi, G. Möller, J. Powers, C. Nindo, Effect of ultrasound frequency on antioxidant activity, total phenolic and anthocyanin content of red raspberry puree, Ultrason. Sonochem. 20 (2013) 1316–1323.
[50] J. Songsungkan, S. Chanthai, Determination of synergic antioxidant activity of the methanol/ethanol extract of allicin in the presence of total phenolics obtained from the garlic capsule compared with fresh and baked garlic clove, Int. Food Res. J. 21 (2014) 2377–2385.
[51] T. Sripakdee, A. Sriwicha, N. Jansam, R. Mahachai, S. Chanthai, Determination of total phenolics and ascorbic acid related to an antioxidant activity and thermal stability of the Mao fruit juice, Int. Food Res. J. 22 (2015) 618–624.
[52] J.-K. Yan, Y.-Y. Wang, H.-L. Ma, Z.-B. Wang, Ultrasonic effects on the degradation kinetics, preliminary characterization and antioxidant activities of polysaccharides from *Phellinus linteus* mycelia, Ultrason. Sonochem. 29 (2016) 251–257.
[53] A.L.B. Dias, C.S. Arroio Sergio, P. Santos, G.F. Barbero, C.A. Rezende, J. Martínez, Effect of ultrasound on the supercritical CO2 extraction of bioactive compounds from dedo de moça pepper (*Capsicum baccatum* L. var. *pendulum*), Ultrason. Sonochem. 31 (2016) 284–294.
[54] A.-G. Sicaire, M.A. Vian, F. Fine, P. Carré, S. Tostain, F. Chemat, Ultrasound induced green solvent extraction of oil from *oleaginous* seeds, Ultrason. Sonochem. 31 (2016) 319–329.
[55] R. Vardanega, D.T. Santos, M.A. De Almeida, Intensification of bioactive compounds extraction from medicinal plants using ultrasonic irradiation, Pharmacogn. Rev. 8 (2014) 88–95.
[56] I.A. Saleh, M. Vinatoru, T.J. Mason, N.S. Abdel-Azim, E.A. Aboutabl, F.M. Hammouda, A possible general mechanism for ultrasound-assisted extraction (UAE) suggested from the results of UAE of chlorogenic acid from *Cynara scolymus* L. (artichoke) leaves, Ultrason. Sonochem. 31 (2016) 330–336.
[57] M. Vinatoru, An overview of the ultrasonically assisted extraction of bioactive principles from herbs, Ultrason. Sonochem. 8 (2001) 303–313.
[58] J. Scalzo, A. Politi, N. Pellegrini, B. Mezzetti, M. Battino, Plant genotype affects total antioxidant capacity and phenolic contents in fruit, Nutrition 21 (2005) 207–213.
[59] K.G. Sweat, J. Broatch, C. Borror, K. Hagan, T.M. Cahill, Variability in capsaicinoid content and Scoville heat ratings of commercially grown Jalapeño, Habanero and Bhut Jolokia peppers, Food Chem. 210 (2016) 606–612.
[60] G.T.S. Sora, C.W.I. Haminiuk, M.V. da Silva, A.A.F. Zielinski, G.A. Gonçalves, A. Bracht, R.M. Peralta, A comparative study of the capsaicinoid and phenolic contents and in vitro antioxidant activities of the peppers of the genus *Capsicum*: an application of chemometrics, J. Food Sci. Technol. 52 (2015) 8086–8094.
[61] C. Maokam, S. Techawongstien, S. Chanthai, Determination of major and minor capsaicinoids in different varieties of the *Capsicum* fruits using GC-MS and their inhibition effect of the chilli extract on α-amylase activity, Int. Food Res. J. 21 (2014) 2237–2243.
[62] Z.A. Al Othman, Y.B.H. Ahmed, M.A. Habila, A.A. Ghafar, Determination of capsaicin and dihydrocapsaicin in *Capsicum* fruit samples using high performance liquid chromatography, Molecules 16 (2011) 8919–8929.
[63] R.S.S. Teixeira, A.S.A. da Silva, V.S. Ferreira-Leitão, E.P.D.S. Bon, Amino acids interference on the quantification of reducing sugars by the 3,5-dinitrosalicylic acid assay mislead carbohydrase activity measurements, Carbohydr. Res. 363 (2012) 33–37.
[64] V. Perla, P. Nimmakayala, M. Nadimi, S. Alaparthi, G.R. Hankins, A.W. Ebert, U. K. Reddy, Vitamin C and reducing sugars in the world collection of *Capsicum baccatum* L. genotypes, Food Chem. 202 (2016) 189–198.
[65] A. Barapatre, K.R. Aadil, B.N. Tiwary, H. Jha, In vitro antioxidant and antidiabetic activities of biomodified lignin from *Acacia nilotica* wood, Int. J. Biol. Macromol. 75 (2015) 81–89.

Food Chemistry 230 (2017) 398–404

Contents lists available at ScienceDirect

Food Chemistry

journal homepage: www.elsevier.com/locate/foodchem

Analytical Methods

Using bio-dispersive solution of chitosan for green dispersive liquid–liquid microextraction of trace amounts of Cu(II) in edible oils prior to analysis by ICP–OES

Nunticha Limchoowong [a], Phitchan Sricharoen [a], Suchila Techawongstien [b], Saksit Chanthai [a,*]

[a] Materials Chemistry Research Unit, Department of Chemistry and Center of Excellence for Innovation in Chemistry, Faculty of Science, Khon Kaen University, Khon Kaen 40002, Thailand
[b] Department of Plant Science and Agricultural Resources, Faculty of Agriculture, Khon Kaen University, Khon Kaen 40002, Thailand

ARTICLE INFO

Article history:
Received 16 October 2016
Received in revised form 21 February 2017
Accepted 11 March 2017
Available online 14 March 2017

Chemical compounds studied in this article:
Chitosan (Pubchem CID: 21896651)
Citric acid (Pubchem CID: 311)
Copper chloride dihydrate (Pubchem CID: 61482)
Hydrochloric acid (Pubchem CID: 313)
Nitric acid (Pubchem CID: 944)
Phosphoric acid (Pubchem CID: 1004)
Sulfuric acid (Pubchem CID: 1118)

Keywords:
Chitosan
Bio-dispersive agent
Dispersive liquid–liquid microextraction
Copper
Edible oils

ABSTRACT

A green approach using chitosan solution as a novel bio-dispersive agent for the dispersive liquid–liquid microextraction (DLLME) of trace amounts of Cu(II) in edible oils is presented. An emulsion was formed by mixing the oil sample with 300 μL of 0.25% (w/v) chitosan solution containing 200 μL of 6 mol L^{-1} HCl. Deionized water was used to induce emulsion breaking without centrifugation. The centrifuged Cu(II) extract was collected and analyzed using an inductively coupled plasma–optical emission spectrometer. The detection and quantitation limits were 2.1 and 6.8 μg L^{-1}, respectively. Trace amounts of Cu(II) in six edible oil samples were tested under optimum conditions for DLLME, with a recovery ranging from 90.3% to 109.3%. Therefore, the new dispersive agent in DLLME offers superior performance owing to the non-toxic nature of the solvent, short extraction time, high sensitivity, and easy operation.

1. Introduction

Although copper (Cu) has been long known as an essential element for physiological functions, it has been classified as one of the common heavy metals, which pollutes the environment due to its toxicity, persistence, and bio-accumulative nature (Karadas & Kara, 2017; Yavuz, Tokalıoglu, Sahan, & Patat, 2016). It can accumulate in the food chain system, representing a significant threat to ecosystems and human health. Humans are frequently exposed to Cu through various sources such as drinking water, air, food consumption (Ali, Ibrahim, Sulaiman, Kamboh, & Sanagi, 2016; Wadhwa, Tuzen, Kazi, Soylak, & Hazer, 2014; Yavuz et al., 2016), or skin contact with particles and/or Cu-containing compounds. Copper toxicity may cause severe health issues in humans, including vomiting, diarrhea, stomach and intestinal distress, liver and kidney damage, and anemia; it can even lead to death (Kozlowski, Luczkowski, Remelli, & Valensin, 2012). According to the WHO, the limit of tolerable daily intake for Cu is 0.5 mg kg^{-1} body weight (WHO, 1982, Shams, Babaei, & Soltaninezhad, 2004). The maximum acceptable Cu concentrations are 1.3 and 2 mg L^{-1} for drinking water and food, respectively (Salmani, Vakili, & Ehrampoush, 2013). The edible oil that is commonly used in cooking has been reported to contain Cu in the range of 0–130 μg kg^{-1} (Llorent-Martinez, Ortega-Barrales, Fernandez-de Cordova, Dominguez-Vidal, & Ruiz-Medina, 2011). However, Cu concentration in peanut oil, rapeseed oil, and olive oil was found to be higher than the recommended legal limits (Zhu, Fan, Wang, Qu, & Yao, 2011). Therefore, it is very essential to determine accurately, precisely, and quickly trace amounts of Cu in real samples.

* Corresponding author at: Khon Kaen University, Department of Chemistry, Faculty of Science, 123 Mittraphab Road, M. 16, T. Ni-Muang, A. Muang, Khon Kean 40002, Thailand.
E-mail address: sakcha2@kku.ac.th (S. Chanthai).

http://dx.doi.org/10.1016/j.foodchem.2017.03.070
0308-8146/

Currently, a variety of analytical methods have been used for monitoring Cu concentrations in drugs, food, and oils, among them, flame atomic absorption spectrometry (FAAS) (Tokay & Bagdat, 2015), graphite furnace atomic spectrometry (GFAAS) (Zhu et al., 2011), and inductively coupled plasma-atomic emission spectrometer (ICP-AES) (Sricharoen et al., 2017) are the most commonly used. The component extraction technique offers improved sensitivity; and the separation phase acts as an efficient step that reduces any interference from sample matrices. For the separation and determination of Cu from environmental matrices, several procedures have been developed such as co-precipitation (Gholivand, Sohrabi, & Abbasi, 2007), solid-phase extraction (SPE) (Tobiasz, Walas, Soto Hernandez, & Mrowiec, 2012), cloud point extraction (Shoaee, Rosgdi, Khanlarzadeh, & Beiraghi, 2012), and liquid–liquid extraction (LLE) (Karadas & Kara, 2014). However, LLE is time-consuming and usually requires large quantities of organic solvents that are potentially toxic, whereas SPE uses much lesser amount of organic solvents than LLE, but it is rather expensive. In addition, to achieve high enrichment of the analyte, the organic extract needs to be evaporated to a small volume. In general, the absorbed solute needs to be eluted after sample loading, and the solvent evaporation and re-dissolution steps are often time consuming. Recently, dispersive liquid–liquid microextraction (DLLME) has been widely used. This technique requires a smaller amount of organic solvent and the extraction time taken is significantly lower. The basic principle of this technique is the dispersion of extraction solvent assisted with a disperser solvent within an organic solution that generates a very high contact area between the extraction and organic phases (Caldas, Costa, & Primel, 2010). In fact, the surface area between two phases becomes very large due to the formation of emulsion solution. Therefore, to achieve good extraction efficiency, it is imperative to use a disperser solvent that empowers the extracting solvent to uniformly partition itself and the emulsifier in the sample phase. To date, studies have been focused on the application of DLLME for the analysis of various organic and inorganic pollutants in aqueous samples (Karadaş, 2014; Kokya, Farhadi, & Kalhori, 2012; Niazi, Habibi, & Ramezani, 2015). However, only a few reports have investigated the determination of heavy metals in lipid samples (Baran & Yasar, 2013; Zhu et al., 2011) because lipidic components get co-extracted with the target analyte. Low miscibility between the two phases (lipid and aqueous extracting phases) is the main problem related to the application of extraction methods. Therefore, it is challenging to use the DLLME method for the analysis of noxious chemicals in lipid or fat samples. However, the dispersive solvents used in conventional DLLME, such as acetone, methanol, and acetonitrile, are generally toxic in nature (Al-Saidi & Emara, 2014; Fernandez, Clavijo, Forteza, & Cerda, 2015). Therefore, an alternative approach on a green extraction method is further developed using biopolymer as the dispersive solvent.

Chitosan, a natural deacetylated polymer, has been widely used in applied fields such as water treatment, pharmacology, and biochemistry, particularly for the removal of dyes, phenols, and metals (Chaudhary, Vadodariya, Nataraj, & Meena, 2015; Li, Duan, Wang, & Luo, 2015; Limchoowong, Sricharoen, Techawongstien, & Chanthai, 2016). It primarily consists of (1–4)-2-amino-2-deox y-d-glucose units and has numerous properties such as non-toxic nature, anti-bacterial, bio-degradable, adsorption and flocculating ability, polyelectrolisity, and regeneration capacity. When dissolved in acidic solution, the amino group (NH_3^+) in its structure does not carry a very high positive charge. The positive charge on the molecule allows binding with negatively charged lipids and fatty acids (Santas, Espadaler, Mancebo, & Rafecas, 2012). In addition, the cross-linked chitosan is used to absorb triglycerides and reactive dyes. It not only acts as a stabilizer for hydrocolloid–lipid mixtures-promoting emulsion formation and interfacial stabilization as its structure composes of both hydrophilic and hydrophobic portions (Payet & Terentjev, 2008) but also facile solutes easily get dissolved in both the lipid and aqueous phases, possibly behaving as a dispersive agent. Therefore, this study is aimed to use the eco-friendly chitosan as a bio-dispersive agent instead of other organic compounds in DLLME.

To the best of our knowledge, thus far, this study for the first time reports the use of chitosan for liquid extraction as an alternative choice of a bio-dispersive agent for trace determination of Cu (II) in edible oil samples using vortex-assisted dispersive liquid–liquid microextraction (VA-DLLME) prior to determination by inductively coupled plasma–optical emission spectrometer (ICP–OES).

2. Materials and methods

2.1. Instruments

All the measurements were carried out using a Perkin-Elmer (Wellesley, USA) OPTIMA 2100 DV inductively coupled plasma-optical emission spectrometer, with an axially viewed plasma system. The instrument and operating conditions for ICP–OES are described in Table 1. A vortex mixer (50 Hz) from Scientific Industries, Inc. (USA) was used for the extraction.

2.2. Chemicals

Shrimp shell chitosan (about 75% degree of deacetylation) was purchased from Sigma-Aldrich (Japan). Copper chloride dihydrate was obtained from INIVAR (New Zealand). Hydrochloric acid, nitric acid and phosphoric acid were obtained from Carlo Erba (France). Sulfuric acid was purchased from QREC™ (New Zealand). Glacial acetic acid was obtained from AnalaR (England). All chemicals and solvents used were of analytical reagent grade (AR grade), and all solutions were prepared with deionized water (Milli Q Millipore 18.2 MΩ cm^{-1}) by Simplicity Water purification system, Model Simplicity 185, Millipore Corporation (USA).

A 1000 mg L^{-1} standard stock solution of Cu(II) was prepared from $CuCl_2{\cdot}2H_2O$. Working solution of Cu(II) was diluted from the stock solution each day. The calibration curve of Cu(II) was constructed between its intensity recorded at 327.393 nm and the concentration range of 10–500 μg L^{-1}. For recovery study, the standard solution of 50 μg L^{-1} Cu(II) was spiked into 1 mL of the oil sample used.

2.3. Sample

Edible oil samples were purchased from a retail store in Khon Kaen, Thailand. Six types of the oils including soybean oil, palm oil, rice bran oil, corn oil, extra virgin olive oil, and chili oil were

Table 1
Working conditions and instrumental parameters of ICP–OES.

Analytical emission line (nm)	327.393
Vision (plasma view)	Axial
RF power (W)	1300
Peristaltic pump flow rate (mL min^{-1})	1.5
Plasma flow rate (L min^{-1})	15.0
Auxiliary flow rate (L min^{-1})	0.20
Nebulizer flow rate (L min^{-1})	0.8
Nebulizer/spray chamber	Sea spray/gas cyclonic
Purge	Normal
Resolution	Normal
Replicate read time (s)	20
Sample uptake delay time (s)	14
Wash time (s)	1
Number of replicates	3

collected and stored in a brown glass bottle at room temperature. Soybean oil was used as a model sample for optimizing extraction.

2.4. DLLME procedure

DLLME was used to extract Cu(II) from edible oil. An oil sample (1 mL) containing different Cu(II) concentrations was added into a conical test tube. Subsequently, 300 μL of 0.25% (w/v) chitosan in 1% (v/v) acetic acid (as bio-disperser solvent) containing 200 μL of 6 mol L^{-1} HCl (as an extraction solvent) were injected rapidly using a microsyringe. After that, it was shaken with a vortex for 30 s for emulsification. The extraction solvent acts not only to extract Cu(II) from the sample mixture but it can also be dissolved in the aqueous phase. Therefore, it was very easy to break an emulsion with 4 mL deionized water without centrifugation. The dispersed extraction solvent was quickly separated into two phases (Fig. 1): the upper phase containing the oil sample and the lower phase containing the aqueous phase with extracted Cu(II). The lower aqueous phase was collected using a 5 mL small syringe with long needle and directly determined of copper by ICP–OES.

2.5. Method validation

Under optimum extraction conditions, this method was used to determine Cu(II) in six plant oil samples. To study their recoveries, the samples were spiked with 50, 100, and 150 μg L^{-1} of Cu(II) and mixed well prior to analysis by DLLME and ICP–OES. The extraction and determination of Cu(II) were performed in triplicate for all oil samples. The percentage recovery was calculated using the following equation (Limchoowong, Sricharoen, Techawongstien, Kongsri, & Chanthai, 2017; Sricharoen, Limchoowong, Techawongstien, & Chanthai, 2016):

$$\text{Recovery } (\%) = [(C_{found} - C_{real})/C_{added}] \times 100 \quad (1)$$

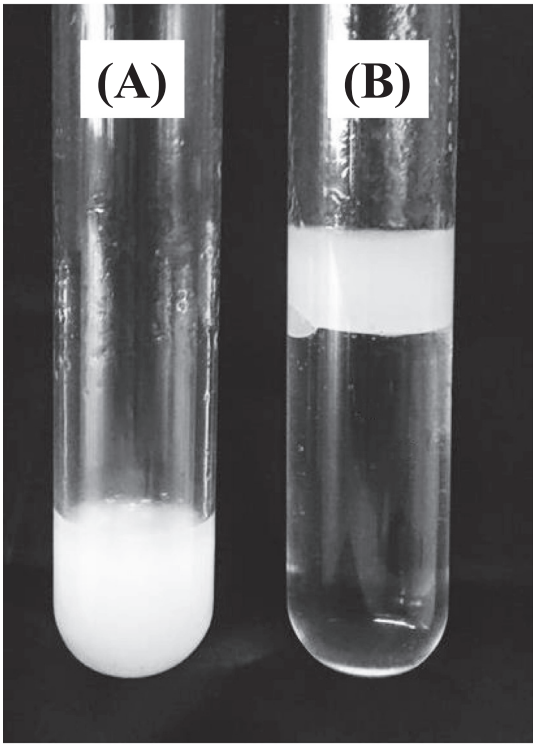

Fig. 1. The emulsion (A) before and (B) after breaking by addition of deionized water.

where C_{found}, C_{real}, and C_{added} are the concentration of Cu(II) after addition of a known amount of the standard in the sample, the concentration of Cu(II) found in the sample, and the concentration of the known amount of the standard that was spiked in the sample, respectively.

3. Results and discussion

3.1. Optimization of DLLME

A chitosan solution was used to get high extraction efficiency for trace Cu(II) determination in the oil samples. The effects of various experimental parameters, such as concentration and volume of chitosan solution; type, concentration, and volume of an extraction solvent; and extraction time after emulsion formation, were investigated. All the experiments were performed in triplicate.

3.1.1. Effects of chitosan concentration and its volume used

The main criterion for choosing a disperser solvent was the capability of being highly miscible with both the extraction solvent (an acidic solution) and oil phase (as an organic part) for the emulsification. Therefore, the disperser solvent plays an important role in decreasing the interfacial tension between the oil and extractant, improving the analyte transfer due to an enhanced contact area between the two phases. Furthermore, the effect of chitosan concentration on DLLME was investigated. In the DLLME procedure, the extractant mixture containing both the extraction solvent and disperser agent is injected into the sample solution to favor the dispersion of the extractant in the sample solution. The dilutions of chitosan solutions was prepared by dissolving 0.05, 0.07, 0.1, 0.25, 0.5, 1.0, or 1.5 g chitosan in 1% (v/v) acetic acid solution with continuous stirring at room temperature. Subsequently, 100 μL of conc. HCl was mixed with 400 μL of each concentration of chitosan using a vortex mixer. As illustrated in Fig. 2(a), 0.05% (w/v) chitosan solution resulted in a very low recovery because the assembly of chitosan on the oil–aqueous interface resulted in insufficient surface coverage. The extraction recovery of Cu(II) increased with the increasing chitosan concentration up to 0.25% (w/v). Increasing the chitosan concentration made the solution more viscous, leading to effective dispersion. The surface area between the oil and extraction solvent phases was essentially large. Moreover, the extraction recovery of Cu(II) decreased with a continuous increase in the chitosan concentration from 0.25% to 1.5% (w/v). An extra-emulsion was observed, probably caused by an over concentration. Furthermore, the emulsion forming rate and height of the creamed layer were strongly dependent on the chitosan concentration, which was affected by their viscosity (Payet & Terentjev, 2008). Therefore, higher concentrations (>0.25%) of chitosan could disturb their solubility and dispersion property. In all subsequent experiments, 0.25% (w/v) of chitosan was chosen as the bio-dispersive agent.

Further, the optimum volume for DLLME was investigated. The effect of volume of the disperser solution was investigated by varying the volume of 0.25% (w/v) chitosan in a range of 100–500 μL along with 100 μL of 6 mol L^{-1} HCl. The extraction efficiency of Cu(II) increased with an increasing volume of the chitosan solution from 100 to 300 μL and then decreased after exceeding 300 μL (Fig. 2(b)). The small amount of chitosan possibly could not properly disperse in the extraction solvent as a tiny emulsion in the aqueous phase, leading to decreased efficiency. The extraction efficiency of the target analyte decreased with the increasing volume of chitosan solution due to the dilution of the extracted analyte in the extraction solvent. Therefore, 300 μL of 0.25% (w/v) chitosan was selected as the optimum disperser solvent for the DLLME procedure.

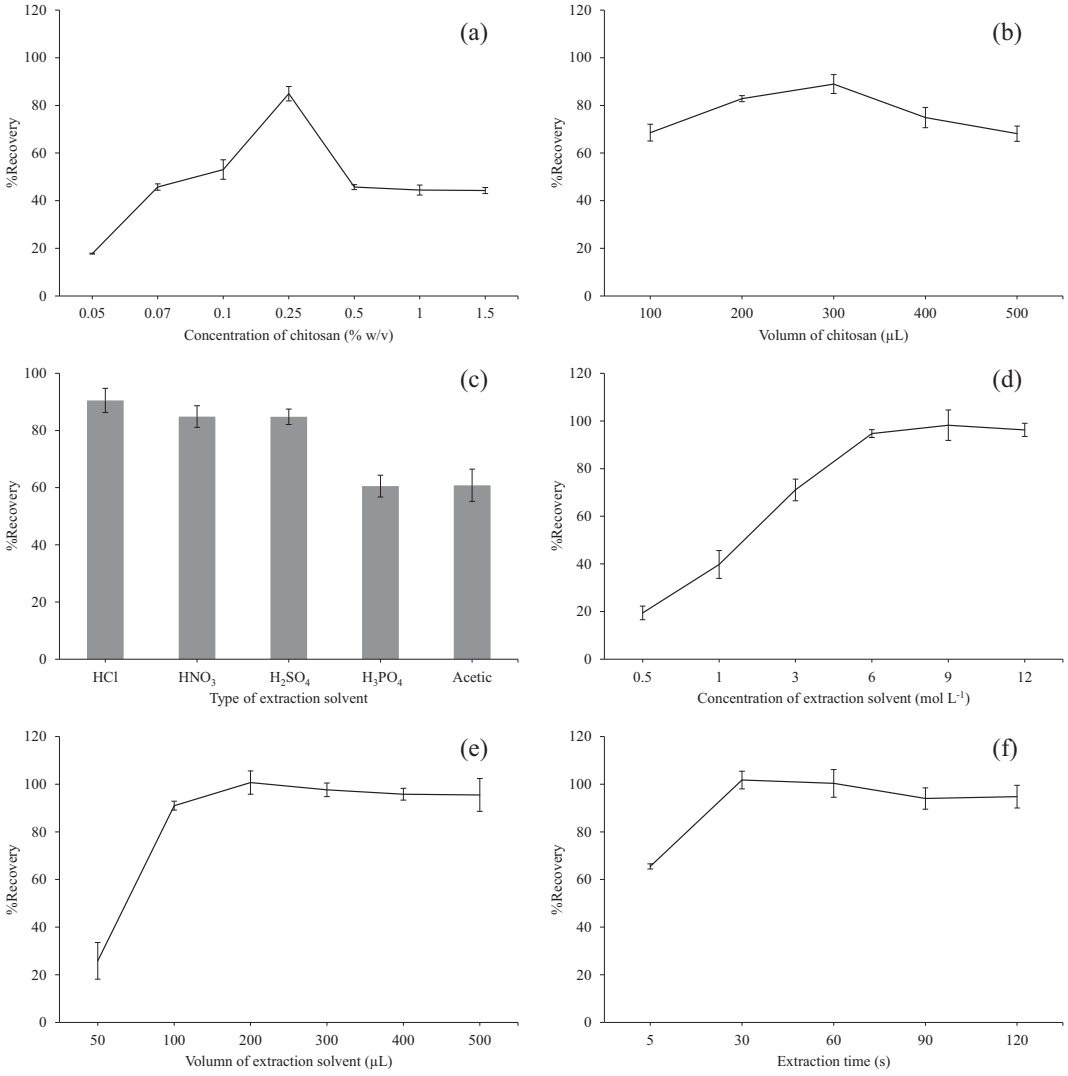

Fig. 2. The optimization of extraction parameters. (a) Effect of different chitosan concentrations on the extraction efficiency. Conditions: Sample containing Cu(II) 50 μg L^{-1}, chitosan 400 μL, concentrated HCl 100 μL, extraction time 30 s, DI water, (b) Effect of different chitosan volume on the extraction efficiency. Conditions: Sample containing Cu(II) 50 μg L^{-1}, 0.25% (w/v) chitosan, concentrated HCl 100 μL, extraction time 30 s, DI water. (c) Effect of the extraction solvent types on the extraction efficiency. Conditions: Sample containing Cu(II) 50 μg L^{-1}, 0.25% (w/v) chitosan 300 μL, extraction solvent 100 μL, extraction time 30 s, DI water. (d) Effect of the extraction solvent concentrations on the extraction efficiency. Conditions: Sample containing Cu(II) 50 μg L^{-1}, 0.25% (w/v) chitosan 300 μL, HCl 100 μL, extraction time 30 s, DI water. (e) Effect of different extraction solvent volumes on the extraction efficiency. Conditions: Sample containing Cu(II) 50 μg L^{-1}, 0.25% (w/v) chitosan 300 μL, 6 mol L^{-1} HCl 100 μL, extraction time 30 s, DI water. (f) Effect of different extraction times on the extraction efficiency. Conditions: Sample containing Cu(II) 50 μg L^{-1}, 0.25% (w/v) chitosan 300 μL, 6 mol L^{-1} HCl 100 μL, DI water.

3.1.2. Effects of type, concentration, and volume of the extraction solvent

For better analytical selectivity of the target analyte, a suitable extraction solvent must be used. This solvent must be immiscible with the oil (organic-like) phase. For better extraction efficiency, the solubility of analyte in the solvent should be higher than the donor phase. Therefore, common extracting solvents for metal ions were evaluated. These weak or strong acidic solvents include concentrated hydrochloric acid, nitric acid, sulfuric acid, phosphoric acid, and acetic acid (Reyes & Campos, 2006). A series of sample solutions were studied using 300 μL of 0.25% (w/v) chitosan and 100 μL of different kinds of the extracting acid solutions. The highest extraction recovery was obtained with HCl (Fig. 2(c)). Therefore, HCl was selected as the extraction solution for all subsequent investigations.

To study the effect of the acid concentration on DLLME, a series of HCl concentrations (0.5–12 mol L^{-1}) in fixed volume of the dispersive solution were investigated. The extraction efficiency increased with the increasing concentration of HCl from 0.5 to 6 mol L^{-1} and then remained constant (Fig. 2(d)). The highest recovery (94.70%) of Cu(II) was obtained with 100 μL of 6 mol L^{-1} HCl. Therefore, 6 mol L^{-1} HCl solution was used for further experiments.

For microextraction, the effect of HCl volume on the extraction recovery was also evaluated. Different volumes of 6 mol L^{-1} HCl (50, 100, 200, 300, 400, and 500 μL) with a fixed minimum volume of the chitosan solution were tested in a similar way. The extraction recovery sharply increased with an increase in the volume of HCl from 50 to 100 μL, following which there was a slight increase from 100 to 200 μL (Fig. 2(e)). The highest recovery of Cu(II) as 100.69% was obtained. Therefore, 200 μL of 6 mol L^{-1} HCl was used in this study.

3.1.3. Effect of extraction time

Extraction time is one of the most important factors for all the extraction methods. DLLME is time independent because of the

Table 2
Analytical characteristics of the developed DLLME for determination of Cu(II).

Analytical parameter	
Linear range ($\mu g\ L^{-1}$)	10–1000
Calibration curve ($\mu g\ L^{-1}$)	10–200
Correlation coefficient (R^2)	0.9994
Limit of detection ($\mu g\ L^{-1}$, $n = 10$)	2.05
Limit of quantification ($\mu g\ L^{-1}$, $n = 10$)	6.82
Relative standard deviation (%) for:	
Intra-day analysis ($n = 5$)	6.40
Inter-day analysis ($n = 5$)	7.04

Table 3
The content ($\mu g\ L^{-1}$) and relative recovery (%) of Cu(II) in six edible oil samples.

Sample	Spiked value	Found value	Recovery ± SD
Soybean oil	–	75.22 ± 2.67	
	50	125.94 ± 1.87	101.45 ± 3.16
	100	167.01 ± 4.90	91.79 ± 1.64
	150	239.17 ± 6.85	109.30 ± 4.79
Palm oil	–	99.89 ± 2.85	
	50	151.41 ± 2.47	103.03 ± 1.65
	100	202.93 ± 6.89	103.03 ± 0.36
	150	249.61 ± 5.80	99.81 ± 4.97
Rice bran oil	–	91.80 ± 1.08	
	50	138.75 ± 3.73	93.90 ± 3.93
	100	182.20 ± 4.49	90.41 ± 4.33
	150	233.63 ± 8.77	94.55 ± 3.99
Corn oil	–	77.53 ± 1.49	
	50	122.67 ± 2.85	90.29 ± 3.60
	100	172.96 ± 5.82	95.44 ± 3.38
	150	241.298 ± 4.57	109.18 ± 9.61
Extra virgin olive oil	–	74.84 ± 1.64	
	50	121.47 ± 6.38	93.27 ± 5.01
	100	165.30 ± 2.76	90.46 ± 3.65
	150	236.30 ± 4.23	107.63 ± 3.02
Chili oil	–	107.83 ± 3.77	
	50	153.17 ± 2.71	90.68 ± 5.14
	100	203.48 ± 3.80	95.65 ± 2.81
	150	252.00 ± 5.64	96.11 ± 1.41

infinitely large surface area between the extraction solvent and its organic phase after the emulsion formation. This leads to a very fast transition of the analyte from the oil phase to the extraction solvent and a quick achievement of the equilibrium state (Chen, Chen, Ying, Huang, & Liao, 2009). The effect of vortex extraction time was investigated in the range of 5–120 s. Fig. 2(f) shows the profiles of extraction time and extraction efficiency for Cu(II). The recoveries of Cu(II) increased with the increase in the extraction time from 5 to 30 s and remained constant with a further increase in the extraction time from 30 to 120 s, indicating that the extraction time >30 s had no significant effect on the extraction efficiency. Therefore, the extraction of Cu(II) from the oil sample into the extraction solution was very fast within 30 s with a high recovery of 100.34%. All the subsequent extraction studies used less than a minute as the extraction time.

3.2. Analytical features of merit

To evaluate the performance of the proposed method, the working concentration range of Cu(II), limits of detection (LOD) and quantification (LOQ), and reproducibility were studied. The spiked samples were analyzed for their recovery. Table 2 shows that the present method exhibits satisfactory linearity in the concentration range of 10–1000 $\mu g\ L^{-1}$ with good correlation coefficients >0.999. A series of the working standard solutions (10, 50, 100, 150, and 200 $\mu g\ L^{-1}$) of Cu(II) was used to construct the calibration curve with a regression coefficient of 0.9994. Both LOD and LOQ, defined as 3SD/m and 10SD/m (where SD is the standard deviation of the low concentration of Cu(II) and m is the slope of the calibration curve), were 2.05 and 6.82 $\mu g\ L^{-1}$, respectively. Precision was expressed as the percent relative standard deviation (%RSD) using the slope of the calibration graph, which was determined in terms of repeatability (data from five independent standard preparations; intra-day%RSD) and reproducibility (work performed during five consecutive days; inter-day%RSD). The intra-day and inter-day precisions were 6.40% and 7.04%, respectively.

3.3. Analysis of real samples

To demonstrate the potential use of this new dispersive solution for the extraction method, six types of edible oil samples were extracted using DLLME prior to determination by ICP-OES. These oil samples were tested using the green approach of the optimized conditions for DLLME. The Cu(II) contents in these samples ranged from 74.84 ± 1.64 to 107.83 ± 3.77 $\mu g\ L^{-1}$. Chili oil had the highest concentration of Cu(II) (107.83 ± 3.77 $\mu g\ L^{-1}$); while those of other five edible oils ranged from 75.22 ± 2.67 to 99.89 ± 2.85 $\mu g\ L^{-1}$. The olive oil sample had the lowest concentration of Cu(II) (74.84 ± 1.64 $\mu g\ L^{-1}$). Moreover, to evaluate the matrix effect, the accuracy of the proposed method was verified by calculating the percentage recovery from the real samples. These oil samples were spiked with Cu(II) concentrations of 50, 100, and 150 $\mu g\ L^{-1}$, and their recoveries were in the range of 91.8–109.3%, 99.8–103.0%, 90.4–94.5%, 90.3–109.2%, 90.5–107.6%, and 90.7–96.1% for soybean oil, palm oil, rice bran oil, corn oil, extra virgin olive oil, and chili oil, respectively (Table 3). The Cu(II) contents in these samples were acceptable to be consumed safely. The natural compositions of these oils did not have any interfering effect on the spiked Cu(II) concentrations (low, medium, and high concentration). Therefore, the proposed method is suitable for trace determination of Cu(II) in real samples and can be easily applied for routine analysis.

Table 4
Comparison of the developed DLLME for the determination of Cu(II) with other methods.

Sample	Extraction method	Dispersive solvent	Extraction time (min)	Recovery (%)	LOD[a] ($\mu g\ L^{-1}$)	Detection	References
Vegetable oil	Microemulsification	Propan-1-ol	30	89–102	–	HR-CSFAAS	Nunes et al. (2011)
Human hair	DLLME-SFO[b]	Ethanol	15	–	3.4	FAAS	Bahar and Zakerian (2012)
Water	DLLME	Acetonitrile	5	93.3–105.6	2.6	Spectrophotometer	Niazi et al. (2015)
Blood serum	DLLME	Chloroform	5	94.5–105	8.6	UV–Visible	Sabzi, Mohseni, Bahram, and Bari, (2015)
Edible oil	DLLME	0.25% (w/v) Chitosan	0.5	90.2–109.3	2.1	ICP–OES	This work

[a] Limit of detection.
[b] Dispersive liquid–liquid microextraction based on solidification of floating organic drop.

Table 4 compares the results obtained with DLLME for Cu(II) determination using chitosan as new bio-dispersive solvent with those obtained in previous reports. Compared with other methods, the proposed method follows a green chemistry approach. Compared to propan-1-ol, ethanol, acetonitrile, and chloroform used in other extraction methods, the chitosan solution used here is not toxic. Therefore, it is advantageous to use this extraction technique. The advantages include higher recovery (90.3–109.3%), less extraction time (30 s), lower LOD (2.05 μg L^{-1}), low cost, and simple methodology.

4. Conclusion

The proposed method is very simple, low cost, and environmental friendly for the extraction and determination of Cu(II) in lipid samples. The replacement of the organic solvent with chitosan as bio-dispersive solvent allows an emulsifier extraction rather than the common DLLME procedure. In addition, this method does not use any toxic organic solvent and the extraction time is as low as 30 s. Under optimum conditions, relative recoveries of Cu(II) were high in the range of 90.2–109.3%. The proposed method was successfully applied for the extraction of Cu(II) from the spiked edible oil samples. Therefore, the proposed method is very useful for determination of heavy metals in all types of food and food products.

Conflicts of interest

The authors declare no conflicts of interest.

Acknowledgements

The authors would like to thank the Higher Education Research Promotion and the National Research University Project of Thailand; the Office of the Higher Education Commission, through the Food and Functional Food Research Cluster of Khon Kaen University; the Materials Chemistry Research Unit, Department of Chemistry, Center of Excellence for Innovation in Chemistry (PERCH-CIC); and the Commission on Higher Education and the Ministry of Education, Thailand for financial support.

References

Ali, L. I. A., Ibrahim, W. A. W., Sulaiman, A., Kamboh, M. A., & Sanagi, M. M. (2016). New chrysin-functionalized silica-core shell magnetic nanoparticles for the magnetic solid phase extraction of copper ions from water samples. *Talanta, 148*, 191–199.

Al-Saidi, H. M., & Emara, A. A. A. (2014). The recent developments in dispersive liquid–liquid microextraction for preconcentration and determination of inorganic analytes. *Journal of Saudi Chemical Society, 18*(6), 745–761.

Bahar, S., & Zakerian, R. (2012). Determination of copper in human hair and tea samples after dispersive liquid-liquid microextraction based on solidification of floating organic drop (DLLME-SFO). *Journal of the Brazilian Chemical Society, 23*(6), 1166–1173.

Baran, E. K., & Yasar, S. B. (2013). Determination of iron in edible oil by FAAS after extraction with a Schiff base. *Food Analytical Methods, 6*(2), 528–534.

Caldas, S. S., Costa, F. P., & Primel, E. G. (2010). Validation of method for determination of different classes of pesticides in aqueous samples by dispersive liquid-liquid microextraction with liquid chromatography-tandem mass spectrometric detection. *Analytica Chimica Acta, 665*(1), 55–62.

Chaudhary, J. P., Vadodariya, N., Nataraj, S. K., & Meena, R. (2015). Chitosan-based aerogel membrane for robust oil-in-water emulsion separation. *ACS Applied Materials & Interfaces, 7*(44), 24957–24962.

Chen, H., Chen, H., Ying, J., Huang, J., & Liao, L. (2009). Dispersive liquid–liquid microextraction followed by high-performance liquid chromatography as an efficient and sensitive technique for simultaneous determination of chloramphenicol and thiamphenicol in honey. *Analytica Chimica Acta, 632*(1), 80–85.

Fernandez, M., Clavijo, S., Forteza, R., & Cerda, V. (2015). Determination of polycyclic aromatic hydrocarbons using lab on valve dispersive liquid–liquid microextraction coupled to high performance chromatography. *Talanta, 138*, 190–195.

Gholivand, M. B., Sohrabi, A., & Abbasi, S. (2007). Determination of copper by adsorptive stripping voltammetry in the presence of calcein blue. *Electroanalysis, 19*(15), 1609–1615.

Karadaş, C. (2014). A new dispersive liquid–liquid microextraction method for preconcentration of copper from waters and cereal flours and determination by flame atomic absorption spectrometry. *Water Air & Soil Pollution, 225*, 2150–2159.

Karadas, C., & Kara, D. (2014). Determination of copper (II) in natural waters by extraction using N–o–vanilidine–2–amino–p–cresol and flame atomic absorption spectrometry. *Instrumentation Science and Technology, 42*(4), 548–561.

Karadas, C., & Kara, D. (2017). Dispersive liquid–liquid microextraction based on solidification of floating organic drop for preconcentration and determination of trace amounts of copper by flame atomic absorption spectrometry. *Food Chemistry, 220*, 242–248.

Kokya, T. A., Farhadi, K., & Kalhori, A. A. (2012). Optimized dispersive liquid-liquid microextraction and determination of sorbic acid and benzoic acid in beverage samples by gas chromatography. *Food Analytical Methods, 5*(3), 351–358.

Kozlowski, H., Luczkowski, M., Remelli, M., & Valensin, D. (2012). Copper, zinc and iron in neurodegenerative diseases (Alzheimer's, Parkinson's and prion diseases). *Coordination Chemistry Reviews, 256*(19–20), 2129–2141.

Li, L., Duan, H., Wang, X., & Luo, C. (2015). Fabrication of novel magnetic nanocomposite with a number of adsorption sites for the removal of dye. *International Journal of Biological Macromolecules, 78*, 17–22.

Limchoowong, N., Sricharoen, P., Techawongstien, S., & Chanthai, S. (2016). An iodine supplementation of tomato fruits coated with an edible film of the iodide-doped chitosan. *Food Chemistry, 200*, 223–229.

Limchoowong, N., Sricharoen, P., Techawongstien, S., Kongsri, S., & Chanthai, S. (2017). A green extraction of trace iodine in table salts, vegetables, and food products prior to analysis by inductively coupled plasma optical emission spectrometry. *Journal of the Brazilian Chemical Society, 28*(4), 540–546.

Llorent-Martinez, E. J., Ortega-Barrales, P., Fernandez-de Cordova, M. L., Dominguez-Vidal, A., & Ruiz-Medina, A. (2011). Investigation by ICP-MS of trace element levels in vegetable edible oils produced in Spain. *Food Chemistry, 127*, 1257–1262.

Niazi, A., Habibi, S., & Ramezani, M. (2015). Preconcentration and simultaneous spectrophotometric determination of copper and mercury by dispersive liquid–liquid microextraction and orthogonal signal correction-partial least squares. *Arabian Journal of Chemistry, 8*(5), 706–714.

Nunes, L. S., Barbosa, J. T. P., Fernandes, A. P., Lemos, V. A., dos Santos, W. N. L., Korn, M. G. A., & Teixeira, L. S. G. (2011). Multi-element determination of Cu, Fe, Ni and Zn content in vegetable oils samples by high-resolution continuum source atomic absorption spectrometry and microemulsion sample preparation. *Food Chemistry, 127*, 780–783.

Payet, L., & Terentjev, E. M. (2008). Emulsification and stabilization mechanisms of O/W emulsions in the presence of chitosan. *Langmuir, 24*(21), 12247–12252.

Reyes, M. N. M., & Campos, R. C. (2006). Determination of copper and nickel in vegetable oils by direct sampling graphite furnace atomic absorption spectrometry. *Talanta, 70*(5), 929–932.

Sabzi, R. E., Mohseni, N., Bahram, M., & Bari, R. M. (2015). Dispersive liquid–liquid microextraction for the preconcentration and spectrophotometric determination of copper(II) in blood serum sample using sodium diethyldithiocarbamate as the complexing agent. *Mediterranean Journal of Chemistry, 3*(6), 1111–1121.

Salmani, M. H., Vakili, M., & Ehrampoush, M. H. (2013). A comparative study of copper (ii) removal on iron oxide, aluminum oxide and activated carbon by continuous down flow method. *Journal of Toxicology and Environmental Health Sciences, 5*(8), 150–155.

Santas, J., Espadaler, J., Mancebo, R., & Rafecas, M. (2012). Selective in vivo effect of chitosan on fatty acid, neutral sterol and bile acid excretion: a longitudinal study. *Food Chemistry, 134*(2), 940–947.

Shams, E., Babaei, A., & Soltaninezhad, M. (2004). Simultaneous determination of copper, zinc and lead by adsorptive stripping voltammetry in the presence of Morin. *Analytica Chimica Acta, 501*(1), 119–124.

Shoaee, H., Rosgdi, M., Khanlarzadeh, N., & Beiraghi, A. (2012). Simultaneous preconcentration of copper and mercury in water samples by cloud point extraction and their determination by inductively coupled plasma atomic emission spectrometry. *Spectrochimica Acta Part A, 98*, 70–75.

Sricharoen, P., Limchoowong, N., Areerob, Y., Nuengmatcha, P., Techawongstien, S., & Chanthai, S. (2017). Fe_3O_4/hydroxyapatite/graphene quantum dots as a novel nano-sorbent for preconcentration of copper residue in Thai food ingredients: optimization of ultrasound-assisted magnetic solid phase extraction. *Ultrasonics Sonochemistry, 37*, 83–93.

Sricharoen, P., Limchoowong, N., Techawongstien, S., & Chanthai, S. (2016). A novel extraction method for β-carotene and other carotenoids in fruit juices using air-assisted, low-density solvent-based liquid–liquid microextraction and solidified floating organic droplets. *Food Chemistry, 203*, 386–393.

Tobiasz, A., Walas, S., Soto Hernandez, A., & Mrowiec, H. (2012). Application of multiwall carbon nanotubes impregnated with 5-dodecylsalicylaldoxime for on-line copper preconcentration and determination in water samples by flame atomic absorption spectrometry. *Talanta, 96*, 89–95.

Tokay, F., & Bagdat, S. (2015). Determination of iron and copper in edible oils by flame atomic absorption spectrometry after liquid–liquid extraction. *Journal of the American Oil Chemists' Society, 92*(3), 317–322.

Wadhwa, S. K., Tuzen, M., Kazi, T. G., Soylak, M., & Hazer, B. (2014). Polyhydroxybutyrate-b-polyethyleneglycol block copolymer for the solid

phase extraction of lead and copper in water, baby foods, tea and coffee samples. *Food Chemistry, 152*, 75–80.

WHO (World Health Organization) (1982). *Evaluation of certain food additives and contaminants*. Geneva: World Health Organization. Technical Report Series: 683.

Yavuz, E., Tokalıoglu, S., Sahan, H., & Patat, S. (2016). Nanosized spongelike Mn_3O_4 as an adsorbent for preconcentration by vortex assisted solid phase extraction of copper and lead in various food and herb samples. *Food Chemistry, 194*, 63–469.

Zhu, F., Fan, W., Wang, X., Qu, L., & Yao, S. (2011). Health risk assessment of eight heavy metals in nine varieties of edible vegetable oils consumed in China. *Food and Chemical Toxicology, 49*(12), 3081–3085.

Food Chemistry 230 (2017) 388–397

Contents lists available at ScienceDirect

Food Chemistry

journal homepage: www.elsevier.com/locate/foodchem

Analytical Methods

Preconcentration and trace determination of copper (II) in Thai food recipes using Fe_3O_4@Chi–GQDs nanocomposites as a new magnetic adsorbent

Nunticha Limchoowong [a], Phitchan Sricharoen [a], Yonrapach Areerob [a], Prawit Nuengmatcha [a,b], Thitiya Sripakdee [a,c], Suchila Techawongstien [d], Saksit Chanthai [a,*]

[a] Materials Chemistry Research Center, Department of Chemistry and Center of Excellence for Innovation in Chemistry, Faculty of Science, Khon Kaen University, Khon Kaen 40002, Thailand
[b] Department of Chemistry, Faculty of Science and Technology, Nakhon Si Thammarat Rajabhat University, Nakhon Si Thammarat 80280, Thailand
[c] Chemistry Program, Faculty of Science and Technology, Sakon Nakhon Rajabhat University, Sakon Nakhon 47000, Thailand
[d] Department of Plant Science and Agricultural Resources, Faculty of Agriculture, Khon Kaen University, Khon Kaen 40002, Thailand

ARTICLE INFO

Article history:
Received 20 September 2016
Received in revised form 17 February 2017
Accepted 11 March 2017
Available online 14 March 2017

Chemical compounds studied in this article:
Chitosan (Pubchem CID: 21896651)
Citric acid (Pubchem CID: 311)
Copper(II) chloride (Pubchem CID: 24014)
Ferric chloride hexahydrate (Pubchem CID: 24810)
Iron(II) sulphate heptahydrate (Pubchem CID: 62662)

Keywords:
Chitosan–graphene quantum dots
Magnetic nanocomposite
Copper
Food recipes

ABSTRACT

This study describes the preparation, characterization, and application of a new magnetic chitosan–graphene quantum dots (Fe_3O_4@Chi–GQDs) nanocomposite as an adsorbent for the preconcentration of Cu (II) in Thai food recipes or the so-called "Som Tam" (green papaya salad) prior to determination by inductively coupled plasma–optical emission spectrometry. The spectroscopic and magnetic properties along with the morphology and thermal property were analyzed using FTIR, EDX, XRD, TGA, VSM, and TEM. Preconcentration optimizations including pH, dosage of adsorbent, adsorption–desorption time, concentration and volume of elution solvent, sample volume and enrichment factor, and reusing time were investigated. Good linearity was obtained ranging from 0.05 to 1500 $\mu g\ L^{-1}$ with correlation coefficient of 0.999. Limit of detection was 0.015 $\mu g\ L^{-1}$. Relative recoveries of 85.4–107.5% were satisfactorily obtained. This Fe_3O_4@Chi–GQDs has high potential to be used as preconcentration method and can be reused 7 times with high extraction efficiency.

1. Introduction

Copper is a well-known inorganic element and possesses many biological characteristics as an essential element as well as a toxic substance. It is one of the most important heavy metals that is broadly used in industrial applications. It is also found as a residual contaminant in agricultural products (Rohani Moghadam, Poorakbarian Jahromi, & Darehkordi, 2016). Based on its widespread applications, Cu(II) can be leached out into the environment from several sources. As a result, it may directly or indirectly enter the food chains and in turn affects human health. Numerous serious diseases caused by its higher doses include an intestinal distress; bladder, brain, liver, and kidney damage; and Alzheimer's, Wilson's, and Menkes and Parkinson's diseases (Karadaş & Kara, 2017). Therefore, the determination of Cu(II) at trace concentration becomes increasingly essential because the heavy-metal contaminants in food products have posed a serious threat to public health and biological systems. The trace amount of Cu in food products must be controlled on a daily basis and the maximum allowable level of 30 $mg\ kg^{-1}$ Cu is recommended internationally (Sricharoen et al., 2017). Consequently, to ensure the public health, the preconcentration and determination of Cu(II) are required to meet its detection limit as well as the trace-to-ultratrace levels. Numerous techniques, such as solid phase extraction (SPE) (Yavuz, Tokalıoğlu, Şahan, &

* Corresponding author at: 123 Mittraphab Road, M. 16, T. Ni-Muang, A. Muang, Khon Kaen University, Department of Chemistry, Faculty of Science, Khon Kean 40002, Thailand.
E-mail address: sakcha2@kku.ac.th (S. Chanthai).

http://dx.doi.org/10.1016/j.foodchem.2017.03.066
0308-8146/

Patat, 2016), and dispersive liquid–liquid microextraction (Shrivas & Jaiswal, 2013) have been reported for the preconcentration of Cu(II). Among these methods, SPE is a well-established method for the preconcentration and separation of metals from matrices because it is simple to operate, fast performance, and various adsorbents are available. Recently, nanoparticles (NPs) have been widely used for the preconcentration and determination of copper because of their high surface-area-to-volume ratio, resulting in high extraction capacity and efficiency as well as rapid extraction dynamics. Nowadays, magnetic nanoparticles (MNPs) have also been used as SPE sorbents because of their distinctive properties including an easy phase separation under an external magnetic field, low toxicity, and short analysis time. However, bare MNPs, normally iron oxide (Fe_3O_4), are easily oxidized and tend to form aggregates (Yin, Zhu, Ju, Liao, & Yang, 2016), indicating that their magnetic properties decrease the sorption efficiency and are not suitable ones. In order to improve their stability, Fe_3O_4 NPs are often modified with functionalized materials or biopolymers before applications.

One of the biopolymers that has attracted much attention is chitosan (Chi). Chitosan (β-(1–4)-linked-d-glucosamine) (Limchoowong, Sricharoen, Techawongstien, & Chanthai, 2016; Zou et al., 2016) is known as an ideal natural support with many useful features such as functionality, biocompatibility, nontoxicity, adsorption property, low price, and eco-friendly. It contains a substantial number of amino and hydroxyl groups, which is useful for metal bindings (Çetinus, Sahin, & Saraydin, 2009). The recent research on chitosan mainly focuses on the enhancement of its property by incorporating chitosan matrix to form chitosan-based NPs (Elgadir et al., 2015). Furthermore, the ionic attractions between chitosan macromolecular chains and Fe_3O_4 may encourage a good dispersion of the NPs (Marroquina, Rheea, & Park, 2013). However, a few reports have addressed the combination of chitosan-based magnetic NPs and chitosan beads as a biosorbent (Luo, Zhou, & Yue, 2017). The literature survey shows that a variety of chemically modified metal chelating ligands, such as citrate (Freitas, Nascimento, Souza, & Silva, 2013), graphene oxide, and graphene quantum dots (Ou et al., 2015), have been successfully applied.

Graphene quantum dots (GQDs) are carbon nanosheets that are smaller than 20 nm in later dimension (Hui, Huang, Chen, Zhu, & Yang, 2016). They have recently attracted much research attention owing to their unique property such as an excellent magnetic property, biocompatibility, and low toxicity (Dong et al., 2012). Since oxygen-containing groups such as hydroxyl (–OH), epoxy (–O), carbonyl (–CO), and carboxyl (–COOH) are present, it has been frequently used in separation processes (Nuengmatcha, Mahachai, & Chanthai, 2014). GQDs are superior to common carbon materials because of their nature of nano-sized single-layer graphene sheets, which endows them with an ultrahigh specific surface and makes them more sensitive to environmental variations (Roy, Chen, Periasamy, Chen, & Chang, 2015).

The green papaya salad or "Som Tam" is a popular Thai dish and eaten throughout the Southeast Asian countries. It can be found everywhere in Thailand from restaurants to food stalls. It possesses spicy, sour, and sweet flavors. The main ingredients are tomato, papaya, carrot, eggplant, garlic, yard long bean, chili pepper, and lime. The previously works reported the levels of copper in different food samples such as tomato, carrot, green beans, green pepper, and lemon (Shrivas & Jaiswal, 2013; Jalbani & Soylak, 2015). Therefore, the determination of Cu(II) in these Thai foods was interested in order to protect human health from its toxicity.

To the best of our knowledge, no analytical study on heavy metals using Fe_3O_4 NPs functionalized with Chi–GQDs has been reported. Thus, this work aims at the synthesis and characterization of the magnetic chitosan–graphene quantum dots (Fe_3O_4@Chi–GQDs) nanocomposite and its first presentation as a new and alternative adsorbent for the preconcentration and determination of Cu(II) traces in such samples. The extraction and dispersion of Cu(II) on magnetic nanocomposites were carried out using the ultrasound-assisted extraction (Sricharoen et al., 2016) prior to determination by inductively coupled plasma–optical emission spectrometry (ICP–OES).

2. Materials and methods

2.1. Chemicals and reagents

All the chemicals and reagents were of analytical grade. Shrimp shell chitosan (degree of deacetylation ≥75%), copper(II) chloride, sodium phosphate monobasic monohydrate, sodium phosphate dibasic anhydrous, and sodium acetate was purchased from Sigma-Aldrich (Japan). Glacial acetic acid was obtained from AnalaR (England). Citric acid was purchased from Carlo Erba (Italy). Sodium hydroxide, iron(II) sulphate heptahydrate, ferric chloride hexahydrate, ammonium hydroxide and paraffin oil were obtained from QRec™ (New Zealand). Acetic acid, hydrochloric acid, and sulfuric acid were purchased from UNILAB (Australia). A Millipore water purification system (Molsheim, France) was used to produce deionized water with a resistivity of 18.2 MΩ cm.

2.2. Instruments

The Fourier transform infrared (FTIR) spectrum was recorded using an infrared (IR) spectrometer (Tensor 27, Bruker Optics, Germany) as a KBr pellet and using an attenuated total reflection (ATR)-FTIR spectrophotometer. The transmission infrared spectra of all samples exhibited broad peaks in the range of 400–4000 cm^{-1} at a resolution of 4 cm^{-1}. The surface morphology image and the energy-dispersive X-ray (EDX) spectrum were obtained by a HITACHI S–3000 N scanning electron microscope (SEM, Hitachi Co. Ltd., Japan). The X-ray diffraction (XRD) pattern was recorded with monochromatic Cu Kα radiation (λ = 0.15406 nm), a 2θ range of 10–80°, and a speed of 4 min^{-1} using a PANalytical Empyrean. Thermogravimetric analysis (TGA) was conducted by a Hitachi STA7200 from 50 to 1000 °C at a heating rate of 10 °C min^{-1}. A JEM–2010 TEM (JEOL, Japan) was used to obtain the transmission electron microscopy (TEM) image. The magnetic property was characterized by a vibrating sample magnetometer (VSM, Lake Shore VSM 7403, USA) at 300 K. A Sonorex Digitec DT 510 H (Bandelin, Germany) ultrasonic bath, operating at 35 kHz, was used to leach Cu(II) from the sample. The Cu(II) extract was determined by a Perkin–Elmer OPTIMA 2100 DV inductively coupled plasma–optical emission spectrometer (ICP–OES) (Wellesley, Massachusetts, USA) with a standard ICP torch, an axially viewed plasma system, and a peristaltic pump. The operational system is controlled with PE Winlab software. The instrument and operating conditions for ICP–OES are described in the Supplementary data, Table S1.

2.3. Synthesis of Fe_3O_4@Chi–GQDs

Fe_3O_4 MNPs were synthesized using the coprecipitation method by the modified procedure described previously (Dong et al., 2012). For the synthesis of GQDs was described in the Supplementary data 1. Briefly, 2.5 g of $FeCl_3{\cdot}6H_2O$ and 1.25 g of $FeSO_4{\cdot}7H_2O$ (ratio 2:1) were dissolved in 50 mL of deionized water and sonicated for 5 min at 80 °C. Then, 7.5 mL of ammonia solution (28%, w/v) was added dropwise to their action mixture. A black precipitate of Fe_3O_4 MNPs was formed instantly and their action was allowed to proceed for another 5 min. An aqueous solution of 25 mL of

acetic acid (2%, v/v) containing 1.5 g L^{-1} chitosan was dissolved in the magnetic iron nanoparticle solution under vigorous stirring for 30 min. On the surface of Fe_3O_4 nanoparticles, the mixed chitosan was formed. Then, 20 mL of GQDs was added to the mixture solution drop by drop under vigorous stirring for 30 min at 80 °C. In order to remove any excess of residue materials such as chloride before being dried in an oven at 60 °C for 6 h and ground with a mortar, the resultant was collected using an external magnet and washed several times with distilled water until the washing showed neutral pH. The as-prepared composites were, namely, Fe_3O_4@Chi−GQDs magnetic nanocomposites.

2.4. Samples

Fresh samples including tomato, papaya, carrot, eggplant, garlic, yard long bean, chili pepper, and lime were purchased from a local market of Khon Kaen, Thailand. Only edible parts of each sample were used for the analysis. The rotted or damaged parts were removed before preparation as a simulation to the real food preparation for human consumption. The samples were completely washed with running tap water and subsequently with deionized water. A fresh sample was cut into small portions and dried at 60 °C for 48 h in an oven. A dry sample was ground in a household grinder and then sieved using a No. 100 sieve (0.15 mm opening size). Otherwise, they were stored in plastic bottles and kept in a desiccator until analysis.

2.5. Ultrasonic assisted extraction (UAE)

Approximately 0.1 g of dried sample powder was accurately weighed and extracted with 10 mL of 1 mol L^{-1} nitric acid by the ultrasonic bath for 5 min under a constant frequency of 35 kHz. Subsequently, the copper extract in the supernatant after centrifuging at 5000 rpm for 5 min was immediately determined using ICP–OES.

2.6. Ultrasonic assisted-magnetic solid phase extraction (UA-MSPE)

In Fig. 1 presents the procedure for the UA-MSPE. First, 10 mL of 50 μg L^{-1} Cu(II) was prepared as a sample model in the phosphate buffer solution (0.1 M, pH 6.0). This solution was added to a PTFE bottle with a screw cap containing 0.02 g of Fe_3O_4@Chi–GQDs. Then, the mixture was sonicated by an ultrasonic bath for 10 min at room temperature to suspend Fe_3O_4@Chi–GQDs throughout the sample. The magnetic adsorbents were isolated with a strong magnet, once the adsorption process was completed. Subsequently, an external magnet was easily and quickly applied to the bottom of the bottle and Fe_3O_4@Chi–GQDs were aggregated from the solution. The supernatant could be easily separated from the sorbent within 1 min. After discarding the supernatant, 5 mL of 1 mol L^{-1} HNO_3 (i.e., the eluent solvent) was added, and the mixture was ultrasonicated for 10 min to desorb Cu(II) from its adsorbent. Finally, the magnetic adsorbent was collected through an external magnet, and the desorbed Cu(II) solution was analyzed using an ICP–OES. High-purity water was used as the blank solution and subjected to the same operation as described above. The magnet nanocomposite was reused again to settle the adsorbent, after a cleaning process with 5 mL of the re-extraction solution (1 mol L^{-1} HNO_3) followed by 10 mL of deionized water.

The residual concentration of Cu(II) was also measured in the aqueous solution. The equilibrium adsorption capacity (q_e, μg g^{-1}) of the magnetic adsorbent was calculated using Eq. (1) (Ali, Ibrahim, Sulaiman, Kamboh, & Sanagi, 2016):

$$q_e = (C_0 - C_e) \times V/m \quad (1)$$

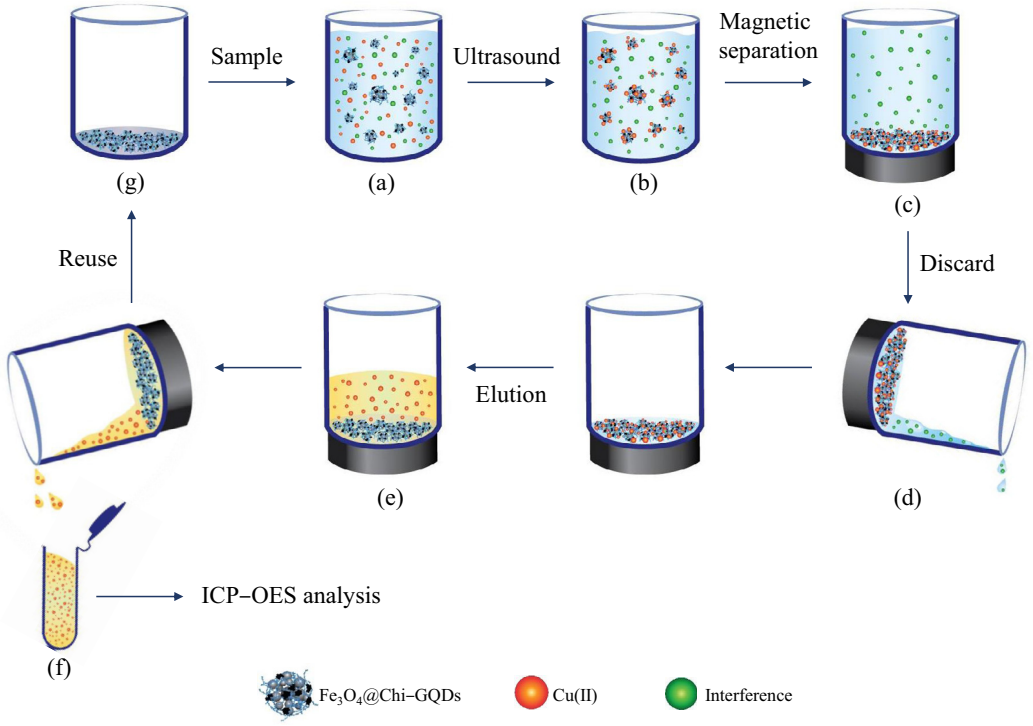

Fig. 1. The procedure for the preconcentration of Cu(II) using UA-MSPE: (a) The adsorbent was added into the aqueous sample, (b) the mixture was adsorbed by ultrasonic bath, (c) the adsorbed Cu(II) was separated from the solution using a magnet, (d) the supernatant was discarded, (e) the adsorbent was desorbed by elution solvent under ultrasonication, (f) The analyte was detected with ICP–OES, and (g) the adsorbent was reused again.

where q_e is the equilibrium adsorption capacity ($\mu g\ g^{-1}$), V is the initial sample volume (mL), m is the mass of the adsorbent (g), and C_0 and C_e are the initial and residual concentrations after equilibrium of Cu(II) ($\mu g\ mL^{-1}$), respectively. The residual concentrations were calculated using the instrument's calibration.

The relative percentage recovery was calculated using Eq. (2) (Limchoowong, Sricharoen, Techawongstien, Kongsri, & Chanthai, 2017; Sricharoen, Limchoowong, Techawongstien, & Chanthai, 2016):

$$\text{Recovery}\ (\%) = [(C_{found} - C_{real})/C_{added}] \times 100 \quad (2)$$

where C_{found}, C_{real}, and C_{added} are the concentration of Cu(II) after addition of the known amount of the standard in the real sample, the concentration of Cu(II) in the real sample, and the concentration of the known amount of the standard that was spiked in the real sample, respectively.

2.7. Statistical analysis

Data results are given as the mean ± standard deviation (SD) of three measurements ($n = 3$). A linear regression analysis was conducted using Microsoft Excel 2013 software.

3. Results and discussion

3.1. Optimization of the UAE procedure

Some of the main parameters that affect the extraction efficiency were studied and optimized including the extraction solvent and its concentration, and the sonication time, whereas the sample mass, solvent volume, and ultrasonic power were fixed at 0.1 g, 10.0 mL, and 35 kHz, respectively. Each experiment was performed in triplicate with a tomato sample. All the detailed optimizations are presented in the Supplementary data 2 (Fig. S1).

3.2. Characterization of Fe_3O_4@Chi–GQDs

3.2.1. Fourier transform infrared spectroscopy

To confirm the functional groups of the as-synthesized magnetic nanoparticles, their FTIR spectra were recorded as shown in Fig. 2(a). The FTIR spectra of Fe_3O_4, Fe_3O_4@Chi, and Fe_3O_4@Chi–GQDs were found comparable. The absorption band around 3420 cm^{-1} revealed the stretching vibration of the N—H bond with O—H in chitosan (Moghimi, 2014), the band around 1654 cm^{-1} could be attributed to the N—H scissoring from the primary amine, due to the free amino group in the cross-linked chitosan (Shen et al., 2014), and around 1068 cm^{-1} resulted from the C—O stretching (Xu et al., 2011). The amino peak shifts from 1654 cm^{-1} for chitosan (Wang et al., 2013) to 1628 cm^{-1} for the magnetic chitosan and Chi–GQDs. Moreover, the C—O stretching position shifts from 1068 to 1072 cm^{-1}, which can be attributed to the hydroxyl functional (–OH) of chitosan that is covalently coordinated with Fe_3O_4, and it is the O atom of the –OH group that forms the coordinate covalent bonds with the Fe atom (Marroquina et al., 2013; Wang et al., 2013). The characteristic absorption peak is validated for Fe–O at 586 cm^{-1}, and it can be observed both in the spectra of Fe_3O_4@Chi and Fe_3O_4@Chi–GQDs, which demonstrates that the composite nanoparticles contain Fe_3O_4 (Shen et al., 2014). From FTIR spectra of the chitosan–GQD MNPs, the C—O peaks shift from 1072 cm^{-1} to 1069 cm^{-1} and 3420 cm^{-1} (O—H stretching vibrations) to 3382 cm^{-1} for chitosan itself because of the hydrogen bonding between the amino group of chitosan and the remaining oxygenated functional groups of the GQDs (Justin et al., 2015). The IR spectrum of the chitosan–GQD MNPs exhibits a layer of the modified Chi–GQDs on the surface of the magnetite nanoparticles.

3.2.2. Energy-dispersive X-ray analysis

As shown in Fig. 2(b), EDX analysis of the magnetic composite material is aimed to investigate the compositions of the element. The EDX spectra showed the strong peaks of Fe and O in the unmodified MNPs. The components of Fe_3O_4 formed by coprecipitation were found to be 71% Fe and 29% O. In addition, the presence of Chi–GQDs on the surface of Fe_3O_4 nanoparticles was verified with the appearance of N and C in the EDX spectrum. Based on the total weight (%) of Fe, O, N, and C on the surface of Fe_3O_4 nanoparticles, their values were found to be about 54.4, 19.9, 2.5, and 23.2%, respectively. Thus, the presence of chitosan and GQDs in the magnetic nanocomposite was confirmed.

3.2.3. X-ray diffraction analysis

To confirm the existence of iron oxide particles (Fe_3O_4), the as-synthesized phase of Fe_3O_4@Chi–GQDs was investigated by using X-ray diffraction. As shown in Fig. 2(c), the XRD patterns were obtained in the 2θ region of 20–80° of Fe_3O_4, Fe_3O_4@Chi, and Fe_3O_4@Chi–GQDs. All characteristic diffraction peaks of Fe_3O_4 (2θ = 30.1, 35.5, 43.3, 53.4, 57.2, and 62.5), marked by their indices (220), (311), (400), (422), (511), and (440), are observed for Fe_3O_4 and Fe_3O_4@Chi–GQDs, which exactly matched with the standard XRD data of the Fe_3O_4 crystal (JCPDS No. 19-06290). Thus, these results demonstrate that the new adsorbent shows good magnetic property and thus can be used for application of magnetic separation.

3.2.4. Thermogravimetric analysis

TGA analysis was used to investigate the thermal degradation and the organic functional groups attached to the MNPs. Fig. 2(d) shows the TGA curves of Fe_3O_4, Fe_3O_4@Chi, and Fe_3O_4@Chi–GQDs determined in an air atmosphere from 50 to 1000 °C. The first step of the TGA analysis from 50 to 100 °C was assigned to the loss of physically adsorbed water. The second step from 250 to 650 °C showed the proportions of chitosan and graphene quantum dots present in the magnetic nanocomposites. The weight losses for both Fe_3O_4@Chi (10.55%) and Fe_3O_4@Chi–GQDs (14.46%) during the major degradation step, caused by the loss of the absorbed moisture, were used to determine Chi–GQDs onto Fe_3O_4.

3.2.5. Vibrating sample magnetometry analysis

Magnetism is an important feature of magnetic materials. Sufficient magnetism can quickly separate materials from the aqueous medium in practical applications. The magnetic property was evaluated using the vibrating sample magnetometer at room temperature. The magnetic hysteresis loops of Fe_3O_4 MNPs, Fe_3O_4@Chi, and Fe_3O_4@Chi–GQDs are shown in Fig. 2(e). The magnetization curves illustrate that all Fe_3O_4 MNPs, Fe_3O_4@Chi, and Fe_3O_4@Chi–GQDs are essentially super paramagnetic with magnetization saturations of 71.77 emu g^{-1}, 64.77 emu g^{-1}, and 59.31 emu g^{-1}, respectively. The decrease in the saturation magnetization is due to the increased amount of Chi-GQDs incorporated in the Fe_3O_4@Chi–GQD nanocomposites. The existence of non-magnetite on surface of Fe_3O_4 nanoparticles decreases the uniformity because of the quenching of surface moments, which results in the reduction of the magnetic moment in such nanoparticles. In this case, the magnetic property of Fe_3O_4@Chi–GQDs remains high enough for the application of magnetic separation (Fan, Luo, Lv, Lu, & Qiu, 2011). The super paramagnetic saturation of 16.3 emu g^{-1} is sufficient for the magnetic separation from the solution with a magnet (Ma, Guan, & Liu, 2005). Because of such high magnetic values (i.e., 59.31 emu g^{-1}), this new adsorbent dispersed in water can be easily and rapidly separated from the aqueous solution by

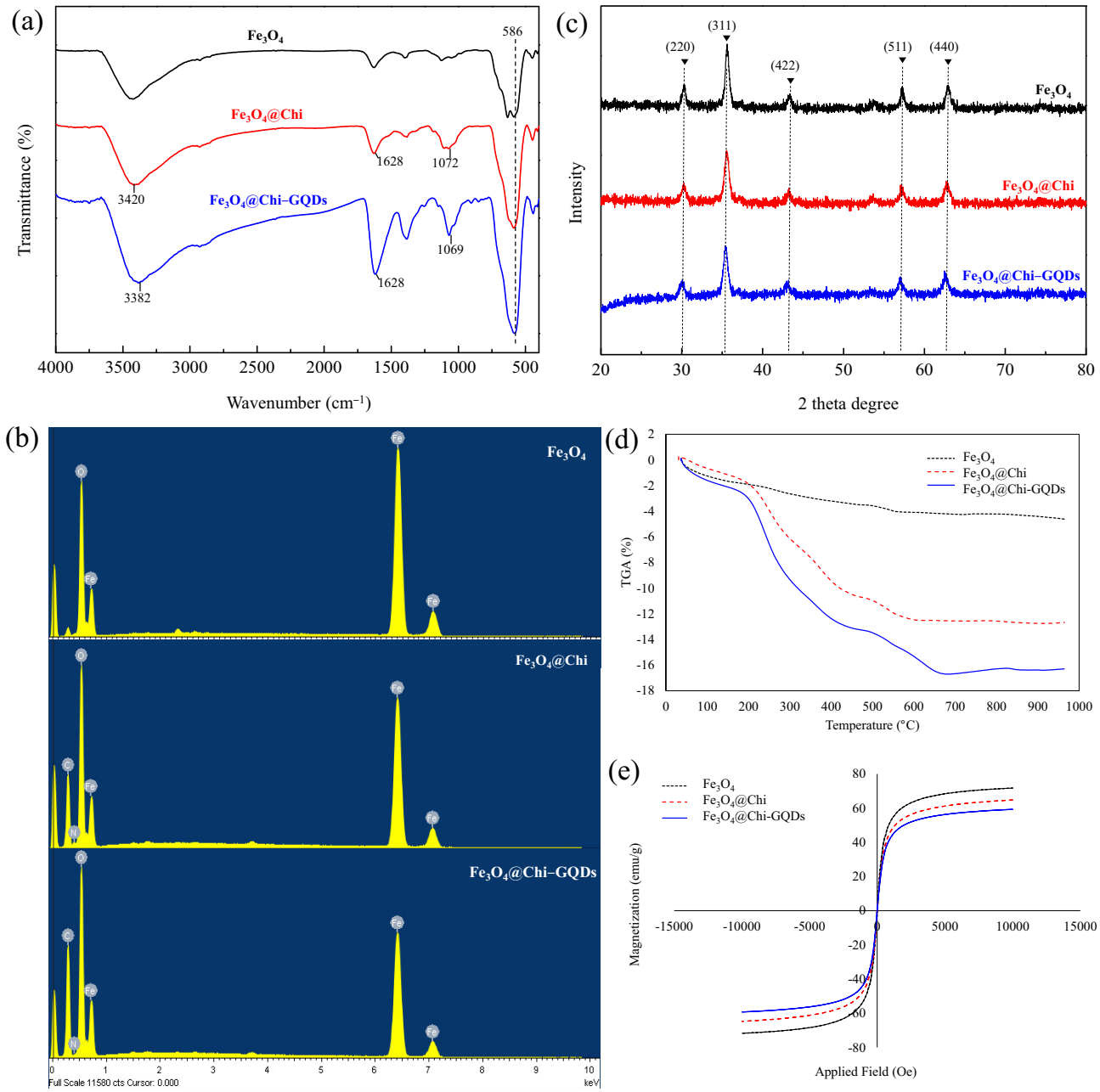

Fig. 2. (a) FT–IR spectra, (b) EDX pattern, (c) XRD pattern, (d) TGA curve, and (e) magnetic hysteresis loops of Fe_3O_4 MNPs, Fe_3O_4@Chi, and Fe_3O_4@Chi–GQDs.

an external magnetic field within 30 s. Thus, with an external magnetic field, Fe_3O_4@Chi–GQDs were attracted to the wall of the vial through strongly binding magnetism.

3.2.6. Transmission electron microscopy analysis

Micrographs of the magnetite were obtained by a transmission electron microscope operated at an accelerating voltage of 100 kV. The typical TEM of MNPs using Image J Software is shown in Fig. 3. It is evident that the morphology of magnetic Fe_3O_4 NPs is spherical with an average particle size of 13.6 nm. This image clearly shows the successful coating of the functionalized iron oxide nanoparticles, Fe_3O_4@Chi–GQDs, as a new chelating agent with an average diameter of 9.0 nm. The particle size of the new magnetic nanocomposite is smaller than those reported in previous works (Hou, Wang, Zhu, & Wei, 2016). Although it is difficult for the magnetic nanocomposite to observe directly the layer of Chi–GQDs on the iron oxide from the TEM image, the dispersing performance of the surface of MNPs was obviously improved as compared with that of the unmodified Fe_3O_4 NPs, which exhibited aggregated morphology. This is caused by the chelating effect of the functional groups on chitosan and graphene quantum dots with iron oxide, thus during the growth process it inhibits the nanocomposite from conglomerating. These results confirmed that the Chi–GQDs were successfully functionalized on the Fe_3O_4 substrate.

3.3. Optimization conditions for the magnetic solid-phase extraction

To validate Fe_3O_4@Chi–GQDs using the magnetic solid-phase extraction (MSPE) method for the determination of Cu(II), various experimental parameters (pH, adsorbent dosage, adsorption time, elution solvent, eluent concentration, desorption time, sample

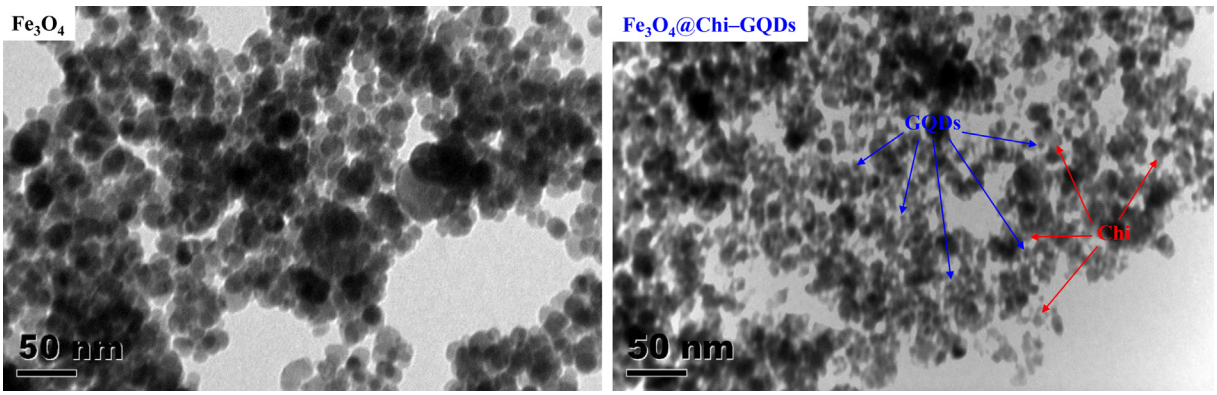

Fig. 3. TEM images of Fe_3O_4 and Fe_3O_4@Chi–GQDs.

volume and the enrichment factor, and reusability of the magnetic adsorbent) were investigated in detail. Each experiment was performed at least in triplicate.

3.3.1. Effect of pH

The pH value of a solution is an important parameter that affects the adsorption of metal ions. It can control an electrostatic or molecular interaction to any extent between the adsorbent surface and the adsorbate due to the charge distribution on materials. The effect of the pH value on the equilibrium adsorption capacity (q_e, $\mu g\, g^{-1}$) of Cu(II) using Fe_3O_4@Chi–GQDs was investigated between pH 2 and pH 8 using 10 mL of the water sample containing 50 $\mu g\, L^{-1}$ of Cu(II) and 0.02 g of MNPs with an adsorption time of 15 min. As shown in Fig. 4(a), a small amount of Cu(II) was adsorbed onto Fe_3O_4@Chi–GQDs at pH 2. Lower q_e, at lower pH levels (pH 2–4), does not favor the adsorption of Cu(II) on the adsorption sites. As chitosan is mostly present in its protonated form (NH_3^+ cation), the chelating group (deprotonated form, NH_2) of the adsorbent for the Cu(II) adsorption decreased considerably. Furthermore, for the Cu(II) adsorption, the carboxylate ion (COO^-) chelating group of the adsorbent decreased because of the protonation of the carboxylate ion to form carboxylic acid. These effects decreased the adsorption of Cu(II) on the magnetic Chi–GQDs adsorbent. The amount of Cu(II) adsorbed increased significantly as the pH values increased from 4 to 6, mostly because of the deprotonation of amino groups of chitosan, which is caused by the increase in the pH value, which substantially enhanced the adsorption of heavy metal ions because of their decrease in binding sites. Furthermore, the high-equilibrium adsorption capacity of Cu (II) might be due to the ionic behavior of Fe_3O_4@Chi–GQDs at pH 6 because the adsorbent has the carboxylic (COO−), amino (NH_2), and hydroxyl (OH) groups that can act as anions. Lone pair electrons of their groups of the sorbent act as anionic binding sites for the cationic metal ion, and Cu(II) is then extracted through metal ion covalent coordination. In fact, Cu(II) in an aqueous medium can exist in various forms. It has been reported that Cu(II) is the predominant species at pH 6 (Liu, Chen, & Hao, 2013). Consequently, q_e at the pH range of 6–8 decreased because of the copper hydroxide ($Cu(OH)_2$) precipitated from the solution when its pH value is greater than 6. This precipitation reduces the concentration of Cu(II) in the solution, generating either an error or a deviation in the adsorbed amount during the adsorption experiment (Marroquina et al., 2013). Thus, the solution with a pH value of 6 was chosen for the subsequent experiments.

3.3.2. Effect of the adsorbent dosage

An adsorbent mass is also a crucial factor for the extraction of the target analyte because the adsorbent dosage provides Cu(II) the ability to be adsorbed with a minimum dosage, subject to beneficial economic point of views. Therefore, the adsorption experiment was performed using 0.02–0.1 g of Fe_3O_4@Chi–GQDs (MNPs) to evaluate the equilibrium adsorption capacity. Other conditions were fixed with 10 mL of the deionized water sample containing 50 $\mu g\, L^{-1}$ Cu(II) at pH 6 for an adsorption time of 15 min. The results (Fig. 4(b)) obtained show that 0.02 g of the MNPs was sufficient for the adsorption of the analytes and an additional amount of the sorbent could cause a decrease in the equilibrium adsorption capacity. The higher amounts of the MNPs may not effectively disperse and work properly, and they may lead to a decrease in the surface area available to Cu(II), which could be resulted from either an overlapping or an aggregation of the adsorption sites (Akar, Altinişik, & Seki, 2013). Therefore, 0.02 g of the MNPs was enough to ensure complete adsorption.

3.3.3. Effect of the adsorption time

The adsorption time is also a key parameter for evaluating the equilibrium adsorption capacity of Cu(II) using Fe_3O_4@Chi–GQDs. To analyze the loading time of Cu(II) onto the adsorbent, the adsorption time was varied from 5 to 30 min using mechanical shaking. As shown in Fig. 4(c), the equilibrium adsorption capacity of Cu(II) continuously increases between 5 and 10 min, and remains constant beyond this time period. Since a rapid diffusion within the nanosorbent would provide a high rate of the adsorption process, the equilibrium state between Cu(II) and the adsorbent surface can be obtained in a shorter contact time. Thus, the adsorption time of 10 min was relatively justified.

3.3.4. Effect of the elution solvent

The eluting solvent is a very important factor that affects the MSPE procedure. To achieve a high enrichment factor, the desorption was studied using different acid eluents. For desorbing Cu(II) from the adsorbent surface, an aliquot of 10 mL of 50 $\mu g\, L^{-1}$ Cu (II) solution was mixed with 0.02 g of Fe_3O_4@Chi–GQDs. As discussed in Section 3.3.1, the adsorption of Cu(II) at a pH value of lower than 4 is negligible; thus, an acidic medium is preferred for the Cu(II) desorption. Of 1 mol L^{-1} typical acid eluents, including hydrochloric acid, nitric acid, sulfuric acid, and acetic acid, 5 mL was used for desorbing the adsorbed Cu(II). The Cu(II) content that back-extracted into the liquid phase by each eluent was determined by ICP–OES. The percent-recovery of Cu(II) was calculated for each sample. Results in Fig. 5(a) show that the dilute nitric acid solution exhibited the highest recovery of Cu(II). Therefore, HNO_3 was considered suitable for the elution solvent.

3.3.5. Effect of the eluent concentration

The effect of the concentration of HNO_3 on the desorption of Cu(II) was also analyzed. For desorbing, Cu(II) adsorbed on 0.02 g of the adsorbent was eluted with 5.0 mL of different nitric acid

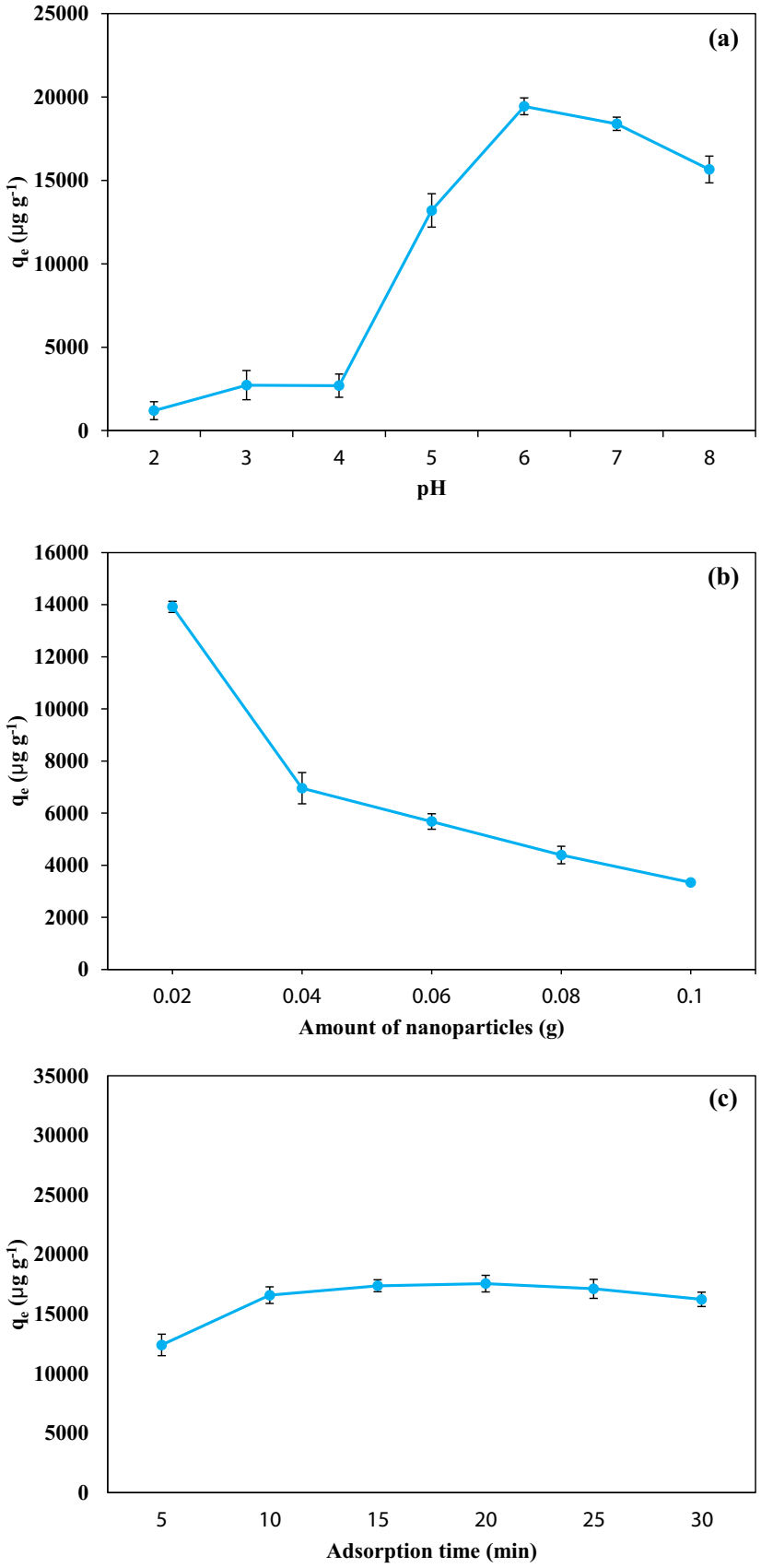

Fig. 4. The optimization of the UA-MSPE parameters: (a) pH, conditions: 0.02 g of adsorbent; 10 mL of 50 µg L^{-1} Cu(II) solution; 15 min of adsorption time, (b) dosage of magnetic adsorbent, conditions: 10 mL of 50 µg L^{-1} Cu(II) solution; pH 6; 15 min of adsorption time, and (c) adsorption time, conditions: 0.02 g of adsorbent; 10 mL of 50 µg L^{-1} Cu(II) solution; pH 6.

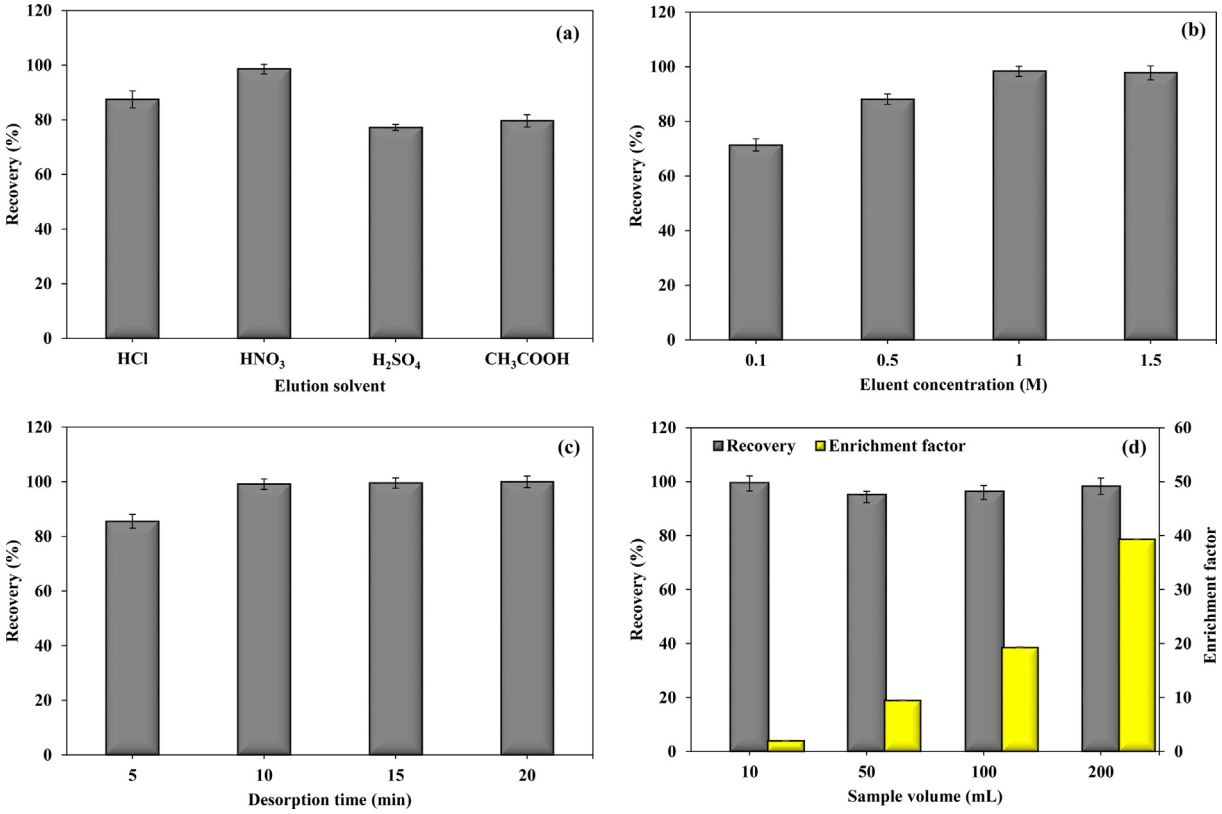

Fig. 5. The optimization of the UA-MSPE parameters: (a) type of the elution solvent, conditions: 0.02 g of adsorbent; 10 mL of 50 μg L^{-1} Cu(II) solution; pH 6; 10 min of adsorption time; 10 min of desorption time; 5.0 mL of 1 mol L^{-1} eluents (b) concentration of the elution solvent, conditions: 0.02 g of adsorbent; 10 mL of 50 μg L^{-1} Cu(II) solution; pH 6; 10 min of adsorption time; 10 min of desorption; 5.0 mL of HNO_3, (c) desorption time, conditions: 0.02 g of adsorbent; 10 mL of 50 μg L^{-1} Cu(II) solution; pH 6; 10 min of adsorption time; 5.0 mL of 1 mol L^{-1} HNO_3, and (d) sample volume and enrichment factor, conditions: 0.02 g of adsorbent; 10 mL of 50 μg L^{-1} Cu(II) solution; pH 6; 10 min of adsorption time; 10 min of desorption; 5.0 mL of 1 mol L^{-1} HNO_3.

concentrations (0.1, 0.5, 1, and 1.5 M). The results showed that the recovery of Cu(II) increases with the increase in the concentration of HNO_3 (Fig. 5(b)). For higher than 1.0 mol L^{-1} of nitric acid, the amount of Cu(II) was completely desorbed from the adsorbent (almost 100% recovery). Thus, only 5 mL of 1 mol L^{-1} HNO_3 was obtained as a mild elution solvent for further study.

3.3.6. Effect of the desorption time

The effect of the desorption time using an ultrasonic shaking was varied in the range of 5–20 min using 5 mL of 1 mol L^{-1} HNO_3 as the eluent. As shown in Fig. 5(c), it is evident that the desorption of Cu(II) was completely achieved within 10 min (almost 100% recovery). Since it is due to nanosize with a high surface area of the adsorbent used, the desorption equilibrium state can therefore be obtained rapidly as well.

3.3.7. Effect of the sample volume and the enrichment factor

In order to obtain a higher enrichment factor (EF), a larger sample volume is required. The MNP-mixed hemimicelle SPE method based on the magnetic carrier technology avoids time consumed for column passing and filtration steps, and shows a great analytical potential in the preconcentration of the large volume of water sample (Faraji, Yamini, & Rezaee, 2010). The effect of the sample volume on the enrichment of Cu(II) was investigated by extracting the sample from 10 to 200 mL of an aqueous solution spiked with 50 μg L^{-1} Cu(II), while the maximum eluting solvent was 5 mL because the flow injection of ICP–OES required at least about 3 mL (Fig. 5(d)). Under the optimal conditions, the recoveries for Cu(II) were still above 90% with sample volumes up to 200 mL. Therefore, it is noted that this step can be performed with all of these sample volumes because they provide an acceptable recovery for the determination of copper. However, the EF increased with the increase in the sample volume up to 200 mL (EF = 34.2–43.0), higher sample volumes were not obtained because of too much of the sample volume used, making the sample preparation difficult and inconvenient. Thus, 200 mL of the sample was used for the analysis of the real sample. The enrichment factor (EF) was calculated using Eq. (3) (Sricharoen, Limchoowong, Techawongstien, & Chanthai, 2017):

$$EF = C_{ext}/C_{ini} \quad (3)$$

where C_{ext} and C_{ini} are the analyte concentration in the extraction phase and the initial analyte concentration in the aqueous phase, respectively.

3.3.8. Reusability of the magnetic adsorbent

The regeneration ability of the adsorbent is one of the main factors in the assessment of the performance of the sorption materials. Such adsorbent has higher adsorption capability as well as better desorption property, which reduces the overall cost of the adsorbent used. For this purpose, the sorption–desorption cycles were repeated eight times by using the same adsorbent. The results in the Supplementary data (Fig. S2) showed that within seven cycles of reuse, the magnetic adsorbent is stable in the operation process without losing its significant adsorption capacity, which indicates a good performance and robustness of the as-prepared Fe_3O_4@Chi–GQDs as an adsorbent for the removal of Cu (II). High recovery was obtained over 84% and decreased to 66.6% thereafter. Therefore, the reusability of the studied metal ion was about seven times. The results strongly demonstrate that the mag-

Table 1
Determination of Cu(II) in vegetable, fruit and herb samples using both UAE and UA-MSPE procedures.

Sample	Scientific name	UAE[a]		UA-MSPE[b]		
		Content ($\mu g\ g^{-1}$ DW)	Recovery (%)	Content ($\mu g\ g^{-1}$ DW)	Recovery (%)	EF[c]
Tomato 1	*Solanum lycopersicum*	19.36 ± 0.15	94.12 ± 3.42	18.68 ± 1.10	93.17 ± 4.04	37.3
Tomato 2	*Solanum lycopersicum*	17.62 ± 0.76	92.57 ± 2.37	16.13 ± 0.78	90.18 ± 7.58	36.1
Papaya	*Carica papaya*	9.88 ± 0.36	97.48 ± 6.26	8.61 ± 0.62	102.28 ± 3.59	40.9
Carrot	*Daucus carota* subsp. *sativus*	10.29 ± 0.52	96.93 ± 3.81	9.57 ± 0.77	95.35 ± 3.31	38.1
Eggplant	*Solanum melongena*	14.70 ± 0.45	104.90 ± 5.68	13.14 ± 0.50	107.47 ± 6.59	43.0
Garlic	*Allium sativum*	11.19 ± 0.30	96.01 ± 4.87	10.32 ± 0.42	98.12 ± 7.50	39.2
Yard long bean	*Vigna unguiculata* subsp. *sesquipedalis*	15.73 ± 0.90	96.95 ± 1.36	15.15 ± 0.68	94.52 ± 4.54	37.8
Chili pepper	*Capsicum annuum*	22.26 ± 1.03	92.14 ± 3.06	19.89 ± 0.48	104.32 ± 6.28	41.7
Lime	*Citrus aurantifolia*	11.55 ± 0.54	93.92 ± 5.43	11.17 ± 1.32	85.38 ± 1.67	34.2

Data are presented as mean ± SD (n = 3).
[a] Ultrasound assisted extraction.
[b] Ultrasound assisted magnetic solid-phase extraction.
[c] Enrichment factor (n = 3).

netic adsorbent can be recycled for the Cu(II) adsorption, and it can be reused several times.

3.4. Method validation

3.4.1. Analytical features of merit

The characteristic calibration data are listed in the Supplementary data, Table S2. A series of working solutions containing Cu(II) was used to prepare the calibration curve for six concentration levels of 1, 5, 10, 20, 40, and 60 $\mu g\ L^{-1}$. Linearity was observed in the range of 0.05–1500 $\mu g\ L^{-1}$ with a regression coefficient of 0.999. The limit of detection (LOD) and the limit of quantification (LOQ), defined as $3 \times SD/m$ and $10 \times SD/m$ (where SD is the standard deviation of the low concentration of copper and m is the slope of the calibration curve), were 0.015 and 0.049 $\mu g\ L^{-1}$, respectively. The precision is expressed as the percent relative standard deviation (%RSD), using the slope of the calibration graph, which was determined in terms of repeatability (data from five independent standard preparations, intraday %RSD) and reproducibility (work performed during five consecutive days, interday %RSD) and found to be 0.87% and 4.47%, respectively. These results show that the proposed method shows high sensitivity and precision. In addition, the EF of this preconcentration method was found to be 39.3.

3.4.2. Analysis of the real samples

To assess the applicability and reliability of the proposed method (UAE and UA-MSPE) to the real samples, the extraction and determination of Cu(II) from 10 mL of different sample extracts were carried out. Moreover, UAE and UA-MSPE were successfully applied to eleven samples of Thai "Som Tam" recipes (green papaya salad) including nine types of fresh vegetables, fruits, and herbs (i.e., tomato, shallot, green papaya, carrot, eggplant, garlic, yard long bean, chili pepper, and lime). As shown in Table 1, the contents of Cu(II) found in each sample were obtained. For UAE, the results confirmed that Cu(II) was found in all samples evaluated and ranged from 10.95 ± 0.34 to 29.38 ± 1.38 $\mu g\ g^{-1}$ DW. Chili pepper contained the highest amount of Cu(II), whereas papaya contained the lowest mount. After UAE, all samples were diluted to 200 mL with 0.1 mol L^{-1} acetate buffer at pH 6 to reduce the concentration of Cu(II) and the matrix effect prior to analysis under the optimal conditions using UA-MSPE. It was found that the contents of Cu(II) using ICP–OES in association with UA-MSPE were in the range of 8.61 ± 0.62 to 19.89 ± 0.48 $\mu g\ g^{-1}$ DW. These results are in agreement (paired t-test) with those obtained using only the UAE method for the sample preparation at the 95% confidence level. In addition, to complement the evaluation of the proposed method and to check matrix effects, the accuracy of the method was verified by evaluating the recovery values in the real samples. Each sample was spiked with 100 $\mu g\ L^{-1}$ of the standard solution of Cu(II) and subjected to the optimized extraction procedure. The recovery was expressed as the mean value of the three independent determinations. The recovery ranges of 92.14 ± 3.06 to 104.90 ± 5.68% for UAE and 85.38 ± 1.67 to 107.47 ± 6.59% for UA-MSPE were comparatively obtained, which indicated that both extraction methods (UAE and UA-MSPE) were free of matrix interferences. These methods provide an acceptable recovery for the determination of copper. This demonstrates that the proposed methods were suitable for analyzing the copper residue in the real samples. Moreover, the performance of the preconcentration in terms of the enrichment factor was also obtained using the UA-MSPE analysis. As a good outcome of this approach, the remarkable EF was obtained in the range of 34.2–43.0, at which the trace determination of the target analyte is ensured.

The comparison of the present extraction and determination of Cu(II) using Fe_3O_4@Chi–GQDs as a new magnetic adsorbent with those of previous reports is summarized in the Supplementary data 3, Table S3.

4. Conclusion

In summary, Fe_3O_4@Chi–GQDs were successfully prepared and applied as a new magnetic adsorbent for the preconcentration and trace determination of Cu(II) in food samples. The adsorbent exhibited an effective and well-dispersed suspension for magnetic Fe_3O_4 NPs. Thus, the preconcentration step was faster than the traditional SPE, which resulted in the reduction of the analysis time because the adsorbent could be easily separated from the sample solution. In addition, the functional groups on the surface of Fe_3O_4@Chi–GQDs provided plenty of active sites for Cu(II) binding, primarily by electrostatic interactions and/or surface complex formation through covalent coordinate binding. Therefore, the new magnetic adsorbent can be applied as a high potential micro-solid-phase extraction for metal separation and analysis.

Acknowledgements

The authors would like to thank the Higher Education Research Promotion and the National Research University Project of Thailand; the Office of the Higher Education Commission, through the Food and Functional Food Research Cluster of Khon Kaen University; the Materials Chemistry Research Unit, Department of Chemistry, Center of Excellence for Innovation in Chemistry (PERCH-CIC); and the Commission on Higher Education and the Ministry of Education, Thailand for financial support.

Appendix A. Supplementary data

Supplementary data associated with this article can be found, in the online version, at http://dx.doi.org/10.1016/j.foodchem.2017.03.066.

References

Akar, E., Altinişik, A., & Seki, Y. (2013). Using of activated carbon produced from spent tea leaves for the removal of malachite green from aqueous solution. *Ecological Engineering, 52*, 19–27.

Ali, L. I. A., Ibrahim, W. A. W., Sulaiman, A., Kamboh, M. A., & Sanagi, M. M. (2016). New chrysin-functionalized silica-coreshell magnetic nanoparticles for the magnetic solid phase extraction of copper ions from water samples. *Talanta, 148*, 191–199.

Çetinus Sahin, E., & Saraydin, D. (2009). Preparation of Cu(II) adsorbed chitosan beads for catalase immobilization Senay Akkus. *Food Chemistry, 114*, 962–969.

Dong, Y., Shao, J., Chen, C., Li, H., Wang, R., Chi, Y., ... Chen, G. (2012). Blue luminescent graphene quantum dots and graphene oxide prepared by tuning the carbonization degree of citric acid. *Carbon, 50*(12), 4738–4743.

Elgadir, M. A., Uddin, M. S., Ferdosh, S., Adam, A., Chowdhury, A. J. K., & Sarker, M. Z. I. (2015). Impact of chitosan composites and chitosan nanoparticle composites on various drug delivery systems: A review. *Journal of Food and Drug Analysis, 23*(4), 619–629.

Fan, L., Luo, C., Lv, Z., Lu, F., & Qiu, H. (2011). Removal of Ag^+ from water environment using a novel magnetic thiourea-chitosan imprinted Ag^+. *Journal Hazardous Materials, 194*, 193–201.

Faraji, M., Yamini, Y., & Rezaee, M. (2010). Extraction of trace amounts of mercury with sodium dodecyle sulphate-coated magnetite nanoparticles and its determination by flow injection inductively coupled plasma-optical emission spectrometry. *Talanta, 81*, 831–836.

Freitas, E. V., Nascimento, C. W., Souza, A., & Silva, F. B. (2013). Citric acid-assisted phyto extraction of lead: A field experiment. *Chemosphere, 92*(2), 213–217.

Hou, C., Wang, Y., Zhu, H., & Wei, H. (2016). Construction of enzyme immobilization system through metal-polyphenol assisted Fe_3O_4/chitosan hybrid microcapsules. *Chemical Engineering Journal, 283*, 397–403.

Hui, L., Huang, J., Chen, G., Zhu, Y., & Yang, L. (2016). Antibacterial property of graphene quantum dots (both source material and bacterial shape matter). *Applied Materials Interfaces, 8*(1), 20–25.

Jalbani, N., & Soylak, M. (2015). Ligandless ultrasonic-assisted and ionic liquid-based dispersive liquid–liquid microextraction of copper, nickel and lead in different food samples. *Food Chemistry, 167*, 433–437.

Justin, R., Roman, S., Chen, D., Tao, K., Geng, X., Grant, R. T., ... Chen, B. (2015). Biodegradable and conductive chitosan–grapheme quantum dot nanocomposite microneedles for delivery of both small and large molecular weight therapeutics. *RSC Advances, 5*(64), 51934–51946.

Karadaş, C., & Kara, D. (2017). Dispersive liquid–liquid microextraction based on solidification of floating organic drop for preconcentration and determination of trace amounts of copper by flame atomic absorption spectrometry. *Food Chemistry, 220*, 242–248.

Limchoowong, N., Sricharoen, P., Techawongstien, S., & Chanthai, S. (2016). An iodine supplementation of tomato fruits coated with an edible film of the iodide-doped chitosan. *Food Chemistry, 200*, 223–229.

Limchoowong, N., Sricharoen, P., Techawongstien, S., Kongsri, S., & Chanthai, S. (2017). A green extraction of trace iodine in table salts, vegetables, and food products prior to analysis by inductively coupled plasma optical emission spectrometry. *Journal of the Brazilian Chemical Society, 28*(4), 540–546.

Liu, Y., Chen, M., & Hao, Y. (2013). Study on the adsorption of Cu(II) by EDTA functionalized Fe_3O_4 magnetic nano-particles. *Chemical Engineering Journal, 218*, 46–54.

Luo, Y., Zhou, Z., & Yue, T. (2017). Synthesis and characterization of nontoxic chitosan-coated Fe_3O_4 particles for patulin adsorption in a juice-pH simulation aqueous. *Food Chemistry, 221*, 317–323.

Ma, Z., Guan, Y., & Liu, H. (2005). Synthesis and characterization of micron-sized monodisperse superparamagnetic polymer particles with amino groups. *Journal of Polymer Science Part A: Polymer Chemistry, 43*(15), 3433–3439.

Marroquina, J. B., Rheea, K. Y., & Park, S. J. (2013). Chitosan nanocomposite films: Enhanced electrical conductivity, thermal stability, and mechanical properties. *Carbohydrate Polymers, 92*(2), 1783–1791.

Moghimi, A. (2014). Separation and extraction of Co(II) using magnetic chitosan nanoparticles grafted with β-cyclodextrin and determination by FAAS. *Russian Journal of Physical Chemistry A, 88*(12), 2157–2164.

Nuengmatcha, P., Mahachai, R., & Chanthai, S. (2014). Thermodynamic and kinetic study of the intrinsic adsorption capacity of graphene oxide for malachite green removal from aqueous solution. *Oriental Journal of Chemistry, 30*, 1463–1474.

Ou, J., Tao, Y., Xue, J., Kong, Y., Dai, J., & Deng, L. (2015). Electrochemical enantiorecognition of tryptophan enantiomers based on graphene quantum dots–chitosan composite film. *Electrochemistry Communications, 57*, 5–9.

Rohani Moghadam, M., Poorakbarian Jahromi, S. M., & Darehkordi, A. (2016). Simultaneous spectrophotometric determination of copper, cobalt, nickel and iron in foodstuffs and vegetables with a new bis thiosemicarbazone ligand using chemometric approaches. *Food Chemistry, 192*, 424–431.

Roy, P., Chen, P. C., Periasamy, A. P., Chen, Y. N., & Chang, H. T. (2015). Photoluminescent carbon nanodots: Synthesis, physicochemical properties and analytical applications. *Materials Today, 18*(8), 447–458.

Shen, M., Yu, Y., Fan, G., Chen, G., Min Jin, Y., Tang, W., & Jia, W. (2014). The synthesis and characterization of monodispersed chitosan-coated Fe_3O_4 nanoparticles via a facile one-step solvothermal process for adsorption of bovine serum albumin. *Nanoscale Research Letters, 9*(1), 1–8.

Shrivas, K., & Jaiswal, N. K. (2013). Dispersive liquid–liquid microextraction for the determination of copper in cereals and vegetable food samples using flame atomic absorption spectrometry. *Food Chemistry, 141*, 2263–2268.

Sricharoen, P., Lamaiphan, N., Patthawaro, P., Limchoowong, N., Techawongstien, S., & Chanthai, S. (2016). Phytochemicals in oleoresin from different varieties of hot chilli peppers with their antidiabetic and antioxidant activities due to some phenolic compounds. *Ultrasonics Sonochemistry*. http://dx.doi.org/10.1016/j.ultsonch.2016.08.018.

Sricharoen, P., Limchoowong, N., Areerob, Y., Nuengmatcha, P., Techawongstien, S., & Chanthai, S. (2017). Fe_3O_4/hydroxyapatite/graphene quantum dots as a novel nano-sorbent for preconcentration of copper residue in Thai food ingredients: Optimization of ultrasound-assisted magnetic solid phase extraction. *Ultrasonics Sonochemistry, 37*, 83–93.

Sricharoen, P., Limchoowong, N., Techawongstien, S., & Chanthai, S. (2016). A novel extraction method for b-carotene and other carotenoids in fruit juices using air-assisted, low-density solvent-based liquid–liquid microextraction and solidified floating organic droplets. *Food Chemistry, 203*, 386–393.

Sricharoen, P., Limchoowong, N., Techawongstien, S., & Chanthai, S. (2017). Ultrasound-assisted emulsification microextraction coupled with salt-induced demulsification based on solidified floating organic drop prior to HPLC determination of Sudan dyes in chili products. *Arabian Journal of Chemistry*. http://dx.doi.org/10.1016/j.arabjc.2016.12.020.

Wang, B., Zhang, P. P., Williams, G. R., Christopher, B. W., Quan, J., Nie, H. L., & Zhu, L. M. (2013). A simple route to form magnetic chitosan nanoparticles from coaxial-electrospun composite nanofibers. *Journal of Materials Science, 9*(11), 3991–3998.

Yavuz, E., Tokalıoğlu, Ş., Şahan, H., & Patat, Ş. (2016). Nanosized spongelike Mn_3O_4 as an adsorbent for preconcentration by vortex assisted solid phase extraction of copper and lead in various food and herb samples. *Food Chemistry, 194*, 463–469.

Yin, Q., Zhu, Y., Ju, S., Liao, W., & Yang, Y. (2016). Rapid determination of copper and lead in *Panax notoginseng* by magnetic solid-phase extraction and flame atomic absorption spectrometry. *Research on Chemical Intermediates, 42*(5), 4985–4998.

Zou, P., Yang, X., Wang, J., Li, Y., Yu, H., Zhang, Y., & Liu, G. (2016). Advances in characterisation and biological activities of chitosan and chitosan oligosaccharides. *Food Chemistry, 190*, 1174–1181.

http://dx.doi.org/10.5935/0103-5053.20160193

J. Braz. Chem. Soc., Vol. 28, No. 4, 540-546, 2017.
Printed in Brazil - ©2017 Sociedade Brasileira de Química
0103 - 5053 $6.00+0.00

Article

A Green Extraction of Trace Iodine in Table Salts, Vegetables, and Food Products Prior to Analysis by Inductively Coupled Plasma Optical Emission Spectrometry

Nunticha Limchoowong,[a] Phitchan Sricharoen,[a] Suchila Techawongstien,[b] Supalak Kongsri[c] and Saksit Chanthai[,a]*

[a]*Materials Chemistry Research Center, Department of Chemistry and Center of Excellence for Innovation in Chemistry, Faculty of Science and* [b]*Department of Plant Science and Agricultural Resources, Faculty of Agriculture, Khon Kaen University, 40002 Khon Kaen, Thailand*

[c]*Nuclear Research and Development Division, Thailand Institute of Nuclear Technology (Public Organization), Chatuchak, 10900 Bangkok, Thailand*

In this study, we report a new method for iodine extraction from table salts, vegetables, and other food products using ultrasound-assisted extraction, prior to the iodine determination by inductively coupled plasma optical emission spectrometry. For the ultrasound-assisted extraction, deionized water as the extraction solvent and an extraction time of 5 min were found to be the most optimum condition. A linear calibration curve was plotted for 0.1 to 200.0 mg L^{-1} iodine convention. The limits of detection and quantification were 0.049 and 0.164 mg L^{-1}, respectively. The precision for intra- and inter-day analyses was 2.75 and 4.54%, respectively. The accuracy of the method was confirmed with certified reference materials. Recoveries in 47 real samples were ranged between 80.48 and 118.1%. Therefore, the proposed method could be considered as a rapid, simple, and environmental-friendly method (the green extraction) to determine the trace amounts of iodine in different kinds of food products.

Keywords: iodine, ultrasound assisted extraction, green extraction, food products, ICP OES

Introduction

Iodine is one of the most essential trace elements for humans and other higher animals.[1] Iodine is physiologically required by thyroid gland to synthesize thyroid hormones, such as thyroxin and triiodothyronine, which are required for several normal metabolic processes.[2] The roles of thyroid hormones include the control of growth, development, and some metabolic processes in the body. These hormones affect physical and intellectual development, functioning of muscles and nerve tissues, circulatory system, regulation of body heat and energy, and the metabolism of all nutrients.[3] Thus, iodine deficiency may lead to various clinical abnormalities including mental retardation, deafness, stunted growth, and neurological problems.[4] Iodine deficiency in human nutrition results in iodine deficiency disorders (IDDs), the most well-known among them is goiter that shows an enlargement of the thyroid gland. World Health Organization reported that IDD affects around 35% of the world's population.[5] Therefore, concentrations of iodine usage need to be controlled on a daily uptake of about 180-200 μg to avoid iodine deficiency and associated disorders.[6]

The analytical method for iodine determination is tedious due to its very low concentrations in foods (few μg L^{-1} at most), and losses also occur due to its high volatility. Therefore, the determination of iodine in food has been a big challenge since a long time.[7] The analytical methods that have been used for the determination of iodine in food samples include mid-infrared (IR) or 1H nuclear magnetic resonance (NMR) spectroscopy,[8] the classic Sandell and Kolthoff kinetic-catalytic method,[9] neutron activation analysis,[10] kinetic spectrophotometry,[11] chemiluminescence,[12] X-ray fluorescence,[13] energy-dispersive X-ray fluorescence spectrometry (EDXRF), electrospray ionization tandem mass spectrometry,[14] inductively coupled plasma optical emission spectrometry (ICP OES),[13] and amperometry.[15] In addition, iodine is not stable in acidic media that may result in low recovery.[16] The determination of iodine in food samples is mostly

*e-mail: sakcha2@kku.ac.th

based on alkaline extraction such as by ammonia solution and tetramethyl ammonium hydroxide (TMAH), which is a toxic substance and poses a serious risk to human health. Therefore, it is highly desirable to conduct TMAH extraction at high temperatures (90 °C).[17-19] The extraction at high temperatures may cause changes in quality and lead to iodine loss, resulting in low extraction efficiency. The disadvantages of the existing extraction methods, such as high temperature, high energy consumption (more than 10% of the total energy required by the process), and the use of harmful chemicals, have forced the food and chemical industries to find environmental-friendly techniques such as ultrasound extraction. The ultrasonic technique has been applied for the extraction of some biological compounds.[20-23] It can be used either as a diagnostic tool or as a source of energy. Ultrasonic treatments are considered efficient for shorter extraction time and lower liquid-solid ratios by increasing the mass transfer rate.[24,25] Thus, it is necessary to find out the green alternatives, efficient and simple methods for iodine extraction from food samples.

The aim of this study was to improve the extraction method for the trace amounts of iodine using ultrasonic-assisted extraction (UAE) with either deionized water or 3% (v/v) ammonia solution. The green extraction method was applied in association with UAE followed by ICP OES for a rapid determination of iodine in food samples.

Experimental

Instruments

The measurement of iodine was carried out with a PerkinElmer (Wellesley, USA) model OPTIMA 2100 DV inductively coupled plasma optical emission spectrometer using a standard ICP torch, axially viewed plasma system and a peristaltic pump. The entire system is controlled by the PE Winlab software. The plasma viewing mode and instrumental condition used are presented in Table 1.

Chemicals

All aqueous solutions were prepared with deionized water (with a resistivity of 18.2 MΩ cm^{-1}; Milli Q Millipore) using a simplicity water purification system, Model Simplicity 185 (Millipore Corporation, USA). An iodine stock solution of 1000 mg mL^{-1} was prepared from potassium iodide (KI; Carlo Erba, France) with deionized water. Because iodide is sensitive to light, its exposure to light was minimized. The stock solution was used to prepare all standard solutions on a daily basis. A series of the calibration solutions (iodide concentrations of 0.1, 0.5, 1.0, 5.0, and 10.0 mg L^{-1}) were made from KI. Ammonia solution with 3% (v/v) was prepared by diluting 10 mL of concentrated ammonia solution (analytical grade was obtained from Carlo Erba, Milan, Italy) with 100 mL of deionized water.

Table 1. Working conditions and parameters of ICP OES spectrometer

Analytical emission line / nm	182.976
Vision (plasma view)	axial
RF power / W	1300
Peristaltic pump flow rate / (mL min^{-1})	1.5
Plasma flow rate / (L min^{-1})	15.0
Auxiliary flow rate / (L min^{-1})	0.20
Nebulizer flow rate / (L min^{-1})	0.8
Nebulizer/spray chamber	sea spray/gas cyclonic
Purge	normal
Resolution	normal
Replicate read time / s	20
Sample uptake delay time / s	14
Wash time / s	1
Number of replicate	3

Sample preparation

The representative iodine samples that include table salts, seaweeds, dried seafoods, rice porridge, seasoning powder, seasoned crispy, and milk were purchased from the convenient retail stores in Khon Kaen City, Thailand. In particular, tomato and chili samples used in this study were obtained from the cultivar areas of Department of Plant Science and Agricultural Resources, Faculty of Agriculture, Khon Kaen University, Thailand. The local names of the six varieties of tomato used are Seeda, Mani Siam, Tor, Black Cherry Kham Kaen, Mo Kho 40, and Phuang, whereas those of five varieties of chili pepper are Akkhani Phirot, Mokho 2, Thapthim Mo Dindaeng, Som, and Ratchaburi. All tomato and chili fruits were washed with distilled water, cut into pieces, and homogenized. The homogenized sample was placed in the polytetrafluoroethylene (PTFE) centrifuge tube and frozen at −20 °C. Then, this frozen puree was freeze-dried (SCANVAC Centrifuge for Vacuum Concentrator Freeze-Dry, China). Further, the sample was enclosed in a container of the laboratory mill and ground into a fine powder. These materials were later stored in a freezer at −20 °C until further analysis. Seaweeds, dried seafoods, rice porridge, seasoning powder, and seasoned crispy were ground in a kitchen grinder (Philips, Indonesia) to pass a 100 mesh sieve and analyzed as soon as they were

brought to the laboratory. Otherwise, they were stored in plastic bottles and kept in a desiccator until analysis.

Ultrasound-assisted extraction

Approximately 0.1 g of the sample was accurately weighed and extracted with 10 mL of two kinds of the extraction solvent (deionized water and 3% (v/v) ammonia solution) by an ultrasonic-assisted extraction method (Sonorex Digitec DT 510 H, Bandelin, Germany) for different extraction times (1, 5, 10, and 15 min) under a controlled temperature of about 35 °C under the protection from light using a commercial foil. The clear extract in the supernatant was immediately analyzed by ICP OES after centrifugation at 5000 rpm (Compact Centrifuge Z 206A, Germany).

Method accuracy evaluation

For a spiked iodine solution, a stock solution (1000 mg L^{-1} iodide) was used to obtain working concentrations. To measure the recovery of iodine from real food samples and to determine the effect of cellular matrix of the sample materials, an optimal condition was chosen and applied by spiking with a standard iodide solution (5 mg L^{-1}) to the samples before ultrasound-assisted extraction. However, only deionized water was ultimately selected as an extraction solvent for the tomatoes, chili peppers, and other food samples. The certified reference material analysis was carried out by weighing 0.1 g of material sample in triplicate followed by the same procedure.

Linearity

The iodine standard solutions (0.1, 0.5, 1, 5, 10, 15, 20, 25, 50, 100, and 200 mg L^{-1}) were used to draw a calibration curve. In order to ensure accuracy, the iodine concentrations of all the analyzed samples were required to fall within the range of the calibration curve. Otherwise, the sample extracts were diluted.

Results and Discussion

Merits of the proposed method

The analytical characteristics of the proposed method were validated under the optimized conditions in terms of linearity, limit of detection (LOD), limit of quantification (LOQ), and precision (expressed as the relative standard deviation (RSD) of the slope of the calibration curve obtained from both intra-day and inter-day analyses) to estimate the efficiency and feasibility of the method using table salts, vegetables, and food products and samples. The results thus obtained are presented in Table 2. A linear calibration curve was obtained by titrating an iodine solution of 0.1 mg L^{-1} to 200 mg L^{-1} ($r^2 > 0.9994$). The equation of the linear calibration curve can be expressed as $y = 690.47x - 53.895$, where y is the analytical signal and x is the concentration of iodine (mg L^{-1}). The limit of detection and limit of quantification calculated for three and ten times standard deviation of an analytical signal of 10 reagent blanks divided by the slope of the standard calibration curve were found to be 0.049 and 0.164 mg L^{-1}, respectively. The LOD was lower than that reported previously (0.280 mg L^{-1}).[26] Precision, expressed as RSD of the slope of the calibration curve, was evaluated in terms of repeatability (data were taken from five independent standard preparations, intra-day RSD) and reproducibility (work performed for five consecutive days, inter-day RSD) and found to be 2.75 and 4.54%, respectively, indicating an acceptable repeatability of the method.

Table 2. Analytical characteristics of UAE-ICP OES for determination of iodine

Analytical parameter	Corresponding range/value
Linear range / (mg L^{-1})	0.1-200
Calibration curve	0.1-30
Linear equation	$y = 690.47x - 53.895$
Correlation coefficient (R^2)	0.9994
Limit of detection (n = 10) / (mg L^{-1})	0.049
Limit of quantification (n = 10) / (mg L^{-1})	0.164
RSD for intra-day analysis (n = 5) / %	2.75
RSD for inter-day analysis (n = 5) / %	4.54

RSD: Relative standard deviation.

Ultrasound-assisted extraction optimization

To optimize the extraction efficiency, following factors were studied. First of all, the effect of ammonia concentration on the extraction of iodine was studied. The iodide solutions (5 mg L^{-1}) with varying ammonia solutions (1-4%, v/v) were tested for an extraction time of 5 min. The results showed that the recovery of iodine increased from about 80 to 100% when extracted with 1-3% NH_3 solution, and then slightly decreased at 4% NH_3 solution (Figure 1). Therefore, in this case, 3% (v/v) NH_3 solution could be chosen as the extraction solvent. However, when deionized water was used as background solvent, the recovery of iodine was found to be better than those of ammonia solutions. The results are presented in

Figure 2. The effect of different extraction times on the iodine extraction was also investigated. The recovery of iodine using deionized water as an extraction solvent was found consistently around 100% for the extraction times of 5 and 15 min, whereas that of 3% NH_3 solution was lower with varying extraction times. The long extraction time with this basic solution may increase volatility of iodine. Thus, we obtained deionized water as solvent and 5 min extraction time as the best condition for iodine extraction.

Therefore, only deionized water was chosen for the green extraction (nontoxic) using an ultrasound-assisted method. The recoveries of the real tomato sample under the extraction conditions were found to be 103.5 ± 2.7% and 117.2 ± 4.4% using deionized water and 3% (v/v) ammonium hydroxide solution, respectively.

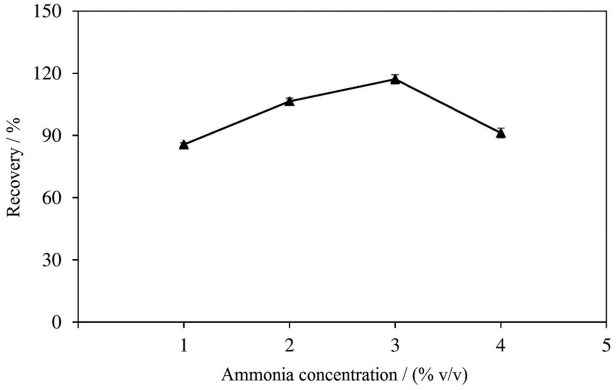

Figure 1. The effect of ammonia concentration on the extraction recovery of iodide in the tomato sample. Conditions: sample mass, 0.1 g; iodide concentration, 5 mg L^{-1}; volume of the extraction solvent, 10 mL; extraction time, 5 min.

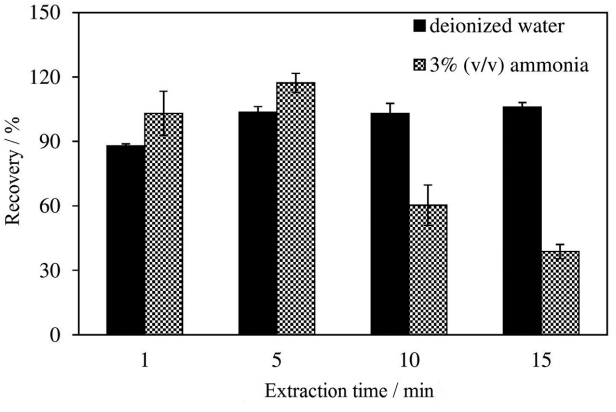

Figure 2. The effect of extraction time on the recovery of iodine in the tomato sample using both deionized water and 3% (v/v) ammonia solution. Conditions: sample mass, 0.1 g; iodide concentration, 5 mg L^{-1}; volume of the extraction solvent, 10 mL.

Ultrasound-assisted extraction mechanism

The ultrasound-assisted extraction (UAE) of the target compounds for a given matrix is a complex mechanism that involves mass transfer and a variety of possible chemical reactions influencing the yield and associated biological activities. In general, the effect of sonication on mass transfer shows a direct relationship with the sound energy introduced in the extraction system and the ultrasonic frequency.[27] UAE in food products is applied for the extraction of organic and inorganic compounds because this provides improved solvent penetration into the plant body and can also break down cell walls. A review of the literature[28] suggests that combinations of various physical, mechanical, chemical, and biochemical processes take place during the application of ultrasound in chemical processing and extraction processes. The mechanism of UAE using a solvent and a solid matrix can be summarized as follows:

(*i*) using ultrasonic waves, a cavitation bubble can be generated close to the material surface;

(*ii*) during a compression cycle, this bubble collapses and a microjet directing toward the plant matrix is created;

(*iii*) the high pressure and temperature applied in this process destroy the cell walls or damage the surface at solvent-matrix interfaces by shock waves and microjets, and its contents or analytes are released into the extraction buffer or solvent.

This is a very effective technique for the extraction of natural products from a biomass. As a consequence, the method of UAE has a number of advantages that include increased mass transfer, better solvent penetration, less dependence on solvent use, extraction at lower temperatures, faster extraction rates, and greater yields of the product.[29]

Working concentration of iodine

The concentration of iodine also has a significant effect on its sensitivity. Figure 3 shows the effect of spiked iodine concentrations using both extraction solvents, which ranges between 1 and 20 mg L^{-1}, resulting in similar recoveries in the range of 90.5-114.0%. However, the iodine concentration of 5 mg L^{-1} was selected for further experiments.

Iodine contents in real samples and recovery

The accuracy of the proposed method was evaluated by analyzing the certified reference materials (NIST SRM 1549 Non-Fat Milk Powder, NIST SRM 1573a Tomato Leaves, and NIES No. 9 Sargasso). The results are presented in Table 3. A comparison between the certified and the obtained concentration values was statistically nonsignificant. It was concluded that the presented

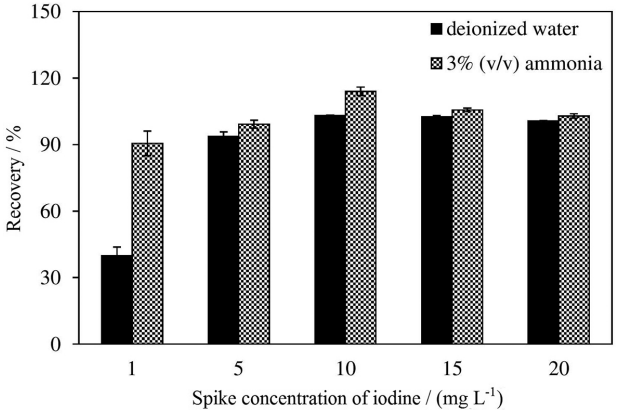

Figure 3. The effect of spiked iodine concentrations on the tomato sample using both deionized water and 3% (v/v) ammonia solution. Conditions: sample mass, 0.1 g; volume of the extraction solvent, 10 mL; extraction time, 5 min.

extraction method can be successfully applied to food samples.

To demonstrate the applicability and reliability of the proposed method, it was successfully applied to 47 samples of food products including salt, seaweed, dried seafood, tomato fruit, chili fruit, milk powder, rice porridge, seasoning powder, and seasoned crispy. Table 4 shows both iodine contents and their recoveries. Salt samples contain rather higher amounts of iodine (40.93-58.77 mg kg^{-1}), which are in good agreement with those previously reported.[30,31] Iodine in seaweeds was found from a non-detectable (n.d.) value to 20.30 mg kg^{-1}, whereas there was a wide range of 16-8,165 mg kg^{-1} iodine depending on the type of the samples.[32,33] Dried seafoods' iodine contents are also contained at trace levels (0.85-6.18 mg kg^{-1}). Milk powder (1.27 mg kg^{-1}) could be supplemented with iodine, whereas some were found between 0.07 and 13.07 mg kg^{-1}.[31] Rice porridge (0.19-2.12 mg kg^{-1}), seasoning powder (0.52-4.29 mg kg^{-1}), and seasoned crispy were unavoidably examined for being commercially available food products. In particular, iodine was not detectable in tomatoes and chili fruits, even in a background amount, probably because of its low detection limit (0.05 mg L^{-1}). Moreover, to test the accuracy and evaluate the effect of the matrix by the green extraction method, the recovery study of all used samples was conducted along with their iodine contents. Each sample was spiked with a concentration (5 mg L^{-1}) of the standard solution of iodide. Then, the relative percentage recoveries were calculated as follows:

$$\% \text{ Recovery} = [(C_{found} - C_{real}) / C_{added}] \times 100 \quad (1)$$

where C_{found}, C_{real}, and C_{added} are the concentration of analyte after the addition of the known amount of the standard in the real sample, the concentration of analyte in the real sample, and the concentration of the known amount of the standard that was spiked in the real sample, respectively.

From the results (Table 4), it can be observed that the recoveries by the proposed method, which are expressed as the mean percentage (n = 3), vary between 80.48 and 118.1%. They are rather found in wide range probably due to the sample matrices, but some are satisfactorily close to 80% observed for several samples (brand 2 of seaweed, Mokho 2 of chili fruits, etc.), however, the I_2 that could be formed by sonication is easily volatile and lost during the sample preparation, leading to low recovery study.[34] This demonstrates that this method provides acceptable recovery (> 80%) for the determination of iodine in real samples and implies that the matrix has a negligible effect on the efficiency of the proposed method. Therefore, the adopted procedure demonstrated that using deionized water as an extraction solvent with ultrasound-assisted extraction for 5 min could be considered as simple, fast, and green extraction conditions in association with ICP OES.

By the way, this UAE method for iodine in various samples was compared with other sample extraction ones in terms of the sample preparation method, type of solvent, extraction time and recovery (Table 5). The accuracy of the method was well lined out within the generally acceptable range. In addition, the proposed method is superior to the others in terms of using green solvent, short extraction time and simple procedure. Therefore, it can be used as an alternative technique to the other complicated extraction methods for analysis of iodine in real samples.

Conclusion

In this study, a new approach for trace iodine extraction based on ultrasound-assisted extraction is proposed. It is a fast (with an extraction time of only 5 min), simple, and safe method, and therefore can be called a green

Table 3. The results for certified reference materials (μg g^{-1}) for the determination of iodine

Element	NIST SRM 1549 Non-fat milk powder		NIST SRM 1573a Tomato leaves		NIES No. 9 Sargasso	
	Certified value	Our value	Certified value	Our value	Certified value	Our value
Iodine	3.38	3.30 ± 0.05[a]	0.85	0.83 ± 0.02[a]	520	519.66 ± 2.11[a]

[a]Measured in triplicate (n = 3) ± standard deviation (SD).

Table 4. The iodine contents and its recovery from salts, vegetables, and other food products

Sample	Content ± SD[a] / (mg kg^{-1})	Recovery / %
Salt		
Brand 1	46.06 ± 3.93	99.37
Brand 2	53.54 ± 6.59	99.21
Brand 3	40.93 ± 3.69	83.73
Brand 4	52.13 ± 9.93	105.7
Brand 5	58.77 ± 2.23	95.51
Seaweed		
Brand 1	13.39 ± 1.78	96.74
Brand 2	5.85 ± 0.05	80.48
Brand 3	10.74 ± 0.57	96.06
Brand 4	15.60 ± 1.65	92.71
Brand 5	20.30 ± 2.61	91.96
Brand 6	9.74 ± 0.04	85.74
Brand 7	n.d.	99.23
Brand 8	7.39 ± 1.92	92.13
Dried Seafood		
Minnow (*Parachela oxygastroides*)	3.65 ± 0.44	102.7
Dried shrimp (*Penaeus* sp.)	1.16 ± 0.11	114.4
Splendid squid (*Loligo duvauceli*)	2.07 ± 0.22	103.0
Splendid Squid Middle (*Teuthida*)	1.91 ± 0.36	87.01
Blue eye Rice fish (*Oryzias Minutillus*)	6.18 ± 0.18	98.01
Octopus (*Coleoidea*)	0.85 ± 0.11	85.60
Tomato fruits		
Seeda	n.d.	93.66
Mani Siam	n.d.	102.6
Tor	n.d.	101.2
Black Cherry Kham Kaen	n.d.	110.2
Mo Kho 40	n.d.	105.0
Phuang	n.d.	103.9
Chili fruits		
Akkhani Phirot	n.d.	93.30
Mokho 2	n.d.	82.57
Thapthim Mo Dindaeng	n.d.	84.81
Som	n.d.	91.14
Ratchaburi	n.d.	87.42
Milk powder	1.27 ± 0.08	82.02
Rice porridge		
Brand 1	0.19 ± 0.01	93.67
Brand 2	2.12 ± 0.23	97.75
Brand 3	1.47 ± 0.50	102.2
Brand 4	0.16 ± 0.02	98.62
Brand 5	1.37 ± 0.18	112.5
Brand 6	0.64 ± 0.07	110.5
Seasoning powder		
Brand 1	2.94 ± 0.90	99.24
Brand 2	4.26 ± 0.01	93.14
Brand 3	2.89 ± 0.21	118.1
Brand 4	2.89 ± 0.20	88.43
Brand 5	0.83 ± 0.13	96.86
Brand 6	0.52 ± 0.10	98.43
Brand 7	4.29 ± 0.05	106.6
Seasoned crispy		
Brand 1	n.d.	111.3
Brand 2	n.d.	100.9
Brand 3	n.d.	81.69

[a]Measured in triplicate (n = 3) ± standard deviation (SD); n.d.: not detectable.

Table 5. Comparison of ultrasound-assisted extraction with other extraction techniques for the determination of the iodine

Sample	Sample preparation	Solvent	Extraction time	Recovery / %	Reference
Leaves of spinach	incubation (90 °C)	25% TMAH	3 h	89.3	35
Vegetable oils	magnetic stirrer	99% ethanol	5 min	–	36
Milk	water bath (40 °C)	3% acetic acid	5 min	87-14	37
Milk whey proteins	microwave	25 mmol L^{-1} NH_4OH	25 min	105	26
Oil	microwave	HNO_3	20 min	–	38
Food	microwave	HNO_3 and H_2O_2	–	85-95	39
Coal	microwave	HNO_3, H_2O_2 and $S_2O_8^{2-}$	–	82-120	40
Food	ultrasound	deionized water	5 min	80.48-118.1	this work

extraction method. This method using only deionized water as extraction solvent was applied for the analysis of the trace amounts of iodine in table salts, tomatoes, chili, and different kinds of other food samples. This method resulted in high iodine recoveries from all samples. Although both the limit of detection and the limit of quantification were lower than 0.2 mg L^{-1}, the amount of iodine in some vegetables could not be detected, indicating that the background residual contents of iodine in these vegetables are quite low for daily food consumption. In summary, our method can effectively be used for the detection of trace levels of iodine in different food products.

Acknowledgments

The authors would like to thank the Higher Education Research Promotion and National Research University Project of Thailand, Office of the Higher Education

Commission, through the Food and Functional Food Research Cluster of Khon Kaen University, Materials Chemistry Research Center, Department of Chemistry, Center of Excellence for Innovation in Chemistry (PERCH-CIC), Thailand, for financial support.

References

1. Rana, R.; Raghuvanshi, R. S.; *J. Food Sci. Technol.* **2013**, *50*, 1212.
2. Haldimann, M.; Alt, A.; Blanc, A.; Blondeau, K.; *Food Compos. Anal.* **2005**, *18*, 461.
3. Erkan, N.; *Int. J. Food Sci. Technol.* **2011**, *46*, 1734.
4. Waszkowiak, K.; Szymandera-Buszka, K.; *Int. J. Food Sci. Technol.* **2008**, *43*, 895.
5. Anderson, M.; Takkouche, B.; Egli, I.; Allen, H. E.; de Benoist, B.; *Bull. W. H. O.* **2005**, *83*, 518.
6. Pop, F.; *Int. J. Food Sci. Technol.* **2010**, *45*, 327.
7. Heckman, M. M.; *J.- Assoc. Off. Anal. Chem*. **1979**, *62*, 1045.
8. Shimamoto, G. G.; Favaro, M. M. A.; Tubino, M.; *J. Braz. Chem. Soc*. **2015**, *26*, 1431.
9. Gasior, R.; Szczypula, M.; Szybinski, Z.; *Ann. Anim. Sci.* **2013**, *13*, 375.
10. El-Ghawi, U. M.; Al-Sadeq, A. A.; *Biol. Trace Elem. Res.* **2006**, *111*, 31.
11. Ni, Y.; Wang, Y.; *Microchem. J.* **2007**, *86*, 216.
12. Fujiwara, T.; Mohammadzai, I. U.; Inoue, H.; Kumamaru, T.; *Analyst* **2000**, *125*, 759.
13. Varga, I.; *Microchem. J.* **2007**, *85*, 127.
14. Minakata, K.; Yamagishi, I.; Kanno, S.; Nozawa, H.; Suzuki, M.; Suzuki, O.; *J. Chromatogr. B* **2010**, *878*, 1683.
15. Souza, F. C.; Da Silva, D. A. I.; Ribeiro, M. S.; Faria, R. B.; Melo, M. A.; Toledo, R. M. M.; D'Elia, E.; *J. Braz. Chem. Soc*. **2013**, *24*, 1582.
16. Julshamn, K.; Dahl, L.; Eckhoff, K.; *J. AOAC Int.* **2001**, *84*, 1976.
17. Fecher, P. A.; Goldmann, I.; Nagengast, A.; *J. Anal. At. Spectrom.* **1998**, *13*, 977.
18. Niedobová, E.; MacHát, J.; Kanický, V.; Otruba, V.; *Microchim. Acta* **2005**, *50*, 103.
19. Tagami, K.; Uchida, S.; Hirai, I.; Tsukada, H.; Takeda, H.; *Anal. Chim. Acta* **2006**, *570*, 88.
20. Perlatti, B.; Fernandes, J. B.; Silva, M. F. G. F.; Ardila, J. A.; Carneiro, R. L.; Souza, B. H. S.; Costa, E. N.; Eduardo, W. I.; Boiça Junior, A. L.; Forim, M. R.; *J. Braz. Chem. Soc*. **2016**, *27*, 475.
21. Dong, J.; Cai, L.; Zhu, X.; Huang, X.; Yin, T.; Fang, H.; Ding, Z.; *J. Braz. Chem. Soc*. **2014**, *25*, 1956.
22. Santos, O. O.; Montanher, P. F.; Bonafé, E. G.; Do Prado, I. N.; Maruyama, S. A.; Matsushita, M.; Visentainer, J. V.; *J. Braz. Chem. Soc*. **2014**, *25*, 1712.
23. Gasmalla, M. A.; Yang, R.; Hua, X.; *J. Food Sci. Technol.* **2015**, *52*, 5946.
24. Kim, Y. U.; Wang, M. C.; *Ultrasonics* **2003**, *41*, 539.
25. Kumcuoglu, S.; Yilmaz, T.; Tavman, S.; *J. Food Sci. Technol.* **2014**, *51*, 4102.
26. Naozuka, J.; da Veiga, M. A. M. S.; Oliveira, P. V.; de Oliveira, E.; *J. Anal. At. Spectrom.* **2003**, *18*, 917.
27. Albero, B.; Sánchez-Brunete, C.; García-Valcárcel, A. I.; Pérez, R. A.; Tadeo, J. L.; *TrAC, Trends Anal. Chem.* **2015**, *71*, 110.
28. Picó, Y.; *TrAC, Trends Anal. Chem.* **2013**, *43*, 84.
29. Tiwari, B. K.; *TrAC, Trends Anal. Chem.* **2015**, *71*, 100.
30. Dasgupta, P. K.; Liu, Y.; Dyke, J. V.; *Environ. Sci. Technol.* **2008**, *42*, 1315.
31. Barikmo, I.; Henjum, S.; Dahl, L.; Oshaug, A.; Torheim, L. E.; *J. Food Compos. Anal.* **2011**, *24*, 637.
32. Teas, J.; Pino, S.; Critchley, A.; Braverman, L. E.; *Thyroid* **2004**, *14*, 836.
33. Romarís-Hortas, V.; Moreda-Piñeiro, A.; Bermejo-Barrera, P.; *Talanta* **2009**, *79*, 947.
34. Nascentes, C. C.; Korn, M.; Sousa, C. S.; Arruda, M. A. Z.; J. Braz. Chem. Soc. 2001, 12, 57.
35. da Silva, S. V.; Picoloto, R. S.; Flores, E. M. M.; Wagner, R.; Richards, N. S. P. S.; Barin, J. S.; *Food Chem.* **2016**, *190*, 364.
36. Shimamoto, G. G.; Aricetti, J. A.; Tubino, M.; *Food Anal. Methods* **2016**, DOI 10.1007/s12161-016-0401-1.
37. Lu, H.; Wei1, C.; Fu, H.; Li, X.; Zhang, Q.; Wang, J.; *J. Am. Oil Chem. Soc.* **2015**, *92*, 1549.
38. Smoleń, S.; Strzetelski, P.; Rożek, S.; Ledwożyw-Smoleń, I.; *Acta Sci. Pol., Hortorum Cultus* **2011**, *10*, 29.
39. Melichercik, J.; Szijarto, L.; Hill, A. R.; *J. Dairy Res.* **2006**, *89*, 934.
40. Sun, M.; Gao, Y.; Wei, B.; Wu, X.; *Talanta* **2010**, *81*, 473.

Submitted: May 25, 2016
Published online: June 28, 2016

Scientia Horticulturae 220 (2017) 20–26

Contents lists available at ScienceDirect

Scientia Horticulturae

journal homepage: www.elsevier.com/locate/scihorti

Inheritance analysis of anthracnose resistance and marker-assisted selection in introgression populations of chili (*Capsicum annuum* L.)

Patcharaporn Suwor[a], Jirawat Sanitchon[a], Petcharat Thummabenjapone[b], Sanjeet Kumar[c], Suchila Techawongstien[a,*]

[a] Plant Breeding Research Center for Sustainable Agriculture, Faculty of Agriculture, Khon Kaen University, Khon Kaen 40002, Thailand
[b] Plant Pathology Section, Faculty of Agriculture, Khon Kaen University, Khon Kaen 40002, Thailand
[c] World Vegetable Center, P.O. Box 42, Shanhua, Tainan 74199, Taiwan

ARTICLE INFO

Article history:
Received 13 January 2017
Received in revised form 20 March 2017
Accepted 22 March 2017
Available online 31 March 2017

Keywords:
Colletotrichum
Disease resistance
Genetic analysis
Marker efficacy
Phenotype selection

ABSTRACT

Two *Capsicum annuum* anthracnose resistant introgression lines P_{R1} (derived from PBC932*C. chinense*) and P_{R2} (derived from PBC80*C. baccatum*) with resistance conferred by different sources were crossed to a susceptible parent (P_S) and F_1, F_2, BC_1P_S, BC_1P_R and F_2 of a three-way populations were generated. Fruits of the populations were inoculated with *Colletotrichum acutatum*-Ca153 using microinjection method at the mature green stage. The SCAR-Indel and SSR-HpmsE032 markers were used for validation in all populations derived from P_{R1} and P_{R2}, respectively. In both resistance sources (P_{R1} and P_{R2}), resistance was controlled by a major recessive gene. The resistant banding pattern amplified by SCAR-Indel and SSR-HpmsE032 markers was 100 bp and 231 bp fragments, respectively. Validation studies of both markers in F_2 populations revealed that individually their ability to correctly predict resistant genotypes (selection efficiency) was 65%. However, when both markers were used together, the selection efficiency increased to 77% as well as the efficacy of individual SSR marker used within F_2 of the three-way populations.

1. Introduction

Anthracnose caused by *Colletotrichum* sp. is a serious disease for chili pepper (*Capsicum* spp.) and has been reported worldwide (Tozze and Massola, 2009; Xia et al., 2011; Liao et al., 2012; Garg et al., 2013). Four species of *Colletotrichum* (*C. coccodes*, *C. truncatum, C. gloeosporioides*, and *C. acutatum*) are known to cause chili anthracnose (Than et al., 2008). In Thailand, three species (*C. truncatum, C. gloeosporioides* and *C. acutatum*) cause significant damage to chili fruits (Mongkolporn et al., 2010). However *C. acutatum* is the most predominant and aggressive species, which can infect all five *Capsicum* species at both mature green and red ripe fruit stages (Mongkolporn et al., 2010). Anthracnose lesions are sunken necrotic tissue on infected fruit, which turns brown and then black due to the formation of setae and sclerotia. Fruit rot reduces marketability and affects quality traits such as dry weight, and capsaicin and oleoresin contents (Mistry et al., 2008). Latent infection can also occur starting from the flowering to fruiting stages (Ahn and Yun, 2009), and the symptoms appear under hot and humid conditions. With that latent infection periods, the pathogen can easily survive until fruit ripening stage, if fungicide spray is delayed by 24 h after infection. (Ahn and Yun, 2009). Fungicide sprays often are washed away by unpredictable rains. Fungicides are misused by the growers leading to increasing cost of production and adversely affect human and environmental health. Host plant resistance is considered to be a more cost-effective and sustainable control measure for anthracnose (Than et al., 2008).

Anthracnose resistance sources PBC80/VI046804, PBC81/VI046805 (*C. baccatum*) and PBC932/VI047018 (*C. chinense*) identified by World Vegetable Center during the late 1990s have been extensively used to breed resistant *C. annuum* introgression lines through conventional breeding and embryo recues technique (Yoon et al., 2006; Bosland and Votava, 2012). The resistant genes in these sources have been characterized i.e., PBC932 possesses recessive genes (*co1-co3*) located on linkage group (LG) P5 (Sun et al., 2015), while PBC80 possesses recessive (*co4*) or dominant (*Co5*) genes (Mahasuk et al., 2009) located on LG12 and LG9. Recently, *C. annuum* introgression lines (called progressive lines) derived from two non-*annuum* sources (PBC932 and PBC80) have been screened against anthracnose and marker analysis confirmed that they contained different resistance loci (Suwor et al., 2015). Resistance in one introgression line derived

* Corresponding author.
E-mail addresses: suctec.kku@gmail.com, suctec@kku.ac.th (S. Techawongstien).

http://dx.doi.org/10.1016/j.scienta.2017.03.032
0304-4238/

from PBC932 was associated with Indel-SCAR marker at 100 bp (resistant locus) and 90 bp (susceptible locus), while resistance in three introgression lines derived from PBC80 was associated with HpmsE032-SSR marker at 231 bp (resistant locus) and 240 bp (susceptible locus) (Suwor et al., 2015). The understanding of inheritance of resistance in two different introgression resistant lines would be desirable. The variable mode of inheritance of anthracnose resistance has been reported, depending on the choice of resistant and susceptible parents, pathogen species and isolates, fruit maturity stages (Temiyakul et al., 2012), and inoculation methods (Mahasuk et al., 2013; Suwor et al., 2016). This highly differential inheritance patterns complicates anthracnose resistance breeding. Application of molecular markers closely linked to anthracnose resistance breeders can bypass traditional phenotype-based selection methods of selection of resistant plants through marker-assisted selection (MAS) (Farkhzadeh and Alifakheri, 2014). Molecular markers associated with major genes and quantitative trait loci (QTLs) controlling chili anthracnose resistance have been developed and mapped (Voorrips et al., 2004; Lee et al., 2010, 2011; Wang, 2011; Sun et al., 2015). As a part of ongoing efforts to improve commercial chili cultivars with enhanced levels of anthracnose resistance, in this communication, we report inheritance of anthracnose resistance in *C. annuum* introgression lines, and share progress made towards combining different resistance genes by advancing resistant seedlings through MAS.

2. Materials and methods

2.1. Plant materials, hybridization and population development

Two anthracnose resistant introgression lines were used as parents. The first parent was a *C. annuum* introgression line 0038-9155-5-1 (AVPP0207) (P_{R1}) derived from *C. chinense* PBC932 (Fig. 1). The second parent was possessing anthracnose resistance from *C. baccatum* PBC80 $BC_2F_4398\times80C5(1)8/14,2/7\text{-}31$ (P_{R2}) (Fig. 1). Both resistant parents were crossed to a susceptible parent (KKU-P31118; P_S) to study inheritance of resistance against *C. acutatum* Ca153 at the mature green fruit stage. The susceptible parent (P_S) was a highly pungent inbred line derived from landrace Perennial. Two F_1 crosses (single cross) involving a common female susceptible parent and two resistant male parents, i.e., population I ($P_S\times P_{R1}$) and populations II ($P_S\times P_{R2}$) were developed during March-October 2011 in a greenhouse at Khon Kaen University (KKU), Thailand. Backcross (backcross to susceptible parent; BC_1P_S), (backcross to resistant parent; BC_1P_R) and three-way cross generations were produced during October 2011-February 2012 at KKU (Fig. 1). For inheritance study, Randomized Complete Block Design (RCBD) with three replications was used. Ten plants of each parent and F_1, 40 F_2 plants of the single cross, and 20 plants of each backcross were used in each replication. One hundred and one seedlings of F_2 of the three-way population were selected based on homozygosity of both markers SCAR-Indel and SSR-HpmsE032 markers. All populations were grown during March-October 2012 under open field conditions at World Vegetable Center, Taiwan. Five mature green fruits were inoculated in laboratory with three replications (totally 15 fruit per plant) (phenotyping).

2.2. DNA extraction

Total DNA was extracted from the leaves using the cetyl trimethyl ammonium bromide (CTAB) method with some modifications (Suwor et al., 2015). The final concentration of the DNA was adjusted to 10 ng/μl and stored at −20 °C. Polymerase chain reaction (PCR) was performed in a thermocycler (BIO-RAD Alpha Unit Block Assembly, Mexico) in a total volume of 25 μl reaction mixture containing 1 μl genomic DNA, 10× PCR buffer, 50 μM dNTPs, 2.5 μM Mg^{2+}, 10 μM of each primer, 1 unit of Taq DNA polymerase with the final volume adjusted with dH_2O. PCR cycling conditions were 3 min at 94 °C, followed by 30 cycles of 30 s at 94 °C, 30 s at 55 °C, 60 s at 72 °C and a final extension at 72 °C for 10 min (Yi et al., 2006). PCR products were separated on 6% polyacrylamide gels, stained with ethidium bromide and visualized under ultraviolet light.

2.3. Segregation analysis of DNA markers (genotyping)

Thirty-day-old seedlings of resistant parents were genotyped. All plants of AVPP0207 (P_{R1}) were genotyped using primers for SCAR-$Indel_{100bp}$ marker and P_{R2} was genotyped using SSR-$HpmsE032_{231bp}$ marker (Table 1). Both co-dominant markers (SCAR-Indel and SSR-HpmsE032) were used to genotype F_1, F_2 and backcross seedlings and the susceptible parent (KKU-P31118) (Table 3).

At each locus, the allele from the susceptible parent (P_S) and resistant parents (P_{R1} and P_{R2}) were denoted as a single dominant gene (*RR*) and recessive gene (*rr*), respectively (Gururania et al., 2012). The expected Mendelian segregation ratio in the F_2 generation was 1:2:1 (*RR*:*Rr*:*rr*), while in BC_1P_S the expected ratio was 1:1 for *RR*:*Rr*, and in BC_1P_{R1} and BC_1P_{R2}, the expected ratio was 1:1 for *Rr*:*rr*. The observed ratio was tested for deviation from the expected ratio with a chi-square for the goodness-of-fit test ($P< 0.05$) for each marker (Table 3).

2.4. Disease inoculation and evaluation (phenotyping)

An aggressive isolate of *C. acutatum*-Ca153 isolated from pepper fruit in Taiwan was used (Liao et al., 2012). The concentration of inoculum was adjusted to 5×10^5 conidia/ml. Five mature green (approximately 35 day after anthesis) fruits per plant were evaluated in inoculation room with three replications. Wounds 1 mm in depth were created with the microinjector at two sites (top and end of the fruit; totally 10 lesions per plant) and 1.0 μl of the conidia suspension was injected into each wound (Suwor et al., 2015). The inoculated fruits were incubated at high relative humidity (95–98%) and 26 °C in a dark room. The severity of the disease was measured from the lesion size five days after inoculation (DAI). Plants with mean lesions diameter less than 4 mm were considered to be resistant; plants with mean lesions diameter more than 4 mm were classified as susceptible (Lin et al., 2007).

2.5. Estimation of the efficacy of the markers to select anthracnose-resistant plants

Co-segregation of the markers with anthracnose resistance was studied in plants of three F_2 populations, population I (tested with SCAR-Indel), population II (tested with SSR-HpmsE032), and also in the three-way population (tested with both markers). Since both markers were co-dominant, plants homozygous for both resistance and susceptible alleles were divided by the total number of resistant plants to calculate the selection efficacy percentage for each marker. Similarly, plants homozygous for susceptibility were used to calculate the selection efficacy of susceptible plants (Table 4). In addition, both markers were tested together in 1000 F_2 seedlings of the three-way population, and 101 seedlings with homozygous for the resistance alleles were classified into three groups: group A/B (homozygous for both markers), group A (homozygous only for SCAR-Indel) and group B (homozygous only for SSR-HpmsE032). These seedlings were transplanted in the field and plants were assessed for disease reaction. Selected plants were advanced.

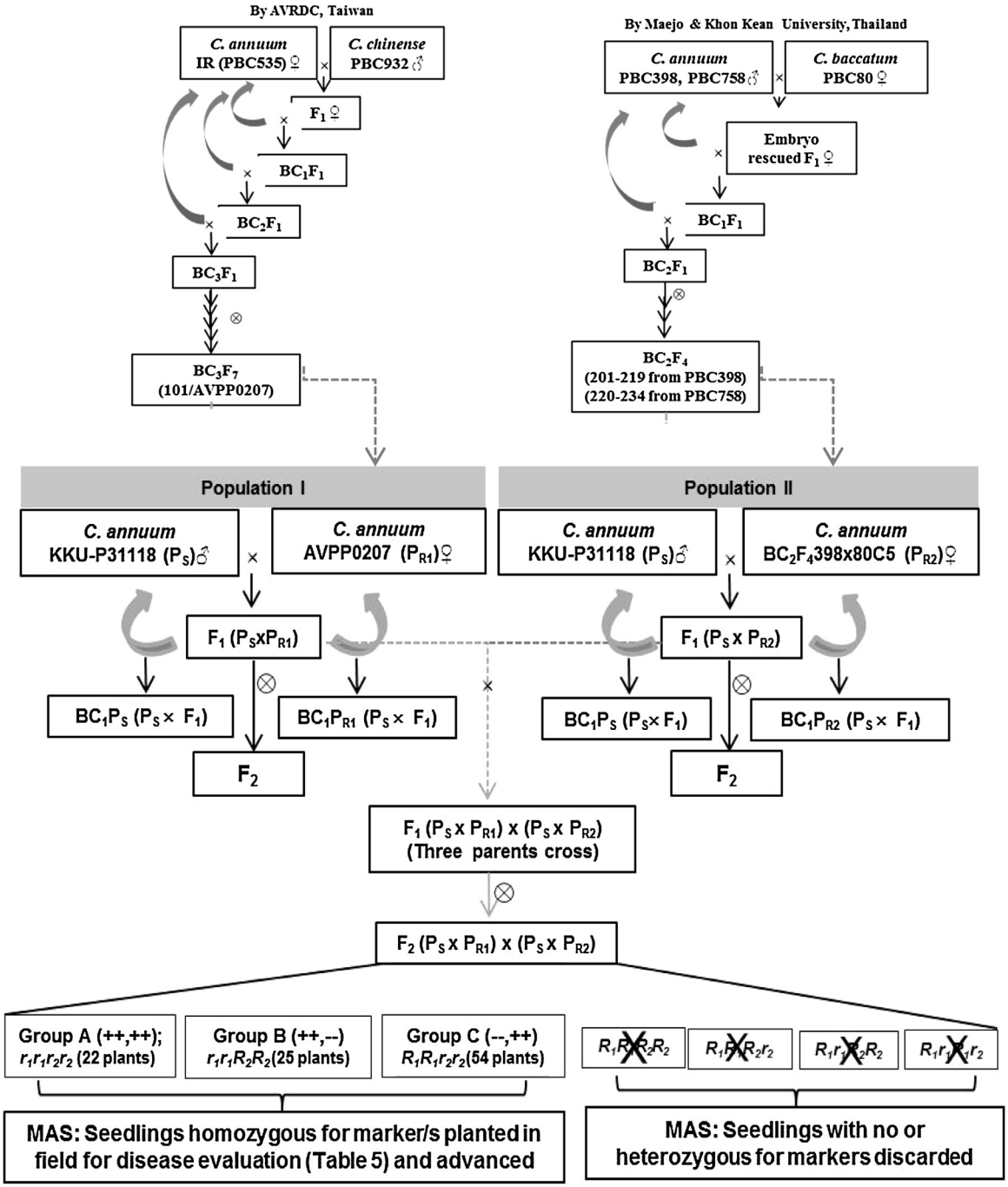

Fig. 1. Developmental description of populations and generation advancement of resistant plants possessing combined resistance from two sources through marker-assisted selection.

Table 1
Sequence-characterized amplified region (SCAR) and simple sequence repeat (SSR) markers associated with anthracnose resistance used in this study.

Marker	Position	Product sizeand sources[a]	Primer sequence	References
SCAR-Indel	P.5	100 bp (R) (AVPP0207 &P_{R1}) 90 bp (S) (AVPP9905 &P_S)	F: GGTATCTTATTTCATAGGGACCAGGCA R:TTTGCGGTAGTGACAACAACTTTACAGCCA	Wang (2011), Suwor et al. (2015)
SSR-HpmsE032	LG12	231 bp (R) (PBC81 & P_{R2}) 240 bp (S) (SP26 & P_S)	F: ATGCGCAAAGGGAGAAAATTCA R: CGAACTAACCGTTCATGGTGGA	Lee et al. (2010), Suwor et al. (2015)

[a] R = resistant variety (parent), S = susceptible variety (parent).

2.6. Statistical analysis for phenotype segregation

The chi-square for goodness-of-fit was used to test agreement between the observed ratio of resistant (R) and susceptible (S) plants in each population. The hypothesis was expected ratio based on the monogenic recessive control of anthracnose resistance. The ratio of 1R:3S of F_2 population, 1R:1S of BC_1P_{R1} and 0R:1S of BC_1P_S were tested using chi-squared (χ^2) values. The χ^2 values were cal-

Table 2
Lesion diameter on mature green fruit of three parents, two single crosses and one three-way population after inoculation with *Colletotrichum acutatum*- Ca153.

Parents[a] and population	Lesion diameter (mm)[b] Mean ± SD
Population I	
P_S (KKU-P31118)	12.81 ± 1.70
P_{R1} (AVPP0207)	1.86 ± 1.06
F_1 ($P_S \times P_{R1}$)	8.27 ± 1.32
Mid-parent	7.33
Population II	
P_S (KKU-P31118)	12.81 ± 1.70
P_{R2} ($BC_2F_4398\times80C_5(1)8/14,17/17\text{-}13$)	1.00 ± 0.00
F_1 ($P_S \times P_{R2}$)	4.52 ± 4.01
Mid-parent	6.90
Three-way population	
F_1 ($P_S \times P_{R1}$) × ($P_S \times P_{R2}$)	10.31 ± 7.80

[a] P_S: susceptible parent, P_{R1}: resistant parent derived from PBC932, P_{R2}: resistant parent derived from PBC80.
[b] Mean ± Standard deviation (SD).

culated for phenotypic and genotypic ratio by using the following formula: Σ (O-E)^2/E, where, Σ-Summation, O and E are observed and expected value, respectively, with 1° of freedom. The significance level was established at $P < 0.05$.

3. Results

The susceptible parent (KKU-P31118) had the greatest mean lesion diameter (12.81 mm), while two resistant parents, P_{R1} and P_{R2}, had smaller mean lesion diameters of 1.86 and 1.00 mm, respectively (Table 2). The F_1 plants of crosses $P_S \times P_{R1}$ and $P_S \times P_{R2}$ were susceptible, with mean lesion diameters of 8.27 and 4.52, respectively. The average lesion diameter of the three-way population was 10.31 mm, thus it was classified as susceptible (Table 2).

3.1. Segregation of anthracnose resistance (phenotypic segregation)

Table 3 provides different disease segregating data of genetic resistant sources derived from PBC80 and PBC 932. The plants in the population I ($P_S \times P_{R1}$), the resistant parent (AVPP0207) showed resistance and all plants of the susceptible parent (KKU-P31118) and F_1 plants showed susceptibility. The F_2 plants segregated into 17 resistant (R) and 85 susceptible (S) plants, which is not fit to theoretical ratio 1R:3S with a chi-squared value of 3.77 (χ^2) with probability (*P*-value) of 0.05. In the BC_1P_S generation, all 56 plants were susceptible, while there were 29 resistant and 26 susceptible plants in the BC_1P_{R1} generation, which was a good fit to 1R:1S ($\chi^2 = 0.163$, $P = 0.68$), as it was in the F_2 generation. Segregation of resistant and susceptible plants in the F_2 generation of the cross $P_S \times P_{R2}$ (populationII) was 34R to 73S with the χ^2 and *P*-value of 2.61 and 0.11 respectively. The segregation ratio in a BC_1P_{R2} generation was 25R:16S—a good fit to the expected segregation ratio 1R:1S. However, in BC_1P_S, the population segregation ratio was 4R:48S, which was not exceptional deviation from the expected 0R:1S ratio or this locus is not controlled by one single gene.

3.2. Segregation of the markers SCAR-Indel and SSR-HpmsE032 (genotypic segregation)

The distribution of both co-dominant markers was examined in the segregating generation. SCAR-Indel primers amplified 100 bp fragments in the resistant parent (AVPP0207; P_{R1}) and 90 bp fragments in the susceptible parent (KKU-P31118; P_S), while SSR-HpmsE032 primers amplified 231 bp fragments in the resistant parent (P_{R2}) and 240 bp fragments in the susceptible parent (P_S) (Table 3, Fig. 2). Segregation analysis of the SCAR-Indel marker in 119 F_2 seedlings of population I was expected ratio for a single locus 1:2:1 (90 bp:90/100 bp:100 bp) as the observed ratio in the seedlings was 28:63:28 ($\chi^2 = 0.41$, $P = 0.81$). In BC_1P_{R1} and BC_1P_S generations, the observed segregation of the marker was 31:28 (90/100 bp:100 bp) and 27:30 (90 bp:90/100 bp), respectively. Both segregation ratios were in agreement with the expected 1:1 ratio for a single locus (Table 3, Fig. 2). Segregation of the SSR-HpmsE032 marker in F_2 progenies of the 231 bp:231/240 bp:240 bp bands was 35:62:23, which was in accordance with the expected ratio of 1:2:1 ($\chi^2 = 2.53$, *P*-value 0.28). The segregation ratio of 231/240 bp:231 bp in BC_1P_{R2} progenies was 26:34; in the BCP_S progenies, 240 bp and 231/240 bp fragments segregated in 17 and 36 plants, respectively (Table 3, Fig. 2).

Table 3
Phenotypic (disease reactions) and genotypic (markers) segregation and test for goodness of fit based on monogenic recessive control of resistance.

Population	Distribution of genotypes or markers (number of plants)					Distribution of phenotypes or disease reactions (number of plants)			
	Expected ratio[a]	Observed number			Chi-square	Expected ratio	Observed Number[b]		Chi-square
	RR:Rr:rr	*RR*	*Rr*	*rr*	χ_i^2(P)	R : S	R	S	χ_i^2(P)
Population I (SCAR-Indel)									
P_S	–	10	0	0	–	–	0	10	–
P_{R1}	–	0	0	10	–	–	10	0	–
F_1 ($P_S \times P_{R1}$)	–	0	10	0	–	–	0	10	–
F_2	1:2:1	28	63	28	0.41 (0.81)	1:3	17	85	3.77 (0.05)
BC_1P_{R1}	0:1:1	0	31	28	0.15 (0.68)	1:1	29	26	0.16 (0.68)
BC_1P_S	1:1:0	27	30	0	0.6 (0.58)	0:1	0	56	
Population II (SSR-HpmsE032)									
P_S	–	10	0	0	–	–	0	10	–
P_{R2}	–	0	0	10	–	–	10	0	–
F_1 ($P_S \times P_{R2}$)	–	0	10	0	–	–	2	8	–
F_2	1:2:1	35	62	23	2.53 (0.28)	1:3	34	73	2.61 (0.11)
BC_1P_{R2}	0:1:1	0	26	34	1.6 (0.30)	1:1	25	16	1.98 (0.16)
BC_1P_S	1:1:0	17	36	0	6.81 (0.01)	0:1	4	48	–

[a] *RR:*susceptible, *Rr:* heterozygous and *rr:* resistant marker genotypes.
[b] R: resistant plant (lesion diameter <4 mm); S:susceptible plant (lesion diameter >4 mm).

Table 4
Phenotyping of F_2 plants homozygous for two tested markers, and marker selection efficacy of single cross.

Marker genotype	SCAR-Indel and phenotypic assay ($P_S \times P_{R1}$)			Efficacy	SSR-HpmsE032 and phenotypic assay ($P_S \times P_{R2}$)			Efficacy
	R	S	Total		R	S	Total	
Positive (++)	18	10	28	64.28%	15	8	23	65.21%
Negative (−−)	1	27	28	96.42%	8	27	35	77.14%
Total	19	37	56		23	35	58	

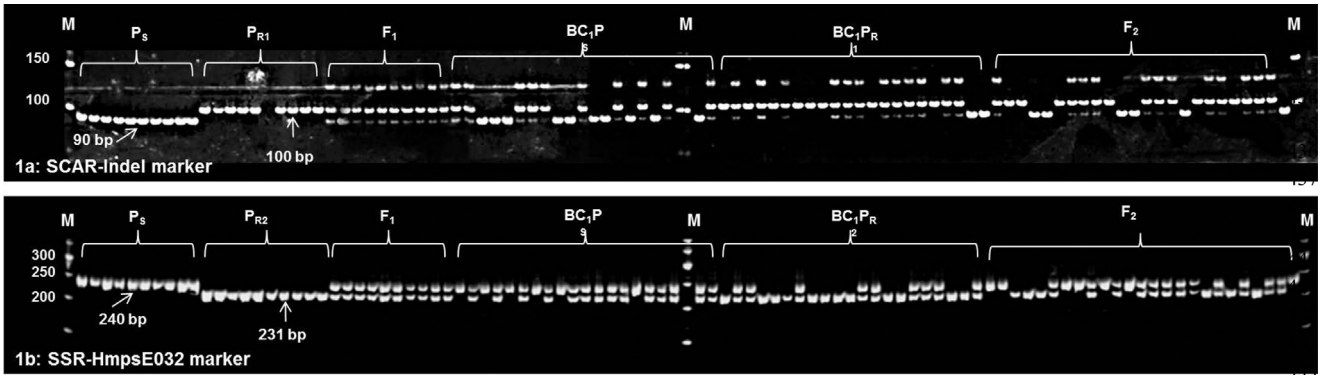

Fig. 2. Segregation patterns of anthracnose associated markers in parents and segregating generations (1a). SCAR-Indelin population I (1b). SSR-HpmsE032 in population II; M marker 50 bp.

Table 5
Grouping of 101 F_2 plants of three-parent cross ($P_S \times P_{R1}$) × ($P_S \times P_{R2}$) and selection efficacy of the markers.

Genotype groups[1/a]: SCAR-Indel/SSR-HpmsE032 (bp)	Number of plants (genotypic and phenotypic assay)			Efficacy
	R	S	Total	
A/B: ++/++ (90/231)	17	4	22	77.2%
A: ++/−− (90/100)	16	9	25	64.0%
B: −−/++ (240/231)	41	13	54	75.9%

[1/]A/B: Seedlings homozygous at both resistant markers; A:seedlings homozygous at resistant loci of SCAR-Indelmarker; B: Seedlings homozygous at one resistant marker of SSR-HpmsE032 marker.

3.3. Efficacy of markers to predict the anthracnose resistance phenotype

The F_2 seedlings of the two single crosses $P_S \times P_{R1}$ (56 plants) and $P_S \times P_{R2}$ (58 plants) and three-way cross (101 plants) were examined at the SCAR-Indel and SSR-HpmsE032 loci, and plants were phenotyped for disease reaction (Table 4). Fifty-six F_2 seedlings of the cross $P_S \times P_{R1}$ were homozygous positive (++, 28 plants) and homozygous negative (−−,28 plants) at the SCAR-Indel locus (Table 4). The selection efficacies of resistant and susceptible seedlings were 64.28% and 96.42%, respectively (Table 4). In the F_2 population II ($P_S \times P_{R2}$), out of 120 seedlings, 58 seedlings were homozygous at the SSR-HpmsE032 locus in resistant (23) and susceptible (35) plants. Thus, selection efficacies for resistant and susceptible plants were 65.21% and 77.14%, respectively (Table 4). From 1000 F_2 seedlings of the three-way cross analyzed with the SCAR-Indel and SSR-HpmsE032 markers, 101 seedlings homozygous for either one or both of the resistance markers were identified and transplanted in the field and eventually, the plants were phenotyped. Based on the homozygosity of the markers, seedlings were classified into three groups. Plant contained DNA 90 bp of SCAR-indel marker and 231 bp of SSR-HpmsE032 marker consisted of 22 seedlings homozygous for both, among which 17 plants turned out to be resistant to anthracnose *C. acutatum* at the mature green fruit stage. The recombination frequency of two loci was 2.2%. The efficacy for resistant plant selection was 77.2%. Plant contained DNA only 90 bp of SCAR-indel marker consisted of 25 seedlings homozygous for only the SCAR-Indel marker at 90 bp, among which 16 plants were resistant, with a selection efficacy of 64% (Table 5, Fig. 1). The remaining 54 seedlings constituted DNA 231 bp of SSR-HpmsE032 marker; 41 plants were resistant, thus the selection efficacy was 75.9% (Table 5, Fig. 1).

4. Discussion

Anthracnose resistance at the mature green fruit stage in two *C. annuum* resistant introgression lines P_{R1} (AVPP0207) and P_{R2} ($BC_2F_4$398/80C5(1)8/14,2/7-31) was contained a different major recessive genes for resistance. Progenies in segregating populations of population I (AVPP0207) showed a good fit to a single gene model for genotypic (DNA markers) segregation, while phenotypic (disease reaction) segregation in F_2 population did not fit to single gene model. In F_2 populations of $P_S \times P_{R1}$, the phenotypic segregation confirm the hypothesis of a major recessive resistant gene to *C. acutatum* at the mature green fruit stage (Mahasuk et al., 2009). However, in one segregating population (BC_1P_S) of the cross $P_S \times P_{R2}$, segregation was also not in agreement with the hypothesis of a single recessive gene control for resistance. This deviation may be either due to the involvement of other minor genes in P_{R2} derived from *C. baccatum* (PBC80) (Lee et al., 2010) or due to incompatibility between host and pathogen known in backcross populations derived from susceptible parents (Yoon et al., 2006). In addition, for the distribution of genotypic data not fit to the single gene, may be due to the fact that resistant parent used was BC_2F_4. Variable inheritance patterns in *Capsicum* germplasm resistance to anthracnose induced by *Colletotrichum* isolates is well known (Park et al.,

2009; Suwor et al., 2015). For example, resistance to *C. acutatum* has been found to be under a single recessive gene (Kim et al., 2007; Kim et al., 2008; Mahasuk et al., 2009), two complementary genes (Lin et al., 2007), and quantitative genes (Lee et al., 2010).

Both parents P_{R1} (derived from PBC932) and P_{R2} (derived from PBC80) were highly resistant to *C. acutatum*-Ca153 compared to susceptible parent KKU-P31118 and the two F_1 crosses derived from them. Therefore, resistant parental lines could potentially serve as donors for improving anthracnose resistance by combining resistance from both *C. chinense* and *C. baccatum* (Suwor et al., 2015). Both single crosses derived from two resistant parents showed variable disease lesion sizes, although in both cases the disease reaction was classified as susceptible. The mean lesion diameter of F_1 plants derived from P_{R2} was smaller than from the F_1 plants derived from P_{R1}. This was expected, as P_{R2} is an introgression line derived from a broad resistance source (PBC80) (Yoon et al., 2004; Montri et al., 2009; Lee et al., 2010). The anthracnose lesion diameter of the three-parent cross was higher than the two single crosses. This may be because resistant genes to *C. acutatum* in both donor parents are presumably non-allelic and located in different chromosome regions (Pakdeevaraporn et al., 2005; Mahasuk et al., 2009).

Both SCAR-Indel and SSR-HpmsE032 markers increased selection efficacy, SSR-HpmsE032 marker seems to be a good marker for selection anthracnose resistant genes similar to use two markers combination together. The mismatches between marker genotype and resistance phenotype can partially be explained due to recombination events such as the distance between marker and recessive resistant genes reported as 1.3 cM for the SCAR-Indel marker (Sun et al., 2015) and 8.1 cM for the interval length of the flanking marker of the HpmsE032-SSR marker (Lee et al., 2010). Nevertheless, selection of desirable putative resistant seedlings based on the two markers with the F_2 of the three-way population was considerable effective inbreeding program. The SSR-HpmsE032 marker developed using the *C. baccatum* (PBC81) resistance source (Lee et al., 2010) has been validated in introgression resistant lines derived from another *C. baccatum* (PBC80) (Suwor et al., 2015). This marker and SCAR-Indel have been used successfully in MAS for early identification of putative resistant and susceptible seedlings from 1000 F_2 progenies of the three-parent cross, which combined two resistant genes derived from P_{R1} and P_{R2}. The SSR-HpmsE032 was also effective in our population used derived from PBC80parental line P_{R2}, which demonstrates case-specific utilization of marker technology in practical plant breeding (Suwor et al., 2015). The combined use of both markers increased the efficacy to 77%, and facilitated identification of more than 90% non-desirable genotypes at the seedling stage in the greenhouse. The remaining10% seedlings were transplanted to the field for disease screening, further evaluation and generation advancement, leading to a significant reduction in costs for land, field labor, and crop management.

In conclusion, the resistant genes in two introgression lines were inherited as monogenic recessive. The SCAR-$Indel_{90}$ marker was validated in introgression line (AVPP0207) derived from PBC932*C. chinese* with selection efficacy of 64%, while SSR-$HpmsE032_{231}$-marker was validated in introgression line (BC_2F_4) of *C. baccatum* derived from PBC80 at 231 bp with selection efficacy of more than 75% as well as the efficacy selection of two markers.

Acknowledgements

The authors are grateful to The Royal Golden Jubilee (RGJ) Ph.D. Program, Thailand Research Fund (TRF); The National Science and Technology Agency (NSTDA); National Research University Project of Thailand, Office of the Higher Education Commission, through the Food and Functional Food Research Cluster of Khon Kaen University (KKU), TRF (project code: IRG5780003) and the Faculty of Agriculture, KKU for providing financial support for manuscript preparation activities. The authors are also grateful to World Vegetable Center, Taiwan and Asst. Prof. Chalermsri Nontaswatsri, Maejo University, Thailand for providing seeds of genotypes used in this study.

References

Ahn, M.I., Yun, S.C., 2009. Epidemiological Investigations to optimize the management of pepper anthracnose. Plant Pathol. 25, 213–219.
Bosland, P.W., Votava, E.J., 2012. Peppers: Vegetable and Spice Capsicums. CABI Publishing, Wallingford, United Kingdom.
Farkhzadeh, S., Alifakheri, B., 2014. Marker-assisted selection for disease resistance: application in breeding. Int. J. Agric. Crop Sci. 7, 1392–1405.
Garg, R., Kumar, S., Kumar, R., Loganathan, M., Saha, S., Kumar, S., Rai, A.B., Roy, B.K., 2013. Novel source of resistance and differential reactions on chilli fruit infected by *Colletotrichum capsici*. Aust. Plant Pathol. 42, 227–233.
Gururania, M.A., Venkatesha, J., Upadhyayab, C.P., Nookarajuc, A., Pandeyc, S.K., Park, S.W., 2012. Plant disease resistance genes: current status and future directions. Physiol. Mol. Plant Pathol. 78, 51–65.
Kim, S.H., Yoon, J.B., Do, J.W., Park, H.G., 2007. Resistance to anthracnose caused by *Colletotrichum acutatum* in chili pepper (*Capsicum annuum* L.). J. Crop Sci. Biotechnol. 10, 277–280.
Kim, S.H., Yoon, J.B., Do, J.W., Park, H.G., 2008. Inheritance of anthracnose resistance in a new genetic resource *Capsicum baccatum* PI594137. J. Crop Sci. Biotechnol. 11, 13–16.
Lee, J., Hong, J.H., Do, J.W., Yoon, J.B., 2010. Identification of QTLs for resistance to anthracnose to two *Colletotrichum* species in pepper. J. Crop Sci. Biotechnol. 13, 227–233.
Lee, J., Do, J.W., Yoon, J.B., 2011. Development of STS markers linked to the major QTLs for resistance to the pepper anthracnose caused by *Colletotrichum acutatum* and *C. capsici*. Hortic. Environ. Biotechnol. 52, 596–601.
Liao, C.Y., Chen, M.Y., Chen, Y.K., Wang, T.C., Sheu, Z.M., Kuo, K.C., 2012. Characterization of three *Colletotrichum acutatum* isolates from *Capsicum* spp. Eur. J. Plant Pathol. 133, 599–608.
Lin, S.W., Gniffke, P.A., Wang, T.C., 2007. Inheritance of resistance to pepper anthracnose by *Colletotrichum acutatum*. Acta Hortic. 760, 329–334.
Mahasuk, P., Taylor, P.W.J., Mongkolporn, O., 2009. Identification of Two new genes conferring resistance to *Colletotrichum acutatum* in *Capsicum baccatum*. Phytopathology 99, 1100–1104.
Mahasuk, P., Chinthaisong, J., Mongkolporn, O., 2013. Differential resistances to anthracnose in *Capsicum baccatum* as responding to two *Colletotrichum* pathotypes and inoculation methods. Breed. Sci. 63, 333–338.
Mistry, D.S., Sharma, L.P., Patel, S.T., 2008. Bio-chemical parameter of chili fruits as influenced by *Colletotrichum capsici* (Sydow) Butler & Bisby infection. Karnataka J. Agric. Sci. 21, 586–587.
Mongkolporn, O., Montri, P., Supakaew, T.T., Taylor, P.W.J., 2010. Differential reactions on mature green and ripe chili fruit infected by three *Colletotrichum* species. Plant Dis. 94, 306–310.
Montri, P.P., Taylor, P.W.J., Mongkolporn, O., 2009. Pathotypes of *Colletotrichum capsici* the causal agent of chili anthracnose in Thailand. Plant Dis. 93, 17–20.
Pakdeevaraporn, P., Wasee, S., Taylor, P.W.J., Mongkolporn, O., 2005. Inheritance of resistance to anthracnose caused *Colletotrichum capsici* in *Capsicum*. Plant Breed. 124, 206–208.
Park, K.S., Kim, S.H., Park, H.G., Yoon, J.B., 2009. *Capsicum* germplasm resistance to pepper anthracnose differentially interacts with Colletotrichum isolates. Hortic. Environ. Biotechnol. 50, 17–23.
Sun, C.Y., Li, M.S., Hai, Z.Z., Alain, P., Hao, W., Xi, Z.B., 2015. Resistances to anthracnose (Colletotrichum acutatum) of Capsicum mature green and ripe fruit are controlled by a major dominant cluster of QTLs on chromosome P5. Sci. Hortic. 181, 81–88.
Suwor, P., Thummabenjapone, P., Sanitchon, J., Kumar, S., Techawongstien, S., 2015. Phenotypic and genotypic responses of chili (*Capsicum annuum* L.) progressive lines with different resistant genes against anthracnose pathogen (*Colletotrichum* spp.). Eur. J. Plant Pathol. 143, 725–736.
Suwor, P., Thummabenjapone, P., Sanitchon, J., Kumar, S., Techawongstien, S., 2016. Role of two inoculation methods in the expression of anthracnose resistance gene in chili (*Capsicum annuum* L.). Acta Hortic. 1144, 207–214.
Temiyakul, P., Taylor, P.W.J., Mongkolporn, O., 2012. Differential fruit maturity plays an important role in chili anthracnose infection. J. KMUTNB 22 (3), 494–504.
Than, P.P., Jeewon, R., Hyde, K.D., Pongsupasamit, S., Mongkolporn, O., Taylor, P.W.J., 2008. Characterization and pathogenicity of *Colletotrichum* species associated with anthracnose disease on chili (*Capsicum* ssp.) in Thailand. Plant Pathol. 57, 562–572.
Tozze, H.J., Massola, N.M., 2009. First report of *Colletotrichum* boninense causing anthracnose on pepper in Brazil. Plant Dis. 93, 106.
Voorrips, R.E., Finkers, R., Sanjaya, L., Groenwold, R., 2004. QTL mapping of anthracnose (*Colletotrichum* spp.) resistance in a cross between *Capsicum annuum* and *C. chinense*. Theor. Appl. Genet. 109, 1275–1282.
Wang, Y.W., 2011. Development of Sequence Characterized Amplified Region (SCAR) Markers Associated with Pepper Anthracnose (Colletotrichum

acutatum) Resistance. Master Thesis. University of National Chiayi University, Taiwan.
Xia, H., Wang, X.L., Zhu, H.J., Gao, B.D., 2011. First report of anthracnose caused by *Glomerella acutata* on chili pepper in China. Plant Dis. 95, 219.
Yi, G., Lee, J.M., Lee, S., Lee, D., Choi, D., Kim, D., Kim, B.D., 2006. Exploitation of pepper EST-SSRs and an SSR-based linkage map. Theor. Appl. Genet. 114, 113–130.
Yoon, J.B., Yang, D.C., Lee, W.P., Ahn, S.Y., Park, H.G., 2004. Genetic resources resistant to anthracnose in the genus *Capsicum*. J. Korean Soc. Hortic. Sci. 45, 318–323.
Yoon, J.B., Yang, D.C., Do, J.W., Park, H.G., 2006. Overcoming two post-fertilization genetic barriers in interspecific hybridization between *Capsicum annuum* and *C. baccatum* for introgression of anthracnose resistance. Breed. Sci. 56, 31–38.

Hortic. Environ. Biotechnol. 58(2):103-110. 2017.
DOI 10.1007/s13580-017-0165-6

ISSN (print) : 2211-3452
ISSN (online) : 2211-3460

Research Report

Light Intensity Affects Capsaicinoid Accumulation in Hot Pepper (*Capsicum chinense* Jacq.) Cultivars

Nakarin Jeeatid[1], Sungcom Techawongstien[1], Bhalang Suriharn[1], Paul W. Bosland[2], and Suchila Techawongstien[1*]

[1]*Department of Plant Science and Agricultural Resources, Faculty of Agriculture, Khon Kaen University, Khon Kaen 40002, Thailand*
[2]*Department of Plant and Environmental Sciences, College of Agriculture, Consumer and Environmental Science, New Mexico State University, New Mexico, 88003, U.S.A.*

*Corresponding author: suctec.kku@gmail.com

Received May 30, 2016 / Revised October 10, 2016 / Accepted October 25, 2016

Abstract. Strong light intensity affects plant growth, fruit yield, and accumulation of capsaicinoids in hot peppers (*Capsicum* spp.) which are important food and medicinal products. Shading improves plant growth and fruit yield in bell pepper (*Capsicum annuum*), but research on the effect of shading on high pungency *C. chinense* cultivars is limited. This study investigated the responses of *C. chinense* cultivars to different light intensities to maximize capsaicinoid production. An experiment to test the effect of shading, i.e., no-shading (full light intensity as control), 50% shade and 70% shade of full light intensity, was conducted in a plastic-net house using four *C. chinense* cultivars with different pungency levels: Bhut Jolokia, Akanee Pirote, Orange Habanero, and BGH1719. The cultivars showed different capsaicinoid production levels depending on the shade level. The highest capsaicinoid yields were found in the F1 hybrid cultivar Akanee Pirote under 50% shading (4,820 mg/plant) and in the Bhut Jolokia cultivar under 70% shading (3,419 mg/plant). By contrast, the BGH1719 plants showed the lowest capsaicinoid production (291 mg/plant) when shade was applied. These results demonstrate that capsaicinoid production in the studied cultivars is affected by light intensity. It is recommended that growers of high pungency cultivars use the appropriate level of shading for the particular cultivar to increase capsaicinoid yield.

***Additional key words*:** capsaicin, environmental factors, heat levels, pharmaceutical product, pungency, shading

Introduction

Capsaicinoids are alkaloids that cause the sensation of heat when hot peppers are eaten, and they are specific to *Capsicum* species (Hoffman et al., 1983; Suzuki and Iwai, 1984). Capsaicinoids are traditionally used in the food industry to enhance the flavor of dishes. In addition, they are increasingly used by the pharmaceutical industry due to their valuable antioxidant, anti-arthritic, gastroprotective, anti-carcinogenic, and analgesic properties (Prasad et al., 2005). Capsaicinoids are also used as a feed additive in swine, poultry and fish production (Erdost et al. 2006), which highlights the importance of capsaicinoid production.

The *Capsicum* genus contains more than 30 species, among which *C. annuum* is the most cultivated and economically important (Bosland and Votava, 2012). The hottest peppers are varieties of the species *C. chinense*, such as Bhut Jolokia (Bosland and Baral, 2007), and 'Trinidad Moruga Scorpion' (Bosland et al., 2012). These varieties represent a good source for capsaicinoid production and extraction. Unfortunately, the poor uniformity found in these high pungency varieties limits their usefulness for this purpose (Bosland et al., 2012). Bosland and Votava (2012) indicated that chili peppers grown from hybrid seeds are highly uniform and usually higher yielding than the parental lines. It would be a beneficial to the food and pharmaceutical industry if such F1 hybrid seed from hot peppers was available to ensure high capsaicinoid production.

In general, hot peppers are grown in the open field where they are subjected to biotic stresses such as diseases and insects, and abiotic stresses such as high temperatures and high light intensities. Rylski and Spigelman (1982) reported that heat stress can inhibit pepper production due to reduced fruit numbers and increased flower abscission. The optimum

temperature for sweet pepper production ranges between 20 and 25°C (Saha et al., 2010) and the optimum light intensity is 1,400 μmol·m^{-2}·s^{-1} (Díaz-Pérez, 2013). However, flower abortion occurs when daytime temperatures rise above 34°C for extended periods of time (Cochran, 1936). In addition, accumulation of capsaicinoids is reduced at high temperatures and high light intensity levels (Gurung et al., 2011).

Shading is generally used to protect agricultural crops from damage caused by high light intensities and high temperatures (Díaz-Pérez, 2013; Möller and Assouline, 2007; Valiente-Banuet and Gutiérrez-Ochoa, 2016). Several reports indicate that plant height, leaf area, and leaf chlorophyll content increase under shading (Rylski and Spigelman, 1982; Díaz-Pérez, 2013) and this results in increased fruit yield. A recent study using bell pepper plants in Tifton, GA, USA, suggested that reducing the sunlight intensity with 30% to 47% resulted in higher yields and increased fruit number compared with plants grown without shade. However, decreasing the light intensity by more than 60% resulted in a decrease in fruit set and yields (Díaz-Pérez, 2014; Valiente-Banuet and Gutiérrez-Ochoa, 2016). Because hot pepper belongs to the nightshade family (DeWitt and Bosland, 2009), shading could improve plant growth, fruit yield, and capsaicinoid accumulation. Although it has been reported that shading increases yield in bell pepper (*C. annuum*), no research on the effects of different light intensities on plant growth and fruit yield in *C. chinense* cultivars has been reported.

Light intensity is an important factor in capsaicinoid formation and accumulation (Iwai et al., 1979). It is well known that capsaicinoid production is affected by the genotype, including species and cultivar, the environment and the genotype-by-environment interaction (Zewdie and Bosland, 2000). Hot pepper plants from different origin and with different pungency levels show different responses under a variety of growing conditions (Gurung et al., 2012). Reducing the light intensity may result in either a positive or a negative effect on hot pepper yield and capsaicinoid accumulation, depending on the species, the degree of shading, and other agricultural practices (Rylski and Spigelman, 1986). Additional research is thus required to determine the influence of environmental factors and specifically light intensity, on the maximum pungency level in hot peppers.

Although previous studies suggested that light intensity does affect morphological and physiological traits such as fruit quality and yield in bell pepper (*C. annuum*), responses in other *Capsicum* species may differ. In particular, appropriate shading may be required for the high pungency cultivars of *C. chinense* to produce maximum capsaicinoid levels. Therefore, the objective of this study was to determine the effect of different levels of shading on plant growth, fruit yield, and pungency in *C. chinense* Jacq. cultivars with different pungency levels.

Materials and Methods

The four cultivars of *C. chinense* used in this experiment are from different origins, and have different growth habits, fruit size, and pungency levels. The F1 hybrid cultivar, Akanee Pirote, was released by Khon Kaen University for capsaicinoid extraction in Thailand and has a perennial growth habit, large canopy size, a relative large leaf size and a mean heat level of 400,000-600,000 Scoville Heat Units (SHU). The Bhut Jolokia cultivar, one of the world's hottest peppers producing cultivar, has a perennial growth habit, big canopy size, and a heat level of 800,000-1,200,000 SHU. The cultivars Orange Habanero and BGH 1719 both have an annual growth habit, small canopy size and a heat level of 100,000-250,000 SHU. Orange Habanero is very popular in the Yucatan region of Mexico, and is grown in many parts of the world (Bosland and Votava, 2012) and this cultivar can be used in the industrial extraction of capsaicinoid. BGH 1719, has a high capsaicinoid yield, which is determined by the fruit heat level and the fruit yield per plant, and is tolerant to water deficit stress (Phimchan et al., 2012).

The experiment was conducted during the main growing season from May to October 2013 under a plastic-net house at the experimental farm of Khon Kaen University, Khon Kaen Province, Thailand (latitude 16° 28' N, longitude 102° 48' E, 200 m above mean sea level). The plastic-net house was 24 m long, 6 m wide, and 2.7 m high with a polyethylene cover of 0.1 mm clear polyethylene film. In order to synchronize the time of flowering for all cultivars, the sowing dates were adjusted based on the growth habits of each cultivar. In May 2013, the seedlings were transplanted to 12 L plastic pots (0.28 × 0.20 m; $W \times H$) filled with a mixture of rice husk, charcoal rice husk, filter cake (organic waste from the sugar industry), and composted cow manure in a ratio of 2:1:1:0.5 (v:v) and placed under the plastic-net house. The pots were placed in rows with 80 cm between the pots and 80 cm between rows. The plants were irrigated daily through a micro-drip irrigation system at field capacity. All plants received the same amount of fertilizer at three-day intervals by fertigation throughout the experiment (adapted from Patricia, 1999). Before the start of the experiment all plants were placed in full sunlight (no shading). At the flowering stage (45 days after transplanting; DAT), the shading material was installed over the plants in a split plot design with three replications and six plants per replication. Three levels of shading were designed as main-plot, i.e. no-shading (S_0), 50% shading (S_{50}), and 70% shading (S_{70}), and four hot pepper cultivars were used as sub-plot.

The light intensity under shade net was measured using a luminance meter (Konica Minolta T-10A, USA) at three locations above the plant canopy. The Lux reading was converted to μmol·m^{-2}·s^{-1} by multiplying the amount of Lux

with the conversion factor (0.0185) to get the Photosythetic Photon Flux value (Thimijan and Heins, 1982). Every two weeks a luminance measurement was taken from 11:00 am to 1:00 pm. Plant height and canopy width were recorded at the time of second fruit harvest, approximately 140 DAT. Roots were separated from shoots and washed to remove the media. Each plant part was oven-dried at 80°C and, subsequently, the dry mass was determined. The total dry mass was calculated as the sum of the shoot and root dry mass, and a root-to-shoot ratio was calculated.

Mature fruits were weekly harvested starting at 133 DAT and the fruits were sundried for 3 days, then oven-dried at 80°C, and their dry weights determined. The total fruit number of each individual plant was recorded at the time of harvest. At the second harvest (140 DAT), the fruit size was recorded and the capsaicinoid levels were analyzed. Capsaicinoids were extracted and quantified according to the 'short run' method using high performance liquid chromatography (HPLC) (Collins et al., 1995). For capsaicinoid extraction, 1 g of hot pepper powder was extracted with 10 mL of acetonitrile at 80°C for 4 hours. The extracted solution was filtered using a 0.45 μL polyamide syringe and 10 μL of the filtered extract was injected for HPLC analysis using a Shimadzu-Model, 10AT-VP series HPLC system (Shimadzu Company, Japan). The mobile phases were methanol: deionized water at a ratio of 80:20 and a flow rate of 1.5 $mL \cdot min^{-1}$ with the ODS C-18 column was used. The wavelength of the detector was set at 284 nm. Extraction standards for capsaicin and dihydrocapsaicin (Fluka #37274; Fluka Chemie, Buchs, Switzerland) were prepared at concentrations of 0, 50, 100, 500, and 1,000 ppm. Capsaicin and dihydrocapsaicin concentrations were converted to Scoville Heat Units (SHU), as described by Collins et al. (1995). Because capsaicin and dihydrocapsaicin are the primary capsaicinoids found in hot peppers, they were pooled as 'capsaicinoids'. The capsaicinoid yield was calculated based on dry fruit yield by multiplying the capsaicinoid amount per plant.

The data were analyzed according to the method described by Gomez and Gomez (1984). All data were analyzed using analysis of variance (ANOVA) in a split-plot randomized complete block design. Treatment means were separated by the Least Significant Difference (LSD) test at a 5% probability level ($p \leq 0.05$).

Results

The environmental conditions of the different shading treatments are shown in Figure 1. The light intensity varied from 1,500 to 1,900 $\mu mol \cdot m^{-2} \cdot s^{-1}$ in the S0 treatment (Fig. 1A). The light intensity under the S50 treatment ranged from 700 to 950 $\mu mol \cdot m^{-2} \cdot s^{-1}$, and as expected, the lowest light intensity was observed under S_{70} treatment where it ranged from 300 to 600 $\mu mol \cdot m^{-2} \cdot s^{-1}$. The mean maximum air temperature under shading conditions ranged from 27 to 43°C for S_{50} treatment, and 27 to 42°C for S_{70} treatment, both of which were lower when compared with S_0 treatment (30 to 48°C). However, the minimum air temperature under the different shading conditions was similar (Fig. 1B). In addition, the mean maximum relative humidity (RH) under shading was higher than in the control treatment without shading (Fig. 1C).

An analysis of variance showed significant differences for

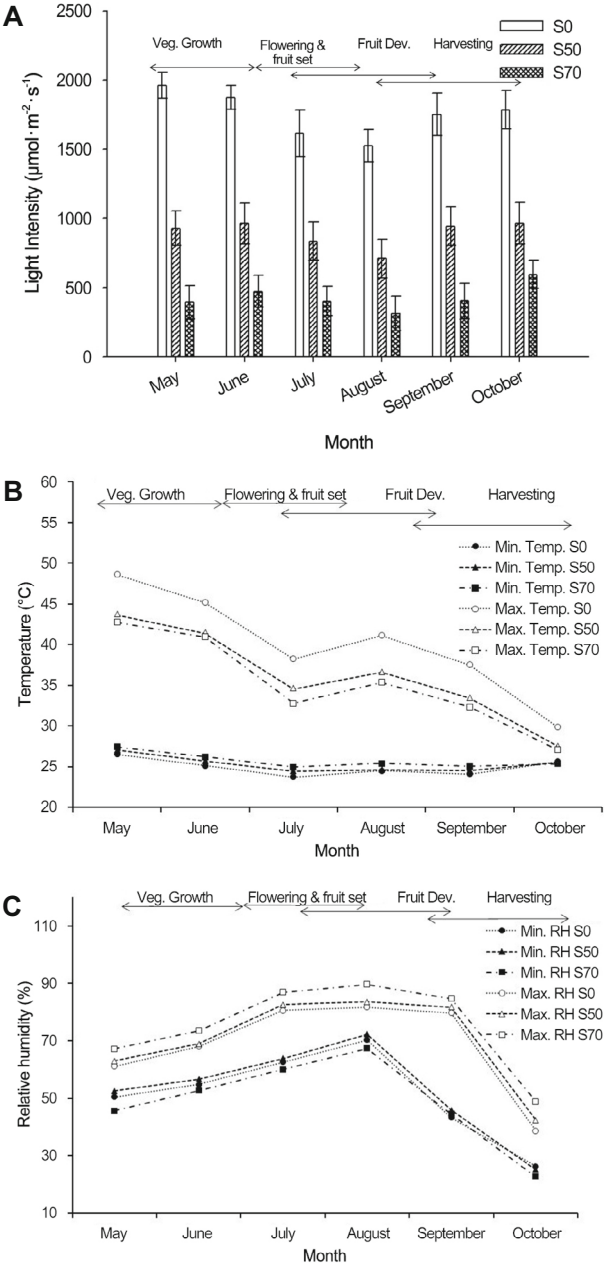

Fig. 1. Light intensity (A), air temperature (B) and relative humidity (C) under different shading conditions from May to October 2013.

Table 1. Plant height, canopy width, shoot dry mass, root dry mass, total dry mass and root to shoot ratio of four hot pepper cultivars grown under different shading treatments from May to October 2013

Treatments		Plant height (cm)	Canopy width (cm)	Total dry mass (g)	Shoot dry mass (g)	Root dry mass (g)	Root to shoot ratio
Cultivar (C)							
Bhut Jolokia		103.6 a[z]	105.2 a	304 a	256 a	46.7 b	0.18 c
Akanee Pirote		104.6 a	100.4 b	293 a	234 b	54.5 a	0.25 b
Orange Habanero		73.3 c	68.2 d	128 b	98 c	29.9 c	0.30 a
BGH 1719		85.5 b	94.6 c	131 b	109 c	22.3 d	0.19 c
Shading (S)							
S_0		82.8 c	86.9 b	242 a	194 a	47.8 a	0.26 a
S_{50}		93.4 b	93.8 a	214 b	174 b	36.1 b	0.23 b
S_{70}		99.0 a	95.7 a	186 c	155 c	31.1 c	0.20 c
Interaction (C x S)							
Bhut Jolokia	S_0	100.0 b	103.7 a	335 a	281 a	53.8 b	0.19 d
	S_{50}	101.0 b	106.3 a	302 b	255 b	43.8 de	0.17 ef
	S_{70}	109.7 a	105.5 a	275 c	233 c	42.6 de	0.18 de
Akanee Pirote	S_0	81.4 de	93.6 c	295 bc	232 c	62.7 a	0.27 bc
	S_{50}	115.0 a	101.1 ab	310 ab	244 bc	53.3 bc	0.26 c
	S_{70}	117.8 a	106.5 a	274 c	227 c	47.4 cd	0.21 d
Orange Habanero	S_0	68.6 f	65.2 f	148 e	114 e	33.8 f	0.29 b
	S_{50}	74.2 ef	65.8 f	132 ef	99 ef	32.8 f	0.33 a
	S_{70}	77.4 de	73.6 e	105 gh	82 fg	23.1 g	0.28 bc
BGH 1719	S_0	81.4 de	85.0 d	190 d	149 d	40.9 e	0.28 bc
	S_{50}	83.5 cd	101.7 ab	114 fg	100 ef	14.7 h	0.15 fg
	S_{70}	91.6 c	97.2 bc	88 h	76 g	11.4 h	0.13 g
Mean		91.0	92.1	214	174	38.3	0.23
Cultivar (C)		**	*	**	**	**	**
Shading (S)		**	**	**	**	**	*
C x S		**	**	**	*	**	**

*,**; Significant at $p \leq 0.05$ and 0.01 P levels, respectively.
[z]Means in the same column followed by the same letter are not significantly different at ($p \leq 0.05$) by least significant difference.

all plant growth traits among cultivars, shading, and cultivar-by-shading interaction (Table 1). Plant height was highest in the Akanee Pirote cultivar under S_{70} (117.8 cm.) and S_{50} (115.0 cm.) treatment, followed by the Bhut Jolokia cultivar under S_{70} shading (109.7 cm.). The shortest plants were observed in the Orange Habanero cultivar under all treatments (68.6-77.4 cm.). Furthermore, Akanee Pirote plants had wider canopies under S_{50} and S_{70} treatments (101.1 and 106.5 cm.) when compared with the control, while no significant differences in canopy width could be observed among treatments in the Bhut Jolokia cultivar (103.7-106.3 cm.). The canopy width of Orange Habanero plants was larger under S_{70} treatment (73.6 cm.) when compared with control plants, but this cultivar had the smallest canopy width under all treatments when compared with the other cultivars.

The total dry mass of Bhut Jolokia plants in the control treatment (335 g/plant) was higher than in the S_{50} and S_{70} treatments (302 and 275 g/plant, respectively) (Table 1). A decrease in total dry mass under shading conditions was also found for the BGH1719 cultivar. However, the total dry mass of Akanee Pirote plants under S_{50} treatment (310 g/plant) was not significantly different from S_0 treatment (295 g/plant), but higher than the dry mass of plants under S_{70} treatment (274 g/plant). The total dry mass of Orange Habanero plants showed a similar trend to Akanee Pirote plants, however the total weight (105-148 g/plant) was lower than the total weight of Akanee Pirote plants.

The shoot dry mass of Akanee Pirote and Orange Habanero plants under S_{50} treatment (244 and 99 g/plant, respectively) was similar to the shoot dry mass of plants grown under S0 treatment (Table 1). In contrast, shoot dry mass of Bhut Jolokia and BGH1719 plants was lower under shading treatment when compared with S_0 treatment. Furthermore, for all cultivars a reduction in root dry mass was observed under both shading treatments when compared with the root dry mass under S_0 treatment, with the exception of the Orange Habanero cultivar under S_{50} treatment (32.8 g/plant). Among the cultivars, Akanee Pirote and Orange Habanero had a relatively high root-to-shoot

Table 2. Dry fruit yield, fruit number, fruit length and fruit width of four hot pepper cultivars grown under different shading treatments from May to October 2013

Treatments		Dry fruit yield (g/plant)	Fruit number	Fruit length (cm)	Fruit width (cm)
Cultivar (C)					
Bhut Jolokia		52.2 c[z]	65.1 c	6.17 a	2.61 b
Akanee Pirote		105.9 b	159.8 b	5.00 b	2.40 c
Orange Habanero		119.8 a	135.0 b	3.79 c	3.07 a
BGH 1719		51.2 c	265.5 a	2.46 c	1.26 d
Shading (S)					
S_0		83.2 b	176.4 a	4.31	2.41
S_{50}		100.6 a	168.2 a	4.38	2.36
S_{70}		62.9 c	124.4 b	4.38	2.23
Interaction (C x S)					
Bhut Jolokia	S_0	57.0 de	66.0 e	6.08	2.67
	S_{50}	51.0 e	63.7 e	6.16	2.69
	S_{70}	49.0 e	66.2 e	6.28	2.54
Akanee Pirote	S_0	77.0 c	113.3 d	5.02	2.24
	S_{50}	155.0 a	222.7 b	4.96	2.52
	S_{70}	85.7 c	143.0 cd	5.03	2.52
Orange Habanero	S_0	128.7 b	137.8 cd	3.71	2.84
	S_{50}	142.3 ab	149.3 cd	3.86	3.18
	S_{70}	88.0 c	118.7 d	3.81	3.21
BGH 1719	S_0	70.7 cd	389.3 a	2.45	1.26
	S_{50}	54.3 de	237.3 b	2.54	1.31
	S_{70}	29.0 f	170.0 c	2.39	1.26
Mean		82.3	156.4	4.36	2.34
Cultivar (C)		**	**	**	**
Shading (S)		**	*	ns	ns
C x S		**	**	ns	ns

ns *, **; Nonsignificant, Significant at $p \leq 0.05$ and 0.01 P levels, respectively.
[z]Means in the same column followed by the same letter are not significantly different at ($p \leq 0.05$) by least significant difference.

ratio. Orange Habanero plants under S_{50} treatment showed a higher root-to-shoot ratio (0.33) than the control (0.29). No significant difference in root to shoot ratio was found in Akanee Pirote plants under S50 treatment (0.26), but a decrease was show under S70 treatment (0.21) when compared with the control.

Analysis of variance showed significant differences among the cultivars for all yield traits studied, between shading treatments and for the cultivar-by-shading interaction for dry fruit yield and fruit number (Table 2). Akanee Pirote plants showed the highest dry fruit yield under S_{50} treatment followed by Orange Habanero plants (155.0 and 142.3 g/plant, respectively), but these values were not significantly different. The fruit number in the Akanee Pirote cultivar was significantly higher under S_{50} treatment (223 fruits) than under control (S_0) treatment (113 fruits) and there was no significant difference between the S_0 and the S_{70} treatments (143 fruits). The fruit number in the Orange Habanero plants was also not significantly different among shading treatments. In contrast, the dry fruit yield in cultivar BGH1719 was slightly reduced under shading conditions when compared with the S_0 treatment. Although, BGH1719 had the highest fruit number of all cultivars, it had the smallest fruit length and fruit width. In addition, the dry fruit yield, fruit number and fruit size of the Bhut Jolokia cultivar were not affected by shading.

The capsaicin, dihydrocapsaicin, and the capsaicinoid levels were increased under shading conditions (Fig. 2A-C). However, the different cultivars did respond differently under the different light intensities in terms of capsaicin, dihydrocapsaicin, and the capsaicinoid accumulation. High pungency cultivars were strongly affected by altered light intensities. Bhut Jolokia plants showed the highest capsaicinoid level under S_{70} treatment (1,111,721 SHU) and this level was significantly higher than observed under S_{50} and S_0 treatments (870,232 and 680,880 SHU, respectively) (Fig. 2C). The Akanee Pirote cultivar showed higher capsaicinoid accumulation under S_{70} treatment (612,852 SHU) when compared with the other two treatments, and the accumulation under S_{50} and S_0 treatments were not significantly different from each other. Under shading treatments, the Orange Habanero and BGH1719

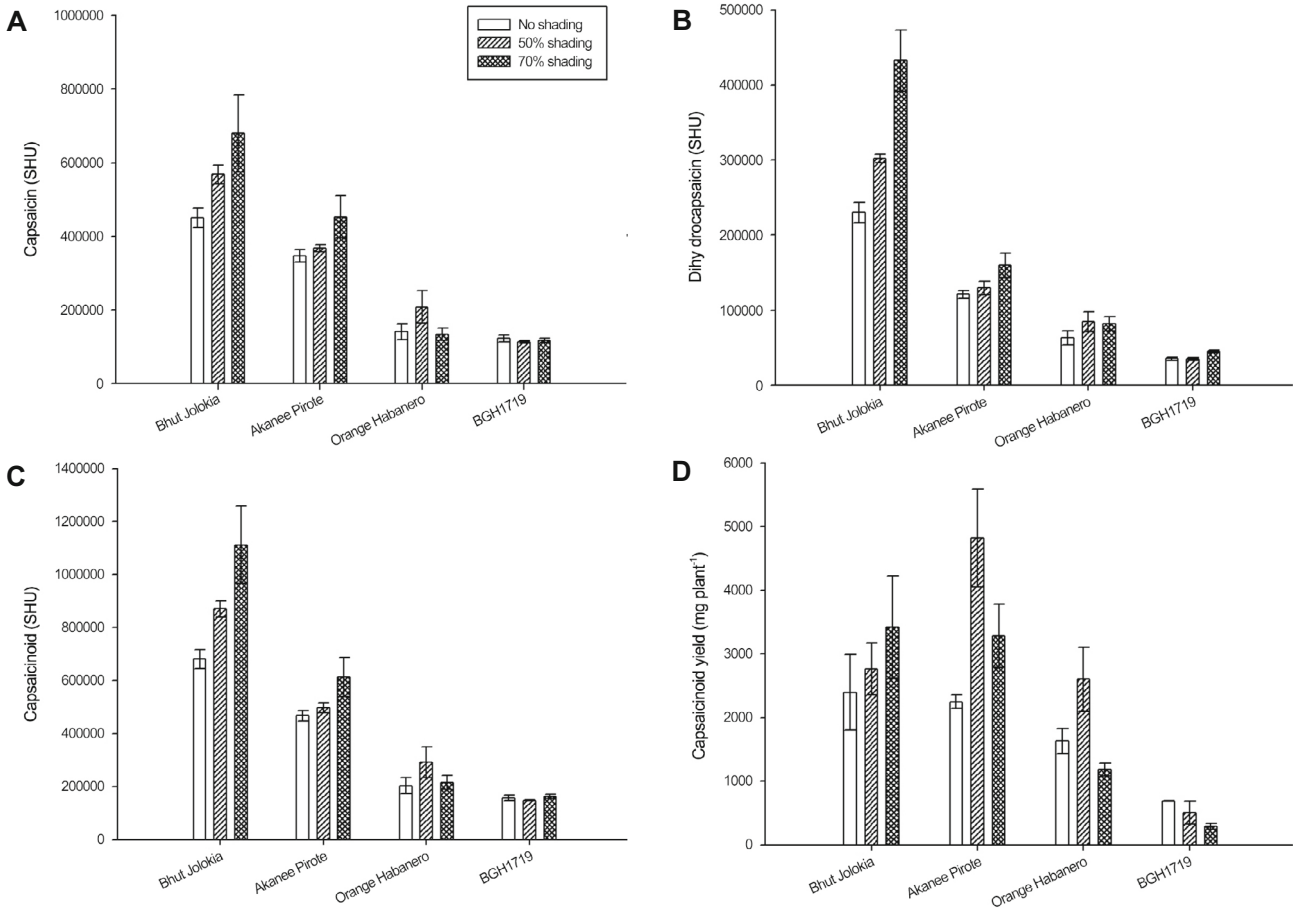

Fig. 2. Capsaicin (A), dihydrocapsaicin (B) and capsaicinoid accumulation (C) in fruit and capsaicinoid yield (D) of four hot pepper cultivars 'Bhut Jolokia', 'Akanee Pirote', 'Orange Habanero' and 'BGH1719' under different shading treatments: no shading, 50% shading and 70% shading. Capsaicin, dihydrocapsaicin and capsaicinoid concentration are expressed in Scoville Heat Units (SHU) and capsaicinoid yield is expressed as mg·plant^{-1}, average ± SD, n = 3. Capsaicinoid = capsaicin + dihydrocapsaicin, capsaicinoid yield = {[capsaicinoid (mg) x fruit dry yield per plant] / sample weight}.

cultivars showed similar capsaicinoid levels. Furthermore, Akanee Pirote plants under S_{50} treatment showed the highest capsaicinoid yield (4,820 mg/plant), a high fruit dry yield per plant and high levels of capsaicinoid accumulation (Fig. 2D).

Discussion

Fruit yield for each cultivar was determined by the combination of fruit number and fruit size. Cultivars with big fruits, such as Akanee Pirote, had higher yield than cultivars with small fruit size, such as BGH1719, despite the higher fruit number. Cultivar Bhut Jolokia with a large fruit size but low fruit number, resulted in the lowest fruit yield. The optimum light intensity for maximum fruit yield for bell peppers (*C. annuum*) ranged from 1,365 to 1,470 μmol·m^{-2}·s^{-1} (Díaz-Pérez, 2014). The results obtained here indicate that the different cultivars of *C. chinense* required different light intensities for maximum fruit yield. The high fruit yield of Akanee Pirote plants under S_{50} treatment (medium shading) as a result of an increase of fruit number, indicates that this cultivar requires less light when compared with BGH1719 plants which had the highest fruit number under S_0 treatment (full light intensity). The fruit yield in BGH1719 plants under S_{70} treatment (high shading) was so low that the light intensity under these shading conditions may be too low to fulfill the photosynthetic requirement (Díaz-Pérez, 2013). However, the fruit number of the Bhut Jolokia and Orange Habanero cultivars was not affected by the shading. In addition, the temperature of 32.8 to 40.0°C under high shading was not optimal for fruit set in any cultivar, because the optimum temperature for fruit set in peppers ranges from 20 to 25°C (Wien, 1997). Taken together, these findings indicate that light intensity has a greater effect on fruit set and yield than air temperature.

The total dry mass seems to be the key characteristic that influences dry fruit yield. The similarity of total and shoot dry mass between full light intensity and medium shading in the Akanee Pirote cultivar indicated that the photoassimilates

in this cultivar are sufficient for maximum dry fruit yield (Turner and Wien, 1994). However, high light intensity in a tropical country like Thailand always occurs in combination with high temperatures. These conditions can severely hamper fruit set and yield in hot pepper cultivars, particularly Akanee Pirote, under full light intensity. In addition, the low total dry mass under high shading means that the low light intensity negatively affected growth and photosynthesis, resulting in senescence in the flower and fruit (Marcelis et al., 2004; Díaz-Pérez, 2013). Medium shading improved canopy size of Akanee Pirote plants indicating that the cultivar was more efficient in using the available light for photosynthesis and the increased number of nodes on the pepper plant lead to increased fruit setting.

Although, high temperature stress can enhance capsaicinoid production (Rahman and Inden, 2012), the four cultivars of hot pepper tested here showed different responses to different shading levels. The Bhut Jolokia and Akanee Pirote cultivars showed high levels of capsaicinoids at low light intensity, even though the average air temperature was lower by 4-5°C under these conditions. This indicated that temperature is not the only factor that does determine capsaicinoid accumulation, but that genetic and environmental factors such as light intensity also play a role in capsaicinoid accumulation. The levels of phenylalanine ammonia lyase (PAL), an enzyme that plays a key role in capsaicinoid biosynthesis in *Capsicum* fruit (Phimchan et al., 2014), increases under low light intensities (Pacheco et al., 2014) and this may be the cause of increased capsaicinoid accumulation in the Akanee Pirote and Bhut Jolokia cultivars. Moreover, full light intensity reduced capsaicinoid accumulation in Bhut Jolokia plants. It is known that under full light intensity, plants prevent cell damage by increasing lignin levels in the cell wall by stimulating the phenylpropanoid pathway (Moura et al., 2010). The phenylpropanoid pathway is also used to synthesize capsaicinoids, however, in a competing manner, which means that under high light intensity cell wall lignification is stimulated, while capsaicinoid production is inhibited. Nevertheless, the increase in capsaicinoid content under shading was dependent on the cultivar and the shade level. The Orange Habanero and BGH1719 cultivars showed an inconsistent increase and decrease of capsaicinoid levels to different shading, while capsaicinoid accumulation was high in high pungency cultivars, i.e., Bhut Jolokia and Akanee Pirote, under low light intensities. This confirms that the high pungency cultivars with bigger fruits (Bhut Jolokia and Akanee Pirote) are sensitive to different environmental factors (Gurung et al., 2012). The sensitivity of these high pungency cultivars to different light intensities might be explained by the fact that the degree of pungency is quantitatively inherited and highly affected by the environment (Zewdie and Bosland, 2000). Thus, the genotype-by-environment interaction may be more strongly affected in high pungency cultivars than in low pungency cultivars.

The Akanee Pirote cultivar under medium shading showed the highest capsaicinoid yield. This may suggest that the increased dry fruit yield is the determining factor of capsaicinoid yield. Although, the highest dry fruit yield was found in Akanee Pirote and Orange Habanero plants under medium shading, the capsaicinoid content in the Akanee Pirote cultivar was 2-fold higher than in the Orange Habanero cultivar which was caused by genetic rather than environmental factors (Zewdie and Bosland, 2000; Gurung et al., 2011). The capsaicinoid content in Bhut Jolokia plants was 2-fold higher than in Akanee Pirote plants, but the dry fruit yield in Bhut Jolokia plants was 3-fold lower than in Akanee Pirote plants resulting in low capsaicinoid yield. These findings confirm that the capsaicinoid yield is determined by fruit weight and pungency.

In conclusion, *C. chinense* cultivars with different heat levels showed different responses to altered light intensities. Cultivar Akanee Pirote exhibited the highest capsaicinoid yield under 50% shading, while cultivar Bhut Jolokia had the highest capsaicinoid yield under 70% shading. These results show that particular shading levels can be used to maximize the capsaicinoid yield for certain high pungency cultivars of *C. chinense*.

Acknowledgements: The authors are grateful to The Royal Golden Jubilee (RGJ) Ph.D. Program, Thailand Research Fund (TRF); National Science of Thailand and Development Association (NSTDA); National Research University Project of Thailand, Office of the Higher Education Commission, through the Food and Functional Food Research Cluster of Khon Kaen University. We also thank the Plant Breeding Research Center for Sustainable Agriculture, Khon Kaen University and, New Mexico State University for financial support. Acknowledgement is extended to the Thailand Research Fund (TRF) (Project code: IRG5780003), Khon Kaen University (KKU) and the Faculty of Agriculture KKU for providing financial support for manuscript preparation activities.

Literature Cited

Bosland PW, Baral JB (2007) 'Bhut Jolokia' The world's hottest known chile pepper is a putative naturally occurring interspecific hybrid. HortScience 42:222-224

Bosland PW, Coon D, Reeves G (2012) 'Trinidad Moruga Scorpion' Pepper is the world's hottest measured chile pepper at more than two million scoville heat units. HortTechnology 22:534-538

Bosland PW, Votava E (2012) Peppers: vegetable and spice capsicums. 2nd ed. CAB International, United Kingdom

Collins MD, Wasmund LM, Bosland PW (1995) Improved method for quantifying capsaicinoids in *Capsicum* using high-performance liquid chromatography. HortScience 30:137-139

Cochran H (1936) Some factors influencing growth and fruit-setting

in the pepper (*Capsicum frutenscens* L.). NY. (Cornell). Agricultural Experiment Station Memoir. 190:1-39

DeWitt D, Bosland PW (2009) The complete chile pepper. Timber Press, Portland, OR

Díaz-Pérez JC (2013) Bell pepper (*Capsicum annuum* L.) crop as affected by shade level: Microenvironment, plant growth, leaf gas exchange, and leaf mineral nutrient concentration. HortScience 48:175-182

Díaz-Pérez JC (2014) Bell pepper (*Capsicum annuum* L.) crop as affected by shade level: fruit yield, quality, and postharvest attributes, and incidence of phytophthora blight (caused by *Phytophthora capsici* Leon). HortScience 49:891-900

Erdost H, Özer A, Yakışık M, Özfiliz N, Zık B (2006) FSH and LH cells in the laying hens and cocks, fed with a diet containing red hot pepper. J Food Agric Environ 4:119-123

Gomez KA, Gomez AA (1984) Statistical procedures for agricultural research. 2nd Ed. Wiley, New York

Gurung T, Techawongstien S, Suriharn B, Techawongstien S (2011) Impact of environments on the accumulation of capsaicinoids in *Capsicum* spp. HortScience 46:1576-1581

Gurung T, Techawongstien S, Suriharn B, Techawongstien S (2012) Stability analysis of yield and capsaicinoids content in chili (*Capsicum* spp.) grown across six environments. Euphytica 187:11-18

Hoffman PG, Lego MC, Galetto WG (1983) Separation and quantitation of red pepper major heat principles by reverse-phase high-pressure liquid chromatography. J Agr Food Chem 31:1326-1330

Iwai K, Suzuki T, Fujiwake H (1979) Formation and accumulation of pungent principle of hot pepper fruits, capsaicin and its analogues, in *Capsicum annuum* var. *annuum* cv. Karayatsubusa at different growth stages after flowering. Agr Biol Chem 43:2493-2498

Marcelis LFM, Heuvelink E, Baan Hofman-Eijer LR, Den Bakker J, Xue LB (2004) Flower and fruit abortion in sweet pepper in relation to source and sink strength. J Exp Bot 55:2261-2268

Möller M, Assouline S (2007) Effects of a shading screen on microclimate and crop water requirements. Irrig Sci 25:171-181

Moura JCMS, Bonine CAV, Viana JOF, Dornelas MCD, Mazzafera P (2010) Abiotic and biotic stresses and changes in the lignin content and composition in plants. J Integr Plant Biol 52:360-376

Pacheco FV, Alvarenga ICA, Ribeiro Junior PM, Pinto JEBP, Avelar RDP, Alvarenga AA (2014) Growth and production of secondary compounds in monkey-pepper (*Piper aduncum* L.) leaves cultivated under altered ambient light. Aust J Crop Sci 8:1510-1516

Prasad NBC, Shrivastava R, Ravishankar GA (2005) Capsaicin: a promising multifaceted drug from *Capsicum* spp. Evid Base Integr Med 2:147-166

Patricia I (1999) Recent techniques in fertigation of horticultural crops in Israel. Available via http://www.ipipotash.org/presentn/rtifohc. Accessed 15 Jan. 2009

Phimchan P, Techawongstien S, Chanthai S, Bosland PW (2012) Impact of drought stress on the accumulation of capsaicinoid in *Capsicum* cultivar with different initial capsaicinoid levels. HortScience 47:1-6

Phimchan P, Chanthai S, Bosland PW, Techawongstien S (2014) Enzymatic changes in phenylalanine ammonia-lyase, cinnamic-4-hydroxylase, capsaicin synthase, and peroxidase activities in *Capsicum* under drought stress. J Agr Food Chem 62:7057-7062

Rahman MJ, Inden H (2012) Effect of nutrient solution and temperature on capsaicin content and yield contributing characteristics in six sweet pepper (*Capsicum annuum* L.) cultivars. J Food Agric and Environ 10:524-529

Rylski I, Spigelman M (1982) Effects of different diurnal temperature combinations on fruit set of sweet pepper. Sci Hortic 17:101-106

Rylski I, Spigelman M (1986) Effect of shading on plant development, yield and fruit quality of sweet pepper grown under conditions of high temperature and radiation. Sci Hortic 29:31-35

Saha SR, Hossain MM, Rahman MM, Kuo CG, Abdullah S (2010) Effect of high temperature stress on the performance of twelve sweet pepper genotypes. Bangladesh J Agric Res 35:525-534

Suzuki T, Iwai K (1984) Constituents of red pepper species: Chemistry, biochemistry, pharmacology, and food science of the pungent principle of *Capsicum* species. In: Brossi, A. (ed.). The alkaloids: Chemistry and pharmacology. Academic Press, Orlando, FL

Thimijan RW, Heins RD (1982) Photometric, radiometric, and quantum light units of measure: a review of procedures for interconversion. HortScience 18:818-822

Turner AD, Wien HC (1994) Dry matter assimilation and partitioning in pepper cultivars differing in susceptibility to stress-induced bud and flower abscission. Ann Bot 73:617-622

Valiente-Banuet JI, Gutiérrez-Ochoa A (2016) Effect of irrigation frequency and shade levels on vegetative growth, yield, and fruit quality of piquin pepper (*Capsicum annuum* L. var. *glabriusculum*). HortScience 51:573-579

Wien HC (1997) Peppers. *In* Wien, H.C. (ed.). The physiology of vegetable crops. CAB International, Ithaca, NY, pp 259-293

Zewdie Y, Bosland PW (2000) Evaluation of genotype, environment, and genotype-by-environment interaction for capsaicinoids in *Capsicum annuum* L. Euphytica 111:185-190

Hindawi
Oxidative Medicine and Cellular Longevity
Volume 2017, Article ID 5187102, 12 pages
https://doi.org/10.1155/2017/5187102

Research Article

Neuroprotective and Memory-Enhancing Effect of the Combined Extract of Purple Waxy Corn Cob and Pandan in Ovariectomized Rats

Woranan Kirisattayakul,[1,2] Jintanaporn Wattanathorn,[2,3] Sittichai Iamsaard,[4] Jinatta Jittiwat,[5] Bhalang Suriharn,[6] and Kamol Lertrat[6]

[1]*Department of Physiology and Graduate School (Neuroscience Program), Faculty of Medicine, Khon Kaen University, Khon Kaen 40002, Thailand*
[2]*Integrative Complementary Alternative Medicine Research and Development Center, Khon Kaen University, Khon Kaen 40002, Thailand*
[3]*Department of Physiology, Faculty of Medicine, Khon Kaen University, Khon Kaen 40002, Thailand*
[4]*Department of Anatomy, Faculty of Medicine, Khon Kaen University, Khon Kaen 40002, Thailand*
[5]*Faculty of Medicine, Mahasarakham University, Maha Sarakham 44150, Thailand*
[6]*Faculty of Agriculture, Khon Kaen University, Khon Kaen 40002, Thailand*

Correspondence should be addressed to Jintanaporn Wattanathorn; jintanapornw@yahoo.com

Received 7 March 2017; Accepted 1 June 2017; Published 9 July 2017

Academic Editor: Luciano Saso

The neuroprotectant and memory enhancer supplement for menopause is required due to the side effects of hormone replacement therapy. Since purple waxy corn cob and pandan leaves exert antioxidant and acetylcholinesterase inhibition (AChEI) effects, we hypothesized that the combined extract of both plants (PCP) might provide synergistic effect leading to the improved brain damage and memory impairment in experimental menopause. To test this hypothesis, female Wistar rats were ovariectomized bilaterally and orally given various doses of the functional drink at doses of 20, 40, and 80 mg/kg for 28 days. The animals were assessed nonspatial memory using object recognition test every 7 days throughout the study period. At the end of study, they were assessed with oxidative stress status, AChEI, neuron density, and ERK1/2 signal in the prefrontal cortex (PFC). Interestingly, all doses of PCP increased object recognition memory and neuron density but decreased oxidative stress status in PFC. Low dose of PCP also decreased AChE activity while medium dose of PCP increased phosphorylation of ERK1/2 in PFC. Therefore, the improved oxidative stress status and cholinergic function together with signal transduction via ERK in PFC might be responsible for the neuroprotective and memory-enhancing effects of PCP.

1. Introduction

To date, the number of menopausal women is continually growing. The World Health Organization (WHO) has estimated that the number of menopausal women worldwide will be 1200 million within 2030 [1]. It has been reported that cognitive decline is one of the important symptoms frequently observed especially in premature menopause [2]. Unfortunately, the current therapeutic strategy is still not in satisfaction level. The effect of hormone replacement therapy (HRT) on the cognitive function of menopausal women is controversial [3–7]. In addition, serious adverse effect such as breast cancer risk is reported in HRT [8, 9]. Therefore, the alternative strategy has gained much attention.

Among various alternative strategies, plant-based therapy is very much popular [10]. In the recent years, the use of plant-based food supplement is increased in Thailand [11]. It has been demonstrated that dietary approaches are regarded as the safe and effective preventive intervention against neurodegeneration [12]. A pile of evidence has

revealed that consumption of the polyphenol-rich supplements can enhance memory impairment [13–15]. Recent findings have demonstrated that the purple corn (*Zea mays* Linn., purple color) cob, an agricultural waste, can be served as an important natural resource of polyphenol [16]. It also exhibits potent antioxidant activity and can improve oxidative stress-related disorders [16, 17]. In addition to purple corn cob, pandan (*Pandanus amaryllifolius*), a commonly used culinary plant in Southeast Asia, also possesses high phenolic compound content and exhibits antioxidant activity [18]. An effervescent powder containing pandan also improves oxidative stress-related damage of the pancreas [19]. Based on these pieces of information and synergistic effect according to traditional folklore concept, the protective effect against oxidative stress-related brain damage and functional disorders of the combined extract of purple corn cob and pandan leaves (PCP) in menopausal women has been considered in order to produce an additive value of both plants. Currently, no data concerning this issue are available until now. Therefore, we aimed to determine the neuroprotective and memory-enhancing effects of the combined extract of purple corn cob and pandan leaves in experimental menopause in ovariectomized rats.

2. Materials and Methods

2.1. Chemicals and Reagents. Thiobarbituric acid (TBA), sodium dodecyl sulfate (SDS), glacial acetic acid, N-butanol, pyridine, 1,3,3-tetraethoxypropane (TEP), cytochrome C, xanthine oxidase, xanthine, glutathione reductase, nicotinamide adenine dinucleotide phosphate (NADPH), hydrogen peroxide, superoxide dismutase, glutathione peroxidase, catalase, acetylthiocholine iodide (ATCI), acetylcholinesterase, 5,5′-dithiobis (2-nitrobenzoic acid) (DTNB), cresyl violet, sodium acetate, sodium carbonate, 2,4,6-tripyridyl-striazine (TPTZ), Folin-Ciocalteu reagent, gallic acid, ascorbic acid, Trizma hydrochloride, potassium chloride, 2,2-diphenyl-1-picrylhydrazyl (DPPH), tris-hydrochloride, and sodium carbonate were purchased from Sigma-Aldrich (St. Louis, MO, USA). Chemicals used in Western blot analysis were purchased from Bio-Rad Laboratories. Methanol and acetic acid (HPLC grade) were purchased from Fisher Scientific.

2.2. Plant Material Preparation and Extraction. The cobs of purple waxy corn (*Zea mays*, open-pollinated cultivar) harvested during November–December 2012 were identified and kindly provided by Professor Kamol Lertrat and Assistant Professor Bhalang Suriharn, Department of Plant Science and Agricultural Resources, Faculty of Agriculture, Khon Kaen University, Khon Kaen, Thailand. Pandan (*Pandanus amaryllifolius*) leaves were harvested at the same period as *Z. mays* from the Khon Kaen province. The plant identification was performed by Mister Winai Somprasong, an expert agricultural scientist in the Botany and Plant Herbarium research group, Plant Varieties Protection Division, Ministry of Agriculture and Cooperatives. The cobs of *Z. mays* and the leaves of *P. amaryllifolius* were cleaned and cut into a small pieces; then, they were force dried by using an oven at 60°C overnight. The dried plants (2 kilograms of each plant) were twice extracted with 5 liters of distilled water. The percent yield of *Z. mays* and *P. amaryllifolius* were 2.4 and 8, respectively.

2.3. Preparation of a Polyphenol-Rich Functional Drink. Powder of various ingredients including 2% (*w*/*v*) combined extract of *Z. mays* and *P. amaryllifolius* (a ratio of both extracts was obtained from our unpublished in vitro data which provided optimum potential and under petit patent), 0.75% (*v*/*v*) sucralose, 1% (*v*/*v*) lemonade, 0.025% (*w*/*v*) salt, and 96.225% (*v*/*v*) water. All ingredients were mixed together and filtered through a cheesecloth, and the filtrate was used for further study.

2.4. Determination of Total Phenolic Compound Contents. The determination of total phenolic compounds content was carried out by using the Folin-Ciocalteu method [20]. In brief, an aliquot of combined extract beverage (20 μl) was added to distilled water (1.58 ml) and 50% (*v*/*v*) Folin-Ciocalteu phenol reagent (0.1 ml) (Sigma-Aldrich). After 8 minutes of incubation, 20% sodium carbonate (0.3 ml) was added and mixed well. The mixture was kept in a dark room and incubated for 2 hours at room temperature. The absorbance was measured at 765 nm with a UV-spectrophotometer (Pharmacia LKB-Biochrom4060). Gallic acid at concentrations of 50–600 mg/l were used for preparing the standard calibration curve. The total phenolic compound was expressed as gallic acid equivalents per mg extract (mg/l GAE).

2.5. Assessment of DPPH Inhibition. The scavenging activity against free radicals of the developed drink was assessed via DPPH assessment. Briefly, 0.15 mM DPPH in methanol (0.5 ml) and the functional drink (1 ml) were mixed and incubated at room temperature for 30 minutes. The absorbance was determined at 517 nm with a UV-spectrophotometer (Pharmacia LKB-Biochrom4060). The DPPH radical scavenging activity was calculated using the following equation:

$$\%\text{Inhibition of DPPH} = \left[\left(\frac{\text{Abs control} - \text{Abs sample}}{\text{Abs control}}\right)\right] \times 100. \quad (1)$$

Abs control was the absorbance of methanol plus DPPH reagent while Abs sample was the absorbance of developed drink or standard. The linear portion of percentage inhibition of combined extract beverage was plotted against its concentration. The half maximal inhibitory concentration (IC_{50}) was calculated by using the equation from its graph [21]. All determinations were performed in triplicate.

2.6. Determination of Ferric-Reducing Antioxidant Power (FRAP) Assay. The assessment of ferric-reducing antioxidant power (FRAP) was performed based on the ability of the tested substance to reduce ferric tripyridyl triazine (Fe III TPTZ) complex to ferrous form (intense blue color) at low pH by using a modified method of Benzie and Strin [22]. FRAP reagent was freshly prepared by mixing solution A (300 mM acetate buffer pH 3.6), solution B (10 mM 2,4,6-

tripyridyl-striazine (TPTZ) in 40 mM HCl), and solution C (20 mM ferric chloride) together at a ratio of A : B : C; 10 : 1 : 1, respectively, and kept in water bath at 37°C. The tested substance (50 μl) was added to FRAP reagent (1.45 ml), mixed thoroughly, and incubated at 37°C for 10 minutes. The absorbance was measured with spectrophotometer at 593 nm (Pharmacia LKB-Biochrom4060). FRAP reagent and L-ascorbic acid (100–1000 μM) were used as blank and standard calibration, respectively. Data were expressed as μM L-ascorbic acid equivalent.

2.7. Determination of Anthocyanin Content. Anthocyanin content was determined according to the official method of the Association of Official Analytical Chemists (AOAC) [23]. The tested sample (1 ml) was mixed with 0.025 M potassium chloride pH 1.0 (2 ml) or 0.4 M sodium acetate pH 4.5 (2 ml). After the incubation at room temperature for 10 minutes, the absorbance was determined at 520 and 720 nm using a UV-spectrophotometer (Pharmacia LKB-Biochrom 4060). All assessments were performed as triplicate. Anthocyanin content was calculated and expressed as mg/l cyaniding-3-glucoside equivalent/mg extract (mg/l CGE) as follows:

$$\text{Anthocyanin content} \left(\frac{\text{cyanindin} - 3 - \text{glucoside equivalent, mg}}{\text{l}}\right) = \frac{\left(\text{A} \times \text{MW} \times \text{DF} \times 10^3\right)}{(\varepsilon \times 1)}, \quad (2)$$

where A = (A 520 nm–A 700 nm) pH 1.0 – (A 520 nm–A 700 nm) pH 4.5, MW (molecular weight) = 449.2 g/mol, DF = dilution factor obtained from the study, ε = 26,900 molar extinction coefficient, in l mol^{-1} cm^{-1}, for cyanindin-3-glucoside, 10^3 = factor for conversion from g to mg, and l = path length of the cuvette in cm (1 cm).

2.8. Assessment of Acetylcholinesterase Inhibitory (AChEI) Activity. Inhibition of acetylcholinesterase of the sample was determined according to the method previously described [24] using acetylthiocholine chloride iodide (ATCI) as a substrate. In brief, combined extract beverage (25 μl) was incubated with 15 mM ATCI (25 μl), 3 mM DTNB (5,5′-dithiobis[2-nitrobenzoic acid]) (75 μl), and 50 mM Tris buffer (pH 8) (50 μl) for 5 minutes at room temperature. The absorbance was measured with a microplate reader (iMark™ Microplate Absorbance Reader) at 415 nm before and after adding 0.25 units/ml acetylcholinesterase (AChE) (25 μl) to the mixture. The elevation of yellow color from the reaction was obtained and the percentage inhibition was calculated by comparing the yellow color of extract to a noninhibition well (Tris buffer). All tests were conducted in triplicate.

2.9. Fingerprint Chromatogram Assessment. The fingerprint chromatogram of the developed drink was analyzed by using gradient high-performance liquid chromatography (HPLC) system. High-performance liquid chromatography (HPLC) system consisted of 515 HPLC pump and 2998 photodiode array detector (Water Company, USA). Chromatographic separation was performed using Purospher®STAR, C-18 endcapped (5 μm), LiChroCART®250-4.6, and HPLC-Cartridge, sorbet lot number HX255346 (Merk, Germany) with guard column (Merk, Germany). Methanol (A) and 7.5% acetic acid in deionized (DI) water (B) were used as mobile phases. The gradient elution was carried out at a flow rate of 1.0 ml/min with the following gradient: 0–17 min, 70%A; 18–22 min, 100%A; 23–25, 50%A; and 26–30 min, 60%A. The sample was filtered (0.45 μm, Millipore), and a direct injection of tested sample at the volume of 20 μl on the column was performed. The chromatograms were recorded at 280 nm using a UV detector and data analysis was performed using EmpowerTM3.

2.10. Experimental Animals and Protocols. Female Wistar rats (Laboratory Animal Center, Salaya, Nakhon Pathom, Thailand), weighing 200–250 g, were used as the experimental animals. They were randomly housed 6 per cage in a temperature-controlled room on a 12 h light/dark cycle with ad libitum access to food and water. All procedures in this experiment were strictly performed in accordance with the internationally accepted principles for laboratory use and care of the European Community (EEC directive of 1986; 86/609/EEC). The experiment protocols were approved by the Institutional Animal Care and Unit Committee, Khon Kaen University, Thailand (record number AEKKU 1/2556).

The experimental rats were divided into 8 groups (n = 6/group) as follows:

Group I: Naïve intact group; all rats received no treatment and were served as the control group.

Group II: Sham operation + vehicle; all rats were subjected to sham operation surgery and received distilled water which was served as the vehicle in this study.

Group III: OVX + vehicle; the experimental animals in this group were subjected to bilateral ovariectomy (OVX) and received the vehicle.

Group IV: OVX + donepezil (3 mg/kg BW); the OVX rats were orally given donepezil, an acetylcholinesterase inhibitor, at a dose of 3 mg/kg and were served as the positive control-treated group.

Group V: OVX + isoflavone; all OVX rats were orally given isoflavone, a well-known polyphenol substance with cognitive enhancing, at a dose of 20 mg/kg BW.

Groups VI–VIII: OVX + PCP20, OVX + PCP40, and OVX + PCP80; the OVX rats in these groups received PCP at doses of 20, 40, and 80 mg/kg BW, respectively.

The treatment programs of the assigned substances for rats in groups II–VIII were started since the first day after surgery and were maintained throughout a 28-day experimental period. All treatments were performed once daily in the morning with the total volume of 1.5 ml. The assessment of nonspatial memory was performed every 7 days throughout the study period while the determinations of oxidative stress markers including malondialdehyde (MDA), superoxide dismutase (SOD), catalase (CAT), glutathione peroxidase (GSH-Px), the activity of acetylcholinesterase (AChE), histology, and ERK1/2 expression in the prefrontal cortex were determined at the end of the study.

2.11. Ovariectomized Surgery Procedure. The experimental animal was anesthetized with sodium thiopental at the dose of 60 mg/kg BW via intraperitoneal route prior to the ovariectomy. The ovariectomized (OVX) procedure was performed according to the method which had been previously described [25]. Briefly, the dorsolateral incisions were performed bilaterally, the ovarian blood vessels were tied off, and the ovaries were removed. Then, the skin was sutured and the rat was returned to their cage after postoperation care. Sham operation was carried out with the same procedures except that both the ovaries were kept intact.

2.12. Object Recognition Test. The object recognition test, the common test for evaluating nonspatial memory in rats, was used to assess the effect of PCP on nonspatial memory. This test was performed as previously described elsewhere with minor modification [26]. In brief, each rat was placed in an open field (80 cm long × 50 cm high × 60 cm wide) with two identical objects for 3 minutes (T1) and then was placed back to its home cage. Both objects should be placed in a symmetric position in the central line of the area. Then, the animal was orally given the assigned substance, and 30 minutes later, the second 3-minute trial was performed. In this session, one of the objects was replaced with the novel object which was totally different in shape and size at the same location. During the intertrial interval, the objects and open-field apparatus object were cleaned with 70% ethanol to avoid a confounding error induced by the influence of odor. The amount of time which the rat spent exploring each object was recorded and calculated as a novel object ratio (NOR) as the following equation:

$$\mathrm{NOR} = \frac{(T_{\mathrm{novel}} - T_{\mathrm{familiar}})}{(T_{\mathrm{novel}} + T_{\mathrm{familiar}})}, \quad (3)$$

where T_{novel} = time spent to explore the novel object and T_{familiar} = time spent to explore the familiar object.

2.13. Histological Study. After perfusion, the brains were removed and fixed with 4% paraformaldehyde solution (pH 7.4) at 4°C. Then, they were cryoprotected in formalin-sucrose (30%) for 2-3 days. Serial sections of tissue containing prefrontal cortex were cut frozen on a cryostat (Thermo Scientific™ HM 525 Cryostat) at 20 μm thick and mounted on slides coated with 0.3% aqueous solution of gelatin containing 0.05% aluminum potassium sulfate. To stain with cresyl violet, the slides were air dried; hydrated by successive immersion in 95, 70, and 50% ethanol; stained in 0.5% cresyl violet for 2 min at room temperature; dehydrated by successive immersion in 50, 70, 95, and 100% ethanol and xylene; and mounted with DPX. Three representative slides containing the prefrontal cortex were selected according to the stereotaxic coordinates anteroposterior 2.5–4.5 mm and mediolateral 0.2–1.0 mm from the rat brain atlas [27]. The analysis was performed by a blinded observer. The evaluation was performed via Olympus light microscope model BH-2 (Japan) at 40x magnification. The density of survival neurons in medial prefrontal cortex area (mPFC) was expressed as number of cells/255 μm^2.

2.14. Determination of Extracellular Signal-Regulated Kinase 1/2 (ERK1/2) Expression. The prefrontal cortex was subjected to a 2-minute homogenization in 1/10 (*w*/*v*) M-PER mammalian protein extraction (Pierce Protein Biology Product, Rockford, IL, USA) containing protease inhibitor cocktail (Sigma-Aldrich). Then, it was centrifuged at 14,000*g* for 10 minutes at 4°C. The supernatant was harvested and used for the determination of ERK1/2 expression. Protein concentration of the supernatant was quantified by using NanoDrop instrument (Thermo Fisher Scientific, Wilmington, Delaware USA). Total 30 μg of brain samples were separated by 10% sodium dodecyl sulfate polyacrylamide gel electrophoresis (SDS-PAGE) at 80 V. All protein bands were transferred.

The determination of ERK1/2 protein was performed according to the method previously described with a minor modification [28]. Total of 30 μg of brain samples were separated by 10% sodium dodecyl sulfate polyacrylamide gel electrophoresis (SDS-PAGE) at 80 V. Proteins from the gel were transferred to a nitrocellulose membrane (Bio-Rad Laboratories) and blocked with 5% nonfat dry milk in 0.1% tween 20 tris-buffered saline (TBS-T) for 30 minutes. After the blocking of a membrane, they were incubated with primary antibody which recognized ERK1/2 or monoclonal rabbit antiphosphorylated p44/p42 mitogen-activated protein kinase (MAPK) (Cell Signaling Technology Inc.; dilution, 1 : 1000) for 2 hours at room temperature. Then, they washed and incubated with secondary antibody conjugated with horseradish peroxidase or anti-rabbit IgG, HRP-linked antibody (Cell Signaling Technology Inc.; dilution, 1 : 2000) for 2 hours at room temperature. The band density was detected with an enhanced chemiluminescent (ECL) system (GE Healthcare, Piscataway, NJ). The analysis was performed using ImageQuant TL analysis software (GE Healthcare, Piscataway, NJ). The expression was normalized using antitotal ERK1/2. Data were presented as a relative density to the naïve control.

2.15. Biochemical Assays. The prefrontal cortex, an important area in learning and memory, was isolated and prepared as brain homogenate by subjecting to homogenization with 50 volume of 0.1 M phosphate buffer saline. Then, the homogenate was used for the determination of acetylcholinesterase (AChE) activity and oxidative stress status including malondialdehyde (MDA) level and the activities of superoxide dismutase (SOD), catalase (CAT), and glutathione peroxidase (GSH-Px). Protein concentration was assessed according to the Lowry method [29] and albumin bovine serum (2–20 mg/ml) was used as a standard.

The determination of AChE was carried out to reflect the cholinergic function in OVX rats by the colorimetric method [30]. A reaction mixture of 200 μl of 0.1 mM sodium phosphate buffer (pH 8.0), 10 μl of 0.2 M DTNB (5,5′-dithio-bis-(2-nitrobenzoic acid)), and 20 μl of the sample solution were incubated for 5 minutes, and the absorbance at 415 nm was recorded via microplate reader (iMark Microplate Absorbance Reader). Then, 10 μl of acetylcholine thiochloride (ACTI) was added, incubated for 3 minutes, and recorded the absorbance at 415 nm. The activity of AChE was

calculated according to the equation below and expressed as mmol/min/g protein.

$$\text{AChE activity} = \left(\Delta A/1.36 \times 10^4\right) \times 1/(20/230)C, \quad (4)$$

where ΔA = the difference of absorbance/minute and C = protein concentration of brain homogenate.

MDA level was assessed according to the method of Thiraphatthanavong et al. [31]. In brief, the mixture of 0.1 ml of brain homogenate, 0.1 ml of 8.1% (*w*/*v*) sodium dodecyl sulfate, 0.75 ml of 20% (*v*/*v*) acetic acid pH 3.5, 0.75 ml of 0.8% (*w*/*v*) thiobarbituric acid, and 0.3 ml of distilled water were mixed thoroughly and boiled at 95°C for 1 hour. After cooling, 0.5 ml of water and 2.5 ml of the mixture of n-butanol and pyridine at the ratio of 15 : 1 were added, mixed together, and centrifuged at 4000 rpm for 10 minutes. The pink layer was harvested and determined the optical density at 532 nm. 1,1,3,3-tetramethoxypropane (2–20 nmol) was served as a standard and MDA level was expressed as nmol/mg protein.

SOD assessment was performed according to the method previously described elsewhere [32]. Briefly, 20 μl of brain homogenate was mixed with the mixture which contained 216 mM potassium phosphate buffer (KH_2PO_4), 10.7 mM ethylenediaminetetraacetic acid, 1.1 mM cytochrome C, and 0.54 mM xanthine solution pH 7.4 at the ratio of 25 : 1 : 1 : 50. Then, 20 μl of 0.05 units/ml of xanthine oxidase was added and incubated for 5 minutes at room temperature. The absorbance was measured at 490 nm using microplate reader. SOD enzyme activities at the concentrations of 0–10 units/ml were used as standards, and the results were expressed as units/mg protein.

The activity of catalase (CAT) was evaluated indirectly by measuring the residual H_2O_2 which was titrated by potassium permanganate. In brief, 10 μl of brain homogenate was mixed with 50 μl of 30 mM H_2O_2, 25 μl of 5 N H_2SO_4, and 150 μl of 5 mM $KMnO_4$. The mixture was shaken and the absorbance was measured at 490 nm. CAT enzyme at the concentration range of 0–10 units/ml was used as a standard and the result was expressed as units/mg protein [32].

Glutathione peroxidase activity was assessed using the colorimetric method. In brief, 10 μl of brain homogenate was mixed with the mixture containing 50 μl of 30 mM H_2O_2, 25 μl of 5 N H_2SO_4, and 150 μl of 5 mM $KMnO_4$. The mixture was shaken and the absorbance was measured at 490 nm. The standard calibration curve was prepared by using CAT enzyme at the concentration range of 0–10 units/ml. CAT activity was expressed as units/mg protein [32].

2.16. Statistical Analysis. Data are presented as mean ± standard error of mean (SEM). The statistical analysis of the experiment was carried out using IBM SPSS Statistics (version 21). Data was analyzed using one-way analysis of variance (ANOVA), followed by Tukey's post hoc test. Probability levels less than 0.05 were accepted as significant.

Table 1: The biological activity of PCP including total phenolic compound, anthocyanin content, DPPH radical activity, FRAP activity, and AChEI activity.

Test	PCP	Standard reference
Total phenolic compound (mg/l GAE)	184 ± 1.91	—
Anthocyanin content (mg/l CGE)	25.66 ± 0.32	—
FRAP activity (μM L-ascorbic acid equivalent)	602.40 ± 2.33	—
DPPH radical activity (IC_{50} μg/ml)	56.37 ± 0.45	Ascorbic acid 2.89 ± 0.01
AChEI activity (IC_{50} μg/ml)	1950 ± 16.02	Donepezil 0.51 ± 0.03

3. Results

3.1. Biological Activities of the Combined Extract. Total phenolic compounds and anthocyanin content together with the biological activities including the antioxidant activity (DPPH and FRAP assay) and acetylcholinesterase inhibition activity of the combined extract were evaluated. The results showed that 1 ml of the combined extract contained the total phenolic compounds and anthocyanin contents of 184.00 ± 1.91 mg/l gallic acid equivalent and 25.66 ± 0.32 mg/l cyanidin-3-glucoside equivalent, respectively. IC_{50} of the antioxidant activity via 2,2-diphenyl-1-picrylhydrazyl (DPPH) assay was 56.37 ± 0.45 μg/ml, whereas the antioxidant activity via ferric-reducing antioxidant power (FRAP) assay was 602.40 ± 2.33 μM L-ascorbic acid equivalent. In addition, AChEI activity showed IC_{50} at a concentration of 1950 ± 16.02 μg/ml as shown in Table 1.

3.2. The Fingerprint of the Combined Extract. Figure 1 shows the fingerprint chromatogram of PCP, the combined extract of purple corn cob and pandan leaves. More than 7 different peaks were observed in the chromatogram. Four of them were anthocyanins (peak 2–peak 5) including cyaniding-3-glucoside (peak 2), pelargonidin-3-glucoside (peak 3), cyanidin 3-O-(6″-malonyl-glucoside) (peak 4), and cyaniding-3-o-B-glucopyranoside (peak 5). It was found that the contents of anthocyanins mentioned earlier in PCP were 3.239 ± 0.014, 2.543 ± 0.011, 2.993 ± 0.024, and 2.335 ± 0.006 mg/ml, respectively. In addition to anthocyanins, gallic acid, rutin, and ferulic acid were observed at the concentrations of 0.180 ± 0.001, 0.337 ± 0.001, and 0.341 ± 0.027 mg/ml, respectively.

3.3. Effect of the Combined Extract on Nonspatial Memory in OVX Rats. Memory-enhancing effect of the combined extract on nonspatial memory was shown in Figure 2. It was found that sham operation rats showed no significant change on novel object ratio (NOR). OVX rats treated with vehicle significantly decreased NOR throughout the study period (p value < 0.01, 0.01, 0.05, and 0.05, resp., compared with the sham operation group). OVX rats with isoflavone treatment attenuated the reduction of NOR induced by OVX throughout the study period (p value < 0.01, 0.05, 0.01, and

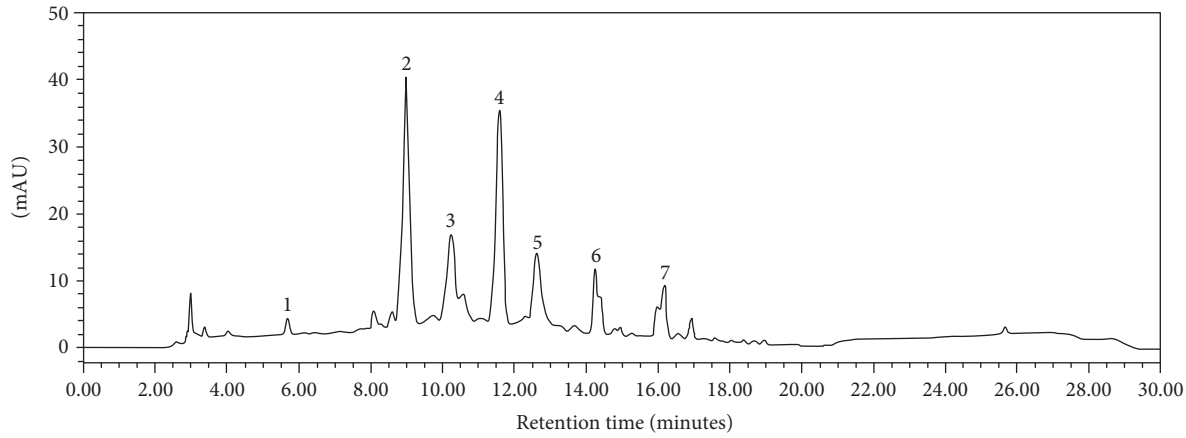

Figure 1: The fingerprint chromatogram of the PCP using HPLC analysis.

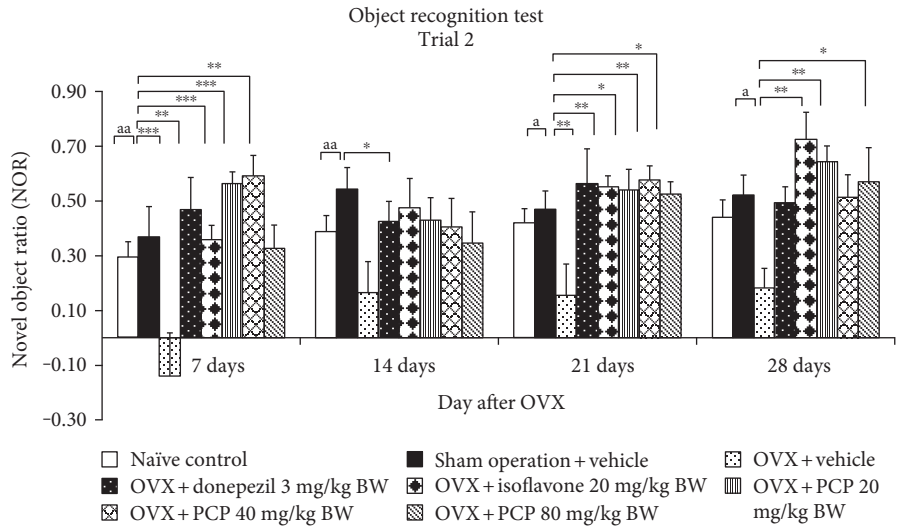

Figure 2: The effect of the PCP on nonspatial memory assessing by the object recognition test ($n = 6$/group). Data were expressed as mean ± SEM. $^{a, aa}p$ value < 0.05, 0.01, respectively, compared with the sham operation group. *, **, $^{***}p$ value < 0.05, 0.01, and 0.001, respectively, compared with the OVX + vehicle-treated group.

0.01, resp., compared with OVX + vehicle). Donepezil also showed the mitigation effect on the reduction of NOR in OVX rats, but significant differences were observed only at 7- and 21-day treatment periods (p value < 0.001 and 0.01, resp., compared with the OVX + vehicle-treated group). The combined extract at doses of 20 and 80 mg/kg BW significantly attenuated the decreased NOR in OVX rats at 7, 21, and 28 days of treatment (p value < 0.001 and 0.01; 0.05 all; and 0.01 and 0.05, resp., compared with the OVX + vehicle-treated group). The significant mitigation effect of PCP at a dose of 40 mg/kg BW on NOR was also observed at 7 and 21 days of treatment (p value < 0.001 and 0.01, resp., compared with the OVX + vehicle-treated group). The increased NOR in the PCP treatment groups were also observed at a 14-day study period, but no significant difference was revealed.

3.4. Histological Change in the Prefrontal Cortex. Based on the previous finding that the prefrontal cortex played a crucial role on working memory in rodents [33], we also investigated the neuron density in this area and results were shown in Figure 3. The current results demonstrated that OVX treated with vehicle significantly reduced the neuron density in PFC (p value < 0.05, compared with the sham operation group). Both donepezil and isoflavone could attenuate the reduction of neuron density in PFC of OVX rats (p value < 0.01 all; compared with the OVX + vehicle-treated group). In addition, combined extract at the dosage range used in this study also significantly attenuated the reduction of neuron density in PFC of OVX rats (p value < 0.01, 0.01, and 0.05; compared with the OVX + vehicle-treated group).

3.5. Biochemical Assays. Table 2 shows the effect of PCP on oxidative stress markers including MDA level and the activities of SOD, CAT, and GSH-Px. Sham operation showed no significant changes of the mentioned parameters. OVX rats which received vehicle significantly increased MDA level (p value < 0.05; compared to the sham operation group) in the prefrontal cortex (PFC). Donepezil treatment

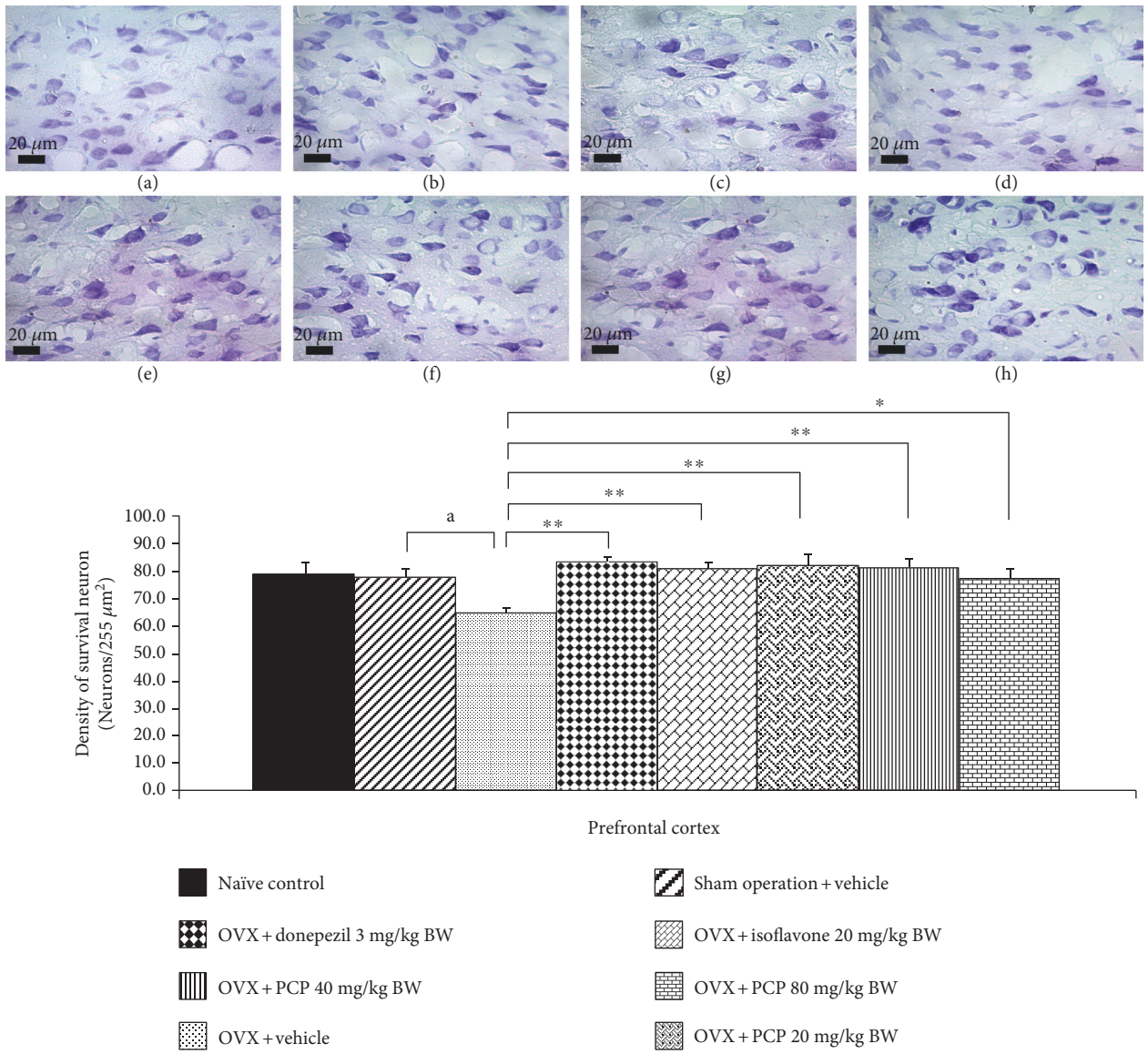

Figure 3: The effect of the PCP on the density of survival neurons in medial prefrontal cortex (mPFC) ($n = 6$/group). The upper panel showed the photomicrograph of the coronal section of rat brains in (a) naïve control, (b) sham operation + vehicle, (c) OVX + vehicle, (d) OVX + donepezil, (e) OVX + isoflavone, (f) OVX + PCP 20 mg/kg BW, (g) OVX + PCP 40 mg/kg BW, and (h) OVX + PCP 80 mg/kg BW. Scale bar: 20 μm. The lower panel demonstrated the density of survival neurons of mPFC. ^{a}p value < 0.05, compared with the sham operation group. *, $^{**}p$ value < 0.05 and 0.01, respectively, compared with the OVX + vehicle-treated group. Data were expressed as mean ± SEM.

failed to produce the significant changes on all parameters just mentioned in OVX rats. However, isoflavone significantly decreased MDA level but enhanced SOD activity (p value < 0.05 and 0.01, resp., compared to the OVX + vehicle-treated group). Interestingly, PCP at all doses used in this study significantly decreased MDA level in PFC (p value < 0.001 all; compared to the OVX + vehicle-treated group). The elevation of SOD activity in PFC was observed in OVX rats which received PCP at the concentrations of 20 and 40 mg/kg BW (p value < 0.001 and 0.01, resp., compared with the OVX + vehicle-treated group).

Since the cholinergic system plays a crucial role on learning and memory [34], we also investigated the effect of PCP on the cholinergic system by using the suppression activity of AChE or AChEI activity as an indirect index, and results were shown in Figure 4. It was found that both sham operation and OVX rats which received vehicle failed to produce the significant changes of AChE. The decreased AChE activity was observed in OVX rats which received donepezil and combined extract at the dose of 20 mg/kg BW (p value < 0.05 and 0.01, resp., compared with the OVX rats + vehicle-treated group). When compared with OVX rats which received vehicle, no significant changes of AChE were observed in the other groups.

3.6. ERK1/2 Signaling Pathway. Based on the crucial role of ERK1/2 on the survival neurons and memory enhancement [28], the effect of PCP on the phosphorylation ERK1/2

Table 2: The effect of PCP on oxidative stress markers in the prefrontal cortex ($n = 6$/group).

Treatment	Oxidative stress markers in the prefrontal cortex			
	MDA (nmol/mg protein)	GSH-Px (Units/mg protein)	SOD (Units/mg protein)	CAT (Units/mg protein)
Naïve control	0.073 ± 0.0.001	0.661 ± 0.034	0.567 ± 0.164	2.707 ± 0.234
Sham operation	0.077 ± 0.007	0.576 ± 0.052	0.834 ± 0.256	2.516 ± 0.237
OVX + vehicle	0.095 ± 0.008[a]	0.523 ± 0.034	0.309 ± 0.100	2.684 ± 0.216
OVX + donepezil 3 mg/kg BW	0.090 ± 0.007	0.714 ± 0.047	1.387 ± 0.344	2.650 ± 0.187
OVX + isoflavone 20 mg/kg BW	0.059 ± 0.005*	0.902 ± 0.111	2.220 ± 0.458**	2.130 ± 0.210
OVX + PCP 20 mg/kg BW	0.047 ± 0.012***	0.866 ± 0.186	3.080 ± 0.352***	2.447 ± 0.359
OVX + PCP 40 mg/kg BW	0.034 ± 0.002***	0.799 ± 0.070	2.047 ± 0.184**	2.151 ± 0.160
OVX + PCP 80 mg/kg BW	0.032 ± 0.004***	0.639 ± 0.029	1.068 ± 0.366	1.921 ± 0.092

[a]p value < 0.05, compared with the sham operation group. *, **, ***p value < 0.05, 0.01, and 0.001, respectively, compared with the OVX + vehicle-treated group. Data were expressed as mean ± SEM.

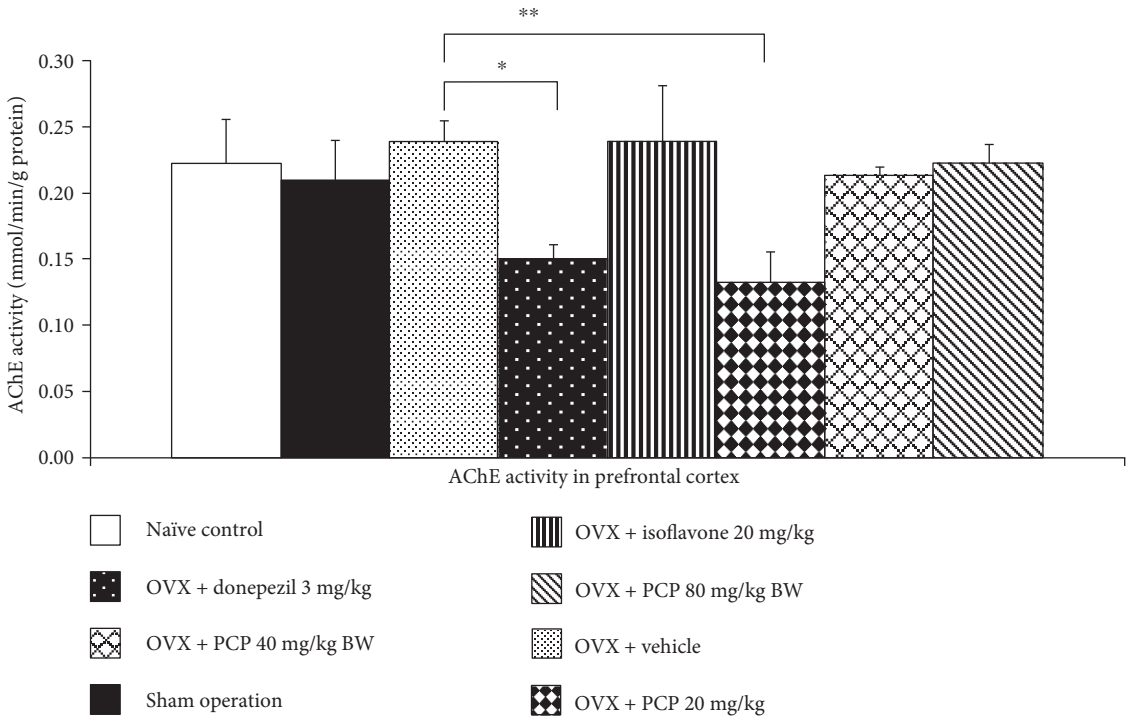

Figure 4: The effect of PCP on the activity of AChE in the prefrontal cortex ($n = 6$/group). *, **p value < 0.05 and 0.01, respectively, compared with the OVX + vehicle-treated group. Data were expressed as mean ± SEM.

was also determined, and results were shown in Figure 5. The current data showed that OVX rats significantly decreased expression of phosphorylation ERK1/2 in PFC (p value < 0.001; compared with the sham operation group). Isoflavone and medium dose of PCP produced the significant attenuation effect induced by OVX (p value < 0.01 and 0.05, resp., compared with the OVX + vehicle-treated group).

4. Discussion

The current data showed that ovariectomy, a widely used model of menopause, increased oxidative stress status, impairment of the cholinergic system, and memory impairment which were in concordance with the previous study [35, 36]. In the present study, it was found that OVX increased MDA without changes of the main scavenger enzymes such as SOD, CAT, and GSH-Px. This was in agreement with the previous study [37]. These results suggested that the elevation of MDA level might occur either via the increased oxidative stress production or via the decreased function of the nonenzymatic antioxidant system. Interestingly, PCP, the combined extract of purple corn cob and pandan leaves attenuated the memory impairment evaluated by using the object recognition test.

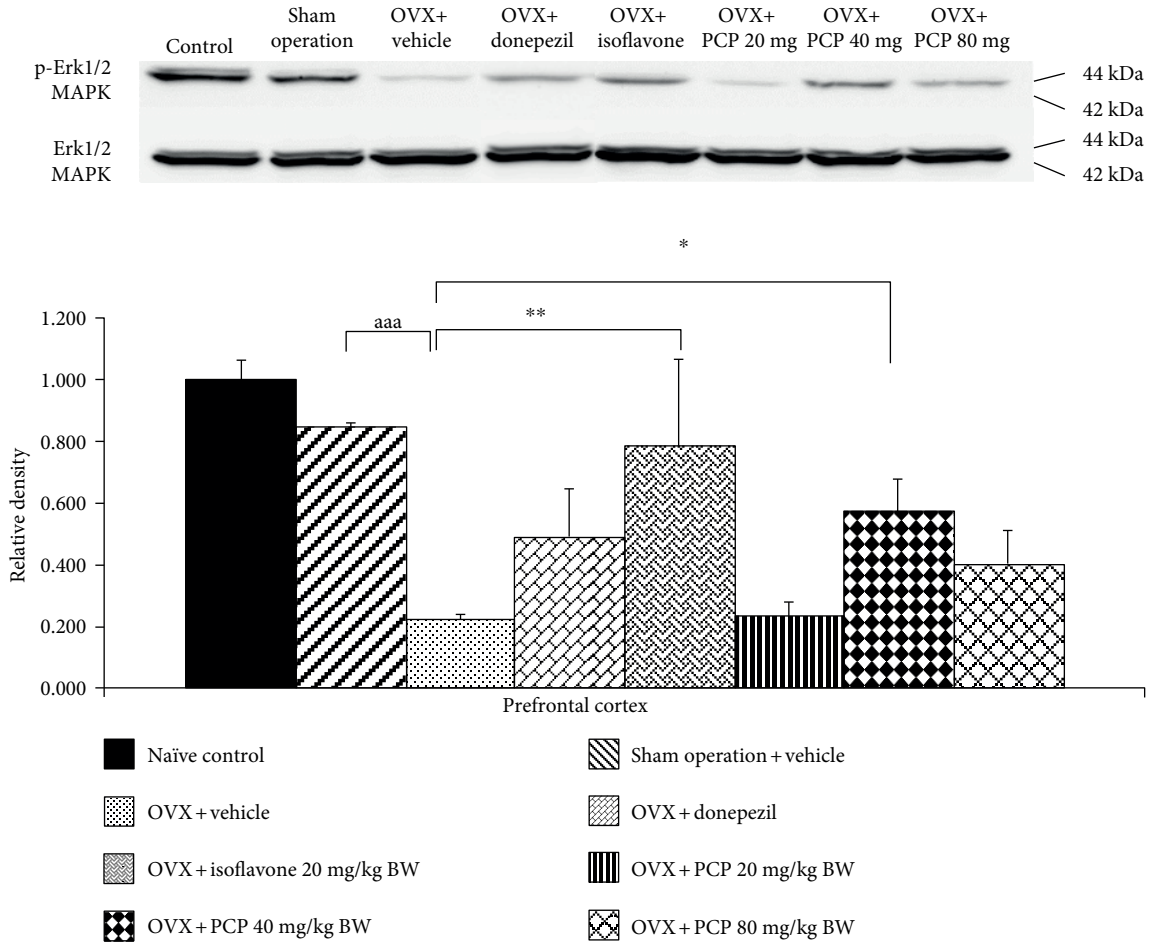

FIGURE 5: The effect of the PCP on the expression of phosphorylation ERK1/2 (p-ERK1/2) protein in the prefrontal cortex ($n = 6$/group). ^{aaa}p value < 0.001, compared with the sham operation group. *, $^{**}p$ value < 0.05 and 0.01, respectively, compared with the OVX + vehicle-treated group. Data were expressed as mean ± SEM.

It has been reported that the prefrontal cortex plays a crucial role on nonspatial memory. Lesion of this area could induce nonspatial memory impairment [38]. In this study, we have found that this impairment was attenuated by both isoflavone and all doses of PCP. The reduction of MDA level which indicated the decreased oxidative stress status and the enhanced neuron density was also observed in OVX rats which received isoflavone and all doses of PCP. Therefore, we suggested that PCP and isoflavone might improve oxidative stress status leading to the enhanced neuron density in PFC resulting in the improved nonspatial memory. The decreased oxidative stress status in PFC observed in this study might occur partly via the enhanced function of a scavenger enzyme especially SOD. Since no closed relationship between the decreased MDA level and the enhanced SOD activity in PFC was observed, other factors such as the decreased nonenzymatic system and the decreased oxidative stress production mentioned earlier might also contribute to the role.

In addition to oxidative stress, the cholinergic system in PFC also plays the crucial role on memory. Depletion of acetylcholine (ACh) together with the elevation of acetylcholinesterase (AChE) in the PFC induces memory impairment both in primates and in rodents [39, 40]. The cognitive-enhancing effect of donepezil, an AChEI, was observed without changes of oxidative stress markers. Our study also demonstrated that both donepezil and low dose of PCP also suppressed AChE activity in PFC. Therefore, the enhanced cholinergic function in PFC by suppressing AChE activity in the mentioned area also contributes to a role on the cognitive-enhancing effect of both substances. It has been reported that polyphenol [14] including anthocyanins [41] can improve memory impairment induced by scopolamine which exerts the effect at muscarinic receptors. Since PCP contains polyphenols and anthocyanins, it is also possible that PCP also exerts its influence on muscarinic receptor. However, this requires further investigation.

Recently, it has been demonstrated that mitogen-activated protein kinase (MAPK) especially ERK1/2 contributes to the pivotal role on learning and memory [42]. The substances which improve ERK signaling also improve the impairment of object recognition memory [43]. Based on this information, we did suggest that the cognitive-enhancing effect of isoflavone and medium dose of PCP might also occur via the enhanced ERK1/2 signaling pathway.

Anthocyanins, a member of flavonoids, have been shown to exert the neuroprotective and cognitive-enhancing effect [44]. Since our fingerprint of PCP showed that the main ingredient in PCP was anthocyanins (peak 2–peak 5), we suggested that the neuroprotective effect and cognitive-enhancing effects of PCP in this study might involve anthocyanins. However, the effect of other ingredients still cannot be omitted.

Our data failed to show a dose-dependent manner of PCP. The possible explanation might be due to the non-simple linear relationship between the concentration of PCP and the observed parameters. Since many factors exert the influences on the observed parameters in this study, no simple linear relationship was observed. In addition, PCP contained many ingredients, so the effect of an active ingredient could be masked by other ingredients.

In this study, we have found that our data showed that although in vitro data showed that IC_{50} of AChEI of PCP was very high, low dose of PCP could exert the cognitive-enhancing effect via the suppression of AChE in the prefrontal cortex while the medium and high doses of PCP failed to exert this effect. The possible explanation might also occur as that mentioned earlier in the lack of a dose-dependent study.

Taken all data together, our study highlights the neuroprotective and cognitive effects of PCP that might occur primarily via the decreased oxidative stress which in turn increased neuron density in the brain especially in PFC, an area playing an important role on learning and memory especially nonspatial memory, resulting in the improved nonspatial memory. However, the improved cholinergic function and signal transduction via ERK1/2 might also exert the roles especially at low and medium doses, respectively.

5. Conclusion

This study is the first study to demonstrate the neuroprotective and cognitive effects of PCP. We have shown that the combined extract of purple corn cob and pandan leaves can be served as functional ingredients for developing neuroprotectant and cognitive enhancer for menopausal women. Therefore, we highlight how to create the value for agricultural waste such as purple corn cob. However, chronic toxicity is required in order to assure the consumption safety before moving forward to a clinical trial study.

Conflicts of Interest

The authors declare that they have no conflicts of interest.

Acknowledgments

This study was supported by the Higher Education Research Promotion and National Research University Project of Thailand, Office of the Higher Education Commission, through the Food and Functional Food Research Cluster of Khon Kaen University, the Integrative Complementary Alternative Medicine Research and Development Center, and the Invitation Research Grant of the Faculty of Medicine (Grant no. IN58219), Khon Kaen University.

References

[1] World Health Organization, *WHO Technical Report Series 866: Research on the Menopause in the 1990s*, WHO Library Cataloguing in Publication Data, Geneva, Switzerland, 1994.

[2] J. R. Sliwinski, A. K. Johnson, and G. R. Elkins, "Memory decline in peri- and post-menopausal women: the potential of mind-body medicine to improve cognitive performance," *Integrative Medicine Insights*, vol. 9, pp. 17–23, 2014.

[3] E. Hogervorst, J. Williams, M. Budge, W. Riedel, and J. Jolles, "The nature of the effect of female gonadal hormone replacement therapy on cognitive function in post-menopausal women: a meta-analysis," *Neuroscience*, vol. 101, no. 3, pp. 485–512, 2000.

[4] M. Sano, "Understanding the role of estrogen on cognition and dementia," *Journal of Neural Transmission Supplementum*, vol. 59, pp. 233–239, 2000.

[5] S. A. Shumaker, C. Legault, L. Kuller et al., "Conjugated equine estrogens and incidence of probable dementia and mild cognitive impairment in postmenopausal women: Women's Health Initiative Memory Study," *The Journal of the American Medical Association*, vol. 291, no. 24, pp. 2947–2958, 2004.

[6] M. A. Espeland, S. R. Rapp, S. A. Shumaker; et al., "Conjugated equine estrogens and global cognitive function in postmenopausal women: Women's Health Initiative Memory Study," *The Journal of the American Medical Association*, vol. 291, no. 24, pp. 2959–2968, 2004.

[7] S. M. Resnick, P. M. Maki, S. R. Rapp et al., "Effects of combination estrogen plus progestin hormone treatment on cognition and affect," *The Journal of Clinical Endocrinology and Metabolism*, vol. 91, no. 5, pp. 1802–1810, 2006.

[8] V. Beral, "Breast cancer and hormone-replacement therapy in the Million Women Study," *Lancet*, vol. 362, no. 9382, pp. 419–427, 2003.

[9] W. Y. Chen, S. E. Hankinson, S. J. Schnitt, B. A. Rosner, M. D. Holmes, and G. A. Colditz, "Association of hormone replacement therapy to estrogen and progesterone receptor status in invasive breast carcinoma," *Cancer*, vol. 101, no. 7, pp. 1490–1500, 2003.

[10] O. H. Franco, R. Chowdhury, J. Troup et al., "Use of plant-based therapies and menopausal symptoms: a systematic review and meta-analysis," *Journal of the American Medical Association*, vol. 315, no. 23, pp. 2554–2563, 2016.

[11] P. Leerasiri, C. Chayachinda, S. Indhavivadhana, T. Wongwananurak, C. Dangrat, and M. Rattanachaiyanont, "Nutritional supplements in health-conscious pre-/post-menopausal Thai women," *Journal of the Medical Association of Thailand*, vol. 93, no. 10, pp. 1128–1136, 2010.

[12] C. W. Cotman, E. Head, B. A. Muggenburg, S. Zicker, and N. W. Milgram, "Brain aging in the canine: a diet enriched in antioxidants reduces cognitive dysfunction," *Neurobiology of Aging*, vol. 23, no. 5, pp. 809–818, 2002.

[13] J. Rubio, W. Qiong, X. Liu et al., "Aqueous extract of black maca (*Lepidium meyenii*) on memory impairment induced by ovariectomy in mice," *Evidence-Based Complementary and Alternative Medicine*, vol. 2011, Article ID 253958, 7 pages, 2011.

[14] Y. S. Juan, S. M. Chuang, Y. L. Lee et al., "Green tea catechins decrease oxidative stress in surgical menopause-induced overactive bladder in a rat model," *BJU International*, vol. 110, no. 6, Part B, pp. E236–E244, 2012.

[15] G. Patki, F. H. Allam, F. Atrooz et al., "Grape powder intake prevents ovariectomy-induced anxiety-like behavior, memory impairment and high blood pressure in female Wistar rats," *PloS One*, vol. 8, no. 9, article e74522, 2013.

[16] F. Ramos-Escudero, A. M. Muñoz, C. Alvarado-Ortíz, Á. Alvarado, and J. A. Yáñez, "Purple corn (*Zea mays* L.) phenolic compounds profile and its assessment as an agent against oxidative stress in isolated mouse organs," *Journal of Medicinal Food*, vol. 15, no. 2, pp. 206–215, 2012.

[17] R. Chaisanam, S. Muchimapura, J. Wattanathorn, W. Thukham-mee, and J. Jittiwat, "Antioxidant and cyclooxygenase-2-inhibiting effect of purple corn cob extract-loaded nanofiber patch on motor recovery in spinal cord injury rats," *North-Eastern Thai Journal of Neuroscience*, vol. 10, no. 4, pp. 14–33, 2015.

[18] S. W. Yan and R. Asmah, "Comparison of total phenolic contents and antioxidant activities of turmeric leaf, pandan leaf and torch ginger flower," *International Food Research Journal*, vol. 17, pp. 417–423, 2010.

[19] T. D. Widyaningsih, I. Z. Zumroh, and N. Rochmawati, "Effect of mixed grass jelly (*Mesona palustris* BL.) and other ingredients effervescent powder in diabetic rats," *International Journal of Technical Research and Applications*, vol. 2, no. 5, pp. 52–55, 2014.

[20] A. L. Waterhouse, "Determination of total phenolics," *Current Protocols in Food Analytical Chemistry*, pp. I1–I8, 2002.

[21] S. Sreelatha and P. R. Padma, "Antioxidant activity and total phenolic content of Moringa oleifera leaves in two stages of maturity," *Plant Foods Human Nutrition*, vol. 64, pp. 303–311, 2009.

[22] I. F. Benzie and J. J. Strin, "The ferric reducing ability of plasma (FRAP) as a measure of antioxidant power: the FRAP assay," *Analytical Biochemistry*, vol. 239, pp. 70–76, 1996.

[23] J. Lee, R. W. Durst, and R. E. Wrolstad, "Determination of total monomeric anthocyanin pigment content of fruit juices, beverages, natural colorants, and wines by the pH differential method: collaborative study," *Journal of AOAC International*, vol. 88, no. 5, pp. 1269–1278, 2005.

[24] M. A. Papandreou, A. Dimakopoulou, Z. I. Linardaki et al., "Effect of a polyphenol-rich wild blueberry extract on cognitive performance of mice, brain antioxidant markers and acetylcholinesterase activity," *Behavioural Brain Research*, vol. 198, no. 2, pp. 352–358, 2009.

[25] S. Sungkamanee, J. Wattanathorn, S. Muchimapura, and W. Thukham-mee, "Antiosteoporotic effect of combined extract of *Morus alba* and *Polygonum odoratum*," *Oxidative Medicine and Cellular Longevity*, vol. 2014, Article ID 579305, 9 pages, 2014.

[26] S. Okuda, B. Roozendaal, and J. L. McGaugh, "Glucocorticoid effects on object recognition memory require training-associated emotional arousal," *Proceedings of the National Academy of Sciences of the United States of America*, vol. 101, no. 3, pp. 853–858, 2004.

[27] G. Paxinos and C. Watson, *The Rat Brain in Stereotaxic Coordinates*, Elsevier, Amsterdam, 2009.

[28] J. Lu, D. M. Wu, Y. L. Zheng, B. Hu, and Z. F. Zhang, "Purple sweet potato color alleviates D-galactose-induced brain aging in old mice by promoting survival of neurons via PI3K pathway and inhibiting cytochrome C-mediated apoptosis," *Brain Pathology*, vol. 20, no. 3, pp. 598–612, 2010.

[29] O. H. Lowry, N. J. Rosebrough, A. L. Farr, and R. J. Randall, "Protein measurement with the folin phenol reagent," *Journal of Biological Chemistry*, vol. 193, no. 1, pp. 265–275, 1951.

[30] G. L. Ellman, K. D. Courtney, V. Andres Jr, and R. M. Feather-Stone, "A new and rapid colorimetric determination of acetylcholinesterase activity," *Biochemical Pharmacology*, vol. 7, pp. 88–95, 1961.

[31] P. Thiraphatthanavong, J. Wattanathorn, S. Muchimapura et al., "Preventive effect of *Zea mays* L. (purple waxy corn) on experimental diabetic cataract," *BioMed Research International*, vol. 2014, Article ID 507435, 8 pages, 2014.

[32] W. Kirisattayakul, J. Wattanathorn, T. Tong-Un, S. Muchimapura, P. Wannanon, and J. Jittiwat, "Cerebroprotective effect of Moringa oleifera against focal ischemic stroke induced by middle cerebral artery occlusion," *Oxidative Medicine and Cellular Longevity*, vol. 2013, Article ID 951415, 10 pages, 2013.

[33] S. M. Courtney, L. Petit, J. V. Haxby, and L. G. Ungerleider, "The role of prefrontal cortex in working memory: examining the contents of consciousness," *Philosophical Transactions of the Royal Society B*, vol. 353, no. 1377, pp. 1819–1829, 1998.

[34] A. Blokland, "Acetylcholine: a neurotransmitter for learning and memory?" *Brain Research Review*, vol. 21, no. 3, pp. 285–300, 1995.

[35] M. Ulas and M. Cay, "The effects of 17beta-estradiol and vitamin E treatments on oxidative stress and antioxidant levels in brain cortex of diabetic ovariectomized rats," *Acta Physiologica Hungarica*, vol. 97, no. 2, pp. 208–215, 2010.

[36] M. Singh, E. M. Meyer, W. J. Millard, and J. W. Simpkins, "Ovarian steroid deprivation results in a reversible learning impairment and compromised cholinergic function in female Sprague-Dawley rats," *Brain Research*, vol. 644, no. 2, pp. 305–312, 1994.

[37] M. Da Silva Morrone, C. E. Schnorr, G. A. Behr et al., "Oral administration of curcumin relieves behavioral alterations and oxidative stress in the frontal cortex, hippocampus, and striatum of ovariectomized Wistar rats," *The Journal of Nutritional Biochemistry*, vol. 32, pp. 181–188, 2016.

[38] C. T. Curtis, "The effects of prefrontal lesions on working memory performance and theory," *Cognitive, Affective & Behavioral Neuroscience*, vol. 4, no. 4, pp. 528–539, 2004.

[39] Z. Alrefaie, "Vitamin D3 improves decline in cognitive function and cholinergic transmission in prefrontal cortex of streptozotocin-induced diabetic rats," *The Medical Journal of Cairo University*, vol. 81, no. 2, pp. 25–31, 2013.

[40] Y. Chudasama, J. W. Dalley, F. Nathwani, P. Bouger, T. W. Robbins, and F. Nathwani, "Cholinergic modulation of visual attention and working memory: dissociable effects of basal forebrain 192-IgG-saporin lesions and intraprefrontal infusions of scopolamine," *Learning & Memory*, vol. 11, no. 1, pp. 78–86, 2004.

[41] J. M. Gutierres, F. B. Carvalho, M. R. Schetinger et al., "Protective effects of anthocyanins on the ectonucleotidase activity in the impairment of memory induced by scopolamine in adult rats," *Life Sciences*, vol. 91, no. 23-24, pp. 1221–1228, 2012.

[42] K. P. Giese and K. Mizuno, "The roles of protein kinases in learning and memory," *Learning & Memory*, vol. 20, no. 10, pp. 540–552, 2013.

[43] B. González, M. Raineri, J. L. Cadet, E. García-Rill, F. J. Urbano, and V. Bisagno, "Modafinil improves methamphetamine-induced object recognition deficits and restores prefrontal cortex ERK signaling in mice," *Neuropharmacology*, vol. 87, no. 1, pp. 188–197, 2014.

[44] P. Kaewkaen, T. Tong-Un, J. Wattanathorn, S. Muchimapura, W. Kaewrueng, and S. Wongcharoenwanakit, "Mulberry fruit extract protects against memory impairment and hippocampal damage in animal model of vascular dementia," *Evidence-Based Complementary and Alternative Medicine*, vol. 2012, Article ID 263520, 9 pages, 2012.

ISSN 1479-2621
Plant Genetic Resources: Characterization and Utilization; 1–10
doi:10.1017/S1479262115000428

Evaluation of the tolerance of Thai indigenous upland rice germplasm to early drought stress using multiple selection criteria

Kittichai Narenoot[1], Tidarat Monkham[1], Sompong Chankaew[1], Patcharin Songsri[1,3], Wattana Pattanagul[2] and Jirawat Sanitchon[1]*

[1]*Department of Plant Science and Agricultural Resources, Faculty of Agriculture, Khon Kaen University, Khon Kaen, Thailand,* [2]*Faculty of of Science, Khon Kaen University, Khon Kaen, Thailand and* [3]*Northeast Thailand Cane and Sugar Research Center, Khon Kaen University, Khon Kaen, Thailand*

Received 11 May 2015; Revised 18 August 2015; Accepted 28 August 2015

Abstract

Drought remains the most important factor that affects rice productivity, especially in rainfed areas, worldwide. Upland rice is one of the crop choices of farmers in the rainfed environment. Although upland rice varieties require less water than lowland rice varieties, yields often remain limited by drought, particularly in the period of early growth. The aims of this study were to identify the traits related to early drought tolerance in upland rice varieties, and to identify the potential sources of germplasm for early drought tolerance. A total of sixty upland rice varieties were planted in a factorial experiment with a randomized complete block design with 3 replications in the rainy seasons of 2011 and 2012, under greenhouse conditions. Based on the drought tolerance index (DTI), the test germplasm sources were classified into three groups: (i) susceptible; (ii) moderately tolerant; (iii) tolerant to drought stress. Grain yield (GY) showed significant negative correlations with the leaf rolling score ($r = -0.623$, $P < 0.01$), the leaf death score (LDS) ($r = -0.673$, $P < 0.01$) and the recovery score ($r = -0.746$, $P < 0.01$), while leaf dry matter ($r = 0.698$, $P < 0.01$) and leaf water potential ($r = 0.618$, $P < 0.01$) had significant positive correlations with GY. These findings indicate the suitability of the DTI as the selection criteria for early drought tolerance in a breeding programme. In addition, the upland rice germplasm accessions KKU-ULR011, KKU-ULR012, KKU-ULR125, KKU-ULR199 and KKU-ULR292 were identified as having high levels of stability for drought tolerance in both the 2011 and 2012 experiments, suggesting their potential for further use for rice variety improvement for drought tolerance.

Keywords: breeding; drought tolerance; DTI; recovery score; water deficit

Introduction

Drought is one of the environmental factors that can cause a great reduction in rice yield. Different types of drought can be classified in relation to rainfall and the growing environment, and the stage of crop development (Kamoshita *et al*., 2008). The main effect of drought is dry matter accumulation (Kumar *et al*., 2006; Beheshti and Behboodi fard, 2010) and/or severe yield reduction (Kumar *et al*., 2008). Drought during the vegetative stage of plant development may reduce yields less than drought during the terminal stage because of the

* Corresponding author. E-mail: jirawat@kku.ac.th

opportunity for plant growth recovery later in the growing season. However, early drought can inhibit vegetative development and reduce tiller number (Bernier *et al.*, 2008), leaf area (Farooq *et al.*, 2010) and dry matter (Kumar *et al.*, 2006). Late heading and flowering, followed by a short grain-filling period, can be associated with higher yields when drought stress is experienced early in the growing season, during the vegetative phase (Van Ginkel *et al.*, 1998; Yang and Zhang, 2006; Cattivelli *et al.*, 2008).

Upland rice can adapt very well to tropical and subtropical areas with aerobic soils and undulating land. However, all upland rice fields are subjected to mild drought stress conditions, with more severe stress developing between major rainfall events, particularly under conditions of high evapotranspiration (Kamoshita *et al.*, 2008). In Asia, around 13 million ha of the total area planted to rice are occupied by upland rice cultivars (Acuña *et al.*, 2008). The chronic low yield of upland rice cultivars is largely due to the limitations of infertile upland soils and/or abiotic stresses, and to the low harvest index of traditional cultivars (George *et al.*, 2001; Saito *et al.*, 2006). However, Srihanoo and Sanitchon (2011) reportedly showed that the yields of indigenous upland rice germplasm in Thailand can range from about 700 to more than 3400 kg/ha, suggesting that some varieties are well adaptive to upland conditions.

The lack of sources of drought tolerance for upland rice has been a major obstacle in upland rice breeding programmes. The advantage of existing genetic resources is that they can assist in the development of drought-resistant cultivars for upland rice field systems. Traditional rice breeding can be slow due to a lack of understanding of the traits and mechanisms that confer adaptation characteristics (Bernier *et al.*, 2009). Leaf rolling (LR) and leaf death (LD) are plant traits during the vegetative stage, which have a high heritability (0.8) but a low association with yield. Leaf water potential (LWP) is a popular trait for use in drought screening programmes (Jongdee *et al.*, 2002; Pantuwan *et al.*, 2002a, b); however, percentage recovery is one of the most important traits related to grain yield (GY) in the evaluation of the impact of early wet season drought. The objectives of this study were (1) to identify different plant traits and their association with early drought tolerance in upland rice varieties, and (2) to identify potential germplasm sources for early drought tolerance.

Materials and methods

Experimental sites, design and genotypes

The experiment was conducted at Khon Kean University under greenhouse conditions. A total of sixty indigenous upland rice varieties supplied by the Research Center for Plant Breeding for Sustainable Agriculture at Khon Kean University were evaluated in rainy seasons (June –December) in 2011 and 2012. The experimental design was a factorial experiment with a randomized complete block (RCB) design with three replications; factor A comprised 2 water regimes and factor B had 60 varieties of upland rice.

Soil and water condition treatments

Soil samples were collected from three randomly selected points, with the sampling being done by an auger at a depth of 0–15 and 15–30 cm from upland rice fields in Ban Wang War village, Banhad district, Khon Kaen province. Soil texture in this locality was loamy sand, with pH 6.3 and 0.28% organic matter. The soil samples were dried at 105°C for 72 h followed by weighing to calculate soil density, based on the method of the International Atomic Energy Agency (IAEA) (2008) and Black (1965). Soil density was 1.32 g/cm^3. The second part of the soil samples was air-dried separately for different soil sampling depths. Then, individual pots (30 cm in diameter and 30 cm in depth) were filled using the soil from different sampling levels. Individual pots had 25 cm depth of soil and 17.5 kg/pot (according to the soil density). Seeds were sown at a rate of four to five seeds/pot and later thinned to two plants/pot at 14 d after sowing (DAS).

Water management in this experiment was based on soil evaporation and plant water use, following the method of Doorenbos and Pruitt (1992). In the control (non-stress) condition, soil water was maintained at field capacity before sowing by calculating crop evapotranspiration (ET_{crop}) and then adding sufficient water to maintain the field capacity throughout the growing period; $ET_{crop} = ET_0 \times K_c$, where ET_{crop} is the crop evapotranspiration (mm/d); K_c is the crop coefficient (dimensionless); ET_0 is the reference crop evapotranspiration (mm/d). Reference crop evapotranspiration (ET_0) was calculated from $E_0 \times K_p$, where E_0 is the water evaporation at the KKU field and $K_p = 0.7$ (constant). The crop coefficient (K_c) of rice is different with the plant growth stage, with months 1 and 2 having 1.1–1.5 mm/d, and months 3 and 4 having 1.1–1.3 mm/d and 0.95–1.05 mm/d in the last component of the growth period (Doorenbos and Kassam, 1986).

In stress conditions, the water was drained out at 28 DAS and then restored at 56 DAS, with soil moisture being maintained in the same non-stress condition as before draining.

Data collection

LR was scored following the method proposed by De Datta *et al.* (1988), using a scale range from 1 to 5,

with 1 = unrolled, turgid, 2 = leaf rim starts to roll, 3 = leaf has a shape of V, 4 = rolled leaf rim covers part of the leaf blade and 5 = leaf is rolled like an onion leaf. LR was measured at 44 (LR1) and 49 (LR2) DAS in 2011 and at 41 (LR1) and 45 (LR2) DAS in 2012.

LD was scored following the method proposed by De Datta *et al*. (1988), using a scale range from 0 to 10, based on the percentage of the estimated total leaf area that was dead, with 0 = no symptom, 1 = dead leaf tip area less than 10%, 2 = 25% of dead leaf area, 3 = 50% of dead leaf area, 4 = more than 50% of dead leaf area and 25% of plant, 5 = 50% of plant was dead, 6 = more than 50% of plant was dead but not exceeding 70% of plant, 7 = 70% of plant was dead, 8 = more than 70% of plant was dead and 9 = all leaves were dead. The LDS was measured in the third expanded leaf at 45 DAS in 2011 and at 50 DAS in 2012.

Recovery (RE) was scored following the method proposed by IRRI (1996), using the following score range: 1 = 90–100% RE; 3 = 70–89% RE; 5 = 40–69% RE; 7 = 20–39% RE; 9 = 0–19% RE. The RE rating score was recorded at 10 d after re-watering (66 DAS) in both 2011 and 2012.

Mid-day LWP (10.00–14.00 h) was determined at 50 DAS in 2011 and at 47 DAS in 2012. For each measurement, one last fully expanded leaf was randomly sampled from each pot. To prevent transpiration, a long-narrow plastic bag (2 cm wide and 20 cm long) was placed over the leaf tip and pulled down to cover the whole leaf blade. Then, the leaf was cut with scissors just above the leaf collar. The leaf sample was immediately taken to measure the rate of LWP using a pressure chamber (Model 3005 Plant Water Status Console; Soilmoisture Equipment, USA).

Drought tolerance index (DTI) was determined after harvesting following the method of Nautiyal *et al*. (2002). This method was used to determine the DTI of groundnut (*Arachis hypogaea* L.), with a slight modification made to take into account the GY, root and shoot dry matter in rice. Dry matter, root dry matter and GY in both experiments were used for estimating the DTI as follows: DTI = stress treatment/non-stress treatment.

Plant stem dry matter was separated from the panicles and oven-dried at 80°C for 72 h; root dry matter was filtered using a sieve to separate out the sand. It was then oven-dried at 80°C for 72 h. GY was based on grain weight at 14% moisture after air-drying.

Data analysis

Yield and yield components were analysed according to the RCB design (Gomez and Gomez, 1984), and means

Table 1. Means, standard deviations (SD) and coefficients of variation (CV) for the tested traits under non-stress and stress conditions in the wet seasons of 2011 and 2012

	2011						2012					
	Mean		SD[a]		CV (%)		Mean		SD		CV (%)	
	Non-stress	Stress	Non-stress	Stress	Non-stress	Stress	Non-stress	Stress	Non-stress	Stress	Non-stress	Stress
LRS1	1.00	2.01	–	0.79	–	39.43	1.00	1.28	–	0.29	–	22.62
LRS2	1.00	3.23	–	1.21	–	37.35	1.00	3.19	–	0.59	–	18.46
LDS1	0.00	2.57	–	2.25	–	87.57	0.00	3.87	–	2.05	–	53.08
RES	1.00	5.72	–	2.26	–	39.49	1.00	2.81	–	1.73	–	61.41
GY (g/plant)	23.27	13.15	3.54	6.65	15.19	50.55	24.35	21.66	2.69	3.77	11.06	17.40
RDW (g/plant)	13.73	14.48	4.73	6.38	34.47	44.03	14.94	5.18	1.94	1.14	13.00	22.06
PDW (g/plant)	44.15	13.97	11.32	8.19	25.65	58.58	39.28	15.93	6.56	3.30	16.71	20.70
LWP2 (MPa)	−1.47	−3.86	0.14	0.92	9.80	23.74	−1.59	−3.67	0.17	0.62	10.45	16.86

LRS1 and LRS2, leaf rolling score at the first and second measurements; LDS, leaf death score; RES, recovery score; GY, grain yield; RDW, root dry weight; PDW, plant dry weight; LWP2, leaf water potential at the second measurement.
[a] SD and CV (%) were not determined under non-stress conditions.

comparisons were made by Duncan's multiple range test. The combined analysis of the 2-year data followed Barlett's test (Gomez and Gomez, 1984). Correlation and linear regression analyses were conducted for the test traits.

Results

Genetic variation as revealed by analysis of variance

The analysis of variance under early drought conditions in a greenhouse in both 2011 and 2012 showed a high level of variation in criteria being reflected by the distribution of the traits representing the different water conditions. Overall, eight traits [except root dry weight (RDW)] showed a significant variation in 2011, with significant differences also being observed under the stress and control conditions. In 2012, the eight criteria traits (except LR1) also exhibited a significant variation (Supplementary Table S1, available online). All the criteria traits in both experiments (except RDW in 2011 and LR1 in 2012) showed significant interactions between genotype and water status. The results indicated that the criteria traits were significantly influenced by genotype, water condition and the interaction of these two factors.

Phenotypic variation among the genotypes for each trait was confirmed by basic statistical parameters including means, standard deviation and coefficient of variation (Table 1). The coefficient of variation under non-stress conditions ranged from 9.80% to 34.47% in 2011 and from 10.45% to 16.71% in 2012. However, under water stress conditions, it ranged from 23.74% to 87.57% and 16.86% to 61.41% in 2011 and 2012, respectively. When compared with non-stress conditions, the mean values of the leaf rolling score (LRS), LDS and recovery score (RES) were increased under stress conditions. In contrast, the LWP, RDW, plant dry weight (PDW) and GY declined in response to the stress conditions.

Genetic correlations among the tested traits

Pearson's correlations among the eight criteria traits were calculated (Table 2). A range of 1–26 correlation pairs reached significance levels under the non-stress and stress conditions, respectively. Leaf-related traits, such as leaf rolling score 2 (LRS2) and LDS, LRS and RES, and LDS and RES, had positive correlations of $r = 0.852$, $r = 0.760$ and $r = 0.870$ under stress conditions, respectively. Under stress conditions, GY was negatively correlated with LRS2, LDS and RES ($r = -0.623$, -0.673 and $r = -0.746$, respectively). In contrast, GY was positively correlated with PDW and LWP2 ($r = 0.698$ and $r = 0.618$, respectively). The results showed relatively high correlations between the criteria traits under the stress conditions. Surprisingly, RDW was not correlated with other criteria under stress conditions, but was correlated with PDW under non-stress conditions.

Drought tolerance indices

The DTI for three traits (RDW, PDW and GY) was calculated in all the tested upland rice genotypes.

Table 2. Correlation coefficients between the traits under early drought conditions using the combined data for two years (2011 and 2012)

	LRS1	LRS2	LDS	RES	GY	RDW	PDW	LWP2
Non-stress								
GY	ND[a]	ND	ND	ND	1.000			
RDW	ND	ND	ND	ND	0.063	1.000		
PDW	ND	ND	ND	ND	0.144	0.279*	1.000	
LWP2	ND	ND	ND	ND	0.219	−0.068	0.061	1.000
Stress								
LRS1	1.000							
LRS2	0.725**	1.000						
LDS	0.514**	0.852**	1.000					
RES	0.509**	0.769**	0.870**	1.000				
GY	−0.585**	−0.623**	−0.673**	−0.746**	1.000			
RDW	0.040	0.101	0.075	0.015	0.071	1.000		
PDW	−0.383**	−0.366**	−0.404**	−0.575**	0.698**	−0.077	1.000	
LWP2	−0.496**	−0.592**	−0.544**	−0.505**	0.618**	−0.079	0.412**	1.000

LRS1 and LRS2, leaf rolling score at the first and second measurements; LDS, leaf death score; RES, recovery score; GY, grain yield; RDW, root dry weight; PDW, plant dry weight; LWP2, leaf water potential at the second measurement.

Values were significant at * $P < 0.05$ and ** $P < 0.01$.

[a] ND indicates that LRS1, LRS2, LDS and RES were not determined under non-stress conditions.

Among these three traits, the DTI for PDW had the lowest value of 0.32, while the DTI for RDW had the highest value of 1.17 in 2011. However, in 2012, the DTI for RDW had the lowest value of 0.35, while the DTI for GY had the highest value of 0.90. The DTI values ranged from 0.29 to 1.06, reflecting different levels of drought tolerance among the genotypes (Fig. 1). Based on the DTI values, the tested upland rice genotypes were classified into three groups. A total of 45 accessions showed drought susceptibility, with DTI values being lower than 0.70 (G1); ten accessions showed moderate drought tolerance, with DTI values between 0.70 and 0.90 (G2); and five accessions showed drought tolerance, with DTI values being greater than 0.90 (G3) (Supplementary Table S2, available online). The mean values and standard deviations for each trait in the three groups are shown in Fig. 2.

Under non-stress conditions, the mean values of LRS1, LRS2, LDS, RES and LWP2 were similar in all the groups. In contrast, under stress conditions, the mean values of LRS1, LRS2, LDS, RES and LWP2 were lowest in G3, moderate in G2 and highest in G1. The mean values of LRS1, LRS2, LDS, RES and LWP2 showed substantial increases from G3 to G2 and G1 (Fig. 2).

The mean values of GY, RDW and PDW were lowest in G3, moderate in G2 and highest in G1 under non-stress conditions, while under stress conditions, the mean values of GY and PDW tended to decrease from G3 to G2 and G1. Surprisingly, the mean value of RDW in G3 increased under stress conditions when compared with non-stress conditions (Fig. 2). The results indicated that classifying the upland rice accessions into three groups based on DTI values could be an effective means for the identification of drought tolerance among the accessions.

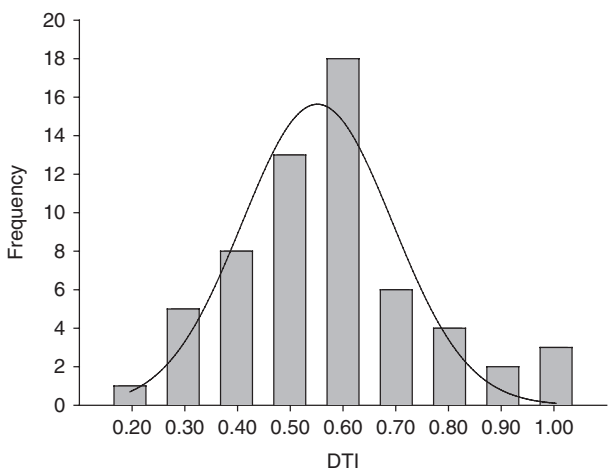

Fig. 1. Frequency distribution of the drought tolerance index (DTI) for drought tolerance in the tested upland rice germplasm.

Relationship of DTI and pre-harvesting traits under the conditions of drought stress

Correlation analysis revealed a significant difference between the criteria traits under both the non-stress and stress conditions (Table 1). Based on harvesting time, the criteria traits can be divided into two stages: pre- and post-harvest. Pre-harvest comprised LRS1, LRS2, LDS, RES and LWP2; post-harvest comprised PDW, RDW and GY. The post-harvested traits were used for the DTI to classify the upland rice accessions in relation to drought tolerance. The relationship was defined within the context of the three groups based on the DTI values. LRS1, LRS2, LDS and RES had a close relationship with DTI ($R^2 = 0.76$, 0.87 and 0.79, respectively) in G3 (tolerant), while the relationship decreased substantially from G3 to G2 and then to G1 (Fig. 3). In contrast, LWP2 in G3 had the R^2 value lower than that in G2 and G1, indicating that the LWP2 value in G3 was more stable than that in the other groups. The results indicated that LRS1, LRS2, LDS, RES and LWP2 were related to post-harvest parameters.

Discussion

Genetic variation for drought tolerance in upland rice genotypes, and the importance of related traits in drought tolerance evaluation

The development of new rice genotypes tolerant to drought stress will increase and stabilize rice yield, and could potentially save water (Zhou *et al.*, 2006). The investigation among primitive cultivars, landraces, wild species and world collections for drought tolerance is the most common approach adopted for identifying potential donors for breeding programmes (Kumar *et al.*, 2009; Thomson *et al.*, 2010). According to the centres of origin, South and Southeast Asia are the areas of origin of rice (*Oryza sativa*), where 90% of world's rice is produced and consumed (Hibberd *et al.*, 2008). In Asia, around 13 million ha of rice-planted area are occupied by upland rice cultivars (Acuña *et al.*, 2008). The ancestors of this crop are semi-aquatic, and they are not yet fully adapted to the aerobic systems, because of its limited tolerance to water deficits.

In this study, 60 upland rice varieties from Thailand were used to identify the traits related to early drought tolerance in upland rice varieties, and to identify the potential sources of germplasm for early drought tolerance. The analysis of variance of data related to early drought conditions in a greenhouse environment in 2011 and 2012 showed high levels of criteria variation reflected by drought. All criteria traits in both experiments,

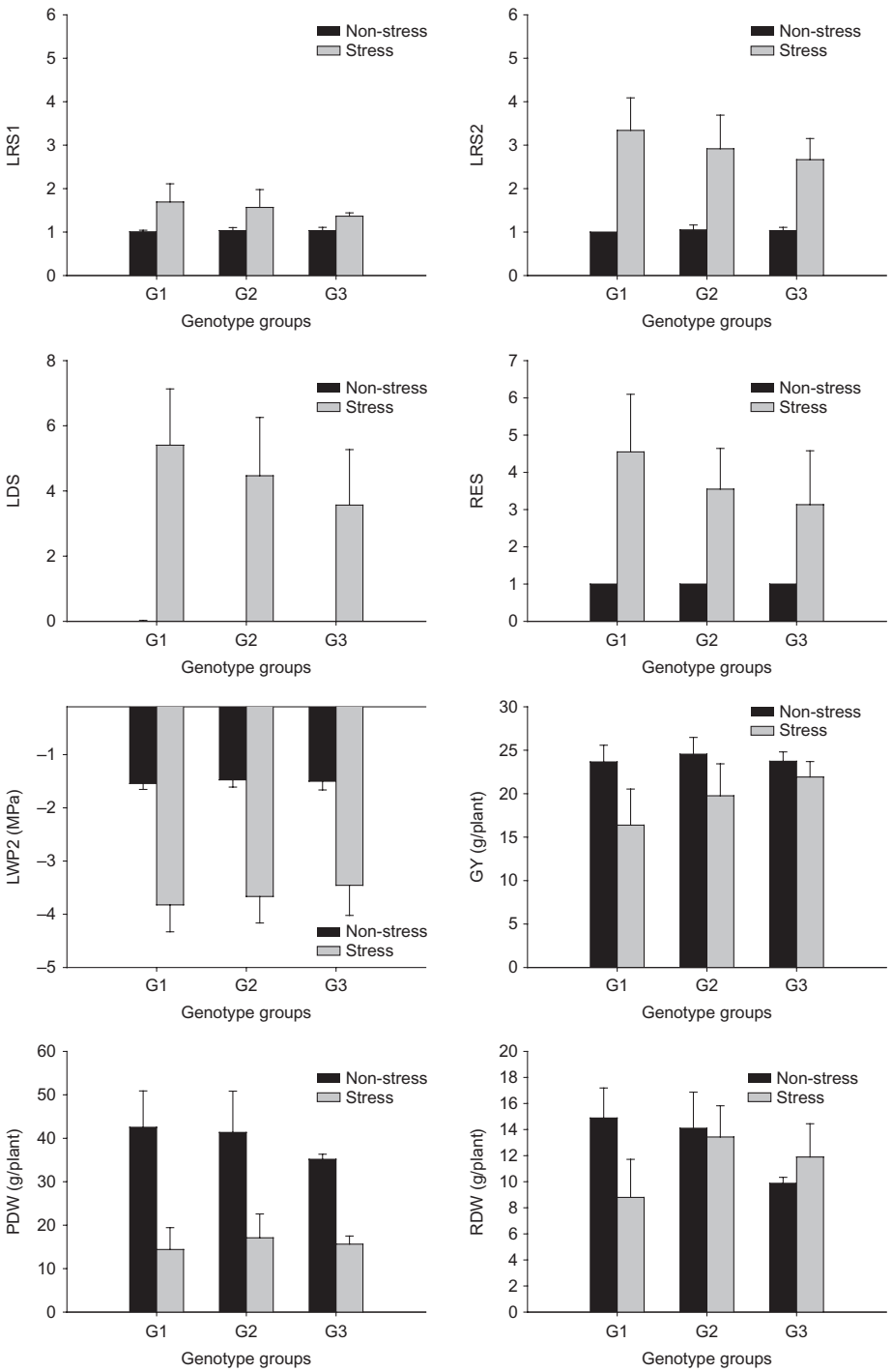

Fig. 2. Mean values and standard deviations for the eight traits in three rice groups under non-stress and stress conditions. Based on the drought tolerance index, the tested rice accessions were classified into three groups. G1, G2 and G3 represent susceptible, moderate tolerance and tolerance of drought conditions, respectively. Bars represent the standard deviation of means in the three groups ($N = 45$, 10 and 5 for G1, G2 and G3, respectively). LRS1 and LRS2, leaf rolling score at the first and second measurements; LDS, leaf death score; RES, recovery score; LWP2, leaf water potential at the second measurement; GY, grain yield; PDW, plant dry weight; RDW, root dry weight.

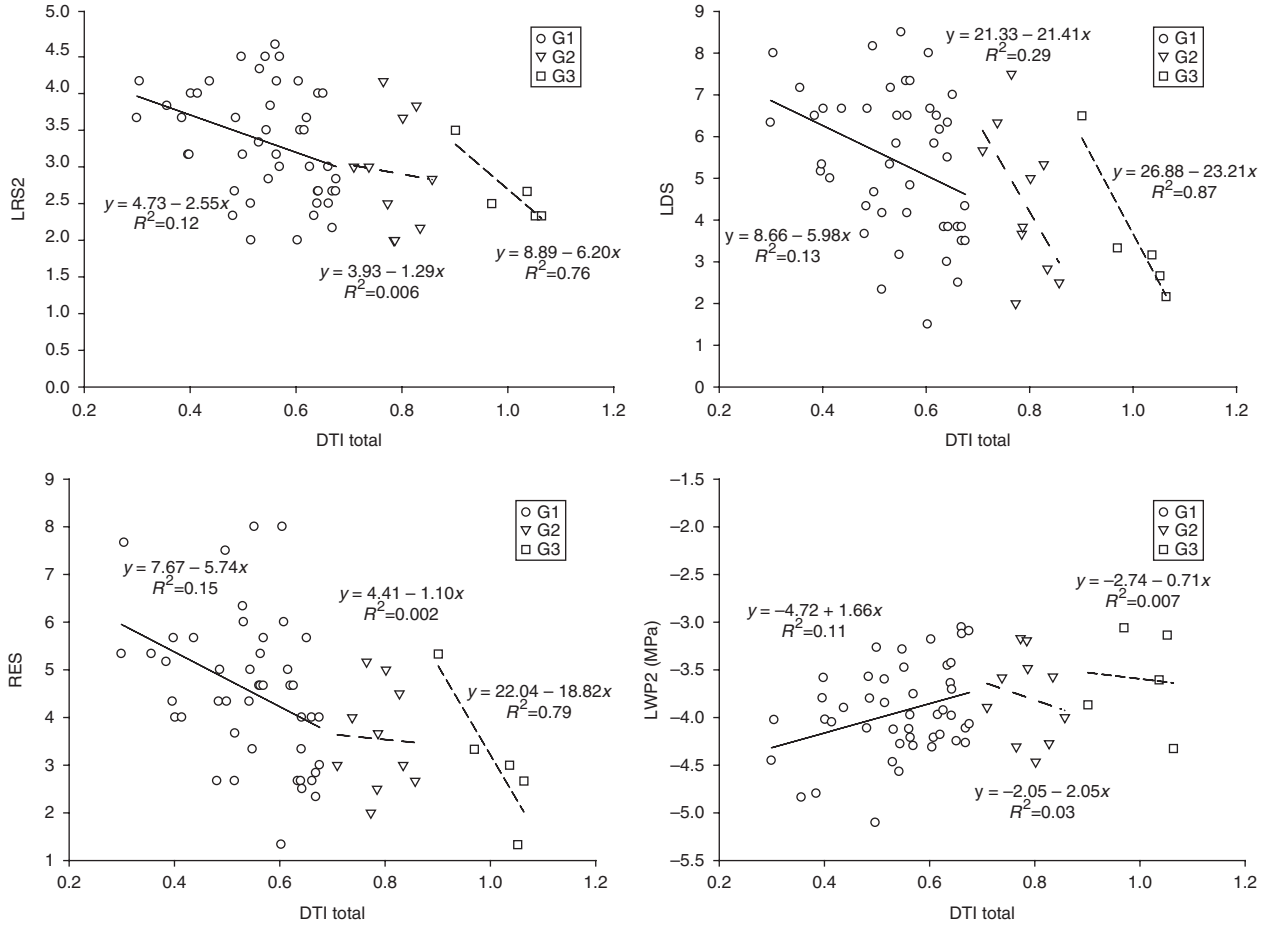

Fig. 3. Relationship between the drought tolerance index (DTI) and leaf rolling score at the second measurement (LRS2), leaf death score (LDS), recovery score (RES) and leaf water potential at the second measurement (LWP2) in the three groups of genotypes (G1, G2 and G3) under stress conditions for the two years combined.

with the exception of RDW in 2011 and LR1 in 2012, showed significant interactions between genotype and water status. The results showed that the criteria traits were significantly influenced by genotype, water conditions and their interaction (Supplementary Table S1, available online), and indicated that drought is complicated and difficult in terms of field management and variation in plant phenology (Manickavelu *et al*., 2006).

The level of drought influenced the root character, with severe conditions leading to increased RDW as a defence mechanism (Almekinders and De Boef, 2000; Kanbar *et al*., 2009). In this study, the experiment conducted in 2011 was associated with greater severity of water stress than that conducted in 2012, with this being reflected in a higher level of final LDS (~6.5) and lower level of genotype recovery (~6) (Supplementary Fig. S1, available online). The Mean RDW of rice germplasm increased in response to drought (Table 1; Supplementary Fig. S1, available online); however, the results of analysis of variance were non-significant (Table 1) due to the measurement of this trait being made after re-watering and of trait plasticity under re-watering.

Some of the plant responses that have been recorded in plants in response to drought have included shortened life cycles, proliferations of roots for improved water uptake (Yue *et al*., 2006), reduced water loss (Blum, 2011), water use efficiency (Zhang *et al*., 2012) and drought tolerance via osmotic adjustment and desiccation tolerance (Yue *et al*., 2006). In the present study, traits related to early drought tolerance were analysed. The results showed that the leaf-related traits LRS, LDS, RES and LWP were associated with GY ($r = -0.623$, -0.673, -0.746 and 0.618, respectively). LR was related to LD ($r = 0.69$, $P < 0.01$) but dependent on the period of drought, with long and severe stress affecting both traits (Kamoshita *et al*., 2008; Gana, 2011; Bunnag and Pongthai, 2013). Rice plants reduce water loss by rolling their leaves under the conditions of low soil moisture (Blum, 2011). The rolling of the leaves is associated with stomata closure to reduce

water loss; it also reduces gas exchange between the plant and the ambient air.

The reduced CO_2 intake after LR results in reduced photosynthesis. This mechanism improves the plant's survival under conditions of drought stress, but is also associated with reduced yield (Bernier *et al.*, 2008; Ping *et al.*, 2011). This is the reason for the negative correlation between GY and LRS, LDS and RES. Upland rice genotypes that can maintain a higher rate of LWP, a lower rate of LR, a lower rate of LD and a higher ability of recovery are associated with higher GY under conditions of early drought, as reported previously (Dingkuhn *et al.*, 1989; Jongdee *et al.*, 2002; Hu *et al.*, 2004; Bunnag and Pongthai, 2013).

Genotypes with the Way Rarem allele (*qtl12.1*) of quantitative trait loci have been shown to exhibit a reduced rate of LR and leaf drying, and a higher LWP, under severe drought conditions (Bernier *et al.*, 2009). Upland genotypic variation in relation to LWP has been shown to exist in this study, and is was negatively correlated with drought score ($r = -0.75$, $P < 0.01$, $n = 42$), which varied in relation to plant size (Mitchell *et al.*, 1998; Jongdee *et al.*, 2002; Pantuwan *et al.*, 2002a, b). Plant recovery was one of the important traits identified in early drought screening, with plants having a higher ability to maintain LWP being associated with a greater ability for recovery after a period of drought stress.

DTI as selection criteria for drought tolerance

The development of drought-resistant cultivars with a higher yield potential is one of the main objectives of rainfed rice breeding programmes. The identification of rice accessions with tolerance to drought is necessary for genetic research and breeding. Drought screening is a complicated trait to be addressed through the conventional approach of selection for yield and its stability over locations and years. The low heritability of yield under stress, the inherent variation under field conditions, and the limitation that there is usually only one experimental drought crop per year is reflected in a slow rate of progress (Eid, 2009; Venuprasad *et al.*, 2009). Studies under greenhouse conditions provide an alternative option for early drought tolerance selection. Plant and root dry matter accumulation could be important traits of the recovery period, leading to higher yields, following early water deficits. However, all three traits are influenced by rice plant growth characteristics. For example, in relation to the value of RDW, it was found that G3 genotypes with high levels of early drought tolerance had high values under stress conditions, but had the lowest values under non-stress conditions (Fig. 2).

In this study, to avoid the potential influence of rice growth characteristics on drought tolerance evaluation, a DTI was calculated from the ratio of the value of three traits (RDW, PDW and GY) under non-stress and stress conditions. Based on the DTI value, the upland rice accessions were classified into three groups: G1 (susceptible); G2 (moderate tolerance); G3 (tolerant).

Compared with the other groups, G3 with a higher DTI value had the lowest mean value for LRS, LDS, RES and LWP under stress conditions. In contrast, PDW and GY showed the least reduction under drought stress conditions. Interestingly, the RDW values in G3 showed an increase under drought stress conditions, while the values decreased in the other groups. The root characteristics, including deeper and thicker roots (Yadav *et al.*, 1997), root pulling resistance (Pantuwan *et al.*, 2002a, b) and greater root penetration (Ali *et al.*, 2000; Clark *et al.*, 2000), could improve the adaptation of rice to drought through enhancing water uptake. The relationship between pre-harvest (leaf-related traits) and the DTI was also determined. LRS1 and LRS2, LDS and RES had a high relationship with DTI ($R^2 = 0.76$, 0.87 and 0.79, respectively) in G3 (Fig. 3), with the pattern of value distribution tending to decrease when the DTI increased. In contrast, LWP2 in G3 showed greater stability than that in the other groups. These results indicated that LRS1 and LRS2, LDS, RES and LWP2 were related to post-harvesting traits (i.e. yield). DTI provides a consistent selection trait for genotypes with potential drought tolerance, although it may differ with different screening methods (Ahadiyat *et al.*, 2012). The traits that were found to be most useful for early drought screening in this experiment were LR, LD, LWP, RE and DTI.

Conclusions

Thai indigenous upland rice genotypes showed variations in their responses to early drought under greenhouse conditions in studies undertaken in 2011 and 2012.Among the criteria traits used to evaluate the association with early drought tolerance, the traits associated with drought tolerance included plant recovery ability, lower LRS and LDS, maintenance of high LWP and high DTI. This information is potentially useful for future breeders in genotype selection for early drought tolerance in upland rice, especially the DTI. In addition, of the 60 test accessions, five were identified as being drought-tolerant varieties, which have the potential for providing a source of drought-tolerant genes in future breeding programmes.

Supplementary material

To view supplementary material for this article, please visit http://dx.doi.org/10.1017/S1479262115000428

Acknowledgements

This research was supported by the Plant Breeding Research Centre for Sustainable Agriculture and Research Center of Agricultural Biotechnology for Sustainable Economy, Khon Kaen University, Thailand. The authors thank Dr John Schiller of the University of Queensland, Australia, for proofreading the manuscript. They also thank the Thailand Research Fund (Project code: IRG5780003) and the Faculty of Agriculture, Khon Kaen University, for providing financial support for manuscript preparation. J. Sanitchon is grateful to Khon Kaen University under Incubation Researcher Project for providing financial support.

References

Acuña TLB, Lafitte HR and Wade LJ (2008) Genotype × environment interactions for grain yield of upland rice backcross lines in diverse hydrological environments. *Field Crops Research* 108: 117–125.

Ahadiyat YR, Hidayat P and Susanto U (2012) Selection of upland rice genotypes on drought tolerance and P efficiency at laboratory and screen house levels. *Journal of Agricultural Technology* 8: 453–463.

Ali ML, Pathan MS, Zhang J, Bai G, Sarkarung S and Nguyen HT (2000) Mapping QTLs for root traits in a recombinant inbred population from two indica ecotypes in rice. *Theoretical and Applied Genetics* 101: 756–766.

Almekinders CJM and De Boef W (2000) *Encouraging Diversity. The Conservation and Development of Plant Genetic Resources*. London: Intermediate Technology Publications.

Beheshti AR and Behboodi fard B (2010) Dry matter accumulation and remobilization in grain sorghum genotypes (*Sorghum bicolor* L. Moench) under drought stress. *Australian Journal of Crop Science* 4: 185–189.

Bernier J, Atlin GN, Serraj R, Kumar A and Spaner D (2008) Breeding upland rice for drought resistance. *Journal of the Science of Food and Agriculture* 88: 927–939.

Bernier J, Serraj R, Kumar A, Venuprasad R, Impa S, Gowda RPV, Oane R, Spaner D and Atlin G (2009) The large-effect drought-resistance QTL *qtl12.1* increases water uptake in upland rice. *Field Crop Research* 110: 139–146.

Black CA (ed.) (1965) Methods of Soil Analysis. Madison, Wisconsin: American Society of Agronomy.

Blum A (2011) Plant water relations, plant stress and plant production. In: Blum A (ed.) *Plant Breeding for Water-Limited Environments*. New York: Springer, 258 pp.

Bunnag S and Pongthai P (2013) Selection of rice (*Oryza sativa* L.) cultivars tolerant to drought stress at the vegetative stage under field conditions. *American Journal of Plant Sciences* 4: 1701–1708.

Cattivelli L, Rizza F, Badeck F-W, Mazzucotelli E, Mastrangelo AM, Francia E, Marè C, Tondelli A and Stanca AM (2008) Drought tolerance improvement in crop plants: an integrated view from breeding to genomics. *Field Crops Research* 105: 1–14.

Clark LJ, Aphale SL and Barraclough PB (2000) Screening the ability of rice roots to overcome the mechanical impedance of wax layers: importance of test conditions and measurement criteria. *Plant Soil* 219: 187–196.

De Datta SK, Malabuyoc JA and Aragon EL (1988) A field screening technique for evaluating rice germplasm for drought tolerance during the vegetative stress. *Field Crops Research* 19: 123–134.

Dingkuhn M, Cruz RT, O'Toole JC and Dörffling K (1989) Net photosynthesis, water use efficiency, leaf water potential and leaf rolling as affected by water deficit in tropical upland rice. *Australian Journal of Agricultural Research* 40: 1171–1181.

Doorenbos J and Kassam AH (1986) Rice. In: Doorenbos J and Kassam AH (eds) *Yield Responses to Water, FAO Irrigation and Drainage Paper No. 33*. Rome, Italy: FAO, pp. 125–130.

Doorenbos J and Pruitt WO (1992) Calculation of crop water requirements. In: Doorenbos J and Pruitt WO (eds) *FAO Irrigation and Drainage Paper No. 24*. Rome, Italy: FAO, pp. 1–65.

Eid MH (2009) Estimation of heritability and genetic advance of yield traits in wheat (*Triticum aestivum* L.) under drought condition. *International Journal of Genetics and Molecular Biology* 1: 115–120.

Farooq M, Kobayashi N, Ito O, Wahid A and Serraj R (2010) Broader leaves result in better performance of indica rice under drought stress. *Journal of Plant Physiology* 167: 1066–1075.

Gana AS (2011) Screening and resistance of traditional and improved cultivars of rice to drought stress at Badeggi, Niger State, Nigeria. *Agriculture and Biology Journal of North America* 2: 1027–1031.

George T, Magbanua R, Roder W, Van Keer K, Trebuil G and Reoma V (2001) Upland rice response to phosphorus fertilization in Asia. *Agronomy Journal* 9: 1362–1370.

Gomez KA and Gomez AA (1984) *Statistical Procedures for Agricultural Research*, 2nd edn. New York: John Wiley & Sons.

Hibberd JM, Sheehy JE and Langdale JA (2008) Using C4 photosynthesis to increase the yield of rice-rationale and feasibility. *Current Opinion in Plant Biology* 11: 228–231.

Hu J, Jiang D, Cao W and Luo W (2004) Effect of short-term drought on leaf water potential, photosynthesis and dry matter partitioning in paddy rice. *Journal of Applied Ecology* 15: 63–67.

International Atomic Energy Agency (IAEA) (2008) Field estimation of soil water content. A practical guide to methods, instrumentation and sensor technology. *Training Course Series No. 30*. Vienna: International Atomic Energy Agency.

IRRI (1996) *Standard Evaluation System for Rice*. Manila, Philippines: The International Rice Research Institute.

Jongdee B, Fukai S and Cooper M (2002) Leaf water potential and osmotic adjustment as physiological traits to improve drought tolerance in rice. *Field Crops Research* 76: 153–163.

Kamoshita A, Babu RC, Boopathi NM and Fukai S (2008) Phenotypic and genotypic analysis of drought-resistance traits for development of rice cultivars adapted to rainfed environments. *Field Crop Research* 109: 1–23.

Kanbar A, Toorchi M and Shashidhar HE (2009) Relationship between root and yield morphological characters in rainfed low land rice (*Oryza sativa* L.). *Cereal Research Communications* 37: 261–268.

Kumar R, Sarawgi AK, Ramos C, Amarante ST, Ismail AM and Wade LJ (2006) Partitioning of dry matter during drought stress in rainfed lowland rice. *Field Crop Research* 98: 1–11.

Kumar A, Bernier J, Verulkar S, Lafitte HR and Atlin GN (2008) Breeding for drought tolerance: direct selection for yield, response to selection and use of drought-tolerant donors in upland and lowland-adapted populations. *Field Crops Research* 107: 221–231.

Kumar A, Verulkar S, Dixit S, Chauhan B, Bernier J, Venuprasad R, Zhao D and Shrivastava MN (2009) Yield and yield-attributing traits of rice (*Oryza sativa* L.) under lowland drought and suitability of early vigor as a selection criterion. *Field Crops Research* 114: 99–107.

Manickavelu A, Nadarajan N, Ganesh SK, Gnanamalar RP and Babu RC (2006) Drought tolerance in rice: morphological and molecular genetics consideration. *Plant Growth and Regulation* 50: 121–138.

Mitchell JH, Siamhan D, Wamala MH, Risimeri JB, Chinyamakobvu E, Henderson SA and Fukai S (1998) The use of seedling leaf death score for evaluation of drought resistance of rice. *Field Crop Research* 55: 129–139.

Nautiyal PC, Nageswara Rao RC and Joshi YC (2002) Moisture-deficit-induced change in leaf water content leaf carbon exchange rate and biomass production in groundnut cultivars differing in specific leaf area. *Field Crops Research* 74: 67–79.

Pantuwan G, Fukai S, Cooper M, Rajatasereekul S and O'Toole JC (2002a) Yield response of rice (*Oryza sativa* L.) genotypes to different types of drought under rainfed lowlands Part 2. Selection of drought resistant genotypes. *Field Crop Research* 73: 169–180.

Pantuwan G, Fukai S, Cooper M, Rajatasereekul S and O'Toole JC (2002b) Yield response of rice (*Oryza sativa* L.) genotypes to different types of drought under rainfed lowlands Part 3. Plant factors contributing to drought resistance. *Field Crop Research* 73: 181–200.

Ping LL, Wen YZ, Dong W, Li ZY and Yu S (2011) Effects of plant density and soil moisture on photosynthetic characteristics of flag leaf and accumulation and distribution of dry matter in wheat. *Acta Agronomica Sinica* 37: 10491059.

Saito K, Linquist B, Atlin GN, Phanthaboon K, Shiraiwa T and Horie T (2006) Response of traditional and improved upland rice cultivars to N and P fertilizer in northern Laos. *Field Crops Research* 96: 216–223.

Srihanoo W and Sanitchon J (2011) Yield evaluation of upland rice germplasm at Khon Kaen [Abstract in English]. *Agricultural Science Journal* 42: 137–140.

Thomson MJ, Ismail AM, McCouch SR and Mackill DJ (2010) Marker assisted breeding. In: Pareek A, Sopory SK and Bohnert HJ (eds) *Abiotic Stress Adaptation in Plants*. Dordrecht, The Netherlands: Springer, pp. 451–469.

Van Ginkel M, Calhoun DS, Gebeyehu G, Miranda A, Tian-you C, Pargas Lara R, Trethowan RM, Sayre K, Crossa L and Rajaram S (1998) Plant traits related to yield of wheat in early, late, or continuous drought conditions. *Euphytica* 100: 109–121.

Venuprasad R, Dalid CO, Valle MD, Zhao D, Espiritu M, Cruz MTS, Amante M, Kumar A and Atlin GN (2009) Identification and characterization of large-effect quantitative trait loci for grain yield under lowland drought stress in rice using bulk-segregant analysis. *Theoretical and Applied Genetics* 120: 177–190.

Yadav R, Courtois B, Huang N and McLaren G (1997) Mapping genes controlling root morphology and root distribution in a doubled-haploid population of rice. *Theoretical and Applied Genetics* 94: 619–632.

Yang J and Zhang J (2006) Grain filling of cereals under soil drying. *New Phytologist* 169: 223–236.

Yue B, Xue W, Xiong L, Yu X, Luo L, Cui K, Jin D, Xing Y and Zhang Q (2006) Genetic basis of drought resistance at reproductive stage in rice: separation of drought tolerance from drought avoidance. *Genetics* 172: 1213–1228.

Zhang Y, Tang Q, Peng S, Xing D, Qin J, Laza RC and Punzalan B (2012) Water use efficiency and physiological response of rice cultivars under alternate wetting and drying conditions. *The Scientific World Journal* 2012: 1–10.

Zhou SX, Tian F, Zhu ZF, Fu YC, Wang XK and Sun CQ (2006) Identification of quantitative trait loci controlling drought tolerance at seedling stage in Chinese Dongxiang common wild rice (*Oryza rufipogon* Griff.). *Acta Genetica Sinica* 33: 551–558.

AGRIVITA Journal of Agricultural Science. 2017. 39(2): 128-136

Stability of Four New Sources of Bacterial Leaf Blight Resistance in Thailand Obtained from Indigenous Rice Varieties

Arthit Sribunrueang, Sompong Chankaew*), Petcharat Thummabenjapone and Jirawat Sanitchon

Department of Plant Science and Agricultural Resources Faculty of Agriculture
Khon Kaen University, Khon Kaen, 40002, Thailand
*) Corresponding author E-mail: somchan@kku.ac.th

Received: August 28, 2016 /Accepted: January 3, 2017

ABSTRACT

Bacterial leaf blight (BLB) disease caused by *Xanthomonas oryzae* pv. *oryzae* (*Xoo*) is one of the most serious diseases in rice production. Breeding varieties specifically for their resistance to BLB disease is therefore an efficient and cost-effective strategy. However, the resistance gene for BLB can be race and non-race specific, meaning it is often overcome by the pathogen. The identification of new sources of resistance genes for *Xoo* is crucial in rice breeding programmes. In this study, six rice varieties were assessed using six *Xoo* isolates in multiple screening conditions. The GGE biplot analysis considers both genotype (G) and genotype environment (GE) interaction effects and demonstrates GE interaction. The first two principal components (PCs) accounted for 95.46% of the total GE variation in the data. Based on lesion length and stability performance, Phaladum was the most ideal genotype against all *Xoo* isolates in the four screening conditions. The results relayed that Phaladum indigenous rice varieties could be considered as new sources of bacterial leaf blight resistance in Thailand. In the future, the BLB resistance gene in this variety will be identified in regard to mode of inheritance and used as parental line in rice breeding programmes for resistance to BLB.

Keywords: Bacterial leaf blight; GGE biplot; rice; stability; *Xanthomonas oryzae*

INTRODUCTION

Rice (*Oryza sativa* L.) is an important source of calories in South and Southeast Asia where annually 90 % of the world's rice is produced. More than 50 % of the world's population consumed rice as a staple food (Khush, 2005; Latif et al., 2011). The major diseases affecting rice yields is bacterial leaf blight (BLB) disease caused by the bacterial pathogen *Xanthomonas oryzae* pv. *oryzae* (*Xoo*). While this bacterial pathogen is infectious all year round, it is particularly so during wet season. BLB is a vascular disease that results in greyish tan to white lesions along the veins of the plants in field conditions. The wounded leaves or root during transplantation usually infected by the pathogen. Therefore, young plants at seedling stage are the most susceptible especially plants that are younger than 21 days old. (Ou, 1985; Reddy & Mohanty, 1981). However, disease incidence increases with stages of plant growth and peaking at the flowering stage. An infection could reduce rice yields by more than 50 % and even lead to a complete crop damaged when it occurs during the tillering stage (Ou, 1985). In several rice production areas in Thailand, BLB has been reported as one of the most destructive diseases in rice (Korinsak et al., 2009). Rice varieties RD6 and KDML105, aromatic rice cultivars with high cooking qualities, are widely grown in the North and Northeast of Thailand. The large-scale and long-term cultivation of these two varieties makes them easy targets for being damaged by the pathogen.

Out of all the available strategies to control BLB disease, breeding for host-plant resistance is effective way. However, BLB disease mainly infects plants in wet conditions, a factor that severely limits the breeding process and selection of plants due to seasonal confounding. However, the limited of seasonal confounding could overcome by marker-assisted selection (MAS) (Collard & Mackill, 2008). The modes of inheritance of resistance to BLB in rice were differences when evaluated in different sources of resistance (Khan, Naeem, & Iqbal, 2014; Das, Sengupta, Prasad, & Ghose, 2014). This suggests a number of different mechanisms or genes may confer resistance to BLB. So far, 40 BLB resistance genes have been reported (Khan,

Cite this as: Sribunrueang, A., Chankaew, S., Thummabenjapone, P., & Sanitchon, J. (2017). Stability of four new sources of bacterial leaf blight resistance in Thailand obtained from indigenous rice varieties. *AGRIVITA Journal of Agricultural Science, 39*(2), 128–136. http://doi.org/10.17503/agrivita.v39i0.1051
Accredited: SK No. 60/E/KPT/2016

Naeem, & Iqbal, 2014). However, resistance was very often overcome by the pathogen, which in turn led to high levels of variability in infections in cultivation areas (Sreewongchai et al., 2009). In addition, more virulent populations of the pathogen emerge and resistant cultivars lose their effective resistance within a short period of time (Thakur, Shetty, & King, 1992). The incorporation of resistant genes was a continuous process to counter evolving pathogens according to the gene-for-gene hypothesis (Flor, 1971).

Mapping several resistance genes or quantitative trait loci (QTLs) shows the same location in a genome region, indicating that some of the resistance genes or QTLs are the same (Das, Sengupta, Prasad, & Ghose, 2014). The use of same resistance gene in large production areas is very often cause resistance breaking by the pathogen. Therefore, rice breeders need to search other natural sources of resistance and subsequently determine additional resistance genes in order to pyramid several genes to achieve durable resistance. New rice resistant sources against *Xoo* were identified in wild related species, namely *O. nivara, O. longistaminata* and *O. punctate*. The use of these species in rice breeding programmes has been recommended (Akhtar et al., 2011). It is important to note, however, that desirable agronomic attributes, such as photoperiod response, plant types and cooking quality, can be found lacking with genetically diverse resistance parents. The increasing use of locally available genetic resistance materials as parents can minimise this problem.

In Thailand, Chanlakhon, Thammabenjapon, & Sanitchon (2012) identified 14 indigenous lowland rice varieties as resistant to three BLB isolates by completing the same resistance checks (IRBB5, IR64 and IR62266). Out of those, Hom Mali Nin, Pet-Retree, LG6822 and Phaladum were considered to have high potentials for the resistance breeding programme. However, an effective breeding for BLB resistance relies on a good understanding of the relationship between host, pathogen and environment.

The resistances testing in difference pathogen isolates and over conditions have significant fluctuations in disease reaction due to GE interaction. The durable resistance varieties could be identified by stability analysis strategies (Jenns, Leonard, & Moll, 1982). In the presence of GE interaction, superior genotypes could be identified using genotypic means across conditions (Kang, 1992). Moreover, the most resistant variety, the most virulent pathogen and the particular environment for differentiating resistance levels among varieties could also be employed by genotype and genotype by environment (GGE) biplot analysis (Yan & Falk, 2002).

The GGE biplot analysis of plant traits focused on identifying a stable genotype for deployment as well as suitable areas for subsequent commercial grain production (Lakew, Tariku, Alem, & Bitew, 2014), stability of disease resistance (Idowu, Salami, Ajayi, Akinwale, & Sere, 2013; Tabien, Samonte, Abalos, & San Gabriel, 2008; Yan & Falk, 2002), stability of F1 hybrid (Akter et al., 2015), cooking quality (Fotokian & Agahi, 2014), and anthocyanin content (Somsana, Wattana, Suriharn, & Sanitchon, 2013). Therefore, the analysis of disease reaction also aims to determine suitable donor parents for the trait and to identify BLB isolates that will be useful in further screening for resistance breeding program. The objectives of this study were (a) to confirm the response of Thai indigenous rice varieties to BLB disease and (b) to identify genotypes with high stability and broad resistance to BLB disease through the use of the GGE biplot method.

MATERIALS AND METHODS

Rice Varieties and BLB Isolates

Four indigenous low land rice varieties, Hom Mali Nin (HMLN), Pet-Retree (PRT), LG6822 and Phaladum (PLD) were identified as BLB resistant (Chanlakhon, Thammabenjapon, & Sanitchon, 2012). These four varieties, together with two susceptible varieties, RD6 and Kao Dok Mali 105 (KDML105), were used as materials to screen against six *Xoo* isolates: two isolates from Ubon Ratchatani (BB2009-758 and BB2009-786), two isolates from Udon Thani (BB2009-928 and BB2009-1066), and two isolates from Khon Kaen (BB2009-1099 and BB2009-1111) (Fig. 1).

Rice Growing Conditions and Inoculum Preparation

Growing conditions were tested using two different approaches: solution and soil cultures. Solution cultures required the seeds to be sown individually in small holes in styrofoam plates with a nylon net providing support underneath. The styrofoam plates floated on water without nutrient solution in rectangular plastic for three days.

Afterwards the plastic trays were filled with nutrient solution following the protocol described by Yoshida, Forno, Cock, & Gomez (1976). The nutrient solution was renewed every four days until 21 days after sowing (DAS) for disease evaluation.

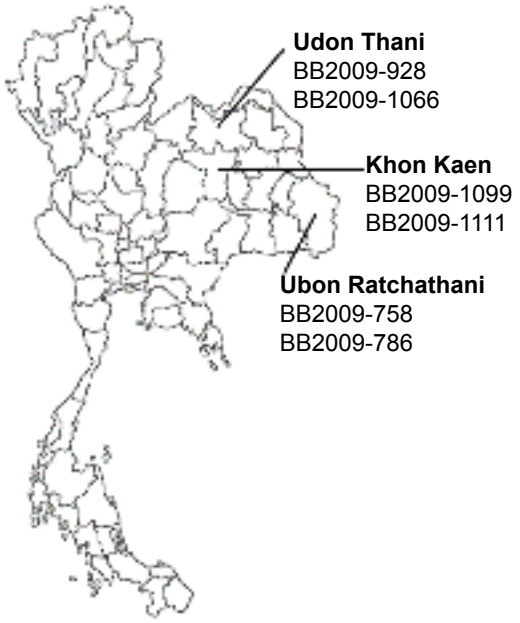

Fig 1. Distribution of sources of six *Xanthomonas oryzae pv. oryzae* isolates used for artificial inoculation in greenhouse conditions

To produce the soil cultures, the procedure described by Gregorio, Dharmawansa, & Mendoza (1997) was applied, with slight modifications. Two-day old seedlings were transferred into 4.7 x 4.7 x 5.0 cm^3 plastic pots filled with soil and soaked in a water tank, with one seedling per pot (four pots/variety). The pots were fertilised with 156 kg ha^{-1} of nitrogen at 15 DAS until inoculation.

To prepare the inoculum, six isolates of *Xoo* were stored with glycerol at a constant of -20°C. Next, *Xoo* isolates were regrown on nutrient agar at 27-30°C for 48 hours. Each bacterial colony was suspended in sterilised, distilled water and adjusted to concentrations of 10^9 cfu ml^{-1} (OD = 0.3 at 600 nm) by spectrophotometer.

Assessments of BLB Resistance

Assessments of BLB resistance were performed from 2013 to 2015 under greenhouse conditions in different seasons and with different screening methods at Khon Kean University in Thailand. The rice varieties HMLN, PRT, PLD, LG6822, RD6 and KDML105 were tested against six *Xoo* isolates under soil culture conditions in the 2013 rainy season, under solution culture conditions in the 2014 winter season, and under soil and solution culture conditions in the 2015 summer season by factorial analysis in a completely randomised design (CRD) with three replications. In all experiments, seeds were sown and remained untouched for 21 days. Afterwards, artificial inoculation was completed using the leaf-clipping method (Sun et al., 2004). Fourteen days after inoculation (DAI), the plant reaction to BLB was examined based on the lesion length in individual plants.

Data Analysis

The lesion length data for six varieties of six isolates in four conditions was used to analyse the variance (ANOVA) to determine the effects of both genotype (G) and environment (E), and their interactions. The mean lesion length data was graphically analysed to interpret GE interaction using the GGE biplot software (Yan, 2001), and then PC1 and PC2 were described to account for the main and minor affects respectively using R v 2.10 (R Development Core Team, 2010).

RESULTS AND DISCUSSION

The analysis of the variance in lesion length (in cm) at 14 DAI in six varieties using six *Xoo* isolates under greenhouse conditions in 2013, 2014 and 2015 is shown in Table 1. Significant ($P<0.01$) differences were found among varieties, isolates and their interaction for BLB disease lesions (Table 1). The mean lesion lengths for all rice varieties, isolates and conditions are shown in Table 2. Out of the six rice varieties, PLD showed the shortest lesion length (1.2 cm), followed by LG6822, PRT and HMLN (2.7, 2.8 and 3.3 cm respectively). In contrast, the longest lesion length was observed in RD6 and KDML105 (8.4 and 7.1 cm). PLD's short lesion length suggests that this variety has a broad resistance to several *Xoo* isolates. It is therefore suitable as a resistance donor parent in the breeding programme. Host-plant resistance is the most economic and sustainable strategy for controlling BLB disease. According to BLB's genetic control, resistance is governed by several genes or QTLs, with major resistance genes consist of *Xa4*, *xa5*, *Xa7*, *xa13* and *Xa21*. The latter, *Xa21*, is the most broad-spectrum resistance to *Xoo* strains, inherited from the wild rice species *O. longestaminata*. It was widely used in rice breeding programmes (Khush, Mackill, & Sidhu, 1989).

Table 1. Summary of ANOVA tests for bacterial leaf blight disease response as measured by lesions length (cm) at 14 days after inoculation in six varieties used six Xanthomonas oryzae pv. oryzae isolates in a greenhouse environment in 2013, 2014 and 2015

SOVa	Soil culture 2013		Solution culture 2014		Soil culture 2015		Solution culture 2015	
	df[b]	MS[c]	df	MS	df	MS	df	MS
Isolate(I)	5	52.5**	5	8.49**	5	37.6*	5	53.8**
Varieties(V)	5	868.8**	4	1.91*	5	210.5**	5	26.9**
I x V	25	17.1**	20	0.82ns	25	25.2**	25	22.9**
Error	58	7.4	48	0.59	56	8.04	57	4.40

Remarks: a) SOV= source of variation, b) df= degree of freedom, c) MS= mean squares, ns, * and ** = non-significant, significant at p<0.05 and p<0.01, respectively

Table 2. Mean lesion lengths in rice varieties and Xanthomonas oryzae pv. oryzae isolates under greenhouse conditions from 2013 to 2015

Conditions	Isolates	Varieties						
		RD6	KDML105	LG6822	PRT	HMLN	PLD	Mean
Soil culture 2013	B786	10.7	12.6	0.6	0.9	1.3	1.1	**4.5**
	B928	11.4	5.2	1.0	0.4	0.7	0.8	**3.2**
	B1111	18.2	18.5	3.5	3.4	2.0	1.2	**7.8**
	B1066	14.8	16.8	0.1	2.2	1.7	0.5	**6.0**
	B1099	19.1	14.5	0.6	4.3	0.3	2.0	**6.8**
	B758	21.7	15.8	1.0	1.7	1.8	0.4	**7.1**
	Mean	**16.0**	**13.9**	**1.1**	**2.1**	**1.3**	**1.0**	**5.9**
Solution culture 2014	B786	0.9	1.1	ND*	0.7	1.1	1	**1.0**
	B928	0.5	0.4	ND	0.2	0.2	0.3	**0.3**
	B1111	0.9	1.6	ND	1	1.2	0.6	**1.1**
	B1066	4	3.2	ND	1.7	1.5	0.3	**2.1**
	B1099	0.2	0.2	ND	0.1	0.2	0.3	**0.2**
	B758	1.6	0.7	ND	0.4	1.1	0.3	**0.8**
	Mean	**1.4**	**1.2**	**ND**	**0.7**	**0.9**	**0.5**	**0.9**
Soil culture 2015	B786	8	3.2	0.5	7	8	6.2	**5.5**
	B928	10.8	12.7	11.5	4	7.8	4.4	**8.5**
	B1111	9.8	9.4	2.8	3.5	8	1.9	**5.9**
	B1066	13.1	14.3	4.3	8.7	11.6	0.2	**8.7**
	B1099	16.6	8.5	5.7	7.4	8.9	0.2	**7.9**
	B758	10.8	8.5	7.8	9.1	11.7	0.2	**8.0**
	Mean	**11.5**	**9.4**	**5.4**	**6.6**	**9.3**	**2.2**	**7.4**
Solution culture 2015	B786	12.7	1.4	1	0.5	1.1	0.3	**2.8**
	B928	1.7	1.2	1.2	0.6	0.7	0.4	**1.0**
	B1111	2.2	0.7	2.1	0.7	2.8	1.8	**1.7**
	B1066	1.8	2.4	1.1	0.5	2.4	0.5	**1.5**
	B1099	1.3	0.6	0.7	1	0.6	0.5	**0.8**
	B758	4.9	15	2.5	5.4	2	4	**5.6**
	Mean	**4.1**	**3.6**	**1.4**	**1.5**	**1.6**	**1.3**	**2.2**
Overall mean		**8.4**	**7.1**	**2.7**	**2.8**	**3.3**	**1.2**	**4.2**

Remarks: ND= non determined

To date, several breeding programmes to improve BLB resistance in Thai rice varieties have been developed (Korinsak et al., 2009; Korinsak, Sirithanya, & Toojinda, 2009; Win et al., 2012; Pinta, Toojinda, Thummabenjapone, & Sanitchon, 2013). In most cases, researchers utilised the resistance lines from introduced varieties, such as IRBB21, IR24, IRBB5 and IR62266. Limitations of this approach included undesirable agronomic attributes and instability of resistance. In contrast, screening indigenous rice varieties are adaptive to local areas and possess desirable agronomic attributes.

Different virulent reactions were observed when examining *Xoo* isolates from different rice varieties. The BB2009-758 isolate from Ubon Ratchatani, BB2009-1066 isolate from Udon Thani and BB2009-1111 isolate from Khon Kaen were more virulent, indicating that these varieties transmit infections to other varieties and in different cultivation conditions. However, some isolates are more virulent in specific conditions, such as BB2009-928 isolate from Udon Thani. This isolate was more virulent in soil cultures in the summer of 2015 than others, suggesting that this isolate was a specific pathogen. However, PLD reported the shortest lesion length in all *Xoo* isolates (Table 2), indicating that PLD has a different BLB resistance gene.

Das, Sengupta, Prasad, & Ghose (2014) have previously reported on divergent genes for BLB resistance. In this study, the reaction to *Xoo* isolates from HMLN, PRT, LG6822 and PLD are different (see Table 1 and 2), indicating different resistance genes. PLD, the indigenous lowland rice variety was collected from Yasothorn province in Northeast Thailand, possessed the broadest resistance, followed by PRT, LG6822 and HMLN, respectively. However, BLB infections were vary from varieties to varieties based on seasonal and screening conditions. The pathogen favours wet conditions (Table 2) and large-scale field tests, which limits breeding programmes' success due to environmental factors. Ultimately, soil cultures in rainy seasons are most suited to BLB pathogenic testing to distinguish susceptible and resistant varieties than other cultures and seasons (Table 2). Artificial inoculation under controlled conditions is neither labour- nor space-intensive and therefore is ideal for large-scale year round screening.

Out of the four conditions tested, the 2015 soil culture had the longest lesion length and the 2014 solution culture had the shortest. Interestingly, the 2013 soil culture showed a higher ability to discriminate amongst varieties than the others. Table 2 suggests that these conditions can be used to select *Xoo* isolates as well as variety in a rice breeding programme. The lesion length for each variety differed among culture conditions due to the correlation of the severity of disease and GXE interaction (Table 1). PLD shows a stable lesion length with a simple regression value of b=0.17. This value lies below the values shown by other varieties (Fig. 2) and indicates that this variety possesses a broad resistance to BLB. However, BLB disease incidence affected by the GE interaction led to confounding results. Therefore, a GGE biplot analysis can also be employed to identify durable resistance, the most virulent pathogen and the particular environment that can be used to distinguish resistance levels among varieties (Yan & Falk, 2002).

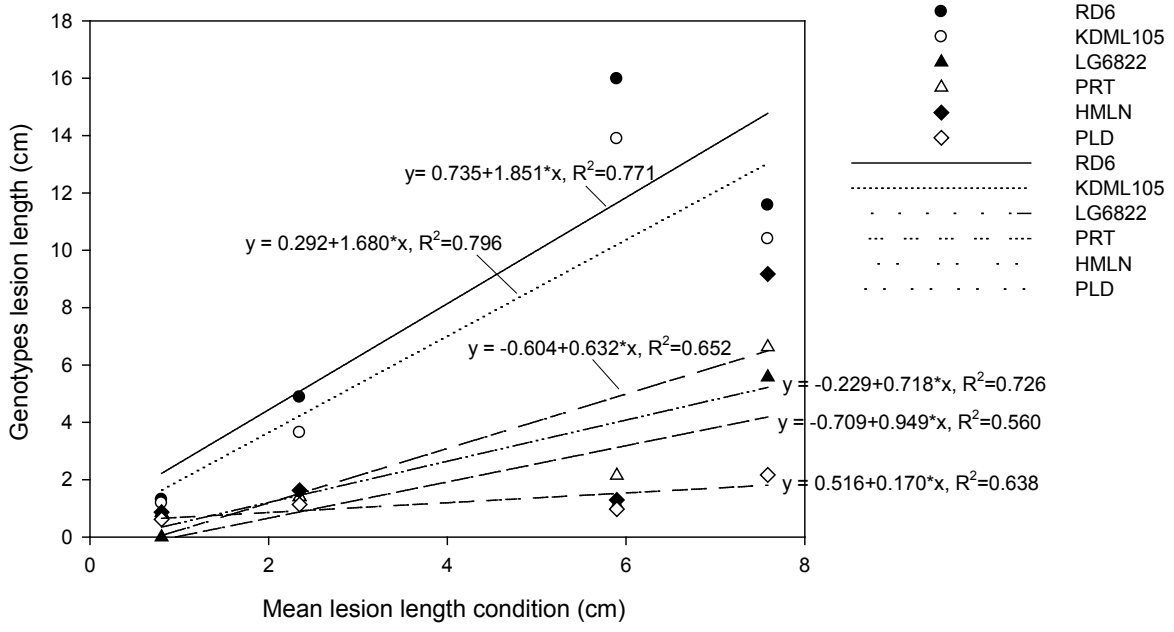

Fig 2. Simple linear regression of disease incidence for different severity of rice varieties under greenhouse conditions

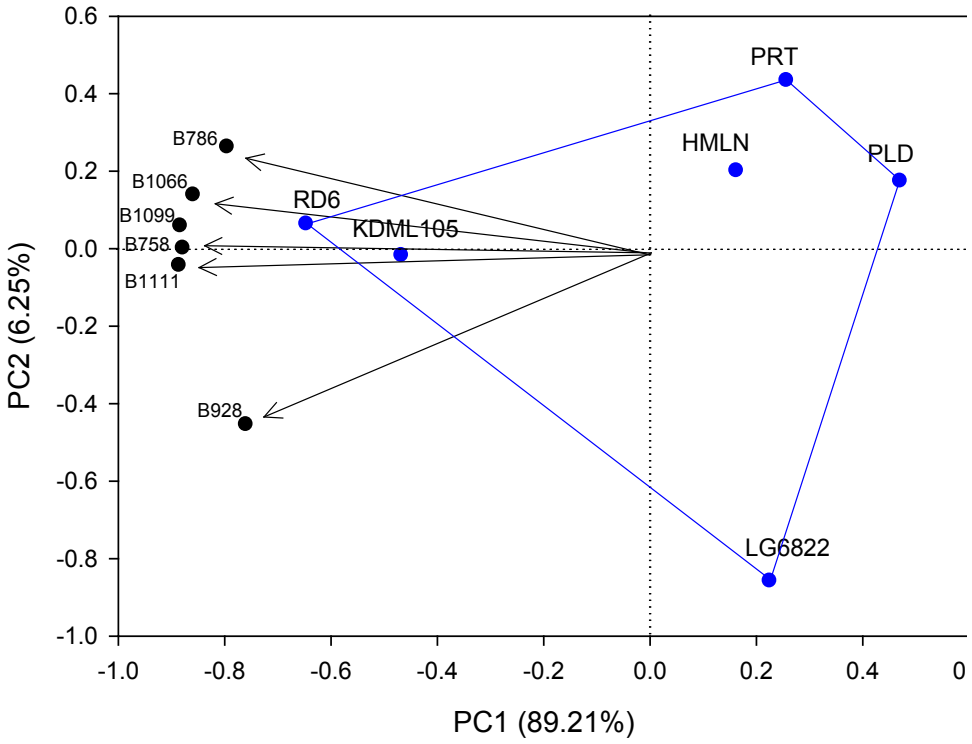

Fig 3. GGE biplot based on BLB lesions length in six rice varieties and six *Xanthomonas oryzae pv. oryzae* isolates. The average environmental axis (AEA) is the straight line that passes through the origin (0.0) and coordinate of the culture condition mean

The GGE biplot analysis shows the grouping of six varieties based on their mean lesion length and stability (Fig. 3) over three screening conditions (2014 soil culture was omitted due to missing data for variety LG6822). Following this, the varieties can be divided into two groups. The first group is represented by *Xoo* isolates and the varieties with the longest lesion length or highest susceptibility, RD6 and KDML105. The second group consists of varieties PLD, PRT, LG6822 and HMLN, which had a shorter lesion length or less resistance to BLB disease. In this graph, the first two PCs accounted for 95.46% (PC1=89.21%, PC2=6.25%) of the total GGE variation among the data (Figure 3). PC1 consistently shows higher values than PC2 with regards to lesion length for the six isolates, demonstrating that the lesion length is majorly affected by genotype rather than GE interaction effects. The varieties located closer to the X-axis show a more stable resistance. In this study, PLD was found to be the best genotype out of all the *Xoo* isolates in the three screening conditions. Based on lesion length and stability performance, PLD came first, followed by PRT, HMLN and LG6822, while RD6 and KDML105 performed the worst.

The GGE biplot was used to identify disease resistance and associated stability in several crops, such as soybean (Twizeyimana et al., 2008), chick pea (Sharma et al., 2012), wheat (Gitonga, Ojwang, Macharia, & Njau, 2016), mung bean (Alam, Somta, Jompuk, Chatwachirawong, & Srinives, 2014) and rice (Idowu, Salami, Ajayi, Akinwale, & Sere, 2013; Tabien, Samonte, Abalos, & San Gabriel, 2008). Moreover, genotype and GE interaction, graphically represented using a GGE biplot to assess the genotypes and environment, play an important role in variety selection (Yan, 2001; Yan & Hunt, 2002). In this study, the GGE biplot analysis identifies ideal conditions and isolates for BLB screening, and also highlights the PLD rice variety as the most stable new source of BLB resistance in Thailand.

CONCLUSION

The overall results of this study confirmed the preliminary results published by Chanlakhon, Thammabenjapon, & Sanitchon (2012) that some of Thai indigenous rice varieties are potential to be a source of BLB resistance. The varieties demonstrate a stable resistance to BLB for all seasonal and screening conditions. This indicates that the resistance varieties, including PLD, PRT, LG6822 and HMLN, are reliable. The four varieties provide an opportunity for breeding with resistance to BLB in Thailand. Further research is needed to identify the genes responsible for resistance in these varieties in order to integrate divergent sources of resistance into commercial cultivation.

ACKNOWLEDGEMENT

This research was supported by the Plant Breeding Research Centre for Sustainable Agriculture and Research Center of Agricultural Biotechnology for Sustainable Economy, Khon Kaen University, Thailand. The authors thank to Cowan Communications GbR for proofreading the manuscript. Our gratitude is also extended to the Thailand Research Fund (TRF) (Project code: IRG5780003) and the Faculty of Agriculture, Khon Kaen University, for providing financial support for manuscript preparation.

REFERENCES

Akhtar, M. A., Abbasi, F. M., Ahmad, H., Shahzad, M., Shah, M. A., & Shah, A. H. (2011). Evaluation of rice germplasm against *Xanthomonas oryzae* causing bacterial leaf blight. *Pakistan Journal of Botany, 43*(6), 3021-3023. Retrieved from http://www.pakbs.org/pjbot/PDFs/ 43(6)/62.pdf

Akter, A., Hasan, M. J., Kulsum, U., Rahman, M. H., Khatun, M., & Islam, M. R. (2015). GGE biplot analysis for yield stability in multi-environment trials of promising hybrid rice (*Oryza sativa* L.). *Bangladesh Rice Journal, 19*(1), 1-8. http://doi.org/10.3329/brj.v19i1.25213

Alam, A. K. M. M., Somta, P., Jompuk, C., Chatwachirawong, P., & Srinives, P. (2014). Evaluation of mungbean genotypes based on yield stability and reaction to mungbean yellow mosaic virus disease. *Plant Pathology Journal*, *30*(3), 261–268. http://doi.org/10.5423/ PPJ.OA.03.2014.0023

Chanlakhon, A., Thammabenjapon, P., & Sanitchon, J. (2012). Evaluation of resistance to bacterial leaf blight in low land rice germplasm. *Khon Kaen Agriculture Journal, 40*(4), 48-52. Retrieved from http://ag2.kku.ac.th/kaj/PDF.cfm?filename=10-Apichat.pdf&id=1049&keeptrack=17

Collard, B. C. Y., & Mackill, D. J. (2008). Marker-assisted selection: An approach for precision plant breeding in the twenty-first century. *Philosophical Transactions of the Royal Society B: Biological Sciences*, *363*(1491), 557–572. http://doi.org/10.1098/rstb.2007.2170

Das, B., Sengupta, S., Prasad, M., & Ghose, T. K. (2014). Genetic diversity of the conserved motifs of six bacterial leaf blight resistance genes in a set of rice landraces. *BMC Genetics, 2014*, 1-15. http://doi.org/10.1186/1471-2156-15-82

Flor, H. H. (1971). Current status of the gene-for-gene concept. *Annual Review of Phytopathology*, *9*(1), 275–296. http://doi.org/10.1146/annurev.py.09.090171.001423

Fotokian, M. H., & Agahi, K. (2014). Biplot analysis of genotype by environment for cooking quality in hybrid rice: A tool for line x tester data. *Rice Science*, *21*(5), 282–287. http://doi.org/10.1016/S1672-6308(13)60193-6

Gitonga, H. W., Ojwang, P. P. O., Macharia, G. K., & Njau, P. N. (2016). Evaluation of advanced bread wheat genotypes for resistance to stem rust and yield stability. *African Journal of Plant Science, 10*(6), 111-120. http://doi.org/10.5897/AJPS2016.1398

Gregorio, G. B., Dharmawansa, S. & Mendoza, R.D. (1997). Screening rice for salinity tolerance. IRRI. Discussion Paper Series No. 22. International Rice Research Institute, Manila, pp.1–30.

Idowu, O. O., Salami, A. O., Ajayi, S. A., Akinwale, R. A., & Sere, Y. (2013). Varietal resistance of rice to blast fungus *Magnaporthe oryzae* at two sites in southwestern Nigeria. *African Journal of Biotechnology, 12*(33), 5173-5182. http://doi.org/10.5897/AJB2012.2959

Jenns, A. E., Leonard, K. J., & Moll, R. H. (1982). Stability analyses for estimating relative durability of quantitative resistance. *Theoretical and Applied Genetics*, *63*(2), 183–192. http://doi.org/10.1007/BF00303707

Kang, M. S. (1992). Simultaneous selection for yield and stability in crop performance trials: Consequences for growers. *Agronomy Journal, 85*(3), 754-757. http://doi.org/10.2134/agronj1993.00021962008500030042x

Khan, M. A., Naeem, M., & Iqbal, M. (2014). Breeding approaches for bacterial leaf blight resistance in rice (*Oryza sativa* L.), current status and future directions. *European Journal of Plant Pathology, 139*(1), 27-37. http://doi.org/10.1007/s10658-014-0377-x

Khush, G. S. (2005). What it will take to feed 5.0 billion rice consumers in 2030. *Plant Molecular Biology*, *59*(1), 1–6. http://doi.org/10.1007/s11103-005-2159-5

Khush, G. S., Mackill, D. J., & Sidhu, G. S. (1989). Breeding rice for resistance to bacterial blight. In *Bacterial of blight rice* (pp. 207-218). Manila, PH: International Rice Research Institute.

Korinsak, S., Sirithanya, P., & Toojinda, T. (2009). Identification of SSR markers linked to a bacterial blight resistance gene in rice cultivar 'Pin Kaset'. *KKU Research Journal, 9*(2), 16-21. Retrieved from http://www.tci-thaijo.org/index.php/gskku/article/view/24247

Korinsak, S., Sriprakhon, S., Sirithanya, P., Jairin, J., Korinsak, S., Vanavichit, A., & Toojinda, T. (2009). Identification of microsatellite markers (SSR) linked to a new bacterial blight resistance gene xa33 (t) in rice cultivar "Ba7." *Maejo International Journal of Science and Technology*, *3*(2), 235–247. Retrieved from https://www.researchgate.net/publication/215750483

Lakew, T., Tariku, S., Alem, T., & Bitew, M. (2014). Agronomic performances and stability analysis of upland rice genotypes in North West Ethiopia. *International Journal of Scientific and Research Publications, 4*(4), 1-9. Retrieved from http://www.ijsrp.org/research-paper-0414/ijsrp-p2838.pdf

Latif, M. A., Rahman, M. M., Kabir, M. S., Ali, M. A., Islam, M. T., & Rafii, M. Y. (2011). Genetic diversity analyzed by quantitative traits among rice (*Oryza sativa* L.) genotypes resistant to blast disease. *African Journal of Microbiology Research*, *5*(25), 4383–4391. http://doi.org/10.5897/AJMR11.492

Ou, S. H. (1985). *Rice Diseases* (2nd ed.). Slough, UK: Commonwealth Agricultural Bureaux.

Pinta, W., Toojinda, T., Thummabenjapone, P., & Sanitchon, J. (2013). Pyramiding of blast and bacterial leaf blight resistance genes into rice cultivar RD6 using marker assisted selection. *African Journal of Biotechnology, 12*(28), 4432-4438. http://doi.org/10.5897/AJB12.202

R Development Core Team. (2010). *R: A language and environment for statistical computing* [Computer programme]. Retrieved from http://www.r-project.org/

Reddy, P. R., & Mohanty, S. K. (1981). Epidemiology of the kresek phase of bacterial blight of rice. *Plant Disease, 65*(7), 578-580. Retrieved from http://www.apsnet.org/publications/plantdisease/backissues/Documents/1981Articles/PlantDisease65n07_578.pdf

Sharma, M., Babu, T. K., Gaur, P. M., Ghosh, R., Rameshwar, T., Chaudhary, R. G., Upadhyay, J. P., Gupta, O., Saxena, D. R., Kaur, L., Dubey, S.C., Anandani, V. P., Harer, P. N., Rathore, A., & Pande, S. (2012). Identification and multi-environment validation of resistance to *Fusarium oxysporum* f. sp. ciceris in chickpea. *Field Crops Research, 135*, 82-88. http://doi.org/10.1016/j.fcr.2012.07.004

Somsana, P., Wattana, P., Suriharn, B., & Sanitchon, J. (2013). Stability and genotype by environment interactions for grain anthocyanin content of thai black glutinous upland rice (*Oryza sativa*). *SABRAO Journal of Breeding and Genetics, 45*(3), 523-532. Retrieved from http://www.sabrao.org/journals/ vol45_3_ dec2014/SABRAOJ%20Breed%20Genet%2045(3)%20523-532%20Somsana.pdf

Sreewongchai, T., Toojinda, T., Thanintorn, N., Kosawang, C., Vanavichit, A., Tharreau, D., & Sirithunya, P. (2009). Development of elite indica rice lines with wide spectrum of resistance to Thai blast isolates by pyramiding multiple resistance QTLs. *Plant Breeding, 129*(2), 176-180. http://doi.org/10.1111/j.1439-0523.2009.01669.x

Sun, X., Cao, Y., Yang, Z., Xu, C., Li, X., Wang, S., & Zhang, Q. (2004). Xa26, a gene conferring resistance to *Xanthomonas oryzae* pv. oryzae in rice, encodes an LRR receptor

kinase-like protein. *The Plant Journal, 37*(4), 517-527. http://doi.org/10.1046/j.1365-313X.2003.01976.x

Tabien, R. E., Samonte, S. O. P. B., Abalos, M. C., & San Gabriel, R. C. (2008). GGE biplot analysis of performance in farmers' fields, disease reaction and grain quality of bacterial leaf blight-resistant rice genotypes. *Philippine Journal of Crop Science, 33*(1), 03-19. Retrieved from http://www.cabi.org/gara/FullTextPDF/2008/20083129674.pdf

Thakur, R. P., Shetty, K. G., & King, S. B. (1992). Selection for host-specific virulence in asexual populations of *Sclerospora graminicola*. *Plant Pathology*, *41*, 626–632. http://doi.org/10.1111/j.1365-3059.1992.tb02463.x

Twizeyimana, M., Ojiambo, P. S., Ikotun, T., Ladipo, J. L., Hartman, G. L., & Bandyopadhyay, R. (2008). Evaluation of soybean germplasm for resistance to soybean rust (*Phakopsora pachyrhizi*) in Nigeria. *Plant Disease*, *92*(6), 947–952. http://doi.org/10.1094/pdis-92-6-0947

Win, K. M., Korinsak, S., Jantaboon, J., Siangliw, M., Lanceras-Siangliw, J., Sirithunya, P., Vanavichit, A., Pantuwan, G., Jongdee, B., Sidhiwong, N., & Toojinda, T. (2012). Breeding the Thai jasmine rice variety KDML105 for non-age-related broad-spectrum resistance to bacterial blight disease based on combined marker-assisted and phenotypic selection. *Field Crops Research, 137*, 186-194. http://doi.org/10.1016/j.fcr.2012.09.007

Yan, W. (2001). GGEbiplot - A windows application for graphical analysis of multienvironment trial data and other types of two-way data. *Agronomy Journal*, *93*(5), 1111–1118. http://doi.org/10.2134/agronj2001.9351111x

Yan, W., & Falk, D. E. (2002). Biplot analysis of host-by-pathogen data. *Plant Disease*, *86*(12), 1396–1401. http://doi.org/10.1094/PDIS.2002.86.12.1396

Yan, W. & Hunt, L. A. (2002). Biplot analysis of diallel data. *Crop Science*, 42, 21-30. Retrieved from http://www.ggebiplot.com/Yan-Hunt2002.pdf

Yoshida, S., Forno, D. A., Cock, J. H., & Gomez, K. A. (Eds.). (1976). Routine procedures for growing rice plants in culture solution. In *Laboratory manual for physiological studies of rice* (pp. 61-66). Laguna, PH: The International Rice Research Institute.

Sugar Tech (Jan-Feb 2017) 19(1):64–71
DOI 10.1007/s12355-016-0437-y

RESEARCH ARTICLE

Sweet Sorghum and Upland Rice: Alternative Preceding Crops to Ameliorate Ethanol Production and Soil Sustainability Within the Sugarcane Cropping System

N. Thawaro[1] · B. Toomsan[1] · W. Kaewpradit[1,2,3]

Received: 1 December 2015 / Accepted: 3 February 2016 / Published online: 1 March 2016

Abstract The objective of this study was to assess the effect of preceding crops (soybeans, sunn hemp, upland rice, and sweet sorghum) on the succeeding sugarcane yield, total bioethanol production, and soil chemical properties within the sugarcane cropping system. Treatments with upland rice and sweet sorghum provided the greatest increase in soil available P, compared to uncultivated land (control) at the final sampling, preceding the sugarcane harvest. Treatments effects were not significantly different for soil organic matter. At sugarcane harvest, the upland rice treatment provided the highest cane yield compared to the unplanted land, yet was not significantly higher than the yield of the sweet sorghum treatment. The highest sugarcane ethanol yields were observed in the sweet sorghum–sugarcane and upland rice–sugarcane treatments. However, the total ethanol yield in both preceding and succeeding crops was found to be highest in the sweet sorghum treatment, followed by the upland rice treatment. Upland rice proved to be most suitable for farming systems which emphasized food security, whereas sweet sorghum was most desirable for farming systems which emphasized alternative biofuel production. Both crops improved the sustainable production of soil and sugarcane.

Keywords Crop residue · Sunn hemp · Soybeans · C/N ratio · Bioethanol

Introduction

The importance of renewable fuel as an alternative energy source has increased significantly in recent years (Saxena et al. 2009). Specifically, bioethanol is one of the most useful forms of automobile fuel (Franceschin et al. 2008), and sugarcane is so far the most commonly used raw material in bioethanol production (Marina et al. 2011), contributing to 60 % of all global ethanol production (Demirbas 2009). Sugarcane is an important crop in many tropical countries including Thailand, where the production area has been reported to be approximately one million ha (Rumpa et al. 2012). Production areas in the Northeast occupy more than 40 % of Thailand's total sugarcane cultivation.

In Thailand's Northeast region, sugarcane is generally planted in October through December and is harvested in December to April of the following year. At the end of the last ratoon crop, there is a fallow period of 6–8 months before planting the next sugarcane crop (Hemwong et al. 2008). The period of inactivity in the sugarcane cropping system covers the duration of the rainy season. A short sugar crop with a short production span such as sweet sorghum can be produced during fallow period in order to increase bioenergy productivity of the upcoming sugarcane cropping system.

Electronic supplementary material The online version of this article (doi:10.1007/s12355-016-0437-y) contains supplementary material, which is available to authorized users.

✉ W. Kaewpradit
wanwka@gmail.com

[1] Agronomy Section, Department of Plant Science and Agriculture Resources, Faculty of Agriculture, Khon Kaen University, Muang, Khon Kaen 40002, Thailand

[2] Northeast Thailand Cane and Sugar Research Center, Khon Kaen University, Khon Kaen 40002, Thailand

[3] Applied Engineering for Important Crops of the North East Group, Khon Kaen University, Khon Kaen 40002, Thailand

Green manure legumes were tried during such a period, but they did not generate an economic return, and were not generally accepted by small farmers with limited resources (Whitmore et al. 2000). Grain legumes, such as groundnuts and soybeans, were more attractive options, as they provided income along with improved soil fertility, due to N_2 fixation. Retention of legume crop residues increases the soil organic matter and nutrient content in cropping systems (Promsakha Na Sakonnakhon et al. 2005). Upland rice is an alternative crop that is grown under rain-fed upland conditions, and is a major staple food crop in the region. Sweet sorghum [*Sorghum bicolor* (L.) Moench] is a crop with high potential for ethanol production and is a good second option for candidate energy crops (Kaien et al. 2012). It produces an ethanol yield of 70 l per ton of fresh stalk, and optimum planting occurs from March to July, which corresponds with sugarcane's fallow period. Production of sweet sorghum in the fallow period may increase the efficiency of bioethanol production in sugarcane cropping system; however, the residual effect of different preceding crops may lead to different impacts on succeeding sugarcane yields and total ethanol production within the sugarcane production system. Moreover, the potential preceding crops for bioenergy production should improve, or at the very least maintain soil fertility within the cropping system. The objective of this study is therefore to assess the effect of different preceding crops on soil chemical properties at the preceding crop's harvest, succeeding sugarcane yield, total bioethanol production, and soil chemical properties at the succeeding sugarcane harvest.

Materials and Methods

Experiment Location

The field experiment was conducted from July, 2011, to February, 2013, in Ban Wang Wha, Khon Kaen, Thailand. Soil samples were collected at 0–15 cm depths for chemical analysis before the preceding crops planting, at the preceding crop harvest, and at the last sugarcane harvest. The soil is classified as Nam Phong soil series (Grossarenic Haplustalfs), with 95.96 % sand, 2.93 % silt, and 1.11 % clay (sandy soil). The soil chemical properties are soil pH 5.49 (1:2.5 H_2O), cation exchange capacity (CEC) 2.50 cmol kg^{-1}, electrical conductivity (EC) 0.011 mS cm^{-1}, organic matter (OM) 3.40 mg g^{-1}, available phosphorus (P) 17.06 µg g^{-1}, exchangeable potassium (K) 31.72 µg g^{-1}, exchangeable calcium (Ca) 92.50 µg g^{-1}, and total nitrogen (N) 0.19 mg g^{-1} (Table 1). Total rainfall during the experimental period (1960 mm), average weekly rainfall, and temperature patterns are also provided (supplementary file).

Management of the Preceding Crops

The preceding treatments including control (fallow), upland rice (*Oryza sativa* L.), sunn hemp (*Crotalaria juncea*), soybeans (*Glycine max*), and sweet sorghum [*Sorghum bicolor* (L.) Moench] were arranged in randomized complete block design (RCBD) with four replications, and a plot size of 9.6 × 6 m. Crops were planted on July 8, 2011. Upland rice cultivar Sew Mae Jan was planted with a spacing of 50 × 25 cm, and N, P, and K fertilizers were applied simultaneously to the rice plots at the rates of 15.0 kg N ha^{-1}, 8.3 kg P ha^{-1}, and 15.6 kg K ha^{-1}. Fertilizer in the form of ammonium sulfate was top-dressed to the rice crop during the panicle initiation (PI) stage at the rate of 6.6 kg N ha^{-1}. Sunn hemp was sown to the plot at the seed rate of 31.3 kg ha^{-1} and harvested at 100 days after sowing (no fertilizer was used). Soybean seeds were inoculated with commercial *Rhizobium* inoculant (Department of Agriculture, Ministry of Agriculture and Cooperatives, Thailand) and planted with a spacing of 50 × 20 cm and received N, P, and K fertilizers at the rates of 18.8 kg N ha^{-1}, 16.5 kg P ha^{-1}, and 15.6 kg K ha^{-1}. Sweet sorghum was planted with a spacing of 50 × 10 cm and received N, P, and K fertilizers in two equal splits each, at the rates of 46.9 kg N ha^{-1}, 20.6 kg P ha^{-1}, and 38.9 kg K ha^{-1}. The first split was done at the time of planting, while the second split occurred 30 days after planting. The preceding crops and weeds in the control plots were evaluated at harvest for dry weight and nutrient content.

Succeeding Crops

Sugarcane variety Khon Kaen 3 was planted on February 7, 2012, after the harvesting of upland rice, sunn hemp, soybeans, and sweet sorghum (as well as weeds in the fallow plots). After each preceding crop harvest, soil was twice plowed to incorporate crop residues into the soil. Sugarcane was subsequently planted 2 weeks after the incorporation of crop residues, with spacing of 120 cm between rows and 30 cm between plants. Two applications of chemical fertilizers were made. The first application was conducted at the time of planting, at the rates of 46.88 kg N ha^{-1}, 20.63 kg P ha^{-1}, and 38.91 kg K ha^{-1}, while the second application of urea was performed 5 months after planting, at the rate of 71.88 kg N ha^{-1}.

Data Collection

Preceding Crop Harvest

Plant samples were harvested in areas of 15 m^2 $plot^{-1}$. Heads of sweet sorghum were cut from the stems, and fresh stem weights were recorded. Twenty stem samples were

Table 1 Chemical properties of soil at depths of 0–15 cm before proceeding crops planting

Chemical properties	
pH (1:2.5 H_2O)	5.49
EC (mS cm^{-1})	0.011
CEC (cmol kg^{-1})	2.50
OM (mg g^{-1})	3.40
Total N (mg g^{-1})	0.19
Available P (μg g^{-1})	17.06
Exchangeable K (μg g^{-1})	31.72
Exchangeable Ca (μg g^{-1})	92.50

also assessed to determine juice yield, total soluble solids (°Brix), and ethanol yield using batch fermentation method (Laopaiboon et al. 2009). Five hundred grams of samples of the remaining stems (after juice extraction) was taken from each plot, oven-dried at 70 °C until constant dry weights were obtained, and then used in dry matter yield calculations. The stover weights of all treatments were recorded. Grain yields, seed yields, and juice yields were recorded in upland rice, soybeans, and sweet sorghum. Residue samples were taken, oven-dried, weighed, ground, and then analyzed for N, P, K, Ca, lignin (L), and polyphenol contents. Crop residues were incorporated into the respective soil plots prior to sugarcane planting.

Soil Data of the Preceding Crops (at Harvest) and Sugarcane (at Harvest), and Soil Mineral N During Sugarcane Growth

Soil samples at 0–15 cm soil depths were collected at preceding crop harvests and at the sugarcane harvest, for chemical analysis. Soil pH (1:2.5 H_2O) was determined using pH meter. CEC by 1 M ammonium acetate extraction, OM by Walkley and Black (wet oxidation), total N by Kjeldahl, available P by Bray II and exchangeable K and Ca by using 1 M ammonium acetate extraction at pH 7 was determined.

Soil samples at 0–15 cm were again taken at 8, 16, 24, 32, 40, and 48 weeks after the sugarcane was planted. Mineral N (NH_4^+ and NO_3^-) was determined from 20 g of fresh soil immediately after sampling. Soil samples were extracted with 100 ml of 1 M KCl, and mineral N was determined colorimetrically, using a flow injection analysis (FIA) (Tecator 1984).

Growth, Yield, and Ethanol Yield of the Succeeding Sugarcane

At final harvest, sugarcane was harvested from an area of 7.2 × 4.2 m in each plot. Recorded data included stalk number, stalk weight, and commercial cane sugar (CCS). Total soluble solids were measured with a hand refractometer on three points per stalk (of five stalks), and each stalk taken from five randomly chosen hills. CCS was calculated according to the method described by Blackburn (1984). Twenty cane stalks were sampled from each plot and subjected to juice extraction. Ethanol yield of sugarcane juice was also analyzed, by batch fermentation (Laopaiboon et al. 2009).

Statistical Analysis

Data were analyzed using a randomized complete block (four replications) analysis of variance (ANOVA). Statistical analyses were achieved using an MSTAT-C (version 1.42), developed by the Crop and Soil Science Division, Michigan State University, Michigan, USA. A single ANOVA factor was used to analyze the main effect of the treatments, and the standard error of mean (SEM) between treatment means is presented.

Results

Yield of the Preceding Crops

At final preceding crop harvest, upland rice had the highest residue of 4.03 tons ha^{-1}, followed by the fallow, sunn hemp, soybean, and sweet sorghum treatments (Table 2). Moreover, upland rice had the highest grain yield of 2.87 tons ha^{-1}, whereas soybeans had a grain yield of 1.95 tons ha^{-1}. The ethanol yield of sweet sorghum was 2111 l ha^{-1}. Upland rice had the highest biomass production of 6.90 tons ha^{-1}, followed by sorghum, soybeans, fallow, and sunn hemp.

Table 2 Yield of preceding crops (seeds and sugar) and dry residues left in the field

Treatment	Ethanol yield (l ha^{-1})	Grain yield (tons ha^{-1})	Residues (tons ha^{-1})
Control (fallow)	0	–	2.98
Soybean[a]	0	1.95	2.18
Sunn hemp	0	–	2.42
Upland rice[a]	0	2.87	4.03
Sweet sorghum[b]	2111	–	2.12
SEM			324.19**
C.V. (%)			23.63

SEM standard error of mean

** = significantly different at $p \leq 0.01$

[a] Seeds were removed from the field

[b] Sugar was removed from the field

Soil Chemical Properties After Preceding Crops' Harvest

Significant differences among treatments were observed for pH, EC, total N, exchangeable Ca ($p \leq 0.05$), available P ($p \leq 0.01$), and CEC ($p \leq 0.10$). Treatments were not significantly different for both OM and exchangeable K (Table 3). The preceding crop treatments demonstrated a decrease in soil pH, in which sweet sorghum had the lowest soil pH ($p \leq 0.05$), compared with the fallow treatment. Those preceding crop treatments that received chemical fertilizers (upland rice, sweet sorghum, and soybean) yielded a higher EC ($p \leq 0.05$) and available P ($p \leq 0.01$), compared with those treatments which received no chemical fertilizers (sunn hemp and fallow). However, preceding crop treatments had a tendency to reduce total N, compared to the fallow treatment ($p \leq 0.05$), in which the highest total N was observed. Although significant differences were observed in both CEC ($p \leq 0.10$) and exchangeable Ca ($p \leq 0.05$), no significant differences were observed between preceding crop treatments and the fallow treatment.

Chemical Properties and Nutrient Contents (N, P, K, and Ca) in Crop Residues Added to the Succeeding Sugarcane Crop'S Soil

Total N concentrations in crop residue ranging from 0.41 % in upland rice to 0.95 % in sunn hemp were observed among residues of the preceding crops (Table 4). Sweet sorghum had a rather low total N in its residue, whereas fallow and soybeans had an intermediate total N of 0.61 and 0.67 %, respectively. Sweet sorghum also had the highest (L + *P*)/N ratio, followed by upland rice, soybeans, fallow, and sunn hemp, as well as the highest *P*/N ratio, followed by upland rice, sunn hemp, fallow, and soybeans. Soybeans had the highest lignin (L) content of 14.52 %, followed by sunn hemp, upland rice, fallow, and sweet sorghum at 9.19, 8.59, 8.44, and 7.03 %, respectively, as well as the highest polyphenol (*P*) content (17.87 %), followed by sweet sorghum, fallow, upland rice, and sunn hemp, and the highest L/N ratio, followed by upland rice, sweet sorghum, and fallow, and sunn hemp. Upland rice had the highest C/N ratio, followed by sweet sorghum, fallow, soybeans, and sunn hemp.

Table 3 pH, EC, CEC, OM, total N, available P, exchangeable K, and Ca of soil at 0–15 cm soil layers at the final harvest of the preceding crops

Treatments	pH (1:2.5 H_2O)	EC (mS cm^{-1})	CEC (cmol kg^{-1})	OM (mg g^{-1})	Total N (mg g^{-1})	Available P (μg g^{-1})	Exchangeable K (μg g^{-1})	Exchangeable Ca (μg g^{-1})
Control (fallow)	5.28	0.007	3.09	4.5	0.24	7.48	27.30	120.00
Soybean	5.16	0.009	3.26	4.2	0.20	12.46	25.20	100.00
Sunn hemp	5.27	0.007	2.79	4.0	0.20	7.44	29.87	115.00
Upland rice	5.25	0.010	3.68	4.3	0.021	25.03	25.44	135.00
Sweet sorghum	5.11	0.010	2.88	4.1	0.20	16.94	23.34	115.25
SEM	0.05*	0.001*	0.29#	0.2^{ns}	0.01*	2.11**	3.26^{ns}	6.67*
C.V. (%)	1.84	25.20	18.94	9.81	11.40	30.34	24.86	11.41

SEM standard error of mean

= significantly different at $p \leq 0.1$, * = significantly different at $p \leq 0.05$

** = significantly different at $p \leq 0.01$, ns = not significantly different at $p \leq 0.1$

Table 4 Percentages of N, lignin (L), polyphenol (*P*), C/N, L/N, *P*/N, and (L + *P*)/N ratios in the tissues of preceding crops at final harvest

Treatment	% N	% L	% *P*	C/N	L/N	$^{b}P/N$	(L + ^{b}P)/N
Control (fallow)	0.61	8.44	8.99	65.39	13.83	14.73	28.57
Soybeans	0.67	14.52	7.72	56.25	21.67	11.52	33.19
Sunn hemp	0.95	9.19	17.87	44.32	9.67	18.81	28.48
Upland rice	0.41	8.59	8.11	90.80	20.74	19.58	40.73
Sweet sorghum	0.45	7.03	14.62	73.33	15.62	32.48	48.11

Table 5 Total N, total P, total K and total Ca in crop residues added to soil

Treatment	Total N (kg N ha^{-1})	Total P (kg P ha^{-1})	Total K (kg K ha^{-1})	Total Ca (kg Ca ha^{-1})
Control (fallow)	18.00	4.00	43.06	13.38
Soybean	14.56	4.25	26.69	5.56
Sunn hemp	23.06	3.19	47.31	8.13
Upland rice	16.69	8.31	102.06	13.94
Sweet sorghum	9.56	1.13	16.06	7.31

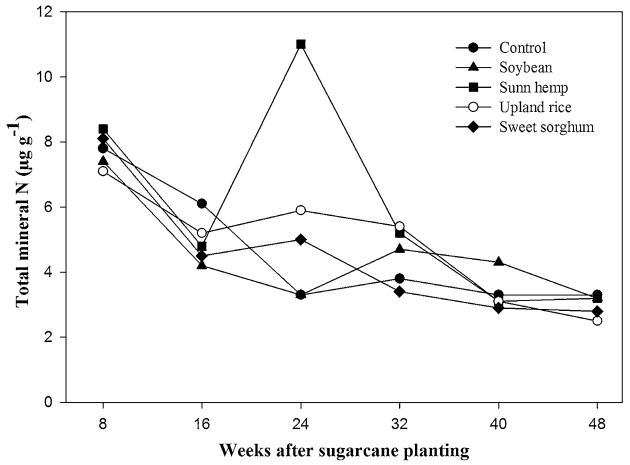

Fig. 1 Soil's total N through various treatments at 8, 16, 24, 32, 40, and 48 weeks after sugarcane planting

The nutrients in crop residues added to the soil were observed to be dependent upon residues types (Table 5). The highest addition of nitrogen (N) was found in sunn hemp (23.06 kg N ha^{-1}), followed by fallow, upland rice, soybeans, and sweet sorghum (9.56 kg N ha^{-1}; Table 5). The highest P added was observed in upland rice (8.31 kg P ha^{-1}) followed by soybean, fallow, sunn hemp, and sweet sorghum (1.13 kg P ha^{-1}). The highest K was also observed in upland rice (102.06 kg K ha^{-1}), followed by sunn hemp, fallow, soybeans, and sweet sorghum (16.06 kg K ha^{-1}). Lastly, the highest Ca added to the soil was found in upland rice (13.94 kg Ca ha^{-1}) followed by fallow, sunn hemp, sweet sorghum, and soybeans (5.56 kg Ca ha^{-1}).

Soil Total N at Sugarcane Planting

After the incorporation of crop residues into the soil, total mineral N was monitored at 0–15 cm of the soil surfaces at 8, 16, 24, 32, 40, and 48 weeks after sugarcane planting. The total N found within all treatments generally decreased from 8 to 48 weeks after sugarcane planting (Fig. 1). However, at 24 weeks after planting, the sunn hemp treatment demonstrated an increase in total mineral N content to 11.0 µg g^{-1} soil, then dropped rapidly at 32 weeks after planting, and continued to decline gradually through the last 48 weeks.

Number of Stalks, Cane Yield, CCS, Total N, and Total Ethanol Yield

Differences ($p \leq 0.05$) among preceding crop treatments were observed for number of stalks, cane yield, total N in tissue, and total ethanol yield, whereas no significant differences were observed for CCS (Table 6). The highest number of stalks was observed in the upland rice treatment, though not significantly greater than the sunn hemp, fallow, and sweet sorghum treatments. The highest cane yield (89.00 tons ha^{-1}) was also achieved by the upland rice treatment. Total N in cane stalks ranged from 106.55 to 186.26 kg ha^{-1} in the sunn hemp and sweet sorghum treatments, respectively. Total ethanol yields from succeeding sugarcane ranged from 3468.8 to 5652.5 l ha^{-1} in the fallow and upland rice treatments, respectively (Table 7). In general, upland rice and sweet sorghum provided higher cane yield, total N, and total ethanol yield, over both the soybean and sunn hemp treatments.

Soil Chemical Properties After Sugarcane Harvest

Soil samples (0–15 cm soil depth) were collected for chemical properties analysis at the succeeding sugarcane's final harvest. The upland rice treatment had the highest soil pH, while sweet sorghum ranked the lowest (and significantly different at $p \leq 0.05$). The soybean and sweet sorghum treatments had the highest CEC, though not significantly different from upland rice. The sunn hemp and fallow treatments maintained the lowest values.

All preceding crops treatments had significantly higher soil total N and OM and higher available P than the fallow treatment. Upland rice had the highest exchangeable K, but not significantly different from soybean, sweet sorghum, and fallow, whereas sunn hemp had the lowest value and significantly higher exchangeable Ca than the other treatments (Table 8).

Table 6 Number of stalks, cane yield, CCS, total N, and total ethanol yield of sugarcane grown after the preceding crops

Treatment	Number of stalks (ha^{-1})	Cane yield ($tonsha^{-1}$)	CCS	Total N ($kg\ ha^{-1}$)	Ethanol yield ($l\ ha^{-1}$)
Control (fallow)	70,106	62.06	17.21	111.99	3468.8
Soybean	64,401	65.49	16.96	114.35	4086.4
Sunn hemp	70,685	61.79	16.34	106.55	3533.3
Upland rice	81,763	89.00	16.88	142.41	5652.5
Sweet sorghum	67,212	76.32	16.83	186.26	5254.4
SEM	6104^{ns}	5.58*	0.35^{ns}	12.79**	317**
C.V. (%)	17.24	15.75	3.79	19.34	14.43

SEM standard error of mean

* = significantly different at $p \leq 0.05$

** = significantly different at $p \leq 0.01$

ns = not significantly different at $p \leq 0.1$

Table 7 Total ethanol yield in each system

Treatment	Ethanol yield ($l\ ha^{-1}$)			Increased ethanol yield (over control) ($l\ ha^{-1}$)
	Preceding crops	Succeeding crops (sugarcane)	Total ethanol yield	
Control (fallow)	–	3468.8	3468.8	–
Soybean	–	4086.4	4086.4	617.7
Sunn hemp	–	3533.3	3533.3	64.5
Upland rice	–	5652.5	5652.5	2183.7
Sweet sorghum	2111	5254.7	7365.4	3896.6
SEM		317**	328**	354**
C.V. (%)		14.43	13.60	41.89

SEM standard error of mean

** = significantly different at $p \leq 0.01$

Table 8 pH, EC, CEC, OM, total N, available P, exchangeable K and Ca, at the final harvest of the sugarcane crops (0–15 cm soil depths)

Treatment	pH (1:2.5 H_2O)	EC ($mS\ cm^{-1}$)	CEC ($cmol\ kg^{-1}$)	OM ($mg\ g^{-1}$)	Total N ($mg\ g^{-1}$)	Available P ($\mu g\ g^{-1}$)	Exchangeable K ($\mu g\ g^{-1}$)	Exchangeable Ca ($\mu g\ g^{-1}$)
Control (fallow)	4.79	0.013	0.62	4.4	0.12	16.67	31.91	22.50
Soybean	4.81	0.013	1.01	6.1	0.21	29.10	40.12	25.00
Sunn hemp	5.02	0.012	0.66	5.6	0.19	21.45	27.09	32.50
Upland rice	5.22	0.013	0.81	5.8	0.19	26.95	42.07	52.50
Sweet sorghum	4.72	0.012	0.99	5.7	0.20	27.52	37.18	25.00
SEM	0.09*	0.0007^{ns}	0.11#	0.3*	0.01*	2.72*	3.03*	7.43#
C.V. (%)	3.71	11.06	29.17	9.52	17.98	37.44	32.68	47.18

SEM Standard error of mean

= significantly different at $p \leq 0.1$

* = significantly different at $p \leq 0.05$

ns = not significantly different at $p \leq 0.1$

Discussion

Soil Sustainability

Soil analysis of the preceding crops' harvest found the upland rice treatment to be highest in soil available P, followed closely by the sweet sorghum treatment. The remaining treatments were significantly lower in value. Data collection occurred before the preceding crop residues were incorporated into the soil. The upland rice treatment also added the highest P, K, and Ca to the soil. The highest N added to the soil was revealed in the sunn hemp treatment's analysis. The amount of nutrients added to the soil as well as the chemical properties of the preceding crop residues also varied according to residue types, thus leading to different decomposition rates and nutrient availability. Sunn hemp residues had the lowest C/N and L + *P*/N ratios, which led to a rapid N release (Vityakon et al. 2000; Kaewpradit et al. 2008). However, the early N released from the sunn hemp residues may be lost before the sugarcane is able to develop enough root system capable of absorbing it. The high L + *P*/N ratios in the upland rice and sweet sorghum residues led to slow N release, and therefore, its prolonged availability.

Soil analysis at sugarcane harvest revealed that soil OM, total N, and available P in the preceding crop treatments differed significantly from the fallow treatment. The highest exchangeable Ca was found in the upland rice treatment and significantly different from the rest of the treatments. Our results indicate that the growth of preceding crops in the fallow period (between the last ratoon cane harvest and the next sugarcane crop planting) may increase the availability of some nutrients and thus became available to the succeeding cane.

Upland Rice and Sweet Sorghum Improved Cane Productivity

The highest succeeding sugarcane yield was achieved in the upland rice treatment, followed closely by the sweet sorghum treatment, while the remaining preceding crop treatments varied insignificantly. While the sweet sorghum treatment yielded lower amounts of N, P, and K in its residue (compared to the upland rice treatment), its addition to the soil increased the sugarcane yield to a level equal to the upland rice treatment, due to its residue having a higher (L + *P*)/N ratio than the upland rice residue (which leads to a slow release and possibly increased retention of nitrogen). The low amounts of N, P, and K in the sweet sorghum residue may also be a result of the juice extraction (for ethanol production) before returning it to the field.

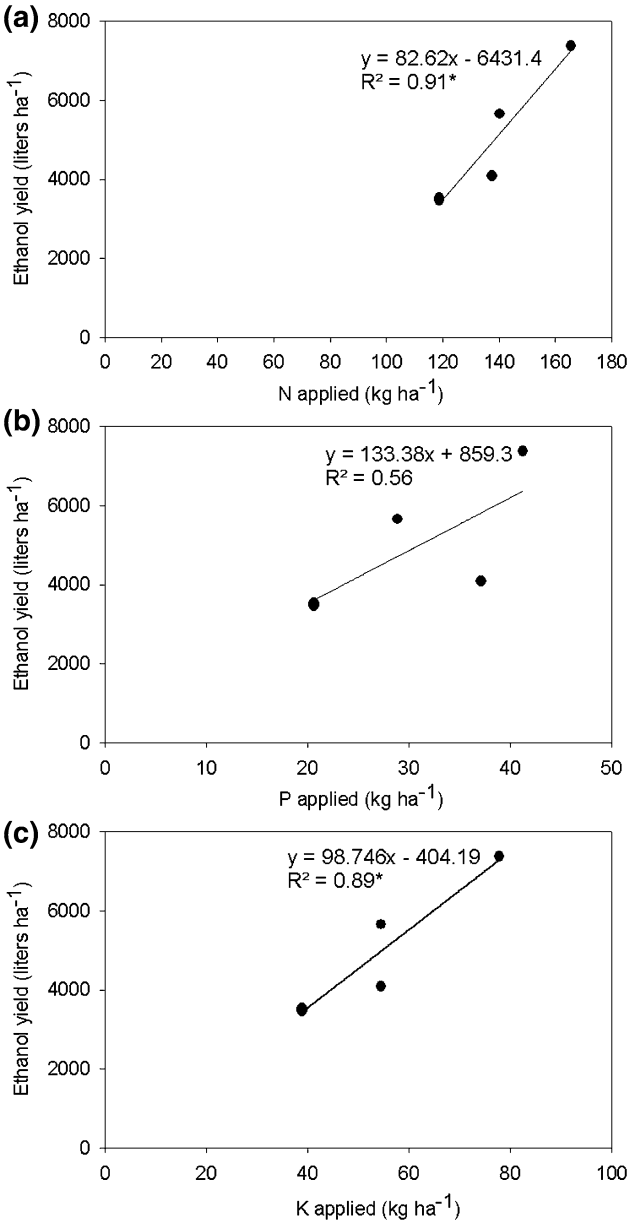

Fig. 2 Relationships between the amounts of N, P, and K applications and the total ethanol yield

Ethanol and Sugarcane Production System Sustainability

Sweet sorghum provided higher ethanol yields than the other treatments, due to the total ethanol yield, comprised of the amount of ethanol produced from both the preceding (sweet sorghum) and succeeding (sugarcane) crops. Even though each of the preceding crops received different types and rates of chemical fertilizers, significant relationships between the amounts of N, P, and K applied and the total ethanol yields were observed (Fig. 2).

Conclusion

Planting upland rice or sweet sorghum as preceding crops during the fallow period of the sugarcane production system improves soil available P at the preceding crop's harvest. The upland rice treatment provided the highest cane yield, though not significantly greater than the sweet sorghum treatment, leading to the highest ethanol yields achieved from sugarcane crops. However, sweet sorghum treatment produced the highest total ethanol yield. At final sugarcane crop harvest, all preceding crop treatments significantly increased soil OM, total N, and available P, compared with the fallow (control) treatment.

This study identifies the two most favorable options for preceding crop selection in the fallow period of sugarcane cropping system, namely upland rice and sweet sorghum. Upland rice is suitable for the system which emphasizes food security, as it provides rice for home consumption, as well as cash income for the farmers. Sweet sorghum is suitable for the system which emphasizes alternative biofuel production, due to its ability to produce ethanol from both preceding and succeeding crops. Both crops significantly improve soil and sugarcane production sustainability. However, the ultimate choice of selection depends on each individual farmer's conditions.

Acknowledgments This research was funded from the generosity of the National Research University Project of Thailand through the Biofuels Research Cluster of Khon Kaen University in part from the Applied Engineering in Agriculture Research Group, and the Northeast Thailand Cane and Sugar Research Center, Khon Kaen University. This manuscript was extended to the Thailand Research Fund (TRF; Project code: IRG5780003) at Khon Kaen University, and the Faculty of Agriculture KKU, in order to provide financial support for manuscript preparation activities.

Author Contributions N. Thawaro carried out the whole experiment under supervision of W. Kaewpradit. They are responsible for the main experimental assignments and data analysis; B. Toomsan advised in manuscript preparation.

Compliance with Ethical Standard

Conflict of interest The authors declare that they have no conflict of interest.

References

Blackburn, F. 1984. *Sugarcane*. Singapore: The Print House (Pte) Ltd.

Demirbas, A. 2009. Biofuels securing the planet's future energy needs. *Energy Conversion Management Journal* 50(9): 2239–2249.

Franceschin, G., A. Zamboni, F. Bezzo, and A. Bertucco. 2008. Ethanol from corn: A technical and economical assessment based on different scenarios. *Chemical Engineering Research and Design* 86: 488–498.

Hemwong, S., G. Cadisch, B. Toomsan, V. Limpinuntana, P. Vityakon, and A. Patanothai. 2008. Dynamics of residue decomposition and N_2 fixation of grain legumes upon sugarcane residue retention as an alternative to burning. *Soil and Tillage Research* 99: 84–97.

Kaewpradit, W., B. Toomsan, G. Cadisch, P. Vityakon, V. Limpinuntana, P. Saenjan, S. Jogloy, and A. Patanothai. 2008. Regulating mineral N release by mixing groundnut residues and rice straw under field conditions. *European Journal of Soil Science* 59: 640–652.

Kaien, R., F. Shiotsu, J. Abe, and S. Morita. 2012. Biomass yield and nitrogen use efficiency of cellulosic energy crops for ethanol production. *Biomass and Bioenergy* 37: 330–334.

Laopaiboon, L., S. Nuanpeng, P. Srinophakun, P. Klanrit, and P. Laopaiboon. 2009. Ethanol production from sweet sorghum juice using very high gravity technology: Effects of carbon and nitrogen supplementations. *Bioresource Technology* 100: 4176–4182.

Marina, O.S., M. Marcelo, V.E. Adriano, A.N. Silvia, M.F. Rubens, and E.V.R. Carlos. 2011. Improving bio-ethanol production from sugarcane: Evaluation of distillation, thermal integration and cogeneration systems. *Energy* 36: 3691–3703.

Rumpa, J., N. Leepipatpiboon, V. Tolieng, V. Kitpreechavanich, T. Srinorakutara, and A. Akaracharanya. 2012. Sugarcane leaves: Pretreatment and ethanol fermentation by *Saccharomyces cerevisiae*. *Biomass and Bioenergy* 39: 283–289.

Promsakha Na Sakonnakhon, S., B. Toomsan, G. Cadisch, E.M. Baggs, P. Vityakon, V. Limpinuntana, S. Jogloy, and A. Patanothai. 2005. Dry season groundnut stover management practices determine nitrogen-cycling efficiency and subsequent maize yields. *Plant and Soil* 272: 183–199.

Saxena, R.C., D.K. Adhikari, and H.B. Goyal. 2009. Biomass-based energy fuel through biochemical routes: A review. *Renewable and Sustainable Energy Reviews* 13: 167–178.

Tecator. 1984. Determination of ammonium nitrogen (ASN 65-32/84) or nitrate nitrogen (ASN 65-31/84) in soil sample extractable by 2 M KCl using flow injection analysis. Application notes. Tecator Höganas, Sweden.

Vityakon, P., S. Meepech, G. Cadisch, and B. Toomsan. 2000. Soil organic matter and nitrogen transformation mediated by plant residues of different qualities in sandy acid upland and paddy soils. *Netherlands Journal of Agricultural Science* 48: 75–90.

Whitmore, A.P., G. Cadisch, B. Toomsan, V. Limpinuntana, V.M. Noordwijk, and P. Purnomosidhi. 2000. An analysis of economic values of novel cropping systems in N.E. Thailand and S. Sumatra. *Netherlands Journal of Agricultural Science* 48: 105–114.

Pak. J. Bot., 49(2): 493-497, 2017.

RAPID ASSESSMENT OF LYCOPENE AND β-CAROTENE IN SPINY BITTER GOURD (*MOMORDICA COCHINCHINENSIS* (LOUR.) SPRENG)

PAWANRAT WIHONG[1], PATCHARIN SONGSRI[1,2*], BHALANG SURIHARN[1,2], KHOMSORN LOMTHAISONG[3] AND KAMOL LERTRAT[1,2]

[1]DepartmentofPlant Science and Agricultural Resources, Faculty of Agriculture, KhonKaenUniversity, KhonKaen 40002, Thailand
[2]Plant Breeding Research Center for Sustainable Agriculture, Khon Kaen University, KhonKaen 40002,Thailand
[3]Department of Biochemistry, Faculty of Science,Khon Kaen University, KhonKaen 40002, Thailand
[*]Corresponding author's email: patcharinso@kku.ac.th

Abstract

A simple spectrophotometric method was developed for the analysis of lycopene, β-carotene and total carotenoids in the spiny bitter gourd. Lycopene, β-carotene and total carotenoids were extracted from spiny bitter gourd aril samples using three accelerated solvent extraction methods. The supernatants of the extracted samples were then analyzed for carotenoids using spectrophotometry at the wavelengths of 450, 470 and 502 nm. The proposed method was validated for its analytical performance parameters including simplicity, accuracy and effectiveness. The method was applied to the determination of lycopene, β-carotene and total carotenoids in 43 spiny bitter gourd genotypes. Over all genotypes, the lycopene, β-carotene and total carotenoidscontents obtained using the proposed spectrophotometric method were not significantly different from those obtained from HPLC methods. A spiny bitter gourd genotype with high lycopene, β-carotene and total carotenoids was identified by the HPLC method, and this result was similar to the results of the spectrophotometric method. The highest positive correlation was found between HPLC and spectrophotometric method III for lycopene ($r = 0.94$; $p \leq 0.01$), β-carotene ($r = 0.92$; $p \leq 0.01$) and total carotenoids ($r = 0.93$; $p \leq 0.01$). The results indicated that the present spectrophotometric method could be used as an alternative to chromatographic analysis for the determination of the lycopene, β-carotene and total carotenoids contents in spiny bitter gourd. This method is reliable, rapid and inexpensive and can be usedto screen a large number of accessions in spiny bitter gourd breeding programs.

Key words: Gac fruit, Spectrophotometer, Indirect selection, Carotenoids, Phytochemical.

Introduction

The modern lifestyle and the consumption of low quality food can cause several health problems such as diabetes, hypertension, heart disease and cancer (Voung & King, 2003; Voung *et al*., 2006; Ishida & Chapman, 2009). Functional food products, including many vegetables and fruits that contain useful phytochemicals, have health benefits beyond ordinary food, and appropriate consumption of these functional food products reduces the risk of many chronic diseases.

Spiny bitter gourd or gac fruit (*Momordica cochinchinensis* (Lour.) Spreng) is an underutilized climbing plant in the Cucurbitaceae family. Its aril is rich in lycopene and β-carotene, which can reduce the risk of several diseases such as cancer of the prostate, colon and stomach as well as coronary heart disease (Vuong *et al*., 2006; Ishida & Chapman, 2009). The species is distributed widely in many Asian countries, including Vietnam, India, Bangladesh, China, Laos, Myanmar, Malaysia and Thailand (Bootprom *et al*., 2012; Bootprom *et al*., 2015). The spiny bitter gourd aril contains higher levels of β-carotene and lycopene than any known fruit crop, and it also contains high quality fatty acids (Ishida *et al*., 2004). The fatty acids in spiny bitter gourd play an important role in the absorption of lycopene and β-carotene (Ishida *et al*., 2004). Thus, arils of the spiny bitter gourd are currently used for the production of many functional food products, such as encapsulated arils, frozen arils, dry arils, beverages, snacks, health foods and cosmetics.

For the quality control of raw materials and breeding of spiny bitter gourd for a high lycopene content, reliable and effective methods for the determination of lycopene are required. The methods available for lycopene analysis include spectrophotometry-based methods and high performance liquid chromatographic (HPLC) methods used in tomato products (Luterotti *et al*., 2013). The spectrophotometric method is simple, rapid and cost-effective and can be used as a tool for the analysis lycopene in other plants. The HPLC method, in contrast, is more effective and accurate, but it is also more complex and time-consuming. The spectrophotometric method is an alternative method for large numbers of samples. A positive and significant correlation between the values obtained with the spectrophotometric method and the HPLC method has been reported in tomato (Davis *et al*., 2003a), vegetables (Barba *et al*., 2006), orange juice (Meléndez-Martínez *et al*., 2011) and yellow maize flour (Luterotti *et al*., 2013). However, the HPLC method is more sensitive for the quantification of lycopene in fruit and vegetable samples, and is more specific than the spectrophotometric method (Càmara *et al*., 2010)

The HPLC method is not appropriate for the evaluation of lycopene in large numbers of accessions or segregating materials in breeding programs because it is difficult, costly and time-consuming. For the spiny bitter gourd, the spectrophotometric method may be useful as an alternative method for screening spiny bitter gourd accessions for high lycopene contents if the results are closely related to those of the HPLC method. Although the spectrophotometric method was developed for the analysis of lycopene and total carotenoid contents in many plant species, the development of this method in

spiny bitter gourd plant is still lacking. Moreover, the relationship between these methods in spiny bitter gourd is not known. The objectives of this study were to evaluate carotenoids, lycopene and β-carotene in spiny bitter gourd accessions using the spectrophotometric and HPLC methods and to determine the relationship between these methods. This information will be useful for the quality control and breeding of spiny bitter gourd with a high lycopene and β-carotene content.

Materials and methods

Plant materials: Forty-three genotypes of spiny bitter gourd were used in this study. Forty-one F_1 plants were obtained from the hybridization of parental plants from various sources of origin and two accessions (KKU ac.11-134 and KKU ac.12-161) were introduced from Vietnam for comparison. These genotypes were planted from seeds as individual plants in May 2013-May 2014 at the Fruit Crop Research Station, Faculty of Agriculture, Khon Kaen University. Agronomic practices, including irrigation, fertilizer application, insecticides and fungicides were applied appropriately and mini-sprinkler irrigation was available to avoid drought. Six months after transplanting, the female flowers were artificially pollinated and tagged to identify the parents and days to maturity. At maturity, or about 60-90 days after pollination, the ripe fruits (identified by the red skin of the fruits) were harvested. Four fruits from each genotype were harvested, and the arils were separated from the fruits and stored separately as four replicates at -20ºC until phytochemical analysis.

Reagents and standards: Butylated hydroxyl toluene (BHT), carotenoid standards for the HPLC method, lycopene and β-carotene were purchased from Sigma Chemical Co. (Louis, MO, USA). Methanol, acetonitrile and dichloromethane used in the extraction of carotenoids and used in the HPLC and spectrophotometer analysis were purchased from Labscan (RCI, Labscan, Thailand). All chemicals and reagents used in the experiments were of analytical grade.

Extraction of carotenoids: Three extraction methods were used for carotenoid analysis for 43 genotypes of spiny bitter gourd. Aril samples (0.1 g) were used for the analysis. These samples were placed in plastic cups and covered with lids. The cups were wrapped in aluminum foil to protect the aril samples from direct sunlight. These samples were used for all extraction methods.

The extraction methods used in this study are described briefly. In method I, the samples were extracted with ethanol in a mortar and ground until the aril samples were pale. The ground samples were then put in a Falcon tube with 3 mL of tetrahydrofuran (Vuong *et al*., 2006). In method II, the samples were mixed with 100 mL of extraction solvent (n-hexane/DW/ethanol, 56:10:34 v/v/v) until the complete exhaustion of color. In method III, the samples were mixed with 100 mL of extraction solvent (n-hexane/acetone/ethanol, 50:25:25 v/v/v) (Bohm *et al*., 2002; Kubola & Siriamornpun, 2011).

The extracted samples were loaded in Falcon tubes and then vortexed (speed 6) for 1 minute. The samples were the supplemented with 5 mL of 95% n-hexane and 5 mL of distilled water and centrifuged at 5000 rpm at 25ºC for 10 minutes. The supernatants of the extracted samples were used for the analysis of carotenoids.

The samples obtained from methods I, II and III were analyzed by a spectrophotometer at the wavelengths of 450, 470 and 502 nm. The samples obtained from method III were also filtered through 0.45 µm membrane filters and sub-samples of 20 µl were injected for HPLC analysis at a wavelength of 450 nm.

Carotenoid analysis by spectrophotometry: A spectrophotometer (10S UV/visible spectrophotometer, Thermo Scientific Genesys, Australia) was used for carotenoid analysis in spiny bitter gourd aril samples. Thespectrophotometer analyzed the samples in the visible spectrum ranging from 190 to 1100 nm. The samples were diluted with hexane, and 3 mL of the diluted samples was used for analysis at the wavelengths of 450, 470 and 502 nm. Hexane was used as the blank. A quartz cuvette was used in the spectrophotometer. The coefficient of $A^{1\%}$ was used for the calculation of lycopene and β-carotene, and the extinction coefficient of 1% was used as the absorbance coefficient for hexane.

Carotenoid analysis by high performance liquid chromatography (HPLC): An HPLC method (Kubola & Siriamornpun, 2011) with minor modifications was used for the analysis of the carotenoid, β-carotene and lycopene contents in the arils of ripe fruits. The composition of the solvents and the isocratic conditions used were described previously (Kubola & Siriamornpun, 2011). Analysis was performed using a Shimadzu (Japan) LC-20AC pump, an SPD-M20A diode array detector and a LUNA C-18 column (4.6 × 250 mm i.d., 5 µM). The mobile phase consisted of acetonitrile l (solvent A)/dichloromethane (solvent B) and methanol (solvent C) at a flow rate of 1 mL/min. At this flow rate, one sample took 30 minutes to pass through the column, and the absorbance was measured at the wavelength of 450 nm.

Statistical analysis: The data were analyzed for the individual methods according to a completely randomized design, and the combined analysis of variance for all methods was performed for all parameters that showed homogeneity of variance. The least significant difference (LSD) test at $p>0.05$ was used to compare means. All calculations were carried out in the STATIX8 software package.

Results

Variations in lycopene, β-carotene and total carotenoid levels: The spectrophotometric and HPLC methods were used for the evaluation of lycopene, β-carotene and total carotenoid levels in 43 spiny bitter gourd genotypes. Significant differences were observed among the 43 genotypes of gac fruit regarding lycopene, β-carotene and carotenoid levels determined using all methods (Table 1). Lycopene levels determined by three different spectrophotometric methods ranged from 94.5 to 3798.0 µg/g fresh weight, whereas it ranged from 300.1 to 4014.7 µg/g fresh weight by the HPLC method (Table 1). Method II had the lowest range (94.5 to 2323.1 µg/g fresh weight), whereas method III had the highest range (172.0 to 3798.0 µg/g fresh weight).

Table 1. Maximum (max), minimum (min) and means for lycopene, Beta-carotene and total carotenoids in 43 spiny bitter gourd genotypes determined by three spectrophotometric methods (method I, II and III) and HPLC method.

	Lycopene (µg/g fresh weight)				Beta-carotene (µg/g fresh weight)				Total carotenoids (µg/g fresh weight)			
	Method I	Method II	Method III	HPLC	Method I	Method II	Method III	HPLC	Method I	Method II	Method III	HPLC
Max.	2543.8	2323.1	3798.0	4014.7	827.5	755.1	884.2	454.4	2705.2	2351.8	3855.3	4179.8
Min.	123.4	94.5	172.0	300.1	8.8	28.7	19.6	121.6	179.7	169.5	271.4	427.8
Mean	890.4	783.9	996.3	951.1	222.1	208.3	214.2	211.0	1112.6	992.1	1210.5	1162.1
SD.	556.0	497.4	697.7	701.1	180.2	189.9	206.5	83.6	577.8	530.4	720.5	715.9
SE.	42.4	37.9	53.2	53.5	13.7	14.5	15.7	6.4	44.1	40.4	54.9	54.6
C.V.(%)	27.4	27.7	34.3	34.2	41.8	46.6	46.4	16.4	23.9	25.7	30.2	29.3
F-test	**	**	**	**	**	**	**	**	**	**	**	**

** = Significant at p<0.01
SD = Standard deviation, SE = Standard errors, C.V. = Calculation from of variance data

Table 2. The simple linear regression, coefficient of determination (R^2) and correlation coefficients between three spectrophotometric methods and HPLC method in analysis of lycopene, β-carotene and total carotenoid content in 43 spiny bitter gourd genotypes.

Method	Equation	R^2	r
Lycopene			
HPLC vs method I	y = 0.95x – 101.84	0.59**	0.77**
HPLC vs method II	y = 1.17x + 32.72	0.71**	0.85**
HPLC vs method II	y = 0.96x – 7.48	0.89**	0.94**
***B*-carotene**			
HPLC vs method I	y = 0.40x + 123.36	0.67**	0.82**
HPLC vs method II	y = 0.40x + 128.32	0.74**	0.86**
HPLC vs method II	y = 0.38x + 129.54	0.85**	0.92**
Total carotenoids			
HPLC vs method I	y = 0.90x + 157.66	0.55**	0.74**
HPLC vs method II	y = 1.07x + 101.91	0.64**	0.80**
HPLC vs method II	y = 0.93x + 26.83	0.87**	0.93**

** Significant at p<0.01

The β-carotene levels determined by the three spectrophotometric methods ranged from 8.8 to 882.5 µg/g fresh weight, while it ranged from 121.6 to 454.4 µg/g fresh weight by the HPLC method. The ranges of β-carotene were rather similar for method I (8.8 to 827.5 µg/g fresh weight) and method III (19.6 to 884.2 µg/g fresh weight); however, it was rather narrow for method II (28.7 to 755.1 µg/g fresh weight).

Total carotenoid levels determined by the three spectrophotometric methods ranged from 169.5 to 3855.3 µg/g fresh weight, while the total carotenoid levels determined by the HPLC method ranged from 427.8 to 4179.8 µg/g fresh weight. Method II had the lowest range (169.5 to 2351.8 µg/g fresh weight), while method III had the highest range (271.4 to 3855.3 µg/g fresh weight). Of note, the range of values provided by spectrophotometric method III were rather similar to those determined by the HPLC method.

Relationship between the HPLC and spectrophotometric methods: The correlation coefficients between the HPLC and spectrophotometric methods for lycopene, β-carotene and carotenoid contents were calculated for 43 spiny bitter gourd genotypes (Table 2).Strong positive correlations were found between the HPLC method and spectrophotometric method I for lycopene (r = 0.77), β-carotene (r = 0.82) and total carotenoids (r = 0.74). There were also positive correlations between the HPLC method and spectrophotometric method II regarding the lycopene (r = 0.85), β-carotene (r = 0.86) and total carotenoid (r = 0.80) contents. Similarly, there was a consistently strong and positive correlation between HPLC and spectrophotometric method III for thelycopene (r = 0.94), β-carotene (r = 0.92) and total carotenoid (r = 0.93)contents. The results show that spectrophotometric method III was more strongly and positively correlated with the HPLC method than spectrophotometric methods I and II.

Thus, we focused on the relationship between HPLC method and spectrophotometric method III for the determination of phytochemicals (Fig. 1).

Discussion

Spectrophotometry-based methods have been used for the analysis of lycopene, β-carotene and total carotenoids in various crops such as tomato (Davis *et al*., 2003a), watermelon (Davis *et al*., 2003b), vegetables (Barba *et al*., 2006) and orange juice (Meléndez-Martínez *et al*., 2011). However, studies have been limited to a small number of genotypes, and information on the development of this method for the analysis of gac fruit is still lacking.

In this study, lycopene, β-carotene and total carotenoids were determined by three spectrophotometry-based methods and an HPLC method in 43 spiny bitter gourd genotypes. The results indicate that the spectrophotometric method can be used to identify different spiny bitter gourd genotypes according to their lycopene, β-carotene and total carotenoid contents, similar to the HPLC method. The carotenoid levels were the highest, the lycopene levels were intermediate, and the β-carotene levels were the lowest. High CV values and F-ratios indicate considerable variations in these phytochemicals.

The average lycopene, β-carotene and total carotenoids contents were 300.1, 121.6 and 427.8 µg/g fresh weight, respectively, determined by HPLC. These levels were similar to the findings of Vuong *et al*. (2006), who reported average lycopene, β-carotene and total carotenoids content of 408, 83 and 497 µg/g fresh weight, respectively. In addition, the lycopene and β-carotene contents were estimated to be 380 and 101 µg/gfresh fruit, respectively, by Aoki *et al*. (2002). In contrast, Ishida*et al*. (2004) reported average lycopene and β-carotene contents of 2300 and 750 µg/g fresh weight, respectively. The differences in these observations could be due to differences in plant materials. In this study, the phytochemical content determined by HPLC was rather similar to the levels provided by the spectrophotometric methods, especially spectrophotometric method III. This result is similar to that of Luterotti *et al*. (2013), reported in tomato products and yellow maize flour.

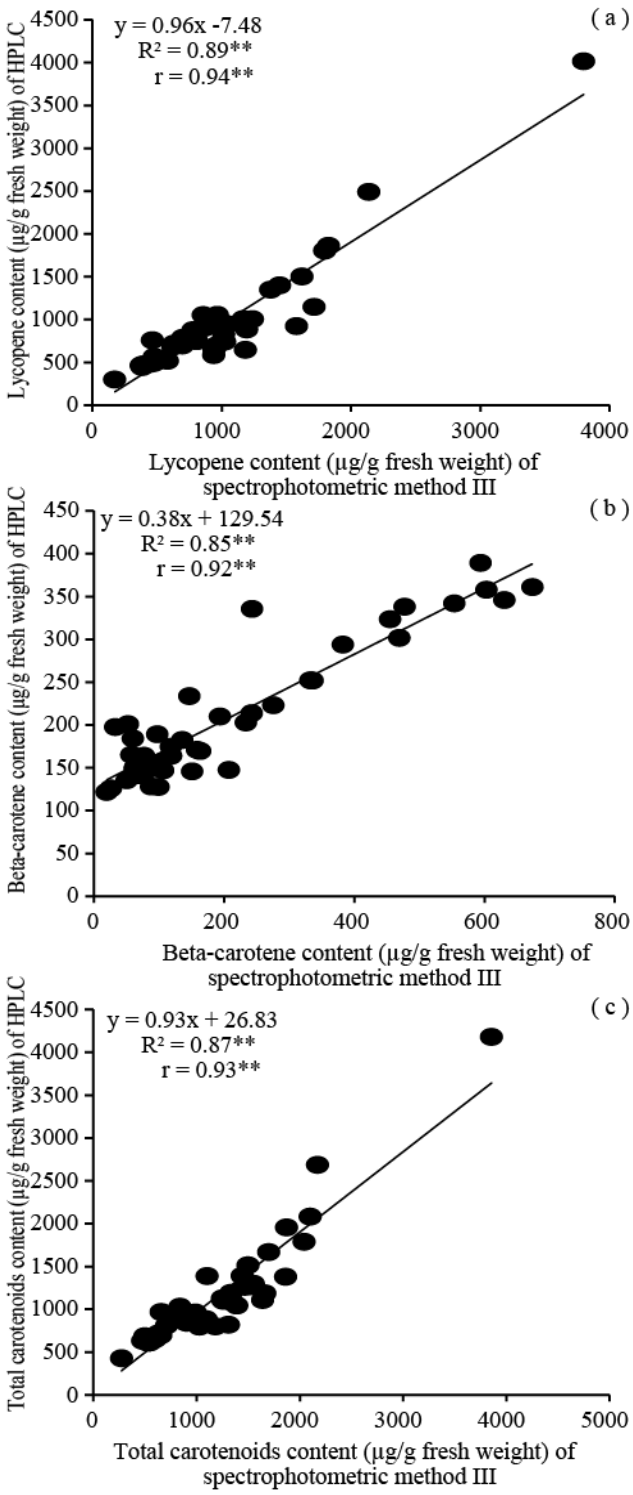

Fig. 1. Relationships between HPLC and spectrophotometric method III for determination of lycopene content (a), β-carotene content (b), and total carotenoid content (c) in 43 spiny bitter gourd genotypes.

Although the application of spectrophotometric methods for the analysis of lycopene, β-carotene and total carotenoids has been investigated in many plant species (Davis *et al*., 2003a; Barba *et al*., 2006; Meléndez-Martínez *et al*., 2011; Luterotti *et al*., 2013), there is limited information on the application of this method to gac fruit. An understanding of the relationship between the HPLC method and spectrophotometric methods may be helpful in choosing a simple method for the determination of phytochemicals in spiny bitter gourd accessions. In the present study, three spectrophotometric methods with different extraction methods were compared with the HPLC method for the determination of lycopene, β-carotene and total carotenoids in the arils of the spiny bitter gourd. All correlation coefficients between the spectrophotometric methods and the HPLC method were positive and significant for the lycopene, β-carotene and total carotenoidcontents. The current study supports previous studies in which that high correlations are found between the HPLC method and the spectrophotometric methods for the analysis of lycopene, β-carotene and total carotenoids in tomato and orange (Melendez-Martinez *et al*., 2011, Luterotti *et al*., 2013).

Interestingly, the correlation coefficients between spectrophotometric method III and the HPLC method had the highest coefficients of determination for lycopene, β-carotene and total carotenoids. Thus, the HPLC method could be largely explained by spectrophotometric method III for the analysis of lycopene (R^2 = 0.89), β-carotene (R^2 = 0.85) and total carotenoids (R^2 = 0.87). This result is in agreement with those observed in which a high positive relationship was found between spectrophotometric method III and the HPLC method, likely because the same extraction method was used for phytochemical analysis.

To the best of our knowledge, this study is be the first report on the relationship between spectrophotometric methods and HPLC methods for the analysis of lycopene, β-carotene and total carotenoids in spiny bitter gourd. The present study demonstrates that spectrophotometry can be used as a tool for the analysis carotenoids, including lycopene and β-carotene in spiny bitter gourd arils. The spectrophotometric method is rapid and accurate for measuring phytochemicals and can be used for screening the spiny bitter gourd germplasm or for large breeding populations.

Conclusions

This study demonstrated that spectrophotometric methods can be developed for the analysis of lycopene, β-carotene and total carotenoids in spiny bitter gourd arils. The results show high correlation coefficients between the spectrophotometric methods and the HPLC method for the analysis of lycopene, β-carotene and total carotenoids. Based on its rapid, precise and inexpensive assessment of phytochemicals, the spectrophotometric method can be used as an alternative to the HPLC method for the determination of lycopene, β-carotene and total carotenoids in spiny bitter gourd. This method can be used in spiny bitter gourd selection programs to increase lycopene, β-carotene and carotenoid levels and to evaluate fruit quality in the functional food industry.

Acknowledgment

This work was supported by the Higher Education Research Promotion and National Research University Project of Thailand, Office of the Higher Education Commission through the Food and Functional Food Research Cluster of Khon Kaen University. Grateful

acknowledgments are made to the Thailand Research Fund (TRF) providing financial support through the New Research Scholar Project (Project no. TRG5780083) and partial support from the Plant Breeding Research Center for Sustainable Agriculture, Faculty of Agriculture, Khon Kaen University. Acknowledgement is extended to the Thailand Research Fund (IRG 5780003), Khon Kaen University and Faculty of Agriculture for providing financial support for manuscript preparation activities.

References

Aoki, H., N.T.M. Kieu, N. Kuze and K. Tomisaka. 2002. Carotenoid pigments in Gac fruit (*Momordica cochinchinensis* Spreng). *Biosci. Biotechnol. Biochem.*, 66: 2479-2482.

Barba, A.I.O., M. Ca´mara Hurtado, M.C. Sa´nchez Mata, V. Ferna´ndez Ruiz and M. Lo´pez Sa´enz de Tejada. 2006. Application of a UV–vis detection-HPLC method for a rapid determination of lycopene and b-carotene in vegetables. *Food Chem.*, 95: 328-336.

Bohm, V., N.L. Puspitasari-Nienaber, M.G. Ferruzzi and S.J. Schwartz. 2002. Trolox equivalent antioxidant capacity of different geometrica isomers of α -carotene, β- carotene, lycopene and zeaxanthin. *Agric. Food Chem.*, 50: 221-226.

Bootprom, N., P. Songsri, B. Suriharn, K. Lomthaisong and K. Lertrat. 2015. Genetics Diversity Based on Agricultural Traits and Phytochemical Contents in Spiny Bitter Gourd (*Momordica cochinchinensis* (Lour.) Spreng). *SABRAO J. Breed. Gen.*, 47(3): 278-290.

Bootprom, N., P. Songsri, B. Suriharn, P. Chareonsap, J. Sanitchon and K. Lertrat. 2012. Molecular diversity among selected *Momordica cochinchinensis* (Lour.) Spreng) accessions using RAPD markers. *SABRAO J. Breed. Gen.*, 44 (2): 406-417.

Càmara, M., J.S. Torrecilla, J.O. Caceres, M.C.S. Mata and V. Fernàndez-Ruiz. 2010. Neural network analysis of spectroscopic data of lycopene and β-Carotene content in food samples compared to HPLC-UV-Vis. *J. Agric. Food Chem*., 58:72-75.

Davis, A.R., W.W. Fish and P. Perkins-Veazie. 2003a. A rapid spectrophotometric method for analyzing lycopene content in tomato and tomato products. *Postharvest Biol. Tec*., 28: 425-430.

Davis, A.R., W.W. Fish, P. Perkins-Veazie. 2003b. A rapid hexane- free method for analyzing lycopene content in watermelon. *J. Food Sci*., 68:328-332.

Iaroslav, M.S., G.N. Valeriy, D.T. Yuriy and A.A. Tyurenkov. 2012. Spectroscopy analysis for simultaneous determination of lycopene and β-carotene in fungal biomass of *Blakeslea trispora*. *Acta Biochem Pol*., 59: 65-69.

Ishida, B.K. and M.H. Chapman. 2009. Carotenoid extraction from plants using a novel, environmentally friendly solvent. *J. Agric. Food Chem*., 57: 1051-1059.

Ishida, B.K., C. Turner, M.H. Chapman and A.T. Mckeon. 2004. Fatty acid and composition of Gac (*Momordica cochinchinensis* Spreng) fruit. *J. Agric. Food Chem*., 52: 274-279.

Kubola, J. and S. Siriamornpun. 2011. Phytochemicals and antioxidant activity of different fruit fractions (peel, pulp, aril and seed) of Thai Gac (*Momordica cochinchinensis* Spreng). *Food Chem*., 127(3): 1138-1145.

Luterotti, S., K. Markovic, M. Franko, D. Bicanic, A. Madzgalj and K. Kljak. 2013. Comparison of spectrophotometric and HPLC methods for determination of carotenoids in foods. *Food Chem*., 140: 390-397.

Meléndez-Martínez, A.J., F. Ayala, J.F. Echцvarri, A.I. Negueruela, M.L. Escudero-Gilete, M.L. Gonzclez-Miret, I.M. Vicario and F.J. Heredia. 2011. A novel and enhanced approach for the assessment of the total carotenoid content of foods based on multipoint spectroscopic measurements. *Food Chem*., 126: 1862-1869.

Vuong, L.T. and J.C. King. 2003. A method of preserving and testing the acceptability of Gac fruit oil, a good source of beta-carotene and essential fatty acids. *Food Nutr. Bull*., 24(2): 224-230.

Vuong, L.T., A.A. Franke, L.J. Custer and S.P. Murphy. 2006. *Momordica cochinchinensis* Spreng. (Gac) fruit carotenoids reevaluated. *J. Food Comp. Anal*., 19: 664-668.

(Received for publication 8 February 2016)

Journal of Agricultural Science (2017), **155**, 978–992. © Cambridge University Press 2017
doi:10.1017/S0021859617000053

CROPS AND SOILS RESEARCH PAPER

Physiological determinants of storage root yield in three cassava genotypes under different nitrogen supply

K. PHUNTUPAN[1] AND P. BANTERNG[1,2]*

[1] *Faculty of Agriculture, Khon Kaen University, Khon Kaen 40002, Thailand*
[2] *Plant Breeding Research Center for Sustainable Agriculture, Faculty of Agriculture, Khon Kaen University, Khon Kaen 40002, Thailand*

(*Received 11 July 2016; revised 5 December 2016; accepted 25 January 2017; first published online 20 February 2017*)

SUMMARY

Physiological traits can be used to improve the efficiency of selecting suitable genotypes to grow under nitrogen (N) limitation. The objective of the current study was to investigate the relationship between physiological characteristics and storage root yield of three cassava genotypes under three rates of N fertilizer. The experiments were conducted from 2014 to 2016 at farm fields in Thailand. A split-plot randomized complete block design with four replications was used. Three different rates of N fertilizer, i.e., 46·9, 90·0 and 133·2 kg N/ha and three cassava genotypes, Rayong 9, Rayong 11 and Kasetsart 50, were used. Kasetsart 50 had the highest mean performance for most crop traits. Growth rate of stem (SGR), storage root (SRGR) and crop (CGR) during 180–210 days after planting (DAP) and leaf area index (LAI) at 120 DAP were related to storage root dry weight for all three rates of N fertilizer. Storage root growth during 90–120 DAP, CGR during 180–210 DAP and specific leaf area (SLA) at 210 DAP contributed most to storage root dry weight of the three genotypes grown at 46·9 kg N/ha, while the combination of SRGR during 90–120 DAP, SRGR during 180–210 DAP, LAI at 210 DAP and SLA at 210 DAP was best for N fertilizer at 90·0 kg N/ha and the combination of leaf growth rate (LGR) during 180–210 DAP and LAI at 210 DAP was best for N fertilizer at 133·2 kg N/ha.

INTRODUCTION

Cassava (*Manihot esculenta*) is an important crop used for human and animal foods as well as for the production of bioenergy. With an increasing human population, the demand for food and energy from cassava could also increase. Thailand is the world's major producer of cassava, and according to the Office of Agricultural Economics, the average storage root yield in 2013/14 was around 22·3 t/ha fresh weight. However, storage root yield of cassava can be improved by using appropriate production technologies, such as planting with high-yielding cultivars, selecting suitable planting dates and applying adequate fertilizer rates. At present, many improved cassava cultivars are recommended for the production system in Thailand, and each cultivar responds and adapts differently to various management practices (Kaweewong *et al.* 2013*a*, *b*). Nitrogen (N) fertilizer application is one of the most important management processes for increasing cassava storage root yield. Significant responses of cassava to N fertilizer have been observed in Asia, especially in Thailand (Howeler 2002). The use of N fertilizer at appropriate rates, meeting the requirements of each cassava cultivar, improves crop growth and ultimately supports the production of high storage root yield.

Previous studies have evaluated the responses of cassava to different application rates of N fertilizer and found that high rates can increase plant height, canopy width (Cenpukdee & Fukai 1991), number of leaves, number of storage roots, weight per storage root, final yield (Olasantan 1999), leaf N concentration (Nguyen *et al.* 2002), chlorophyll concentration, chlorophyll a/b ratio, stomatal conductance, photorespiration rate, net carbon assimilation rate, specific leaf area (SLA) (Cruz *et al.* 2003) and above-ground dry weight (Kaweewong *et al.* 2013*a*, *b*). However,

* To whom all correspondence should be addressed. Email: bporam@kku.ac.th

studies on the other physiological characteristics, such as crop growth rate (CGR), stem growth rate (SGR), leaf growth rate (LGR), storage root growth rate (SRGR), leaf area index (LAI), SLA and harvest index (HI) together with final storage root yields of different cassava branching types under different rates of N fertilizer applications are rare. Such studies could provide additional information concerning growth habit and crop adaptation, leading to a better understanding of the response of different cassava cultivars to N fertilizer as well as advanced knowledge of physiological determinants of cassava storage root yield. Physiological traits have been used to explain yield performances under different management practices and environments in various crops, for example soybean (Yusuf *et al*. 1999), triticale (Czerednik & Nalborczyk 2001), peanut (Banterng *et al*. 2003; Arunyanark *et al*. 2009; Puangbut *et al*. 2010), safflower (Koutroubas *et al*. 2009), maize, sunflower (Massignam *et al*. 2009), linseed (Dordas 2010) and Jerusalem artichoke (Ruttanaprasert *et al*. 2016). However, studies on evaluating growth and physiological determinants of cassava storage root yield under different rates of N supply are still lacking. Such studies could be valuable in determining appropriate criteria with the overall aim of increasing crop productivity under N-limitation. Therefore, the objective of the current study was to investigate the relationship between physiological characteristics and storage root yield of three cassava genotypes under the three rates of N fertilizer.

MATERIALS AND METHODS

Plant materials

Three improved genotypes of cassava with different branching patterns were used for the current study: Rayong 9 (non-forking), Rayong 11 (forking) and Kasetsart 50 (forking). These three cultivars are high-yielding genotypes with high starch (%). They are also suitable as raw materials for industrial starch production in Thailand. Kasetsart 50 is currently the most popular cassava cultivar in Thailand and was introduced by Kasetsart University, Thailand. Rayong 9 and Rayong 11 cultivars were released by the Department of Agriculture, Thailand.

Experimental details

The experiments were conducted under rain-fed conditions at two sites of cassava production area (Ban Khok Sri; 16°32′14·9″N, 102°46′05·6″E, 177·3 m a.s.l., during 2014/15 and Ban Kham Pom; 16°08′50·8″N, 102°46′34·9″E, 199·4 m a.s.l., during 2015/16) in Khon Kaen province, Thailand. For both experimental sites, a randomized complete block split-plot design with four replications was used. Three different N fertilizer rates, i.e., 46·9 (minimum rate from the general recommendation of the Department of Agriculture, Thailand), 90·0 and 133·2 kg N/ha, were randomized in main plots and the three different cassava genotypes were allocated to sub-plots. The individual plot size was 120 m^2 (20 × 6 m) with 1 m between plots. Land preparation was conducted following normal procedures for experimental cassava cropping. The stems of 9-month old cassava were cut as sticks to 0·2 m in length and soaked with thiamethoxam 25% water dispersible granules at a rate of 4 g per 20 litres of water for 5–10 min to prevent mealy bug infestation. The representative planting dates for cassava production in Ban Khok Sri and Ban Kham Pom were 18 December 2014 (the dry season planting date) and 18 June 2015 (the rainy season planting date), respectively, with a spacing of 1 × 1 m^2 for each cassava stick. Since there was no rain during the first month after planting on the 18 December 2014 (Fig. 1), supplementary irrigation was applied immediately after planting, at 7 days after planting (DAP) and at 14 DAP in order to facilitate germination. Weeds were controlled manually throughout the experiment and a commercial compound fertilizer grade 15–15–15 at the rate of 312·5 kg/ha was applied to all experimental plots at 30 DAP that was equivalent to 46·9 kg/ha of N, 46·9 kg/ha of phosphorus pentoxide (P_2O_5) and 46·9 kg/ha of potassium oxide (K_2O) (minimum recommended rate for the Department of Agriculture, Thailand). In order to improve the productivity, at 60 DAP, additional N fertilizer at rates of 0, 43·1 and 86·3 kg N/ha was applied to the main plots. Additional K_2O fertilizer was applied to all experimental plots at a rate of 56·3 kg/ha.

Data collection

Soil physical and chemical properties for the two experimental years were determined before planting. Soil samples were taken from three points in each experimental site at 15 cm depths up to 1·05 m for soil texture, pH, cation exchange capacity (CEC), total N and exchangeable phosphorus (P) and potassium (K) analysis. Table 1 shows the soil analysis

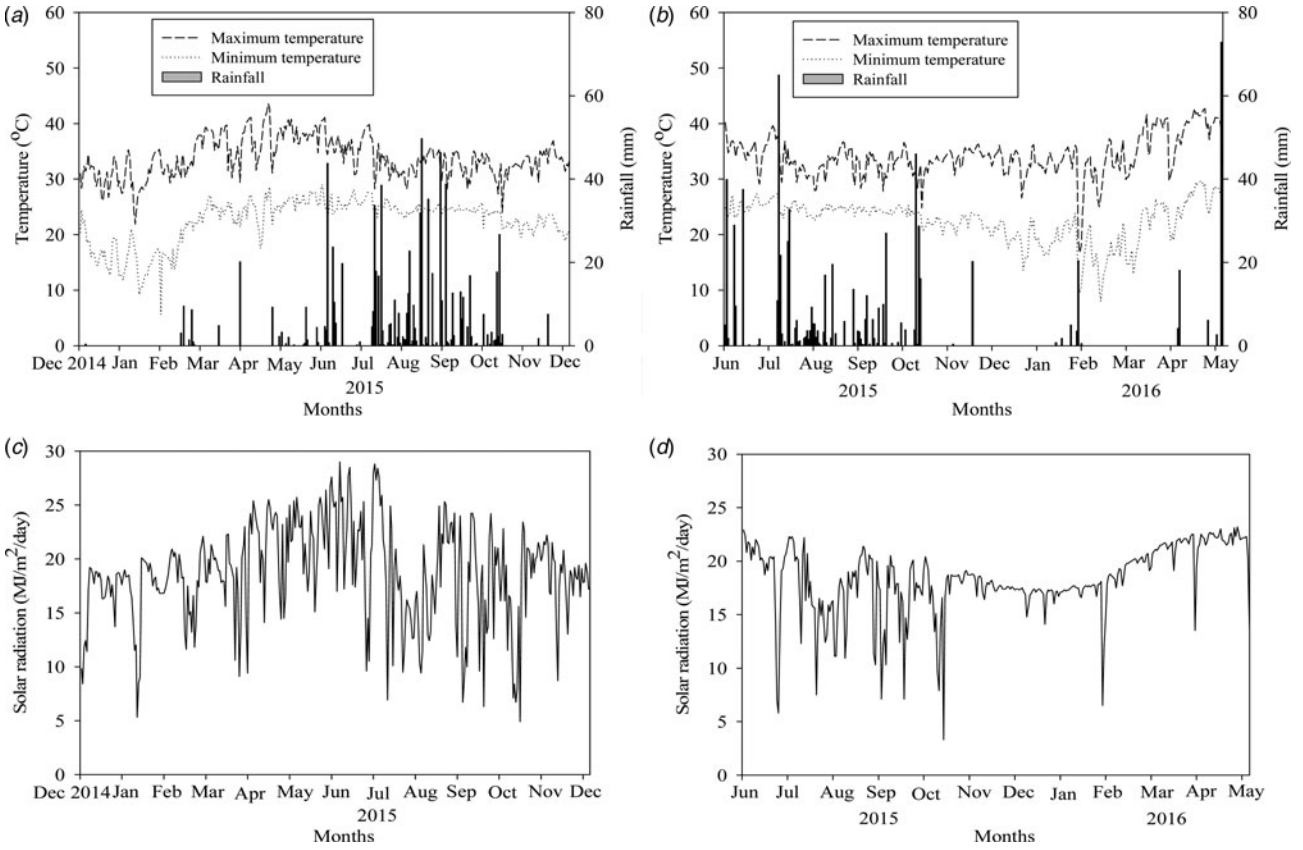

Fig. 1. Maximum and minimum temperatures, rainfall and solar radiation for the growing periods of (*a* and *c*) 2014/15 and (*b* and *d*) 2015/16.

Table 1. *Soil properties prior to land preparation for the two experimental years*

	Soil textural class		pH 1:1 H_2O		CEC (cmol/kg)		Total nitrogen (g/kg)		Available phosphorus (mg/kg)		Available potassium (mg/kg)	
Soil depth (m)	2014/15	2015/16	2014/15	2015/16	2014/15	2015/16	2014/15	2015/16	2014/15	2015/16	2014/15	2015/16
0–0·15	Sandy	Sandy	5·0	5·6	3·4	2·3	0·0022	0·0013	7·6	7·9	45·4	133·8
0·15–0·30	Loamy sand	Sandy	5·0	5·3	4·2	2·4	0·0014	0·0005	4·3	5·5	23·9	173·5
0·30–0·45	Loamy sand	Sandy	4·8	5·4	6·8	2·5	0·0014	0·0008	2·9	5·6	28·2	111·6
0·45–0·60	Loamy sand	Loamy sand	4·8	5·5	7·0	2·1	0·0010	0·0004	2·6	4·4	30·6	58·7
0·60–0·75	Loamy sand	Loamy sand	4·8	5·8	8·6	2·3	0·0008	0·0004	2·3	3·6	26·2	47·1
0·75–0·90	Loamy sand	Sandy loam	4·8	5·8	7·8	2·6	0·0008	0·0004	2·7	2·1	32·5	37·0
0·90–1·05	Loamy sand	Sandy loam	4·8	5·8	8·7	3·5	0·0010	0·0002	2·6	2·3	33·5	88·1

results; soil texture at 0–0·15 m for both experimental years was sandy, with low total N values, indicating low soil fertility.

Crop growth data in each experimental plot were recorded from four cassava plants per plot at 90, 120, 180 and 210 DAP. At final harvest (300 DAP), crop data were recorded for eight plants per plot. The plants were separated into leaves, stem and storage root, and all plant organs were then sub-sampled (about 0·10 total fresh weight of each organ). The sub-samples of green leaf were used to measure leaf area using a leaf area scanning meter (LI-cor3100). Sub-samples of all plant organs were oven-dried at 70 °C to constant weight to determine the dry weight of individual plant organs. Total leaf area and its corresponding dry weight at 120 and 210 DAP then used to calculate SLA, which was subsequently used to convert leaf weight into total leaf area and LAI. The physiological traits, i.e., CGR, SGR, LGR and SRGR during 90–120 DAP (early growth stage) and 180–210 DAP (late growth stage) were derived based on the function of changed dry weight per unit time. The value for HI was calculated based on the ratio of storage root dry weight to total crop dry weight (Yusuf *et al*. 1999; Banterng *et al*. 2003; Koutroubas *et al*. 2009). Starch content of storage roots at final harvest was determined by the specific gravity method. In addition, meteorological data were also recorded, i.e., daily maximum and minimum temperatures, amount of solar radiation and rainfall.

Statistical analysis

Separate analyses of variance for each experimental year and combined analysis with orthogonal polynomial contrasts for the data from the two experimental years were performed. Least significant difference was used for the mean comparisons. The relationship between physiological traits and final storage root yield was examined by single and multiple regression analyses. The stepwise regression technique was conducted to search for the best multiple regressions (Gomez & Gomez 1984). The analysis of variance (ANOVA) and the mean comparisons were performed in MSTAT-C Version 1.42 (Freed & Nissen 1992). Partition of the variances into linear and non-linear contrasts and regression analysis were performed using Statistix 8 (Analytical Software, Tallahassee, Florida, USA).

RESULTS

Crop traits for the 2014/15 growing period

In 2014/15 with a planting date of 18 December 2014, representing the planting date of cassava for the dry season (Fig. 1) in Thailand, growth rates during 180–210 DAP in terms of LGR, SGR, SRGR and CGR for all different N fertilizer rates, cassava genotypes and combinations of N fertilizer and genotype were mostly higher than those during 90–120 DAP (Table 2). Significant interactions ($P < 0{\cdot}01$) between genotypes and N fertilizer applications were found for LGR, SGR during 180–210 DAP, SRGR and CGR. The responses of the three cassava genotypes to the three different N fertilizer applications were different for those crop traits. There were significant differences among three rates of N fertilizer application for LGR during 90–120 DAP ($P < 0{\cdot}05$), LGR during 90–120 DAP ($P < 0{\cdot}01$), SGR during 180–210 DAP ($P < 0{\cdot}01$), SRGR ($P < 0{\cdot}01$) and CGR ($P < 0{\cdot}01$), but not for SGR during 90–120 DAP, and high rates of N fertilizer application produced increased values for most crop traits in Table 2. Significant differences ($P < 0{\cdot}01$) between the three cassava genotypes were also recorded for LGR during 180–210 DAP, SRGR and CGR, and Kasetsart 50 showed improved performance for almost all crop traits when compared with the other two genotypes (Table 2).

The values of LAI at 210 DAP for all additional N fertilizer rates, cassava genotypes and combinations of N fertilizer applications and genotypes were mostly higher than those at 120 DAP (Table 3). Interactions between genotypes and N fertilizer applications ($P < 0{\cdot}01$) were also found for LAI at 210 DAP, storage root dry weight, total dry weight and HI. There were significant differences ($P < 0{\cdot}01$) among the three rates of N fertilizer for LAI at 210 DAP, SLA at 210 DAP, storage root dry weight, total dry weight, HI and total starch content, but not for LAI at 120 DAP and SLA at 120 DAP, and high rates of N fertilizer application produced higher values for most crop traits (Table 3). Comparing the three cassava genotypes, there were significant differences for LAI ($P < 0{\cdot}05$), SLA at 210 DAP ($P < 0{\cdot}01$), storage root dry weight ($P < 0{\cdot}01$), total dry weight ($P < 0{\cdot}01$), HI ($P < 0{\cdot}01$) and total starch content ($P < 0{\cdot}01$). Kasetsart 50 had higher values for these crop traits (except for SLA) than the other two genotypes (Table 3).

Crop traits for the 2015/16 growing period

For 2015/16 with a planting date of 18 June 2015, representing cassava planting date for the rainy season in Thailand (Fig. 1), the growth rate values during 180–210 DAP with regard to LGR, SRGR and CGR for all N fertilizer rates, cassava genotypes and the combination of N fertilizer applications and genotypes were mostly lower than those during 90–120 DAP (Table 4). Non-significant differences for genotypes × N fertilizer applications in SGR during 90–120 DAP, SRGR during 180–210 DAP and CGR during 180–210 DAP in Table 4 indicate that the three different cassava genotypes responded similarly to the three rates of N fertilizer. Significant differences among the three rates of N fertilizer application were observed for LGR during 180–210 DAP ($P < 0{\cdot}01$), SGR during 90–120 DAP ($P < 0{\cdot}01$), SRGR during 90–120 DAP ($P < 0{\cdot}01$), SRGR during 180–210 DAP ($P < 0{\cdot}05$) and CGR during 90–120 DAP ($P < 0{\cdot}01$) (Table 4), except for LGR during 90–120 DAP, SGR during 180–210 DAP and CGR during 180–210 DAP. Comparing the three genotypes, there were significant differences for SGR during 180–210 DAP ($P < 0{\cdot}05$), SRGR during 90–120 DAP ($P < 0{\cdot}01$), CGR during 90–120 DAP ($P < 0{\cdot}01$) and CGR during 180–210 DAP ($P < 0{\cdot}05$) (Table 4).

Leaf area index at 210 DAP for all N fertilizer rates, cassava genotypes and the combinations of N fertilizer and genotype was mostly lower than at 120 DAP (Table 5). Non-significant differences for genotypes × N fertilizer applications in LAI, SLA and starch content were recorded. Significant differences among the three rates of N fertilizer application were observed for LAI ($P < 0{\cdot}01$), SLA at 210 DAP ($P < 0{\cdot}05$), storage root dry weight ($P < 0{\cdot}01$), total dry weight ($P < 0{\cdot}01$), HI ($P < 0{\cdot}01$) and starch content ($P < 0{\cdot}05$) (Table 5), except for SLA at 120 DAP. Application of higher additional N fertilizer rates gave high values of almost all crop traits (Table 5). There were also significant differences among the three cassava genotypes in LAI ($P < 0{\cdot}01$), SLA at 210 DAP ($P < 0{\cdot}01$), storage root dry weight ($P < 0{\cdot}01$), total dry weight ($P < 0{\cdot}01$), HI ($P < 0{\cdot}01$) and starch content ($P < 0{\cdot}01$). Kasetsart 50 showed the highest performance for most crop traits (Table 5).

Combined analysis and physiological determinants of storage root dry weight

The results from the combined analysis (Tables 6 and 7) indicate that there were significant differences ($P < 0{\cdot}01$) for almost all crop traits between the two experimental years or growing periods, except for SLA at 120 DAP. According to the final harvest data, the growing

Table 2. *Means for leaf growth rate (LGR), stem growth rate (SGR), storage root growth rate (SRGR) and crop growth rate (CGR) during 90–120 and 180–210 days after planting (DAP) of three cassava genotypes under three nitrogen (N) fertilizer rates in 2014/215*

	LGR (kg/day)		SGR (kg/day)		SRGR (kg/day)		CGR (kg/day)	
Treatment	90–120 DAP	180–210 DAP	90–120 DAP	180–210 DAP	90–120 DAP	180–210 DAP	90–120 DAP	180–210 DAP
Nitrogen fertilizer								
46·9 kg N/ha (N1)	1·7	3·3	4·0	28·0	52·2	70·7	62·0	106·5
90·0 kg N/ha (N2)	2·9	7·6	4·4	45·3	72·1	118·5	82·2	176·9
133·2 kg N/ha (N3)	4·5	10·8	4·6	43·9	74·7	170·3	87·5	235·9
S.E. (n = 12)	0·49	0·64	0·30	0·92	0·60	1·06	0·80	1·26
LSD	1·70	3·35	–	4·81	3·13	5·53	4·22	6·61
P level (N)	$P < 0·05$	$P < 0·01$	NS	$P < 0·01$	$P < 0·01$	$P < 0·01$	$P < 0·01$	$P < 0·01$
C.V. for main plots (%)	56·41	30·64	23·78	8·13	3·12	3·05	3·61	2·52
Genotype (G)								
Rayong 9 (G1)	3·0	6·4	4·78	38·5	54·5	114·2	64·7	165·7
Rayong 11 (G2)	2·8	4·4	4·29	38·5	53·5	108·6	64·4	158·0
Kasetsart 50 (G3)	3·2	10·8	3·94	40·2	91·1	136·7	102·6	195·6
S.E. (n = 12)	0·25	0·73	0·32	0·65	0·54	1·73	0·81	2·42
LSD	–	2·97	–	–	2·19	7·03	3·28	9·86
P level (G)	NS	$P < 0·01$	NS	NS	$P < 0·01$	$P < 0·01$	$P < 0·01$	$P < 0·01$
G × N								
N1 × G1	1·4	3·9	4·7	30·5	52·4	74·4	61·4	113·7
N1 × G2	2·0	4·6	4·0	26·2	51·6	56·0	60·7	90·7
N1 × G3	1·6	1·3	3·4	27·3	52·7	81·8	63·8	115·0
N2 × G1	3·4	6·0	4·6	43·7	53·4	96·5	64·8	153·6
N2 × G2	3·0	5·7	4·6	46·6	55·2	133·5	66·0	189·0
N2 × G3	2·1	10·9	4·1	45·8	107·7	125·5	115·8	188·2
N3 × G1	4·4	9·3	5·1	41·4	57·6	171·7	67·9	229·9
N3 × G2	3·2	2·9	4·3	42·7	53·6	136·2	66·4	194·3
N3 × G3	6·0	20·3	4·3	47·5	112·9	202·9	128·2	283·6
S.E. (n = 4)	0·44	1·27	0·55	1·13	0·93	2·99	1·40	4·19
LSD	1·78	5·15	–	4·60	3·80	12·18	5·69	17·07
P level (G × N)	$P < 0·01$	$P < 0·01$	NS	$P < 0·01$	$P < 0·01$	$P < 0·01$	$P < 0·01$	$P < 0·01$
C.V. for sub-plot (%)	29·12	35·10	25·21	5·77	2·81	5·00	3·62	4·85

C.V., coefficient of variation; NS, not significant; S.E., standard error; n, number of observations; LSD, least significant difference.

period of 2014/15 resulted in higher values of total dry weight (27·17 t/ha) and storage root dry weight (18·55 t/ha) than the 2015/16 growing period (17·50 and 12·10 t/ha for total and storage dry weights, respectively). However, the 2014/15 season had lower values of HI (0·68) and starch content (24·5%) than the 2015/16 season (0·69 and 30·2% for HI and starch content, respectively).

Significant differences ($P < 0·05$ and $< 0·01$) for the effect of N fertilizer applications in different years (years × N fertilizer) were found for almost all crop traits, except for SLA at 120 DAP, HI and starch content (Tables 6 and 7). For the performance of genotypes in different years (years × genotypes), non-significant differences were recorded for LGR during 90–120 DAP, SGR, SLA at 120 DAP and starch content. Significant differences in both linear and quadratic terms ($P < 0·05$ and $< 0·01$) for the effect of N fertilizer were observed for almost all crop traits, except for LGR during 90–120 DAP and SLA at 120 DAP (Tables 6 and 7). Both linear and quadratic parts of the effect of N fertilizer varied significantly with years or growing periods ($P < 0·05$ and $< 0·01$), except for SLA at 120 DAP and HI. Non-significant

Table 3. *Means for leaf area index (LAI) and specific leaf area (SLA) at 120 and 210 days after planting (DAP) and storage root dry weight, total dry weight, harvest index (HI) and starch content at harvest of cassava genotypes under three nitrogen (N) fertilizer rates in 2014/15*

Treatment	LAI (mm^2/mm^2)		SLA (mm^2/g)		Storage root dry weight (t/ha)	Total dry weight (t/ha)	HI	Starch content (%)
	120 DAP	210 DAP	120 DAP	210 DAP				
Nitrogen fertilizer								
46·9 kg N/ha (N1)	0·2	0·6	17701	10278	14·0	20·2	0·69	23·1
90·0 kg N/ha (N2)	0·3	1·9	19532	16138	20·2	29·0	0·70	25·0
133·2 kg N/ha (N3)	0·3	2·0	13224	14883	21·5	32·3	0·67	25·4
S.E. ($n = 12$)	0·02	0·04	2528·3	341·5	0·12	0·11	0·002	0·28
LSD	–	0·20	–	1790·0	0·64	0·57	0·026	1·48
P level (N)	NS	$P < 0·01$	NS	$P < 0·01$	$P < 0·01$	$P < 0·01$	$P < 0·01$	$P < 0·01$
C.V. for main plots (%)	32·55	8·78	52·13	8·66	2·28	1·38	4·63	3·99
Genotype (G)								
Rayong 9 (G1)	0·3	1·4	18215	12411	17·8	25·7	0·69	25·3
Rayong 11 (G2)	0·2	1·5	15269	16076	16·4	24·5	0·67	23·5
Kasetsart 50 (G3)	0·3	1·6	16979	12811	21·6	31·3	0·69	24·8
S.E. ($n = 12$)	0·02	0·04	1368·5	413·8	0·09	0·10	0·002	0·30
LSD	0·05	0·13	–	1684·0	0·38	0·42	0·012	1·23
P level (G)	$P < 0·05$	$P < 0·05$	NS	$P < 0·01$	$P < 0·01$	$P < 0·01$	$P < 0·01$	$P < 0·01$
G × N								
N1 × G1	0·3	0·7	20601	8990	15·5	21·4	0·73	23·5
N1 × G2	0·2	0·7	15692	11946	12·4	18·6	0·67	22·0
N1 × G3	0·2	0·5	16828	9898	14·0	20·8	0·67	23·8
N2 × G1	0·3	1·9	19405	15598	18·0	26·0	0·69	25·5
N2 × G2	0·2	1·8	14955	17689	17·8	26·2	0·68	24·5
N2 × G3	0·4	1·9	24236	15127	24·9	34·7	0·72	25·0
N3 × G1	0·3	1·7	14639	12646	19·7	29·8	0·66	26·8
N3 × G2	0·2	1·9	15161	18595	19·0	28·6	0·66	24·0
N3 × G3	0·2	2·3	9872	13409	25·8	38·4	0·67	25·5
S.E. ($n = 4$)	0·03	0·08	2370·2	716·7	0·16	0·18	0·003	0·52
LSD	–	0·32	–	–	0·67	0·73	0·020	–
P level (G × N)	NS	$P < 0·01$	NS	NS	$P < 0·01$	$P < 0·01$	$P < 0·01$	NS
C.V. for sub-plots (%)	21·18	10·36	28·21	10·52	1·76	1·32	0·93	4·27

C.V., coefficient of variation; NS, not significant; S.E., standard error; n, number of observations; LSD, least significant difference.

differences for N fertilizer (both linear and quadratic functions) × genotypes were recorded for SGR during 90–120 DAP, SLA at 120 DAP and starch content (Tables 6 and 7).

Based on the results of simple regression analyses with data from both experimental years, the growth rate values during 180–210 DAP in respect of SGR, SRGR and CGR contributed greatly to the variation in storage root dry weight at final harvest for all three rates of N fertilizer application, as indicated by high values of determination coefficients (R^2) (Table 8). Stem growth rate accounted for 61–83% of the variation in storage root dry weight at final harvest (Y (storage root yield) = 8·8 + 0·17 SGR during 180–210 DAP, Y = 9·1 + 0·24 SGR during 180–210 DAP and Y = 9·7 + 0·27 SGR during 180–210 DAP for N fertilizer of 46·9, 90·0 and 133·2 kg N/ha, respectively). The total variation in storage root dry weight at final harvest can be explained by SRGR, which ranged from 74 to 88% (Y = 8·6 + 0·07 SRGR during 180–210 DAP, Y = 10·4 + 0·08 SRGR during 180–210 DAP and Y = 12·0 + 0·06 SRGR during 180–210 DAP for N fertilizer of 46·9, 90·0 and 133·2 kg N/ha, respectively). Crop growth rate during 180–210 DAP accounted for 76–90% of the variation in storage root dry weight at final harvest (Y = 8·7 + 0·05 CGR during

Table 4. *Means for leaf growth rate (LGR), stem growth rate (SGR), storage root growth rate (SRGR) and crop growth rate (CGR) during 90–120 and 180–210 days after planting (DAP) of three cassava genotypes under three nitrogen (N) fertilizer rates in 2015/16*

	LGR (kg/day)		SGR (kg/day)		SRGR (kg/day)		CGR (kg/day)	
Treatment	90–120 DAP	180–210 DAP	90–120 DAP	180–210 DAP	90–120 DAP	180–210 DAP	90–120 DAP	180–210 DAP
Nitrogen fertilizer								
46·9 kg N/ha (N1)	7·2	−4·8	12·1	12·7	154·7	30·1	180·3	38·1
90·0 kg N/ha (N2)	4·9	−3·3	11·1	14·0	196·2	21·2	220·6	32·0
133·2 kg N/ha (N3)	5·3	−7·6	18·6	13·9	247·7	25·4	283·5	32·1
S.E. ($n = 12$)	0·83	0·44	1·19	0·97	6·16	1·73	6·48	1·68
LSD	–	2·31	6·25	–	32·29	6·00	33·95	–
P level (N)	NS	$P < 0·01$	$P < 0·01$	NS	$P < 0·01$	$P < 0·05$	$P < 0·01$	NS
C.V. for main plots (%)	49·74	−28·98	29·64	24·74	10·69	23·48	9·83	17·11
Genotype (G)								
Rayong 9 (G1)	4·6	−4·9	12·8	16·8	173·4	27·8	198·2	39·7
Rayong 11 (G2)	6·5	−4·8	15·4	12·0	183·7	24·8	214·7	32·4
Kasetsart 50 (G3)	6·3	−6·1	13·6	11·7	241·5	24·1	271·4	30·0
S.E. ($n = 12$)	0·64	0·60	1·16	1·24	4·68	2·70	5·28	2·54
LSD	–	–	–	3·70	19·05	–	21·51	7·56
P level (G)	NS	NS	NS	$P < 0·05$	$P < 0·01$	NS	$P < 0·01$	$P < 0·05$
G × N								
N1 × G1	4·8	−7·0	9·8	18·0	104·2	32·2	123·4	43·1
N1 × G2	6·4	−1·7	16·8	8·5	134·9	25·9	164·6	33·4
N1 × G3	10·4	−5·8	9·7	11·4	224·9	32·3	253·0	37·8
N2 × G1	5·3	−1·9	9·3	18·9	200·1	24·5	222·6	41·3
N2 × G2	5·3	−2·9	10·8	14·7	172·9	21·6	197·3	33·4
N2 × G3	4·3	−5·4	13·1	8·5	215·7	17·4	241·8	21·3
N3 × G1	3·7	−5·8	19·1	13·4	216·1	26·6	248·6	34·7
N3 × G2	7·8	−9·8	18·7	12·9	243·3	26·8	282·4	30·5
N3 × G3	4·3	−7·4	18·0	15·3	283·8	22·7	319·4	31·0
S.E. ($n = 4$)	1·11	1·04	2·01	2·16	8·11	4·68	9·15	4·41
LSD	3·30	4·23	–	6·40	33·00	–	37·25	–
P level (G × N)	$P < 0·05$	$P < 0·01$	NS	$P < 0·05$	$P < 0·01$	NS	$P < 0·01$	NS
C.V. for sub-plots (%)	38·37	−39·43	28·88	31·90	8·13	36·64	8·02	25·89

C.V., coefficient of variation; NS, not significant; S.E., standard error; n, number of observations; LSD, least significant difference.

180–210 DAP, $Y = 10·2 + 0·06$ CGR during 180–210 DAP and $Y = 12·0 + 0·04$ CGR during 180–210 DAP for N fertilizer of 46·9, 90·0 and 133·2 kg N/ha, respectively). Leaf area index in the early growth stage (at 120 DAP) was also able to explain storage root dry weight at harvest. However, the determination coefficients from simple regression analyses were not very high (0·57–0·70; $Y = 14·5–3·76$ LAI at 120 DAP, $Y = 22·4–8·74$ LAI at 120 DAP and $Y = 22·6–5·24$ LAI at 120 DAP for N fertilizer of 46·9, 90·0 and 133·2 kg N/ha, respectively).

Multiple regression analyses using data from the two experimental years and three cassava genotypes indicated that there were different physiological combinations for describing the storage root yield of cassava grown under three different rates of N fertilizer. Storage root dry weight at final harvest of three cassava genotypes grown with N at a rate of 46·9 kg N/ha could be explained by the combination of SRGR during 90–120 DAP, CGR during 180–210 DAP and SLA at 210 DAP (accounted for 87%; $Y = 9·0 + 0·01$ SRGR during 90–120 DAP + 0·06 CGR

Table 5. *Means for leaf area index (LAI) and specific leaf area (SLA) at 120 and 210 days after planting (DAP) and storage root dry weight, total dry weight, harvest index (HI) and starch content at harvest of cassava genotypes under addition nitrogen (N) fertilizer rates in 2015/16*

Treatment	LAI (mm^2/mm^2)		SLA (mm^2/g)		Storage root dry weight (t/ha)	Total dry weight (t/ha)	HI	Starch content (%)
	120 DAP	210 DAP	120 DAP	210 DAP				
Nitrogen fertilizer								
46·9 kg N/ha (N1)	0·9	0·7	14530	11750	10·7	15·3	0·70	29·3
90·0 kg N/ha (N2)	1·1	1·0	16308	11772	12·0	17·2	0·70	31·0
133·2 kg N/ha (N3)	1·7	1·3	16372	13258	13·6	20·0	0·68	30·4
S.E. ($n = 12$)	0·05	0·03	674·1	304·6	0·18	0·23	0·003	0·33
LSD	0·25	0·15	–	1054·0	0·93	1·19	0·010	1·15
P level (N)	$P < 0·01$	$P < 0·01$	NS	$P < 0·05$	$P < 0·01$	$P < 0·01$	$P < 0·01$	$P < 0·05$
C.V. for main plots (%)	13·12	9·94	14·84	8·69	5·07	4·50	4·56	3·80
Genotype (G)								
Rayong 9 (G1)	1·2	0·8	16613	11179	11·7	16·7	0·70	30·5
Rayong 11 (G2)	1·3	1·0	16013	11573	11·7	17·1	0·69	29·2
Kasetsart 50 (G3)	1·3	1·2	14584	14029	12·9	18·7	0·69	31·1
S.E. ($n = 12$)	0·04	0·03	625·1	392·6	0·14	0·17	0·003	0·29
LSD	0·17	0·12	–	1598·0	0·58	0·67	0·010	1·18
P level (G)	$P < 0·01$	$P < 0·01$	NS	$P < 0·01$	$P < 0·01$	$P < 0·01$	$P < 0·01$	$P < 0·01$
G × N								
N1 × G1	0·7	0·6	13703	11958	10·8	15·1	0·71	29·0
N1 × G2	1·1	0·8	15699	9968	10·1	14·8	0·69	29·0
N1 × G3	1·0	0·9	14189	13323	11·3	16·0	0·70	30·0
N2 × G1	1·1	0·8	18634	10217	11·7	16·3	0·72	32·0
N2 × G2	1·2	1·0	16280	12019	11·3	16·7	0·68	29·5
N2 × G3	1·1	1·1	14009	13081	13·0	18·5	0·70	31·5
N3 × G1	1·5	1·1	17503	11363	12·7	18·7	0·68	30·5
N3 × G2	1·7	1·2	16059	12731	13·7	19·8	0·70	29·0
N3 × G3	1·9	1·6	15554	15682	14·4	21·6	0·67	31·8
S.E. ($n = 4$)	0·07	0·05	1082·7	679·9	0·25	0·29	0·005	0·50
LSD	–	–	–	–	0·67	1·16	0·020	–
P level (G × N)	NS	NS	NS	NS	$P < 0·05$	$P < 0·05$	$P < 0·01$	NS
C.V. for sub-plots (%)	11·79	10·60	13·74	11·10	4·10	3·27	1·50	3·32

C.V., coefficient of variation; NS, not significant; S.E., standard error; n, number of observations; LSD, least significant difference.

during 180–210 DAP – 2·1 SLA at 210 DAP). Under the N fertilizer rate of 90·0 kg N/ha, the combination of SRGR during 90–120 DAP, SRGR during 180–210 DAP, LAI at 210 DAP and SLA at 210 DAP accounted for 97% of total variation in storage root dry weight at final harvest ($Y = 6·0 + 0·04$ SRGR during 90–120 DAP + 0·07 SRGR during 180–210 DAP + 13·16 LAI at 210 DAP – 13·4 SLA at 210 DAP). The combination of LGR during 180–210 DAP and LAI at 210 DAP had the highest correlations to storage root dry weight at final harvest of three cassava genotypes grown at a rate of 133·2 kg N/ha (accounted for 95%; $Y = 11·2 + 0·30$ LGR during 180–210 DAP + 3·55 LAI at 210 DAP).

DISCUSSION

The larger values in growth rate during 180–210 DAP and LAI at 210 DAP (the late growth period) for the 2014/15 season were probably due to higher rainfall and temperature during the late growth stages. Optimum temperature for cassava photosynthesis varies between 30 and 40 °C for hot-climate genotypes (El-Sharkawy *et al.* 1992*b*). In field experiments,

Table 6. *Mean square values from combined analysis for leaf growth rate (LGR), stem growth rate (SGR), storage root growth rate (SRGR) and crop growth rate (CGR) during 90–120 and 180–210 days after planting (DAP) of three cassava genotypes under three nitrogen (N) fertilizer rates*

Source of variation	Degree of freedom	LGR (kg/day)		SGR (kg/day)		SRGR (kg/day)		CGR (kg/day)	
		90–120 DAP	180–210 DAP	90–120 DAP	180–210 DAP	90–120 DAP	180–210 DAP	90–120 DAP	180–210 DAP
Year (Y)	1	139 ($P<0·01$)	2805 ($P<0·01$)	1658 ($P<0·01$)	11758 ($P<0·01$)	319390 ($P<0·01$)	159947 ($P<0·01$)	409840 ($P<0·01$)	348112 ($P<0·01$)
Replication/Y	6	3	6	8	16	83	34	104	95
Nitrogen	2	6 (NS)	56 ($P<0·01$)	108 ($P<0·01$)	644 ($P<0·01$)	20055 ($P<0·01$)	13626 ($P<0·01$)	24866 ($P<0·01$)	22873 ($P<0·01$)
N linear	1	3 (NS)	68 ($P<0·01$)	148 ($P<0·01$)	876 ($P<0·01$)	40058 ($P<0·01$)	26957 ($P<0·01$)	49674 ($P<0·01$)	45719 ($P<0·01$)
N quadratic	1	9 (NS)	45 ($P<0·01$)	69 ($P<0·05$)	413 ($P<0·01$)	52 (NS)	295 ($P<0·01$)	59 (NS)	27 (NS)
Y × N	2	37 ($P<0·05$)	172 ($P<0·01$)	93 ($P<0·01$)	471 ($P<0·01$)	7848 ($P<0·01$)	16376 ($P<0·01$)	9741 ($P<0·01$)	27710 ($P<0·01$)
Y × N linear	1	69 ($P<0·01$)	322 ($P<0·01$)	107 ($P<0·01$)	645 ($P<0·01$)	14957 ($P<0·01$)	32668 ($P<0·01$)	18067 ($P<0·01$)	55109 ($P<0·01$)
Y × N quadratic	1	5 (NS)	22 ($P<0·05$)	79 ($P<0·05$)	298 ($P<0·01$)	739 (NS)	84 (NS)	1416 ($P<0·05$)	311 ($P<0·01$)
Genotype (G)	2	6 (NS)	39 ($P<0·01$)	10 (NS)	36 (NS)	20145 ($P<0·01$)	1192 ($P<0·01$)	21595 ($P<0·01$)	1871 ($P<0·01$)
N × G	4	9 ($P<0·05$)	96 ($P<0·01$)	15 (NS)	72 ($P<0·01$)	612 ($P<0·01$)	976 ($P<0·01$)	836 ($P<0·01$)	1595 ($P<0·01$)
N linear × G	2	5 (NS)	188 ($P<0·01$)	18 (NS)	91 ($P<0·01$)	21 (NS)	239 ($P<0·05$)	21 (NS)	1115 ($P<0·01$)
N quadratic × G	2	14 ($P<0·05$)	5 (NS)	13 (NS)	52 ($P<0·05$)	1203 ($P<0·01$)	1713 ($P<0·01$)	1652 ($P<0·01$)	2076 ($P<0·01$)
Y × G	2	7 (NS)	98 ($P<0·01$)	15 (NS)	71 (NS)	1516 ($P<0·01$)	1523 ($P<0·01$)	1869 ($P<0·01$)	3153 ($P<0·01$)
Error for main plots	12	6	4	9	11	230	25	225	27
Error for sub-plots	36	3	5	9	12	133	62	171	74

NS, not significant.

Table 7. *Mean square values from combined analysis for leaf area index (LAI) and specific leaf area (SLA) at 120 and 210 days after planting (DAP) and storage root dry weight, total dry weight, harvest index (HI) and starch content at harvest of cassava genotypes under three nitrogen (N) fertilizer rates*

Source of variation	Degree of freedom	LAI (mm^2/mm^2)		SLA (mm^2/g)		Storage root dry weight (t/ha)	Total dry weight (t/ha)	HI	Starch content (%)
		120 DAP	210 DAP	120 DAP	210 DAP				
Year (Y)	1	17·83 ($P < 0·01$)	4·13 ($P < 0·01$)	21170000 (NS)	40840000 ($P < 0·01$)	749·5 ($P < 0·01$)	1681·4 ($P < 0·01$)	0·00200 ($P < 0·01$)	595 ($P < 0·01$)
Replication/Y	6	0·01	0·01	6937636	2167175	0·6	0·8	0·00010	1
Nitrogen	2	0·89 ($P < 0·01$)	6·09 ($P < 0·01$)	58950000 (NS)	71950000 ($P < 0·01$)	173·7 ($P < 0·01$)	428·9 ($P < 0·01$)	0·00435 ($P < 0·01$)	25 ($P < 0·01$)
N linear	1	1·74 ($P < 0·01$)	11·10 ($P < 0·01$)	20900000 (NS)	112000000 ($P < 0·01$)	325·5 ($P < 0·01$)	837·8 ($P < 0·01$)	0·00558 ($P < 0·01$)	35 ($P < 0·01$)
N quadratic	1	0·05 (NS)	1·07 ($P < 0·01$)	97000000 (NS)	31900000 ($P < 0·01$)	21·9 ($P < 0·01$)	19·9 ($P < 0·01$)	0·00312 ($P < 0·01$)	14 ($P < 0·01$)
Y × N	2	0·87 ($P < 0·01$)	1·61 ($P < 0·01$)	80185000 (NS)	50995000 ($P < 0·01$)	47·0 ($P < 0·01$)	101·5 ($P < 0·01$)	0·00029 (NS)	3 (NS)
Y × N linear	1	1·50 ($P < 0·01$)	1·60 ($P < 0·01$)	119500000 (NS)	28600000 ($P < 0·01$)	65·5 ($P < 0·01$)	161·0 ($P < 0·01$)	0·00032 (NS)	5 ($P < 0·05$)
Y × N quadratic	1	0·25 ($P < 0·01$)	1·61 ($P < 0·01$)	40870000 (NS)	73390000 ($P < 0·01$)	28·6 ($P < 0·01$)	42·0 ($P < 0·01$)	0·00025 (NS)	1 (NS)
Genotype (G)	2	0·07 ($P < 0·05$)	0·44 ($P < 0·01$)	23320000 (NS)	27690000 ($P < 0·01$)	66·7 ($P < 0·01$)	129·4 ($P < 0·01$)	0·00300 ($P < 0·01$)	20 ($P < 0·01$)
N × G	4	0·02 (NS)	0·16 ($P < 0·01$)	20751409 (NS)	5417500 ($P < 0·05$)	14·0 ($P < 0·01$)	21·1 ($P < 0·01$)	0·00179 ($P < 0·01$)	1 (NS)
N linear × G	2	0·01 (NS)	0·31 ($P < 0·01$)	7549493 (NS)	10230000 ($P < 0·05$)	19·7 ($P < 0·01$)	34·0 ($P < 0·01$)	0·00229 ($P < 0·01$)	2 (NS)
N quadratic × G	2	0·04 ($P < 0·05$)	0·01 (NS)	33953325 (NS)	605000 (NS)	8·3 ($P < 0·01$)	8·3 ($P < 0·01$)	0·00128 ($P < 0·01$)	1 (NS)
Y × G	2	0·12 ($P < 0·01$)	0·06 ($P < 0·05$)	15970000 (NS)	49440000 ($P < 0·01$)	25·5 ($P < 0·01$)	43·2 ($P < 0·01$)	0·00030 ($P < 0·05$)	2 (NS)
Error for main plots	12	0·02	0·01	41080000	1256148	0·3	0·4	0·00009	1
Error for sub-plots	36	0·01	0·02	13580000	1952009	0·2	0·2	0·00007	1

NS, not significant.

Table 8. *Determination coefficient (R^2) of simple and multiple regressions for physiological traits and storage root dry weight at harvest of cassava grown under three different nitrogen (N) fertilizer rates*

	R^2		
Physiological trait	46·9 kg N/ha	90·0 kg N/ha	133·2 kg N/ha
$LGR_{90–120\ DAP}$ (kg/day)	0·35 ($P<0·01$)	0·43 ($P<0·01$)	0·00 (NS)
$LGR_{180–210\ DAP}$ (kg/day)	0·43 ($P<0·01$)	0·77 ($P<0·01$)	0·91 ($P<0·01$)
$SGR_{90–120\ DAP}$ (kg/day)	0·42 ($P<0·01$)	0·53 ($P<0·01$)	0·68 ($P<0·01$)
$SGR_{180–210\ DAP}$ (kg/day)	0·61 ($P<0·01$)	0·66 ($P<0·01$)	0·83 ($P<0·01$)
$SRGR_{90–120\ DAP}$ (kg/day)	0·33 ($P<0·01$)	0·43 ($P<0·01$)	0·49 ($P<0·01$)
$SRGR_{180–210\ DAP}$ (kg/day)	0·76 ($P<0·01$)	0·74 ($P<0·01$)	0·88 ($P<0·01$)
$CGR_{90–120\ DAP}$ (kg/day)	0·37 ($P<0·01$)	0·47 ($P<0·01$)	0·51 ($P<0·01$)
$CGR_{180–210\ DAP}$ (kg/day)	0·79 ($P<0·01$)	0·76 ($P<0·01$)	0·90 ($P<0·01$)
$LAI_{120\ DAP}$ (mm^2/mm^2)	0·57 ($P<0·01$)	0·63 ($P<0·01$)	0·70 ($P<0·01$)
$LAI_{210\ DAP}$ (mm^2/mm^2)	0·08 (NS)	0·74 ($P<0·01$)	0·78 ($P<0·01$)
$SLA_{120\ DAP}$ (mm^2/g)	0·32 ($P<0·01$)	0·18 ($P<0·05$)	0·36 ($P<0·01$)
$SLA_{210\ DAP}$ (mm^2/g)	0·19 ($P<0·05$)	0·39 ($P<0·01$)	0·03 (NS)
$SRGR_{90–120\ DAP}$ and $CGR_{180–210\ DAP}$ and $SLA_{210\ DAP}$	0·87 ($P<0·05$)	–	–
$SRGR_{90–120\ DAP}$ and $SRGR_{180–210\ DAP}$ and $LAI_{210\ DAP}$ and $SLA_{210\ DAP}$	–	0·97 ($P<0·05$)	–
$LGR_{180–210\ DAP}$ and $LAI_{210\ DAP}$	–	–	0·95 ($P<0·05$)

NS, not significant.

$LGR_{90–120\ DAP}$ and $LGR_{180–210\ DAP}$ = leaf growth rate during 90–120 and 180–210 days after planting, respectively; $SGR_{90–120\ DAP}$ and $SGR_{180–210\ DAP}$ = stem growth rate during 90–120 and 180–210 days after planting, respectively; $SRGR_{90–120\ DAP}$ and $SRGR_{180–210\ DAP}$ = storage root growth rate during 90–120 and 180–210 days after planting, respectively; $CGR_{90–120\ DAP}$ and $CGR_{180–210\ DAP}$ = crop growth rate during 90–120 and 180–210 days after planting, respectively; $LAI_{120\ DAP}$ and $LAI_{210\ DAP}$ = leaf area index at 120 and 210 days after planting, respectively; $SLA_{120\ DAP}$ and $SLA_{210\ DAP}$ = specific leaf area index at 120 and 210 days after planting, respectively.

Keating *et al.* (1982*a*, *b*) demonstrated that average temperatures above 24 °C are associated with high CGRs and storage root accumulation. In contrast, temperatures below 20 °C lead to decreased photosynthesis capacity, growth and storage root weight (El-Sharkawy 2012). However, in the current study results for the 2014/15 growing period stand in contrast to the results obtained during the 2015/16 growing period. Based on previous studies, higher temperatures (Keating *et al.* 1982*a*, *b*; El-Sharkawy *et al.* 1992*b*; El-Sharkawy 2012) and higher amounts of rainfall during the early growth period positively impact photosynthetic potential and growth in cassava. The negative values of LGR during 180–210 DAP in the 2015/16 season were due to leaf abscission (Fageria *et al.* 1991) resulting from drought and low temperatures.

Higher N fertilizer rates resulted in higher values for most crop traits in both the 2014/15 and 2015/16 growing seasons, indicating a positive effect of N fertilizer application on crop growth with both linear and quadratic functions. This result is similar to the report from Kaweewong *et al.* (2013*a*, *b*), who indicated that N fertilizer influences cassava growth in certain production areas in Thailand and that increasing N fertilizer up to 250 kg/ha can increase aboveground biomass and storage root dry weights. Cruz *et al.* (2003) reported that cassava grown under higher N-treatments (12 mM NO_3^-) had higher photosynthetic capacities and SLA values than cassava grown under lower N-treatments (3 mM NO_3^-).

The combined ANOVA results showed non-significant differences for N fertilizer (both linear and quadratic parts) × genotypes in SGR during 90–120 DAP, SLA at 120 DAP and starch content. This indicates that the responses of the three genotypes to different rates of N fertilizer for those crop traits are not linear and quadratic functions. Significant differences for years × genotypes in most crop traits indicate that the performances for those crop traits of the three

genotypes vary with years or growing seasons. Comparison of the results from individual growing season analysis among the three cassava genotypes, however, showed that Kasetsart 50 had the highest performance for most crop traits in both the 2014/15 and 2015/16 growing seasons. Therefore, this genotype is particularly recommended for cassava production with additional N fertilizer applications. It is also suitable as a parental source for improving cassava in order to maximize storage root dry weight under N-limiting conditions.

The experiment in 2014/15 produced more values with statistical significance in total and storage root dry weights when compared with the experiment in 2015/16. Higher total amounts of rainfall (789·0 mm) and solar radiation (5731·0 MJ/m^2/day) during the 2014/15 growing period compared with 2015/16 (540·4 mm for total rain fall and 5511·7 MJ/m^2/day for solar radiation) can probably explain this result (Fukai *et al*. 1984; Banterng *et al*. 2010; El-Sharkawy 2012; Vilayvong *et al*. 2015). There was a significant difference in HI between the two growing seasons (data not shown), with the 2014/15 season having lower values than 2015/16. High amounts of rainfall in the 2014/15 season (especially during the late growing period) supported above-ground growth rather than growth of storage root. El-Sharkawy *et al*. (1992*a*) reported that growth of leaves and stems was restricted under water stress conditions, but storage root yields were increased or remained unaffected.

The close relationship between storage root dry weight at final harvest and single growth rate trait during 180–210 DAP regarding SGR, SRGR and CGR for all three different rates of N fertilizer application indicates that an increase of storage root dry weight might be accompanied by an increase of these three physiological traits in the late growth period (6–7 months after planting). It seemed that LAI in the early growth stage (at 120 DAP) was also able to explain storage root dry weight at harvest. High storage root biomass at final harvest was associated with high mean LAI in both wet and stressed environments (El-Sharkawy *et al*. 1992*a*). Storage root yield, shoot and total biomass were significantly correlated with seasonal average LAI under rain-fed conditions (El-Sharkawy & de Tafur 2010). Considering the performance of the three cassava genotypes, the current results clearly demonstrate that Kasetsart 50 is superior in terms of storage root dry weight at final harvest, which is also related to high values of growth rates during 180–210 DAP with regard to SGR, SRGR and CGR as well as LAI at 120 DAP. Therefore, improving storage root yield of cassava under different N fertilizer applications should also aim to increase the values of these four physiological traits.

Based on the results from multiple regression analyses using data from two experimental years and three cassava genotypes, it is noteworthy that LAI at 210 DAP is a component of physiological determinants of storage root yield under high N fertilizer. The physiological traits that relate to leaf growth during the late growth period (LGR during 180–210 DAP and LAI at 210 DAP) are also able to explain storage root yield of cassava grown under the highest rate of N fertilizer (133·2 kg N/ha). More leaf growth and high LAI values of cassava were related to high rates of N fertilizer applications (Sangakkara & Wijesinghe 2014) and associated with higher crop photosynthesis, growth and final storage root yield (El-Sharkawy *et al*. 1992*a*; El-Sharkawy & de Tafur 2010). In addition, the results from multiple regression analysis also indicated that SLA at 210 DAP is a component of physiological determinants of storage root yield for cassava grown under N fertilizer at rates of 46·9 and 90·0 kg N/ha. However, when compared with the results of simple regression, single physiological traits of SLA could not be able to describe the variation of storage root dry weight at final harvest. This crop trait would be more useful as a component of physiological combinations.

In order to improve storage root yield of cassava and to better understand the responses of different cassava cultivars to N fertilizer, the current results suggest that SGR, SRGR and CGR during 180–210 DAP as well as LAI at 120 DAP are useful selection criteria to help select desirable cassava genotypes under N-limitation. The physiological combinations proposed from the current study would also be an alternative option to support decision-making in identifying suitable cassava genotypes under N-limitation. Selection of the best crop genotypes under different growing conditions based on only final yield is inefficient and analysis on physiological determinants of yield can provide useful information on how particular genotypes perform within given environments (Banterng *et al*. 2003; Arunyanark *et al*. 2009; Puangbut *et al*. 2010; Ruttanaprasert *et al*. 2016). In addition, the current results regarding physiological determinants of storage root yield of cassava offer valuable information for further improvement of

cassava modelling as a tool to help with decision-making (Jones *et al*. 2003).

CONCLUSION

The genotype Kasetsart 50 was best suited for the three different N fertilizer treatments. Stem growth rate, SRGR and CGR in the late growth period (during 180–210 DAP) and LAI at 120 DAP were identified as the best measurements associated with storage root dry weight for all three different rates of additional N fertilizer. Storage root dry weight of the three genotypes grown under N fertilizer application at a rate of 46·9 kg N/ha could be adequately described by the physiological combination of SRGR during 90–120 DAP, CGR during 180–210 DAP and SLA at 210 DAP, while at 90·0 kg N/ha could be explained by the physiological combination of SRGR during 90–120 DAP, SRGR during 180–210 DAP, LAI at 210 DAP and SLA at 210 DAP and at 133·2 kg N/ha could be illustrated by the physiological combination of LGR during 180–210 DAP and LAI at 210 DAP. Using these single traits and physiological combinations can be useful to improve the efficiency of identifying suitable cassava genotypes to grow under N-limiting conditions.

This study was supported by Khon Kaen University, Thailand. Assistances in conducting the work were also received from the Plant Breeding Research Center for Sustainable Agriculture, Khon Kaen University and from National Science and Technology Development Agency (NSTDA), Thailand. Acknowledgement is extended to the Thailand Research Fund (Project code: IRG5780003) and Faculty of Agriculture, Khon Kaen University for providing financial support for manuscript preparation.

REFERENCES

Arunyanark, A., Jogloy, S., Wongkaew, S., Akkasaeng, C., Vorasoot, N., Wright, G. C., Rachaputi, R. C. N. & Patanothai, A. (2009). Association between aflatoxin contamination and drought tolerance traits in peanut. *Field Crops Research* **114**, 14–22.

Banterng, P., Patanothai, A., Pannangpetch, K., Jogloy, S. & Hoogenboom, G. (2003). Seasonal variation in the dynamic growth and development traits of peanut lines. *Journal of Agricultural Science, Cambridge* **141**, 51–62.

Banterng, P., Hoogenboom, G., Patanothai, A., Singh, P., Wani, S. P., Pathak, P., Tongpoonpol, S., Atichart, S., Srihaban, P., Buranaviriyakul, S., Jintrawet, A. & Nguyen, T. C. (2010). Application of the cropping system model (CSM)-CROPGRO-Soybean for determining optimum management strategies for soybean in tropical environments. *Journal of Agronomy and Crop Science* **196**, 231–242.

Cenpukdee, U. & Fukai, S. (1991). Effects of nitrogen supply on cassava/pigeonpea intercropping with tree contrasting cassava cultivars. *Fertilizer Research* **29**, 275–280.

Cruz, J. L., Mosquim, P. R., Pelacani, C. R., Araujo, W. L. & DaMatta, F. M. (2003). Photosynthesis impairment in cassava leaves in response to nitrogen deficiency. *Plant and Soil* **257**, 417–423.

Czerednik, A. & Nalborczyk, E. (2001). Physiological factors affecting yield formation in the canopy of traditional and new morphotypes of triticale plant (*Triticosecale* Wittmack). *Acta Physiologiae Plantarum* **23**, 87–93.

Dordas, C. A. (2010). Variation of physiological determinants of yield in linseed in response to nitrogen fertilization. *Industrial Crops and Products* **31**, 455–465.

El-Sharkawy, M. A. (2012). Stress tolerant cassava: the role of integrative ecophysiology breeding research in crop improvement. *Open Journal of Soil Science* **2**, 162–186.

El-Sharkawy, M. A. & de Tafur, S. M. (2010). Comparative photosynthesis, growth, productivity, and nutrient use efficiency among tall- and short-stemmed rain-fed cassava cultivars. *Photosynthetica* **48**, 173–188.

El-Sharkawy, M. A., Hernandez, A. D. P. & Hershey, C. (1992*a*). Yield stability of cassava during prolonged mid-season water stress. *Experimental Agriculture* **28**, 165–174.

El-Sharkawy, M. A., de Tafur, S. M. & Cadavid, L. F. (1992*b*). Potential photosynthesis of cassava as affected by growth conditions. *Crop Science* **32**, 1336–1342.

Fageria, N. K., Baligar, V. C. & Jones, C. A. (1991). *Growth and Mineral Nutrition of Field Crops*. New York: Marcel Dekker, Inc.

Freed, R. D. & Nissen, O. (1992). *MSTAT-C Version 1.42*. East lansing, Michigan: Michigan State University.

Fukai, S., Alcoy, A. B., Llamelo, A. B. & Patterson, R. D. (1984). Effects of solar radiation on growth of cassava (*Manihot esculenta* Crantz.). I. Canopy development and dry matter growth. *Field Crops Research* **9**, 347–360.

Gomez, K. A. & Gomez, A. A. (1984). *Statistical Procedures for Agricultural Research*. New York: John Wiley and Sons.

Howeler, R. H. (2002). Cassava mineral nutrition and fertilization. In *Cassava: Biology, Production and Utilization* (Eds R. J. Hillocks, J. M. Thresh & A. C. Bellotti), pp. 115–147. Wallingford, UK: CAB International.

Jones, J. W., Hoogenboom, G., Porter, C. H., Boote, K. J., Batchelor, W. D., Hunt, L. A., Wilkens, P. W., Singh, U., Gijsman, A. J. & Ritchie, J. T. (2003). The DSSAT cropping system model. *European Journal of Agronomy* **18**, 235–265.

Kaweewong, J., Tawornpruek, S., Yampracha, S., Yost, R., Kongton, S. & Kongkaew, T. (2013*a*). Cassava nitrogen requirements in Thailand and crop simulation model predictions. *Soil Science* **178**, 248–255.

Kaweewong, J., Kongkeaw, T., Tawornprek, S., Yampracha, S. & Yost, R. (2013*b*). Nitrogen requirements of cassava in selected soils of Thailand. *Journal of Agriculture and Rural Development in the Tropics and Subtropics* **114**(1), 13–19.

Koutroubas, S. D., Papakosta, D. K. & Doitsinis, A. (2009). Phenotypic variation in physiological determinants of yield in spring sown safflower under Mediterranean condition. *Field Crops Research* **112**, 199–204.

Keating, B. A., Evenson, J. P. & Fukai, S. (1982*a*). Environmental effects on growth and development of cassava (*Manihot esculenta* Crantz.). II. Crop growth rate and biomass yield. *Field Crops Research* **5**, 283–292.

Keating, B. A., Evenson, J. P. & Fukai, S. (1982*b*). Environmental effects on growth and development of cassava (*Manihot esculenta* Crantz.). III. Assimilate distribution and storage organ yield. *Field Crops Research* **5**, 293–303.

Massignam, A. M., Chapman, S. C., Hammer, G. L. & Fukai, S. (2009). Physiological determinants of maize and sunflower grain yield as affected by nitrogen supply. *Field Crops Research* **113**, 256–267.

Nguyen, H., Schoenau, J. J., Nguyen, D., Van Rees, K. & Boehm, M. (2002). Effects of long-term nitrogen, phosphorus, and potassium fertilization on cassava yield and plant nutrient composition in north Vietnam. *Journal of Plant Nutrition* **25**, 425–442.

Olasantan, F. O. (1999). Nitrogen fertilization of okra (*Abelmoschus esculentus*) in an intercropping system with cassava (*Manihot esculenta*) and maize (*Zea mays*) in south-western Nigeria. *Journal of Agricultural Science, Cambridge* **133**, 325–334.

Puangbut, D., Jogloy, S., Toomsan, B., Vorasoot, N., Akkasaeng, C., Kesmala, T., Rachaputi, R. C. N., Wright, G. C. & Patanothai, A. (2010). Physiological basis for genotypic variation in tolerance to and recovery from pre-flowering drought in peanut. *Journal of Agronomy and Crop Science* **196**, 358–367.

Ruttanaprasert, R., Banterng, P., Jogloy, S., Vorasoot, N., Kesmala, T. & Patanothai, A. (2016). Diversity of physiological traits in Jerusalem artichoke genotypes under non-stress and drought stress. *Pakistan Journal of Botany* **48**, 11–20.

Sangakkara, U. R. & Wijesinghe, D. B. (2014). Nitrogen fertilizer affects growth, yield, and N recovery in cassava (*Manihot esculenta* L. Crantz). *Communications in Soil Science and Plant Analysis* **45**, 1446–1452.

Vilayvong, S., Banterng, P., Patanothai, A. & Pannangpetch, K. (2015). CSM-CERES-Rice model to determine management strategies for lowland rice production. *Scientia Agricola* **72**, 229–236.

Yusuf, R. I., Siemens, J. C. & Bullock, D. G. (1999). Growth analysis of soybean under no-tillage and conventional tillage systems. *Agronomy Journal* **91**, 928–933.

doi: 10.17221/51/2016-CJGPB

Pyramiding of Four Blast Resistance QTLs into Thai Rice Cultivar RD6 through Marker-assisted Selection

*Teerawat SUWANNUAL, Sompong CHANKAEW, Tidarat MONKHAM, Weerasak SAKSIRIRAT and Jirawat SANITCHON**

Department of Plant Science and Agricultural Resources, Faculty of Agriculture, Khon Kaen University, Khon Kaen, Thailand

**Corresponding author: jirawat@kku.ac.th*

Abstract

Suwannual T., Chankaew S., Monkham T., Saksirirat W., Sanitchon J. (2017): Pyramiding of four blast resistance QTLs into Thai rice cultivar RD6 through marker-assisted selection. Czech J. Genet. Plant Breed., 53: 1–8.

Thai rice cultivar RD6 is well known for its cooking and eating qualities. However it is susceptible to blast disease, a major rice disease caused by the fungus *Magnaporthe oryzae*. This study focused on the pyramiding of four QTLs for blast resistance located on chromosomes 1, 2, 11 and 12, from two RD6 introgression lines. Marker-assisted selection was performed and facilitated the selection with 8 microsatellite flanking markers to enable the selection in $BC_2F_{2:3}$ lines. All possible combinations of the four QTL alleles were assessed for blast resistance by artificial inoculation using 8 diverse isolates in a greenhouse and under field conditions using the upland short row method. The results showed that the RD6 introgression lines carrying a high number of QTLs for blast resitance achieved from pyramiding have high levels of blast resistance and broad spectrum of resistance to the blast pathogens prevalent in the region. Only one of the *M. oryzae* isolates, THL185, was virulent to all the breeding lines, suggesting that the identification of new blast resistance genes or QTLs and pyramiding them into RD6 for durable blast resistance and no yield penalty should be the focus of further research.

Keywords: broad spectrum; introgression lines; *Magnaporthe oryzae*; *Oryza sativa*; severity index

The rice cultivar RD6 has high cooking and eating qualities and rich aroma. It is widely grown through the North and Northeastern regions of Thailand. However, this cultivar is usually susceptible to blast disease, one of the diseases of rice that is widespread in Asia and Africa (Liu *et al.* 2010). Rice blast is caused by the fungus *Magnaporthe oryzae* (anamorph *Pyricularia oryzae*). The severity of rice blast is dependent on many factors, including cultural practices, cultivars, climate and nitrogen fertilizer (Ou 1985). The disease can reduce grain yield by up to 90% (Khush & Jena 2009).

The utilization of host resistant rice cultivars is the most economical and efficient strategy to control this disease. Blast resistance in rice is controlled by multiple genetic loci (Saka 2006). Currently, more than 90 disease resistance genes and 347 QTLs have been identified for blast resistance (Liu *et al.* 2010) and used for rice variety improvement. However, the cultivation of varieties with single resistant genes on a large scale may enable the pathogen to overcome blast resistance in the longer term. This possibility can potentially be delayed by the introgression of multiple resistant genes through gene pyramiding in rice cultivars, to enable rice varieties to achieve broad-spectrum resistance (Servin *et al.* 2004).

Due to the genetic basis of blast disease resistance, phenotypic selection is compromised by many factors. The availability of molecular markers, along with marker-assisted selection (MAS) strategies, is essential for the development of rice varieties with durable blast resistance against different races of *M. oryzae* (Ashkani *et al.* 2012). The pyramiding of three blast R genes, *Pi1*, *Piz-5* and *Pita-2*, into cultivars

doi: 10.17221/51/2016-CJGPB

was undertaken to provide broad-spectrum resistance to many isolates of *M. oryzae* (Hittalmani *et al.* 2000). Moreover, the pseudo-backcrossing approach is the method for increasing the recurrent genetic background of the pyramiding population (Rueng-phayak *et al.* 2015). The objective of this study was to determine the resistance level conferred by four QTLs in an introgression line by pyramiding of blast resistance QTLs into the rice cultivar RD6 to provide a variety with durable blast resistance in Thailand.

MATERIAL AND METHODS

Plant materials and marker-assisted selection for blast resistance QTLs

The two RD6 near isogenic lines (NILs), NIL RD6 (2, 12) and NIL RD6 (1, 11), were used for the development of the pyramided lines. Both NILs maintained the genetic background of the RD6 variety by MAS (Figure 1). NIL RD6 (2, 12) harbour the resistance QTLs on chromosomes 2 and 12 from the P0489 recombinant line (Theeraamphon, personal communication). P0489, a recombinant line derived from Azucena × IR64, had been identified as a blast resistant line due to carrying QTLs on chromosomes 2 and 12 (Silprakhon 2004). NIL RD6 (1, 11) contained the major resistance QTLs located on chromosomes 1 and 11 from the Jao Hom Nil (JHN) variety (Noenplab *et al.* 2006). Both of the RD6 NILs lines were crossed for the development of the pyramided lines. The F_1 plants (containing the QTLs located on chromosomes 1, 2, 11 and 12) were crossed with RD6 (the recurrent parent of both NILs) through $BC_2F_{2:3}$ and MAS (Figure 1) with flanking SSR markers was used, following Korinsak (2009) (Table 1). Selected lines containing all possible QTL combinations were classified into 16 groups and subsequently evaluated for blast resistance.

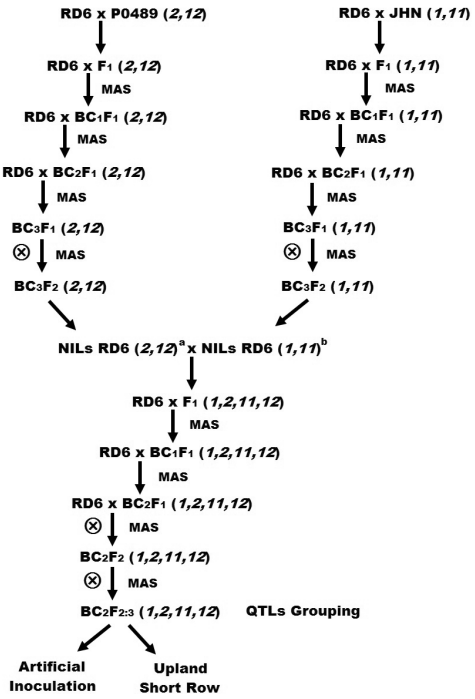

Figure 1. Breeding scheme of gene pyramiding for improved RD6 NILs resistant to rice blast disease through marker-assisted selection (MAS) with flanking markers located on chromosomes 2/12 and 1/11, respectively ([a]Theeraamphon, personal communication; [b]Noenplab *et al.* 2006)

Phenotypic evaluation of resistance to *M. oryzae*

Greenhouse conditions. Eight virulent *M. oryzae* isolates from diverse outbreak areas (Figure 2) (Sirithanya *et al.* 2008) were used for evaluation against 16 combination groups of resistance QTLs. Fungal isolates used in the pathogenicity test were grown on rice flour agar media (Korinsak 2009). The $BC_2F_{2:3}$ population, the parents and control varieties were laid out in a randomized complete block design (RCBD) with three replications, in the wet season (August to October) of 2010 at Khon Kaen University, Khon Kaen, Thailand. At 21 days after sowing (DAS), the plants

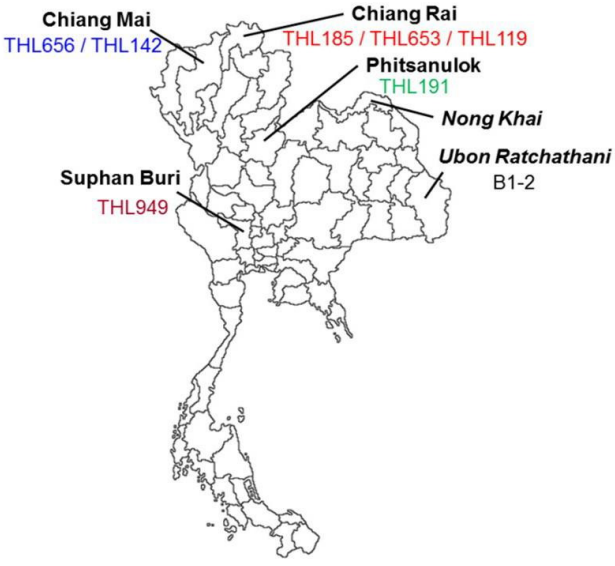

Figure 2. Distributions of 8 *Magnaporthe oryzae* isolates used for artificial inoculation in greenhouse conditions (the provinces in italics were the location for later upland short row tests)

doi: 10.17221/51/2016-CJGPB

were inoculated with single isolate spore suspensions (5×10^5 spore/ml). The inoculated seedlings were kept in an incubation chamber at 26 ± 1°C for 24 h, under conditions of saturated humidity; they were subsequently transferred to growth chambers until disease scores were recorded. The reactions to the disease were scored on a scale from 0 (no lesions) to 6 (coalescence of > 4 mm lesions or 50% of the leaves killed and without dark margins) using a standard evaluation method (Roumen *et al.* 1997).

Field conditions. The $BC_2F_{2:3}$ lines and control varieties were planted in RCBD with two replications during the wet season of 2010 in experimental fields in the provinces Nong Khai and Ubon Ratchathani in Northeast Thailand. In each experiment, seed of each genotype was sown in a single row 1 m long with a 30 cm inter-row spacing. Fourteen days prior to planting, the highly susceptible rice cultivar KDML105 was sown as a trap around and between the experimental plots. At 30 DAS the infection on the leaves of each plant was scored for the blast reaction on a scale of 0–9 (IRRI 1996).

Data analysis

Analysis of variance of the rice blast disease scores data was done. Mean and SD of the blast scores for each line and variety were calculated, and the means of all lines were compared by Tukey's HSD using the R program Version 2.10 (R Development Core Team 2008). Based on the blast score, the severity index (SI) was estimated using the formula reported by Sirithanya (1998). Then the broad-spectrum resistance (BSR) was calculated using the formula of Ahn (1994). In addition, the probability of orthogonal comparison between the groups of $BC_2F_{2:3}$ populations carrying different combinations of the four QTLs, including the control and control varieties, was examined using all isolates with the exception of B1-2, an *M. oryzae* isolate from Ubon Ratchathani province.

RESULTS

Reaction to blast disease. The $BC_2F_{2:3}$ progenies of each of the RD6 lines homozygous for each of the single QTLs and those having different combinations, together with the control varieties, were screened for their reaction to the eight *M. oryzae* isolates prevalent in Thailand. The ANOVA showed a significant difference between the introgression lines with differences among the segments of QTLs (data not shown). The mean comparisons are shown in Figure 3. The JHN cultivar showed more resistance to the *M. oryzae* isolates (with an average blast

Table 1. Specific PCR primers used for the identification of four different QTLs with resistance to *Magnaporthe oryzae*

Marker	Chromosome	Sequence	Specific alleles for individual QTLs (bp)		
			P0489	JHN	RD6
RM319	1	5'ATCAAGGTACCTAGACCACCAC 3' 3'TCCTGGTGCAGCTATGTCTG 5'	–	123	120
RM212	1	5'CCACTTTCAGCTACTACCAG3' 3'CACCCATTTGTCTCTCATTATG5'	105	–	110
RM48	2	5'TGTCCCACTGCTTTCAAGC3' 3'CGAGAATGAGGGACAAATAACC5'	225	–	220
RM207	2	5'CCATTCGTGAGAAGATCTGA3' 3'CACCTCATCCTCGTAACGCC5'	170	–	180
RM224	11	5'ATCGATCGATCTTCACGAGG3' 3'TGCTATAAAAGGCATTCGGG5'	–	85	90
RM144	11	5'TGCCCTGGCGCAAATTTGATCC3' 5'GCTAGAGGAGATCAGATGGTAGTGCATG3'	–	130	125
RM313	12	5'TGCTACAAGTGTTCTTCAGGAC3' 3'GCTCACCTTTTGTGTTCCAC5'	120	–	115
RM277	12	5'CGGTCAAATCATCACCTGAC3' 3'CAAGGCTTGCAAGGGAAG5'	120	–	130

– not amplified

doi: 10.17221/51/2016-CJGPB

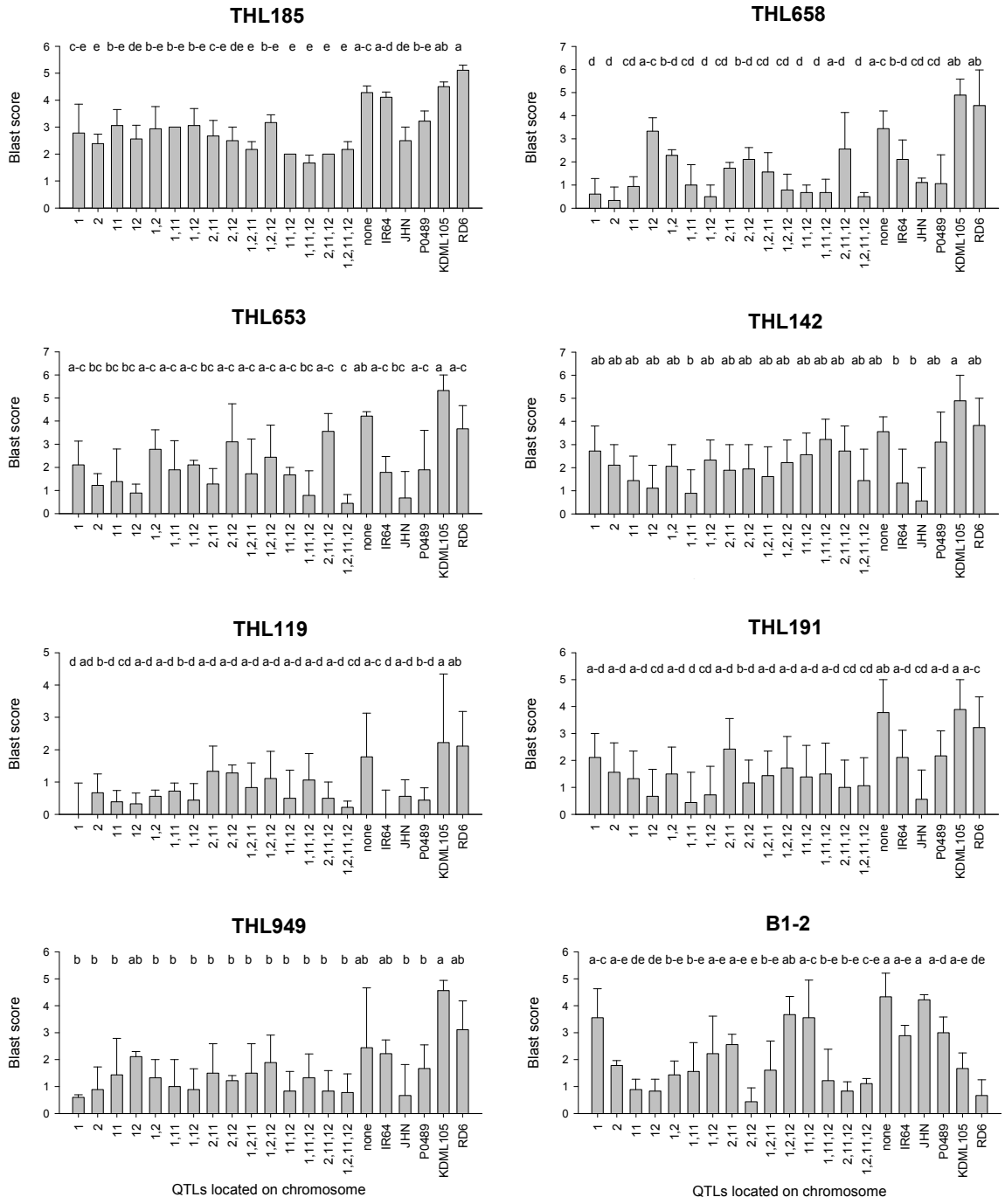

Figure 3. Rice blast disease scores of RD6 introgression NILs containing 15 combinations of rice blast resistance QTLs and their parents and control varieties; different small letters indicate that are significantly different at the 95% confidence level using Tukey's HSD

score of 1.35) than P0489 (with an average blast score of 2.07), while RD6 was very susceptible to the *M. oryzae* isolates (with an average blast score of 3.27). The RD6 introgression lines with single QTLs on chromosome 11 provided more effective resistance against the predominant *M. oryzae* isolates in Thailand, as reflected in the resistant reaction (with blast scores < 2.00) to 7 isolates, whereas lines with a single QTL on chromosomes 1, 2 and 12 showed a resistant reaction to 3, 6 and 5 isolates, respectively.

In this study, the RD6 introgression lines with both single QTL and combinations of resistance QTLs showed resistance to the *M. oryzae* isolates. However, the THL185 isolate produced the high blast

doi: 10.17221/51/2016-CJGPB

Table 2. Severity index (SI) and broad-spectrum resistance (BSR) of NILs of RD6 introgression lines containing 15 combinations of rice blast resistance QTLs, their parents and control varieties

Lines, varieties	QTLs located on chromosome	SI and reaction to rice blast disease[a]								BSR
		THL185	THL658	THL653	THL142	THL119	THL191	THL949	B1-2	
BC_2F_2 9-1/15-1-33	1	39.46 (MR)	8.03 (R)	33.74 (MR)	26.60 (MR)	0.54 (R)	29.46 (MR)	8.03 (R)	50.83 (MS)	0.38
BC_2F_2 16-1/15-38	2	46.60 (MS)	30.89 (MR)	22.32 (MR)	20.89 (MR)	9.46 (R)	32.32 (MR)	13.75 (R)	48.03 (MS)	0.25
BC_2F_2 6-1/15-1-50	11	43.73 (MS)	12.32 (R)	9.46 (R)	19.46 (R)	5.17 (R)	12.32 (R)	15.17 (R)	12.32 (R)	0.88
BC_2F_2 6-1/15-1-43	12	36.60 (MR)	46.60 (MS)	12.32 (R)	15.17 (R)	3.75 (R)	9.46 (R)	28.03 (MR)	10.89 (R)	0.63
BC_2F_2 19-1/15-1-34	1, 2	40.89 (MS)	32.32 (MR)	39.46 (MR)	30.89 (MR)	8.03 (R)	20.89 (MR)	18.03 (R)	19.46 (R)	0.38
BC_2F_2 6-1/15-1-20	1, 11	42.32 (MS)	13.75 (R)	15.17 (R)	12.32 (R)	9.46 (R)	5.17 (R)	13.75 (R)	22.32 (MR)	0.75
BC_2F_2 6-1/15-1/16	1, 12	43.74 (MS)	6.60 (R)	23.74 (MR)	18.03 (R)	5.17 (R)	9.46 (R)	12.32 (R)	30.89 (MR)	0.63
BC_2F_2 9-1/15-1-31	2, 11	38.03 (MR)	23.74 (MR)	18.03 (R)	12.32 (R)	10.89 (R)	39.46 (MR)	20.89 (MR)	36.60 (MR)	0.38
BC_2F_2 6-1/15-2-24	2, 12	35.17 (MR)	29.46 (MR)	29.46 (MR)	26.6 (MR)	18.03 (R)	23.74 (MR)	16.60 (R)	5.17 (R)	0.38
BC_2F_2 6-1/15-1-22	1, 2, 11	30.89 (MR)	22.32 (MR)	12.32 (R)	10.89 (R)	9.46 (R)	18.03 (R)	16.60 (R)	22.32 (MR)	0.63
BC_2F_22 6-1/15-1-41	1, 2, 12	45.17 (MS)	10.89 (R)	19.46 (R)	15.17 (R)	10.89 (R)	23.74 (MR)	16.60 (R)	52.31 (MS)	0.63
BC_2F_2 6-1/15-1-13	11, 12	28.03 (MR)	9.46 (R)	23.74 (MR)	36.6 (MR)	6.60 (R)	19.46 (R)	10.89 (R)	50.89 (MS)	0.50
BC_2F_2 16-1/15-1-9	1, 11, 12	23.74 (MR)	9.46 (R)	5.17 (R)	26.60 (MR)	15.17 (R)	16.60 (R)	18.03 (R)	16.60 (R)	0.75
BC_2F_2 19-1/15-2-4	2, 11, 12	28.03 (MR)	36.60 (MR)	30.89 (MR)	19.46 (R)	6.60 (R)	18.03 (R)	10.89 (R)	16.60 (R)	0.63
BC_2F_2 9-1/15-1-27	1, 2, 11, 12	30.89 (MR)	6.60 (R)	5.17 (R)	19.46 (R)	2.32 (R)	16.60 (R)	10.8 (R)	15.17 (R)	0.88
Control BC_2F_2	none	60.89 (S)	48.03 (MS)	59.46 (MS)	59.46 (MS)	25.17 (MR)	59.46 (MS)	52.31 (MS)	55.17 (MS)	0.00
IR64	R control	58.03 (MS)	19.46 (R)	20.17 (MR)	10.89 (R)	0.54 (R)	19.46 (R)	30.89 (MR)	40.89 (MS)	0.50
JHN	donor (1, 11)	35.17 (MS)	15.17 (R)	3.75 (R)	8.03 (R)	8.03 (R)	8.03 (R)	9.46 (R)	59.46 (MS)	0.75
KDML105	S control	63.74 (S)	69.46 (S)	76.60 (S)	69.46 (S)	30.89 (MR)	59.46 (MS)	65.17 (S)	28.03 (MR)	0.00
P0489	donor (2, 12)	45.17 (MS)	8.03 (R)	36.60 (MR)	32.32 (MR)	5.17 (R)	20.89 (MR)	19.74 (R)	39.46 (MR)	0.38
RD6	recurrent	72.31 (S)	73.74 (S)	56.60 (MS)	62.31 (S)	29.46 (MR)	50.89 (MS)	43.74 (MS)	13.75 (R)	0.13

[a]HR – highly resistant (SI = 0); R – resistant (0 < SI ≤ 20); MR – moderately resistant (20 < SI ≤ 40); MS – moderately susceptible (40 < SI ≤ 60); S = susceptible (60 < SI ≤ 80), S – susceptible (80 < SI ≤ 100)

doi: 10.17221/51/2016-CJGPB

score in all lines, indicating that the THL185 isolate was virulent to all four resistance QTLs (Figure 3). Surprisingly, B1-2 isolate, the *M. oryzae* isolate from Ubon Ratchathani province, produced blast in all check varieties contrary to the expectations. The resistant control varieties and donor parents had high blast scores, while the susceptible control varieties and recurrent parent had low blast scores. However, most of the backcross lines showed resistance to the B1-2 isolate. The results indicate that RD6 might have transferred the resistance genes against *M. oryzae* isolate B1-2 into the backcross lines.

Based on the severity index (SI) and BSR values, JHN and P0489, the donor parents, had a low average SI (18.39 and 25.92) but a high BSR value (0.75 and 0.38). In contrast, RD6 had a high average SI (50.35) and low BSR value (0.13) (Table 2). The RD6 introgression lines with single QTLs on chromosome 11 showed the highest resistance reaction, followed by lines with a single QTL on chromosomes 12, 1 and 2, respectively. Therefore, the RD6 introgression lines with combinations of QTLs on chromosome 11 showed higher values than lines carrying single QTLs. The results indicate that the lines with a combination of QTLs located on chromosomes 11 and 12 were more effective in providing resistance against the pathogen than single QTLs. However, the BSR of lines with combinations of 4 resistance QTLs did not have greater BSR than the line with a single QTL on chromosome 11. These results indicate that the BSR cannot be extended beyond the genetic background of the parents. The BSR can be confirmed by the orthogonal comparison between lines with different combinations of blast QTLs (Table 3). The results also support the fact that the QTL effects on chromosome 11 are greater than on the other chromosomes. However, based on blast scores and SI values, the results suggest that the lines with combination of QTLs had greater resistance against the pathogen than a single QTL (Figure 3 and Tables 2, 3 and 4).

Field evaluation of resistance to *M. oryzae*. The $BC_2F_{2:3}$ progenies were evaluated under field conditions by using the upland short row method. Introgression lines carrying single QTLs and pyramid combinations of the QTLs were grown in two rows in two locations (in Nong Khai and Ubon Ratchathani provinces) (Table 4). Based on the results, the virulence of blast disease is greater in Ubon Ratchathani province than in Nong Khai province. The QTL on chromosome 11 was the most effective single locus against the naturally prevalent pathogen in both regions. The blast score at different sites for all the tested lines showed the same response, indicating that the QTLs on chromosomes 1, 2, 11 and 12 are broadly effective against blast disease in both regions

Table 3. Orthogonal comparison of introgression lines carrying different numbers of QTLs

Class comparisons	Rice blast score	Probability
1QTL : 2QTLs	1.466 : 1.620	0.236
1QTL : 3QTLs	1.466 : 1.744	0.052
1QTL : 4QTLs	1.466 : 0.944	0.022
2QTLs : 3QTLs	1.620 : 1.744	0.334
2QTLs : 4QTLs	1.620 : 0.944	0.003
3QTLs : QTLs	1.744 : 0.944	< 0.001
JHN : 4QTLs	0.944 : 0.944	1.000
P0489 : 4QTLs	1.937 : 0.944	< 0.001
KDML105 : 4QTLs	4.325 : 0.944	< 0.001
RD6 : 4QTLs	3.643 : 0.944	< 0.001
IR64 : 4QTLs	1.918 : 0.944	0.001

Table 4. Rice blast disease scores of resistant RD6 introgression QTLs and control varieties tested under field conditions in Nong Khai and Ubon Ratchathani provinces

Lines, varieties	QTLs located on chromosome	Rice blast severity score (0–9)	
		Nong Khai	Ubon Ratchathani
BC2F2 9-1/15-1-33	1	3	5
BC2F2 16-1/15-38	2	3	4.5
BC_2F_2 6-1/15-1-50	11	2	5
BC2F2 6-1/15-1-43	12	2.5	5.5
BC_2F_2 19-1/15-1-34	1, 2	8	6
BC_2F_2 6-1/15-1-20	1, 11	5	4
BC_2F_2 9-1/15-1-31	2, 11	3	6.5
BC_2F_2 6-1/15-2-24	2, 12	8	7
BC_2F_2 6-1/15-1-22	1, 2, 11	4.5	4.5
$BC_2F_2$2 6-1/15-1-41	1, 2, 12	4	5.5
BC_2F_2 9-1/15-1-27	1, 2, 11, 12	3	5.5
Hangyi71	R control	3	3
KDML105	S control	9	9
RD23	R control	1	9
Supanburi60	R control	1	1
RD7	R control	1	9

doi: 10.17221/51/2016-CJGPB

(Table 4). Again, surprisingly, in Ubon Ratchathani province, the two resistant control varieties (RD23 and RD7) showed susceptibility to blast disease, whereas in Nong Khai province they showed resistance (Table 4).

DISCUSSION

Although, work on improving the blast resistance of rice varieties in Thailand has been undertaken for several decades, to date no commercial cultivars with high stability of resistance over years and seasons have become available. In this study, success was demonstrated in improving blast resistance through pyramiding of respective QTLs in the cultivar RD6, using marker-assisted pseudo-backcrossing. The introgression lines showed a high level of resistance when they possessed a high number of QTLs for resistance.

Historically, several major blast resistance genes *Pib*, *Pita*, *Pia*, *Pi1*, *Pikh*, *Pi2* and *Pi4* have been introduced into rice varieties for blast resistance, through conventional breeding programs (Koizumi 2007). The rice cultivar Koshihikari, which is widely cultivated in Japan, was developed for blast resistance by crossing with several resistance genes including *Pia*, *Pii*, *Pita-2*, *Piz*, *Pik*, *Pik-m*, *Piz-t* and *Pib* (Ishizaki *et al*. 2005). Various strategies in conventional breeding programs have been used in rice variety improvement, including the combining of several genes to provide durable resistance. However, a major disadvantage of the conventional breeding methods is that it is time consuming, leading to a considerable time lag between the emergence of virulent pathotypes of the causal pathogen and the development of new resistant cultivars (Miah *et al*. 2013). In addition, the pyramiding of blast resistance genes with similar reactions to more than one race or isolate, using conventional breeding methods, is difficult due to the dominance and epistasis effects of genes. Currently, molecular markers closely linked to blast resistance genes/QTLs have been widely used for MAS to improve the resistance of rice varieties (Arunakanthi *et al*. 2008).

In this study, success was achieved in the pyramiding of four blast resistance QTLs with similar reactions to more than one isolate. This is difficult to achieve, using conventional breeding methods. The reaction of the pyramided lines to almost all isolates can be explained by the additive effect of QTLs on chromosomes 1, 2, 11 and 12 (Figure 3, Tables 2 and 3). Similarly to the results reported by Koide *et al*. (2009), it was found that there was no reduction in the resistance caused by combining the resistance QTLs. This suggests that the pyramiding of QTLs is potentially useful for improving the blast resistance of RD6. Based on the disease resistance reaction, if the blast resistance genes have similar reactions to more than one race or dominant isolate, the epistatic effect of the genes could affect the disease resistance (Korinsak 2009) that is shown in Figure 3 and Tables 2, 3 and 4, in which some single QTLs are more resistant than the QTL combinations. However, the use of a single QTL as a source of resistance may be more easily overcome by the pathogen, which can be explained by the gene-for-gene theory (Flor 1971). Moreover, the high genetic variation in the blast fungus may be the main reason for numerous resistance genes having evolved and been identified in rice (Koide *et al.* 2009). In this study, there were no parents or breeding lines with resistance to the THL185 isolate. Therefore, the identification of new sources of blast resistance would be necessary for the further variety improvement against this *M. oryzae* isolate.

Interestingly, B1-2 isolate, the *M. oryzae* isolate from Ubon Ratchathani province, showed virulence to all resistant parents, while it was avirulent to varieties RD6 and KDML105. According to the pedigree of RD6, this variety was derived from KDML105 by gamma radiation, with selection in the M_2 population for glutinous and blast-resistant mutants (Khambanonda 1978). The gene with resistance to the *M. oryzae* isolate B1-2 of RD6 and KDML105 is governed by an isolate specific QTL on chromosome 8 (Korinsak 2009).

The evaluation of the RD6 introgression lines with pyramided genes for resistance to the blast pathogen under field conditions was accomplished by using the upland short row method. Natural infection occurred in both locations. However, the pathogens in Ubon Ratchathani province are more virulent than in Nong Khai province, which indicates the prevalence of a highly virulent isolate in the former province (Table 4). Unfortunately, the parental lines P0489, RD6 and JHN were not included in this evaluation. However, the KDML105 variety, which has a very close genetic background to the RD6 recurrent parent, was used as the susceptible standard control. Broad-spectrum and durable resistance suggested in this case that most of the RD6 introgression lines are resistant to blast disease, especially the lines containing the QTLs on chromosome 11 which showed stable resistance in both locations (Table 4), confirming that the QTL on chromosome 11 has broad-spectrum resistance to the blast pathogen in Thailand. In addition, only one of the *M. oryzae* isolates, THL 185, was virulent to all of

doi: 10.17221/51/2016-CJGPB

the breeding lines, suggesting that the identification of a new blast resistance gene or QTLs, and pyramiding them into RD6 for durable blast resistance and no yield penalty should be the focus of further research.

Acknowledgements. This research was supported by the Plant Breeding Research Centre for Sustainable Agriculture, and the Research Centre of Agricultural Biotechnology for Sustainable Economy, Khon Kaen University, Khon Kaen, Thailand. The authors thank Dr. J. Schiller of the University of Queensland, Australia, for proofreading the manuscript. Thanks are also extended to the Thailand Research Fund (TRF) (Project code: IRG5780003) and the Faculty of Agriculture, Khon Kaen University, for providing financial support for the manuscript preparation.

References

Ahn S.W. (1994): International collaboration on breeding for resistance to rice blast. In: Zeigler R.S., Leong S.A., Teng P.S. (eds): Rice Blast Disease. Wallingford, Madison, CABI, CABI UK: 137–153.

Arunakanthi B., Srinivasprasad M., Madhanmohan K., Balachandran S.M., Madhav M.S., Reddy C.S., Viraktamath B.C. (2008): Introgression of major blast resistance genes *Pi-1*, *Pi-2* and *Pi-kh* in *Indica* rice cultivars Samba Mahsuri and Swarna. The Journal of Mycology and Plant Pathology, 38: 625–630.

Ashkani S., Rafii M.Y., Rusli I., Sariah M., Abdullah S.N.A., Harun A.R., Latif M.A. (2012): SSRs for marker-assisted selection for blast resistance in rice (*Oryza sativa* L.). Plant Molecular Biology Reporter, 30: 79–86.

Flor H.H. (1971): Current status of the gene-for-gene concept. Annual Review of Phytopathology, 9: 275–296.

Hittalmani S., Parco A., Mew T.V., Zeigler R.S., Huang N. (2000): Fine mapping and DNA marker-assisted pyramiding of the three major genes for blast resistance in rice. Theoretical and Applied Genetics, 100: 1121–1128.

IRRI (1996): Standard Evaluation System for Rice. 4th Ed. Manila, IRRI.

Ishizaki K., Hoshi T., Abe S., Sasaki Y., Kobayashi K., Kasaneyama H., Matsui T., Azuma S. (2005): Breeding of blast resistant isogenic lines in rice variety "Koshihikara" and evaluation of their characters. Breeding Science, 55: 371–377.

Khambanonda P. (1978): Mutation breeding in rice for high yield and better blast resistance. Thai Journal of Agricultural Science, 11: 263–271.

Khush G.S., Jena K.K. (2009): Current status and future prospects for research on blast resistance in rice (*Oryza sativa* L.). In: Wang G.L., Valent B. (eds): Advances in Genetics. Genomics and Control of Rice Blast Disease. New York, Springer: 1–10.

Koide Y., Kobayashi N., Xu D., Fukuta Y. (2009): Resistance genes and DNA selection markers for blast disease in rice *Oryza sativa* L. Japan Agricultural Research Quarterly, 43: 255–280.

Koizumi S. (2007): Durability of resistance to rice blast disease. Japan International Research Center for Agricultural Sciences Working Report, 53: 1–10.

Korinsak S.(2009): Identification of blast resistance QTLs in two rice RIL populations and marker-assisted selection for pyramiding of four QTLs in RD6 rice variety. [M.S. Thesis.] Bangkok, Kasetsart University.

Liu J., Wang X., Mitchell T., Hu Y., Liu X., Dai L., Wang G.L. (2010): Recent progress and understanding of the molecular mechanisms of the rice-*Magnaporthe oryzae* interaction. Molecular Plant Pathology, 11: 419–427.

Miah G., Rafii M.Y., Ismail M.R., Puteh A.B., Rahim H.A., Asfaliza R., Latif M.A. (2013): Blast resistance in rice: a review of conventional breeding to molecular approaches. Molecular Biology Reports, 40: 2369–2388.

Noenplab A., Vanavichit A., Toojinda T., Sirithunya P., Tragoonrung S., Sriprakhon S., Vongsaprom C. (2006): QTL mapping for leaf and neck blast resistance in Khao Dawk Mali105 and Jao Hom Nin recombinant inbred lines. Science Asia, 32: 133–142.

Ou S.H. (1985): Blast. In: Rice Disease. 2nd Ed., Kew, Commonwealth Mycological Institute: 109–201.

Roumen E., Levy M., Nottegham J.L. (1997): Characterization of the European pathogen population of *Magnaporthe grisea* by DNA fingerprinting and pathotype analysis. European Journal of Plant Pathology, 103: 363–371.

Ruengphayak S., Chaichumpoo E., Phromphan S., Kamolsukyunyong W., Sukhaket W., Phuvanartnarubal E., Korinsak S., Korinsak S., Vanavichit A. (2015): Pseudo-backcrossing design for rapidly pyramiding multiple traits into a preferential rice variety. Rice, 8: 7.

Saka N. (2006): A rice (*Oryza sativa* L.) breeding for field resistance to blast disease (*Pyricularia oryzae*) in mountainous region agricultural research institute, Aichi agricultural research center of Japan. Plant Production Science, 9: 3–9.

Servin B., Martin O.C., Mézard M., Hospital F. (2004): Toward a theory of marker-assisted gene pyramiding. Genetics, 168: 523–523.

Silprakhon S. (2004): Identification and mapping genes controlling leaf blast resistance in double haploid lines IR64 × Azucena population. In: Vanavichit A. (ed.): Proc.1st Conf. Rice for the Future, Bangkok.

Sirithanya P. (1998): Mapping gene controlling blast resistance in rice (*Oryza sativa* L.). [Ph.D. Thesis.] Bangkok, Kasetsart University.

Sirithanya P., Sreewongchai T., Sriprakorn S., Toojinda T., Pimpisithavorn S., Kosawang C., Smitamana P. (2008): Assessment of genetic diversity in Thai isolates of *Pyricularia grisea* by random amplification of polymorphic DNA. Journal of Phytopathology, 156: 196–204.

Received for publication April 20, 2016
Accepted after corrections December 21, 2016

Agricultural Water Management 188 (2017) 29–35

Contents lists available at ScienceDirect

Agricultural Water Management

journal homepage: www.elsevier.com/locate/agwat

Association of photosynthetic traits with water use efficiency and SPAD chlorophyll meter reading of Jerusalem artichoke under drought conditions

Darunee Puangbut[a,b], Sanun Jogloy[a,b,*], Nimitr Vorasoot[a]

[a] Department of Plant Science and Agricultural Resources, Faculty of Agriculture, Khon Kaen University, Khon Kaen, 40002, Thailand
[b] Peanut and Jerusalem Artichoke Improvement for Functional Food Research Group, Khon Kaen University, Khon Kaen, Thailand

ARTICLE INFO

Article history:
Received 27 November 2016
Received in revised form 19 March 2017
Accepted 1 April 2017
Available online 11 April 2017

Keywords:
Gas exchange
SCMR
Water stress
Helianthus tuberosus L.

ABSTRACT

The impact of water stress on plant growth, tuber yield and inulin content has been widely studied but there is limited information on the effect of drought on photosynthetic characteristics. Therefore, this study was to investigate the effect of water stress on photosynthetic characteristics in Jerusalem artichoke genotypes with different levels of drought tolerance. Two experiments were conducted in rhizobox under greenhouse conditions during August to October in 2015 and 2016. A factorial experiment in randomized complete block design with three replications was used. Factor A were two water regimes (irrigated = field capacity; (FC) and water stress) and factor B were three Jerusalem artichoke genotypes. Data were recorded for relative water content, SPAD chlorophyll meter reading (SCMR), photosynthetic characteristics and water use efficiency (WUE) at 7 and 30 days after imposing drought. Leaf area and dry matter was recorded at 30 days after imposing drought. Our results revealed that drought caused a greater reduction in stomatal conductance (g_s), net photosynthetic rate (P_n), leaf area and biomass production than in other traits measured. In contrast, WUE and SCMR were increased under drought conditions. However, g_s and P_n decreases were less in resistant Jerusalem artichoke genotypes than in susceptible genotypes. Also, resistant genotypes had higher WUE increases than susceptible genotypes. Improved P_n combined with high WUE could contribute to higher biomass production. Interestingly, SCMR was associated with P_n and this trait could be used as surrogate trait for improved P_n under drought conditions.

1. Introduction

Jerusalem artichoke is used for many purposes such as human food, animal feedstock, and ethanol production (Yang et al., 2015). Recently Jerusalem artichoke tuber has also been reported as functional food high in inulin (Radovanovic et al., 2015) and other traits thought to reduce the risk of diabetes, cardiovascular diseases, obesity, stroke and cancer (Watzl et al., 2005; Roberfroid, 2007).

Large areas of Jerusalem artichoke are grown under rain-fed conditions. The crop is grown successfully under rain-fed conditions in the semi-arid tropics in Thailand, where drought is a major contributor to production losses. Although Jerusalem artichoke has been reported as hardy plant, drought causes severe yield loss. Irrigation is still necessary for commercial production (Pimsaen et al., 2010; Ruttanaprasert et al., 2016a).

Drought is expected to increase in frequency and severity in the future as a result of climate change, mainly as a consequence of decreases in regional precipitation but also because of increasing evaporation driven by global warming. Drought stress not only reduces yield and quality, it also may reduce inulin accumulation in tubers (Monti et al., 2005a; Gao et al., 2011; Ruttanaprasert et al., 2014; Puangbut et al., 2015). While drought induced yield reductions of 20–98% had been reported (Conde et al., 1991; Ruttanaprasert et al., 2014, 2016a), drought's effect on inulin content varies dependent on severity and length of the drought, with some studies showing increased inulin content when grown under mild water stress (Monti et al., 2005b; Vandoorne et al., 2012; Puangbut et al., 2015).

Most previous research on effects of drought has been focused on growth, yield and inulin content, with few studies of drought effects on photosynthetic characteristics. Monti et al. (2005a)

* Corresponding author at: Department of Plant Science and Agricultural Resources, Faculty of Agriculture, Khon Kaen University, Khon Kaen, 40002, Thailand.
E-mail address: sjogloy@gmail.com (S. Jogloy).

http://dx.doi.org/10.1016/j.agwat.2017.04.001
0378-3774/

reported that leaf net photosynthesis was slightly reduced by moderate water stress under rain-fed conditions. Studies on the effect of severe water stress on photosynthesis and on genotypic variation under water-limited control environments are lacking.

Water use efficiency (WUE) and chlorophyll density have been identified as drought resistant traits and could be used as selection criteria for drought resistance trait in peanut (Arunyanark et al., 2008; Songsri et al., 2009; Puangbut et al., 2009). SPAD chlorophyll meter reading (SCMR) is a tool for rapid assessment of chlorophyll density in several crops (Songsri et al., 2009; Jangpromma et al., 2010; Darkwa et al., 2015). Therefore, SCMR can be used as a screening tool for drought resistant traits in many plant species. However, there were a few studies in Jerusalem artichoke. Recent report has demonstrated that SCMR could be used as a selection tool for harvest index and tuber yield in Jerusalem artichoke (Ruttanaprasert et al., 2016b). Very limited information has been available for the relationships between drought resistant traits and photosynthetic rate under drought conditions.

A better understanding of drought resistant traits associated with photosynthesis should be useful in improving yield under drought conditions. Selection of superior Jerusalem artichoke genotypes for their ability to maintain high photosynthesis under water stress may help breeders to identify Jerusalem artichoke genotypes with drought tolerance. The objective of this study was to investigate the effect of water stress on photosynthetic characteristics in three Jerusalem artichoke genotypes.

2. Materials and methods

2.1. Experiment conditions and plant materials

Two experiments were conducted in rhizobox under greenhouse conditions during August to October 2015 and August to October 2016 at the Field Crop Research Station of Khon Kaen University located in Khon Kaen province, Thailand.

The experimental treatments were arranged in a 2×3 factorial experiment in randomized complete block design with three replications. Factor A consisted of two water regimes including irrigated (field capacity; FC) and water stressed, and factor B included three Jerusalem artichoke genotypes (JA 5, JA 60 and HEL 65) with differences in their drought tolerant index (DTI) and tuber yield reduction (Ruttanaprasert et al., 2014, 2015). JA 5 is drought resistant genotype with high DTI for root traits and high reduction in tuber yield under drought conditions. JA 60 was identified as a drought resistant genotype with high DTI for root traits coupled with low reduction in tuber yield under drought conditions. HEL 65 is susceptible genotype with low DTI for root traits combined with high reduction in tuber yield under drought conditions.

2.2. Rhizobox preparation and crop management

Rhizobox with the dimension of 10 cm in thickness, 50 cm in width and 120 cm in height was used. Rhizoboxs were filled with 92 kg of dry soil up to a height of 115 cm. The soil was uniformly packed from the top to the bottom of the box. Seedlings were transplanted into a rhizobox at the V4 stage (4th leaf sprouted, Paungbut et al., 2015). Seedlings were grown at the center of rhizobox. Fertilizer (15-15-15) was applied at 15 days after transplanting (DAT) at a rate of 1.56 g per rhizobox.

Before planting, each rhizobox was watered to FC to a depth of 35 cm for crop establishment and continued until 15 DAT. At 16 DAT, the water stress treatment was imposed by withholding water for 30 days. The irrigated treatment was maintained at FC throughout the crop growth cycle at 1-day intervals. Soil moisture contents at FC and permanent wilting point (PWP) were determined to be 14.08% and 4.66%, respectively, using the pressure plate method. The amount of water applied was based on crop water requirements using the Doorenbos and Pruitt (1992) methodology along with water loss from surface evaporation as described by Singh and Russell (1981).

Crop water requirement was calculated using the methods described by Doorenbos and Pruitt (1992):

$$\text{ET crop} = \text{ETo} \times \text{Kc}$$

where ET crop = crop water requirement (mm/day), ETo = evapotranspiration of a reference plant under specified conditions calculated by pan evaporation method, Kc = the crop water requirement coefficient for sunflower, which varies with genotype and growth stage. As crop coefficient for Jerusalem artichoke is not available in the literature, the crop coefficient for sunflower (Monti et al., 2005a) was used because sunflower and Jerusalem artichoke are closely related species and their morphological characters are similar.

Soil evaporation (Es) was calculated as (Singh and Russell, 1981):

$$Es = \beta \times \left(\text{Eo}/\text{t}\right)$$

where Es = soil evaporation (mm), β = light transmission coefficient measured depending on crop cover, Eo = evaporation from class A pan (mm/day), t = days from the last irrigation

2.3. Soil moisture content

Soil moisture content was measured by gravimetric method using micro auger at 30 days after imposing drought at 10, 25, 45, 65, and 85 cm of soil depths as 10 cm in thick-ness of rhizobox. The soil samples were collected and soil fresh weights were taken immediately. The soil samples were oven dried at 105 °C until for 72 h or until weights were constant and soil dry weight was determined. Soil moisture content for each rhizobox was calculated as:

$$\text{Soil moisture content} = \left[\frac{\text{wet weight} - \text{dry weight}}{\text{dry weight}}\right] \times 100$$

2.4. Relative water content (RWC)

Relative water content (RWC) was measured at was measured at 7 and 30 days after imposing drought. The third fully-expanded leaf from the top of the main stem was sampled between 10:00 h to 12:00 h. After recording the fresh weight, turgid weight was measured by placing the leaf sample in water for 8 h, blotting dry and weighing. Leaf dry weight was measured after oven-drying at 80 °C for 48 h. RWC was computed by the following formula:

$$\text{RWC} = \left[\frac{\text{fresh weight} - \text{dry weight}}{\text{turgid weight} - \text{dry weight}}\right] \times 100$$

2.5. Leaf gas exchange

Leaf gas exchange was measured at 7 and 30 days after imposing drought by using a LI-6400XT portable measuring system (LiCor, Inc., Lincoln, NE, USA) with a 6400-02B LED source providing a PPFD of 1500 μmol m^{-2} s^{-1} and temperature was set at 25 °C. CO_2 concentration was set at 400 μmol m^{-2} s^{-1} and relative humidity at 70%. Net photosynthetic rate (P_n), transpiration rate (E), and stomatal conductance (g_s) were collected from six plants per treatment. Water use efficiency (WUE) was computed as net photosynthetic rate divided by transpiration rate.

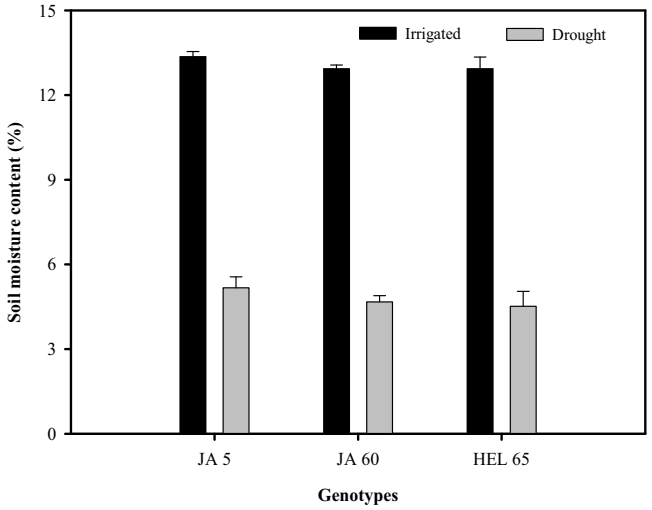

Fig. 1. Soil moisture content under irrigated and drought conditions at 30 days after imposing drought. Means of three replications ± SD.

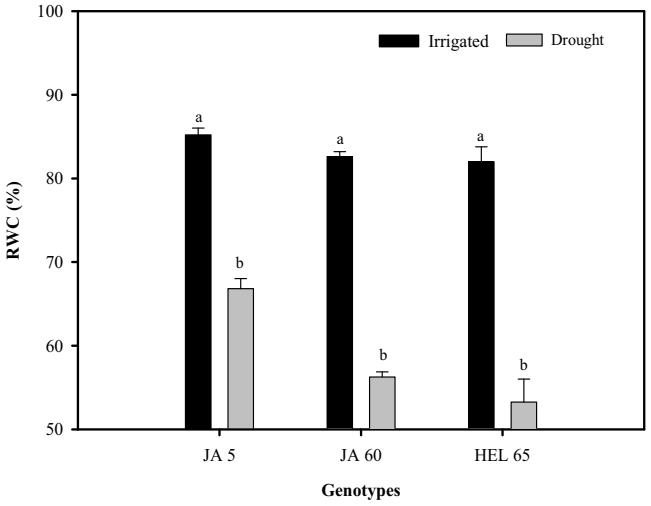

Fig. 2. Relative water content (RWC) of three Jerusalem artichoke under irrigated and drought conditions at 30 days after imposing drought. Means of three replications ± SD.

2.6. SPAD chlorophyll meter reading (SCMR)

SPAD chlorophyll meter reading (SCMR) was measured at 7 and 30 days after imposing drought. The third fully-expanded and intact leaf from the top of the main stem was sampled for each plant between 09:00–11:00 h. A Minolta SPAD-502 m was used in recording SCMR on either side of the midrib and the data were averaged as a single value for each leaf.

2.7. Leaf area and dry matter accumulation

Leaf area (LA) and dry matter were measured at 30 days after imposing drought. Plants were cut at the soil surface and separated into leaf and stem. LA was determined using a leaf area meter (LI-3100 area meter, LI-COR, Inc., USA), and then leaf and stems were oven-dried at 80 °C for 48 h, or until the weight was constant, and weighed.

2.8. Statistical analysis

Individual analysis of variance was performed for each character for each year followed a factorial in randomized complete block design (RCBD) design. Error variances for the two years were tested for homogeneity by Bartlett's test (Hoshmand, 2006). Combined analyses of variance were done for those characters whose error variances for the two years were homogeneous. Due to significance of water regime × genotype interaction (data not shown), data for each water regime were analyzed separately and a Least Significant Difference (LSD) test was used to compare means using a STATISTIX 8 software program.

3. Results and discussion

3.1. Soil moisture and plant water status

Soil moisture at FC was 12.7% and permanent wilting point was 3.6% as measured by pressure plate method. The soil moisture levels were clear distinction between irrigated and drought conditions, which averaged 4.8% (Fig. 1). The results revealed that the levels of drought stress were reasonably well managed. Relative water content (RWC) at 7 days after imposing drought (DAD) was similar between irrigated and drought conditions (data not presented) and this could be due to short time duration of stress. However, RWC differed significantly between irrigated and drought treatments at 30 DAD (Fig. 2). It is clear that RWC in stressed plants were lower than in non-stressed plants. Drought reduced RWC to 42% of irrigated treatment. There were significant differences among genotypes under drought conditions with JA5 having the highest RWC, while the reported susceptible HEL 65 the lowest (Fig. 2). HEL 65 also had a high reduction in transpiration rate or high water loss (64%) under drought conditions. HEL 65 has also been reported to have a high reduction in root growth under drought conditions (Ruttanaprasert et al., 2015), which may have reduced water uptake and thus lower leaf relative water content.

3.2. Genotypic variation and genotype × environment interactions

Difference in years (Y) was significant for relative water content (RWC), SPAD chlorophyll meter reading (SCMR), net photosynthetic rate (P_n), stomatal conductance (gs), and biomass but not for leaf area (LA), transpiration rate (E) and water use efficiency (WUE) (Table 1). Significant differences between water regimes (W) were observed for all traits and significant differences among Jerusalem artichoke genotypes (G) were observed for all traits except biomass. The interactions between water regime and Jerusalem artichoke genotype (W × G) were significant for LA, Pn and gs. Genotypes × year (G × Y) interactions were not significant for all traits, demonstrating that the genotypic ranking for these traits was more stable across environment. Genotype × year × water interactions (G × Y × W) interactions were also not significant for all traits, indicating that the genotypic rankings for photosynthetic traits were stable across years and water regimes.

3.3. SPAD chlorophyll meter reading (SCMR)

SPAD Chlorophyll meter reading (SCMR) was similar between irrigated and drought conditions at 7 DAD (Table 2). However, drought increased SCMR by an average 6% compared with irrigated treatment at 30 DAD. There were significant differences among Jerusalem artichoke genotypes under drought conditions with JA 60 and JA 5 having the highest SCMR, indicating that drought resistant genotypes maintained SCMR higher than those in susceptible genotype under drought conditions.

The result indicated that Jerusalem artichoke genotypes subjected to drought had dark leaf color than did Jerusalem genotypes grown under irrigated conditions. Several researches indicated

Table 1
Mean squares from the combine analysis of variance for relative water content (RWC), SPAD chlorophyll meter reading (SCMR), leaf area (LA) and net photosynthetic rate (Pn), Stomatal conductance (gs), Transpiration rate (E), Water use efficiency (WUE) and biomass (BIO) at 30 days after imposing drought observed in year1 and year 2.

Source of variation	DF	RWC	SCMR	LA	Pn	gs	E	WUE	BIO
Year (Y)	1	829.4**	138.8**	29469.4 ns	109.2**	0.29**	41.7 ns	10.8 ns	19.0*
Reps. within Y	4	2.5	1.24	162975	4.51	0.01	12.1*	4.4	0.64
Water regimes (W)	1	2714.4**	14.8*	2.887E+07**	3964.1**	9.92	616.2**	9.1**	1135.7**
Genotype (G)	2	133.9**	425.9 **	1225449*	97.1**	0.60**	3.69*	0.74*	9.45 ns
W × G	2	84.2 ns	0.48 ns	789454**	48.8**	0.35**	5.01 ns	0.09 ns	0.39
G × Y	1	100.0 ns	14.3 ns	75796.4 ns	16.5 ns	0.08 ns	0.93 ns	0.56 ns	0.83 ns
G × Y × W	2	23.2 ns	2.24 ns	7921.75 ns	15.84 ns	0.04 ns	1.85 ns	0.72 ns	0.13 ns
Pooled Error	20	17.6	3.34	84169.0	4.37	0.02	1.31	0.21	1.91

ns, *,** Non significant and significant at P < 0.05 and P < 0.01, respectively.

Table 2
SPAD chlorophyll meter reading (SCMR) of three Jerusalem artichoke under irrigated and drought conditions at 7 and 30 days after imposing drought (DAD).

Genotypes	SPAD chlorophyll meter reading					
	7 DAD			30 DAD		
	Irrigated	Drought	LSD	Irrigated	Drought	LSD
JA 5	33.9 b	32.4 b	ns	43.2 a	46.1 a	*
JA 60	35.6 a	36.8 a	ns	44.4 a	46.8 a	*
HEL 65	30.1 c	30.5 b	ns	35.3 b	38.0 b	*
Mean	33.2	33.2		40.9	43.6	

Means in the same column with the same letters are not significantly different by LSD ($p \leq 0.05$).
ns and * non- significant and significant at $p \leq 0.05$, respectively by LSD for testing the effect of water.

SCMR was associated with chlorophyll density in Jerusalem artichoke and other plants (Arunyanark et al., 2008; Papasavvas et al., 2008; Jangpromma et al., 2010; Ruttanaprasert et al., 2012). SCMR increased with drought because chlorophyll density was increased under drought conditions. The increase in chlorophyll density due to the thicker leaves of plants exposed to drought stress (Arunyanark et al., 2008; Nageswara Rao and Wright, 1994), causing higher chlorophyll per unit area. Previous studies indicated that chlorophyll density was associated with photosynthetic capacity in many crop such as coffee (Netto et al., 2005), Arabidopsis (Ling et al., 2011) and sugarcane (Silva et al., 2013). Therefore, selection of Jerusalem artichoke genotype with high SCMR may relate to increased chlorophyll density and could maintain high photosynthetic capacity under drought conditions.

3.4. Leaf area (LA) and net photosynthetic rate (P_n)

Imposition of drought reduced leaf area (LA) to 57% of the irrigated treatment at 30 DAD (Table 3). There were significant differences among genotypes for LA under drought conditions with JA 5 and JA 60 having the highest LA and HEL 65 the lowest. Net photosynthetic rate (P_n) of irrigated and drought treatments was not significant at 7 DAD (Table 3). However, drought reduced P_n an average of 62% over the irrigated treatment at 30 DAD. There were significant P_n differences among genotypes under drought conditions with JA 60 having the highest, and HEL 65 the lowest. The reduction in P_n was lower in tolerant genotype JA 60 (52%), with JA 5 and HEL 65 at 60% and 78% respectively. As a result, LA and photosynthetic capacity was reduced, resulting in decreased biomass production. Lu et al. (2015) reported that decreased photosynthetic rate is an important factor affecting growth and biomass production.

Our results revealed that drought reduced LA and P_n in both tolerant and susceptible genotypes, similar to the findings of Subrahmanyam et al. (2006) in wheat. In contrast, Monti et al. (2005a) reported a lesser effect of drought on P_n in Jerusalem artichoke under rain-fed conditions. The differences in the observations could be due to difference in severity of drought. Generally, LA is associated with photosynthetic capacity. It could be hypothesized that Jerusalem artichoke genotypes with high LA have more photosynthetic efficiency under drought conditions. Increased LA also enhances photosynthesis which in turn contributes to yield according to Richards (2000). Therefore, it could be hypothesized that Jerusalem artichoke genotypes which maintain high photosynthetic rate might exhibit improved resistance to water deficit. JA 60 could be identified as a drought resistant genotype because it had high photosynthetic potential and low reduction in photosynthetic rate under drought conditions.

3.5. Stomatal conductance (g_s) and transpiration rate (E)

Stomatal conductance (g_s) and transpiration rate (E) of irrigated and drought treatments were not significant at 7 DAD (Tables 4 and 5). However, drought resulted in an average reduced g_s and E by 64% and 62%, respectively at 30 DAD. Stomatal conductance and transpiration rate differed significantly among genotypes under both irrigated and drought conditions. The reduction in g_s and E was more pronounced in HEL 65, the genotype thought more sensitive to drought. JA 60 was more tolerant to drought, its g_s and E declined less.

Stomatal closure is among the earliest responses to drought and will result in a decrease in photosynthesis (Galmés et al., 2007; Ashraf and Harris, 2013). Therefore, genotypes having relatively

Table 3
Leaf area and net photosynthetic rate (P_n) of three Jerusalem artichoke under irrigated and drought conditions at 7 and 30 days after imposing drought (DAD).

Genotypes	Leaf area (cm^2 $plant^{-1}$)			P_n ($\mu mol\ m^{-2}\ s^{-1}$)					
	30 DAD			7 DAD			30 DAD		
	Irrigated	Drought	LSD	Irrigated	Drought	LSD	Irrigated	Drought	LSD
JA 5	2710b	1348a	**	28.7 a	28.4 ab	ns	32.7a	13.1b	**
JA 60	2439b	1203a	**	30.6 a	30.5 a	ns	34.7a	16.5a	**
HEL 65	3195a	1059b	**	25.9 b	25.2 b	ns	24.6b	5.3c	**
Mean	2782	1204		28.3	28.3		30.7	11.6	

Means in the same column with the same letters are not significantly different by LSD ($p \leq 0.05$).
ns and ** non-significant and significant at $p \leq 0.01$, respectively by LSD for testing the effect of water.

Table 4
Stomatal conductance (g_s) of three Jerusalem artichoke under irrigated and drought conditions at 7 and 30 days after imposing drought (DAD).

Genotypes	Stomatal conductance [mol (H_2O) m^{-2} s^{-1}]					
	7 DAD			30 DAD		
	Irrigated	Drought	LSD	Irrigated	Drought	LSD
JA 5	1.03 b	1.02 a	ns	1.45b	0.53b	**
JA 60	1.16 a	1.11a	ns	1.63a	0.70a	**
HEL 65	1.01 b	0.98 a	ns	0.46c	0.12c	**
Mean	1.06	1.03		1.18	0.45	

Means in the same column with the same letters are not significantly different by LSD ($p \leq 0.05$).
ns and ** non-significant and significant at $p \leq 0.01$, respectively by LSD for testing the effect of water.

Table 5
Transpiration rate (E) of three Jerusalem artichoke under irrigated and drought conditions at 7 and 30 days after imposing drought (DAD).

Genotypes	Transpiration rate [mmol(H_2O) m^{-2} s^{-1}]					
	7 DAD			30 DAD		
	Irrigated	Drought	LSD	Irrigated	Drought	LSD
JA 5	12.26 a	11.20 a	ns	8.74a	3.21a	**
JA 60	13.13 a	12.73 a	ns	8.98a	3.68a	**
HEL 65	12.10 a	11.80 a	ns	5.85b	1.53b	**
Mean	12.39	12.01		7.85	2.81	

Means in the same column with the same letters are not significantly different by LSD ($p \leq 0.05$).
ns and ** non-significant and significant at $p \leq 0.01$, respectively by LSD for testing the effect of water.

high stomatal conductance under water deficit could indicate a potential drought resistant genotype with a relatively high photosynthetic rate under drought conditions.

3.6. Water use efficiency (WUE)

Drought increased water use efficiency (WUE) by an average of 21% when compared with irrigated treatment (Table 6). JA 60 was highest WUE under both irrigated and drought conditions, and drought increased WUE by 31%, significantly more than the susceptible genotype (10%).

Drought increased WUE in all genotypes, which is similar to a previous study that found WUE increased under drought treatment (Conde et al., 1991). These findings are in contrast to those of Janket et al. (2013) who noted that WUE was reduced under both mild and severe drought. This contrast in differences may be due to differences in the severity and duration of drought.

WUE has been identified as drought resistant trait in several crop such as peanut (Songsri et al., 2009), wheat (Condon et al., 2004; Blum, 2005), rice (Luo, 2010), maize (Hund et al., 2009), cassava (Olanrewaju et al., 2009) and bean (Mathobo et al., 2017). There are a few published reports suggesting the WUE as a drought resistant trait in Jerusalem artichoke (Puangbut et al., 2015; Ruttanaprasert et al., 2016a). Plants can decrease water use or transpiration by reducing stomatal conductance, which, when combined with large root systems, would enhance the plant's ability to withstand a drought. Therefore, improvement of WUE may have helped maintain higher photosynthetic rates which contributed to higher yields. This finding is similar to others that suggested that improved WUE, combined with large root systems, contributed to higher yield under drought conditions (Songsri et al., 2009; Puangbut et al., 2009; Janket et al., 2013; Ruttanaprasert et al., 2015, 2016a,b).

3.7. Biomass production

Significant differences among Jerusalem artichoke genotypes were found for biomass production under well-watered and drought conditions (Table 6). Drought significantly decreased biomass production an average of 46% over the irrigated control, yet the reduction was less in the drought resistant genotype JA 60 – a potential parent for high yielding varieties with improved drought resistance. These genotypic differences in response to drought could be associated with several physiological traits that influence biomass production and yield performance (Zhang et al., 2010).

Recent reports have demonstrated that root dry weight and WUE are important traits related to tuber yield under drought conditions (Ruttanaprasert et al., 2015, 2016a). The current study supports earlier findings that JA 60 was drought resistant, in part due to high g_s, high P_n and high WUE under drought conditions. Both our results and previous researches suggested that selection Jerusalem artichoke genotypes with maintain high g_s, P_n, a good root system and high WUE under drought are good selection criteria for drought resistance breeding programs. It is evident that improving Jerusalem artichoke under drought conditions requires a whole plant growth and function approach.

3.8. Relationship between P_n with SCMR and WUE

There was a consistent strong and positive correlation between P_n and SCMR under irrigated and drought conditions (Fig. 3). Under drought conditions, the highest positive correlation was found between P_n and SCMR ($r = 0.80$; $p \leq 0.01$). It was a new finding in Jerusalem artichoke. The correlation coefficient between WUE and P_n was significant under drought conditions but not in the irrigated treatment (Fig. 4). Under drought conditions, the highest positive correlation was found between P_n and WUE ($r = 0.70$; $p \leq 0.05$).

In addition, highest positive correlation was found between SCMR and biomass ($r = 0.98$, $p \leq 0.01$) and P_n and biomass ($r = 0.99$; $p \leq 0.01$) under drought conditions (data not presented), indicating the contribution of P_n to biomass was most important under drought conditions. It was apparent that selection of genotypes for high SCMR coupled with maintains high P_n might help to improve biomass under drought conditions. It was apparent that selection

Table 6
Water use efficiency (WUE) and biomass of three Jerusalem artichoke under irrigated and drought conditions at 7 and 30 days after imposing drought (DAD).

Genotypes	WUE [mol (CO_2) mol (H_2O)$^{-1}$]						Biomass (g plant^{-1})		
	7 DAD			30 DAD			30 DAD		
	Irrigated	Drought	LSD	Irrigated	Drought	LSD	Irrigated	Drought	LSD
JA 5	2.45a	2.61a	ns	3.74b	4.08a	*	23.73a	13.14a	**
JA 60	2.36a	2.44b	ns	3.86b	4.48a	*	24.76a	13.89a	**
HEL 65	2.20a	2.20c	ns	4.21a	3.46b	*	23.37a	11.80a	**
Mean	2.33	2.42		3.93	4.00		23.93	12.95	

Means in the same column with the same letters are not significantly different by LSD ($p \leq 0.05$).
ns, * and ** non-significant, significant at $p \leq 0.05$ and significant at $p \leq 0.01$, respectively by LSD for testing the effect of water.

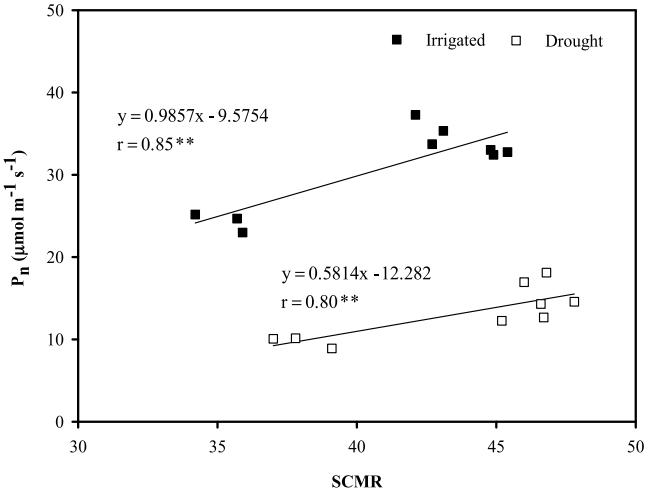

Fig. 3. Relationship between SPAD chlorophyll meter reading (SCMR) and net photosynthetic rate (P_n) under irrigated and drought conditions.

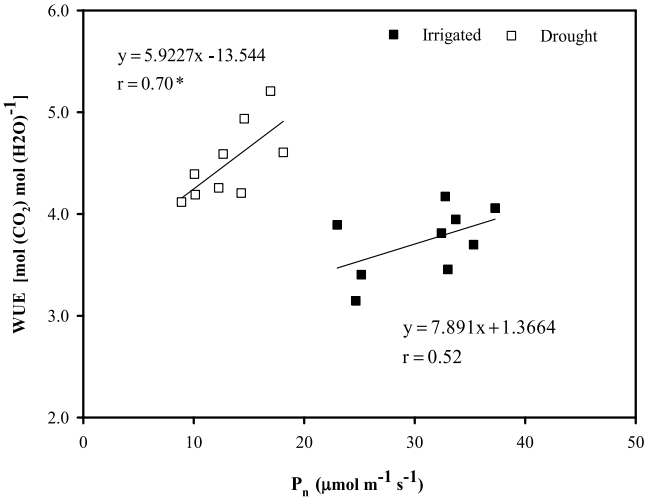

Fig. 4. Relationship between net photosynthetic rate (P_n) and water use efficiency (WUE) under irrigated and drought conditions.

of genotypes for high SCMR coupled with maintains high P_n might help to improve biomass under drought conditions.

Previous studies indicated that SCMR was correlated with chlorophyll density under well-watered conditions (Ruttanaprasert et al., 2012). They also suggested that SCMR can be used as a surrogate trait for chlorophyll density to screen a large number of accessions in Jerusalem artichoke breeding programs. An understanding of the traits associated with P_n such as SCMR to increase leaf chlorophyll content should be useful in improving photosynthetic capacity under drought conditions. However, very limited information has been available for the relationships between SCMR and P_n in Jerusalem artichoke under drought.

Although, P_n can be directly measured by LI-6400XT portable measuring system, in a large-scale breeding program, it is difficult to complete P_n observations within a specified time, especially under drought conditions. Interaction between Pn and time of observation was significant (data not presented). SCMR is easy measure, reliable and fairly stable across different time under drought conditions (Nigam and Aruna, 2008). The present study revealed that an increased SCMR under drought conditions was associated with higher P_n. Thus, SCMR could be used as a tool for rapid assessment of relative for P_n and as well as for the indirect selection of drought tolerance in Jerusalem artichoke.

Furthermore, the results demonstrated that P_n was associated with WUE under drought conditions. It was apparent that improvements in P_n coupled with high WUE could be accomplished by selecting for high SCMR under drought conditions. This information should provide a better understanding on how genotypes could achieve high P_n coupled with enhance WUE under drought, and could have important implications on breeding for drought resistance in Jerusalem artichoke.

4. Conclusion

Plant responses to drought are complex, expression of which depends on action and interaction of different morphological and physiological traits. Drought significantly reduced LA, g_s, P_n and biomass production in all genotypes while WUE was increased. However, considering the genotype was more resistance to drought would have maintained high photosynthetic characteristics and high WUE under drought conditions. JA 60 showed maintained high SCMR, g_s and P_n under drought conditions, and should be useful as a parent in breeding for drought resistance. Plant breeding programs need rapid, accurate screening tools that will identify promising genetic material at a reasonable cost. The present study suggested that increased P_n coupled with high WUE in Jerusalem artichoke could be achieved by selecting for improved SCMR under drought conditions.

Acknowledgements

This work was supported by the Higher Education Research Promotion and National Research University Project of Thailand, Office of the Higher Education Commission, through the Food and Functional Food Research Cluster of Khon Kaen University, Thailand. Grateful acknowledgments are made to the Peanut and Jerusalem artichoke Improvement for Functional Food Research Group and Plant Breeding Research Center for Sustainable Agriculture, Khon Kaen University, and to the Thailand Research Fund for providing financial supports to this research through the Senior Research Scholar Project of Professor Dr. Sanun Jogloy (Project no. RTA 5880003). Acknowledgement is extended to the Thailand Research Fund (IRG 5780003), Khon Kaen University and Faculty of Agriculture, KKU for providing financial support for manuscript preparation activities.

References

Arunyanark, A., Jogloy, S., Akkasaeng, C., Vorasoot, N., Kesmala, T., Nageswara Rao, R.C., Wright, G.C., Patanothai, A., 2008. Chlorophyll stability is an indicator of drought tolerance in peanut. J. Agron. Crop Sci. 194, 113–125.

Ashraf, M., Harris, P.J.C., 2013. Photosynthesis under stressful environments – an overview. Photosynthetica 51, 163–190.

Blum, A., 2005. Drought resistance, water-use efficiency, and yield potential-are they compatible, dissonant, or mutually exclusive? Aust. J. Agric. Res. 56, 1159–1168.

Conde, J.R., Tenorio, J.L., Rodriguez-Maribona, B., Ayerbe, L., 1991. Tuber yield of Jerusalem artichoke (*Helianthus tuberosus* L.) in relation to water stress. Biomass Bioenerg. 3, 131–142.

Condon, A.G., Richards, R.A., Rebetzke, G.J., Farquhar, G.D., 2004. Breeding for high water-use efficiency. J. Exp. Bot. 55, 2447–2460.

Darkwa, K., Ambachew, D., Mohammed, H., Asfaw, A., Blair, M.W., 2015. Evaluation of common bean (*Phaseolus vulgaris* L.) genotypes for drought stress adaptation in Ethiopia. Crop J. 4, 367–376.

Doorenbos, J., Pruitt, W.O., 1992. Guideline for Predicting Crop Water Requirements. FAO Irrigation and Drainage Paper. Food and Agriculture Organization of the United Nations, Rome.

Galmés, J., Medrano, H., Flexas, J., 2007. Photosynthetic limitations in response to water stress and recovery in Mediterranean plants with different growth forms. New Phytol. 175, 81–93.

Gao, K., Zhu, T., Han, G., 2011. Water and nitrogen interactively increased the biomass production of Jerusalem artichoke (*Helianthus tuberosus* L.) in semi-arid area. Afr. J. Biotechnol. 10, 6466–6472.
Hoshmand, A.R., 2006. Design of Experiments for Agriculture and the Natural Sciences. Chapman & Hall, Florida.
Hund, A., Ruta, N., Liedgens, M., 2009. Rooting depth and water use efficiency of tropical maize inbred lines, differing in drought tolerance. Plant Soil 318, 311–325.
Jangpromma, N., Songsri, P., Thammasirirak, S., Jaisil, P., 2010. Rapid assessment of chlorophyll content in sugarcane using a SPAD chlorophyll meter across different water stress conditions. Asian J. Plant Sci. 9, 368–374.
Janket, A., Jogloy, S., Vorasoot, N., Kesmala, T., Holbrook, C.C., Patanothai, A., 2013. Genetic diversity of water use efficiency in Jerusalem artichoke (*Helianthus tuberosus* L.) germplasm. Aust. J. Crop Sci. 7, 1670–1681.
Ling, Q., Huang, W., Jarvis, P., 2011. Use of a SPAD-502 meter to measure leaf chlorophyll concentration in *Arabidopsis thaliana*. Photosynth. Res. 107, 209–214.
Lu, H.B., Qiao, Y.M., Gong, X.C., Li, H.Q., Zhang, Q., Zhao, Z.H., Meng, L.L., 2015. Influence of drought stress on the photosynthetic characteristics and dry matter accumulation of hybrid millet. Photosynthetica 53, 306–311.
Luo, L.J., 2010. Breeding for water-saving and drought-resistance rice (WDR) in China. J. Exp. Bot. 61, 3509–3517.
Mathobo, R., Marais, D., Steyn, J.M., 2017. The effect of drought stress on yield, leaf gaseous exchange and chlorophyll fluorescence of dry beans (*Phaseolus vulgaris* L.). Agric. Water Manage. 180, 118–125.
Monti, A., Amaducci, M.T., Venturi, G., 2005a. Growth response, leaf gas exchange and fructans accumulation of Jerusalem artichoke (*Helianthus tuberosus* L.) as affected by different water regimes. Eur. J. Agron. 23, 136–145.
Monti, A., Amaducci, M.T., Pritoni, G., Venturi, G., 2005b. Growth, fructan yield, and quality of chicory (*Cichorium intybus* L.) as related photosynthetic capacity, harvest time, and water regime. J. Exp. Bot. 56, 1389–1395.
Nageswara Rao, R.C., Wright, G.C., 1994. Stability of the relationship between specific leaf area and carbon isotope discrimination across environments in peanut. Crop Sci. 34, 98–103.
Netto, A.T., Campostrini, E., Oliveira de, J.G., Bressan-Smith, R.E., 2005. Photosynthetic pigments, nitrogen, chlorophyll a fluorescence and SPAD-502 readings in coffee leaves. Sci. Hortic. 104, 199–209.
Nigam, S.N., Aruna, R., 2008. Stability of soil plant analytical development (SPAD) chlorophyll meter reading (SCMR) and specific leaf area (SLA) and their association across varying soil moisture stress conditions in groundnut (*Arachis hypogaea* L.). Euphytica 160, 111–117.
Olanrewaju, O.O., Olufayo, A.A., Oguntunde, P.G., 2009. Water use efficiency of *Manihot esculenta* Crantz under drip irrigation system in southwestern Nigeria. Eur. J. Sci Res. 27, 576–587.
Papasavvas, A., Triantafyllidis, V., Zervoudakis, G., 2008. Correlation of SPAD-502 meter readings with physiological parameters and leaf nitrate content in *Beta vulgaris*. J. Environ. Prot. Ecol. 9, 351–356.
Paungbut, D., Jogloy, S., Vorasoot, N., Patanothai, A., 2015. Growth and phenology of Jerusalem artichoke (*Helianthus tuberosus* L). Pak J. Bot. 47, 2207–2214.
Pimsaen, W., Jogloy, S., Suriharn, B., Kesmala, T., Pensuk, V., Patanothai, A., 2010. Genotype by environment (G × E) interactions for yield components of Jerusalem artichoke (*Helianthus tuberosus* L.). Asian J. Plant Sci. 9, 11–19.
Puangbut, D., Jogloy, S., Vorasoot, N., Akkasaeng, C., Kesmala, T., Rachaputi Rao, C.N., Wright, G.C., Patanothai, A., 2009. Association of root dry weight and transpiration efficiency of peanut genotypes under early season drought. Agric. Water Manage. 96, 1460–1466.
Puangbut, D., Jogloy, S., Vorasoot, N., Srijaranai, S., Holbrook, C.C., Patanothai, A., 2015. Variation of inulin content, inulin yield and water use efficiency for inulin yield in Jerusalem artichoke genotypes under different water regimes. Agric. Water Manage. 152, 142–150.
Radovanovic, A., Stojceska, V., Plunkett, A., Jankovic, S., Milovanovic, D., Cupara, S., 2015. The use of dry Jerusalem artichoke as a functional nutrient in developing extruded food with low glycemic index. Food Chem. 177, 81–88.
Richards, R.A., 2000. Selectable traits to increase crop photosynthesis and yield of grain crops. J. Exp. Bot. 51, 447–458.
Roberfroid, M.B., 2007. Inulin-type fructans: functional food ingredients. J. Nutr. 137, 2493S–2502S.
Ruttanaprasert, R., Jogloy, S., Vorasoot, N., Kesmala, T., Kanwar, R.S., Holbrook, C.C., Patanothai, A., 2012. Relationship between chlorophyll density and SPAD chlorophyll meter reading for Jerusalem artichoke (*Helianthus tuberosus* L.). SABRAO J. Breed. Genet. 44, 149–162.
Ruttanaprasert, R., Banterng, P., Jogloy, S., Vorasoot, N., Kesmala, T., Kanwar, R.S., Holbrook, C.C., Patanothai, A., 2014. Genotypic variability for tuber yield, biomass and drought tolerance in Jerusalem artichoke germplasm. Turk. J. Agric. For. 38, 570–580.
Ruttanaprasert, R., Jogloy, S., Vorasoot, N., Kesmala, T., Kanwar, R.S., Holbrook, C.C., Patanothai, A., 2015. Root responses of Jerusalem artichoke genotypes to different water regimes. Biomass Bioenerg. 81, 369–377.
Ruttanaprasert, R., Jogloy, S., Vorasoot, N., Kesmala, T., Kanwar, R.S., Holbrook, C.C., Patanothai, A., 2016a. Effects of water stress on total biomass, tuber yield, harvest index and water use efficiency in Jerusalem artichoke. Agric. Water Manage. 166, 130–138.
Ruttanaprasert, R., Banterng, P., Jogloy, S., Vorasoot, N., Kesmala, T., Patanothai, A., 2016b. Diversity of physiological traits in Jerusalem artichoke genotypes under non-stress and drought stress. Pak. J. Bot. 48, 11–20.
Silva, M.A. de, Jifon, J.L., Santos dos, C.M., Jadoski, C.J., Silva, J.A.G. da, 2013. Photosynthetic capacity and water use efficiency in sugarcane genotypes subject to water deficit during early growth phase. Braz. Arch. Biol. Technol. 56, 735–748.
Singh, S., Russell, M.B., 1981. Water use by maize/pigeonpeas intercrop on a deep vertisol. In: Proceedings of the International Workshop on Pigeonpeas, ICRISAT Center, pp. 271–282.
Songsri, P., Jogloy, S., Holbrook, C.C., Kesmala, T., Vorasoot, N., Akkasaeng, C., Patanothai, A., 2009. Association of root, specific leaf area and SPAD chlorophyll meter reading to water use efficiency of peanut under different available soil water. Agric. Water Manage. 96, 790–798.
Subrahmanyam, D., Subash, N., Haris, A., Sikka, A.K., 2006. Influence of water stress on leaf photosynthetic characteristics in wheat cultivars differing in their susceptibility to drought. Photosynthetica 44, 125–129.
Vandoorne, B., Matheiu, A.S., Van den Ende, W., Vergauwen, R., Périlleux, C., Javaux, M., Lutts, S., 2012. Water stress drastically reduces root growth and inulin yield in *Cichorium intybus* (var. *sativam*) independently of photosynthesis. J. Exp. Bot. 63, 4359–4373.
Watzl, B., Girrbach, S., Roller, M., 2005. Inulin, oligofructose and immunomodulation. Brit. J. Nutr. 93, 49–55.
Yang, L., He, Q.S., Corscadden, K., Udenigwe, C.C., 2015. The prospects of Jerusalem artichoke in functional food ingredients and bioenergy production. Biotechnol. Rep. 5, 77–88.
Zhang, M., Chen, Q., Shen, S., 2010. Physiological responses of two Jerusalem artichoke cultivars to drought stress induced by polyethylene glycol. Acta Physiol. Plant. 33, 313–318.

Breeding Science 67: 207–212 (2017)
doi:10.1270/jsbbs.16146

Research Paper

Variability of arginine content and yield components in Valencia peanut germplasm

Chorkaew Aninbon[1)], Sanun Jogloy*[1)], Nimitr Vorasoot[1)], Suporn Nuchadomrong[2)], C. Corley Holbrook[3)], Craig Kvien[4)], Naveen Puppala[5)] and Aran Patanothai[1)]

[1)] *Department of Plant Science and Agricultural Resources, Faculty of Agriculture, Khon Kaen University*, Khon Kaen 40002, Thailand
[2)] *Department of Biochemistry, Faculty of Science, Khon Kaen University*, Khon Kaen 40002, Thailand
[3)] *Research Geneticist: USDA-ARS*, Tifton, GA, USA
[4)] *Crop & Soil Sciences, The University of Georgia*, Tifton, GA 31793, USA
[5)] *Agricultural Science Center at Clovis, New Mexico State University*, Clovis, New Mexico, 88101, USA

Peanut seeds are rich in arginine, an amino acid that has several positive effects on human health. Establishing the genetic variability of arginine content in peanut will be useful for breeding programs that have high arginine as one of their goals. The objective of this study was to evaluate the variation of arginine content, pods/plant, seeds/pod, seed weight, and yield in Valencia peanut germplasm. One hundred and thirty peanut genotypes were grown under field condition for two years. A randomized complete block design with three replications was used for this study. Arginine content was analyzed in peanut seeds at harvest using spectrophotometry. Yield and yield components were recorded for each genotype. Significant differences in arginine content and yield components were found in the tested Valencia peanut germplasm. Arginine content ranged from 8.68–23.35 µg/g seed. Kremena was the best overall genotype of high arginine content, number of pods/plant, 100 seed weight and pod yield.

Key Words: groundnut, *Arachis hypogaea*, amino acids, diversity, agronomic traits.

Introduction

Peanut (*Arachis hypogaea* L.) is a legume crop grown mostly in the tropics and semi-arid tropics. The cultivated peanut is an allotetraploid species with a chromosome number of 2n = 40 (Seijo *et al.* 2007). Peanut seed is a rich source of protein, fatty acids, vitamins, fiber, and phytochemicals (Win *et al.* 2011). Arginine, an important amino acid with several health benefits, is found at higher concentrations in peanut seeds than in many other nut crops (Venkatachalam and Sathe 2006). Consumption of arginine at the level of 3–6 g/day has been found to improve the cardiovascular system, reduce intestinal permeability and activate the immune system (Field *et al.* 2000).

Defining the genetic variability in economically important traits is an important step in breeding programs. Information on the variation in arginine content in peanut germplasm is limited. To the best of our knowledge, only one paper, arginine content in 108 accessions of the core collection of peanut germplasm has been published. In this study, arginine contents in peanut seeds ranged from 15–43 µg/g fresh weight (Dean *et al.* 2009). Amino acid profiles were studied in 17 peanut genotypes and the arginine content ranged from 8.98–11.2 µg/g (Anderson *et al.* 1998).

Amino acids in cotyledons of peanut genotypes were higher in Virginia and Valencia types than in other market types, with the arginine content of Valencia types ranging from 11.98–13.01% of total amino acid (Hovis *et al.* 1982). The range of protein content in peanut gerplasm is also large, as seen in a 152 accession study of peanut genotypes in China, where total proteins ranged from 18.93% to 30.22% (Wang *et al.* 2011). From previous study, a large population which study about the variation of arginine content was reported only one (Dean *et al.* 2009). However, this study was not specific to the Valencia type of peanut. So the objective of the present study was to evaluate arginine content and yield components of a large, diverse group of Valencia peanut accessions for the purpose of identifying lines that would be useful in a breeding programs targeting high arginine content and pod yield.

Communicated by J. Michael Bonman
Received August 30, 2016. Accepted January 23, 2017.
First Published Online in J-STAGE on May 23, 2017.
*Corresponding author (e-mail: sjogloy@gmail.com)

Materials and Methods

Plant materials and experimental design

One hundred and twenty eight accessions from the peanut "core" collection for Valencia, one Spanish (KKU 40) and one Virginia (KKU 60) peanut genotype were used for this study. These accessions were maintained in the genebanks of New Mexico State University, US, the International Crops Research Institute for the Semi-Arid-Tropics (ICRISAT) and Khon Kaen University, Thailand. Two varieties (KS 1 and KS 2) from Thailand were also used as Valencia peanut checks. The experiment was conducted at the Field Crop Research Station, Khon Kean University, Thailand during February–June 2012 and repeated during February–June 2013. A randomized completed block design (RCBD) with three replications was used. Plot size was 2 × 5 m and the spacing between row and plant was 50 and 20 cm, respectively.

Crop management

The soil was plowed three times before planting. Sprinkler irrigation system was installed before planting. The seeds of each genotype were treated with Captan (3a, 4, 7, 7 a-tetrahydro-2-((trichloromethyl) thio)-1H-isoindole) at the rate of 5 g/kg seeds for controlling *Aspergillus niger*. At planting, three seeds per hill were sown and pre-emergent weed control herbicide (Alachor) was applied immediately after sowing. Rhizobium (mixture of strains THA 201 and THA 205; Department of Agriculture, Ministry of Agriculture and Cooperatives, Bangkok, Thailand) was applied in a liquid mixture on the day after planting. Seedlings were thinned to one plant per hill at 14 days after planting (DAP). Fertilizer (0, 56.25, 37.5 kg/ha of N: P_2O_5: K_2O, respectively) was applied 15 DAP. Gypsum ($CaSO_4$) was applied at 312 kg/ha 40 DAP. Fields were scouted weekly for insects, weeds and diseases and treated as needed. Sprinkler irrigation was applied at two-day intervals to maintain soil moisture close to field capacity.

Yield and yield components

At harvest time, total pods of each genotype were harvested from a 2 × 5 m^2, and air-dried until reaching 8% moisture content and total pod yield was recorded. Twenty plants were randomly selected and the number of pods per plant, the number of seeds per pod and 100 seed weight of each genotype were recorded.

Arginine content analysis

Seeds from each plot were sub-divided to get 150 g. The 150 g samples of seeds were ground in a blender and a 10 g sub-sample was further ground using a mortar and a pestle. The sub-samples were then extracted using 30 ml of distilled water and filtered through No. 1 Wattman papers. To 5 ml of each sample, 6 M NaCl was added and heated at 90 ± 2°C for 90 minutes for protein precipitation. After heating, the samples were centrifuged for 10 minutes at 5,000 rpm and a 1 ml supernatant was transferred to a microtube and set aside at 4°C until analysis. Free arginine content was then analyzed using the Sakaguchi reaction as follows: to the sub samples, 0.1% α-naphthol (1 ml), 10% KOH (1 ml), 5% urea (1 ml) and 0.4% K-hypobromite (2 ml) were added (Basha *et al.* 1976), the reactions were incubated at room temperature for 20 min and then measured for absorbance at 520 nm using a spectrophotometer.

Statistical analysis

Data were analyzed as a randomized complete block design using Statistix 8 (Statistix8 2003). The correlations between arginine content and yield and yield components were also analyzed using Statistix 8. A data matrix of the 130 accessions was constructed using the mean of yield and yield component characters and arginine content. The cluster analysis based on Ward's method and squared Euclidian distance was performed and the dendrogram was constructed. All calculations were performed in SAS 6.12 software (SAS 2001).

Results

Combined analysis of variance

The year was significantly different ($P \leq 0.05$) for number of pods per plant and pod yield, whereas genotypes were significantly different for all traits (**Table 1**). The interactions between year and genotype were significant for most traits except for number of pods per plant.

Arginine, yield and yield components

The peanut genotypes with highest and lowest arginine content and agronomic traits are shown in **Table 2**. Arginine

Table 1. Mean squares from combined analysis of arginine content (Arg; µg/g), number of pods per plant (P/plant), number of seeds per pod (S/pod), 100 seed weight (100 SW; g) and pod yield (g/plant) of 130 peanut accessions across two years (2012 and 2013)

Source	df	Arg	P/plant	S/pod	100 SW	Pod yield
Year (Y)	1	0.2 ns	36550.2**	0.9 ns	17782.8 ns	42763.9**
Y*REP	4	32.3	216.0	0.1	53	101.1
Genotype (G)	129	50.4**	114.9**	0.6**	140.2**	51.2**
Y*G	129	25.1**	43.6ns	0.1**	28.9**	37.3**
Error	516	3.8	36.1	0.1	17.0	20.8
Total	779					
CV (%)		12.0	25.8	12.7	10.4	25.1

ns = not significant; * $P \leq 0.05$, ** $P \leq 0.01$.

Table 2. Means for arginine content (Arg; μg/g seed), number of pods per plant (P/plant), number of seeds per pod (S/pod), 100 seed weight (100 SW; g) and pod yield (g/plant) of the ten highest and lowest genotypes based on arginine content in 2012 and 2013. Values with different letters within the same column in each group (high and low arginine groups) are significantly different at $P \leq 0.05$ by DMRT

Entry	Accession	2012					Entry	Accession	2013				
		Arg	Pods/plant	Seeds/pod	100 SW	Yield			Arg	Pods/plant	Seeds/pod	100 SW	Yield
Ten highest varities for arginine content													
82	New BG	25.90	33.41 B	2.18 BC	45.30 CD	24.78	78	DC2120 (S3873)	25.02	13.66 AB	2.35 ABC	38.60 BC	14.10 AB
83	S 3881	25.69	25.80 BC	2.06 C	53.08 BC	19.13	85	Kremena	24.02	17.20 AB	1.90 C	47.36A	15.43 A
80	S-3653	23.10	27.80 BC	2.56 AB	45.53 CD	25.31	103	ICG 5475	23.17	20.26 AB	2.11 BC	32.05 C	7.24 CD
85	Kremena	22.68	45.46 A	1.98 C	57.05 ABC	28.95	52	PI493405	22.86	14.80 AB	2.33 ABC	32.95 C	6.97 CD
18	PI536307	22.47	23.40 BC	2.95 A	52.58 BC	24.62	69	PI493630	22.60	12.86 B	2.15 BC	33.87 C	8.84 BCD
9	PI493381	22.46	25.93BC	2.93 A	47.28 CD	25.63	3	PI475921	22.35	12.86 B	1.95 C	36.86 BC	5.00 D
105	ICG 6022	22.28	19.26 C	3.00 A	63.66 AB	29.96	105	ICG 6022	22.24	11.13 B	2.73 A	44.60 AB	11.94 ABC
63	PI493565	22.07	28.26 BC	2.80 A	35.81 D	20.26	45	PI493325	22.07	22.86 A	2.45 ABC	35.36 C	8.87 BCD
129	KKU 60	21.84	31.26 B	1.80 C	65.81 A	33.76	44	PI468208	21.78	23.06 A	2.10 BC	38.26 BC	15.10 AB
53	PI493415	21.71	26.06 BC	2.63 AB	54.99 AB	22.18	4	PI475925	21.65	12.86 B	2.55 AB	34.71 C	10.41 ABCD
Ten lowest varieties for arginine content													
47	PI493340	10.70	27.53	2.60 B	41.83 A	27.33	106	ICG 6201	10.93	13.80	2.85 A	34.61 AB	7.50
41	PI576604	10.61	22.20	1.80 C	44.03 A	27.86	35	PI493518	10.66	15.46	2.70 AB	32.37 AB	10.84
2	PI475913	10.26	40.93	3.20 A	32.48 B	25.57	109	ICG 7181	10.59	12.13	2.70 AB	38.69 A	9.31
106	ICG 6201	10.23	23.73	2.60 B	43.37 A	25.62	114	ICG 10474	10.48	16.20	2.83 A	39.08 A	10.73
119	ICG 13856	10.14	34.00	2.40 B	41.62 A	27.34	72	PI493688	10.45	17.86	2.41 AB	28.64 B	7.38
98	ICG 2738	10.01	34.86	2.50 B	40.01 A	26.04	57	PI493458	10.23	11.40	2.83 A	28.54 B	6.86
60	PI493484	9.91	28.66	2.50 B	42.53 A	26.03	62	PI493523	10.02	16.20	2.56 AB	29.65 B	8.88
76	PI494019	9.87	31.93	2.50 B	45.89 A	27.72	73	PI493810	9.64	17.60	2.16 B	30.54B	11.74
26	PI338337	9.85	34.33	2.70 B	44.71 A	24.63	55	PI493446	8.51	18.33	2.45 AB	38.91 A	11.60
55	PI493446	9.35	30.46	2.20 BC	43.35 A	24.81	60	PI493484	7.44	17.60	2.90 A	34.07 AB	11.99
	Min	**9.35**	**15**	**1.78**	**32.48**	**11.71**			**7.44**	**6.40**	**1.20**	**24.47**	**5.00**
	Max	**25.90**	**51.13**	**3.23**	**65.80**	**37.74**			**25.02**	**30.26**	**3.45**	**52.16**	**19.26**
	Mean	**16.13**	**30.17**	**2.51**	**44.51**	**25.57**			**16.10**	**16.15**	**2.58**	**34.96**	**10.77**

contents ranged from 9.35–25.90 µg/g seed in 2012 and 7.44–25.02 µg/g seed in 2013. The top five accessions for arginine content in 2012 were New BG, S3881, S3653, Kremena and PI 536307 with arginine contents being 25.90, 25.69, 23.10, 22.68 and 22.47 µg/g, respectively, whereas the five highest accessions in 2013 were DC 2120 (S3873), Kremena, ICG 5475, PI 493405 and PI 493630 with arginine contents being 25.02, 24.02, 23.17, 22.86 and 22.60 µg/g, respectively.

Numbers of pods per plant ranged from 15.0–51.13 pods/plant in 2012 and 6.4–30.26 in 2013, whereas the numbers of seeds per pod ranged from 1.78–3.23 to 1.20–3.45 seeds/pod in 2012 and 2013, respectively. One hundred seed weight ranged from 32.48–65.80 g in the first year and 24.47–52.16 g in the second year and pod yield (g/plant) ranged from 11.71–37.74 and 5.00–19.26 in the first and second year, respectively.

Correlation between arginine content and agronomic traits

In this study, the arginine content was not correlated with any trait except 100 seed weight; however the correlation coefficient was low (r = 0.2758) (**Fig. 1**). This indicated that a breeding program to develop a peanut line with a high arginine content and high pod yield is possible because the arginine content did not depend on the yield.

Cluster analysis

One hundred and thirty peanut accessions were grouped into 10 clusters ($R^2 = 0.70$) (**Fig. 2**) based on arginine content, number of pods per plant, number of seeds per pod, 100-seed weight and pod yield. The clusters should aid plant breeders in the development of new peanut lines with multiple desirable, yet unrelated, traits such as arginine content and yield.

Cluster one included 13 accessions originating from Bolivia, Argentina, Costa Rica, Kenya, Zimbabwe and USA. This cluster represented moderate arginine content (15.66 µg/g), high number of pods per plant (29 pods/plant), moderate number of seeds per pod (2.52 seeds/pod), low 100 seed weight (35.86 g) and moderate pod yield (18.95 g/plant). Cluster two consisted of 6 accessions originating from Argentina and Zaire and this cluster represented moderate arginine content (15.66 µg/g), high number of pods per plant (35 pods/plant), low number of seeds per pod (2.17 seeds/pod), low 100 seed weight (34.83 g) and moderate for pod yield (17.74 g/plant). Cluster three consisted of 23 accessions originating from Bolivia, Peru, Argentina, Venezuela, Zimbabwe, New Mexico State, Brazil, Zaire, Cameroon, Srilanka, Africa and one unknown accession. This cluster represented moderate arginine content, moderate number of pods per plant, moderate 100 seed weight and moderate pod yield, and high number of seeds per pod. Cluster four consisted of 14 accessions originating from Uruguay, Bolivia, Argentina, Benin, USA, Uganda and India. This cluster was characterized by low arginine content (12.51 µg/g), high number of pods per plant, high number of seeds per pod, high 100 seed weight and moderate pod yield.

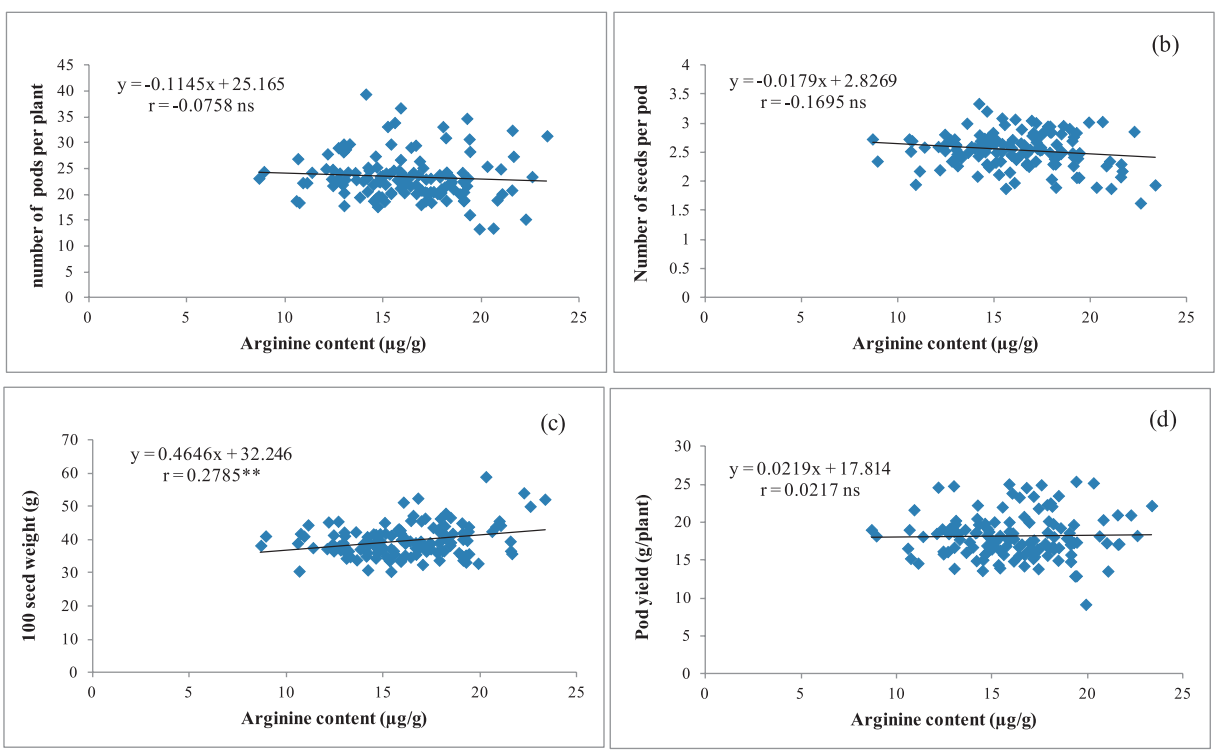

Fig. 1. Relationship between arginine content and number of pods per plant (a), number of seeds per pod (b), 100 seeds weight (c) and pod yield (g/plant) (d) of 130 peanut accessions across two years. ns,** = not significant and significant at ** $P \leq 0.01$, respectively

Breeding Science
Vol. 67 No. 3 BS

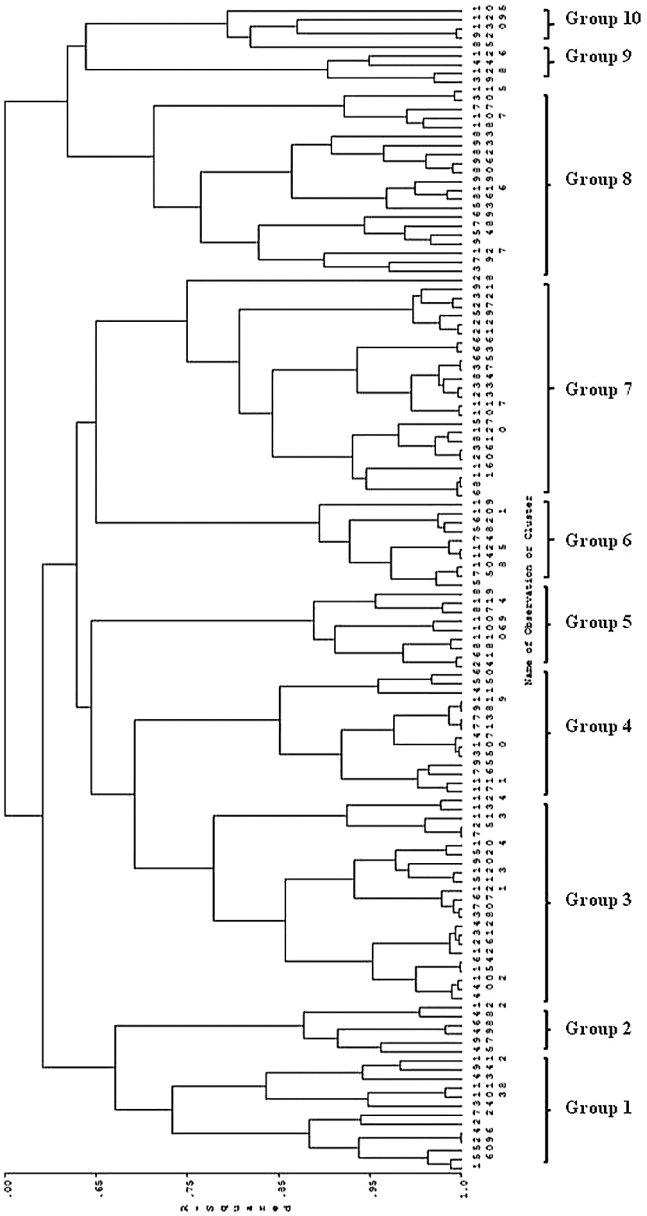

Fig. 2. Dendrogram from cluster analysis of 130 peanut genotypes based on arginine content, number of pods per plant, number of seeds per pod, 100 seed weight and pod yield across two years.

Cluster five consisted of 9 accessions originating from the Russian Federation, Argentina, New Mexico State, Peru, Cuba and India. This cluster represented low arginine content (12.78 µg/g), number of pods per plant and pod yield, whereas the number of seeds per pod and 100 seed weight were high. Cluster six consisted of 10 accessions originating from Brazil, Argentina, Bolivia and Sudan. This cluster represented moderate arginine content (15.04 µg/g), moderate number of pods per plant (23.27 pods/plant), high number of seeds per pod (2.66 seeds/pod), low 100 seed weight (34.28 g) and low pod yield (16.38 g/plant). Cluster seven consisted of 25 accessions originating from Brazil, Argentina, Peru, Uruguay, Uganda, Israel, New Mexico State, USA, Jamaica, Australia, Zimbabwe, India and Ecuador. This cluster represented moderate arginine content, low number of pods per plant, high number of seeds per pod, moderate 100 seed weight and low pod yield.

Cluster eight consisted of 21 accessions originating from Bolivia, New Mexico State, Thailand, Argentina, Congo, Korea, Indonesia, Brazil, Uruguay, Ecuador and unknown. This cluster represented high arginine content (18.58 µg/g), low number of pods per plant, moderate number of seeds per pod, high 100 seed weight (43.97 g) and moderate pod yield. Cluster nine consisted of four accessions originating from Ecuador, Bolivia and Thailand. This cluster represented moderate arginine content (15.24 µg/g), high number of pods per plant (28.97 pods/plant), low number of seeds per pod (2.28 seeds/pod), high 100 seed weight (43.99 g) and moderate for pod yield (24.52 g/plant). Cluster ten consisted of five accessions originating from New Mexico State, Mauritius, India and Thailand. This cluster represented high arginine content (19.75 µg/g), 100 seed weight (53.83 g), and pod yield (23.34 g/plant), whereas the number of pods per plant was moderate (23.67 pods/plant) and the number of seeds per pod was low (2.19 seeds/pod).

Discussion

In a peanut breeding program for high arginine, the diversity of the germplasm for arginine is important for improving this trait. In this study, arginine contents ranging from 8.68 µg/g (PI 493484) to 23.35 µg/g (Kremena) were observed in the Valencia peanut germplasm, core collection. In a previous study, arginine content in 17 peanut cultivars and breeding lines ranged from 8.98–11.20 µg/g (Andersen 1998). In another investigation, the range of arginine contents was between 15 µg/g and 43 µg/g (Dean *et al.* 2009). Arginine diversity in this study was consistent with those in previous studies. The larger number of peanut accessions in this study provides plant breeders with additional peanut germplasm information useful to breeding programs trying to advance multiple traits, such as arginine content and yield.

Arginine concentrations in other nut seeds such as almond, Brazil nut, cashew nut, hazelnut, macadamia nut, pecan, pine nut, pistachio, walnut and peanut (Virginia type) have been reported to average 10.09, 12.91, 9.84, 12.51, 12.53, 12.45, 15.41, 9.15, 13.80 and 11.04 g/100 g of protein, respectively (Venkatachalam and Sathe 2006). Moreover, Phaseolus, which is a legumes food, arginine content in wild type was 5.86, and in cultivated types including Potato, Siena and big Lima were 6.62, 6.38 and 6.13% of total amino acids (Baudoin and Maquet 1999).

From the results, the arginine content differed among years and changed with the order of varieties. Thus, the arginine content may be a quantitative trait that is controlled by several genes (Slocum 2005). However, some varieties, such as Kremena and ICG 6022, still have high arginine contents in both years and they had high potential for use as

parental lines in high arginine content breeding programs.

In this study, arginine content in Valencia peanut was not correlated with the number of pods per plant, number of seeds per pod, 100 seed weight and pod yield. The results indicated that arginine and yield traits segregate independently. Therefore, breeding for both high arginine and high yield should be successful.

The objective of this study was to evaluate the diversity of arginine content and identify lines for use in breeding programs that would aid the development of cultivars superior in yield and arginine by grouping the peanut accessions into 10 clusters based on arginine content, number of pods per plant, number of seeds per pod, 100 seed weight and pod yield. Breeders should be able to study the heritability of these traits and develop superior cultivars for them. For example, cluster five accessions were characterized as having low arginine content (12.78 µg/g) and pod yield. Cluster ten accessions were characterized as having high arginine content (19.75 µg/g) and pod yield. Cluster ten included Kremena, ICG 297, KKU 40, KKU 60 and ICG 6022. Kremana and ICG 6022 should be particularly interesting for breeding programs because they have high arginine content (23.35 and 22.26 µg/g), large seeds (52.2 and 54.13 g/100 seed) and high yield (22.19 and 20.95 g/plant). The origins of peanut plants in each cluster were different. For example, cluster ten with a high arginine content in the seed originated from New Mexico State, Mauritius, India and Thailand. Cluster four and five with low arginine contents also differed in origin. The result indicated that high or low arginine content in peanut seed was not related to their origin.

In conclusion, significant variation of arginine content was found within the Valencia germplasm core collection. Peanut genotypes Kremena and ICG 6022 had high arginine content, pod yield and a good agronomic trait. These two genotypes would be promising parents in breeding programs targeting improved arginine content and yield.

Acknowledgments

The authors are grateful for the jointed financial support of the Royal Golden Jubilee Ph.D. program and Khon Kaen University, the peanut and Jerusalem Artichoke Improvement for Functional Food Research Group, Khon Kaen University, The Higher Education Promotion and National Research University Project of Thailand of the Office of Higher Education Commission were also acknowledged for funding support through the Food and Functional Food Research Cluster of Khon Kaen University, Plant Breeding Research Center for Sustainable Agriculture, The Thailand Research Fund for providing financial supports to this research through the Senior Research Scholar Project of Professor Dr. Sanun Jogloy (Project no. RTA 5880003). Acknowledgment is extended to the Thailand Research Fund (TRF, Project no. IRG 5780003), Khon Kaen University (KKU) and the Faculty of Agriculture KKU for providing financial support for manuscript preparation activities.

Literature Cited

Andersen, P.C. (1998) Fatty acid and amino acid profiles of selected peanut cultivars and breeding lines. J. Food Compost. Anal. 11: 100–111.

Basha, S.M., J.P. Cherry and C.T. Young (1976) Change in free amino acids, carbohydrates, and protein of maturing seeds from various peanut (*Arachis hypogaea* L.) cultivars. Cereal Chem. 53: 586–597.

Baudoin, J.P. and A. Maquet (1999) Improvement of protein and amino acid contents in seeds of food legumes. A case study in *Phaseolus*. Biotechnol. Agron. Soc. Environ. 3: 220–224.

Dean, L.L., K.W. Hendrix, C.C. Holbrook and T.H. Sanders (2009) Content of some nutrients in the core of the core of the peanut germplasm collection. Peanut Sci. 36: 104–120.

Field, C.J., I. Johnson and V.C. Pratt (2000) Glutamine and arginine: Immunonutrients for improved health. Med. Sci. Sports Exerc. 32: 77–88.

Hovis, A.R., C.T. Young and P.Y.P. Tai (1982) Variation in total amino acid percentage in different portions of peanut cotyledons. Peanut Sci. 9: 44–46.

SAS Institute (2001) SAS/STAT user's guide, 2nd edn. SAS Institute Inc., Cary.

Seijo, G., G.I. Lavia, A. Fernandez, A. Krapovickas, D.A. Ducasse, D.J. Bertioli and E.A. Moscone (2007) Genomic relationships between the cultivated peanut (*Arachis hypogaea*, Leguminosae) and its close relatives revealed by double GISH. Am. J. Bot. 94: 1963–1971.

Slocum, R.D. (2005) Genes, enzymes and regulation of arginine biosynthesis in plants. Plant Physiol. Biochem. 43: 729–745.

Statistix8 (2003) Statistix8: analytical software user's manual. Tallahassee, Florida.

Venkatachalam, M. and S.K. Sathe (2006) Chemical composition of selected edible nut seeds. J. Agric. Food Chem. 54: 4705–4714.

Wang, C.T., Y.Y. Tang, X.Z. Wang, D.X. Chen, F.G. Cui, Y.C. Chi, J.C. Zhang and S.L. Yu (2011) Evaluation of groundnut genotypes from China for quality traits. J. SAT Agr. Res. 9: 1–5.

Win, M.M., A. Abdul-Hamid, B.S. Baharin, F. Anwar, M.C. Sabu and M.S. Pak-Dek (2011) Phenolic compounds and antioxidant activity of peanut's skin, hull, raw kernel and roasted kernel flour. Pak. J. Bot. 43: 1635–1642.

Euphytica (2017) 213:164
DOI 10.1007/s10681-017-1950-0

Genotypic diversity of Jerusalem artichoke for resistance to stem rot caused by *Sclerotium rolfsii* under field conditions

Chutsuda Junsopa · Sanun Jogloy · Weerasak Saksirirat · Patcharin Songsri · Thawan Kesmala · Barbara B. Shew

Received: 7 March 2017 / Accepted: 24 June 2017 / Published online: 8 July 2017

Abstract Stem rot caused by *Sclerotium rolfsii* is a major problem in Jerusalem artichoke production. Breeding of Jerusalem artichoke for stem rot resistance is a promising method for disease control, and identification of sources of resistance is necessary to initiate Jerusalem artichoke breeding programs. The objective of this study was to characterize the diversity of Jerusalem artichoke germplasm for resistance to stem rot under field conditions. Forty Jerusalem artichoke genotypes were evaluated in a randomized complete block design with four replications in two environments that differed in soil fertility. Jerusalem artichoke plants were inoculated with *S. rolfsii* at 40 days after transplanting using a single colonized sorghum seed per plant as inoculum. Data were recorded for disease incidence, lesion length, days to permanent wilting, area under disease progress curve and severity index. The Jerusalem artichoke genotypes were classified into three clusters based on traits related to disease resistance. Cluster 1 had eight resistant genotypes, cluster 2 included 15 moderately resistant genotypes, and cluster 3 consisted of 17 susceptible genotypes. The field resistance of Jerusalem artichoke is important to be use as source of resistance to stem rot disease. Jerusalem artichoke genotypes HEL65, HEL246, HEL293, HEL69 and JA98 were identified as source of resistance under field conditions. These genotypes can be used as sources of stem rot resistance in Jerusalem artichoke breeding programs.

Keywords Sunchoke · *Helianthus tuberosus* L. · Southern blight · Disease resistance · Sclerotia · Soilborne plant pathogens

C. Junsopa · S. Jogloy (✉) · W. Saksirirat · P. Songsri · T. Kesmala
Department of Plant Science and Agricultural Resources, Faculty of Agriculture, Khon Kaen University, Khon Kaen 40002, Thailand
e-mail: sjogloy@gmail.com

S. Jogloy
Peanut and Jerusalem Artichoke Improvement for Functional Food Research Group, Khon Kaen University, Khon Kaen 40002, Thailand

B. B. Shew
Department of Entomology and Plant Pathology, North Carolina State University, Raleigh, NC, USA

Introduction

Jerusalem artichoke (*Helianthus tuberosus* L.) is a good source of the carbohydrate inulin, and is produced as a food for human consumption, animal feed (Farnworth et al. 1995; Yildiz et al. 2006) and bio-ethanol (Sung et al. 2014; Kim and Kim 2014; Gunnarsson et al. 2014). Stem rot caused by *Sclerotium rolfsii* is an important problem in Jerusalem artichoke production worldwide and yield losses up to 60% have been reported (McCarter and Kays

1984). The pathogen can survive in field soils and infect Jerusalem artichoke crowns and tubers (Koike 2004).

Diseases caused by this soilborne pathogen can be controlled by several methods, including chemical application (Augusto et al. 2010; Khan and Javaid 2015), cultural practices (Cilliers et al. 2003), antagonistic organisms (Sennoi et al. 2013a; Singh and Gaur 2016) and plant resistance (Sennoi et al. 2013a). Because Jerusalem artichoke is sought after as a health food crop (Milner 1999; Kays and Nottingham 2008; Slavin 2013), chemical control is undesirable, making biological control and host plant resistance the most promising methods for control. Furthermore, these methods are safe and sustainable. Therefore, breeding for stem rot resistance in Jerusalem artichoke is necessary, and sources of resistance are required for crop improvement.

In other crop species such as peanut (*Arachis hypogaea* L.), screening of resistance has been carried out under greenhouse (Eslami et al. 2015) and field conditions (Branch 1987). In general, rankings of most peanut genotypes evaluated under greenhouse and fields conditions differ. However, some genotypes showed consistently high levels of resistance under both conditions (Shew et al. 1987). Previously, resistance to stem rot was evaluated in the greenhouse on 91 genotypes of Jerusalem artichoke (Sennoi et al. 2013b), but resistance of Jerusalem artichoke to stem rot has not been evaluated extensively under field conditions, probably because the crop is rather new to most farmers and agronomists.

It is very important to evaluate resistance under field conditions because the crop ultimately is produced in the field. Identification of superior genotypes must be carried out in the field before cultivars can be released to growers. The objectives of this study were to evaluate resistance of Jerusalem artichoke germplasm under field conditions. This information will help breeders identify and select superior genotypes in breeding programs.

Materials and methods

Plant materials and experimental design

Forty genotypes of Jerusalem artichoke were evaluated in the field for resistance to stem rot caused by *S. rolfsii*. These genotypes were among the 91 genotypes previously evaluated in the greenhouse and were selected to provide a range in resistance based on differences in days to permanent wilting (Sennoi et al. 2013b) (Table 1). The genotypes were planted in two trials with different fertility environments at the Khon Kaen University agronomy farm during the rainy season of March–June 2015. The fertility environments included one environment (E1) in which 15-15-15 NPK fertilizer was applied 25 days after transplanting (DAT) at the rate of 156.125 kg ha^{-1} and one environment (E2) without fertilizer application. Genotypes were arranged in a randomized complete block design with four replications in each environment.

Crop management

The soil was prepared conventionally and raised beds of 2 × 5 m (plots) were created after soil preparation. Uniform and healthy tubers were selected for seedling preparation. Tubers were cut into small pieces with 2–3 active buds and the cut tuber pieces were incubated in moist charred rice husk. After 3 days, seedlings 2–3 cm in length were transferred into plug trays containing soil and charred rice husk at a ratio of 1:1 (*v:v*) for 7 days until the seedlings had 4–6 leaves. Four rows of uniform seedlings of a single genotype were transplanted into each replicate 2 × 5 m plot on a spacing of 50 × 50 cm. Weeds were controlled manually at 15 DAT.

Preparation and inoculation of *Sclerotium rolfsii*

An isolate of *S. rolfsii* previously identified as a causal agent of stem rot in Jerusalem artichoke (Sennoi et al. 2010) was cultured on potato dextrose agar (PDA) in an incubator at 25 ± 2 °C for 3 days. Sorghum seed was soaked in water for 12 h and then steamed until the seeds were expanded and soft (about 1 h). The steamed sorghum seed then was loaded in polypropylene bags, autoclaved at 121 °C for 30 min, and cooled to room temperature. The colonized PDA medium was cut with a cork borer into 0.5 cm diameter plugs and four plugs were transferred into the cooled autoclaved bag of sorghum seed. The sorghum seed medium was then incubated at room temperature (30 ± 2 °C) for 7 days (Junsopa et al. 2016).

At 40 DAT, sixteen plants in the two middle rows of the plots were inoculated at 15:00. Water was applied

Table 1 Jerusalem artichoke genotypes, sources of origin and genetic resources

Genotype no.	Name of genotype	Origin	Genetic resources	Genotype no.	Name of genotype	Origin	Genetic resources
HEL246^{R}	–	Unknown	IPK	HEL6^{MR}	TambovskijKrasnyi	Russian Federation	IPK
HEL278^{R}	BS–83–22	Unknown	IPK	JA10^{MR}	HM Hybrid A	Canada	PGRC
HEL288^{R}	RA9	Poland	IPK	JA107^{MR}	83-001-2 (37 9 6)	Canada	PGRC
HEL293^{R}	–	Unknown	IPK	JA116^{MR}	83-001-11(37 9 6)	Canada	PGRC
HEL65^{R}	Sejanec 19	Russian Federation	IPK	JA127^{MR}	83-006-1 (40 9 39)	Canada	PGRC
HEL69^{R}	–	Unknown	IPK	JA9^{MR}	7513	Canada	PGRC
JA1^{R}	7305	Canada	PGRC	JA35^{MR}	W–97	Canada	PGRC
JA76^{R}	#4	Canada	PGRC	JA58^{MR}	Intress	USSR	PGRC
JA77^{R}	#5	Canada	PGRC	JA49^{S}	7513A	Canada	PGRC
JA98^{R}	242-62	France	PGRC	JA7^{S}	7312	Canada	PGRC
JA36^{R}	W–106	Canada	PGRC	JA134^{S}	83-007-5 (69 9 3)	Canada	PGRC
JA47^{R}	DHM–14–6	Canada	PGRC	JA59^{S}	Volzskij–2	USSR	PGRC
JA93^{R}	Leningradskii (NC10–65)	USSR	PGRC	HEL256^{S}	–	Unknown	IPK
JA60^{R}	Jamcovskijkrashyj	USSR	PGRC	HEL265^{S}	D19–63–340	France	IPK
JA72^{R}	TUB–676USD–ARS–SR	USA	PGRC	HEL316^{S}	–	Unknown	IPK
JA37^{MR}	Comber	Canada	PGRC	HEL317^{S}	–	Unknown	IPK
JA89^{MR}	Waldspindel	France	PGRC	JA12^{S}	HM Hybrid C	Canada	PGRC
JA133^{MR}	83-007-4 (69 9 3)	Canada	PGRC	JA122^{S}	83-004-2 (6 9 20)	Canada	PGRC
CN52867^{MR}	PGR–2367	USSR	PGRC	JA23^{S}	DHM–3	Canada	PGRC
HEL272^{MR}	Voelkenroder Spindel	Unknown	IPK	JA27^{S}	DHM-7	Canada	PGRC

Kays and Nottingham (2008)

IPK Leibniz Institute of Plant Genetics and Crop Plant Research, Germany, *PGRC* Plant Gene Resources of Canada, *R* resistant, *MR* moderately resistant, *S* susceptible were identified based on days to permanent wilting under greenhouse condition (Sennoi et al. 2013a)

for 30 min through a mini sprinkler system before inoculation to create the high humidity that favors high inoculation success. Then a single seed of sorghum inoculum was placed on the crown of each plant. The seed was further covered with a piece of cotton wool and then fastened with cellophane tape. After inoculation, water was applied again for 15 min to maintain high moisture (Junsopa et al. 2016).

Data collection

Relative humidity

The relative humidity under the canopies was recorded at 7:00, 12:00 and 16:00 on 1–7 days after inoculation (DAI) with wet and dry hygrometer. Humidity was record for irrigation management. When humidity was low, water was applied to maintain favorable humidity for *S. rolfsii* infection.

Soil data and meteorological data

Soil samples were collected to a depth of 30 cm before planting and on the days of inoculation (20 days after fertilizer application in E1). The soil samples were analyzed for pH, cation exchangeable capacity (CEC), electrical conductivity (EC), organic matter (OM), total nitrogen, available phosphorus, exchangeable potassium, exchangeable calcium and soil texture. Meteorological data were recorded for relative

humidity, temperature and rainfall throughout the experiment. The meteorological station is located about 500 m from the experimental field.

Disease assessment

Sixteen inoculated plants of each plot were assessed for disease incidence, lesion length and days to permanent wilting at 3-day intervals from 1 DAI until 46 DAI. A disease score of 0–5 (0 = healthy plant, 1 = lesion without wilting, 2 = 1–2 leaf wilting, 3 = wilting more than 2 leaves, 4 = plant damped off and 5 = plant dead) was used for assessment of resistance to *S. rolfsii* (Sennoi et al. 2010). The disease score assessment was carried out at 3-day intervals from 1 DAI until 46 DAI. Disease score data were converted to severity index (SI) as follows (Anfok 2000):

$$\mathrm{SI} = [\Sigma\,(\textit{rating score} \times \textit{number of plants in rating}) \times 100\%]/(\textit{total number of plants} \times \textit{highest rating}).$$

The data for disease incidence recorded every 3 days were transformed to area under disease progress curve (AUDPC) as follows (Shaner and Finney 1977);

$$\mathrm{AUDPC} = \sum_{i=1}^{n}[(x_i + x_{i+3})/2](t_{i+3} - t_i)$$

where x_i is disease incident at day i, x_{i+3} is disease incident at day $i + 3$, t_i is disease incidence assessment day and t_{i+3} is disease incidence assessment day +3.

Statistical analysis

Collected data of each day on each environment were analyzed according to a randomized complete block design. The data for giving a F-ratio and low CV were selected for combined analysis of two environments. The differences in error variances between environments were less than three-fold. Therefore, error variances were considered homogeneous and combined analysis of variance of the two environments was performed (Statistix8 2003). Means were separated by least significance difference (LSD). Jerusalem artichoke genotypes were clustered based on traits related to stem rot resistance (disease incidence, lesion length, days to permanent wilting, area under disease progress curve and severity index) by SAS 6.12 software (SAS 2001).

Results

Soil and meteorological data

Before fertilizer was applied to the environment with fertilizer (E1), the two test sites were similar for all soil properties (Table 2). After application of fertilizer, the soil from E1 (with fertilizer) had higher pH, total nitrogen, exchangeable potassium and exchangeable calcium than the soil from E2 (without fertilizer). The environments were also similar for meteorological data because planting dates differed by only a few days. Temperatures ranged between 19 to 42.4 °C,

Table 2 Soil pH, cation exchange capacity (CEC), electrical conductivity (EC), organic matter (OM), total nitrogen (N), available phosphorus (P), exchangeable potassium (K), exchangeable calcium (Ca) and soil texture before and after fertilizer application

Environments	PH	CEC (c mol kg^{-1})	EC (dS m^{-1})	OM (%)	Total N (%)	Available P (mg kg^{-1})	Exchangeable K (mg kg^{-1})	Exchangeable Ca (mg kg^{-1})	Texture Class
Before fertilizer application									
E1	6.40	1.671	0.057	0.498	0.0262	49.26	32.59	325	Loamy-sand
E2	6.71	2.129	0.055	0.486	0.0250	48.02	33.56	365	Loamy-sand
After fertilizer application									
E1	6.83	1.521	0.064	0.490	0.0250	53.59	30.64	360	Loamy-sand
E2	6.57	1.568	0.067	0.458	0.0226	54.83	27.24	330	Loamy-sand

E1 Environment 1 with application of recommended fertilizer rate (15-15-15 NPK at the rate of 156.125 kg ha^{-1}), *E2* Environment 2 with no fertilizer application

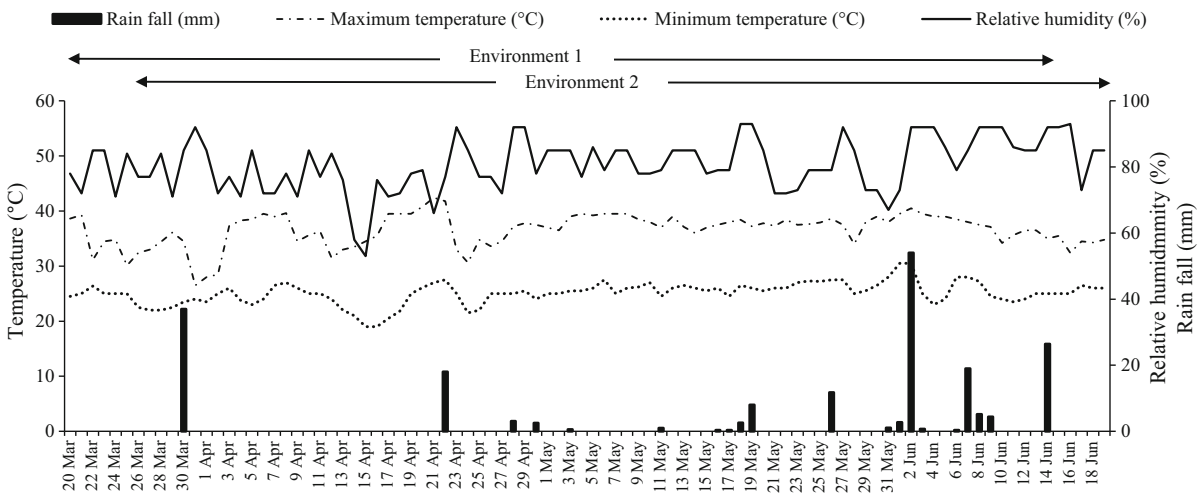

Fig. 1 Rainfall, relative humidity, maximum temperature and minimum temperature for the experiment conduct from 20 March to 19 June, 2015. Environment 1 trial (recommended fertilizer rate: 15-15-15 NPK at the rate of 156.125 kg ha^{-1}) was conducted from 20 March to 14 June, 2015, and environment 2 trial (no fertilizer application) was conducted from 25 March to 19 June, 2015

total rainfall was 199.3 mm and relative humidity was in the range of 53–93% in both environments (Fig. 1).

The relative humidity of the canopy was high in the morning and low in the midday and the afternoon. The field with fertilizer had canopy relative humidity values ranging from 77 to 93, 71 to 82 and 60 to 63% at 7.00, 12.00 and 16.00 respectively, whereas the field without fertilizer had canopy relative humidity values ranging from 77 to 93, 63 to 77 and 58 to 61% at 7.00, 12.00 and 16.00, respectively.

Combined analysis of variance

Environments were significantly different for lesion length ($P \leq 0.05$), days to permanent wilting ($P \leq 0.05$) and severity index ($P \leq 0.01$), whereas genotypes were significantly different for disease incidence ($P \leq 0.01$), lesion length ($P \leq 0.01$), days to permanent wilting ($P \leq 0.01$), area under disease progress curve ($P \leq 0.01$) and severity index ($P \leq 0.01$) (Table 3). The interactions between environment and genotype were significant for disease incidence ($P \leq 0.01$), days to permanent wilting ($P \leq 0.01$), area under disease progress curve ($P \leq 0.05$) and severity index ($P \leq 0.01$). We did compare effect of the interaction between environments and genotypes (E x G) to the main effect (genotypes) and the effect of the interaction was relatively low. The data across two environments were presented.

Disease resistance variation

Genotypes were significantly different in all traits related to stem rot resistance (Table 4). Disease incidence was lowest in HEL65, HEL246, HEL293, JA134 and HEL61, whereas incidence was highest in JA93, JA36, JA12, JA59 and JA116. Lesion length was least in HEL293, HEL65, HEL246, JA116 and JA134, whereas genotypes HEL265, JA89, JA72, JA36 and JA76 had among the greatest lesion lengths.

The genotypes JA107, CN52867, JA9, HEL293 and HEL246 took the most days to reach permanent wilting, and HEL316, JA47, JA49, JA27 and JA58 reached permanent wilting in the fewest days. HEL65, HEL246, HEL293, HEL69 and JA107 had the smallest area under disease progress curve, whereas JA36, JA59, JA116, JA7 and JA27 had the largest AUDPC. The severity index was lowest in HEL246, HEL293, JA107 HEL65 and JA134, and was highest in JA9, JA27, JA72, JA59 and JA36.

Relationship between field conditions

Although environments (with fertilizer application and without fertilizer application) were significantly

Table 3 Mean squares of combined analysis for disease incidence (DI), lesion length (LL), days to permanent wilting (DTW), area under disease progress curve (AUDPC) and severity index (SI)

Source of variance	DF	DI (%)[a]	LL (cm)[b]	DTW[c]	AUDPC[d]	SI (%)[e]
Environments (E)	1	335.79	44.3275*	195.313*	390951	26103.9**
Rep within environments	6	8044.52	5.1368	27.924	1154939	1803.7
Genotypes (G)	39	1295.09**	2.1107**	20.351**	149639**	1777.5**
E × G	39	440.55**	0.7873 ns	6.095**	55704*	455.9**
Pooled error	234	259.33	0.6155	2.517	36766	191.5
Total	319					
CV (%)		22.12	30.26	11.41	12.54	20.78

[a] Disease incidence at 13 DAI

[b] Lesion length at 13 DAI

[c] Days to permanent wilting were observed every 3 days

[d] AUDPC was calculated from disease incidence observed every 3 days $\left(\text{AUDPC} = \sum_{i=1}^{n}[(x_i + x_{i+3})/2](t_{i+3} - t_i)\right)$

[e] Severity index at 19 DAI (SI = [Σ *(rating score* × *number of plants in rating)* × *100%]/(total number of plants* × *highest rating)*)

**, * Significant at 1 and 5% respectively

different for lesion length, days to permanent wilting and severity index (Table 3), the correlations for traits related to disease resistance of genotypes in two environments were significant (Fig. 2): disease incidence (r = 0.50*), lesion length (r = 0.46**), days to permanent wilting (r = 0.52**), area under disease progress curve (r = 0.47**) and severity index (r = 0.60**).

Cluster analysis

Jerusalem artichoke genotypes were classified based on traits related to disease resistance including disease incidence, lesion length, days to permanent wilting, area under disease progress curve and severity index (Fig. 3). The 40 genotypes were classified into three clusters. Cluster I consisted of the eight resistant genotypes that had low disease incidence, short lesion length, long days to permanent wilting, low area under disease progress curve and low severity index including HEL65, HEL246, HEL293, HEL69, JA10, HEL316, JA134 and JA98. Cluster II contained 15 genotypes with intermediate resistance and those that exhibited resistance in some traits but were susceptible in other traits including HEL278, JA12, HEL256, JA60, JA116, JA133, JA58, CN52867, HEL265, HEL61, HEL288, JA107, JA127, JA122 and JA76. Cluster III was formed by the most susceptible genotypes period. Those exhibiting were high disease incidence, long lesion length, short days to permanent wilting, high area under disease progress curve and high severity index including JA23, JA49, JA47, HEL317, JA77, JA37, JA89, JA9, JA1, JA35, HEL272, JA59, JA93, JA27, JA7, JA72 and JA36.

Discussion

The diversity in Jerusalem artichoke has been reported for many important traits such as flowering date and duration (Kays and Kultur 2005), yield components (Pimsaen et al. 2010), inulin content (Puttha et al. 2012), water use efficiency (Janket et al. 2013), and morphological and agronomic traits (Diederichsen 2010; Puttha et al. 2013). A previous study reported the diversity of resistance to ring spot viruses and powdery mildew caused by *Oidium neolycopersici* (Serieys et al. 2010). Diversity in resistance to stem rot caused by *S. rolfsii* also has been evaluated under greenhouse conditions (Sennoi et al. 2013b).

In this study, genetic diversity of Jerusalem artichoke for traits related to stem rot resistance was high, but only a few genotypes HEL65, HEL246, HEL293, HEL69, JA10, HEL316, JA134 and JA98) showed high levels of disease resistance for all traits examined. This group of genotypes can be used as a

Table 4 Means of disease incidence (DI), lesion length (LL), days to permanent wilting (DTW), area under disease progress curve (AUDPC) and severity index (SI) for 40 genotypes of Jerusalem artichoke in 2 environments

Genotypes	DI (%)[a]	LL (cm)[b]	DTW (days)[c]	AUDPC[d]	SI (%)[e]
HEL65	46.0 m	1.6 lm	16 abc	1237.3 n	48.6 op
HEL246	47.8 lm	1.6 lm	18 a	1257.5 mn	24.2 r
HEL293	49.2 klm	1.5 m	17 ab	1283.8 lmn	34.9 qr
JA134	50.7 klm	2.0 i–m	16 bcd	1375.9 h–n	50.9 nop
HEL69	53.0 j–m	2.3 d–l	14 e–j	1308.7 k–n	55.4 l–p
HEL61	53.0 j–m	2.2 e–m	15 c–f	1396.6 g–n	51.6 nop
JA107	60.5 i–m	2.5 c–k	16 b–e	1361.7 j–n	42.4 pq
HEL278	62.6 i–l	2.4 c–k	16 b–f	1511.8 c–j	58.8 k–o
HEL256	63.5 h–l	3.0 a–d	13 h–m	1459.0 e–l	65.9 f–m
JA98	63.5 g–l	2.7 a–j	14 e–j	1387.1 h–n	57.5 k–o
JA122	64.1 f–k	3.0 a–d	15 d–h	1426.6 f–m	61.8 i–o
JA10	64.0 f–k	2.3 d–l	16 b–f	1368.8 i–n	52.6 m–p
CN52867	67.9 e–j	2.8 a–g	16 b–f	1490.0 c–k	56.1 l–o
JA127	68.8 e–j	2.1 g–m	15 c–g	1469.6 e–l	63.1 h–n
HEL288	70.1 e–i	2.8 a–i	14 e–j	1497.4 c–k	63.0 h–n
JA76	70.9 d–i	3.4 a	13 j–o	1425.7 f–n	61.1 i–o
HEL316	71.1 d–i	2.0 j–m	12 l–o	1473.8 e–k	67.5 e–l
JA133	73.8 c–i	2.8 a–h	15 c–f	1480.7 d–k	55.8 l–p
JA23	73.1 c–i	2.3 d–l	14 h–m	1601.2 a–f	70.8 c–k
JA37	74.8 b–i	2.3 d–l	14 f–k	1552.2 a–i	65.9 f–m
JA9	75.0 b–i	3.1 abc	16 b–f	1523.3 b–j	59.4 j–o
JA36	87.6 abc	3.3 a	12 l–o	1706.1 ab	87.3 a
JA60	79.0 a–h	2.7 a–j	14 e–j	1612.7 a–f	65.6 g–m
JA58	79.4 a–g	2.8 a–g	12 l–o	1602.3 a–f	79.6 a–e
JA89	79.7 a–f	3.3 ab	15 d–i	1590.1 a–f	65.8 f–m
HEL272	79.5 a–f	3.1 abc	12 l–o	1612.8 a–f	79.6 a–e
JA1	80.8 a–e	2.8 a–g	14 f–k	1645.2 a–e	72.6 b–j
JA77	80.8 a–e	3.1 abc	14 g–l	1606.6 a–f	68.4 d–l
JA47	82.2 a–e	2.4 c–k	12 l–o	1642.7 a–e	79.9 a–e
JA35	81.8 a–e	3.1 abc	13 j–o	1627.2 a–e	79.3 a–f
JA49	80.4 a–e	2.5 b–k	12 mno	1584.8 a–g	78.4 a–g
JA7	82.2 a–e	2.0 h–m	13 i–n	1720.2 a	83.2 abc
HEL265	81.8 a–e	3.2 abc	13 j–o	1558.0 a–h	73.7 a–i
HEL317	83.3 a–e	2.8 a–f	12 o	1592.3 a–f	76.4 a–h
JA72	86.2 a–d	3.3 a	12 l–o	1664.3 a–d	86.4 a
JA27	86.3 a–d	2.7 a–j	12 l–o	1721.3 a	85.8 ab
JA93	87.5 abc	3.0 a–e	12 no	1678.0 abc	85.0 ab
JA12	87.7 abc	2.2 f–m	13 k–o	1665.2 a–d	81.4 a–d
JA59	90.7 ab	2.8 a–h	12 l–o	1710.8 ab	86.7 a
JA116	91.4 a	1.9 klm	13 j–o	1712.1 ab	81.3 a–d
Max	91.4	3.4	18.0	1721.3	87.3
Min	46.0	1.5	12.0	1237.3	24.2

Table 4 continued

Genotypes	DI (%)[a]	LL (cm)[b]	DTW (days)[c]	AUDPC[d]	SI (%)[e]
Mean	72.8	2.6	13.9	1528.5	66.6
SD	13.25	0.53	1.75	142.36	16.10
F-test	**	**	**	**	**

Common letter in the same column are not significantly different at 5% level by LSD

[a] Disease incidence at 13 DAI

[b] Lesion lengths at 13 DAI

[c] Days to permanent wilting were observed every 3 days

[d] AUDPC was calculated from disease incidence observed every 3 days $\left(\text{AUDPC} = \sum_{i=1}^{n}[(x_i + x_{i+3})/2](t_{i+3} - t_i)\right)$

[e] Severity index at 19 DAI (SI = [Σ *(rating score* × *number of plants in rating)* × *100%]/(total number of plants* × *highest rating)*)

** Significant at 1%

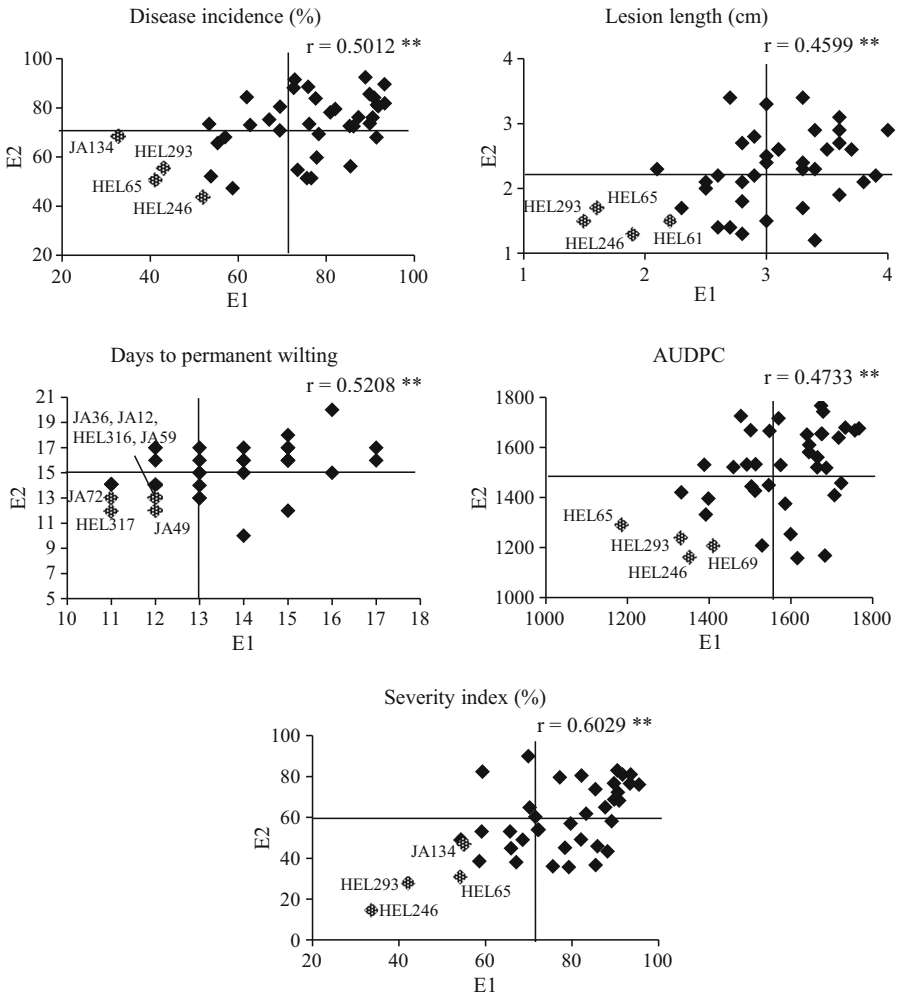

Fig. 2 Correlation of E1 = environment 1 (high fertility; 15-15-15 NPK at the rate of 156.125 kg ha^{-1}) and E2 = environment 2 (no fertilizer application) for disease incidence, lesion length, days to permanent wilting, area under disease progress curve (AUDPC) and severity index. The vertical and horizontal lines in figures are the means for each environment

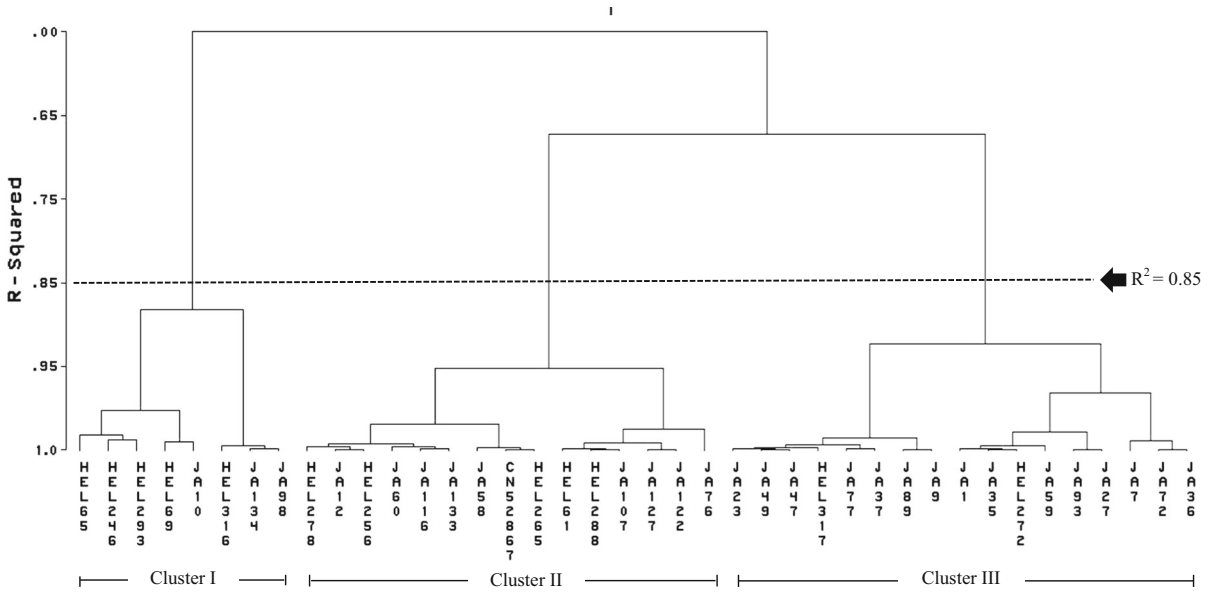

Fig. 3 Dendrogram of 40 Jerusalem artichoke genotypes for resistance to *S. rolfsii* showing 3 cluster groups ($R^2 = 0.85$) based on the similarity of their resistance

source of resistance for breeding programs to improve stem rot resistance in Jerusalem artichoke. HEL65, HEL246, HEL293, HEL69, JA10, HEL316, JA134 and JA98 were the most resistant to stem rot in both field environments, and HEL293 and JA98 also showed the highest resistance in the previous greenhouse trials (Sennoi et al. 2013b). In the greenhouse, HEL65, HEL293, HEL69 and JA98 were classified in a resistant group of ten genotypes in the first season and HEL246, HEL293 and JA98 were identified in a resistant group of ten genotypes in the second season (Sennoi et al. 2013b). Although the greenhouse and field data were only moderately correlated, screening under both conditions identified similar resistant genotypes. Based on the information obtained from the greenhouse studies (Sennoi et al. 2013b) and from this field study, HEL293 and JA98 can be used as standard resistant checks, and JA49 can be used as a standard susceptible check in future resistance evaluations.

Some Jerusalem artichoke genotypes performed differently under greenhouse and field conditions. The main reason for these differences is the difference in testing conditions. In the greenhouse experiments, the soil was sterilized, and the plants were inoculated by wounding (Sennoi et al. 2013b), whereas, in this field study, the soil was not sterilized and the plants were inoculated without wounding. Soil microorganisms and wounding might affect the resistance of plants or infection by *S. rolfsii*. Rain, light and humidity also differed. However, in similar pathosystems, plant morphology can affect how some genotypes show resistance under different conditions (Shew et al. 1987; Kim et al. 2000). The identified genotypes in these studies should be used as a source of stem rot resistance and screening of disease resistance should be carried out under field conditions to identify the resistant genotypes correctly.

In this study, environment (soil fertility) affected lesion length, days to permanent wilting and severity index. Soil fertility was the main cause of difference as meteorological conditions were similar between the two fields, and the fields were conducted within a few days. High fertility can favor disease outbreaks. However, application of calcium and nitrogen could reduce disease (Punja et al. 1986). Although environments were different for disease incidence, the correlations between environments were significant for all disease parameters (Fig. 2). Therefore, screening of stem rot disease resistance in Jerusalem artichoke could be conducted in both low fertility and high fertility field conditions.

Days to permanent wilting is a good parameter for screening Jerusalem artichoke for resistance to stem rot

caused by *S. rolfsii*. Previous studies under greenhouse conditions (Sennoi et al. 2010, 2012, 2013b) and field conditions (Junsopa et al. 2016) and this study indicated that days to permanent wilting could clearly identify resistant genotypes of Jerusalem artichoke.

Conclusion

High variations for traits related to stem rot resistance were observed in 40 Jerusalem artichoke genotypes. Based on five disease resistance parameters including disease incidence, lesion length, days to permanent wilting, area under disease progress curve and severity index, these genotypes were classified into three groups. HEL65, HEL246, HEL293, HEL69, JA10, HEL316, JA134 and JA98 were clustered into the resistance group, and these genotypes were also resistant under greenhouse conditions. These genotypes can be used as sources of resistance to Jerusalem artichoke improvement for resistance to *S. rolfsii*.

Acknowledgements The research project was financially supported by the Royal Golden Jubilee Ph.D. Program (jointly funded by Khon Kaen University and the Thailand Research Fund) (grant no. PHD/0110/2554), the Higher Education Research Promotion and National Research University Project of Thailand, Office of the Higher Education Commission, through the Food and Functional Food Research Cluster of Khon Kaen University and the Thailand Research Fund through the Senior Scholar Project of Professor Dr. Sanun Jogloy (RTA 5880003). The Plant Breeding Research Center for Sustainable Agriculture at Khon Kaen University is acknowledged for partially financial support. The authors would like to extend their gratitude to the Thailand Research Fund (TRF) (Project code: IRG5780003), Khon Kaen University (KKU) and the Faculty of Agriculture, KKU for providing financial support for manuscript preparation activities.

References

Anfok GH (2000) Benzo-(1,2,3)-thiadiazole-7-carbothioic acid S-methyl ester induces systemic resistance in tomato (*Lycopersicon esculentum*. Mill cv. Vollendung) to cucumber mosaic virus. Crop Prot 19(6):401–405

Augusto J, Brenneman TB, Culbreath AK, Sumner P (2010) Night spraying peanut fungicides I. Extended fungicide residual and integrated disease management. Plant Dis 04:676–682

Branch WD (1987) Evaluation of peanut cultivars for resistance to field infection by *Sclerotium rolfsii*. Plant Dis 71:268–270

Cilliers AJ, Pretorius ZA, van Wyk PS (2003) Integrated control of *Sclerotium rolfsii* on groundnut in South Africa. J Phytopathol 151:249–258

Diederichsen A (2010) Phenotypic diversity of Jerusalem artichoke (*Helianthus tuberosus* L.) germplasm preserved by the Canadian genebank. Helia 33(53):1–16

Eslami AA, Khodaparast SA, Mousanejad S, Padasht Dehkaei F (2015) Evaluation of the virulence of *Sclerotium rolfsii* isolates on *Arachis hypogaea* and screening for resistant genotypes in greenhouse conditions. HPPJ 8:1–11. doi:10.1515/hppj-2015-0001

Farnworth ER, Modler HW, Mackie DA (1995) Adding Jerusalem artichoke (*Helianthus tuberosus* L.) to weanling pig diets and the effect on manure composition and characteristics. Anim Feed Sci Technol 55(1–2):153–160

Gunnarsson IB, Svensson SE, Johansson E, Karakashev D, Angelidaki I (2014) Potential of Jerusalem artichoke (*Helianthus tuberosus* L.) as abiorefinery crop. Ind Crops Prod 56:231–240

Janket A, Jogloy S, Vorasoot N, Kesmala T, Holbrook CC, Patanothai A (2013) Genetic diversity of water use efficiency in Jerusalem artichoke (*Helianthus tuberosus* L.) germplasm. AJCS 7(11):1670–1681

Junsopa C, Jogloy S, Saksirirat W, Songsri P, Kesmala T, Shew BB, Patanothai A (2016) Inoculation with *Sclerotium rolfsii*, cause of stem rot in Jerusalem artichoke, under field conditions. Eur J Plant Pathol 146:47–58

Kays JS, Kultur F (2005) Genetic variation in Jerusalem artichoke (*Helianthus tuberosus* L.) flowering date and duration. HortScience 40(6):1676–1678

Kays SJ, Nottingham SF (2008) Biology and chemistry of Jerusalem artichoke *Helianthus tuberosus* L. Taylor & Francis, Boca Raton

Khan IH, Javaid A (2015) Chemical control of collar rot disease of chickpea. Pak J Phytopathol 27(01):61–68

Kim S, Kim CH (2014) Evaluation of whole Jerusalem artichoke (*Helianthus tuberosus* L.) for consolidated bioprocessing ethanol production. Renew Energy 65:83–91

Kim HS, Hartmanb GL, Manandharc JB, Graefd GL, Steadmane JR, Diers BW (2000) Reaction of soybean cultivars to sclerotinia stem rot in field, greenhouse, and laboratory evaluations. Crop Sci 40(3):665–669

Koike ST (2004) Southern blight of Jerusalem artichoke caused by *Sclerotium rolfsii* in California. Plant Dis 88:769

McCarter SM, Kays SJ (1984) Disease limiting production of Jerusalem artichoke in Georgia. Plant Dis 68:299–302

Milner JA (1999) Functional foods and health promotion. J Nutr 129:1395S–1397S

Pimsaen W, Jogloy S, Suriharn B, Kesmala T, Pensuk V, Patanothai A (2010) Genotype by environment (g × e) interactions for yield components of Jerusalem artichoke (*Helianthus tuberosus* L.). Asian J Plant Sci 9(1):11–19

Punja ZK, Carter JD, Campbell GM, Rossell EL (1986) Effects of calcium and nitrogen fertilizers, fungicides, and tillage practices on incidence of *Sclerotium rolfsii* on processing carrots. Plant Dis 70:819–824

Puttha R, Jogloy S, Wangsomnuk PP, Srijaranai S, Kesmala T, Patanothai A (2012) Genotypic variability and genotype by environment interactions for inulin content of Jerusalem artichoke germplasm. Euphytica 183:119–131

Puttha R, Jogloy S, Suriharn B, Wangsomnuk PP, Kesmala T, Patanothai A (2013) Variations in morphological and agronomic traits among Jerusalem artichoke (*Helianthus tuberosus* L.) accessions. Genet Resour Crop Evol 60:731–746

SAS Institute (2001) SAS/STAT user's guide, 2nd edn. SAS Institute Inc., Cary

Sennoi R, Jogloy S, Saksirirat W, Patanothai A (2010) Pathogenicity test of *Sclerotium rolfsii*, a causal agent of Jerusalem artichoke (*Helianthus tuberosus* L.) stem rot. Asian J Plant Sci 95:281–284

Sennoi R, Jogloy S, Saksirirat W, Kesmala T, Singkham N, Patanothai A (2012) Levels of *Sclerotium rolfsii* inoculum influence identification of resistant genotypes in Jerusalem artichoke. AJMR 6(38):6755–6760

Sennoi R, Jogloy S, Saksirirat W, Kesmala T, Patanothai A (2013a) Genotypic variation of resistance to southern stem rot of Jerusalem artichoke caused by *Sclerotium rolfsii*. Euphytica 190(3):415–424

Sennoi R, Singkham N, Jogloy S, Boonlue S, Saksirirat W, Kesmala T, Patanothai A (2013b) Biological control of southern stem rot caused by *Sclerotium rolfsii* using *Trichoderma harzianum* and arbuscular mycorrhizal fungi on Jerusalem artichoke (*Helianthus tuberosus* L.). Crop Prot 54:148–153

Serieys H, Souyris I, Gil A, Poinso B, Berville A (2010) Diversity of Jerusalem artichoke clones (*Helianthus tuberosus* L.) from the INRA-Montpellier collection. Genet Resour Crop Evol 57:1207–1215

Shaner G, Finney RE (1977) The effect of nitrogen fertilization on the expression of slow-mildewing resistance in knox wheat. Phytopathology 67:1051–1056

Shew BB, Wynne JC, Beute MK (1987) Field microplot and greenhouse evaluations for resistance to *Sclerotium rolfsii* in peanut. Plant Dis 71:188–191

Singh SP, Gaur R (2016) Evaluation of antagonistic and plant growth promoting activities of chitinolytic endophytic actinomycetes associated with medicinal plants against *Sclerotium rolfsii* in chickpea. J Appl Microbiol 121:506–518

Slavin J (2013) Fiber and prebiotics: mechanisms and health benefits. Nutrients 5:1417–1435

Statistix8 (2003) Statistix8: analytical software user's manual. Tallahassee

Sung M, Seo YH, Han S, Han JI (2014) Biodiesel production from yeast *Cryptococcus* sp. using Jerusalem artichoke. Bioresour Technol 115:77–83

Yildiz G, Sacakli P, Gungor T (2006) The effect of dietary Jerusalem artichoke (*Helianthus tuberosus* L.) on performance, egg quality characteristics and egg cholesterol content in laying hens. Czech J Anim Sci 51(8):349–354

J Food Sci Technol (March 2017) 54(3):698–706
DOI 10.1007/s13197-017-2508-9

ORIGINAL ARTICLE

Fructan:fructan 1-fructosyltransferase and inulin hydrolase activities relating to inulin and soluble sugars in Jerusalem artichoke (*Helianthus tuberosus* Linn.) tubers during storage

Sukanya Maicaurkaew[1] · Sanun Jogloy[2] · Bruce R. Hamaker[3] · Suwayd Ningsanond[1]

Revised: 17 November 2016 / Accepted: 25 January 2017 / Published online: 14 February 2017

Abstract Influences of harvest time and storage conditions on activities of fructan:fructan1-fructosyltransferase (1-FFT) and inulin hydrolase (InH) in relation to inulin and soluble sugars of Jerusalem artichoke (*Helianthus tuberosus* L.) tubers were investigated. Maturity affected 1-FFT-activity, inulin contents, and inulin profiles of the tubers harvested between 30 and 70 days after flowering (DAF). Decreases in 1-FFT activity, high molecular weight inulin, and inulin content were observed in late-harvested tubers. The tubers harvested at 50 DAF had the highest inulin content (734.9 ± 20.5 g kg^{-1} DW) with a high degree of polymerization (28% of DP >30). During storage of the tubers, increases in InH activity (reached its peak at 15 days of storage) and gradual decreases in 1-FFT activity took placed. These changes were associated with inulin depolymerization, causing decreases in inulin content and increases in soluble sugars. As well, decreasing storage temperatures would retain high inulin content and keep low soluble sugars; and freezing at −18 °C would best retard 1-FFT, InH, and inulin changes.

Keywords Fructan · Inulin content · 1-FFT activity · InH activity · Soluble sugars

✉ Suwayd Ningsanond
suwayd@yahoo.com

[1] School of Food Technology, Institute of Agricultural Technology, Suranaree University of Technology, Nakhon Ratchasima 30000, Thailand

[2] Department of Plant Science and Agricultural Resources, Peanut and Jerusalem Artichoke for Functional Food Research Group, Khon Kaen University, Khon Kaen 40000, Thailand

[3] Whistler Center for Carbohydrate Research, Purdue University, West Lafayette, IN 47907, USA

Introduction

Jerusalem artichoke (*Helianthus tuberosus* Linn.) is one of the primary sources for inulin from higher plants. Inulin is a polydisperse fructan which has 2–60 or higher degree of polymerization (DP) with fructosyl units linked by ß (2 → 1) linkages and an end glucose residue (AACC 2009; Coussement 1999). Inulin is used as a raw material for fiber fortification of processed foods, as a prebiotic, a sweetener, substrate for bio-ethanol and in animal feed. In Thailand, this plant is becoming a commercial crop for extraction of inulin as an ingredient in processed foods and health foods. Jerusalem artichoke and chicory have inulin content of >150 g kg^{-1} fresh weight basis (FW) and >750 g kg^{-1} dry weight basis (DW). The DP of inulin varies according to species, cultivar, production conditions, physiological age, and other factors (De Leenheer 1996). As a health-related supplement, inulin is a prebiotic to stimulate the growth of probiotic microorganisms in the intestinal tract and to suppress putrefactive pathogens. As well, inulin is purported to reduce glucose, cholesterol, phospholipids, and triglycerides in blood (Campbell et al. 1997).

Inulin is synthesized in the plant in two steps according to the model of Edelman and Jefford (1968). The initial step is the conversion of two molecules of sucrose into 1-kestose and glucose by sucrose:sucrose 1-fructosyltransferase (1-SST). In the next step, 1-kestose is converted to higher DP inulin by fructan:fructan 1-fructosyltransferase (1-FFT). Thus, 1-kestose is considered to be an important intermediate for the production of inulin. On the other hand, inulin depolymerization takes place by the action of fructan 1-exohydrolase (1-FEH), releasing free fructose, which in turn is used for sucrose synthesis (Itaya et al. 2002). Therefore, 1-SST, 1-FFT, and 1-FEH are key enzymes in inulin metabolism. Inulin hydrolase (InH) is

localized in the cell's vacuole of Jerusalem artichoke tubers and is developmentally regulated. It is low in growing tubers but increases during dormancy and sprouting. During sucrose depletion, InH activity would increase to breakdown fructans, resulting in fructose, sucrose, kestose, and nystose accumulation (Gupta and Kaur 2000).

Inulin content of Jerusalem artichoke tubers depends on climate, growing conditions, and harvest maturity (Saengthongpinit and Sajjaanantakul 2005). After harvest, the tubers have a short storage life because of rapid onset of rotting. Low temperature storage normally helps reduce inulin losses. For most fleshy products, freezing is not used as it can cause cell damages depending on cultivars, seasons, preconditioning, rate of freezing and others factors (Kays and Nottingham 2007).

Changes in inulin profiles, inulin content, 1-FFT activity, and InH activity in Jerusalem artichoke tubers cultivated in the northeast of Thailand during harvest and low temperature storage have not been fully investigated for maximizing commercial value of the crop. This study aimed to identify suitable harvest time and low temperature storage of Jerusalem artichoke tubers for the highest inulin content, and more broadly to conditions to obtain high DP of inulin to increase the value of the produce and its products.

Materials and methods

Plant materials and harvest time

Jerusalem artichoke (*Helianthus tuberosus;* Accession no. CN52867, Name of accession: PGR-2367, Origin: USSR, Genetic resources: the Plant Gene Resource of Canada) used in this work was obtained from the Department of Plant Science and Agricultural Resources, Faculty of Agriculture, Khon Kaen University, Khon Kaen, Thailand. It had high yield and high inulin content (Pimsaen et al. 2010). Jerusalem artichoke tubers were grown at the Khon Kaen University Farm from July to November, 2010. Tubers were harvested at different maturities; 30, 40, 50, 60 and 70 days after flowering (DAF). All tubers were washed to remove soil and soaked in sodium hypochlorite solution (280 ppm available chlorine) for 30 min to reduce microbial load and then rewashed with distilled water. Tubers of 200 g were sampled on the harvest date for fresh tuber analyses. The tubers were peeled, sliced, and freeze dried before milling with an IKA M 20 Universal mill. Each ground sample was passed through a 150 μm sieve. Prepared samples were vacuum-packed in high density polyethylene (HDPE) bags, then kept in an aluminum-laminated polyethylene bag and stored at −20 °C for further analyses of inulin profiles, inulin content, soluble sugars, and 1-FFT activity.

Storage temperature

Jerusalem artichokes were again grown at the Khon Kaen University Farm from September 2010 to January 2011 for the storage study. At 50 DAF, the tubers were harvested, disinfected in sodium hypochlorite solution (280 ppm available chlorine) for 30 min, drained, washed, packed and sealed in polyethylene bags (200 g each), and then kept at different temperatures: −18, 0, 5, 10, 15, and 25 °C. The tubers were stored for 0, 5, 10, 15, 20, 25, and 30 days. Fresh tubers were sampled from each pack for the analyses before the rest was freeze-dried, ground, packed, and stored in the same manner as above. The samples were analyzed for 1-FFT activity, InH activity, inulin, fructose, glucose, sucrose, kestose, and nystose.

Enzyme extraction

Enzyme extraction was conducted according to the method of Henson and Livingston (1996). Thawed Jerusalem artichoke tubers (5 g) were homogenized in 30 mL of ice-cold 10 mM sodium phosphate buffer containing 2 mM dithiothreitol (pH 6.5) using an ACE homogenizer (model AM4), at full speed. Homogenates were squeezed through 3 layers of cheesecloth and centrifuged at 10,000*g* for 20 min. This extraction was conducted in triplicate. Supernatants were then collected and brought to 100 mL with extraction buffer. Aliquots of 12 mL were concentrated to 1 mL via centrifugation at 3000*g* using an Amicon Ultra15-10,000 NMWL filter (Amicon Bioseparation, Millipore, Bedford, MA, USA). Concentrates were diluted to 10 mL with extraction buffer and re-concentrated twice in the same manner. The extracts were used for enzyme assays.

1-FFT activity assay

1-FFT activity was assayed according to the method of Ishiguro et al. (2010). One unit of 1-FFT activity is defined as the amount of the enzyme which catalyzes the fructosyl transfer from 1-kestose to another 1-kestose to synthesize 1 nmol of nystose in 1 min under the following conditions. A mixture of enzyme (100 μL), 0.05 g kg^{-1} 1-kestose solution (200 μL), and McIlvaine buffer (pH 5.5, 200 μL) was incubated at 30 °C for 3 h. The reaction was stopped in boiling water for 10 min. The activity of 1-FFT was calculated from the amount of nystose formed in the filtered supernatant and analyzed by a high-performance anion exchange chromatography unit with a pulsed-amperometric detector (HPAEC-PAD), Dionex BioLC (Sunnyvale, CA, USA) with a CarboPac PA200 column (2 mm × 250 mm) and a guard column. The injection volume was 25 μL using an autosampler (Dionex AS50) and 150 mM sodium hydroxide was used as the eluent at a

flow rate of 0.25 mL min^{-1}. Nystose content was calculated based on the peak areas from the chromatograms, as integrated by the Chromeleon software version 6.2 from Dionex. An appropriate dilution of nystose standard solution was used for calibration.

lnH activity assay

InH activity was determined by the method of Ishiguro et al. (2010). One unit of InH activity is defined as the amount of enzyme which catalyzes the hydrolysis of 1 nmol of inulin in 1 min. A mixture of enzyme (100 μL), 0.05 g kg^{-1} inulin solution (200 μL), and McIlvaine buffer (pH 5.5, 100 μL) was incubated at 30 °C for 5 h. The reaction was stopped in boiling water for 10 min. InH activity was calculated from the amount of fructose released as analyzed by HPAEC-PAD in the same manner, as described above. The amount of free fructose was calculated from peak areas of the chromatograms, calibrated with an appropriate dilution of fructose standard solution.

Determination of inulin contents

Inulin was extracted using hot deionized water according to the method of Raessler et al. (2008) with modification. Each ground sample (500 mg) was weighed in a centrifuge tube. Deionized water (50 mL) was added, and then the tube was shaken in a water bath at 80 °C for 30 min (Raessler et al. 2008). The sample was cooled to room temperature and transferred in to centrifuge tubes before centrifuging at 10,000g for 20 min. After centrifugation, the supernatant (10 mL) was transferred to another centrifugation tube. To this solution, 340 μL of 300 g L^{-1} HCl solution was added before the tube was again placed in a shaking water bath at 85 °C for 60 min to obtain complete hydrolysis of inulin. After cooling to room temperature, the supernatant was transferred to a 50 mL volumetric flask and filled to volume with deionized water. The aliquot was filtered and transferred to sample vials. Products from inulin hydrolysis, i.e. fructose and glucose were analyzed by HPAEC-PAD, as described in 1-FFT activity assay. Peak areas of the chromatograms were used for sugar calculation. An appropriate dilution of a standard solution containing glucose and fructose was used for calibration with subtractive correction for fructose from sucrose. The inulin final content was obtained from 0.91 × fructose.

Determination of inulin profiles

Fresh tubers of 150 g were sampled from each pack and homogenized with a homogenizer (AM4 model, ACE, Nihon Seiki Kaisha Ltd., Tokyo). Inulin was extracted with hot deionized water (Van Waes et al. 1998). Eighty-five grams of deionized water were added to a flask containing 11.5 g homogenized sample, and then the flask was shaken at 130 rpm for 1 h in a hot (85 °C) water bath. After cooling to room temperature, the total weight was adjusted to 100 g with deionized water before the slurry was centrifuged for 20 min at 10,000*g* and then the supernatant was collected and stored at −20 °C until use. Prior to inulin profile analysis, the sample was thawed in a 40 °C water bath. Inulin profiles were obtained from HPAEC-PAD, as described above. Two gradient eluents were 150 mM sodium hydroxide (eluent A) and 150 mM sodium hydroxide/500 mM sodium acetate (eluent B) running at a flow rate of 0.25 mL min^{-1}. The system was equilibrated with eluent A for 10 min before analysis. The elution gradient was programmed at 0–15 min with 100% eluent A, 15–45 min with 0–60% eluent B, 45–90 min with 60–90% eluent B, 90–110 min with 90–100% eluent B, and 110–120 min with 100–0% eluent B. The relative percentage of inulin DPs was calculated from peak areas of the chromatograms, as shown in Fig. 1.

Determination of fructose, glucose, sucrose, kestose, and nystose

Each ground Jerusalem artichoke sample (500 mg) was weighed into a flask. Deionized water (50 mL) was added, and the preparation steps until centrifugation were the same as described in the inulin determination. Supernatants were collected in a 200 mL volumetric flask and filled to volume with deionized water. Aliquots were filtered and transferred to sample vials. Fructose, glucose, sucrose, kestose and nystose were analyzed by HPAEC-PAD, as described above. Sugar contents were calculated from the peak areas of the chromatograms. An appropriate dilution of a standard solution containing glucose, fructose, sucrose, 1-kestose and nystose was used for calibration.

Statistical analysis

Statistical analyses were performed using SPSS version 16 for Windows. Data were analyzed using one-way fixed factor analysis of variance (ANOVA) with Duncan's multiple range test for mean comparison at the significance level of $P < 0.05$.

Results and discussion

Influence of harvest time

Activity of 1-FFT

Activity of fructan:fructan 1- fructoslytransferase (1-FFT) in harvested tubers continuously decreased from 30 to 70

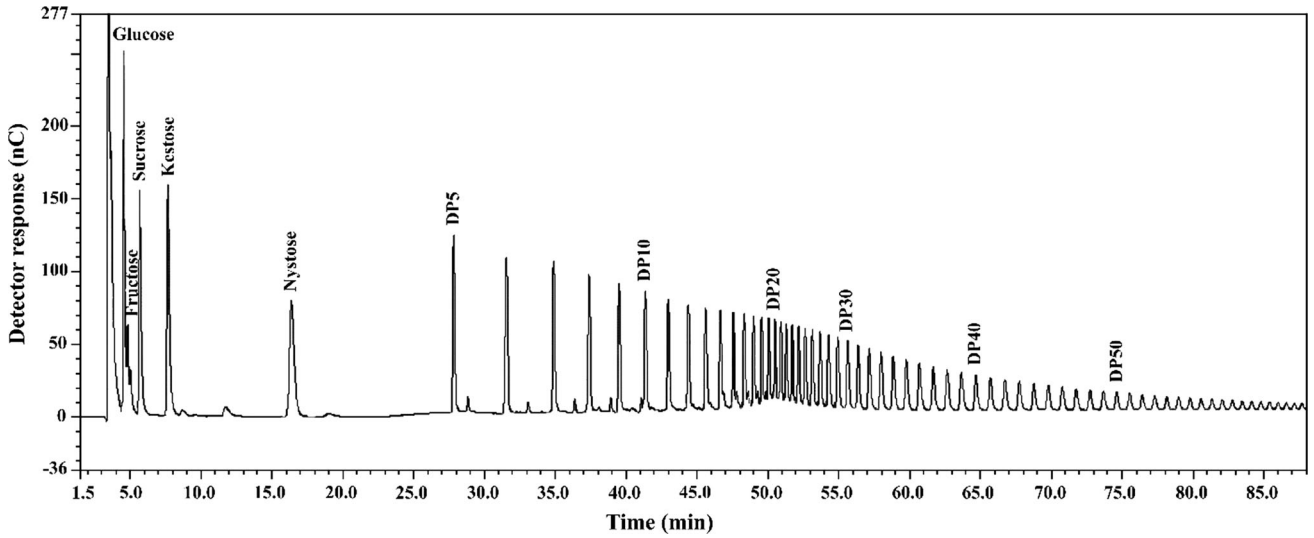

Fig. 1 HPAEC-PAD chromatograms of inulin in Jerusalem artichoke tubers

Table 1 Activity of fructan:fructan 1-fructosyltransferase (1-FFT) and Inulin content in Jerusalem artichoke tubers at different harvest time

Harvest time (DAF)	1-FFT activity (Ug^{-1} DW)	Inulin (g kg^{-1} DW)
30	79.9 ± 5.6^{a}	640.9 ± 15.0^{c}
40	57.0 ± 3.1^{b}	715.6 ± 13.4^{ab}
50	43.3 ± 0.8^{c}	734.9 ± 20.5^{a}
60	35.9 ± 0.6^{d}	710.0 ± 29.9^{ab}
70	28.0 ± 0.6^{e}	681.3 ± 17.8^{b}

Values are the mean ± standard deviation

Different letters indicate significant difference at $P < 0.05$

DAF in a progressively pseudo-linear regression scheme, from 79.9 to 28.0 Ug^{-1} DM (65.0% decrease), as shown in Table 1. From the activity of 1-FFT and inulin content, results suggested that 1-FFT was active before 30 DAF and its remaining activity continued catalyzing the formation of inulin as demonstrated by rising inulin levels until 60 DAF. It was reported that fructan synthesis was controlled by 1-SST and 1-FFT (Edelman and Jefford 1968). The DP of fructans produced by the plant depended mainly on the enzymatic activity of 1-FFT which provided a wide range of DP, from small amounts of short-chain oligomers to large amounts of high-DP fructans (Van Laere and Van Den Ende 2002). In addition, the action of 1-SST and 1-FFT resulted in the formation of fructans with different chain lengths. In Jerusalem artichoke tubers, both 1-SST and 1-FFT were observed to be active during fructan accumulation (Pollock 1986). Starting from sucrose, 1-SST produced 1-ketose which would then be elongated by 1-FFT, resulting in the formation of inulin (Vijn and Smeekens 1999).

Inulin content

Inulin content trended to a peak at 50 DAF with an average of 735 g kg^{-1} DW and gradually decreased in tubers harvested at 60 and 70 DAF (by 7.3% from 50 to 70 DAF) (Table 1). There were no significant differences among inulin contents in tubers harvested during 40–60 DAF, though 50 DAF seemed to be a good harvest time considering that long chain polymerized fructans were also highest at this time point.

Inulin profile

The harvest time for Jerusalem artichoke tubers affected DP of inulin, as shown in Fig. 2a. The inulin profile was significantly different during the period of 30–70 DAF. DP of inulin increased both in proportion and in chain length during 30–50 DAF. The DP >30 relatively reached by 28% at 50 DAF and then decreased with sharp increases in DP <10 at 60 and 70 DAF. The decrease in higher DP

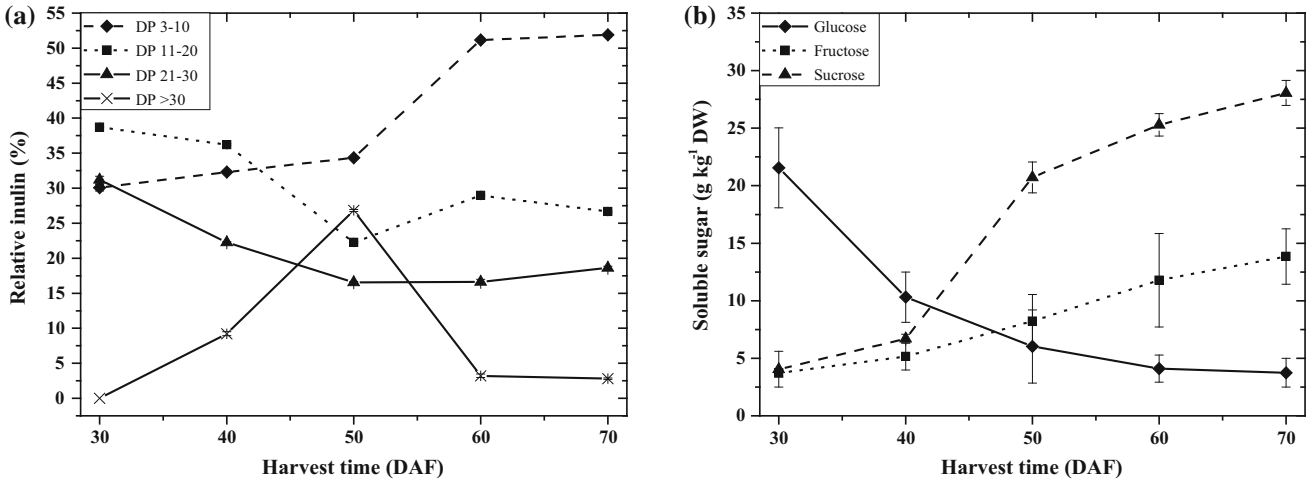

Fig. 2 Inulin profile (**a**), glucose, fructose, and sucrose (**b**) in Jerusalem artichoke tubers at different harvest time

inulin at 60–70 DAF was likely caused by the depolymerization of fructans by fructan 1-exohydrolase (1-FEH) (Edelman and Jefford 1968). Similar changes were reported in Jerusalem artichoke tubers harvested at 56 DAF or 20 weeks maturity (Saengthongpinit and Sajjaanantakul 2005). It was reported that the drying period of Jerusalem artichoke leaves and stems in the field was accompanied by a slight increase in reducing sugars that resulted from depolymerization of high molecular weight carbohydrates (Schorr-Galindo and Guiraud 1997). Results from the present study suggest that tubers harvested at 50 DAF would be preferable for the production of long chain inulin, because the tubers contained the highest DP of fructans among 30–70 DAF harvested tubers.

Soluble sugar content

Soluble sugar contents were significantly different over harvest times (Fig. 2b). After 50 DAF, free glucose decreased while free fructose and sucrose increased. These results were similarly found in more mature (from 16 to 20 weeks) Jerusalem artichoke tubers measured as relative percentage of sugars (Saengthongpinit and Sajjaanantakul 2005). Decreases in free glucose could be explained by its utilization in the respiration process and through metabolic activities of the tubers (Jaime et al. 2000). 1-SST catalyzes the first step of fructan synthesis in the growing tuber, using sucrose as the primary source of the fructosyl donor and releasing free glucose. Thus, glucose usually appears in growing tubers and decreases to a low level in mature tubers.

Increasing in fructose and sucrose at 60 and 70 DAF was coincident with increasing in low DP inulin. This was the result of high molecular weight inulin hydrolysis as shown in Fig. 2a. Jerusalem artichoke tubers use free fructose and sucrose for metabolic activities as glucose substitutes. Changes in soluble sugars were the result of inulin depolymerization catalyzed by 1-FEH and 1-FFT to release free fructose. The released fructose would then be used for the synthesis of sucrose supply to other plant tissues (Itaya et al. 2002).

Changes during low temperature storage

Activity of 1-FFT

Activity of 1-FFT in the tubers harvested at 50 DAF was significantly different over the whole range of temperatures, −18, 0, 5, 10, 15, and 25 °C during 30 days storage (Fig. 3a). Storage at −18 °C provided the highest retention of 1-FFT activity compared with other higher storage temperatures. It should be noted that freezing storage at −18 °C could best maintain 1-FFT activity with gradual decreases in 1-FFT activity during the assigned period. This implied that 1-FFT was still active at this storage temperature. In addition, activity of this enzyme could be further reduced during thawing and storing at higher temperatures above freezing point. The enzyme could be denatured at the ice-liquid interface during freezing due to additional interfacial tension on the entrapped enzyme from ice recrystallization during thawing (Cao et al. 2002). During storage, 1-FFT activity increasingly decreased at high temperatures (Fig. 3a). The higher storage temperature applied led to greater 1-FFT activity loss. The loss of 1-FFT activity at all storage temperatures would be the results of gene 1-FFT transcription and expression affected by soluble sugars changes in the tubers. It was found that carbon deficit in the inulin producing plant, *Chrysolaena obovata* (Less.) Dematt., inhibited transcription of the gene 1-FFT and that sugar supplementation provided negative correlation between 1-FFT activity and gene expression (Trevisan et al. 2015). Supplemented sugars were glucose,

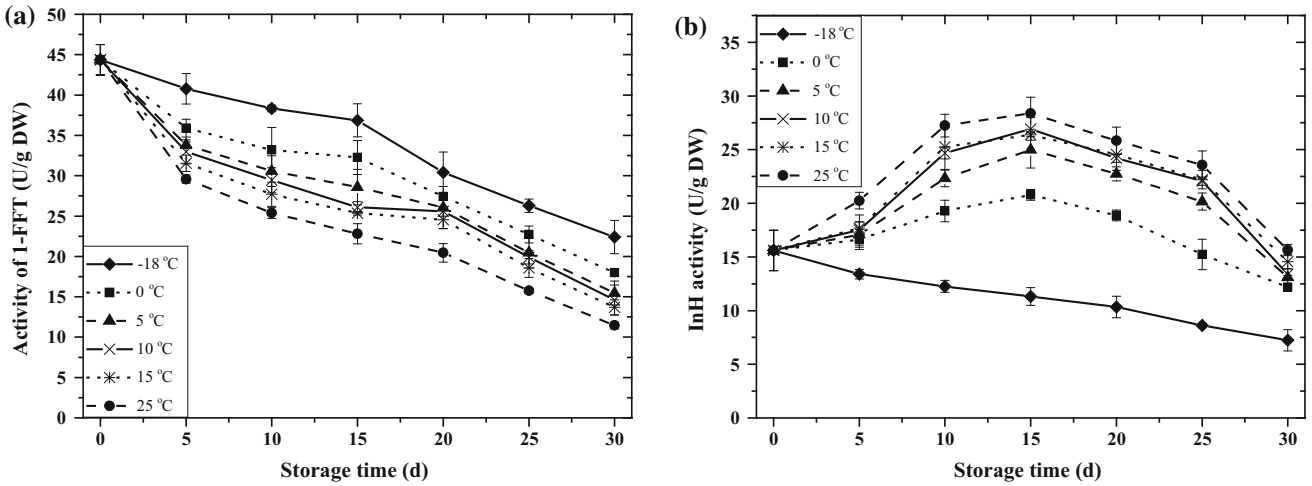

Fig. 3 Activities of 1-FFT (**a**) and InH (**b**) in Jerusalem artichoke tubers stored at different temperatures for 30 days

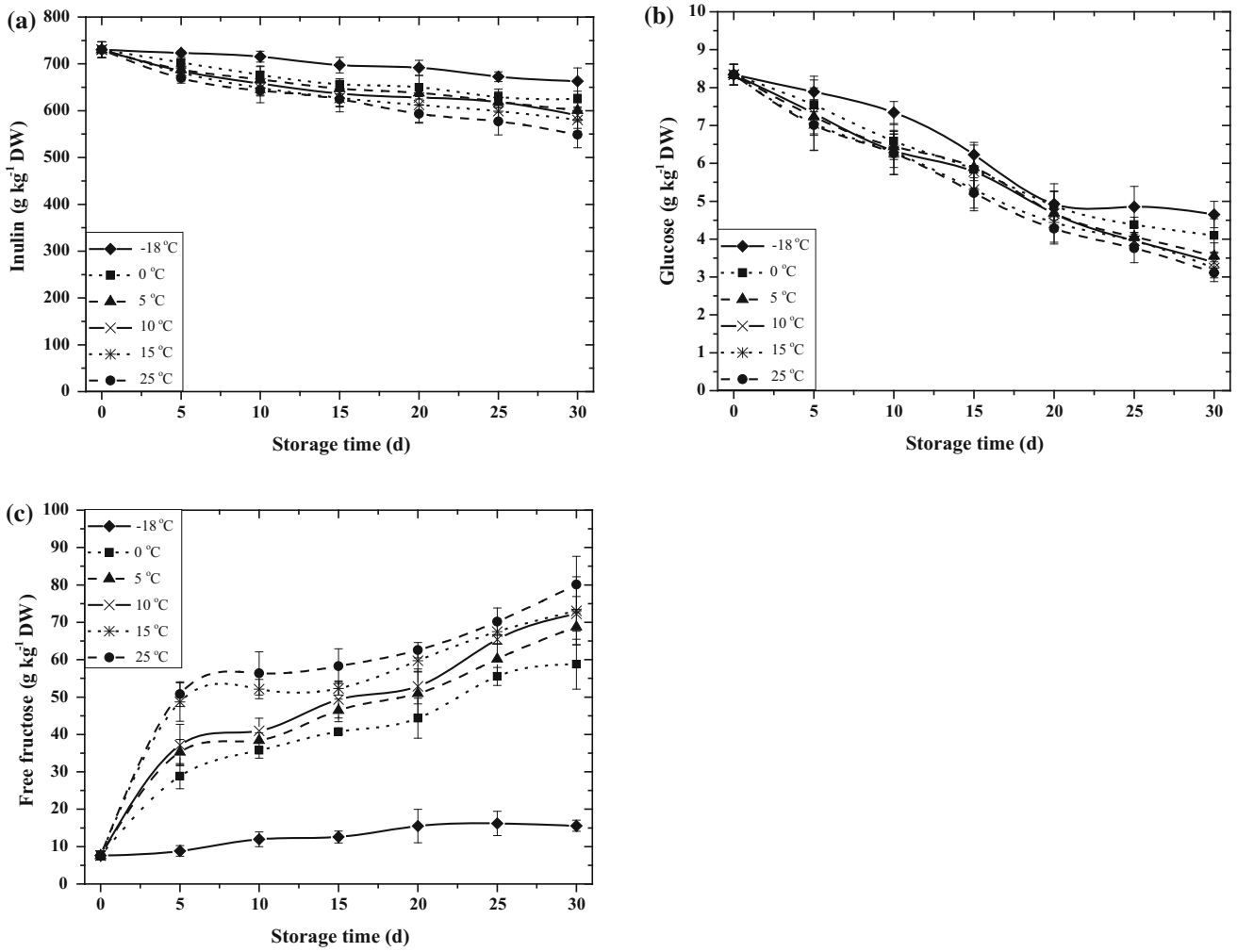

Fig. 4 Inulin content (**a**), glucose (**b**), and free fructose (**c**) in Jerusalem artichoke tubers harvested at 50 DAF and stored at different temperatures for 30 days

fructose, and sucrose, all of which decreased 1-FFT activity. Among these sugars, fructose markedly exhibited 1-FFT activity reduction. Evidently, soluble sugars rise (Figs. 4c, 5a) supported 1-FFT activity loss during storage.

Activity of 1-FFT decreased progressively in a pseudo-linear regression manner as found in fresh tubers during growing. During 30 days storage, 1-FFT activity reduced from 44.4 to 22.4 and to 11.5 Ug^{-1} DM at −18 and 25 °C, respectively. Similar results that the activity of 1-FFT decreased progressively in a pseudo-linear regression scheme were reported in burdock roots stored at 0, 15, and 25 °C (Ishiguro et al. 2010). In Jerusalem artichoke tubers, 1-SST and 1-FFT were active during fructan accumulation (Pollock 1986), though 1-FFT involving both inulin synthesis and hydrolysis decreased during storage (Fukai et al. 1997). At appropriate conditions for synthesis, 1-FFT catalyzes inulin chain elongation. However, depolymerization would be catalyzed by 1-FFT to move fructosyls from the longer-chain inulin to obtain free sucrose (Luscher et al. 1993). In the current work, 1-FFT activity continuously reduced from the first maturity stage being studied (30 DAF) to the end of postharvest storage, but the enzyme was still able to contribute to changes in inulin content.

Activity of InH

Activity of inulin hydrolase (lnH) was significantly different at all temperatures during 30 days storage (Fig. 3b). At −18 °C, lnH steadily lost its activity during storage which was similar to 1-FFT, though was unlike storage at 0, 5, 10, 15, and 25 °C where lnH activity steadily increased over the first 15 days of storage with the maximum increase on day 15 regardless of storage temperature. After InH activity reached its peak, the activity at all storage temperatures on day 25 was higher or similar to day 0. On the other hand, activity of InH progressively increased as storage temperatures increased. Similar results were reported in burdock roots stored in modified atmosphere packaging at 2, 8 and 20 °C where activity of inulinase (InH) also increased sharply after 1 week storage

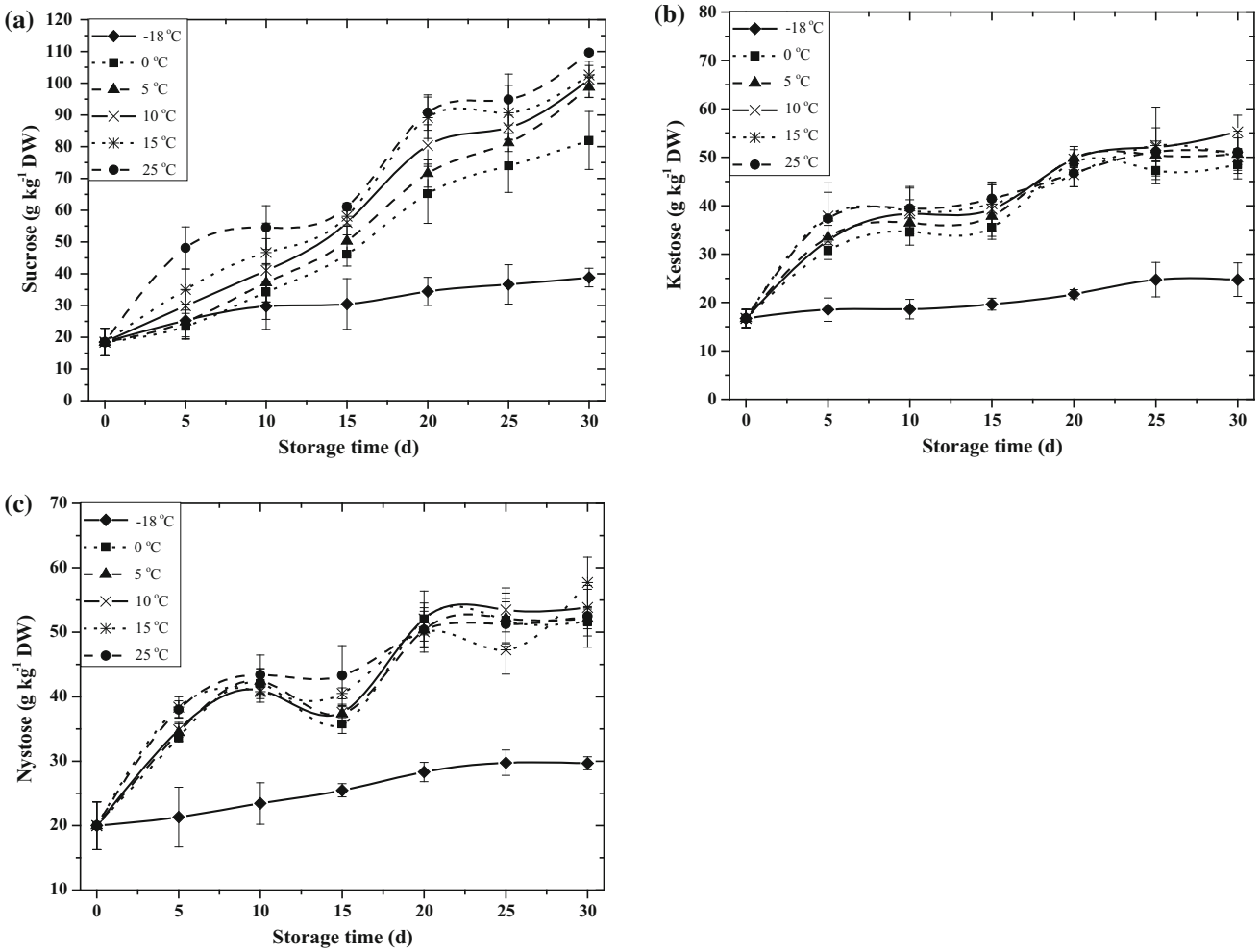

Fig. 5 Sucrose (**a**), kestose (**b**), and Nystose (**c**) in Jerusalem artichoke tubers stored at different temperatures for 30 days

regardless of temperature (Ishimaru et al. 2004). The activity of lnH at the end of 30 days storage changed from 15.6 to 7.2 and to 15.4 Ug^{-1} DW at −18 and 25 °C, respectively. With increased InH activity up to 15 days and relatively high activity at the end of storage, high increases in soluble sugars (fructose, sucrose, kestose, and nystose) were correspondingly observed in the tubers after maximum InH activity. Therefore, InH played an important role in storage changes of sugars in the tubers. This indicated that, storage for first 5 days could maintain quality of the tubers with minimal changes. To avoid high soluble sugars in the tubers, storage should be at 10 °C or below and for no longer than 15 days unless lower DP inulin is desirable for specific uses.

Inulin content

At 50 DAF, inulin content in the Jerusalem artichoke tubers averaged 734.2 g kg^{-1} DW (Fig. 4a). Inulin content varied significantly with different storage temperatures over the 30 days. Jerusalem artichoke tubers stored at −18 °C had the highest content of inulin, though inulin content decreased slightly (9.7% reduction) after 5 days of storage. During storage at 0, 5, 10, and 15, inulin contents only slightly decreased after 5 days, though showed significant loss when stored at 25 °C and linearly reduced to the end of the storage period. Final inulin contents at 30 days were reduced by 14.9, 18.2, 19.6, 20.9, and 25.2% for storage at incremental temperatures between 0 and 25 °C, respectively. This could be due to depolymerization of fructans catalyzed by 1-FEH. Depolymerization of inulin was found to be nearly complete within the first 6 weeks of cold storage and changes in DP of inulin were more pronounced at higher storage temperatures (Rutherford and Weston 2001; Modler et al. 1993). The abiotic stress of low temperature seemed to affect Jerusalem artichoke tubers during the growth period in the same manner. The amount of inulin in overwintered Jerusalem artichoke tubers was found to decrease, because of inulin conversion to sucrose together with forming lower DP inulin (Clausen et al. 2012).

Hydrolysis of inulin is necessary to obtain soluble sugars for metabolic activities of the tubers. Storage at low temperature would slow down respiration rate and delay changes of inulin contents. For long term storage of Jerusalem artichoke tubers, −18 °C would clearly be the best choice.

Soluble sugar content

During 30 days of storage, changes of fructose, sucrose, kestose, and nystose were significantly different at all storage temperatures (Figs. 4b, c, 5a–c). Glucose content gradually decreased during storage whereas fructose, sucrose, kestose, and nystose contents noticeably increased, especially after storage for 15 days except for the −18 °C storage temperature. Increases in fructose and sucrose in the tubers stored at 5 °C for 30 days were similar to those found in mature Jerusalem artichoke tuber stored at the same temperature for 4 weeks, expressed as relative percentage (Saengthongpinit and Sajjaanantakul 2005). Glucose decreased during storage as a result of respiration and metabolic activities of the tubers (Jaime et al. 2001). Increased levels of free fructose, sucrose, kestose, and nystose in the stored tubers could have been caused by inulin hydrolysis as catalyzed by 1-FEH and 1-FFT to produce free fructose and sucrose as glucose substitutes for metabolic activities (Itaya et al. 2002). At low temperature storage, Jerusalem artichoke tubers would be essentially in dormancy and 1-SST activity was found idle, yet 1-FEH was active enough to catalyze the removal of fructosyl residues from the stored fructans, providing sucrose in vacuoles (Gupta and Kaur 2000). However, it is well recognized that enzyme activity is retarded at −18 °C since the majority of water becomes ice which limits movement of the enzyme and its substrates. Slight increase in soluble sugars of the tubers stored at −18 °C would, therefore, be due to the activity of hydrolytic enzymes prior to freezing and during thawing. During storage of the tubers, InH would work in concert with 1-FEH and 1-FFT, resulting in increased soluble sugars. On the basis of fructose released from inulin (Fig. 4c), storage below 10 °C for 10 days would be suitable for controlling the combined effects of these key enzymes.

Conclusion

Jerusalem artichoke tubers harvested at 50 DAF had the highest concentration of inulin and the highest proportion of long chain inulin polymers. Therefore, 50 DAF would be the optimum harvest time for commercial production of the tubers and for industrial uses of inulin. Inulin contents in the tubers were strongly influenced by storage temperatures. During storage of Jerusalem artichoke tubers, inulin depolymerization caused decreases in inulin content associated with increases in fructose, sucrose, kestose, and nystose. These changes were in association with increased InH and decreased 1-FFT activities, indicating high hydrolysis and low synthesis of inulin. Decreasing storage temperatures would slow down the loss of inulin and the rise in soluble sugars, except glucose. Particularly, freezing storage at −18 °C would best minimize changes of inulin contents, soluble sugars, and the activity of 1-FFT and InH.

Acknowledgements This research was supported by Suranaree University of Technology, Suratthani Rajabhat University, Khon Kaen University, Postharvest Technology Innovation Center, the Office of Higher Education, Thailand, and Whistler Center for Carbohydrate Research, Purdue University, USA.

References

AACC International (2009) Approved methods of analysis, 11th Ed, Method 32-31,01 Fructans in foods and food products—ion exchange chromatographic method. AACC International, Minnesota

Campbell JM, Bauer LL, Fahey GC Jr, Hogarth AJ, Wolf BW, Hunter DE (1997) Selected fructooligosaccharide composition of foods and feeds. J Agric Food Chem 45:3076–3082

Cao E, Chen Y, Cui Z, Foster PR (2002) Effect of freezing and thawing rates on denaturation of proteins in aqueous solutions. Biotechnol Bioeng 82:684–690

Clausen MR, Bach V, Edelenbos M, Bertram HC (2012) Metabolomics reveals drastic compositional changes during overwintering of Jerusalem artichoke (*Helianthus tuberosus* L.) tubers. J Agric Food Chem 60:9495–9501

Coussement P (1999) Inulin and oligofructose as dietary fiber: analytical, nutritional and legal aspects. In: Prosky L, Sungsoo Cho S, Dreher M (eds) Complex carbohydrates in foods. Marcel Dekker, New York, pp 203–212

De Leenheer L (1996) Production and use of inulin: industrial reality with a promising future. In: Van Bekkum H, Roper H, Voragen F (eds) Carbohydrates as organic raw materials III. Wiley-VCH Verlag GmbH, Weinheim, pp 67–92

Edelman J, Jefford TG (1968) The mechanism of fructosan metabolism in higher plants exemplified in *Helianthus tuberosus*. New Phytol 67:517–531

Fukai K, Ohno S, Goto K, Nanjo F, Hara Y (1997) Seasonal fluctuations in fructan content and related enzyme activities in yacon (*Polymnia sonchiolia*). Soil Sci Plant Nutr 43:171–177

Gupta AK, Kaur N (2000) Fructan metabolism in Jerusalem artichoke and chicory. Dev Crop Sci 26:223–246

Henson CA, Livingston DP (1996) Purification and characterization of an oat fructan exohydrolase that preferentially hydrolases 2,6-fructans. Plant Physiol 110:639–644

Ishiguro Y, Onoderaa S, Benkebliab N, Shiomia N (2010) Variation of total FOS, total IOS, inulin and their related-metabolizing enzymes in burdock roots (*Arctium lappa* L.) stored under different temperatures. Postharvest Biol Technol 56:232–238

Ishimaru M, Kagoroku K, Chachin K, Imahori Y, Ueda Y (2004) Effects of the storage conditions of burdock (*Arctium lappa* L.) root on the quality of heat processed burdock sticks. Sci Hortic 101:1–10

Itaya NM, Carvalho MA, Figueiredo-Ribeiro RCL (2002) Fructosyltransferase and hydrolase activities in rhizophores and tuberous roots upon growth of *Polymnia sonchifolia* (Asteraceae). Physiol Plant 116:451–456

Jaime L, Martinez F, Martin-Cabrejas MA, Molla E, Lopez-Andreu FJ, Waldron KW, Esteban RM (2000) Study of total fructan and fructooligosaccharide content in different onion tissues. J Sci Food Agric 81:177–182

Jaime L, Martinez F, Martin-Cabrejas MA, Molla E, Lopez-Andreu FJ, Esteban RM (2001) Effect of storage on fructan and fructooligosaccharide of onion. J Agric Food Chem 49:982–988

Kays SJ, Nottingham SF (2007) Storage. In: Kays SJ, Nottingham SF (eds) Biology and chemistry of Jerusalem artichoke. CRC Press, Florida, pp 401–406

Luscher M, Frehner M, Nosberger J (1993) Purification and characterization of fructan:fructan fructosyltransferase from Jerusalem artichoke (*Helianthus tuberosus* L.). New Phytol 123:717–724

Modler HW, Jones JD, Mazza G (1993) Observations on long-term storage and processing of Jerusalem artichoke tubers (*Helianthus tuberosus*). Food Chem 48:279–284

Pimsaen W, Jogloy S, Suriharn B, Kesmala T, Pensuk V, Patanothai A (2010) Genotype by environment (GxE) interactions for yield components of Jerusalem artichoke (*Helianthus tuberosus* L.). Asian J Plant Sci 9:11–19

Pollock CJ (1986) Fructans and the metabolism of sucrose in vascular plants. New Phytol 104:1–24

Raessler M, Wissuwa B, Breul A, Unger W, Grimm T (2008) Determination of water-extractable nonstructural carbohydrates, including inulin, in grass samples with high-performance anion exchange. J Agric Food Chem 56:7649–7654

Rutherford PP, Weston EW (2001) Carbohydrate changes during cold storage of some inulin-containing roots and tubers. Phytochemistry 7:175–180

Saengthongpinit W, Sajjaanantakul T (2005) Influence of harvest time and storage temperature on characteristics of inulin from Jerusalem artichoke (*Helianthus tuberosus* L.) tubers. Postharvest Biol Technol 37:93–100

Schorr-Galindo S, Guiraud JP (1997) Sugar potential of different Jerusalem artichoke cultivars according to harvest. Bioresour Technol 60:15–20

Trevisan F, Oliveira VF, Carvalho MAM, Gaspar M (2015) Effects of different carbohydratesources on fructan metabolism in plants of *Chrysolaena obovata* grown in vitro. Front Plant Sci 6:1–13

Van Laere A, Van Den Ende W (2002) Inulin metabolism in dicots: chicory as a model system. Plant Cell Environ 25:803–813

Van Waes C, Baert J, Carlier L, Van Bockstaele EA (1998) Rapid determination of the total sugar content and the average inulin chain length in root of chicory (*Cichorium intybus* L). J Sci Food Agric 76:107–110

Vijn I, Smeekens S (1999) Fructan: more than a reserve carbohydrate. Plant Physiol 120:351–359

Chiang Mai J. Sci. 2017; 44(1) : 83-93
http://epg.science.cmu.ac.th/ejournal/
Contributed Paper

Rhizobacterial Candidates Isolated from Jerusalem Artichoke (*Helianthus tuberosus* L.) Rhizosphere for Host Plant Growth Promotion

Kamon Sritongon [a,b], Wiyada Mongkolthanaruk [b], Sophon Boonlue [b], Sanun Jogloy [c,d], Darunee Puangbut [c,d] and Nuntavun Riddech*[b]

[a] Graduate school of Microbiology, Faculty of Science, Khon Kaen University, Khon Kaen 40002, Thailand.
[b] Department of Microbiology, Faculty of Science, Khon Kaen University, Khon Kaen 40002, Thailand.
[c] Department of Plant Science and Agricultural Resources, Faculty of Agriculture, Khon Kaen University, Khon Kaen 40002, Thailand.
[d] Peanut and Jerusalem artichoke Improvement for Functional Food Research Group and Plant Breeding Research Center for Sustainable Agriculture, Khon Kaen University, Khon Kaen 40002, Thailand.
*Author for correspondence; e-mail: nunrid@kku.ac.th

Received: 8 April 2015
Accepted: 16 March 2016

Abstract

The objective of this work was to isolate and characterize rhizobacteria from Jerusalem artichoke in order to evaluate their abilities to promote early growth of the plant *in vivo*. Characterization of plant growth promoting activities such as nitrogen fixation, phosphate and potassium solubilization, indole-acetic acid production (IAA), siderophore and phytopathogenic inhibition was conducted. A total of 46 isolates gave positive results for either direct or indirect plant growth promoting activity. Selected stains were identified on the basis of 16s rRNA gene sequences, evaluated individually by being mixed in liquid media which was then used to inoculate pots containing Jerusalem artichoke. Strains identified as *Pseudomonas azotoformans* (N3-903 and C2-114) and *Rhodococcus cercidiphylli* (S1-903) were evaluated in pot experiments under greenhouse conditions. Inoculation of strain C2-114 showed increased shoot dry weight (up to 52.6%), root dry weight (up to 58.5%), and biomass (up to 54.7%). The result of association of IAA activity with plant growth was significant. We provide the first report of plant growth promoting activity by *R. cercidiphylli*. *Pseudomonas* strains has the potential to be use in field-grown Jerusalem artichoke.

Keywords: plant growth promoting rhizobacteria, indole-acetic acid, *Pseudomonas azotoformans*, *Rhodococcus cercidiphylli*

1. Introduction

Jerusalem artichoke (*Helianthus tuberosus* L.) is becoming popular as a new crop in Thailand. Its tuber containing inulin can reduce the risk of colon cancer, by suppressing tumour growth [1]. Moreover, the tuber is a source of novel prebiotic foods for human consumption, bioethanol, fructose syrup and animal feed [2]. Given these promising uses, it is important to

develop sustainable strategies for cultivation, including organic production.

It is possible that organic products can find uses as fertilizers, growth regulators and livestock feed additive, substituting partially or completely for synthetic compounds, and thereby improving agricultural sustainability [3]. Biofertilizers and biological control agents have potential as less damaging substitutes [4]. For example, plant growth promoting rhizobacteria (PGPR) can be a part of new, more ecological based agricultural system [5].

Numerous soil bacteria that prosper in the plant rhizosphere, can enhance plant growth with a plethora of mechanisms; these are known collectively as PGPR [6]. They stimulate plant growth via production of the phytohormones indole-acetic acid (IAA), gibberellins and cytokinins as well as mineral solubilization, asymbiotic nitrogen fixation, antibiosis against phytopathogenic microorganisms, and production of hydrogen cyanide, siderophores as well as antagonistic activity [7]. PGPR is the most important population providing available substrate and mineral exchange into vicinity of root system [8].

Previous research revealed endophytic nitrogen fixing bacteria from the root of Jerusalem artichoke in China [9]. However, there are limitations on use of indigenous microorganisms for enhancement of plant productivity, as PGP activity may vary due to environmental factors including climate, weather, soil characteristics or activity of the indigenous microbes of the soil [7]. Thus, the aim of our work was to 1) discover novel plant growth promoting microbial species associated with the rhizosphere of Jerusalem artichoke and 2) to evaluate the potential of representative strains to act as biofertilizers. To the best of our knowledge, this is the first report of effective PGPR isolated from Jerusalem artichoke in Thailand.

2. MATERIALS AND METHODS

2.1 Isolation and Selection

Samples of soil adhering to Jerusalem artichoke roots were collected from various fields in Thailand during August-September, 2012 and soil was removed by shaking. The 18 rhizosphere soil samples from fields located in Nakhon Ratchasima, Saraburi, Udonthani, Phetchabun and Chaiyaphum provinces were analyzed chemical characters (Table 1). Ten grams of the each sample was transferred to 90 mL in sterile distilled water to shake on a gentle shaker for 10 min. Serial dilutions were spread on soil-extract peptone agar [10]. After that, the petri dishes were incubated at 30°C for 48-72 h. Different characters of colony were selected, then these colonies were purified on nutrient agar (NA) by cross-streak technique and maintained on agar slants at 4-7°C.

2.2 Assays for Direct Plant Growth Promotion Activity

Nitrogen fixation was assayed in Ashbey's nitrogen-free mannitol broth [11], which was dissolved in deionized water before sterilization. National Botanical Research Institute Phosphate medium (NBRIP) agar [12] was used for testing capacity of strains to solubilize tricalcium phosphate. Potassium solubilizing bacteria were detected by Aleksandrov agar supplemented with potassium aluminium silicate powder [13]; a clear zone around the colony, indicated to positive solubilization after 7 days of incubation at room temperature (25 to 30°C). Salkowski's reagent [4] was used to screen for IAA production in nutrient medium broth (NB) (with and without 1 g L^{-1} L-tryptophan) and incubation period was 72 h at room temperature. These experiments were performed in triplicate.

2.3 Assays for Indirect Plant Growth Promotion Assay

Siderophore production: Siderophore production was investigated using chrome

Table 1. Description of the rhizosphere soil samples.

Province	Area	Soil texture	% OM	Total elements (g kg^{-1})			Available elements (mg kg^{-1})		pH[a]	Ec[b] (ds m^{-1})
				N	P	K	P	K		
Nakhon Ratchasima	Mueang Pak Chong	S SL	0.53 2.19	0.33 1.32	0.12 0.44	0.47 0.88	41.92 35.33	107.01 108.45	5.72 7.14	0.30 0.33
Saraburi	Ban Mo	SL	2.99	1.45	0.38	0.89	17.29	414.59	7.67	0.40
Udonthani	Mueang	S	0.64	0.39	0.09	0.40	16.47	34.55	4.42	0.15
Phetchabun	Nam Nao	SL	3.52	1.37	0.33	5.54	8.34	119.48	4.10	0.20
Chaiyaphum	Chulabhorn Dam	LS	2.76	1.15	0.88	1.35	343.78	216.89	4.55	0.41

OM: Organic matter, N: Nitrogen, P: Phosphorus, K: Potassium, S: Sand, SL: Sandy loam, LS: Loamy sand

[a] 1:2 (Soil:Distilled water)

[b] 1:5 (Soil:Distilled water)

azurol S (CAS) agar [14]. Briefly, each isolate was transferred by dissecting needle to the surface of a petri dish containing CAS agar, then incubated overnight for 7 days at 28°C to detect the presence of an orange-yellow halo zone denoting siderophore production.

Antipathogenic fungal assay: A phytopathogenic, isolate of the soilborne fungus *Sclerotium rolfsii* obtained from an infected Jerusalem artichoke in a field at Khon Kaen University, was paired with the rhizosphere inhabiting strains of bacteria on potato dextrose agar (PDA) in dual culturing assays. A PDA disc (5 mm diameter) containing the fungus was placed up at the center of the plate and incubated for 24 h. The candidate bacterial strain was then streaked onto the plate 2 cm away from the center. *Sclerotium rolfsii* cultured alone on PDA served as a control. All Petri dishes were incubated at room temperature for 72 h, after which the percentage of radial growth inhibition of *S. rolfsii* by each candidate strain was calculated using the formula of Sarathambal et al. [15].

2.4 16S rDNA Sequencing and Phylogenetic Tree

Genomic DNA was extracted by using a genomic DNA mini kit (Geneaid Biotech Ltd., Taiwan). Amplification of DNA coding 16S ribosomal RNA regions was carried out by PCR with *Taq* polymerase, using two primers, 20F (5'-GAG TTT GAT CCT GGC TCA G-3'), positions 9-27 and 1500R (5'-GTT ACC TTG TTA CGA CTT-3'), position 1509-1492 [16]. Purified PCR products were directly sequenced with an ABI PRISM® BigDye™ Terminator Ready Reaction Cycle Sequencing Kit (Applied Biosystems). Sequencing of 16s rDNA was obtained by using the primers 27F (5'-AGA GTT TGA TCM TGG CTC AG-3') and 800R (5'-TAC CAG GGT ATC TAA TCC-3'), and addition 518F (5'-CCA GCA GCC GCG GTA ATA CG-3') and 1492R (5'-TAC GGY TAC CTT GTT ACG ACT T-3'). An ABI Prism® 3730XL DNA Sequence (Applied Biosystems) was used for DNA sequencing. The nucleotide sequences derived from all primers were entered to BioEdit (Cap contig assembly). Alignment

algorithm was used for the calculation of pairwise sequence similarity [17], which was implemented on the EzTaxon-e server [18]. The MEGA 5.10 program was applied for phylogenetic trees.

2.5 Quantitative Analysis *in vitro* of Direct Plant Growth Activity

Selected strains were assessed for bio-compatibility using a modified version of the methods of Yu et al. [19]. Each culture was streaked simultaneously across the central culture line of a 9 cm-diameter petri plate, perpendicular to the central culture, for its bio-compatibility on tryptone soya agar (HiMedia®, India) and incubated at 30°C for 48 h. Occurrence of an antagonistic zone at the intersections of cultures inferred bio-incompatibility of the isolates. Individual strain was grown in 50 mL NB in Erlenmeyer flask, cultured on a shaker (150 rpm) for 18 h. The bacterial cells were suspended in distilled water and diluted to 10^8 CFU mL^{-1}. An equal volume of each single inoculum was mixed and used as a mixture suspension. One milliliter of individual and mixture suspensions was transferred to media for quantitative estimations:

Nitrogen fixation: The inoculum was transferred to Ashbey's nitrogen-free broth, and then incubated on a rotary shaker at 30°C for 72 h. Nitrogen content was processed using micro-kjeldahl method and measured with a Flow Injection Analyzer (FIA5012, Tecator, Sweden).

Phosphate and potassium solubilization: For this assay, 40 mL NBRIP broth was added to 125 mL Erlenmeyer flasks and potassium solubilizing ability was detected in Aleksandrov liquid medium supplemented with potassium aluminium silicate as inorganic potassium source. Both experiments were carried out at 30°C for 7 days with a rotary shaker. After incubation, the supernatant was collected and centrifuged twice at 4,000 rpm for 30 min. For quantitation, soluble phosphate in supernatant was measured by the vanadomolybdate method [20]. Solubilized potassium content in the supernatant was estimated in each of the samples by a flame photometry apparatus at 766.5 nm wavelength.

IAA production: The colorimetric quantification procedure was used following the modified method of Ribeiro and Cardoso [4]. One mL of the culture was inoculated in an Erlenmeyer flask (aperture aluminum foil) containing 40 mL NB amended with L-tryptophan (final concentration of 1 g L^{-1}), and incubated at 30°C for 24 h on a rotary shaker (150 rpm). IAA was separated by centrifugation at 4,000 rpm for 30 min, a 1 mL aliquot was then mixed vigorously with an equivalent volume of Salkowski's reagent, and incubated in darkness for 25 min at room temperature. A pinkish color developed, and was quantified using a spectrophotometer (530 nm) against with an IAA standard.

2.6 Plant Material and Pot Experiment

The Kaentawan 50-4 cultivar (JA102×89) of Jerusalem artichoke was used, supplied by Faculty of Agriculture, Khon Kaen University. Young plants were prepared with tubers following the method of Sennoi et al. [21]. One of two true leaves per plant was transplanted to a 14.5 cm-diameter plastic pot filled with nonsterile sandy soil (Table 2). The experiment was conducted in an open-sided greenhouse at the Faculty of Agriculture (Field Crop Division), Khon Kaen University, in March, 2014. It was designed in a randomized complete block with four replications (three pots per unit). Plant biomass (shoot and root dry weight) and height was determined 30 days after transplantation.

Five treatments included both pure and mixed strains and a non-inoculated control treatment was added. Each inoculum mixture was prepared individually in NB, then incubated overnight at 30°C with shaking at 150 rpm.

Table 2. Description of the characteristics of the soil used for potted experiment.

Soil texture	% OM	Total elements (mg kg^{-1})			Available elements (mg kg^{-1})		CEC (cmol kg^{-1})	pH[a]	Ec[b] (ds m^{-1})
		N	P	K	P	K			
sandy soil	0.36	144.02	67.96	291.45	6.02	47.03	2.57	5.5	0.02

OM: Organic matter, N: Nitrogen, P: Phosphorus, K: Potassium, CEC: Cation exchange capacity

[a] 1:2 (Soil:Distilled water)

[b] 1:5 (Soil:Distilled water)

Viable cells were collected by centrifugation at 4,000 rpm for 20 min, washed with sterile distilled water, thoroughly re-washed again and re-suspended in sterile tap water, and adjusted to a final concentration of 10^8 CFU mL^{-1} (equivalent volume of each strain as mixture treatment). An autopipette was used for transferring 5 mL of bacterial inoculum and inoculated into plant; sterile tap water was applied to pots as control.

2.7 Statistical Analysis

Data analysis was conducted with analysis of variance (ANOVA), using STATISTIX 8 software program (Analytical Software, Tallahassee, Florida, USA). The least significant difference (LSD) test was analyzed with separation of means at $P < 0.05$ and $P < 0.01$ for *in vitro* and potted experiments.

3. Results and Discussion

3.1 Characteristics of Bacterial Isolates Exhibiting Plant Growth Promoting Activity

Forty-six isolates exhibited evidence of direct plant growth promotion (Table 3). Of this total, 21 (45.7 %) were able to grow in liquid nitrogen free medium, and were therefore considered to be diazotrophic bacterial isolates. Solubilization of phosphate and potassium occurred for 26 strains (56.5%), whereas 11 (23.9%) colonies grew on Aleksandrov agar. Only eight strains (17.4%) were positive for IAA. Whole isolates possessing direct plant growth promotion activities were used in indirect activity assays (siderophore and antagonistic plant pathogen); results showed >50% inhibition of *S. rolfsii* mycelia growth for S2-801 and U4-90101 on evaluated agar plates and obtained 23 isolates that exhibited a yellow halo zone on CAS agar. Ribeiro and Cardoso [4] reported that rhizosphere microbes had multiple mechanisms for promoting growth of *Araucaria angustifolia*.

3.2 16S rDNA Sequence and Phylogenetic Tree

Rhizobacteria isolates S1-903, C2-114 and N3-903 had multiple functions for promoting plant growth, so we selected these microbes for characterization by 16s rRNA gene sequences. The full sequences analyzed on homology with available sequences deposited in the database, revealing 99.58% similarity of C2-114 and N3-903 with *Pseudomonas azotoformans* in a clade with type strain (Figure 1.). *Pseudomonas azotoformans* has been found in the potato endosphere, and may support to plant growing [22]. PGP attributes of fluorescent *P. azotoformans* such as nitrogen fixation, solubilization of mineral phosphate and sulphur were reported in work of Levenfors et al. [23], and we report here IAA production, potassium solubilization and siderophore production of *P. azotoformans* N3-

Table 3. Characterization of bacterial isolates for nitrogen fixation, phosphate and potassium solubilization, IAA production, siderophore and phytopathogen inhibition.

Isolate	Nitrogen fixation	Phosphate solubilization	Potassium solubilization	IAA production		Siderophores	Antagonism against *S. rolfsii* (% inhibition)
				with L-tryptophan	without L-tryptophan		
H1-607	-	+	-	-	-	-	-
H1-1003	+	-	-	-	-	-	-
H1-702	+	+	-	-	-	-	-
H1-606	+	-	-	-	-	-	-
H1-801	+	-	-	-	-	-	-
H2-801	-	+	-	-	-	-	-
H2-703	-	-	-	+	-	-	-
H2-606	-	-	-	+	-	-	-
H3-603	-	-	-	+	-	+	-
H3-1002	+	-	-	-	-	-	-
P1-50102	-	+	-	-	-	+	-
P1-702	-	+	-	-	-	-	-
P1-5092	+	-	-	-	-	-	-
P1-504	-	+	+	-	-	+	-
P1-5091	+	-	-	-	-	+	-
P1-5071	+	+	-	-	-	+	-
P2-601	+	-	-	-	-	-	-
P2-502	+	-	-	-	-	+	-
P2-508	+	-	-	-	-	-	-
P3-703	+	-	-	-	-	-	-
S1-1002	+	-	-	-	-	-	-
S1-1003	-	-	-	+	-	-	-
S1-903	**+**	**+**	**+**	**+**	**-**	**+**	**30.24**
S2-1003	-	+	-	-	-	-	-
S2-801	+	-	-	-	-	+	52.37
S2-1002	-	+	-	-	-	+	-
S2-802	-	-	+	-	-	-	-
S2-1001	-	+	+	-	-	+	-
U1-805	-	+	+	-	-	+	-
U1-90101	+	-	-	-	-	+	-
U3-80201	-	+	-	-	-	+	-
U3-9021	-	+	-	-	-	+	-

Table3. (Continued).

Isolate	Nitrogen fixation	Phosphate solubilization	Potassium solubilization	IAA production		Siderophores	Antagonism against *S. rolfsii* (% inhibition)
				with L-tryptophan	without L-tryptophan		
U4-90101	-	+	-	-	-	+	50.67
U4-804	+	-	-	-	-	-	-
U4-100202	+	+	-	-	-	-	-
U4-100201	-	+	-	-	-	+	-
C1-112	-	+	+	+	-	+	-
C1-11201	+	-	-	-	-	-	-
C2-110201	-	+	+	-	-	+	-
C2-114	**+**	**+**	**+**	**+**	**-**	**+**	**-**
N1-90101	-	+	-	-	-	+	-
N2-1042	-	+	+	-	-	+	-
N3-904	-	-	+	-	-	-	-
N3-90102	-	+	+	-	-	-	-
N3-906	-	-	+	-	-	+	-
N3-903	**+**	**+**	**+**	**+**	**-**	**+**	**-**

+ or – indicate positive or negative result respectively

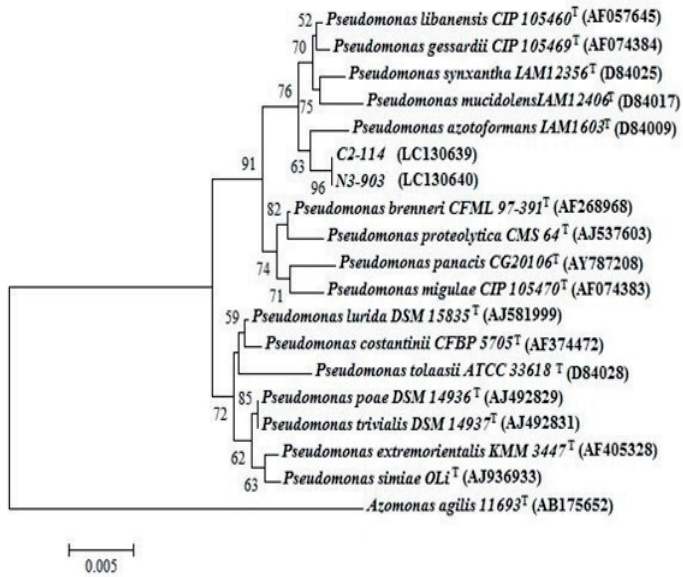

Figure 1. The evolutionary history of C2-114 and N3-903 strains was carried out by using the Neighbor-Joining method with the bootstrap test (1000 replicates) and *Azomonas agilis* 11693^{T} as outgroup.

903 and C2-114. S1-903 had 99.56% similarity *Rhodococcus cercidiphylli* YIM 65003^{T} (Figure 2.). *R. cercidiphylli* first discovered by Li et al. [24] as an endophyte of *Cercidiphyllum japonicum* leaves, was examined as part of research for new bioactive secondary metabolites. This *Rhodococcus* species has not been established in PGPR group. To our knowledge, we present the first evidence that *R. cercidiphylli* displays attributes of PGPR.

Our results showed that *Pseudomonas* sp. was not as antagonistic against *S. rolfsii* under the conditions tested. However, Ahmad et al. [7] found that fluorescent *Pseudomonas* strains had both siderophore synthesis and antagonistic activity against the other fungal phytopathogens *Aspergillus* sp., *Fusarium solani*, *F. ciceri* and *F. oxysporum*. *S. rolfsii*, the causal agent of southern blight, was first reported on Jerusalem artichoke in California, USA [25], and has also caused widespread damage on this crop in Thailand. Future work in our group will focus more explicitly on interaction of PGPR with *S. rolfsii* with the goal of improving southern blight management on Jerusalem artichoke.

3.3 Plant Growth Promoting Activity

There was no evidence of formation of antagonistic zones among strains. Activities of selected bacterial strains in quantitative estimation following screening liquid media showed values (Table 4). We obtained no significant differences among treatments on the amount of available P and K in the crude extract samples. Deceased

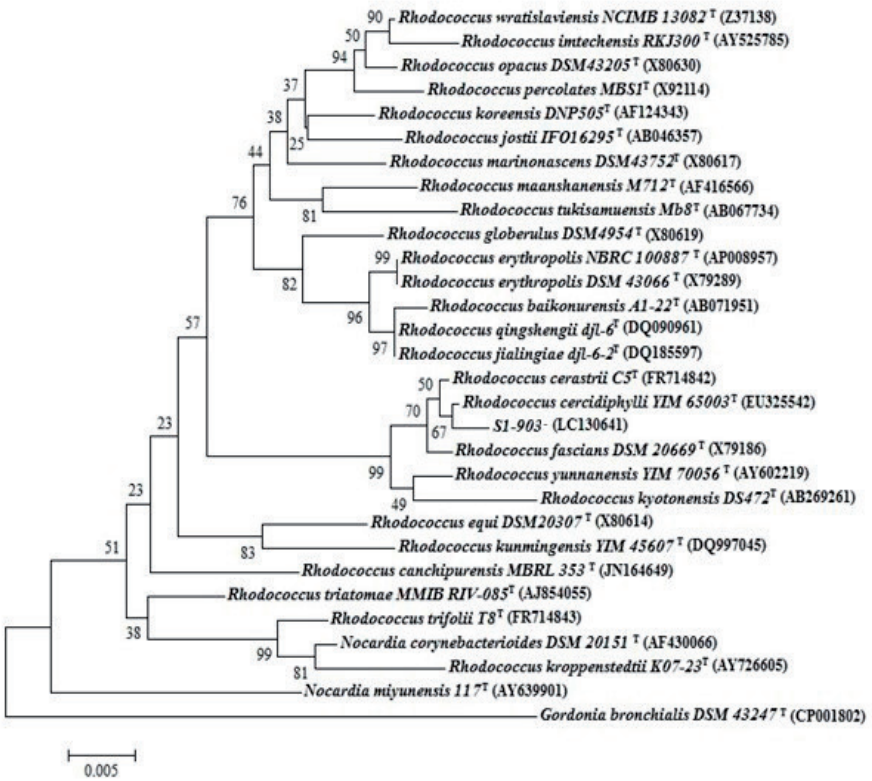

Figure 2. Estimation of the evolutionary history of strain S1-903 was carried out by using the Neighbor-Joining method with the bootstrap test (1000 replicates) and *Gordonia bronchialis* DSM 43247^{T} as outgroup.

Table 4. Plant growth promoting activities of rhizobacterial treatments.

Treatment	Total N ($\mu g\ mL^{-1}$)	Phosphate solubilization		Potassium solubilization		IAA ($\mu g\ mL^{-1}$)
		Available P ($\mu g\ mL^{-1}$)	pH	Available K ($\mu g\ mL^{-1}$)	pH	
P. azotoformans N3-903	11.0 bc	170.68	4.51	4.56	5.02	80.15 a
P. azotoformans C2-114	13.73 ab	169.38	4.60	4.80	5.18	78.75 b
R. cercidiphylli S1-903	17.38 a	166.15	4.26	4.94	5.13	9.81 d
Mixture[a]	6.47 c	174.40	4.58	4.51	5.17	12.38 c
F-test	**	ns		ns		**

[a] Mixture of *P. azotoformans* N3-903*, R. cercidiphylli* S1-903 and *P. azotoformans* C2-114.
ns: non-significant, **: Mean values followed by the different letters in the same column are significant (P<0.01), according to least significant difference (LSD) test .

pH of media was evidence of release of acids that simultaneously increase phosphate and potassium solubilization. Similar results of Hu et al. [13] that described efficiency of mineral solubilizations depending on organic acids and capsule production. Moreover, exopolysaccharide release with the acids (oxalic, gluconic, malic, lactic, citric succinic and fumaric acids) can increase phosphate solubilization activity [26]. Strain S1-903 of *R. cercidiphylli* was shown to excrete more total N in the N free broth than another non-symbiotic nitrogen fixing species (Table 4). Many rhizosphere-associated bacteria act as N fixers that can contribute available nitrogen forms such as ammonium, nitrate and amino acids in N-depleted soils [27]. Both N3-903 and C2-114 *Pseudomonas* strains showed high amount of production of an IAA analog, ranging from 78.74 to 80.15 $\mu g\ mL^{-1}$, which was significantly different (P<0.01) from other treatments in the column (Table 4). It is unclear whether *P. azotoformans* has the ability to produce IAA as no evidence has been reported [23]. The genera *Azospirillum*, *Azotobacter*, *Bacillus*, *Burkholderia*, *Enterobacter*, *Erwinia*, *Pantoea*, *Pseudomonas*, and *Serratia* have been reported as IAA biosynthesizing PGPR by using amino tryptophan [28]. Some microbes (*Azotobacter* spp. and *Pseudomonas* spp.) had IAA production activity without tryptophan [29], but our data on IAA production in the absence on tryptophan showed a negative result.

3.4 Pot Experiment

Inoculation of pots with the *P. azotoformans* strains resulted in significantly (P<0.01) greater root dry weight, shoot dry weight and biomass than the control, whereas *R. cercidiphylli* had no significant impact on growth (Figure 3.). The mixture of the three strains resulted in significantly greater shoot growth but not greater root growth than the control. This association of PGPR-induced IAA levels and biomass accumulation was also observed by Khalid et al. [30]. It was clear that the presence of some PGPR strains enhanced biomass accumulation by Jerusalem artichoke. We found significant positive correlations in IAA production and total nitrogen production of these strains *in vitro* (Table 4) for plant parameters (Table 5); IAA production and root dry weight (r=0.73, P<0.01), shoot dry weight (r=0.48, P<0.05), biomass (r=0.64, P<0.01); total nitrogen related with plant height (r=0.47, P<0.05). In the

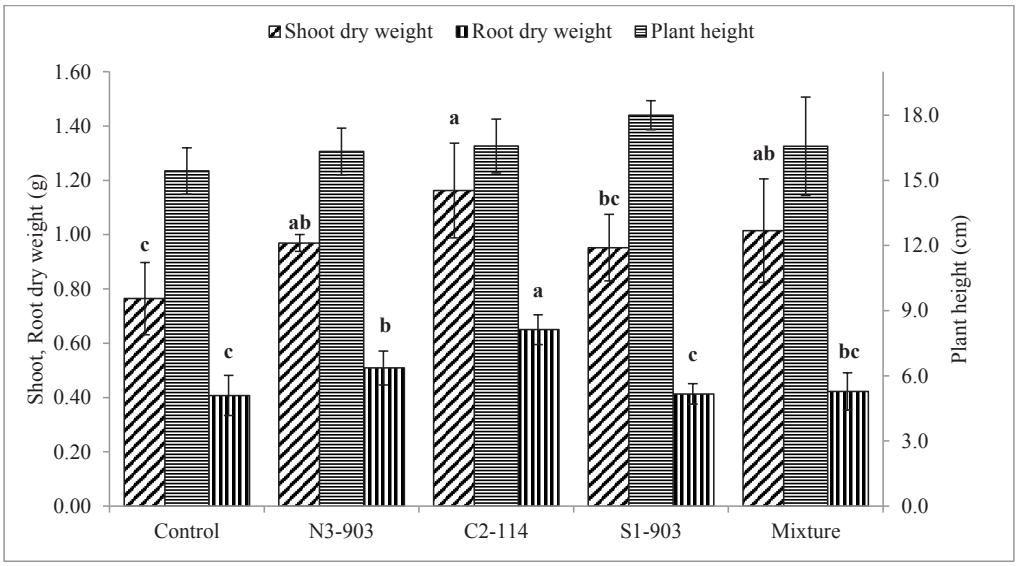

Figure 3. Effect of bacterial treatments (Single inoculum: *P. azotoformans* N3-903; *P. azotoformans* C2-114; *R. cercidiphylli* S1-903; Mixture inoculum: *P. azotoformans* N3-903, *R. cercidiphylli* S1-903 and *P. azotoformans* C2-114) on plant growth parameters of Jerusalem artichoke in pot condition. Bar represents mean ± SD of four replications.

present study, there was a statistically strong association between IAA levels and greater root and shoot development of growth. Similar to Khalid et al. [30] who reported that *in vitro* IAA production correlated with root and shoot growth of wheat. The production of IAA by PGPR enhances plant growth, particularly root development. PGPR may perform via multiple plant growth promoting mechanisms, such as nitrogen fixation and phosphate solubilization, simultaneously with IAA biosynthesis, for plant growth enhancement [7, 15].

4. Conclusion

To our knowledge, we present the first evidence that *R. cercidiphylli S1-903* act as PGPR. *P. azotoformans* C2-114 and N3-903 promoted shoot and root dry weight of Jerusalem artichoke. Thus, these strains could use for development of bio-fertilizer.

Acknowledgments

This work was financially supported by Khon Kaen University. The author would like to gratefully acknowledge Dr. Mark L. Gleason, Department of Plant Pathology and Microbiology, Iowa State University, Ames, Iowa, USA for revision of the manuscript. The authors are grateful for the Thailand Research Fund (TRF) for providing financial support for manuscript preparation through the Senior Research Scholar Project of Professor Dr. Sanun Jogloy (Project no. RTA 5880003).

References

[1] Pool-Zobel B.L., *Br. J. Nutr.*, 2005; **93**: S73-S90. DOI 10.1079/BJN20041349.

[2] Pimsaen W., Jogloy S., Suriharn B., Kesmala T., Pensuk V. and Patanothai A., *Asian J. Plant Sci.*, 2010; **9(1)**: 11-19. DOI 10.3923/ajps.2010.11.19.

[3] Esitken A., Yildiz H.E., Ercisli S., Donmez M.F., Turan M. and Gunes A., *Scientia Horticulturae*, 2010; **124**: 62-66. DOI 10.1016/j.scienta.2009.12.012.

[4] Ribeiro C.M. and Cardoso E.J.B.N., *Microbiol. Res.*, 2012; **167**: 69-78. DOI 10.1016/j.micres.2011.03.003.

[5] Bhattacharyya P.N. and Jha D.K., *World J. Microbiol. Biotechnol.*, 2012; **28**: 1327-1350. DOI 10.1007/s11274-011-0979-9.

[6] Vessey J.K.., *Plant Soil*, 2003; **255**: 571-586. DOI 10.1023/A:1026037216893.

[7] Ahmad F., Ahmad I. and Khan M.S., *Microbiol. Res.*, 2008; **163**: 173-181. DOI 10.1016/j.micres.2006.04.001.

[8] Hartmann A., Schmid M., van Tuinen D. and Berg G., *Plant Soil*, 2009; **321**: 235-257. DOI 10.1007/s11104-008-9814-y**.**

[9] Meng X., Long X., Kang J., Wang X. and Liu Z., *Acta Prataculturae Sinica*, 2011; **20**: 157-163.

[10] Bunt J.S. and Rovira A.D., *J. Soil Sci.*, 1955; **6**: 199-288. DOI 10.1111/j.1365-2389.1955.tb00836.x.

[11] Atlas R.M., *Handbook of Microbiological Media*, 3rd Edn., CRC Press, Boca Raton, 2004.

[12] Nautiyal C.S., *FEMS Microbiol. Lett.*, 1999; **170**: 265-270. DOI 10.1111/j.1574-6968.1999.tb13383.x.

[13] Hu X., Chen J. and Guo J., *World J. Microbiol. Biotechnol.*, 2006; **22**: 983-990. DOI 10.1007/s11274-006-9144-2.

[14] Schwyn B. and Neilands J.B., *Anal. Biochem.*, 1987; **160**: 46-56. DOI 10.1016/0003-2697(87)90612-9.

[15] Sarathambal C., Ilamurugu K., Balachandar D., Chinnadurai C. and Gharde Y., *Appl. Soil Ecol.*, 2015; **87**: 1-10. DOI 10.1016/j.apsoil.2014.11.004.

[16] Kawasaki H., Hoshino Y., Hirata A. and Yamasato K., *Arch. Microbiol.*, 1993; **160**: 358-362. DOI 10.1007/BF00252221.

[17] Myers E.W. and Miller W., *Comput. Appl. Biosci.*, 1988; **4**: 11-17. DOI 10.1093/bioinformatics/4.1.11.

[18] Kim O.S., Cho Y.J., Lee K., Yoon S.H., Kim M., Na H., Park S.C., Jeon Y.S., Lee J.H., Yi H., Won S. and Chun J., *Int. J. Syst. Evol. Microbiol.*, 2012; **62**: 716-721. DOI 10.1099/ijs.0.038075-0.

[19] Yu X., Liu X., Zhu T.H., Liu G.H. and Cui M., *Eur. J. Soil Biol.*, 2012; **50**: 112-117. DOI 10.1016/j.ejsobi.2012.01.004.

[20] Barton C.J., *Anal. Chem.*, 1948; **20**: 1068-1073. DOI 10.1021/ac60023a024.

[21] Sennoi R., Jogloy S., Saksirirat W., Kesmala T. and Patanothai A., *Euphytica*, 2012; **190**: 415-424. DOI 10.1007/s10681-012-0813-y.

[22] Andreote F.D., de Araújo W.L., de Azevedo J.L., van Elsas J.D., da Rocha U.N. and van Overbeek L.S., *Appl. Environ. Microbiol.*, 2009; **75**: 3396-3406. DOI 10.1128/AEM.00491-09.

[23] Levenfors J., Welch C.F., Fatehi J., Wikstrom M., Rasmussen S. and Hökeberg M., *United States Pat. No.* US 20130005572 A1 (2013).

[24] Li J., Zhao G.Z., Chen H.H., Qin S., Xu L.H., Jiang C.L. and Li W.J., *Syst. Appl. Microbiol.*, 2008; **31**: 108-113. DOI 10.1016/j.syapm.2008.03.004.

[25] Koike S.T., *Plant Dis.*, 2004; **88**: 769. DOI 10.1094/PDIS.2004.88.7.769B.

[26] Yi Y., Huang W. and Ge Y., *World J. Microbiol. Biotechnol.*, 2008; **24**: 1059-1065. DOI 10.1007/s11274-007-9575-4.

[27] Richardson A.E., Barea J.M., McNeill A.M. and Prigent-Combaret C., *Plant Soil*, 2009; **321**: 305-339. DOI 10.1007/s11104-009-9895-2.

[28] Dastager S.G., Deepa C.K. and Pandey A., *Plant Physiol. Biochem.*, 2010; **48**: 987-992. DOI 10.1016/j.plaphy.2010.09.006.

[29] Ahmad F., Ahmad I. and Khan M.S., *Turk. J. Biol.*, 2005; **29**: 29-34.

[30] Khalid A., Arshad M. and Zahir Z.A., *J. Appl. Microbiol.*, 2004; **96:** 473-480. DOI 10.1046/j.1365-2672.2003.02161.x.

Cah. Agric. 2017, 26, 25001

DOI: 10.1051/cagri/2017006

Cahiers Agricultures

Available online at:
www.cahiersagricultures.fr

Les agricultures face au changement climatique.
Coordonnateur : Emmanuel Torquebiau

RESEARCH ARTICLE / ARTICLE DE RECHERCHE

OPEN ACCESS

Long-term change in rainfall distribution in Northeast Thailand: will cropping systems be able to adapt?

Guillaume Lacombe[1,*], Anan Polthanee[2] and Guy Trébuil[3]

[1] International Water Management Institute (IWMI), Southeast Asia Regional Office, PO Box 4199, Vientiane, Lao Democratic People's Republic
[2] Department of Plant Science and Agricultural Resources, Faculty of Agriculture, Khon Kaen University, Khon Kaen 40002, Thailand
[3] Centre de coopération internationale en recherche agronomique pour de développement (Cirad), UMR innovation, 34398 Montpellier cedex 5, France

Abstract – Climate vagaries and the lack of irrigation, frequently combined with coarse-textured sandy and unevenly distributed saline soils, explain low crop yields and the endemic relative poverty of the rural population in Northeast Thailand (NET). Local and regional trends in agriculturally-relevant rainfall variables were investigated using the Mann-Kendall test, modified to account for serial correlation, and applied to 17 stations across NET, and the regional average Kendall's statistic. Limited changes in rainfall frequency, intensity and seasonality are observed at individual stations over the study period (1953–2004). But we found a significant regional trend toward a wetter dry season. Based on an intimate knowledge of the local farming systems, we discuss the cropping systems adaptation to these rainfall changes. If the wetting of the dry season extends in the future, as expected according to most climate projections, households would not find it difficult to adapt, except for the problems caused by temperature rise, mainly due to their renowned adaptive capacity and high mobility that historically produced diverse and resilient rural livelihood systems.

Keywords: climate change adaptation / cropping systems / rainfall patterns / Thailand / trend

Résumé – Évolution de la pluviométrie au Nord-Est de la Thaïlande : les systèmes de culture pourront-ils s'adapter ? Les irrégularités climatiques combinées à des conditions édaphiques défavorables expliquent les faibles rendements agricoles du Nord-Est de la Thaïlande, la région la plus pauvre du pays où l'agriculture est majoritairement non irriguée. Des tendances locales et régionales sont recherchées dans des variables pluviométriques contrôlant la production agricole. Une version modifiée du test de Mann-Kendall prenant en compte l'autocorrélation est appliquée aux chroniques de 17 stations dans cette région. La statistique régionale moyenne de Kendall est utilisée pour les tests régionaux. Quasiment aucune tendance locale n'est observée dans la fréquence, l'intensité et la saisonnalité des pluies sur la période d'étude (1953–2004). En revanche, la saison sèche est devenue significativement plus pluvieuse à l'échelle régionale. La capacité des systèmes de culture locaux à s'adapter à ce changement climatique est discutée. Si, comme la plupart des modèles climatiques le prévoient, l'augmentation des pluies de saison sèche se confirme dans le futur, les agriculteurs n'éprouveront probablement pas de difficultés pour s'y adapter, à l'exception des problèmes liés à l'augmentation des températures. Leur capacité d'adaptation, forgée par des siècles de pratiques agricoles en régime pluvial incertain, et le recours aux migrations saisonnières ont permis l'établissement de systèmes agraires diversifiés et résilients.

Mots clés : adaptation aux changements climatiques / système de culture / régime de précipitation / Thaïlande / tendance

* Corresponding author: g.lacombe@cgiar.org

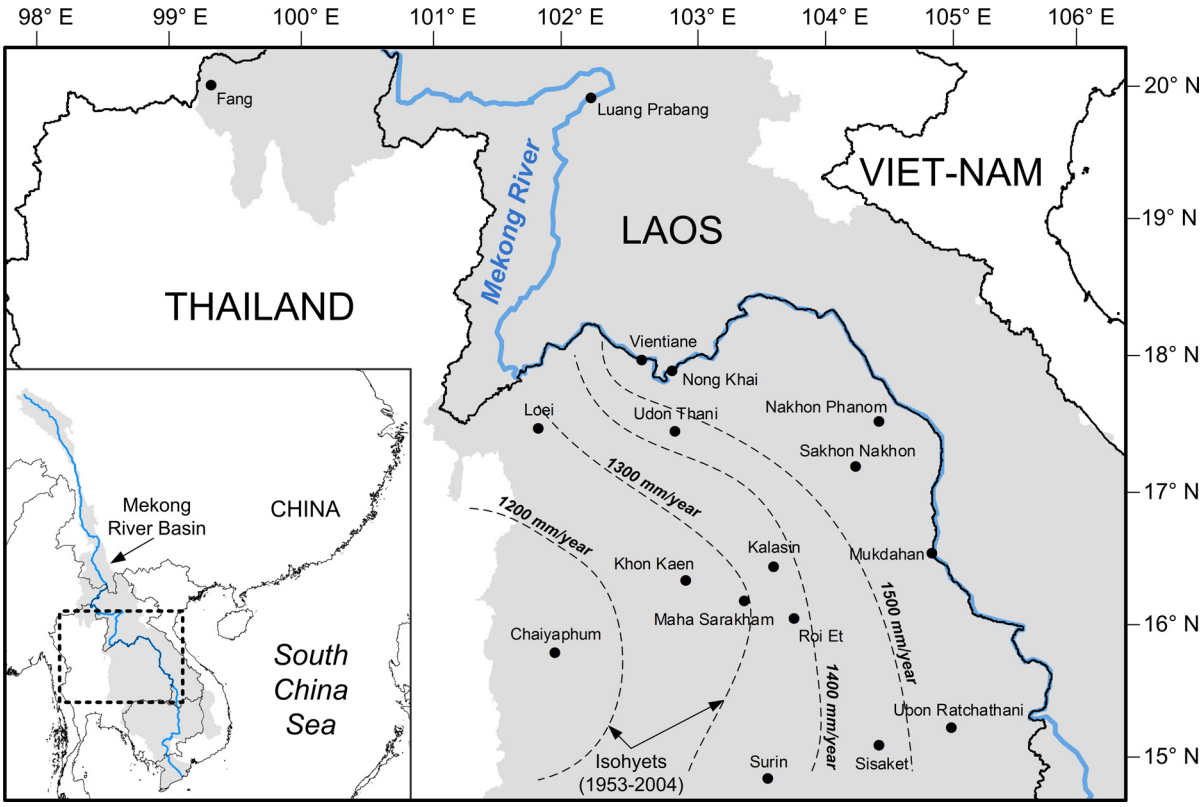

Fig. 1. Study area and location of the rainfall stations.
Fig. 1. *Région d'étude et emplacement des stations pluviométriques.*

1 Introduction

Globally, climate change is expected to have tremendous effects on agriculture through changes in temperature, rainfall patterns, and the frequency and intensity of extreme weather events (IPCC, 2014). While temperature projections exhibit consistencies between climate models, rainfall projections are still contradicting in many instances, despite significant improvements in climate sciences and computational capacity (Knutti and Sedlacek, 2013). Although the Mekong is one of the few large basins where climate models perform best in reproducing the monsoon, there is an overall uncertainty in projections of the Southeast Asian summer monsoon (Hasson *et al.*, 2016). Against this background, insights into historical rainfall are necessary for both agricultural and water development planning. Detection of trends in rainfall time series is not straightforward, particularly in the Mekong where historic records are scarce, and rainfall generating mechanisms are complex (Hasson *et al.*, 2013). The objectives of this study were thus to assess local and regional trends in agriculturally-relevant rainfall variables over the last half century in Northeast Thailand (NET), which is the Mekong sub-region where the longest rainfall records are available, and infer future challenges for cropping systems adaptation.

2 Study area

NET covers one third of the kingdom and is home to about 21 million inhabitants (Fig. 1). It is a sandstone plateau undulating between 100 and 500 m above sea level, characterized by erratic rainfall and poor coarse-textured sandy and unevenly distributed saline soils leading to low crop yields and endemic rural population poverty. About 80% of the population live in rural areas, mainly from agriculture and remittances received from millions of seasonal and permanent migrants.

2.1 Climate

Due to the Southeast Asian summer monsoon blowing humid air masses from the Indian Ocean, the rainy season concentrates about 80–90% of annual rainfall between May and October. The dry season caused by the East Asian winter monsoon brings dry and cold northeasterlies wind from November to April. The occurrence of the rainy season onset mainly relates to the surface temperature of the Pacific and Indian Oceans (Singhrattna *et al.*, 2005). The multi-decadal variability of rainfall is partly due to the El Niño–Southern Oscillation (Räsänen and Kummu, 2013) and the North Pacific Oscillation (Wang *et al.*, 2007).

2.2 Cropping systems

The staple food crop in NET is aromatic rainfed lowland rice (RLR) making 75% of the paddy area in the country, 95% of it being located in NET where only 7% of the farm land has access to irrigation (OAE, 2011). A single RLR cycle is performed annually with rice seedlings prepared in May and transplanted when there is sufficient amount of ponded water in the fields (Fig. 2). Typical problems possibly occurring during the same

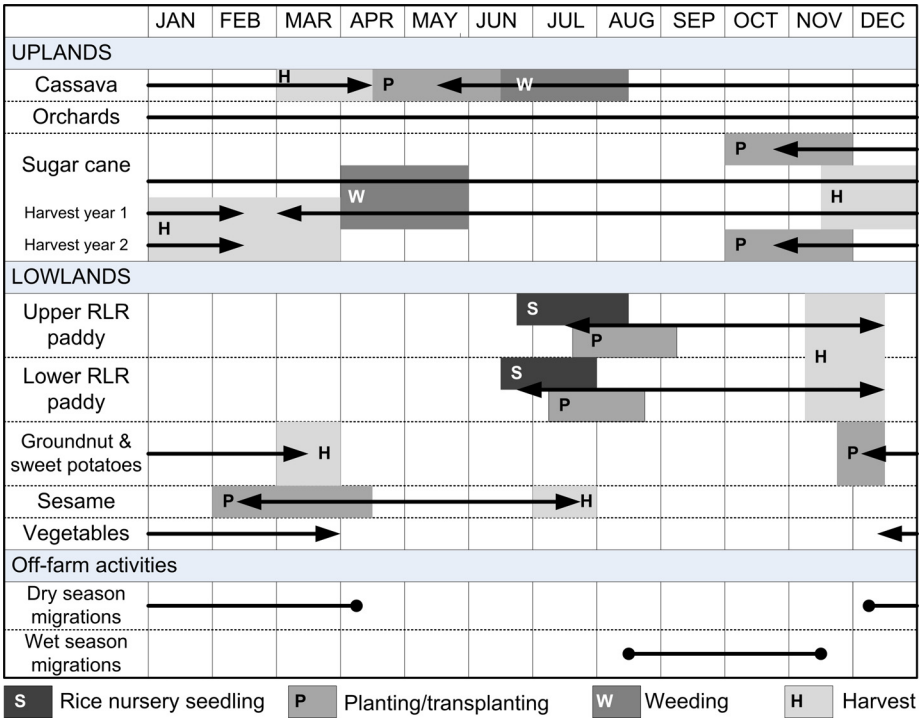

Fig. 2. Calendars of major crops in Northeast Thailand, adapted from Barnaud (2002) and Devillers and Cousinou (2003).
Fig. 2. *Calendriers des principaux cycles culturaux dans le Nord-Est de la Thaïlande, adapté de Barnaud (2002), et Devillers et Cousinou (2003).*

crop year include dry spells in the early rainy season and deep flooding at the peak of the wet monsoon in September. Farmers usually sow several rice seedling nurseries at different dates and elevations to minimize risks of total crop failure. If the rainy season is delayed or too weak, farmers do not transplant rice but practice direct-seeding, which produces lower yields mainly due to weed infestation (Sanusan *et al.*, 2010). Double cropping systems are limited to groundnut and sweet potato after RLR, and sesame before RLR (Polthanee and Marten, 1986). While the initial stage of the cycle (December–January) relies on residual soil moisture, light rainfall during the second part (February–March) provides yields up to 2 and 6 t.ha^{-1} for groundnuts and sweet potatoes, respectively (Polthanee, 1991). Sesame, planted between February and April, and harvested in late July, relies on a mix of residual moisture from the previous rainy season and pre-rainy season light rainfall (Fig. 2). These double-cropping systems tend to be abandoned because of unfavourable climatic constraints including erratic rainfall, especially during the earliest stages of the rainy season, and rising temperature depleting soil moisture through increased evapotranspiration (Polthanee and Marten, 1986; Polthanee and Promkhambut, 2014).

The main industrial crops are sugarcane and cassava. Sugarcane is usually located above the paddies where the soil productivity is too low for RLR. It is planted at the end of the rainy season when the soil moisture decreases but still allows ploughing with reduced efforts. The development then stops at the peak of the dry season. Harvest extends from December to March. Ratooning starts as soon as there is enough water after harvest (mostly in April) and can last two years allowing two additional harvests. Cassava is usually preferred to sugarcane in water deficient areas on sandy soils because of its higher drought-tolerance (Polthanee *et al.*, 2014). A diverse range of mainly vegetable and horticultural crops are traditionally planted on the bank of rivers after water recedes at the end of the rainy season. This small-scale dry season production is for home-consumption and local markets (Fig. 2).

The conversion of forest to RLR began centuries ago in lowland areas. In 1950, forests covered more than half of NET (Sutthipibul, 1987). Thereafter, deforestation extended to upland areas where cash crops stimulated the emerging market economy. In 2009, 36% of NET was covered by RLR, 16% by forest, 10% by annual crops, 4% by tree plantations, most of the remaining land being non-agricultural surface (MOA, 2010). Despite the lack of scientific evidence, the rapid deforestation that occurred over the last half century is often blamed as a major cause for the recurrent droughts that have been faced by farmers in the region.

3 Material and methods

3.1 Rainfall variables

Quality-controlled daily rainfall time series were provided by the Mekong River Commission for 17 stations in NET covering the period January 1953–December 2004 (Tab. 1). Thirty annual variables were derived from the daily data to capture the main climate features that control rainfed agricultural production. They are grouped into five categories.

3.1.1 Timing of the rainy season (variables 1 to 3)

These variables correspond to the ordinal dates (number of days since January 1st) of the onset and retreat of the

Table 1. Rainfall stations.
Tableau 1. *Stations pluviométriques.*

Stations	Latitude North	Longitude East	Elevation m	Mean annual Rainfall (mm)
Chaiyaphum	15°48′	101°51′	250	1,133
Fang	19°58′	99°14′	470	1,312
Kalasin	16°26′	103°31′	142	1,344
Khon Kaen	16°20′	102°51′	157	1,220
Loei	17°27′	101°44′	251	1,238
Luang Prabang	19°53′	102°08′	301	1,297
Maha Sarakham	16°11′	103°18′	150	1,219
Mukdahan	16°32′	104°44′	138	1,500
Nakhon Phanom	17°30′	104°20′	140	2,289
Nong Khai	17°52′	102°45′	173	1,597
Roi Et	16°03′	103°41′	140	1,375
Sakhon Nakhon	17°10′	104°09′	160	1,563
Sisaket	15°07′	104°20′	124	1,478
Surin	14°53′	103°29′	145	1,347
Ubon Ratchathani	15°15′	104°53′	127	1,596
Udon Thani	17°26′	102°46′	178	1,434
Vientiane	17°57′	102°31′	170	1,625

rainy season (variables 1 and 2, respectively), and of the first day of the rainiest 5-day period (variable 3), which coincides, with the rainfall peak of the rainy season. The onset of the rainy season was defined as the first day of the first 10-day period that meets two conditions: the 10-day rainfall depth is higher than the mean 10-day rainfall depth averaged over the period 1953–2004, and at least two of the next three 10-day periods satisfy the first condition. Because of the high rainfall variability, the variations between consecutive 10-day rainfall depths were first smoothed by a 3-time-step moving average. The retreat of the rainy season was defined by symmetrical conditions, starting from the end of the calendar year and moving backward through the 10-day periods. Figure 3 in Lacombe *et al.* (2012) illustrates how variables 1 and 2 are defined. Farming practices and crop yields are closely related to the occurrence of the rainy season, particularly its onset. A delayed rainy season onset may result in delayed transplanting of RLR seedlings or poor emergence and early vegetative growth of crops. A delayed retreat of the rainy season may result in excess soil moisture before and during rice harvest with risks of yield and grain quality losses.

3.1.2 Extreme events (variables 4 and 5)

Variable 4 is the total rainfall depth of the rainiest 5-day period. Variable 5 corresponds to the greatest number of consecutive rainy season days with less than 1 mm of rainfall per day. It reflects farmers' drought definition, which associates drought to extended dry spells during the wet season (Amir Faisal *et al.*, 2014). These extreme events create anoxic conditions through prolonged flood submersion, or drought stress, reducing crop yields.

3.1.3 Intensity index (variable 6)

The intensity index is the number of rainiest days that cumulate 67% of annual rainfall depth (Sun *et al.*, 2006). A low index is associated to a rainfall pattern with few but heavy rainy days while a large index reflects a more regular distribution of rain events in the year.

3.1.4 Seasonal rainfall depths (variables 7 to 18)

These 12 variables correspond to the cumulative rainfall depth for different pairwise associations of three periods (whole year, rainy season and dry season) and four ranges of daily rainfall depths (whole range, low, medium and high rainfall). The low, medium and high ranges of daily rainfall were determined so that the cumulative daily rainfall depths within each of these three ranges are the same over the study period.

3.1.5 Seasonal numbers of rainy days (variables 19 to 30)

These 12 variables correspond to the number of rainy days (rain >1 mm/day) for the similar pairwise combinations of periods and daily rainfall ranges as those defined for variables 7–18.

3.2 Local and regional trend tests

Each of the 510 annual time series (30 variables at 17 stations) were tested for the presence of trends with the Mann-Kendall test (Mann, 1945; Kendall, 1975), one of the most frequently used trend detection tests applied to hydro-meteorological time series. This non-parametric test is robust as it does not require the data to follow any particular statistical

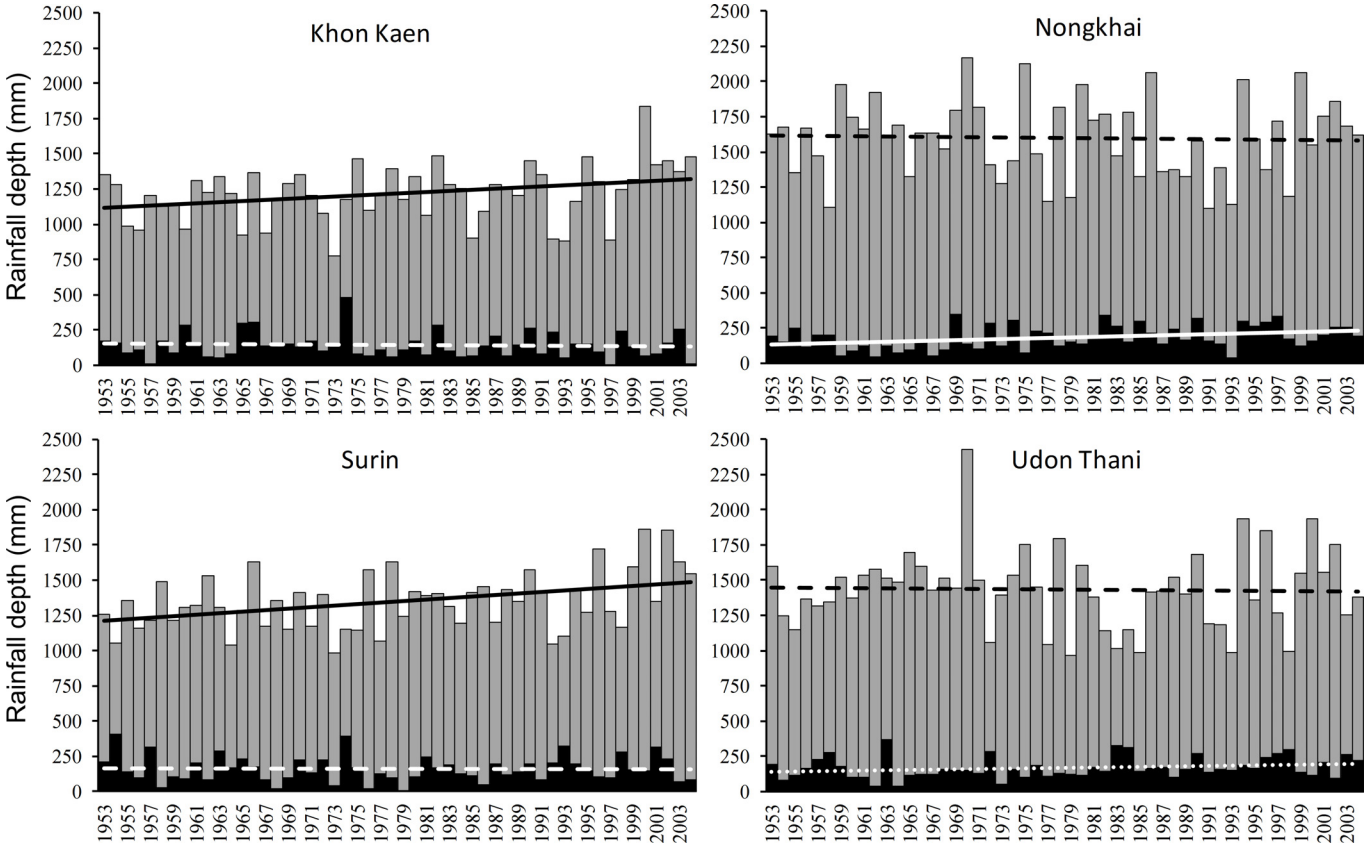

Fig. 3. Time series for annual (grey) and dry season rainfall (black). Solid trend line is significant at 95% confidence level. Dotted trend line is significant at 90% confidence level. Dashed trend line is statistically insignificant.

Fig. 3. *Chroniques des pluies annuelles (gris) et de saison sèche (noir). Ligne continue : tendance significative au seuil de 95 %. Ligne pointillée : tendance significative au seuil de 90 %. Ligne en tirets : tendance non significative.*

distribution and it has low sensitivity to outliers. A modified version of this test (Hamed, 2008) was used to account for possible auto-correlations and to minimize the related overestimation of trend significance. Trend slopes were calculated with the Sen's slope estimator (Sen, 1968).

This modified Mann-Kendall test determines whether a trend exists locally but does not confirm if a trend is evident throughout an entire region. The field significance (Vogel and Kroll, 1989), equivalent to the statistical significance of a regional trend, indicates whether a trend emerges from a group of stations in the same region. It was calculated as follows. Possible auto-correlation was first removed by pre-whitening the rainfall time series, *i.e.* by assuming a first-order auto-correlation structure and removing it from the time series (Hamed, 2009). A regional average Kendall's statistic (Douglas *et al.*, 2000) was calculated for each one of the 30 rainfall variables using a re-sampling technique (Kundzewicz and Robson, 2004). The field significance associated with the regional Kendall's statistic was finally derived from the re-sampled time series using the Weibull plotting position formula. Two confidence levels of trend significance (90% and 95%) were considered at both local and regional scales.

It should be noted that different auto-correlation structures are considered in this analysis: long-term persistence at local level and first-order auto-correlation at regional level. Assuming a first-order auto-correlation at both local and regional levels would enable an accurate comparison of local and regional significances of trends, as performed in Lacombe *et al.* (2012). However, this alternative approach, although more consistent, might be less accurate. Indeed, the long-term persistence, not easily accountable in the regional trend test, better reflects the natural behaviour of meteorological time series at the local level, hence our proposed approach.

4 Results

Out of the 510 tested time series, only 44 and 63 exhibit a trend significant at the 95% and 90% confidence levels, respectively (Tabs. 2, 3 and 4). Significant trends in the timing of the rainy season (variables 1–3), in the intensity of extreme events (variable 4), and in the intensity index (variable 6) are almost inexistent. Only four stations exhibit significant trends in the duration of dry spells (variable 5) (Tab. 2). Among the 24 significant trends in cumulative rainfall depths, 20 are positive. Among the 26 significant trends in the number of rainy days, 21 are positive. The few negative trends are observed during the rainy season only, indicating that rainy season trends are more heterogeneous in direction than those, uniformly positive, observed during the dry season (Tabs. 3 and 4).

Table 2. Sen's slopes and significance of trends in variables 1–6.
Tableau 2. *Pentes et significativités des tendances pour les variables 1–6.*

		Timing of the rainy season			Extreme events		Intensity index
Variable number		1	2	3	4	5	6
Rainfall stations	Chaiyaphum					−0.08[b]	
	Fang	−0.27[a]					0.16[b]
	Kalasin						
	Khon Kaen						
	Loei						
	Luang Prabang		0.27[a]		0.61[a]		
	Maha Sarakham						
	Mukdahan					0.04[b]	
	Nakhon Phanom					0.02[a]	
	Nong Khai					−0.05[a]	0.14[b]
	Roi Et						
	Sakhon Nakhon						
	Sisaket						
	Surin	−0.26[a]		−1.00[b]			
	Ubon Ratchathani				1.22[b]		
	Udon Thani						
	Vientiane			−0.80[a]			
Field significance							

[a] 90% significance.
[b] 95% significance.

Table 3. Sen's slopes and significance of trends in variables 7–18.
Tableau 3. *Pentes et significativités des tendances pour les variables 7–18.*

		Rainfall depth											
		Whole year				Rainy season				Dry season			
		All	Low	Medium	High	All	Low	Medium	High	All	Low	Medium	High
Variable number		7	8	9	10	11	12	13	14	15	16	17	18
Rainfall stations	Chaiyaphum				−3.49[b]								
	Fang				−3.82[b]								
	Kalasin										0.63[b]		
	Khon Kaen	4.19[b]			3.36[b]	3.51[b]			2.74[a]				
	Loei				2.60[a]								
	Luang Prabang	6.05[b]				5.98[a]		3.32[b]					
	Maha Sarakham												
	Mukdahan												
	Nakhon Phanom												
	Nong Khai				−4.01[a]				−4.18[a]	2.00[b]	1.00[b]	1.05[b]	
	Roi Et												
	Sakhon Nakhon	5.01[a]			5.55[b]				5.00[b]				
	Sisaket												
	Surin	5.12[b]			5.45[b]	5.64[b]			5.46[b]				
	Ubon Ratchathani												
	Udon Thani									1.33[a]			
	Vientiane												
Field significance										>0[a]		>0[a]	>0[a]

[a] 90% significance.
[b] 95% significance.

Table 4. Sen's slopes and significance of trends in variables 19–30.
Tableau 4. *Pentes et significativités des tendances pour les variables 19–30.*

		Number of rainy days											
		Whole year				Rainy season				Dry season			
		All	Low	Medium	High	All	Low	Medium	High	All	Low	Medium	High
Variable number		19	20	21	22	23	24	25	26	27	28	29	30
Rainfall stations	Chaiyaphum								−0.04[a]			0.01[a]	
	Fang				−0.06[b]						0.09[b]		
	Kalasin	0.31[b]	0.30[b]							0.14[b]	0.14[b]		
	Khon Kaen				0.05[b]				0.05[b]				
	Loei				0.06[b]								
	Luang Prabang	0.23[b]				0.30[b]		0.13[b]					
	Maha Sarakham											0.02[a]	
	Mukdahan												
	Nakhon Phanom												
	Nong Khai									0.26[b]	0.20[b]	0.06[b]	
	Roi Et			−0.04[a]									
	Sakhon Nakhon												
	Sisaket	0.82[b]				0.75[b]					0.08[b]		
	Surin				0.08[b]				0.08[b]				
	Ubon Ratchathani												
	Udon Thani						−0.14[b]						
	Vientiane								−0.03[a]				
Field significance		>0[a]								>0[a]	>0[a]	>0[a]	>0[a]

[a] 90% significance.
[b] 95% significance.

Figure 3 displays annual and dry season rainfall time series at four stations where contrasting trends are observed. In Nongkhai and Udon Thani, dry season rainfall has significantly increased while annual rainfall does not exhibit any significant trend. In contrast, in Surin and Khon Kaen, annual rainfall has significantly increased while dry season rainfall does not exhibit any significant trend. This comparison illustrates two types of heterogeneities:

- the complex behaviour of climate trends which can reveal contrasting trend significances across seasons, though at the same location;
- the high spatial variability of rainfall trends directions between stations distant by less than 200 km.

Despite insignificant trends at most stations in the onset and retreat of the rainy season (Tab. 2), Figure 4 shows that high inter-annual variability exists. The variability of the onset (standard deviation = 17 and 22 days in Nakhon Phanom and Surin, respectively) is greater than that of the retreat (standard deviation = 11 and 13 days, respectively). This difference illustrates the difficulty for farmers to determine the appropriate sowing time while harvesting time is mainly determined by the photoperiodicity of their RLR cultivars.

Figure 5 shows that the few 90%-field significant regional trends correspond to increases in rainfall depths and numbers of rainy days during the dry season mainly (Tabs. 3 and 4). Except for the timing of the rainy season onset and of the 5-day rainiest period (variables 1 and 3) exhibiting insignificant declining regional trends, all other variables exhibit rising regional trends, revealing an overall increase of rainfall depths and number of rainy days during both seasons. This highlights the importance of evaluating regional trends, which not only indicate the spatial extent of a changing pattern but also enable the detection of long-term changes that remain insignificant at individual stations due to the high variability of small-scale rainfall events and related sampling issues.

5 Discussion

The ability of the Mann-Kendall test to detect true trend in climate time series might be reduced when the tested variable is discrete and includes several ties as in the case of variable 5 (duration of longest dry spells). We plotted the statistical significance of the local trends in this variable against their slope and found that the lower detection threshold (90%) corresponds to a slope equivalent to an additional 1.6 day of mean longest dry spell over the 52-year study period. This result confirms the ability of the test to detect slight changes in the studied rainfall variables.

Increased dry season rainfall in NET was found to be consistent with wider on-going climate dynamics observed in East Asia and explained by the weakening of the East Asian winter monsoon (Zhou, 2011). These changes were attributed to global warming (Zhang *et al.*, 2011), indicating that rainfall is likely to continue increasing in the future. This wetting tendency may appear counterintuitive. 2015 has been the driest

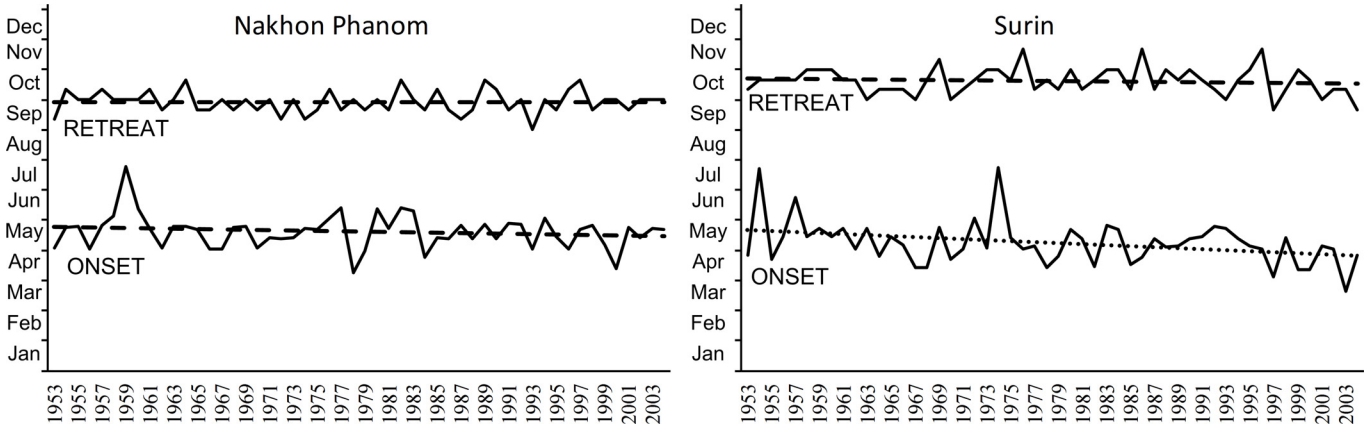

Fig. 4. Occurrence of the onset and retreat of the rainy season. Dotted trend line is significant at 90% confidence level. Dashed trend lines are statistically insignificant.

Fig. 4. *Évolution de la date de début et de fin de la saison des pluies. Ligne pointillée : tendance significative au seuil de 90 %. Ligne en tirets : tendance non significative.*

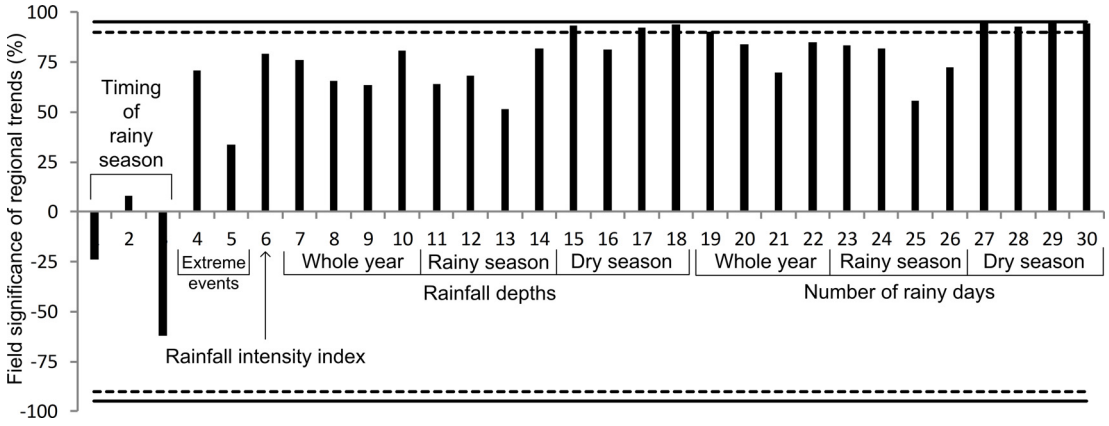

Fig. 5. Field significances of regional trends. Positive and negative values correspond to positive and negative trends, respectively. Solid horizontal line: 95% significance level. Dotted horizontal line: 90% significance level. NB: field significance = statistical significance of regional trend.

Fig. 5. *Significativité des tendances régionales. Les valeurs positives et négatives correspondent aux tendances positives et négatives, respectivement. Les lignes horizontales continues et pointillées correspondent aux seuils de significativité de 95 % et 90 %, respectivement.*

year since 1995 in Southeast Asia, due to an extreme El Niño event (FAO, 2015). Such episodes remain in the memories while insignificant and gradual increases in rainfall go unnoticed, thus possibly giving the impression that rainfall has reduced over recent decades (Amir Faisal *et al.*, 2014).

Mean dry season rainfall increased by 12 mm from 1953 to 2004. Although it is statistically significant at the regional level, this slight increase corresponds to about 7% of the mean total dry season rainfall, far lower than the typical crop water requirements in NET which vary from 500 mm to 1,500 mm per cropping cycle (Allen *et al.*, 1998).

No effect of increased dry season rainfall is expected on RLR since rice quality is mainly controlled by the number of rainy days during the rainy season (Polthanee and Promkhambut, 2014), which did not vary significantly (Tab. 4). Due to the absence of regional trends in the rainy season retreat, the increase in dry season rainfall is unlikely to occur in its earliest phase, leading to no change in the risk of damaged quality of the paddy at harvest. Similarly, the absence of regional trend in the rainy season onset is unlikely to accelerate the switch from RLR transplanting to direct seeding. Increased rainfall in the early dry season is unfavourable for groundnut plantation because it creates a hard soil surface and soil crusting leading to poor germination, more weeds, and often the need to plough again and replant the crop. But additional rainfall in February–March is favourable after pegging and during pod filling stage. Additional rainfall at the end of the dry season could contribute to secure the establishment of sesame before RLR but this system remains risky due to the highly variable rainy season onset (Fig. 4).

The deep rooting system and fast crop establishment of sugarcane will be favoured by additional rain at the beginning

of the dry season. The limited additional dry season rainfall combined with coarse textured soils in these uplands should not hamper the harvest and the transport of the cane by trucks. No significant impact of additional rainfall in the dry season on cassava is expected as most of the crop growth occurs during the wet season (Fig. 2). Recently, rubber plantations have been established in the more humid areas of the region and a wetter dry season will benefit this relatively new perennial crop.

Vegetables and horticultural crops planted on the bank of rivers will benefit from a wetter dry season, especially during its cooler first half. A moderate increase in dry season rainfall may sustain river base-flow at a higher level than currently observed, thus benefiting gardens grown on river banks. But at this stage, the detected increase in rainfall seems too limited to help recharge the shallow aquifers and small ponds on which these systems depend frequently to expand their planted areas.

6 Conclusions

While positive effects of the detected change in rainfall pattern on the existing cropping systems dominate, it is still far too limited to stimulate farmers' switch to new types of mono or double cropping systems, or to use more external inputs, in order to increase crop yields. Benefit from additional dry season rainfall remains marginal but more remarkable effects are expected in the future if these trends persist, as expected according to the most updated climate projections for the East Asian winter monsoon (Xu *et al.*, 2016). The benefit of additional rainwater for crop production should also be considered in light of the expected warming trend. Above 35 °C, a temperature threshold that tends to be exceeded more frequently at rice flowering time in NET (Pornamnuaylap *et al.*, 2014), pollen fertility decreases, inducing yield declines. Several naturally spontaneous adaptations include early anthesis time, panicle cooling through transpiration, and the selection of heat-tolerant varieties (Lafarge *et al.*, 2016). Increased temperature also depletes soil water reserves through enhanced evapotranspiration. The benefit from additional rainfall is enhanced if drought risks are moderated by supplemental irrigation water resources, such as the expansion of thousands of small and multipurpose on-farm ponds installed across NET during the past two decades. They allow the practice of integrated farming systems combining rice, fish rearing, fruit and vegetable production and contribute to food security at the household level across this region. For centuries, the very adaptive and resilient Lao-Isan population in NET has been facing climate uncertainties with up to six-month dry season with scorching temperatures in March–April forcing them to practice internal seasonal migrations to wet spots and to secure part of their food from non-timber forest products. More recently migrations head to urban centres and foreign countries to generate off-farm incomes supporting the continuation of small-scale family farming. Gaining from this traditional flexibility, there is no doubt that NET farmers will find ways to adapt to the limited change in rainfall distribution reported here.

Acknowledgements. This study was funded by the CGIAR Research Program on Climate Change, Agriculture and Food Security (CCAFS). The authors are grateful to the Mekong River Commission for the provision of rainfall data.

References

Allen RG, Pereira LS, Raes D, Smith M. 1998. Crop evapotranspiration – guidelines for computing crop water requirements. In: *Irrigation and drainage paper 56*. Rome (Italy): FAO, 326 p.

Amir Faisal AH, Polthanee A, Promkhambut A. 2014. Farmers' perception of drought and its impact on a community livelihood in rural Northeastern Thailand. *Khon Kaen Agric J* 42(3): 427–442.

Barnaud C. 2002. Analyse diagnostic de la situation agraire du village de Ban Hin Lad, Nord-Est de la Thaïlande. INAP-G, 41 p.

Devillers E, Cousinou L. 2003. Analyse-diagnostic comparative des systèmes agraires de Kut Chieng Mee et Nong Saeng, deux villages dans La Province de Khon Kaen, Nord-Est de la Thaïlande. INAP-G, 89 p.

Douglas EM, Vogel RM, Kroll CN. 2000. Trends in floods and low flows in the United States: impact of spatial correlation. *J Hydrol* 240: 90–105.

FAO. 2015. El Niño in Asia. Prolonged dry weather in several countries affecting plantings and yield potential of the 2015 main season food crops. GIEWS update. Rome (Italy): FAO, 10 p.

Hamed KH. 2008. Trend detection in hydrologic data: the Mann-Kendall trend test under the scaling hypothesis. *J Hydrol* 349: 350–363.

Hamed KH. 2009. Enhancing the effectiveness of prewhitening in trend analysis of hydrologic data. *J Hydrol* 368: 143–155.

Hasson S, Lucarini V, Pascale S. 2013. Hydrological cycle over South and Southeast Asian river basins as simulated by PCMDI/CMIP3 experiments. *Earth Syst Dyn* 4: 199–217.

Hasson S, Pascale S, Lucarini V, Böhner J. 2016. Seasonal cycle of precipitation over major river basins in South and Southeast Asia: a review of the CMIP5 climate models data for present climate and future climate projections. *Atmos Res* 180: 42–63.

IPCC. 2014. Climate change 2014: synthesis report. In: *Contribution of working groups I, II and III to the Fifth Assessment Report of the Intergovernmental Panel on Climate Change*. Geneva (Switzerland): IPCC, 151 p.

Kendall MG. 1975. Rank correlation methods. London (England): Griffin.

Knutti R, Sedlacek J. 2013. Robustness and uncertainties in the new CMIP5 climate model projections. *Nature Climate Change* 3: 369–373. doi: 10.1038/NCLIMATE1716.

Kundzewicz ZW, Robson AJ. 2004. Change detection in hydrological records-a review of the methodology. *Hydrol Sci J* 49(1): 7–19.

Lacombe G, McCartney M, Forkuor G. 2012. Drying climate in Ghana over the period 1960–2005: evidence from the resampling-based Mann-Kendall test at local and regional levels. *Hydrolog Sci J* 57(8): 1594–1609.

Lafarge T, Julia C, Baldé A, Ahmadi N, Muller B, Dingkuhn M. 2016. Rice adaptation strategies in response to heat stress at flowering. In: Torquebiau E, ed. Climate change and agriculture worldwide. Netherlands: Springer/Cirad, p. 31–43.

Mann HB. 1945. Nonparametric tests against trend. *Econometrica* 13: 245–259.

MOA. 2010. Agriculture statistics. Bangkok: Ministry of Agriculture (MOA). Available at http://www.web.nso.go.th/ [2016/05/09].

OAE. 2011. Agricultural statistics of Thailand 2011. Office of Agricultural Economics (OAE). Available at http://www.oae.go.th/ [2016/07/09].

Polthanee A. 1991. Cultivation of peanuts after rice in rainfed areas of Northeast Thailand: farmers' approach. *AGRIS* 7(1): 70–76.

Polthanee A, Marten G. 1986. Rainfed cropping systems in Northeast Thailand. In: Maten G, ed. Traditional agriculture in Southeast Asia.Boulder and London (United Kingdom): Westview Press, p. 103–131.

Polthanee A, Promkhambut A. 2014. Impact of climate change on rice-based cropping systems and farmers' adaptation strategies in Northeast Thailand. *Asian J Crop Sci* 6(3)262–272. doi: 10.3923/ajcs.2014.

Polthanee A, Janthajam C, Promkhambut A. 2014. Growth, yield and starch content of cassava following rainfed lowland rice in Northeast Thailand. *Int J Agric Res* 9(6): 319–324.

Pornamnuaylap D, Limsakul A, Limtong P, Chidthaisong A. 2014. Evaluating the potential impacts of high temperature on rice production in Northeast Thailand. *J Sustain Energ Environ* 5, 65–74.

Räsänen TA, Kummu M. 2013. Spatiotemporal influences of ENSO on precipitation and flood pulse in the Mekong River Basin. *J Hydrol* 476: 154–168.

Sanusan S, Polthanee A, Audebert A, Seripong S, Mouret JC. 2010. Suppressing weeds in direct-seeded lowland rainfed rice: effect of cutting dates and timing of fertilizer application. *Crop Prot* 29: 927–935.

Sen PK. 1968. Estimates of the regression coefficient based on Kendall's tau. *J Am Stat Assoc* 63: 1379–1389.

Singhrattna N, Rajagopalan B, Kumar KK, Clark M. 2005. Interannual and interdecadal variability of Thailand summer monsoon season. *J Climate* 18: 1697–1708.

Sun Y, Solomon S, Dai A, Portmann RW. 2006. How often does it rain? *J Climate* 19: 916–934.

Sutthipibul V. 1987. Effects of diminishing forest area on rainfall amount and distribution in Northeast Thailand. Master Thesis, Kasetsart University (Bangkok), 133 p.

Vogel RM, Kroll CN. 1989. Low-flow frequency analysis using probability plot correlation coefficients. *J Water Res Pl-ASCE* 115 (3): 338–357.

Wang L, Chen W, Huang R. 2007. Changes in the variability of North Pacific Oscillation around 1975/1976 and its relationship with East Asian winter climate. *J Geophys Res* 112: D11110.

Xu M, Xu H, Ma J. 2016. Responses of the East Asian winter monsoon to global warming in CMIP5 models. *Int J Climatol* 36: 2139–2155.

Zhang Q, Singh VP, Sun P, Chen X, Zhang Z, Li J. 2011. Precipitation and streamflow changes in China: changing patterns, causes and implications. *J Hydrol* 410: 204–216.

Zhou LT. 2011. Impact of East Asian winter monsoon on rainfall over Southeastern China and its dynamical process. *Int J Climatol* 31(5): 677–686.

Cite this article as: Lacombe G, Polthanee A, Trébuil G. 2017. Long-term change in rainfall distribution in Northeast Thailand: will cropping systems be able to adapt? *Cah. Agric.* 26: 25001.

Expl Agric.: page 1 of 13 © *Cambridge University Press 2017*
doi:10.1017/S0014479717000023

EFFECTS OF CUTTING LENGTH AND BUD REMOVAL ON ROOT YIELD AND STARCH CONTENT OF CASSAVA UNDER RAINFED CONDITIONS

By MAPITA PRASITSARN†, ANAN POLTHANEE†,§, VIDHAYA TRELO-GES† *and* ROBERT W. SIMMONS‡

†*Department of Plant Science and Agricultural Resources, Faculty of Agriculture, Khon Kaen University, Khon Kaen, 40002, Thailand and* ‡*School of Water Energy and Environment, Cranfield University, Cranfield, Bedfordshire, MK43 0AL, UK*

(*Accepted 23 January 2017*)

SUMMARY

Bud removal of the cuttings at underground level has been claimed by cassava growers in Thailand as a method to increase cassava yield. This practise should be tested experimentally to explain the reason for yield increase. The objective of this study was to investigate the effects of bud removal and cutting length on storage root yield and starch content of three cassava varieties. Field experiment was conducted in a split–split plot design with four replications in 2010 and 2011, under rainfed conditions. Three cassava varieties (KU50, RY9 and HB60) were assigned as main plot. Two cutting lengths (15 cm and 30 cm) were assigned as sub plots, and two treatments of buds (buds cut and not cut) were assigned as sub–sub plots. The buds on the cuttings that were inserted into the soil were removed. In 2010, the plants from 15-cm long cuttings subjected to bud removal had higher fresh storage root yield (88.4 Mg ha^{-1}) than did plants from 30-cm long cuttings subjected to bud removal (75.8 Mg ha^{-1}). Cutting of buds also had higher fresh storage root yield (89.1 Mg ha^{-1}) than did non bud-cutting (75.0 Mg ha^{-1}). KU50 had the highest fresh storage root yield (91.4 Mg ha^{-1}), dry root yield (48.4 Mg ha^{-1}) and starch yield (20.1 Mg ha^{-1}). Cutting length of 15 cm had higher starch concentration in storage roots (25.6%) than did cutting length of 30 cm (24.2%). HB60 had the highest starch concentration (27.0%) among cassava varieties tested. The data in 2011 were similar to the data in 2010. The responses of varieties to bud removal and cutting length are discussed.

INTRODUCTION

Cassava (*Manihot esculenta* Crantz) originated in the tropical areas of South America and it is grown widely in tropical areas of the world due to its starch containing roots (Alves, 2002; Scott *et al.*, 2000). Globally, the area planted with cassava was recently estimated at 20.4 million ha with a total production of 262.5 million tonnes (MT) (FAO, 2014a). Thailand ranks third for world cassava production with an average total production of 22.5 MT year^{-1}, with the areas in the north-eastern region accounting for approximately 51.3% of the country's entire cassava production (OAE, 2014a). The national average yield in 2006 was about 20 MT ha^{-1}, which is higher than the world average but lower than the potential of the crop (FAO, 2014a). The main causal

§Corresponding author. Email: panan@kku.ac.th

factors driving low yields in Thailand are infertile soils and drought (FAO, 2014b), as well as inappropriate agronomic practises (Jones *et al.*, 2013).

It has been reported previously that cassava yield depends on plant population density, number of roots and tuber root weight per plant (Hahn and Hozyo, 1984). In cassava cultivation, the cuttings from the stems are used as planting materials for the succeeding crop (Leihner, 2002; Nassar and Teixeira, 1983). The number of cassava roots can be increased by adopting a vertical planting position and using longer cuttings (Osiru *et al.*, 1997). However, no significant difference in root yield between cuttings with 10 cm and 50 cm length has been reported (Velasco, 1982). Short cuttings produced better yields than long cuttings (Villamayor *et al.*, 1992) and cuttings with 20-cm length have higher root yield than longer cuttings with 25-cm length (Tongglum *et al.*, 1992).

One local agronomic practise that the farmers in north-eastern Thailand claim to considerably increase root yield of cassava is to cut the buds off the section of the cuttings to be inserted into the soil. However, the yield components that contribute to root yield have not been clearly investigated. The hypothesis underlying this research is that bud removal increases storage root yield and modifies yield components of cassava. The reason for yield increase of this local practise has not been verified experimentally. Therefore, the objective of this research was to evaluate the effects of cutting length and bud removal on plant growth, root yield and starch content of three cassava varieties grown under rainfed conditions in north-eastern Thailand.

MATERIALS AND METHODS

Crop management and experimental design

Field experiments were conducted at the Agronomy Experimental Fields of Khon Kaen University, Khon Kaen, Thailand (16°28′N, 102°48′E, 200 m above sea level) under rainfed conditions in two consecutive years (2010 and 2011). The crops were planted in June and harvested after 12 months for both years. Soil type is loamy sand in texture. Soil samples were collected from 0–30 cm depth before planting and analysed for selected chemical and physical properties (Supplementary Table S1, available online at https://doi.org/10.1017/S0014479717000023).

Rainfall, maximum and minimum air temperature were recorded daily and summarized on a monthly basis for entire growing period (Figure 1). Total rainfall in 2010 and 2011 during the growing period was recorded as 1 099 mm and 1 620 mm, respectively. The highest monthly rainfalls observed were 404 mm in August 2010 and 356 mm in September 2011. The experiment was subjected to water stress during the growing period for 4 months in 2010 (starting at 6 months after planting, MAP) and 3 months in 2011 (Figure 1). The experiment also encountered intermittent water-logging events for 5 months in 2011, starting at one MAP.

The experimental fields were ploughed twice with a 3-disk tractor and a 7-disk tractor. Ridging was undertaken with a 7-disk tractor forming a ridge height of 30 cm. The distance between planting rows and cassava plants was 1 m. Pre-emergence

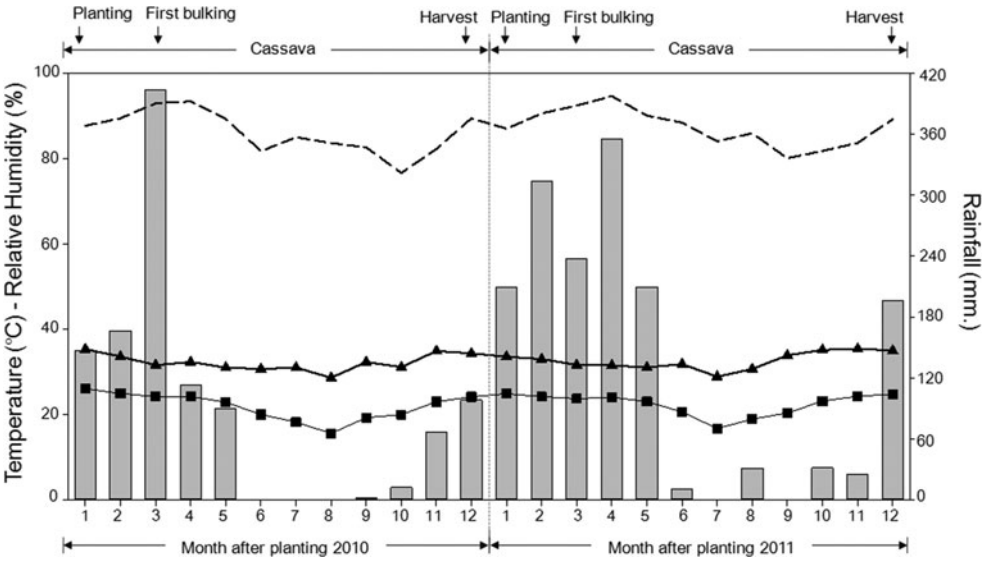

Figure 1. Rainfall (▭), relative humidity (▬ ▬), minimum temperature (—■—) and maximum temperature (—▲—) entire the growing period in 2010 and 2011. Khon Kaen, Thailand.

herbicide (metholachor) was sprayed immediately after planting at the rate of 1.5 kg a.i. ha^{-1}. A split–split plot design with four replications and plot size of 11 × 12 m was adopted in this study.

Three cassava varieties (Kasetsart 50 [KU50], Rayong 9 [RY9] and Huay Bong 60 [HB60]), two cutting lengths of 15 cm and 30 cm and two bud removal treatments (bud cut and not cut) were assigned in main plots, sub-plots and sub–sub-plots, respectively. Three buds on the cutting of 15-cm length (from six normal buds) and five buds on the cutting of 30-cm length (from 10 normal buds) were removed using a sharp knife. The buds, bark and cambium layer were removed (Figure S1). The cuttings were inserted vertically into the soil with two-third of the length exposed on top of ridges. Chemical fertilizer of grade 15-15-15 (N, P_2O_5, K_2O) at the rate of 312.5 kg ha^{-1} (31.3 g $plant^{-1}$) was applied 1 month after planting. The granule fertilizer was dropped into the hole made using a hand hoe 15 cm from the cassava plant and covered with soil.

Hand weeding was undertaken only one time at 1 month after planting and no weeding was done for the rest of cropping period in both years. No insecticide or fungicide was used in these experiments for the entire growing period over both years.

Data collection

Four plants from each plot were selected randomly outside the harvesting area of the experimental plots at 120, 240, 300 and 360 days after planting (DAP) and shoot dry weight per plant, storage root dry weight per plant and storage root number per plant were evaluated. The harvested plants were separated into leaves, stems and roots. Twenty leaves of each plant from each plot were randomly chosen and leaf area

was determined by an automatic leaf area metre (model AAC-400, Hayashi Denkoh Co., Ltd., Bunkyo-ku, Tokyo, Japan). The leaf samples were subsequently oven-dried at 80 °C to a constant weight and leaf dry weight was measured. Leaf dry weight and leaf area of 20 leaves were converted to leaf dry weight and leaf area of total sample using the relationship; total leaf area equals leaf area of 20 leaves × total leaf dry weight/leaf dry weight of 20 leaves. Leaf area index (LAI) was calculated by leaf area per plant divided by ground area covered (Ekanayake, 1994).

Fresh storage root yield and dry storage root yield were measured at 360 DAP in the harvesting area of 6 × 4 m (24 plants). Subsequently, fresh and dry storage root yield were calculated in Mg ha^{-1}. Harvest index (HI) was calculated by storage root dry weight divided by total plant dry weight (Ekanayake, 1994). Starch content was measured using a Riemann scale balance (Bainbridge *et al.*, 1996) and starch yield was calculated by multiplying the actual starch content with the fresh root weight per hectare and divided by 100 (Knutsson, 2012).

Data analysis

The data for each year were analysed statistically according to a split–split plot design using Statistica Ver. 11 (Statsoft Inc., Tulsa, USA) and the error variances were tested for variance homogeneity. As some error variances were three-fold different, means were separated by *post-hoc* Fisher's least significant difference (LSD) at 0.05 probability level.

RESULTS

Fresh storage root yield, dry storage root yield and harvest index

Cutting lengths affected ($P \leq 0.05$) fresh storage root yield, dry storage root yield and HI across years (Table 1). Cutting of 15-cm length caused higher values than that of 30 cm for these traits. Significant differences ($P \leq 0.05$) between bud removal treatments were also observed and cutting with bud removal induced the highest fresh storage root yield, dry storage root yield and HI across years (Table 1). Cassava varieties were also significantly different ($p \leq 0.05$) for these traits across years, with KU50 presenting the highest fresh storage root yield (91.4 Mg ha^{-1} in 2010 and 87.4 Mg ha^{-1} in 2011), dry storage root yield (48.4 Mg ha^{-1} in 2010 and 44.7 Mg ha^{-1} in 2011) and HI (0.53 in 2010 and 0.52 in 2011).

Starch yield and starch content

Significant differences ($P \leq 0.05$) between cutting lengths were observed for starch yield and starch concentration (Table 1). Cutting of 15-cm length determined the highest starch yields (22.6 Mg ha^{-1} in 2010 and 18.5 Mg ha^{-1} in 2011) and starch concentrations (25.6% in 2010 and 25.1% in 2011). Cutting with bud removal induced the highest ($p \leq 0.05$) starch yields (22.5 Mg ha^{-1} in 2010 and 18.6 Mg ha^{-1} in 2011) and starch concentration (25.3% in 2010 and 24.8% in 2011). Cassava varieties were also significantly different ($P \leq 0.05$) for starch yield and starch concentration across years. KU50 had the highest starch yields of 20.1 and 18.7

Table 1. Fresh storage root yield (FRY), dry storage root yield (DRY), starch yield (SY), starch content (SC) and harvest index (HI) of cassava with differences in cutting lengths, bud removal treatments and varieties at 360 days after planting (DAP) in 2010 and 2011.

	2010					2011				
	FRY (Mg ha^{-1})	DRY (Mg ha^{-1})	SY (Mg ha^{-1})	SC (%)	HI	FRY (Mg ha^{-1})	DRY (Mg ha^{-1})	SY (Mg ha^{-1})	SC (%)	HI
Cutting length										
15 cm	88.4*	43.3*	22.6*	25.6*	0.54*	74.0*	38.2*	18.5*	25.1*	0.52*
30 cm	75.8†	32.4†	18.3†	24.2†	0.51†	61.0†	32.4†	14.4†	23.7†	0.50†
Bud removal										
Cut	89.1*	44.1*	22.5*	25.3*	0.53*	75.2*	38.1*	18.6*	24.8*	0.52*
Not cut	75.0†	37.6†	18.3†	24.5†	0.52†	59.9†	31.5†	14.3†	24.0†	0.50†
Variety										
KU50	91.4*	48.4*	20.1*	22.0†	0.53*	87.4*	44.7*	18.7*	21.5†	0.52*
HB60	70.8‡	38.1†	19.1†	27.0*	0.51†	57.1†	31.0†	15.1†	26.5*	0.50†
RY9	82.6†	39.0†	21.2*	25.7*	0.53*	62.0†	32.6†	15.6*†	25.2*	0.51*†

Means of the same category in the same column followed by different symbols are significantly different at 0.05 probability level by LSD.
Means without a symbol indicate non-significance.

Mg ha^{-1} in 2010 and 2011, respectively, whereas HB60 and RY9 had the highest starch concentration of 27.0% and 25.7% in 2010 and 26.5% and 25.2% in 2011, respectively.

Leaf area index (LAI)

Cutting lengths were only significantly different ($P \leq 0.05$) for LAI at 360 DAP in 2010 and 2011 (Table 2). The cuttings of 15-cm length had the highest LAI across varieties and bud removal treatments. Bud removal treatments did not affect LAI across growth stages. Significant differences ($P \leq 0.05$) among cassava varieties were observed for LAI at 300 and 360 DAP in 2010 and 2011, with. KU50 showing the highest LAI at 360 DAP regardless cutting lengths, bud removal treatments and years.

Shoot dry weight

Shoot dry weight increased with time for all treatments, with cutting of 30-cm length causing ($P \leq 0.05$) higher shoot dry weight than cutting of 15-cm length at 360 DAP (Table 3). At 360 DAP, the highest shoot dry weight for the cutting 30-cm length was 2 370 and 2 321 g plant^{-1} in 2010 and 2011, respectively, whereas the highest shoot dry weight for the cutting of 15-cm length were 2 196 and 2 149 g plant^{-1}.Cutting without bud removal caused higher shoot dry weight ($P \leq 0.05$) than cutting with bud removal at 120, 240 and 300 (DAP). Significant differences ($P \leq 0.05$) among cassava varieties were also observed for shoot dry weight at 120, 240, 300 and 360 DAP across years. HB60 had consistently and significantly the highest shoot dry

Table 2. Leaf area index (LAI) of cassava with differences in cutting lengths, bud removal treatments and varieties evaluated at 120, 240, 300 and 360 days after planting (DAP) in 2010 and 2011.

	2010				2011			
	120 DAP	240 DAP	300 DAP	360 DAP	120 DAP	240 DAP	300 DAP	360 DAP
Cutting length								
15 cm	4.03	1.40	1.64	4.51*	3.95	1.32	1.56	4.43*
30 cm	3.93	1.21	1.57	3.76†	3.85	1.13	1.49	3.68†
Bud removal								
Cut	4.10	1.34	1.62	4.24	4.03	1.27	1.54	4.16
Not cut	3.86	1.27	1.59	4.03	3.78	1.19	1.51	3.96
Variety								
KU50	4.25	1.39	2.37*	4.94*	3.64	1.32	2.29*	4.86*
HB60	3.71	1.29	0.81‡	3.56‡	4.17	1.22	0.74‡	3.48‡
RY9	3.99	1.23	1.63†	3.91†	3.91	1.16	1.55†	3.84†

Means of the same category in the same column followed by different symbols are significantly different at 0.05 probability level by LSD.
Means without a symbol indicate non-significance.

Table 3. Shoot dry weight per plant (g) of cassava with differences in cutting lengths, bud removal treatments and varieties evaluated at 120, 240, 300 and 360 days after planting (DAP) in 2010 and 2011.

	2010				2011			
	120 DAP	240 DAP	300 DAP	360 DAP	120 DAP	240 DAP	300 DAP	360 DAP
Cutting length								
15 cm	772†	1670†	1819†	2196†	639†	1652†	1811†	2149†
30 cm	876*	1876*	2027*	2370*	734*	1858*	2017*	2321*
Bud removal								
Cut	789†	1730†	1881†	2259	652†	1708†	1871†	2231
Not cut	859*	1815*	1965*	2307	721*	1799*	1957*	2239
Variety								
KU50	815†	1791†	1939†	2285†	697†	1783†	1924†	2234*†
HB60	848*	1812*	1966*	2291*	715*	1796*	1960*	2247*
RY9	808‡	1716‡	1864‡	2272‡	648‡	1697‡	1857‡	2224†

Means of the same category in the same column followed by different symbols are significantly different at 0.05 probability level by LSD.
Means without a symbol indicate non-significance.

weight across sampling times followed by KU50 and RY9. The highest values of shoot dry weight (2 291 g plant^{-1} in 2010 and 2 247 g plant^{-1} in 2011) were obtained from HB60 at 360 DAP.

Table 4. Storage root dry weight (g) per plant of cassava with differences in cutting lengths, bud removal treatments and varieties evaluated at 120, 240, 300 and 360 days after planting (DAP) in 2010 and 2011.

	2010				2011			
	120 DAP	240 DAP	300 DAP	360 DAP	120 DAP	240 DAP	300 DAP	360 DAP
Cutting length								
15 cm	867	1996*	2840*	3333*	446	1442*	2139*	2723*
30 cm	922	1633†	2353†	2838†	475	1206†	1855†	2238†
Bud removal								
Cut	948	1928*	2912*	3407*	468	1494*	2440*	2807*
Not cut	840	1701†	2280†	2764†	454	1155†	1555†	2154†
Variety								
KU50	990	2485*	3680*	4337*	543	1928*	3057*	3574*
HB60	824	1395‡	1846‡	2097‡	423	985‡	1326‡	1703‡
RY9	870	1564†	2263†	2822†	416	1060†	1611†	2165†

Means of the same category in the same column followed by different symbols are significantly different at 0.05 probability level by LSD.
Means without a symbol indicate non-significance.

Storage root dry weight

Significant differences ($P \leq 0.05$) between cutting lengths were observed for storage root dry weight at 240, 300 and 360 DAP across years (Table 4), with the highest values being found in cuttings of 15-cm length. Cutting with bud removal had higher ($P \leq 0.05$) storage root dry weight than cutting without bud removal at 240, 300 and 360 DAP across years. At final harvest (360 DAP), cutting with bud removal had the highest storage root dry weight of 3 407 and 2 807 g plant^{-1} in 2010 and 2011, respectively. Cassava varieties were significant different ($P \leq 0.05$) for storage root dry weight at 240, 300 and 360 DAP across years. KU50 had the highest storage root dry weight at 240, 300 and 360 DAP in both years. At 360 DAP, KU50 had the highest storage root dry weight of 4 337 and 3 574 g plant^{-1} in 2010 and 2011, respectively.

Storage root number per plant

Significant differences ($P \leq 0.05$) between cutting lengths were observed for storage root number per plant at 120, 240, 300 and 360 DAP in both years (Table 5). Cutting of 15-cm length caused higher storage root number per plant than that of 30-cm length. Bud removal treatments were significantly different ($P \leq 0.05$) for storage root number per plant across sampling times, and cutting with bud removal had higher storage root number per plant than cutting without bud removal. Cutting with bud removal also had the highest numbers of storage roots at 360 DAP (14.9 and 13.5 roots in 2010 and 2011, respectively). Cassava varieties were significantly different ($P \leq 0.05$) for storage root number per plant for most sampling times and across years. At 360 DAP, KU50 had the highest storage root number per plant (14.7 roots in 2010 and 13.7 roots in 2011).

Table 5. Storage root number per plant of cassava with differences in cutting lengths, bud removal treatments and varieties evaluated at 120, 240, 300 and 360 days after planting (DAP) in 2010 and 2011.

	2010				2011			
	120 DAP	240 DAP	300 DAP	360 DAP	120 DAP	240 DAP	300 DAP	360 DAP
Cutting length								
15 cm	8.6*	11.7*	13.7*	14.6*	6.3*	10.2*	12.3*	13.2*
30 cm	8.3†	10.9†	12.8†	13.8†	5.4†	9.4†	11.3†	12.4†
Bud removal								
Cut	9.2*	11.9*	13.9*	14.9*	6.5*	10.5*	12.4*	13.5*
Not cut	7.7†	10.7†	12.6†	13.6†	5.2†	9.1†	11.2†	12.1†
Variety								
KU50	9.4*	12.0	13.8*	14.7*	6.7*	10.6*	12.7*	13.7*
HB60	7.6‡	10.7	12.7‡	13.7‡	5.0‡	9.0‡	11.0‡	11.9‡
RY9	8.5†	11.2	13.2*†	14.2†	5.8†	9.8†	11.8†	12.8†

Means of the same category in the same column followed by different symbols are significantly different at 0.05 probability level by LSD.
Means without a symbol indicate non-significance.

DISCUSSION

Sustainable improvements in crop yield and quality are always the main purpose of crop production. This can be achieved by modifying the genetics of crop plants as well as altering agronomic practises favouring optimum crop productivity. This research focussed on altering agronomic practise by removing buds of cassava cuttings and adjusting cutting length to increase storage roots number and ultimately increasing economic root yields. The assumptions of this study are that the increase in root yield is proportional to the increase in root number and this yield component can be modified by bud removal. In addition, long cuttings should have higher root number than short cuttings and cassava genotypes may respond differently to bud removal. As the practise of bud removal is not common for cassava production, this research should be beneficial to cassava growers especially the small cassava growers.

Bud removal

Cutting with bud removal significantly increased fresh storage root yield and dry storage root yield (Table 1) and these results confirmed the claim of cassava growers in Thailand. These gains were associated with storage root dry weight per plant and storage root number per plant (Tables 4 and 5). As other studies on bud removal experiment are not available, the direct comparison of the results with others is not possible. Hypothetically, fibrous roots arise from the basal cut surface of the cuttings and occasionally from the buds. Some of these fibrous roots start to bulk and became storage roots (Knoth, 1993). Cutting with bud removal may produce a higher number of fibrous roots than those of non-cutting bud treatment. This is probably due to the

accumulation of assimilates transported from other parts of the cuttings at the wounds created by bud removal. The wounds may develop more fibrous roots and increase the possibility of these roots to become storage roots.

In a classical experiment conducted in 1686, phloem tissue was cut by removing the bark. The assimilates produced in leaves were transported along the phloem tissue and stopped at the wound, resulting in high accumulation of assimilates at the wound and the development of roots (Malpighi, 1686). Wound-induced roots have been reported in geranium (Cline and Neely, 1983; Davies *et al.*, 1982) and woody plant (Jackson, 1986). This knowledge is commonly used for plant propagation such as cutting and layering. Stem cuttings with removal of buds, bark (phloem tissue) and cambium layer at underground level increased root number and also increased the possibility of these roots (fibrous roots) to become storage roots. As consequences, bud-removal treatment caused higher fresh storage root yield, dry storage root yield, starch yield, starch content, HI, storage root dry weight and storage root number per plant (Tables 1, 4 and 5). However, the experiment focussed on storage roots and aerial growth and the formation of fibrous roots at early growth stages was not investigated. Further deliberate experiments are required to verify the hypothesis for yield increase as affected by bud removal.

Cutting length

The question underlying this research is what length is suitable for bud removal practise and then cuttings of 15- and 30-cm length were compared as these lengths are commonly used for cassava production. In this study, cutting of 15 cm caused higher storage root yield than that of 30 cm and this is partially explained by higher LAI, storage root dry weight per plant and storage root number (Tables 2, 4 and 5). The results were in agreement with those of Tongglum *et al.* (1992), who found that cutting of 20 cm had higher storage root yield than that of 25 cm. Another work also reported the advantage of short cuttings over long cuttings (Villamayor *et al.*, 1992). Ganado (1956) found that short cuttings were better than long cuttings when the cuttings were planted vertically, and long cuttings were better than short cuttings when the cuttings were planted horizontally. However, cuttings of 10 and 50 cm were not significantly different for root yield (Velasco, 1982). Long cuttings with more than 10 nodes had a better chance of conserving their viability, and stem cuttings of five to seven nodes and minimum length of 20 cm were recommended to obtain optimum yield (Carvalho *et al.*, 1993). Cuttings with four to seven nodes were not different with respect to mean storage root length, radius of storage root tip and the number of major stem per plant (Onwueme, 1978). However, longer cuttings produced a faster growing canopy (Lahai *et al.*, 1999). The differences among above studies would be due to differences in planting methods (vertical insert and horizontal insert) and environments (tillage and soil moisture).

In this study, cutting of 30 cm had higher shoot dry weight per plant than that of 15 cm, which was associated with higher stem dry weight (data not shown). However, higher shoot dry weight of cutting of 30-cm length did not cause root yield advantage

and this would be due to lower starch content, HI and root number (Tables 1, 3 and 5). The assumption is that a longer cutting has higher sprouting and development due to the presence of more buds. Storage root number and root yield were shown to be affected by cutting length and root yield was associated with the number of storage roots (Didier and El-Sharkawy, 1994). The higher LAI associated with cutting of 15 cm indicates that plants can produce higher levels of photosynthate, which has been correlated positively with root yield (Lahai *et al.*, 2013; Lebot, 2009; Lenis *et al.*, 2005). During the period of 120 to 180 DAP, plants maintained LAI above 4.0 (2010) and 3.9 (2011), with LAI subsequently declining to 1.4 in 2010 and 1.3 in 2011 for the remainder of their growth cycle. This pattern is due to leaf senescence and abscision during rainless period (Figure 1). Following the onset of rainy season, new leaves were produced and LAI values above 4.5 (2010) and 4.4 (2011) were recorded (Table 2; Figure 1).

In the present study, the long cutting (30 cm) had higher shoot dry weight (Table 3) due to the presence of higher reserved carbohydrate. However, lower LAI in long cutting might be attributed to the limitation of nutrients applied to the soil. The application of chemical fertilizer formula 15-15-15 (N_2, P_2O_5, K_2O) at the rate of 312.5 kg ha^{-1} is generally recommended for cuttings of 15 to 20 cm. Long cutting produced higher branch number, but it had lower LAI possibly due to poor partitioning of assimilates to the branches. Although long cutting produced higher number of fibrous roots, the formation of storage roots was low due to low LAI (Table 2). Shoots depend on roots for nutrient and water uptake, while the continued root growth is reliant on photosynthates produced by leaves (Kramer and Boyer, 1995). Crop performance in 2011 was generally lower than in 2010 for most parameters investigated. The reduction in crop performance was in large part due to rainfall amount and distribution during the growing season. The crop received a total rainfall of 1 621 mm in 2011 and 1 099 mm in 2010. Then, water logging occurred during high rainfall intensity in September 2011, and resulted in the reduction in crop growth and yield as compared to 2010 (Figure 1).

Cassava variety

KU50 had the highest fresh storage root yield and dry storage root yield in 2010 and 2011, which was associated with the highest LAI, storage root dry weight per plant and storage root number (Tables 1, 2, 4 and 5). In previous investigations, high LAI is an important factor leading to high yield in cassava varieties (Enyi, 1973; Lahai *et al.*, 1999). On the other hand, HB60 had the highest starch content in storage root. Accordingly, Vichukit *et al.* (2004) reported that HB60 had higher starch content than RY5, RY72 and KU50. Herein, KU50 produced the highest starch yield due to the highest fresh storage root yield. KU50 also had higher HI than did HB60, indicating that KU50 was highly efficient in transporting photoassimilates for storage in tuber roots. KU50 is popular among cassava growers in the Northeast, Thailand, being widely adapted to unfavourable growing conditions (Rojanaridpiched *et al.*, 1995). In this study, only three cassava varieties were investigated to understand

the responses to bud removal and cutting lengths. The results indicated that the varieties responded similarly in terms of rooting and formation of storage roots. However, more cassava varieties should be investigated to reach a recommendation of management practise to cassava growers. In addition, the experiment was conducted in the early rainy season planting date and results do not cover the planting date in the late rainy season. This is the main planting date for cassava growing in Thailand and such seasonal influence on cassava management should be further investigated.

CONCLUSIONS

Bud removal practise did increase cassava yield in all evaluated varieties and the combination for the best yield was bud removal with cutting of 15 cm. The interaction between cutting length and environment should be considered. KU50 had the highest fresh storage root yields.

Acknowledgements. This work was supported by the Royal Golden Jubilee Ph.D. Program under the Thailand Research Fund. The authors would like to thank the Department of Plant Science and Agricultural Resources, Faculty of Agriculture, Khon Kaen University, Khon Kaen, Thailand and School of Water Energy and Environment, Cranfield University, United Kingdom for their cooperation during the experimentation.

SUPPLEMENTARY MATERIAL

For supplementary material for this article, please visit https://doi.org/10.1017/S0014479717000023.

REFERENCES

Alves, A. A. C. (2002). Cassava botany and physiology. In *Cassava: Biology, Production and Utilization*, 67–90 (Eds R. J. Hillocks, J. M. Thresh and A. Bellotti). Wallingford, UK: Centre for Agriculture and Biosciences International.

Bainbridge, Z., Tomlins, K., Wellings, K. and Westby, A. (1996). *Methods for Assessing Quality Characteristics of Non-Grain Starch Staples*. (Part 2. Field Methods.). Chatham, UK: Natural Resources Institute.

Bouyoucos, G. J. (1962). Hydrometer method improved for making particle size analysis of soils. *Agronomy Journal* 54:464–465.

Bray, R. H. and Kurtz, L. T. (1945). Determination of total, organic and available forms of phosphorus in soils. *Soil Science* 59:39–45.

Bremner, J. M. (1965). Total nitrogen. In *Methods of Soil Analysis. Part 2: Chemical and Microbiological Properties*, 1149–1178 (Ed C. A. Black). Wisconsin, USA: Madison.

Carvalho, L. J. C. B., Cascardo, J. C. M., Ferreria, M. A. and Loureiro, M. E. (1993). Studies on proteins and enzymes related to tuberization and starch biosynthesis in cassava roots. In *International Scientific Meeting of the Cassava Biotechnology Network*, 234–238 (Eds W. Roca and A. Thro). Proc. 1st, held in Cartagena de Indias, Colombia, January 1992. Cali, Colombia: CIAT.

Cline, M. N. and Neely, D. (1983). The histology and histochemistry of the wound healing process in geranium cuttings. *Journal of the American Society for Horticultural Science* 108:450–496.

Davies, F. T., Lazarte, J. E. and Joiner, J. N. (1982). Initiation and development of roots in juvenile and mature leaf bud cuttings of *Ficus pumila* L. *American Journal of Botany* 69:804–811.

Didier, P. and El-Sharkawy, M. A. (1994). Sink-source relations in cassava effects of reciprocal grafting on yield and leaf photosynthesis. *Experimental Agriculture* 30:359–367.

Ekanayake, I. J. (1994). Terminology for growth analysis of cassava. *Tropical Root and Tuber Crops Bulletin* 8:2–3.

Enyi, B. A. C. (1973). Growth rates of three cassava varieties (*Manihot esculenta* Crantz) under varying population densities. *The Journal of Agricultural Science* 81:15–28.

FAO. (2014a). Food and agriculture organization. Corporate Document Repository. Available at: http://faostat.fao.org/site/339/default.aspx, verified 19 November, 2014.

FAO. (2014b). Food and agriculture organization. FAO 2014 Database. Available at: http://www.fao.org/docrep/007/y2413e/y2413e0i.htm., verified 20 November, 2014.

Ganado, Z. S. (1956). *The Effect of Length of Cassava Cutting on Yield*. B.Sc. Thesis, Central Philippine University (CPU), Iloilo City.

Hahn, S. K. and Hozyo, Y. (1984). Sweet potato. In *The Physiology of Tropical Field Crops*, 551–576 (Eds P. R. Goldsworthy and N. M. Fisher). New York: John Wiley and Sons.

Jackson, M. B. (ed.) (1986). *New Root Formation in Plants and Cuttings*. Dordrecht: Martinus Nijhoff Publishers.

Jones, S., Robin, G., Garry, J., Johnson, L. and Benn, A. (2013). Production, productivity, quality standards and product mixes of roots and tubers crops in the CFC-funded project. Publication DO/029/12. Available at: http://www.cardi.org/cfc-rt/files/downloads/2013/09/Publ-9-Production-Productivity-RT-Jones-et-al.pdf. verified 19 February, 2016.

Knoth, J. (1993). Traditional storage of yams and cassava and its improvement. Deutsche Gesellschaft fur Technische Zusammenarbeit (GTZ) GmbH, Postfach 5180, D-65726 Federal Republic of Germany. Available at: http://www.fastonline.org/CD3WD_40/INPHO/VLIBRARY/GTZHTML/X0066E/EN/X0066E00.HTM, verified 19 February, 2016.

Knutsson, J. (2012). Long-term storage of starch potato and its effect on starch yield. MSc. thesis. Swedish University of Agricultural Sciences. Available at: http://stud.epsilon.slu.se/4996/1/knutsson_j_121023.pdf, verified 19 February, 2016.

Kramer, P. J. and Boyer, J. S. (1995). Roots and root systems. In *Water Relations of Plants and Soil*, 115–166 (Eds P. J. Kramer and J. S. Boyer). San Diego, CA: Academic Press, Inc.

Lahai, M. T., George, J. B. and Ekanayake, I. J. (1999). Cassava (*Manihot esculenta* Crantz) growth indices, root yield and its components in upland and inland valley ecologies of Sierra Leone. *Journal of Agronomy and Crop Science* 182:239–248.

Lahai, M. T., Ekanayake, I. J. and Koroma, J. P. C. (2013). Influence of canopy structure on yield of cassava cultivars at various toposequences of an inland valley agro ecosystem. *Journal of Agricultural Biotechnology and Sustainable Development* 5:36–47.

Lebot, V. (2009). *Tropical Root and Tuber Crops: Cassava, Sweet Potato, Yam and Aroids*, Wallingford, UK: Centre for Agriculture and Biosciences International publication. Available at: http://Amazon.com.

Leihner, D. (2002). Agronomy and cropping systems. In *Cassava: Biology, Production and Utilization*, 91–112 (Eds R. J. Hillocks, J. M. Thresh and A. Bellotti). Wallingford, UK: Centre for Agriculture and Biosciences International.

Lenis, J. I., Cali, F., Jaramillo, G., Perez, J. C., Ceballos, H. and Cock, J. H. (2005). Leaf retention and cassava productivity. *Field Crops Research* 95:126–134.

Malpighi, M. (1686). *Opera Omnia*, London: Royal Society of London.

McKeague, J. A. (1978). *Manual on Soil Sampling and Methods of Analysis*, 2nd edn. Ottawa, Canada: Canadian Society of Soil Science, Suite 907, 151 Slater St.

Nassar, N. M. A. and Teixeira, R. P. (1983). Seed germination of wild cassava species (*Manihot spp.*). *Ciencia e Cultura* 35:630–632.

OAE. (2014). Office of agricultural economics. Thai Economics Database 2014. Available at: http://www.oae.go.th/download/prcai/DryCrop/amphoe/casava-amphoe57.pdf, verified 16 November, 2014.

Onwueme, I. C. (1978). *The Tropical Tuber Crops: Yam, Cassava, Sweet Potato and Cocoyam*, New York: John Wiley and Sons.

Osiru, D. S. O., Porto, M. C. M. and Ekanayake, I. J. (1997). Physiology of cassava. *IITA Research Guide 55. Training Program, IITA, Ibadan, Nigeria.*

Rojanaridpiched, C., Limsila, A., Supraharn, D., Boonseng, O., Poolsanguan, P., Tiraporn, C. and Kawano, K. (1995). Recent progress in cassava varietal improvement in Thailand. In *Cassava Breeding, Agronomy Research and Technology Transfer in Asia*, 124–134 (Ed R. H. Howeler). Proc. 4th Regional Workshop, held in Trivandrum, Kerala, India. 2-6 November 1993. Cali, Colombia: CIAT.

Scott, G. J., Rosegrant, M. W. and Ringler, M. W. (2000). Roots and Tubers for the 21st Century: Trends, projections and policy options. Food, Agriculture and the environment discussion paper 31. International Food Policy Research Institute. Available at: http://pdf.usaid.gov/pdf_docs/Pnach747.pdf, verified 19 February, 2016.

Tongglum, A., Vichukit, V., Jantawat, S., Sittibusaya, C., Tiraporn, C., Sinthuprama, S. and Howeler, R. H. (1992). Recent progress in cassava agronomy research in Thailand. In *Cassava Breeding, Agronomy and Utilization Research in Asia*, 199–223 (Ed R. H. Howeler). Proc. 3rd Regional Workshop, held in Malang, Indonesia. Oct 22–27, 1990.

Velasco, O. L. (1982). The effects of different lengths of cutting on the growth and yield of cassava. B.Sc. thesis. WLAC, San Marcelino, Zambales.

Vichukit, V., Rodjanaridpiched, C., Poonsaguan, P., Sarobol, E., Cheamchamnuncha, C., Changlek, P., Piyachomkwan, K. and Sriroth, K. (2004). Huay Bong 60: New developed Thai cassava (*Manihot esculenta* Crantz) variety with improved starch yield and quality. In *The 6th International Scientific Meeting of the Cassava Biotechnology Network (CBN). March 8–14, 2004. Cali, Colombia.*

Villamayor, F. G., Dingal, A. G., Evangelio, F. A., Ladera, J. C., Medellin, A. C., Sajise, G. E. and Burgos, G. B. (1992). Recent progress in cassava agronomy research in the Philippines. In *Cassava Breeding, Agronomy and Utilization Research in Asia*, 245–259 (Ed R. H. Howeler). Proc. 3rd Regional Workshop, held in Malang, Indonesia.

Walkley, A. and Black, I. A. (1934). An examination of Degtjareff method for determining soil organic matter and a proposed modification of the chromic acid titration method. *Soil Science* 37:29–37.

UNDERSTANDING LODGING RESISTANT TRAITS FROM DIVERSE SUGARCANE LINES

NUNTAWOOT JONGRUNGKLANG[1,2,*], PRAWEENA MANEERATTANARUNGROJ[3], SANUN JOGLOY[1,2], PATCHARIN SONGSRI[1,2] AND PRASIT JAISIL[1]

[1] Northeast Thailand Cane and Sugar Research Center, Khon Kaen University, Khon Kaen, Thailand

[2]Department of Plant Science and Agricultural Resources, Faculty of Agriculture, Khon Kaen University, Khon Kaen Thailand

[3]Department of Biology, Faculty of Science, Khon Kaen University, Khon Kaen, Thailand

[*] Corresponding author

Nuntawoot Jongrungklang, Department of Plant Science and Agricultural Resources, Faculty of Agriculture, Khon Kaen University, Muang, Khon Kaen 40002, Thailand.

Tel.: +66 43 364 637

Fax: +66 43 364 637

E-mail address: nuntawootjrk@gmail.com

Keywords root length density, stalk height, stalk diameter, stalk weight, root anatomy

ABSTRACT

Lodging decreases sugarcane productivity due to a reduction in biomass production and cane quality. One strategy to overcome this problem is the breeding of lodging resistant lines. This implies that lodging resistant traits in sugarcane are first identified. Therefore, the objective of this study was to identify lodging resistant traits in diverse sugarcane lines and their relationships with lodging. Eight diverse sugarcane lines were planted during the period from January 2012 to January 2013 at the experimental farm Mitr Phuwiang Sugar Mill, Thailand. A randomized complete block design with four replications was used. After 12 months, canes in each plot were randomly measured for lodging, stalk height, stalk diameter, leaf and stalk weight, root length density (RLD), root length density percentage (%RLD), and root anatomy. High stalk dry weight is a key factor to induce lodging in cane. Lodging resistant cultivars had low stalk heights (range 248.2-263.7 cm) and stalk dry weights (range 4,884.6-5,482.8 g m^{-2}) as well as a good partition of the root in the upper soil layer, providing a strong root structure. The appropriate balance between shoot and root parts is possibly contributing to low lodging incidences and maintains high yield productivity. Therefore, breeding programs should focus on the selection of cultivars with large root systems in the upper soil layer which correspond appropriately with the aerial part.

INTRODUCTION

Sugarcane provides a juice which is used for the production of sugar. Moreover, sugarcane trash in farm has many benefits to improve soil properties such can reduce fertilizer use and increase water retention in soil (Mendoza et al 2001) and to use as renewable biomass fuel for sugarcane milling (Mendoza & Samson 2002). Sugarcane is widely grown and distributed in the tropics and subtropics and plays a major role in the economy of many countries such as Brazil, Australia and Thailand. There are many problems in sugarcane production that reduces cane yield such as downy mildew diseases (Baer & Lalusin 2013), drought (Jangpromma et al 2012), flooding (Jaiphong et al 2016) and

lodging (Berding & Hurney 2005). Lodging poses a general problem in the production of sugarcane. Lodging contributes to a decline in the rate of biomass accumulation in the late stages of sugarcane growth, leading to reduction in biomass production (Berding & Hurney 2005; Singh et al 2002), it also decreases yield component of sugarcane as stalk length, and stalk fresh mass (Van Heerden et al 2015), and internode volume of some cultivar (Sinclair et al 2005). In addition, lodging reduces cane quality (Hurney & Berding 2000) and can reduce cane yield by 11-15%, commercial cane sugar (CCS) by 3-12%, and sugar yield by 15-35% (Singh et al 2002)

The lodging of sugarcane is closely associated with planting depth level and seeding density, as an appropriate planting depth can reduce lodging occurrence and improve germination efficiency (Aslam et al 2008; Bashir & Saeed 2001). Nevertheless, the strategy to solve this obstacle using only the management practices in field conditions might not be achievement, since the variation in different location such as soil properties, soil environments and land level. Another strategy to solve the obstacle is breed lodging resistant line. This would be success, if the lodging resistant traits in sugarcane are firstly identified.

Agronomic traits such as stalk diameter, number of leaves, leaf size, stalk weight, leaf weight, stalk height, stalk straight, and root system might be associated with sugarcane lodging. Sugarcane cultivars with shorter leaves, lower leaf numbers and larger stalks are more resistant to lodging (Berding & Hurney 2005), and also high fiber content in stalk is a traits for the resistance (Babu et al 2009; White et al 2006). Conversely, traits which reduce lodging incidence represent a reduction in cane productivity. Berding & Hurney (2005) assumed that below ground parameters, such as root architecture, and their possible interaction with above ground components should be considered to understand lodging resistance in cane, but this is not addressed in the previous study. Rooting traits of sugarcane were only identified that involve with resistance to drought and flooding conditions (Jangpromma et al 2012; Jaiphong et al 2016). In maize, a larger root system provides more resistance to lodging than a small root system (Foerster 2012). For cereal crops, lodging

resistant traits are determined as a co-ordinate system between stalk mass, elasticity, and root system (Baker et al 2014). Moreover, lodging in sugarcane may be involved with the strength of root structure. High lignin accumulation in root tissue might contribute to resistance against lodging due to its strengthening effects on plant tissue (Taiz & Zigger 2006). In stem of wheat, lignin and cellulose play an important role in lodging resistance, as correlation was detected between resistance to lodging and width of mechanical tissue (Kong et al 2013).

However, the relationship between lodging resistant traits and lodging events in diverse sugarcane cultivars is not well understood. Root distribution and root anatomical traits might be involved in sugarcane lodging, but studies dealing with these factors are limited. The objective of this study was to identify lodging resistant traits in diverse sugarcane cultivars and their relationships with lodged cane. The results could provide information about lodging resistant traits of sugarcane cultivars which is useful for selection processes in breeding programs.

MATERIALS AND METHODS

Experimental details

Five pre-release sugarcane lines from the Mitr Phol Sugarcane Research Center, MP1, MP3, MP07-309, MP02-2-226, MP02-665 and three commercial cultivars, LK92-11, KK3, and K88-92 were used during January 2012 to January 2013 at the experimental farm Mitr Phuwiang Sugar Mill in Phuwiang, District of Khon Kaen Province, Thailand (lat16° 17.7′ N, 102°12.7′ E, 240 masl). The soil texture was a fine-loamy, siliceous, isohypothermic, Oxic Paleustults. A randomized complete block design with four replications was used with sugarcane lines and cultivars as treatments. A plot consisted of four rows, 10 m long, with a spacing of 1.3 m between rows and 0.3 m between plants. Soil was prepared following the usual procedure for sugarcane yield trials. Single bud sets of each genotype were manually planted. The cane was only irrigated after planting, and the field was then settled into rain-fed conditions. After planting, each plot was sprayed with a pre-emergence herbicide for

weed control. Fertilizer was applied with basal application at the rate of 50 kg N, 50 kg P, and 25 kg K ha^{-1}. Additional 175 kg N, 58 kg P, and 150 kg K ha^{-1} were applied as top dressing at tilling stages (four months after planting). Weed, insect, and disease control were performed as necessary to keep the plants free from pests throughout the experimental period.

Data collection

Lodging event and agronomic traits

At 12 months, five plants in each plot were randomly measured for lodging by recording the mean of the angle in degree from horizontal to vertical axis for all cane stalks in the tiller (0 = totally lodged and 90 = erectness). Before measuring the lodging degree, the ground around randomly marked tillers was leveled. For all cane stalks in a tiller, we determined the angle in degree from horizontal to vertical axis and then calculated the mean of the displacement.

Simultaneously, we measured agronomic traits Stalk height was randomly recorded from the ground to the last exposed dewlap as described by Berding & Hurney (2005). The center two rows with a length of 4 m (10.4 m^2) in each plot were cut at ground level. A sub-sample of five shoots per plot was randomly taken to determine fresh and dry weights of leaves and stalks, and the rest of the sample separated into leaves and stalks to determine fresh weight. The sub-samples were oven-dried at 80˚C for 48 h or until constant weight and dry weight of each leaf and stalk parts was measured. Leaf and stalk dry weights were calculated as dry weight per area (g m^{-2}). Stalk diameter was taken from the ground to the top of stalk level, as internodes appear at the base, middle, and top of the stalk.

Root length density (RLD) and root length density percentage (%RLD)

RLD was measured simultaneously to lodging using a monolith with a size of 20 x 20 cm and a depth of 20 cm; the common square monolith method was used for root collection. Root samples were taken at three layers consisting of 0-20, 20-40, and 40-60 cm. Nine positions were collected in each layer into 60 x 60 cm, including the center of the plant, right and left of the center of the plant and three upper and three lower positions of the center

position. Root samples of each position were washed manually with tap water to remove soil and analyzed with the Winrhizo program (Winrhizo Pro (s) V. 2004a, Regent Instruments, Inc) to determine total root length per sample. RLD was calculated as the ratio between root length (cm) and soil volume (cm^3). RLD values from all monolith positions within a soil depth layer were combined and defined as a single value, thus RLD was finally separated into three layers based on soil depth. i.e. upper, middle, and lower layers. Root length density percentage (%RLD) was calculated from RLD in each layer and whole RLD derived from three soil layers within the cultivar.

Cane root anatomy

At the time of harvest, root samples were randomly collected from the upper layer and separated from the soil with tap water. Measurement of root histological characteristics was carried out using cross sections with four repetitions within a replicate. All root samples were cut into suitable specimens as around 20 mm lengths (from 10 to 30 mm of root apex). Root samples were fixed in FAA 70 (1:1:8 formaldehyde, glacial acetic acid, and ethyl alcohol 70%). Transverse sections were prepared by free hand cross section and stained with 1% safranin. Sugarcane root samples were dehydrated in a graded ethanol series and mounted by DPX. Photomicrographs were taken with a Leica® DMLB photomicroscope equipped with a Leica® DC 300F camera. From the root anatomical picture in each cultivar, we measured the distance from the center of the pith through the outer rim of the pith and the distance from the center of the pith through the outer stele tissue; we then calculated the ratio of pith radial to the radial of pith and stele (ratio P/PS).This ratio was used for determining root strength.

Statistical analysis

The statistical analysis was conducted using the Statistix 8. Data were subjected to analysis of variance according to a RCB design. Comparison among genotypes for all parameters was performed based on the Least Significant Difference (LSD) test at $p<0.05$.

Simple correlation analysis was used to determine the relationship between lodging and agronomic traits, lodging and root traits, and lodging and anatomical traits.

RESULTS AND DISCUSSION

Classification of lodging resistant lines

The sugarcane cultivars were categorized into two groups based on the mean of the angle in degree from the horizontal to the vertical axis for all cane stalks in five tillers of each plot; the difference of two groups was based on the LSD at $p<0.05$. MP02-2-226, K88-92, LK92-11, KK3, and MP02-665 were classified as an erect cultivar (Table 1). They had significantly high mean values of the angle compared to the other three cultivars. MP1, MP3, and MP07-309 could be classified as lodging cultivars (Table 1).

There are various methodologies to identify lodging in sugarcane. For example, Van Heerden (2011) indicated lodging of cane by rating the degree of lodging that ranged from 1 to 9, where 1 = fully erect cane and 9 = completely lodged cane. Another method was investigated by Berding & Hurney (2005) and uses rating proportions of plot displacement and displacement severity which are then used to calculate the erectness index. However, in the previous report, rating was used as a criterion for determining lodging appearance, which might lead to biased results based on different personal perspectives. Using qualitative data with angle degrees is a way to reduce the error. Currently, the angle degrees method was used and reported in Singkham et al (2016).

The effect of lodging has been addressed in previous reports. Lodging has negative impacts on sugarcane crop quality and yield (Berding & Hurney 2005; Singh et al 2002), reduces the rate of biomass accumulation (Park et al 2005), and suppresses cane stalks (Van Heerden et al 2010). It is also able to induce dying of the stalk after lodging of around 60 days due to poor intercepted radiation (Singh et al 2002).

Agronomic traits and their relationship with lodging

The cane lines with different lodging resistant groups showed varying responses to agronomic traits. Cane height, leaf dry weight, and stalk dry weight generally showed higher values in lodging cultivars than in erect cultivars, whereas stalk diameter did not show significant differences between cultivars (Table 2). The diverse cane cultivars within the same lodging incidence group were different in their agronomical traits (Table 2). Lodging resistant cultivars, such as MP02-2-226, obtained low cane height, leaf dry weight, and stalk dry weight, and some cultivars, such as K88-92 and KK3, showed low values for cane height and stalk dry weight, but not for leaf dry weight. LK92-11 showed rather low values for stalk dry weight and stalk height, but high values for leaf dry weight. However, line MP02-665 showed high stalk height and leaf dry weight and relatively high stalk dry weight. Consequently, as lodging is a complex trait, several characteristics, including the performance of a below-ground part with the ability to resist lodging, may be involved.

The relationship between agronomic traits and lodging was investigated in order to identify lodging resistant traits. Stalk dry weight was significantly negatively correlated with lodging resistance, whereas other variables had no significant correlation (Figure 1).The relationship between stalk dry weight and lodging indicates that stalk dry weight is a key trait contributing to resistance to lodging in sugarcane. Moreover, simple correlation coefficients between the traits most related to lodging, such as stalk dry weight and the component traits, were also determined. There were no significant correlations for cane height, stalk diameter, and leaf dry weight (data not shown).

Berding & Hurney (2005) examined three traits, cane height, stalk diameter, and stalk number, and reported that only cane height was involved in lodging resistance. However, the disagreement between cane height in this study and the previous report (Berding & Hurney 2005) might be a result of different management conditions. The previous study was performed under high fertility and water input conditions, leading to different cane height values. In contrast, the present study tried to understand lodging of contrasted cane cultivars in rain-fed conditions, as the most farmer field condition in tropical zone. In addition, the previous study did not address stalk dry weight; however, this parameter should be

addressed when considering lodging resistance. Reduction of stalk dry weight might be a strategy to decrease lodging in sugarcane. Nevertheless, these traits would certainly affect a cane production. Below-ground parameters, such as rooting, possibly support resistance to lodging along with maintaining yield performance, and their possible interaction with above-ground components is necessary to approach a better understanding of lodging resistant cane.

Root length density and relationship with lodging

The RLD of cane cultivars differed among soil depth such as the upper middle and lower soil layers. Erect and lodging cultivars showed variations in high and low values for actual RLD. However, different cane cultivars had a different genetic potential to produce the size of the root system, therefore, we cannot compare actual RLD among cane cultivars. Root data in this experiment were calculated to be root length density percentage (%RLD), as the proportion of the root was derived from three soil layers within the cultivar.Within soil layers, %RLD revealed significant differences (Table 3). In the upper, middle, and lower layers, %RLD showed highly significant differences. In the upper soil layer, %RLD was found lower for lodging cultivars than for erect cultivars, whereas %RLD in the middle layer was higher for lodging cultivars.

The sugarcane cultivars within the same lodging incidence group were different in their rooting traits (Table 3). Erect cultivars, LK92-11 and KK3, had high %RLD in the upper layer, whereas MP02-2-226 and MP02-665 showed rather high %RLD in the soil surface layer, and low %RLD in the same layer was found for K88-92. Lodging cultivars such as MP1, MP3, and MP07-309 had low %RLD in the upper layer. In the middle layer, %RLD was high in lodging cultivars and low for erect cultivars. High variations in %RLD were found in the lower soil layer, lodging cultivars had high %RLD values and cultivars in erect groups showed variation. These consequences revealed that lodging resistant cultivars should have a high proportion of RLD in upper soil layers. So far, there is only limited information about RLD and its distribution associated with lodging in cane. In sunflower, rooting traits such as

root length, root number, root biomass and root axial breakage force connected with tolerance to lodging (Manzur et al 2014). Around 85% of the root biomass appears in the top 60 cm of the soil and 50% in the top 20 cm (Smith et al 2005). This investigation revealed the %RLD at soil depths of 0-20, 20-40 and 40-60 cm (Table 3), in accordance to the previous report. It is likely that RLD at the three soil layers analyzed in this study represent almost the entire RLD in the field; therefore, RLD in upper layers should be emphasized.

RLD was not significantly correlated with lodging at all three soil layers. The %RLD in the upper layer was significantly positively correlated with lodging resistance, whereas %RLD in middle and lower layers were significantly negatively correlated (Figure 2). This suggests that high proportions of RLD in the upper soil layer support the shoot and that RLD has an impact on lodging in sugarcane.

Root anatomy and lodging

Root anatomy in this experiment was represented by photographs to determine root strength, which might possibly be a resistant lodging trait. Some erect cultivars, such as MP02-2-226, KK3, and K88-92, showed low P/PS values (Table 4), indicating that they had a strong root structure due to a higher area occupied by tissue with accumulated lignin. Lignin is found in vascular tissue and controls the transportation of liquids in plants (Taiz & Zigger 2006). In most dicots, lignin units occur those in vessels and structural xylem fibers (Bonawitz & Chapple 2010). Higher sclerenchyma layer width and sclerenchyma layer number are capable to lodging resistance in Wheat (Karim & Jahan 2013). However, the erect cultivar MP02-665 revealed a high P/PS value.The lodging cultivars MP3 and MP1 showed rather high P/PS values (Table 4), indicating weak root tissue. Although MP07-309 was classified as lodging cultivar, it exposed a high area occupied by vascular tissue.The previous result that was reported by Kong et al (2013) showed no significant correlation between lodging and lignin or cellulose contents in stem of wheat.

The correlation between lodging incidence and ratio P/PS was not significant in this experiment (data not shown), therefore, we assume that root anatomical traits might not be used to evaluate resistance to lodging in sugarcane.

Characteristics contributing to lodging resistance in sugarcane

Since lodging is able to reduce cane yield and quality, choosing sugarcane varieties with a resistance to lodging is an important strategy for increasing cane yield. Our study clearly shows that high stalk dry weight is a major parameter which induces cane lodging. Low stalk weights provide resistance to lodging, however, they impede high cane yields. It is therefore important to understand the relationships between lodging resistant traits and sugarcane yields.

Lodging resistant cultivars, such as MP02-2-226, LK92-11, KK3 and K88-92, had low above-ground growth in terms of cane height and stalk weight values and small root systems revealed by actual RLD, but they had a relatively large part of their roots in the upper soil layer (represented by %RLD) and provided a strong root structure (revealed by ratio P/PS, except for LK92-11). Hence, these genotypes are resistant to lodging. MP02-665 is a genotype with resistance to lodging, but it has relatively high stalk height and cane weight values. This might be due to its rather large root system together with a good distribution in the upper soil layer. The appropriate balance between shoot and root parts is possibly contributing to low lodging incidences and maintains high yield productivity. In cereal crops, traits resisting lodging include canopy and stalk mass, elasticity, and root system (Baker et al 2014). Resistance to lodging by an equilibrium between shoot and root system was proposed for wheat (Crook et al 1994).Therefore, breeding programs should focus on the selection of cultivars with large root systems in the upper soil layer which correspond appropriately with the aerial part.

CONCLUSION

The sugarcane cultivars were categorized into two groups based on the mean of the angle from the horizontal to the vertical axis. Cultivars MP02-2-226, K88-92, LK92-11, KK3, and MP02-665 were classified as erect cultivars, whereas MP1, MP3, and MP07-309 could be classified as lodging cultivars. The major findings in this study were that stalk dry weight is the main trait that contributes to sugarcane lodging resistance. High stalk dry weight was clearly identified as a key trait to induce cane lodging. High %RLD in the upper soil layer was a lodging resistance trait, as determined by a good partition of the root in the upper soil layer in the lodging resistant cultivars. However, %RLD values in lodging and erect cultivars in this study showed variation. Thus, RLD in different sugarcane lines and the distribution of RLD in different soil depths needs further investigation. Therefore, clonal selection for lodging resistance inbreeding programs need to focus on the root system in the upper soil layer and appropriate correspondence with the shoot part.

ACKNOWLEDGMENTS

Grateful acknowledgement is made to Northeast Thailand Cane and Sugar Research Center, Faculty of Agriculture, Khon Kaen University and Thailand Research Fund (TRG5880086, IRG 5780003) for providing financial support for data collections, and Mitr Phol Sugarcane Research Center for field experiment preparations.

LITERATURE CITED

Aslam M, Hameed A, Chattha, AA. 2008. Effect of sowing depth and earthing up on lodging in pre sown sugarcane. Pak Sugar J. 23: 20-23.

Babu C, Koodalingam K, Natarajan US, Shanthi RM, Govindaraj P. 2009. Assessment of rind hardness in sugarcane (*Sacharum* Spp. Hybrids) genotypes for development of non-lodging erect canes. Adv Biol Res. 3: 48-52.

Baer OT, Lalusin AG. 2013. Molecular markers associated to Downy Mildew *Peronosclerospora philippinensis* (W. Weston) C.G. Shaw] Resistance in Sugarcane

(*Saccharum officinarum* L.) Hybrids (CP 57-604 X PHIL 84-77). Philipp J Crop Sci. 38 (3): 37-45.

Baker CJ, Sterling M, Berry PA. 2014. Generalized model of crop lodging. J Theor Biol. 36: 31-12.

Bashir S, Saeed M. 2001. Effect of planting pattern and seeding density on yield, weed mass production and crop lodging in sugarcane CV. SPSG.394. Pak Sugar J. 16: 9-13.

Berding N, Hurney AP. 2005. Flowering and lodging, physiological based traits affecting cane and sugar yield. What do we know of their control mechanisms and how do we manage them? Field Crops Res. 92: 261-275.

Bonawitz ND, Chapple C. 2010. The genetics of lignin biosynthesis: connecting genotype to phenotype. Annu Rev Genet. 44: 337–363.

Crook MJ, Eonnos AR, Sellers EK. 1994. Structural development of the shoot and root systems of two winter cultivars, *Triticum aestivum* L. J Exp Bot. 45: 857-863.

Foerster J, Prust I, Kaeppler S. 2008. Effect of root mechanics on lodging resistance in Maize. In: Central for Biology Education. http://cbe.wisc.edu/assets/docs/pdf/srp bio/2008/Foersterj1.pdf. accessed July 2012.

Hurney AP, Berding N. 2000. Impact of suckering and lodging on productivity of cultivars in the wet tropics. Proc Aust Soc Sugar Cane Technol. 22: 328-333.

Jaiphong T, Tominaga J, Watanabe K, Nakabaru M, Takaragawa H, Suwa R, Ueno M, Kawamitsu Y. 2016. Effects of duration and combination of drought and flood conditions on leaf photosynthesis, growth and sugar content in sugarcane. Plant Prod Sci. 19(3): 427-437.

Jangpromma N, Thammasirirak S, Jaisil P, Songsri P. 2012. Effects of drought and recovery from drought stress on above around and root growth, and water use efficiency in sugarcane (*Saccharum officinarum* L.). Aust J Crop Sci. 6: 1298-1304.

Karim MDH, Jahan MA. 2013. Study of lodging resistance and its associated traits in bread wheat. ARPN J Agric Biol Sci. 8: 683-687.

Kong E, Liu D, Guo X, Yang W, Sun J, Li X, Zhan K, Cui D, Lin J, Zhang A. 2013. Anatomical and chemical characteristics associated with lodging resistance in wheat. Crop J. 1: 43-49.

Manzur ME, Hall AJ, Chimenti CA. 2014. Root lodging tolerance in *Helianthus annuus* (L.): associations with morphological and mechanical attributes of roots. Plant Soil. 381: 71–83.

Mendoza TC, Samson R. 2002. Energy costs of sugar reduction in the Philippine context. Philipp J Crop Sci. 27(2): 17-26.

Mendoza TC, Samson R, Helwig T. 2001. Evaluating the many benefits of sugarcane trash farming systems. Philipp J Crop Sci. 27(1): 43-51.

Park SE, Robertson M, Inman-Bamber NG. 2005. Decline in the growth of a sugarcane crop with age under high input conditions. Field Crops Res. 92: 305-320.

Smith DM, Inman-Bamber NG, Thorburn PJ. 2005. Growth and function of the sugarcane root system. Field Crops Res. 92: 169-183.

Sinclair TR, Gilbert RA, Perdomo RE, Shine JM, Powell G, Montes G. 2005. Volume of individual internodes of sugarcane stalks. Field Crops Res. 91: 207-215.

Singh G, Chapman SC, Jackson PA, Lawn RJ. 2002. Lodging reduces sucrose accumulation of sugarcane in the wet and dry tropics. Aust J Agric Res. 53: 1183-1194.

Singkham N, Songsri P, Jaisil P, Jogloy S, Klomsa-Ard P, Jonglangklang N, Patanothai A. 2016. Diversity of characteristics associated with lodging resistance in sugarcane germplasm. SABRAO J Breed Genet. 48: 97-104.

Taiz L, Zeiger E. 2006. Plant Physiology. 4th ed. Sunderland, Massachusetts: Sinauer Associates, Inc. 293 p.

Van Heerden PDR. 2010. Biomass accumulation in sugarcane: unravelling the factors underpinning reduced growth phenomena. J Exp Bot. 61: 2877-2887.

Van Heerden PDR. 2011. Effects of lodging and anti-lodging chemicals on the productivity of variety n25: preliminary findings. Proc S Afr Sugar Technol Assoc. 84: 169-172.

Van Heerden PDR, Singels A, Paraskevopoulos A, Rossler R. 2015. Negative effects of lodging on irrigated sugarcane productivity an experimental and crop modeling assessment. Field Crops res. 180: 135-142.

White WH, Tew TL, Richard EP. 2006. Association of sugarcane pith, rind hardness, and fiber with resistance to the sugarcane borer. J Amer Soc Sugar Cane Technol. 26: 87-100.

Table 1. Classification of lodged sugarcane using the mean of the angle from horizontal to vertical axis (˚) of eight sugarcane cultivars.

group	cultivars	the mean of the angle from horizontal to vertical axis (˚)	
erect cultivars	MP02-2-226	88.23	a
	LK92-11	89.53	a
	KK3	81.22	ab
	MP02-665	77.29	ab
	K88-92	72.50	b
lodging cultivars	MP1	40.63	c
	MP3	40.83	c
	MP07-309	43.96	c
F-test		**	

Different letters adjacent to data of a cultivar within a season in the same column show significance at $P < 0.05$ by LSD

Table 2. Stalk diameter (bottom, middle and top in stalk), height, leaf and stalk dry weight of eight sugarcane cultivars with different lodging event.

group	cultivars	stalk diameter at the different stalk parts			stalk height (cm)		leaf dry weight (g m^{-2})		stalk dry weight (g m^{-2})	
		bottom	middle	top						
erect cultivars	MP02-2-226	27.36	27.84	26.66	248.2	d	301.3	c	4,884	d
	LK92-11	32.60	30.86	28.31	251.6	cd	397.4	ab	5,230	cd
	KK3	31.08	30.15	26.54	250.5	cd	359.0	bc	5,025	d
	MP02-665	32.91	30.73	27.31	263.7	abc	361.0	abc	5,482	cd
	K88-92	31.18	30.92	28.01	254.5	bcd	401.3	ab	4,974	d
lodging cultivars	MP1	28.92	27.59	26.11	272.0	a	439.7	a	6,004	bc
	MP3	31.98	32.38	28.03	253.7	bcd	371.8	abc	6,645	ab
	MP07-309	31.98	33.93	30.70	267.4	ab	346.2	bc	6,816	a
F-test		ns	ns	ns	*		*		**	

Different letters adjacent to data of a cultivar within a season in the same column show significance at $P < 0.05$ by LSD

Table 3. Root length density (RLD) and root length density percentage (%RLD) in upper soil layer (0-20 cm), in middle soil layer (20-40 cm) and in lower soil layer (40-60 cm) of eight sugarcane cultivars with different lodging event.

group	cultivars	RLD in different soil layer			%RLD in different soil layer		
		upper	middle	lower	upper	middle	lower
erect cultivars	MP02-2-	0.68 bc	0. c	0. cd	57.4 ab	27.4 bc	15.1 bc
	LK92-11	0.74 bc	0. c	0. d	64.7 a	22.4 cd	12.8 c
	KK3	0.74 bc	0. c	0. d	64.6 a	22.0 d	13.2 bc
	MP02-	0.88 b	0. c	0. b	57.2 ab	24.4 bc	18.2 ab
	K88-92	0.83 b	0. c	0. bc	56.1 b	25.3 bc	18.5 ab
lodging cultivars	MP1	0.78 b	0. b	0. ab	45.8 c	32.7 a	21.4 a
	MP3	1.37 a	0. a	0. a	55.6 b	27.6 b	16.7 ab
	MP07-	0.50 c	0. c	0. cd	51.7 bc	29.1 ab	19.1 ab
F-test		**	**	**	**	**	*

Different letters adjacent to data of a cultivar within a season in the same column show significance at $P < 0.05$ by LSD

Table 4. Ratio of pith radial to the radial of pith and stele (ratio P/PS) and cross section root photographic of eight sugarcane cultivars with different lodging event.

group	cultivars	ratio P/PS		cross section root photographic	
erect cultivars	MP02-2-226	0.516	c	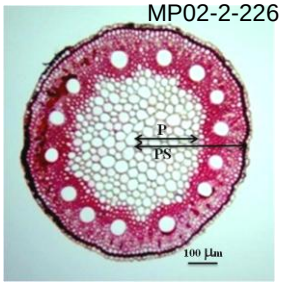	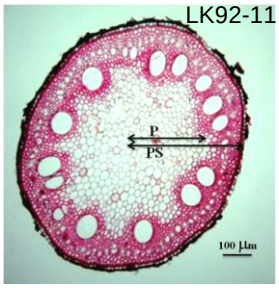
	LK92-11	0.598	a		
	KK3	0.513	c	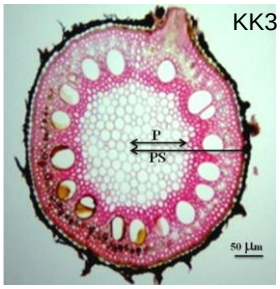	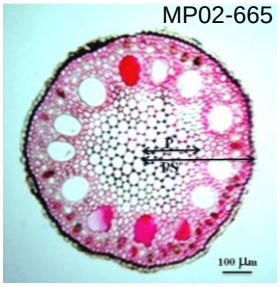
	MP02-665	0.558	ab		
Lodging cultivars	K88-92	0.513	c	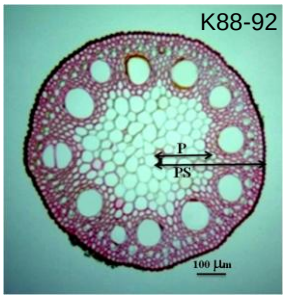	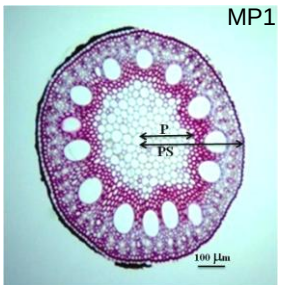
	MP1	0.525	bc		
	MP3	0.620	a	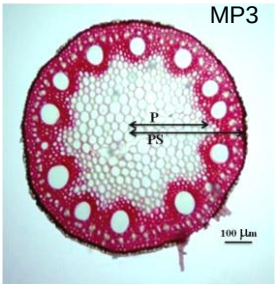	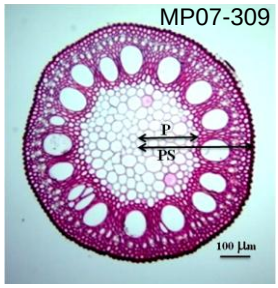
	MP07-309	0.518	c		
F-test		**			

Different letters adjacent to data of a cultivar within a season in the same column show significance at $P < 0.05$ by LSD

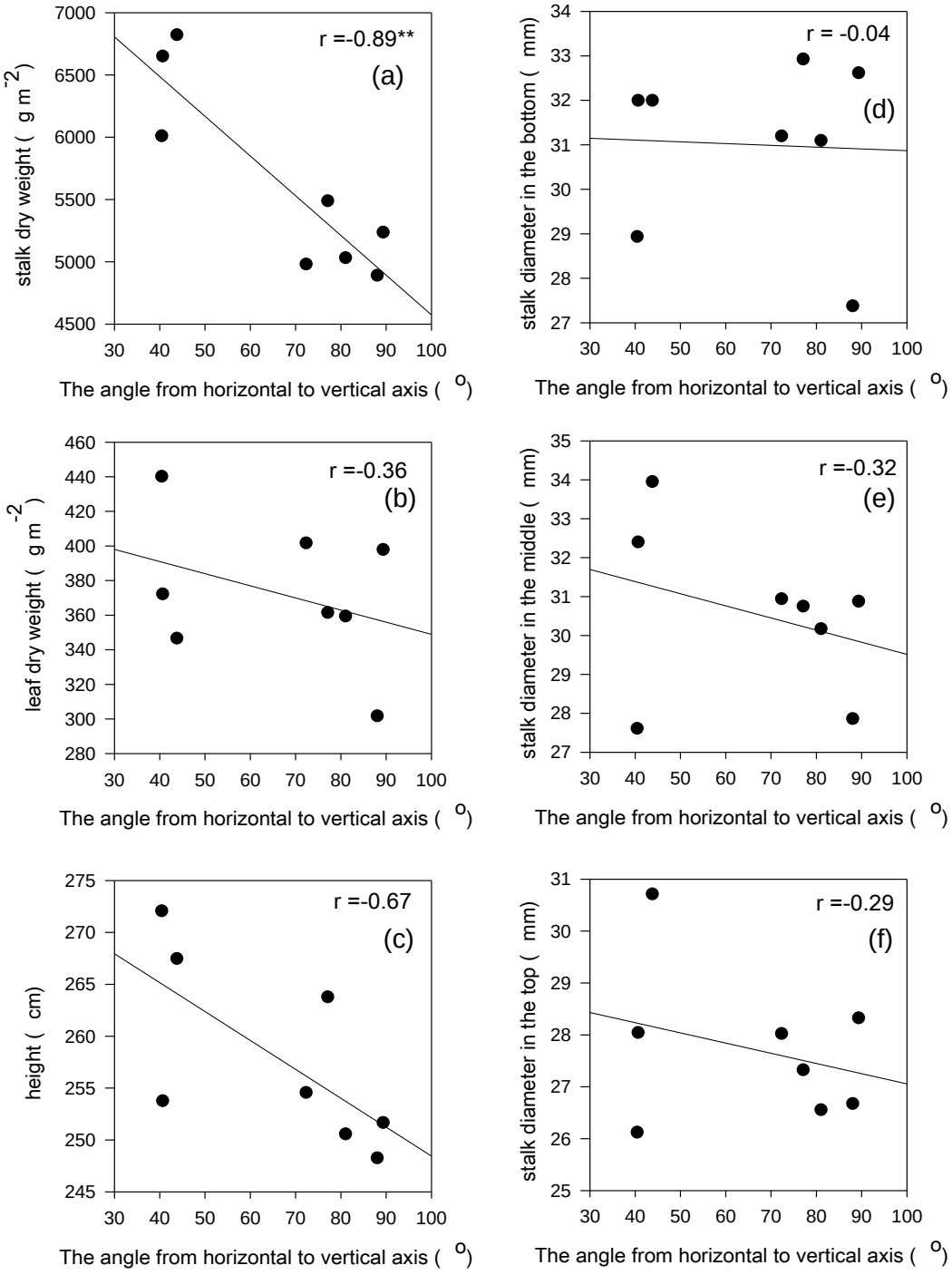

Figure 1. The mean of the angle from horizontal to vertical axis (˚), related agronomic traits including stalk dry weight (a), leaf dry weight (b), stalk height (c), stalk diameter at the bottom (d) middle (e) and top (f) of eight sugarcane cultivars with different lodging event.

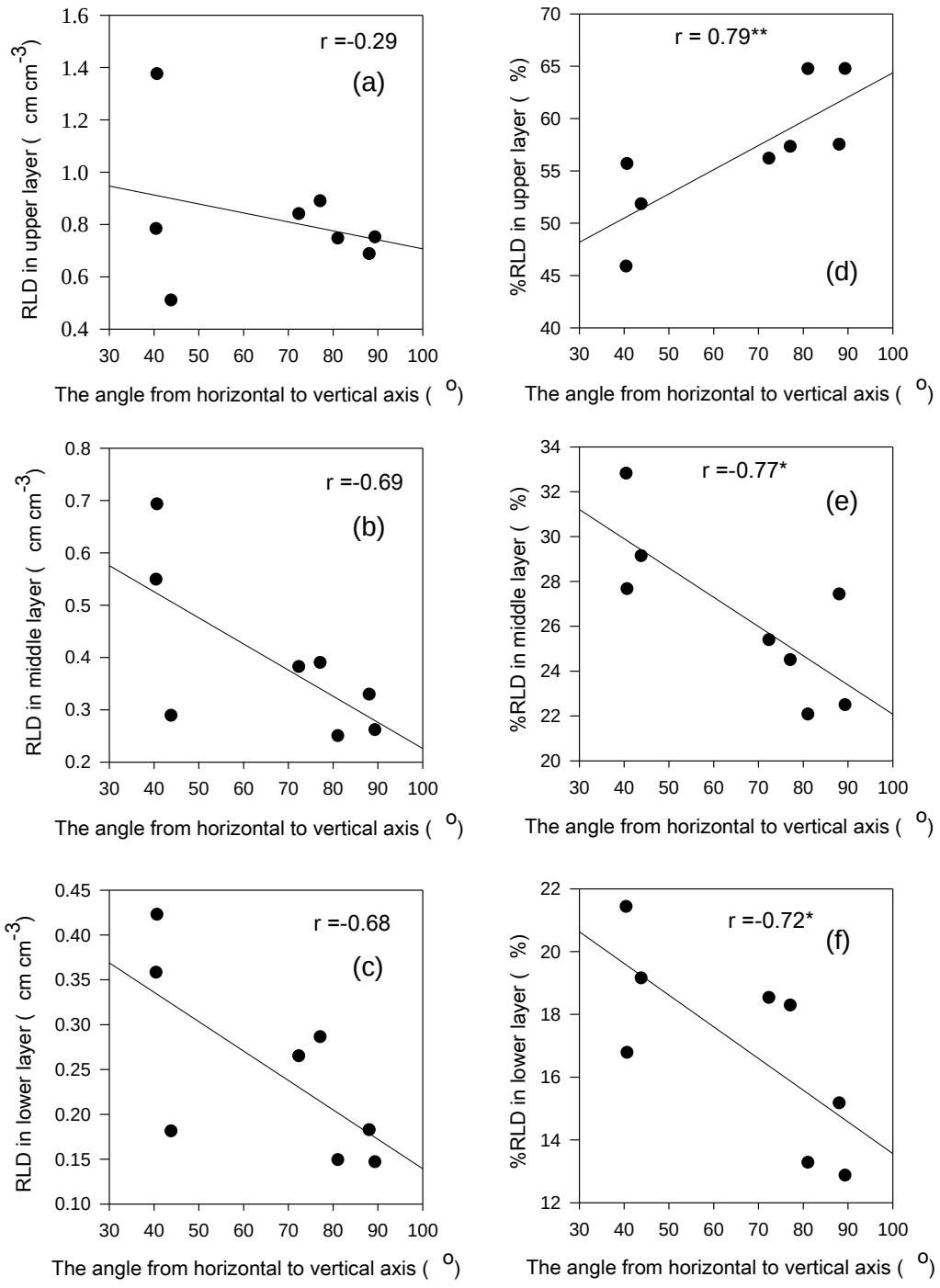

Figure 2. The mean of the angle from horizontal to vertical axis (˚) related rooting traits including root length density (RLD) in upper soil layer (a), middle soil layer (b), and lower soil layer (c), and root length density percentage (%RLD) in upper soil layer (d) middle soil layer (e) and lower soil layer (f) of eight sugarcane cultivars with different lodging event.

International Food Research Journal 24(2): 490-497 (April 2017)
Journal homepage: *http://www.ifrj.upm.edu.my*

Phenolic compound, anthocyanin content, and antioxidant activity in some parts of purple waxy corn across maturity stages and locations

[1]Mohamed, G., [1,2]Lertrat, K. and [1,2*]Suriharn, B.

[1]*Department of Plant Science and Agricultural Resources, Faculty of Agriculture, Khon Kaen University, Khon Kaen 40002, Thailand*
[2]*Plant Breeding Research Center for Sustainable Agriculture, Khon Kaen University, Khon Kaen 40002, Thailand*

Article history

Received: 7 December 2015
Received in revised form: 5 April 2016
Accepted: 8 April 2016

Keywords

Zea mays L.
Waxy maize
Phytochemicals
Environmental effects
Growth stages

Abstract

The understanding on growth stage of purple waxy corn and location effect is very important for anthocyanin production systems. Therefore, the objective of this study was to evaluate phenolic compounds, anthocyanins and antioxidant activity in corn components at immaturity (22 days after pollination (DAP)) and maturity (36 DAS) stages at different growing locations. Two varieties of purple waxy corn were evaluated at two locations during the dry season 2014/2015. Total phenolic (TPC), total anthocyanin (TAC) and antioxidant activity by DPPH free-radical-scavenging assay and TEAC trolox equivalent antioxidant capacity assay were recorded. Significant differences among corn components (C) were observed for all parameters. Location (L) x Variety (V), LxC, VxC and LxVxC interactions were significant for TAC in both stages. Silk and tassel had the highest TPC at immaturity stage but husk of KND and FC111 at KK had the highest at maturity stage. Silk of KND had the highest TAC at KK at immaturity stage but cob and husk of KND had the highest at maturity stage at KK. In general, corn cob and silk had high DPPH at immaturity stage and seed, cob and husk of KND at KK had high DPPH at maturity stage. However, cob and silk had the highest TEAC at immaturity stage and cob and husk especially KND had high TEAC at maturity stage. This information is useful for use waxy corn as food, food supplement and functional food products for corn consumers and food industry.

Introduction

Research on anthocyanins content and phenolic compounds is increasing due to important bioactive properties contributing to health benefits such as antioxidative activities, even though these compounds are not nutritive (Rice-Evans and Miller, 1996; Heinonen *et al*., 1998; Setchell and Aedin, 1999). Nutrient antioxidants are compounds that should be given through foods because they cannot be produced in the human body such as anthocyanin and other phenolic compounds (Huy *et al.*, 2008). The potential health benefits of anthocyanins and other phenolic compounds have been reported in many investigations. Anthocyanins have a wide range of bioactivities conducive to human health such as super antioxidant ability, anti-diabetic capacity, proliferative quality, inflammatory effects and the effects that protect against cancer and stroke (Yang *et al.*, 2010). Previous investigations reported a significant application of anthocyanins in food industry as food natural colorants in beverage, snacks and dairy products (de Pascual-Teresa and Sanchez-Ballesta, 2008).

The phytochemicals in different parts of corn have been reported in previous studies. Corn kernel contains a wide range of colors such as white, yellow, orange, purple and black. This pigmented corn is a rich source of phytochemicals and many secondary metabolites such as anthocyanins and other phenolic compounds (Žilić *et al.*, 2012). Study showed that corn cob provides phenolic compounds and natural antioxidants, which are used for the functional food (Cevallos-Casals and Cisneros-Zevallos, 2003). Corn silk is an excellent source of flavonoid compounds and many bioactive compounds (Ren *et al*., 2009) and silk of purple waxy corn at immaturity stage has high phenolic, flavonoids, anthocyanin and antioxidant activity (Sarepoua *et al*., 2015). Corn husk of purple corn is an excellent source of anthocyanins (Li *et al*., 2008). Moreover, corn tassel included a valuable raw source of phenols and could be used to increase the shelf life of fats and oils (Mohsen and Ammar, 2009).

Waxy or glutinous corn (*Zea mays* L.var. ceratina) is a special cultivated type of corn and an important vegetable crop in East and Southeast Asia countries

*Corresponding author.
Email: *bsuriharn@gmail.com*
Tel: +6643342949; Fax: +6643364636

due to consumer awareness of their health benefits. Waxy corn harvested at immaturity stage is consumed as fresh food similar to sweet corn. Generally, waxy corn has shorter maturity than sweet corn. Waxy corn is also harvested at maturity stage for food industry. Furthermore, waxy corn is a good source of anthocyanins, phenolics and antioxidant activity (Hu and Xu, 2011). Kernels and cobs of purple corn possess an excellent antioxidant activity (Li *et al*., 2008). Kernels of purple waxy corn had higher anthocyanins and antioxidant activity in both milky and maturity stages than did kernels of white waxy corn, super sweet corn and field corn (Khampas *et al*., 2013). The information on systematic evaluation of anthocyanins, phenolic compounds and antioxidant activity in purple waxy corn is very limited in the literature. Furthermore, the information on the quantities of these compounds in different tissues such as kernels, cob, silk, husk and tassel in purple waxy corn is lacking and further investigations are required. Therefore, we aimed to evaluate the total content of anthocyanins, phenolic compounds and antioxidant activity in several parts of purple waxy corn at immaturity and physiological maturity stages at different locations. These information will be valuable for food researchers, who work on functional food products, and consumers, who will have benefits from the products.

Materials and Methods

Plant materials

Two varieties of purple waxy corn (FC111 and KND) were used in this study. FC111 was obtained from Pacific Seeds, Thailand. KND was obtained from Plant Breeding Research Center for Sustainable Agriculture, Khon Kaen University, Thailand. These two varieties were selected because the difference of purple colors in ear parts. Moreover, previous study showed that FC111 and KND had high anthocyanin in cob (Khampas *et al*., 2015).

Two corn varieties were evaluated in a randomized complete block design with three replications at two locations in Uthai thani province (UT), Thailand, and Experimental Farm of Khon Kaen University (KK), Thailand, in the dry season 2014/2015. The soil type in UT was loamy and the soil in KK was sandy. Soil pH at KK was 6.4 but soil pH at UT was 5.5. UT had organic matter of 1.4% but organic matter at KK was lower (0.7%). Both locations had similar solar radiation and rainfall at vegetative period (0-60 days), but KK had lower maximum and minimum than UT.

The agronomic practices used in the experiment followed the recommendations for commercial production of waxy corn. Briefly, the varieties were planted in six-row plots with five meters in length and spacing of 80 cm x 25 cm. Five plants from two middle rows of each variety were selected randomly and harvested at immaturity stage (22 days after pollination) and at maturity stage (36 days after pollination). Ears were manually harvested from 5 randomly selected plants, whereas tassels were cut from the same plants at pollination. Husks and silks were speared from ears, while kernels were manually separated from cobs. Each sample was fragmented into smaller fractions separately and placed in plastic bags with lock court, consisting of two different stages in two sites. The samples (tassel, husk, silk, kernel and cob) were weighed as gram and directly frozen in liquid nitrogen to stop enzymatic activity, freeze-dried and stored at -22°C until analysis.

Sample extraction

Collected plant samples were grinded through electric mixer to obtain extract powder for used as the extracts. The extraction methods for total anthocyanins, phenolic compounds and antioxidant activity were described previously (Singh *et al.*, 2013) with slight modifications. Briefly, 2 g of each sample powder was taken into a flask containing 20 mL methanol and shaken on a platform shaker (LabScientific Inc., Livingston, NJ, USA) at 200 rpm for 1 hour in room temperature. The extracts were filtrated through Whatman No.1 filter paper in order to remove the debris. The procedure was repeated two times. To remove solvent, the filtrate was evaporated using a rotary flash evaporator (BUCHI Operations India Private Limited, 394230-Surat/India) at 40°C (5-10 minutes). The residue was reconstituted with 10 mL methanol and stored at -22°C until determination of total contents.

The extracted samples were analyzed using a spectrophotomerer (10S UV-Vis, Themo Scientific Genesys, Australia) to determine total anthocyanin contents (TAC) and total phenolic contents (TPC), and antioxidant activity was assayed by two methods, DPPH assay (free-radical-scavenging activity) and TEAC assay (trolox equivalent antioxidant capacity).

Determination of total anthocyanin contents (TAC)

Total anthocyanin content was determined following the pH differential method described by Mezadri *et al.* (2008) with minor modification. In brief, 0.5 mL from each sample was mixed with 4.5 mL of KCL buffers (pH 1.0) and 4.5 mL $NaCH_3$ buffers (pH 4.5). After mixing in Vortex, all samples were stored in the dark for 30 minutes. Absorbance at 510 and 700 nm was read in a spectrophotometer and

compared against blank. The blank consisted of 0.5 mL methanol and the same amount of all chemical except for the extracted sample. The determination of anthocyanin was made as the following formula:

(A x Mw x Dilution factor x 1000)/(Ɛ x 1),

where A was absorbance calculated accordance with (A510 – A700) pH1.0 - (A510 – A700) pH4.5, 1000 was converting factor from molar to ppm, Mw was molecular weight equal 449.2 g/ mol. Ɛ was molar extinction coefficient equal 26,900 $M^{-1}cm^{-1}$. For quantification Mw and Ɛ were used for external calibration for cyaniding-3-glucoside. The anthocyanin content was expressed as microgram of cyaniding-3-glucoside equivalents per gram of sample weight (mg C3G/100 g sample).

Determination of total phenolic contents (TPC)

The total phenolic contents were determined using the Folin– Ciocalteu according to the method reported previously (Reddy *et al*., 2010) with slight modifications. Initially, 0.5 mL Folin–Ciocalteu reagent was mixed with 2.5 mL distilled water to make the ratio of 1:5. Briefly, 0.5 of each sample was mixed with 3 mL diluted Folin–Ciocalteu reagent. The mixture was allowed to stand for 3 minutes at room temperature before adding 1.5 mL Na_2CO_3. The solution was stored in the dark for 30 minutes. The absorbance of the resulting mixture with blue color was measured at 765 nm against blank, using a spectrophotometer. The total phenolic contents were determined using curve of standard calibration and expressed as microgram of gallic acid equivalents per gram of dry weight (mg GAE/100 g sample weight).

Determination of antioxidant activities

Antioxidant activities were determined using the DPPH free radical scavenging assay, which was performed according to the method described by Liu *et al.* (2011) with slight modifications. In short, 0.2 mL from extract sample was mixed with 1 ml of 0.2 mM DPPH methanol solution, which was prepared immediately. The mixture was left to stand for 30 minutes in dark conditions. The absorbance of the resulting mixture was measured at 517 nm against blank using a spectrophotometer. The blank included 0.2 mL methanol and the same amount of all reagents except for the extracted sample. The absorbance was calculated and plotted as a function of concentration of standard and the extracted sample to determine the ascorbic acid equivalent concentration of antioxidant. The percentage of DPPH activity was calculated as the following equation:

DPPH radical scavenging activity (%Inhibition) = (1-Asample/A control) x100,

where A sample is the absorbance of extract or the standard, A control is the absorbance of the control.

The Trolox equivalent antioxidant capacity (TEAC) assay measures the antioxidant capacity of a given substance compared to the standard. Trolox antioxidant capacity is measured using the ABTS Decolorization Assay, which measures the reduction of radical cations of ABTS by antioxidants. This method was used as described by Kriengsak *et al.* (2006) with minor adjustments. Briefly, 0.0192 gram from ABTS was added to 5 mL distilled water. Potassium persulphate (0.0033 gram) was added to 5 mL distilled water and then two solutions were mixed for preparing TEAC. The mixture was allowed to stand for 24 hours in dark condition. Then 1 mL of TEAC was added to 60 mL methanol for preparing the final mixture. The extracted sample (0.03 mL) was added to 3 mL of final mixture. The absorbance of the resulting mixture was read at 734 nm against blank, using a spectrophotometer. The results were expressed in µmol of Trolox equivalents per g of dry weight (µmol TE/g sample weight).

Statistical analysis

Combined analysis of variance across the locations was carried out separately in accordance with a randomized complete block design for each character under study for milky stage and maturity stage. Least significant differences (LSD) for mean comparison test were set at $P \leq 0.05$.

Results and Discussion

Sources of variation

At immaturity stage, locations (L) were significantly different ($P \leq 0.01$) for total anthocyanin content (TAC) and antioxidant activity determined by DPPH method, whereas locations were not significant different for total phenolic compound (TPC) and antioxidant activity determined by TEAC method (Table 1). However, varieties (V) were significantly different ($P \leq 0.01$) for TAC and antioxidant activity determined by TEAC method, but TPC and antioxidant activity determined by DPPH method were not significant different. The results indicated that selection of suitable purple waxy corn for TAC and antioxidant activity determined by TEAC is important.

Components (C) were significantly different ($P \leq 0.01$) for all characters. The results showed that accumulations of phytochemical were different in

Table 1. Mean square for total phenolic compound (TPC), total anthocyanin content (TAC) and antioxidant activity determined by DPPH and TEAC methods in purple waxy corn at two growth stages

d.f.	2	1	1	4	1	4	4	4	38	
Traits	Mean squares									C.V. (%)
	Block	Location (L)	Variety (V)	Component (C)	LxV	LxC	VxC	LxVxC	Pooled error	
Immaturity stage										
TPC	106.9 ns	22.6 ns	1,197.6 ns	80,533.9 **	0.4 ns	290.6 ns	219.5 ns	231.0 ns	307.7	9.3
TAC	48 ns	4,669 **	85,054 **	42,756 **	4,929 **	1,567 **	8,780 **	1,461 **	181	15.7
DPPH	30.4 ns	355.3 **	0.1 ns	1,336.3 **	2.8 ns	158.6 **	219.9 **	8.5 ns	20.3	5.8
TEAC	0.11 ns	1.24 ns	21.09 **	150.32 **	2.29 *	0.14 ns	14.04 **	0.19 ns	0.35	6.1
Maturity stage										
TPC	27 ns	1,322 *	5,114 **	43,237 **	1,557 *	4,421 **	3,608 **	1,835 **	231	9.2
TAC	140 ns	5,744 **	60,964 **	76,922 **	777 *	1,393 **	9,423 **	739 *	150	13.7
DPPH	73 ns	39 ns	484 **	2,610 **	19 ns	274 **	126 *	40 ns	35	9.9
TEAC	0.4 ns	0.7 ns	12.4 **	132.2 **	5.9 *	0.4 ns	28.9 **	1.8 ns	0.9	10.5

ns = non-significant different
d.f. = degree of freedom; C.V. = coefficient of variation
*, ** significant different at P≤ 0.05 and 0.01 probability levels, respectively

corn components. The interactions between location and variety were significant (P≤0.01) for TAC and antioxidant activity determined by TEAC method, whereas the interactions between location and component were significant (P≤0.01) for TAC and antioxidant activity determined by DPPH method. The interactions between variety and component were significant (P≤0.01) for most characters except for TPC. In contrast, the interactions among location, variety and component were significant (P≤0.01) for TAC only.

At maturity stage, locations were significant different for TPC (P≤0.01) and TAC (P≤0.05) (Table 1). The differences among varieties and components were significant (P≤0.01) for all characters. The interactions between location and variety were significant (P≤0.05) for most characters except for antioxidant activity determined by DPPH method. However, the interactions between location and component were significant (P≤0.01) for most characters except for antioxidant activity determined by TEAC. The interactions variety and component were significant (P≤0.05 and 0.01) for all characters. The interactions among location, variety and component were significant (P≤0.01 and 0.05) for TPC and TAC.

Total phenolic compound (TPC)

Locations and varieties were not significantly different for TPC at immaturity stage and their interactions were not significant (Table 1). Silk and tassel had the highest TPC from two varieties across two locations (283 and 271 mg/100 g sample, respectively) (Figure 1a). At maturity stage, husk of KND variety at UT location and KK location had the highest TPC (284 and 303 mg/100 g sample, respectively, respectively) followed by husk of FC111 variety at KK location (278 mg/100 g sample) (Figure 1b).

UT location and KK location in the dry season represented the main growing areas of purple waxy corn in Thailand, which are located in the Central Plain and the Northeast of the country. KK location had higher TPC than did UT location for husk of FC111. This can be explained by higher solar radiation (12-17 MJ m^{-2} d^{-1} for UT and 15-19 MJ m^{-2} d^{-1} for KK) and lower temperature (23-32 °C for UT and 22-28 °C for KK) at KK location during seed filling duration or phenolic accumulation (41-115 days after planting). Although, UT location had low temperature at 61-75 days after planting, the period of low temperature was very short and, lather, the temperature increased again.

Normally, waxy corn, as a vegetable corn, is consumed at immaturity stage like sweet corn. However, purple waxy corn can be used at two seed stages including immaturity and maturity stages. At maturity stage or dry stage, purple waxy corn is good for food industry because it does not spoil rapidly and has longer shelf-life than at immaturity stage.

Silk and tassel had the highest TPC at immaturity but they decreased TPC at maturity stage. Husk was only one component that increased TPC very rapidly after immaturity stage and it had the highest TPC at maturity stage. Seed did not change TPC from immaturity to maturity stage. In previous study, seed of purple waxy corn at maturity had higher TPC than at immaturity stage (Khampas *et al*., 2013). The discrepancy of the results from different studies

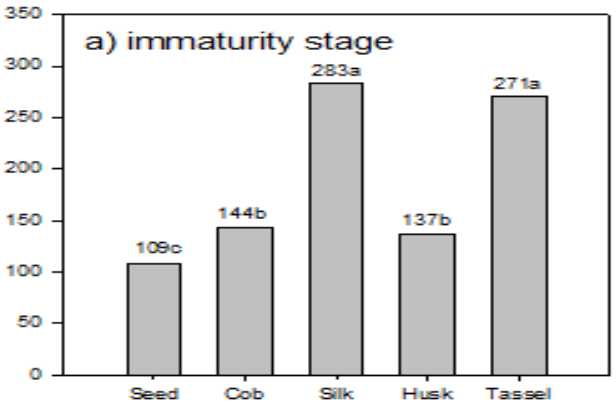

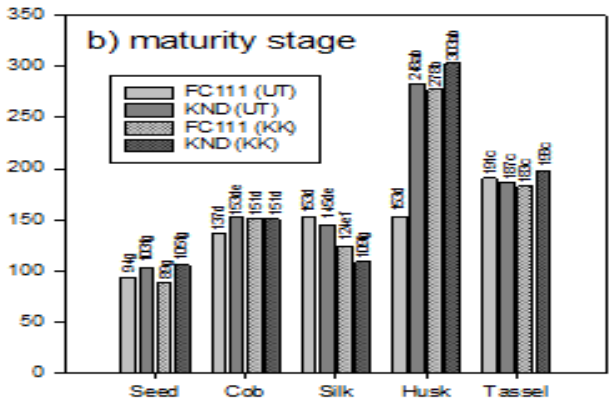

Figure 1. Total phenolic compound (TPC) (mg/100 g sample) in purple waxy corn components at two growth stages (UT is Uthai Thani and KK is Khon Kean). Means with the same letter(s) in each growth stage are not significantly different (P<0.05) by LSD.

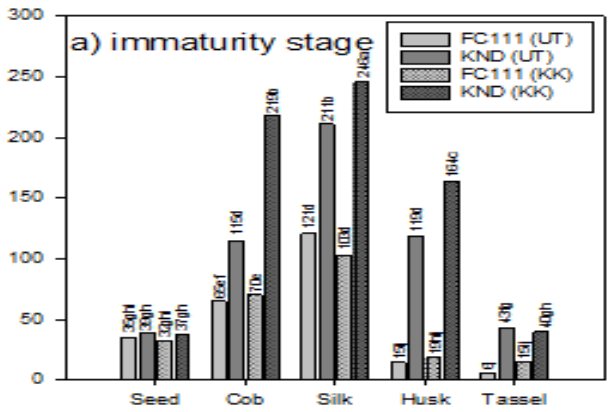

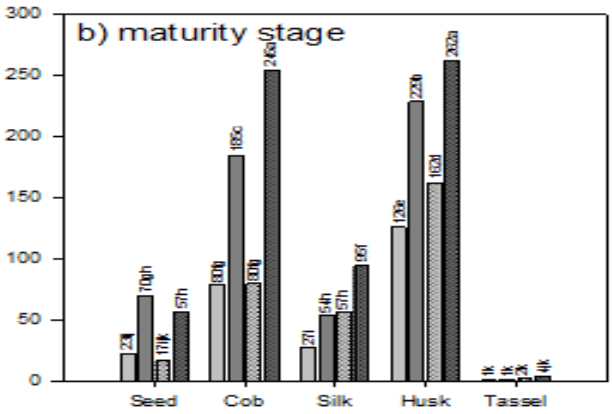

Figure 2. Total anthocyanin content (TAC) (mg/100 g sample) in purple waxy corn components at two growth stages (UT is Uthai Thani and KK is Khon Kean). Means with the same letter(s) in each growth stage are not significantly different (P<0.05) by LSD.

should be possibly due to the differences in materials used. It should be noted here that all components should be harvested at immaturity stage except for husk that it needs to be collected at maturity stage.

Total anthocyanin content (TAC)

At immaturity stage, silk of KND variety had the highest TAC at KK location (246 mg/100 g sample) followed by cob of KND variety (219 mg/100 g sample) at KK location and silk of KND variety at UT location (211 mg/100 g sample), respectively (Figure 2a). However, at maturity stage, husk and cob of KND variety at KK location had the highest TAC (262 and 254 mg/100 g sample, respectively) followed by husk and cob of KND variety at UT location (229 and 185 mg/100 g sample, respectively) (Figure 2b).

KK location had had higher TAC than did UT location at both maturity stages due to the higher solar radiation and lower temperature during anthocyanin accumulation. In previous study, low temperature might be the cause of high TAC in waxy corn cob (Khampas *et al.*, 2015). The results of two studies were rater different. In tomato tubers, phenolics and anthocyanin were increased with higher light intensity and low temperature (Reyes *et al*., 2004), but, in strawberry fruits, high temperature enhanced phenolics, flavonoids and anthocyanin (Wang and Zheng, 2001). The results of this study indicated that KK was a good location for phenolic and anthocyanin production.

Anthocyanins in corn are presented in all tissues and found at high concentrations in kernel skin and cobs (Moreno *et al*., 2005). The variation of maize and waxy corn germplasm in anthocyanins has been reported (Chander *et al.*, 2008; Harakotr *et al*., 2014). FC111 and KND are purple waxy corn varieties that were selected based on high TAC content in seed (Khampas *et al*., 2013) and in cob and good adaptation under growing conditions in Thailand (Khampas *et al*., 2015). Del Pozo-Insfram *et al.* (2007) suggested that corn genotypes with purplish black and blue kernels had very high phenolic compounds compared to corn genotypes with light-colored kernels. Moreover, corn genotypes with purple kernels showed the highest phenolic levels followed by corn genotypes with red and black kernels, respectively (Lopez-martinez *et al*., 2009).

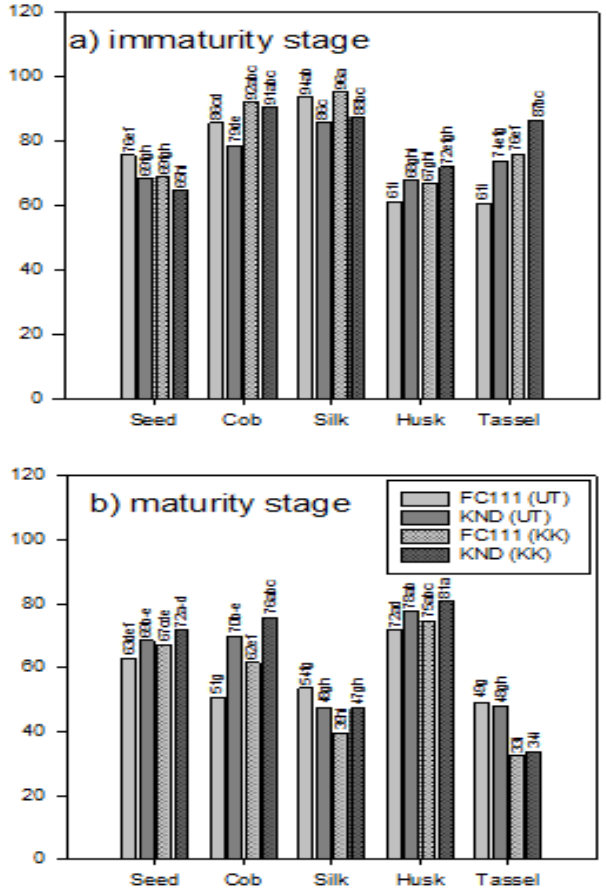

Figure 3. Antioxidant activities determination by DPPH assay (%) in purple waxy corn components at two growth stages (UT is Uthai Thani and KK is Khon Kean). Means with the same letter(s) in each growth stage are not significantly different (P<0.05) by LSD.

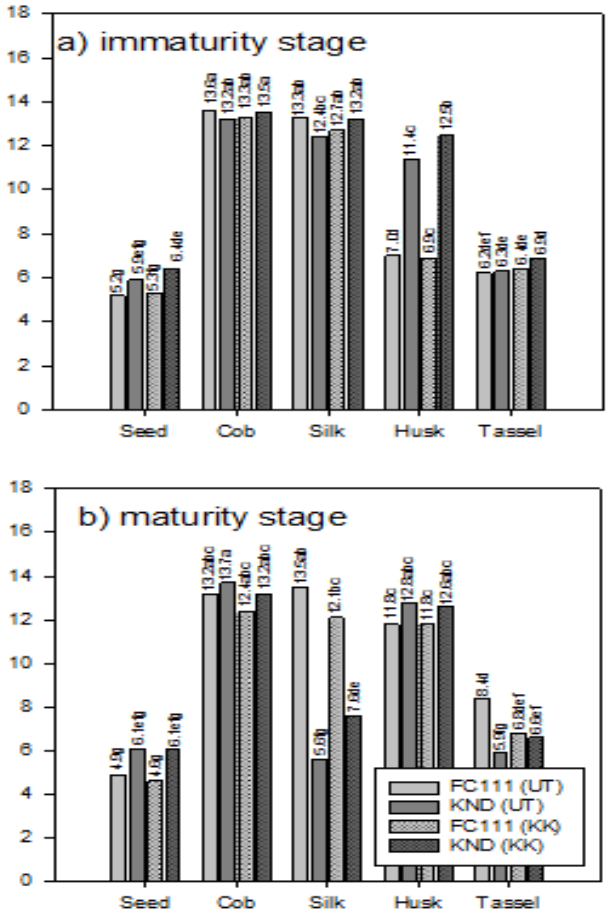

Figure 4. Antioxidant activities determination by TEAC assay (%) in purple waxy corn components at two growth stages (UT is Uthai Thani and KK is Khon Kean). Means with the same letter(s) in each growth stage are not significantly different (P<0.05) by LSD.

In this study, KND had higher TAC than did FC111 in most components except for seed at immaturity stage and tassel at maturity stage. The results were also supported by previous studies of purple waxy corn in seed (Khampas *et al.*, 2013) and cob (Khampas *et al*., 2015) at maturity stage.

Cob, silk, husk and tassel are waste products of waxy corn. In general, corn ears with seed, cob, silk and husk are sold on the market like sweet corn after that corn ears with husk or without husk are boiled or steamed. The consumers eat corn only seed and discard other components. Previous studies reported that corn seed (Khampas *et al*., 2013; Harakotr *et al.*, 2014) and cob (Khampas *et al*., 2015) were good sources of anthocyanin and antioxidant activity. Moreover, waxy corn seed is a good source of carotenoids (Kuhnen *et al*., 2010; Hu and Xu, 2011), anthocyanins, phenolics and antioxidant activity (Hu and Xu, 2011). In this study, silk and tassel were good sources of TPC at immaturity stage, but husk had the highest TPC at maturity stage.

Silk of KND variety had very high TAC at immaturity but cob and husk had high TPC at maturity stage. The results also supported by the results of Sarepoua *et al*. (2015), who found that silk of purple waxy corn genotypes at immaturity stage had higher TPC than at maturity stage. The results suggested that selection suitable corn components at the correct growing stage is very important for both TPC and TAC production.

In general, silk and tassel had high TAC at immaturity then they decreases very fast at maturity stage. However, other components including seed (for KND), cob and husk increased TAC after immaturity stage. The results supported by previous findings of Khampas *et al.* (2013) and Harakotr *et al*. (2014), who found that maturity stage had higher anthocyanin in corn seed than at immaturity stage. Accumulation of TAC in husk was very fast for almost two times compared with the husk at immaturity stage. The results suggested that silk and tassel should be harvested at immaturity stage, but other components especially husk should be collected at maturity stage.

Antioxidant activity determined by DPPH assay

At immaturity stage, silk of FC111 variety (96%),

cob of FC111 variety (92%), cob of KND variety (91%) at KK location and silk of FC111 variety (94%) at UT location had the highest DPPH followed by silk of KND variety (88%) and tassel of KND variety at KK location (87%) (Figure 3a). Husk (81%), cob (76%) and seed (72%) of KND variety, husk of FC111 variety (75%) at KK location, husk of KND variety (78%) and husk of FC111 variety (72%) at UT location had the highest DPPH at maturity stage (Figure 3b).

Location had very low effect on antioxidant activity determined by DPPH and TEAC methods except for DPPH at immaturity stage. In previous studies, low temperature enhanced antioxidant in corn cob (Khampas *et al*., 2015) and potato tuber (Lachman *et al*., 2008). The results in this study did not supported previous findings.

At maturity stage antioxidant activity determined by DPPH reduced in silk and husk but this parameter did not change in other components. The results indicated that silk and husk should be harvested for DPPH at immaturity stage.

Antioxidant activity determined by TEAC assay

Cob (13.6%), silk (13.3%) of FC111 variety, cob (13.2%), silk (12.4%) of KND variety at UT location, cob (13.5%), silk (13.2%) of KND variety, cob (13.3%) and silk of FC111 variety (12.7%) at UT had the highest TEAC followed by husk (12.5%) of KND variety at KK location and silk (12.4%) of KND variety at UT location at immaturity stage (Figure 4a). At maturity stage, cob (13.7%), husk (12.8%) of KND variety, silk (13.5%), cob (13.2%) of FC111 variety at UT location, cob (13.2%), husk (12.6%) of KND variety and cob (12.4%) of FC111 variety at KK location had the highest TEAC (Figure 4b). The results showed that at immaturity stage, KND had higher antioxidant activity determined by TEAC assay than did FC111 variety for corn husk, but FC111 variety increased TEAC until the value was similar to that of KND variety at maturity stage. The values of antioxidant activity determined by TEAC were almost the same as those determined by DPPH accept for TEAC in silk of FC111 variety, which did not decrease from immaturity to maturity stages.

Conclusion

Silk and tassel had high TPC, TAC, DPPH and TEAC at immaturity but husk had the high at maturity. KK had higher TEAC and TAC than UT. Cob, silk and husk of KND at KK location had high TAC at immaturity but cob and husk of KND were good sources at maturity. Cob and silk had high DPPH and TEAC at immaturity but cob and husk had high DPPH and TEAC at maturity.

Acknowledgments

This work was supported by the Plant Breeding Research Center for Sustainable Agriculture, Department of Plant Science and Agricultural Resources, Faculty of Agriculture, Khon Kaen University, Thailand. The authors would like to thanks the Faculty of Agriculture, Khon Kaen University for providing financial support for manuscript preparation activities.

References

Chander, S., Meng, Y., Zhang, Y., Yan, J. and Li, J. 2008. Comparison of nutritional traits variability in selected eighty-seven inbreds from Chinese maize (*Zea mays* L.) germplasm. Journal of Agricultural and Food Chemistry 56: 6506-6511.

Cevallos-Casals, B.A. and Cisneros-Zevallos, L. 2003. Stoichiometric and kinetic studies of phenolic antioxidants from Andean purple corn and red-fleshed sweet potato. Journal of Agricultural and Food Chemistry 51: 3313-3319.

de Pascual-Teresa S. and Sanchez-Ballesta, M.T. 2008. Anthocyanins: from plant to health. Phytochemistry Reviews 7: 281-299.

Del Pozo-Insfram, D., Saldivar, S.O., Brenes, C.H. and Talcott, S.T. 2007. Polyphenolics and antioxidant capacity of white and blue corn processed into tortillas and chips. Cereal Chemistry 84: 162-168.

Harakotr, B., Suriharn, B., Tangwongchai, R., Scott, M.P. and Lertrat, K. 2014. Anthocyanins and antioxidant activity in coloured waxy corn at different maturation stages. Journal of Functional Foods 9: 109-118.

Heinonen, M., Rein, Satué-Gracia, D.M.T., Huang, S., German, B. and Frankel, E.N. 1998. Effect of protein on the antioxidant activity of phenolic compounds in a lecithin-liposome oxidation system. Journal of Agricultural and Food Chemistry 46, 917-922.

Hu, Q.P. and Xu, J.G. 2011. Profiles of carotenoids, anthocyanins, phenolics, and antioxidant activity of selected color waxy corn grains during maturation. Journal of Agricultural and Food Chemistry 59: 2026-2033.

Huy, L., He, A.P.H. and Pham-Huy, C. 2008. Free Radicals, antioxidants in disease and health. International Journal of Biomedical Science 4: 89-96.

Khampas, S., Lertrat, K., Lomthaisong, K. and Suriharn, B. 2013. Variability in phytochemicals and antioxidant activity in corn at immaturity and physiological maturity stages. International Food Research Journal 20: 3149-3157.

Khampas, S., Letrat, K., Lomthaisong, K., Silmla, S. and Suriharn, B. 2015. Effect of location, genotypes and their interactions for anthocyanins and antioxidant

activities of purple waxy corn cobs. Turkish Journal of Field Crops 20(1): 15-23.

Kriengsak, T., Unaroj, B., Kevin, C., Luis, C.Z. and David, H.B. 2006. Comparison of ABTS, DPPH, Frap, and ORAC assays for estimating antioxidant activity from guava fruit extracts. Journal of Food Composition and Analysis 19: 669-675.

Kuhnen, S, Lemos, P.M.M, Campestrini, L.H, Ogliari, J.B., Dias, P.F. and Maraschin, M. 2011. Carotenoid and anthocyanin contents of grains of Brazilian maize landraces. Journal of the Science of Food and Agriculture 9: 1548-1553.

Lachman, J., Hamouz, K., Orsák, M., Pivec, V. and Dvořák, P. 2008. The influence of flesh colour and growing locality on polyphenolic content and antioxidant activity in potatoes. Scientia Horticulturae 117: 109-114.

Lopez-Martinez, L.X., Oliart-Ros, R.M., ValerioAlfaro, G., Lee, C., Parkin, K.L. and Garcia, H.S. 2009. Antioxidant activity, phenolic compounds and anthocyanins content of eighteen strains of Mexican maize. Journal of Food Science and Technology 42: 1187-1192.

Li, C.-Y., Kim, H.-W.,Won, S.-R., Min, H.-K., Park, K.-J., Park, J.-Y., Ahn, M.-S. and Rhee, H.-I. 2008. Corn husk as potential source of anthocyanins. Journal of Agricultural and Food Chemistry 56: 11413-11416.

Liu, J., Wang, C., Wang, Z., Zhang, C., Lu, S. and Liu, J. 2011. The antioxidant and free radical scavenging activities of extract and fractions from corn silk (*Zea mays* L.) and related flavone glycosides. Food Chemistry 126: 261-269.

Mezadri, T., Villano, D., Fernandez-Pachon, M.S., Garcia-Parrilla, M.C. and Troncoso, A.M. 2008. Antioxidant compounds and antioxidant activity in acerola (*Malpighia emarginata* DC.) fruits and derivatives. Journal of Food Composition and Analysis 21: 282-290.

Mohsen, S.M. and Ammar, A.S.M. 2009. Total phenolic contents and antioxidant activity of corn tassel extracts. Food Chemistry 112(3): 595-598.

Moreno, Y.S., Sánchez, G.S., Hernández, D.R. and Lobato, N.R. 2005. Characterization of anthocyanin extracts from maize kernels. Journal of Chromatographic Science 43: 483-487.

Reddy, C.V.K., Sreeramulu, D. and Raghunath, M. 2010. Antioxidant activity of fresh and dry fruits commonly consumed in India. Food Research International 43(1): 285-288.

Ren, S.C., Liu, Z.L. and Ding, X.L. 2009. Isolation and identification of two novel flavone glycosides from corn silk *(Stigma maydis)*. Journal of Medicinal Plants Research 3: 1009-1015.

Reyes, L.E., Miller, J.C. and Cisneros-Zevallos, L. 2004. Environmental conditions influence the content and yield of anthocyanins and total phenolics in purple- and red-flesh potatoes during tuber development. American Journal of Potato Research 81: 187-193.

Rice-Evans, C.A. and Miller, N.J. 1996. Antioxidant activities of flavonoids as bioactive components of food. Biochemical Society Transactions 24: 790-795.

Sarepoua, E., Tangwongchai, R., Suriharn, B. and Lertrat, K. 2015. Influence of variety and harvest maturity on phytochemical content in corn silk. Food Chemistry 169: 424-429.

Setchell, K.D.R. and Cassidy, A. 1999. Dietary Isoflavones: Biological Effects and Relevance to Human Health. Journal of Nutrition 129(3): 758S-767S.

Singh, A., Bajaj, R.V.K., Sekhawatb, P.S. and Singh, K. 2013. Phytochemical estimation and Antimicrobial activity of Aqueous and Methanolic extract of Ocimum Sanctum L. Journal of Natural Product and Plant Resources 3(1): 51-58.

Wang, S.Y. and Zheng, W. 2001. Effects of plant growth temperature on antioxidant capacity in strawberry. Journal of Agricultural and Food Chemistry 49: 4977-4982.

Yang, Z. and Zhai, W. 2010. Identification and antioxidant activity of anthocyanins extracted from the seed and cob of purple corn (*Zea mays* L.). Innovative Food Science and Emerging Technologies 11: 169-176.

Žilić, S., Serpen, A., Akıllıoğlu, G., Gökmen, V. and Vančetović, J. 2012. Phenolic compounds, carotenoids, anthocyanins, and antioxidant capacity of colored maize (*Zea mays* L.) kernels. Journal of Agricultural and Food Chemistry 60: 1224-1231.

International Food Research Journal 24(2): 552-558 (April 2017)
Journal homepage: *http://www.ifrj.upm.edu.my*

Germination process increases phytochemicals in corn

[1]Chalorcharoenying, W., [2]Lomthaisong, K., [1,3*]Suriharn, B. and [1,3]Lertrat, K.

[1]Department of Plant Science and Agricultural Resources, Faculty of Agriculture, Khon Kaen University, Khon Kaen 40002, Thailand
[2]Department of Biochemistry, Faculty of Science, Khon Kaen University, Khon Kaen 40002, Thailand
[3]Plant Breeding Research Center for Sustainable Agriculture, Khon Kaen University, Khon Kaen 40002, Thailand

Article history

Received: 7 December 2015
Received in revised form: 29 March 2016
Accepted: 4 April 2016

Keywords

Zea mays L.
Maize
Vegetable corn
Germinated corn
GABA content
Phytochemical

Abstract

Sprouts and seedlings increase nutritional value of seeds as they increase phytochemicals that are beneficial to health. Corn sprouts and seedlings can be consumed as germinated grains, vegetable and used as food additive. The objective of this study was to compare of phytochemical compounds from seeds, sprouts and seedlings of four small ear waxy corns, three waxy corns, three field corn, three sweet corns and three glutinous rice cultivars. sprouts and seedlings increased carotenoid content, gamma amino butyric acid (GABA) content, total phenolic content and total anthocyanin content, and the highest increases in these phytochemicals were found in seedlings. The levels of carotenoid content, GABA content, total phenolic content and total anthocyanin content among corn genotypes were low in seeds and sprouts but very high in seedlings. The correlation coefficients among Total anthocyanin content, carotenoid GABA and total phenolic content were high and significant ($P \leq 0.01$), ranging from $r=0.711$ to $r=0.871$. The results suggested that field corn is most suitable for germination at seedling stage in order to obtain the highest nutritional values. The utilization of sprouts and seedlings as vegetable and food additive is discussed.

Introduction

Germination process improves nutritional value of grains in many crops (Chavan and Kadam, 1989). Sprouted seeds and seedlings contain higher protein, vitamins, sugar, minerals and nutrient content than normal grains (Lorenz, 1980; Khalil *et al*., 2007). In rice, phytochemical compounds such as gamma amino butyric acid (GABA), vitamin B1, total phenolic and total anthocyanin significantly increased during germination process (Khampang *et al*., 2009; Chatsuwan and Areekul. 2010; Vongsudin et al., 2011). These phytochemicals have several health benefits such as reductions in the risk of cardiovascular disease, cancer, diabetes and aging, and they are also effective in controlling blood pressure, preventing the clogging and hardening of the arteries, reducing obesity and promoting better health for consumers (Hu *et al*., 2003; Tsuda *et al*., 2003; Jones, 2005).

Utilization of germinated seeds could be both at sprouted stage and seedling stage. In rice, hulled grains are germinated, dried and cooked alone or with normal rice to improve nutritional value. In other crop species such as beans, peanut and sunflower, the sprouted seeds are consumed as fresh or cooked vegetables. Another utilization is to make flour from both sprouted seeds and seedlings, and the flour provides both nutritional value and dietary fiber.

Ample information is available for the merit of germinated seeds that can improve nutritional value of the seeds in many crop species, and sprouted seeds have been extensively utilized. However, this information is not available for different types of corn. Which types of corn and germination stages are suitable for germinated seed production is still not clear.

Several distinct types of specialty corns are available (popcorn, sweet corn, high-protein quality corn, high waxy corn, high oil corn, etc.) (Hallauer, 2001.), and they are also different in kernel colors. The kernel colors would be white, brown, yellow, red, purple and black. Environmental conditions also affect the amount of this pigment, phytochemical compounds in corn kernels and seeds of other cereals (Adom and Liu, 2002). However, the information on the changes in phytochemicals during germination process in different types of corn is lacking. The

*Corresponding author.
Email: *bsuriharn@gmail.com*

Table 1. Corn and rice varieties/cultivars used in this study

Varieties/cultivars	Type of corn	Kernel color	Source
Tein Kaow	Small ear waxy corn	White	Khon Kaen University
Tein Luang	Small ear waxy corn	Yellow	Khon Kaen University
Tein Salubsee	Small ear waxy corn	Yellow and white	Khon Kaen University
Tein Line	Small ear waxy corn	Yellow, white and violet	Khon Kaen University
Samlee-Esaan	Waxy corn	White	Khon Kaen University
Khao Niew Khao kam	Waxy corn	Violet	Khon Kaen University
KKU-WX111031	Waxy corn	Violet	Khon Kaen University
Field corn check 1	Field corn	Yellow	Pacific Seeds Company Limited
Suwan 1	Field corn	Yellow	National Corn and Sorghum Research Center
Suwan 2	Field corn	Yellow	National Corn and Sorghum Research Center
Wandokkoon	Sweet corn	Yellow	Khon Kaen University
Sweet corn check 1	Sweet corn	Yellow and white	Syngenta Seeds Company Limited
Sweet corn check 2	Sweet corn	Yellow and white	Chia Tai Company Limited
Khao Maled Phai	Glutinous rice	Violet	Khon Kaen University
Khao Niew Dum Mong	Glutinous rice	Violet	Khon Kaen University
Khao Jao Hawm Nin	Rice	Violet	Kasetsart University

objective of this study was to evaluate phytochemicals in different types of corn at seed, sprouted and seedling stages. The information obtained from this study is useful for selection of suitable corn types and germination stages for production of sprouted corn.

Materials and Methods

Thirteen corn varieties including four small ear waxy corns, three waxy corns, three field corns and three sweet corns were used in this study, and three black rice cultivars were also used for comparison. The corn varieties used in this study were representatives of white, yellow and purple kernel types, and the details for these varieties are presented in (Table 1).

Sample preparation

Dry and well-filled seeds of corn and rice were used in the experiment. The seeds were soaked in water for 6 hours and germinated on moist filter paper in plastic trays at ambient temperature in the dark until shoot tips were about 0.5-1 mm in length or 24 hours. The seeds that germinated completely were cleaned and planted in sterilized sand for 7 days until the seedlings had green leaves. The sprouted seeds and the seedlings (Figure 1) were stored in liquid nitrogen to block the enzymatic activities at -20ºC until the samples were freeze-dried. Then the samples were ready for analysis.

Sample extraction

Sample extraction was carried out according to the modified method of Hu and Xu (2011). Briefly, 50 mg for each of the powder of seeds, sprouted seeds and seedlings was loaded in a flask of 250 ml containing 40 mI of methanol. Hydrochloric of 1% was added onto the flask and the sample was mixed thoroughly. The flask and the mixture was shaken stirrer (Diligent, Thailand) for two hours at

Figure 1. (A) dry kernels, (B) germinated kernels (24 hours), and (C) seedlings (7 days)

ambient temperature and in the absence of light. The homogenates were then centrifuged for 15 minutes in a centrifuge (Universal 30 RF) at 4,000 g and 4ºC. After centrifugation, the supernatants was filtered through Whatman #1 filter paper, evaporated under vacuum at 40ºC, and the resulting precipitates were re-suspended in 10 mL of 1% HCl/MeOH solvents (1 vol of 12.1 M HCl in 100 vol of methanol). The extracts of supernatant fluid were stored at -20ºC in the dark until further analysis for total anthocyanins and total phenolics.

Total anthocyanin content analysis

Total anthocyanin was determined using the spectrophotometric method as described by Hu and Xu (2011). Absorbance of appropriately diluted extracts at 535 nm was immediately measured to detect anthocyanins. Anthocyanin levels were expressed as milligrams of cyanidin 3-glucoside equivalents (CGE) per 100 g of dry weight (DW), using the reported molar extinction coefficient of 25 965 M^{-1} cm^{-1} and a molecular weight of 449.2 g/mol.

Total phenolics content analysis

The total phenolic content was determined based on the Folin-Ciocalteau colorimetric method as described by Hu and Xu (2011). Briefly, the extracted sample of 0.5 ml was mixed with 2.5 ml of distilled water and 0.5 ml of 1.0 M Folin – Ciocalteau phenol

reagent. After incubation for 8 min, 1.5 ml of 7.5% sodium carbonate was added, mixed well and stored in the dark for two hours at room temperature. The samples were then vortexed, and the absorbance was measured at 765 nm using a UV spectrophotometer (Genesys 10S UV-VIS; Thermo scientific). Methanol was used as the blank, and gallic acid (GA) was used for calibration of standard curve (0-500mg/L). Phenolic content was expressed as milligrams of gallic acid equivalents (GAE) per 100 g on dry matter basis (DM).

Carotenoid content analysis

Analysis of carotenoids was carried out according to the modified method of Schaub *et al.* (2004). The samples of seeds, sprouted seeds and seedlings were ground into very fine powder. The powder samples of 0.5 g each were loaded into 15ml blue cap plastic tubes (Falcon tube). EtOH:BHT of 6 ml was added into each tube, and the samples were mixed thoroughly by vortexing.

The samples were then incubated at 85°C in a water bath for 6 minutes, and, after incubation for 3 minutes, the samples were vortexed for 10 seconds. Care must be taken to make sure that the caps were not closed tightly during heating, and the caps were closed tightly during vortexing. KOH of 120 µl (1g/ml H_2O, prepared fresh daily) was added into the tubes and the samples were vortexed thoroughly for 20 seconds.

For saponification, the samples were later Incubated for 5 minutes at 85ºC, vortexed for 10 seconds and further incubated for 5 minutes at 85ºC. After incubation, the samples were allowed to cool in ice bath. Distilled water (H_2O) of 4ml and PE:DE (2+1,v,v of 3 ml as added into the tubes. The samples were shaken or vortexed and centrifuged for 10 minutes at 1400g. Phase separation of the samples was visible.

The upper phase of each tube was transfer to a new 15 ml tube. Care must be taken not to transfer all portion of upper phase, and it is better to leave a little portion for recovering in the next steps. The recovering of upper phase was repeated two times. The organic epiphases from three extraction times were mixed together in the new tubes. This should produce approximately a total of 8-9 ml of the extract. The supernatants of each sample were added with 10 ml of PE:DE (2+1,v,v) and mixed well. The optical density (O.D.) was then measured at 450nm in a spectrophotometer with the appropriate blank (PE:DE (2+1,v,v) and Lambert-Beer's equation was used for calculation of carotenoids.

GABA content analysis

GABA content was determined using method described previously (Kitaoka and Nakano, 1969) with a minor modification. The powder samples of 1.5 g of corn and rice (seeds, sprouted seeds and seedlings) were extracted in 30 ml of 80% ethanol. The tubes were vortexed to mix the powder with ethanol. The samples were then filtered through a number 1 filter paper and dried in vacuum at 40ºC. The resulting precipitates were resuspended in 3 ml of water.

In order to determine GABA content, the sample extracts of 0.2 ml were added with 0.2 ml of borate buffer (0.2 mol boric acid 50 ml with 0.2 mol sodium borate 59 ml); 1ml of 6% phenol. The mixtures were allowed to cool at room temperature. After cooling, the samples were then added with 0.4 ml of 7.5% NaOCl and mixed well. The samples were heated in a hot water bath for 10 minutes, and they were cooled immediately in an ice bath for 5 minutes. The absorbance was measured at 630 nm using a UV spectrophotometer. GABA content was then compared with the graphs of the standard solution. The standard curve was constructed by GABA at concentrations of 0, 50, 100, 150, 200, 250, 300,350, 400, 450 500 mg/I) and the concentrations of standard samples were calculated using the standard curve equation;

$$y=0.0009x-0.0091,$$

where x is the concentration of GABA, y for the 630 nm visible light absorbance, R^2=0.983 derived GABA content.

Statistical analysis

The data of three replications were analyzed statistically according to a completely randomized design. Where main effect was significant, least significant differences (LSD) at 0.05 probability level was used to compare means. Correlation coefficients among carotenoid content, GABA content, total phenolic content and total anthocyanin content were computed to determine the relationships among these phytochemicals.

Results

Significant differences ($P\leq0.01$) among germination stages were observed, and germination stage was the largest source of variations for carotenoid content, GABA content, total phenolic content and total anthocyanin content (Table 2). Significant differences ($P\leq0.01$) among varieties were observed

Table 2. Mean squares for carotenoid content, GABA content, total phenolic content and total anthocyanin content of different corn types and rice evaluated at three germination stages (seed, sprout and seedling)

Source of variation	df	Carotenoid content	GABA content	Total phenolic content	Total anthocyanin content
Germination stage (S)	2	11013.2**	0.2518**	142.568**	42.276**
Variety (V)	15	132.7**	0.00262**	0.858**	0.9501**
S×V	30	122.6**	0.00545**	0.707**	0.5573**
Error	64	2.2	0.00001	0.174	0.0489

** Significant at 0.01 probability level

Table 3. Carotenoid content, GABA content, total phenolic content and anthocyanin content of different corn types and rice evaluated at seed stage, sprout stage and seedling stage

Variety	Carotenoid (mg/g)			GABA (mg/100g)			Total phenolic (mg/100g)			Anthocyanin (mg/g)		
	Seeds	Sprouts	Seedlings	Seed	Sprouts	Seedlings	Seeds	Sprouts	Seedlings	Seeds	Sprouts	Seedlings
Corn												
Tein Kaow	0.008	0.018	15.093	0.030	0.028	0.231	0.126	0.186	3.568	0.049	0.091	2.302
Tein Luang	0.087	0.156	10.253	0.016	0.022	0.145	0.130	0.205	3.396	0.045	0.166	2.024
Tein Salubsee	0.065	0.097	10.347	0.023	0.020	0.199	0.123	0.200	3.358	0.052	0.113	2.129
Tein Line	0.065	0.086	19.160	0.028	0.021	0.202	0.081	0.213	4.034	0.094	0.190	2.053
Samlee-Esaan	0.025	0.032	23.653	0.026	0.040	0.212	0.162	0.247	3.537	0.052	0.051	1.704
Khao Niew Khao kam	0.025	0.033	29.693	0.021	0.033	0.224	0.234	0.221	3.445	0.151	0.682	2.165
KKU-WX111031	0.491	0.658	33.707	0.038	0.053	0.209	0.004	0.006	3.400	1.471	1.051	2.070
Field corn check 1	0.531	0.708	30.373	0.038	0.036	0.232	0.129	0.147	2.842	0.059	0.045	1.917
Suwan 1	0.390	0.602	30.053	0.066	0.038	0.173	0.145	0.151	3.697	0.113	0.115	1.858
Suwan 2	0.384	0.675	34.760	0.047	0.031	0.150	0.105	0.148	1.359	0.098	0.130	1.097
Wandokkoon	0.241	0.398	37.627	0.035	0.090	0.092	0.003	0.006	3.527	0.068	0.069	1.841
Sweet corn check 1	0.341	0.522	51.560	0.028	0.041	0.184	0.004	0.008	3.725	0.082	0.127	2.219
Sweet corn check 2	0.160	0.286	37.013	0.033	0.027	0.164	0.005	0.007	3.287	0.068	0.059	1.879
Mean	0.216	0.329	27.946	0.033	0.037	0.186	0.096	0.134	3.321	0.185	0.222	1.943
Rice												
Khao Maled Phai	0.029	0.048	23.133	0.026	0.068	0.110	0.002	0.006	3.096	0.669	1.048	1.834
Khao Niew Dum Mong	0.024	0.028	20.880	0.021	0.053	0.034	0.003	0.007	1.106	1.089	1.231	0.826
Khao Jao Hawm Nin	0.050	0.044	16.120	0.064	0.085	0.056	0.003	0.005	1.894	0.944	0.447	3.443
Mean	0.034	0.040	20.044	0.037	0.069	0.067	0.003	0.006	2.032	0.901	0.909	2.034
Overall mean	0.182	0.274	26.464	0.034	0.043	0.164	0.079	0.110	3.079	0.319	0.351	1.960
$LSD_{(0.05)}$	0.112	0.012	4.277	0.002	0.003	0.011	0.040	0.038	1.196	0.278	0.141	0.653
C.V.(%)	37.13	2.55	9.72	3.27	3.79	3.99	31.23	42.71	23.35	52.47	24.15	20.01

** Significant at 0.01 probability level

for carotenoid content, GABA content, total phenolic content and total anthocyanin content. The significant interactions (P≤0.01) between germination stage and varieties were observed for carotenoid content, GABA content, total phenolic content and total anthocyanin content. Although differences among varieties and the interactions between variety and germination stage were significant, these variations contributed much smaller portion to total variations in carotenoid content, GABA content, total phenolic content and total anthocyanin content compared to germination stage. As differences in germination stages for these phytochemicals were much higher than differences in genotypes, germination stages should be considered for use of colored corn and rice for functional food products.

In comparison among seeds, sprouts and seedlings for overall means of corn and rice, sprouts were slightly higher than seeds for carotenoid content (0.274 and 0.182 mg/g), GABA content (0.043 and 0.034 mg/100g), total phenolic content (0.110 and 0.079 mg/100g) and anthocyanin content (0.351 and 0.319 mg/g), but they were significantly much lower than seedlings (26.464 mg/g, 0.164 mg/100g, 3.079 mg/100g and 1.960 mg/100g for carotenoid content, GABA content, total phenolic content and anthocyanin content, respectively) (Table 3). The results indicated that increases in carotenoid content, GABA content, total phenolic content and anthocyanin content were low at sprout stage but exceptionally high and significant at seedling stage.

Significant differences among corn genotypes and rice genotypes were found for caroteniod content, GABA content, total phenolic content and anthocyanin content in seeds, sprouts and seedlings. Carotenoid content values ranged from 0.008 to 0.531 mg/g in seeds, 0.018 to 0.708 mg/g in sprouts and 10.253 to 51.560 mg/g in seedlings. In general, corn genotypes with yellow kernels had the highest carotenoid contents in seeds, sprouts and seedlings with the ranges of 0.160 to 0.531, 0.296 to 0.708 and 30.053 to 51.560 mg/g, respectively, compared to corn genotypes and rice genotypes with white endosperm. These corn genotypes with high carotenoid content included KKU-WX111031, field corn check 1, Suwan 1, Suwan 2, Wandokkoon, Sweet corn check 1 and

Table 4. Correlation coefficients among carotenoid, GABA, total phenolic content (TPC) and total anthocyanin content (TAC)

	TAC	Carotenoid	GABA
Carotenoid	0.711**		
GABA	0.741**	0.769**	
TPC	0.771**	0.837**	0.871**

** significant at 0.01 probability level

Sweet corn check 2. It is interesting to note here that KKU-WX111031 with waxy endosperm and purple kernels was also had high carotenoid content.

GABA contents ranging from 0.016 to 0.066, 0.020 to 0.090 and 0.034 to 0.232 mg/100g in seeds, sprouts and seedlings, respectively, were observed among corn genotypes and rice genotypes. Suwan 1 had the highest GABA content (0.066 mg/100g) at seed stage. Wandokkoon had the highest GABA content (0.090 mg/100g) at sprout stage, and Field corn check 1 had the highest GABA content (0.232 mg/100g) at seedling stage. It is important to note here that, although GABA content increased with sprouts and seedlings, GABA contents at seed stage, sprout stage and seedling stage were not related.

Total phenolic content values ranging from 0.002 to 0.234, 0.005 to 0.247 and 1.106 to 4.034 mg/100g in seeds, sprouts and seedlings, respectively, were observed among corn genotypes and rice genotypes. Khao Niew Khao Kam had the highest total phenolic content (0.234 mg/100g) at seed stage. Samlee-Esaan had the highest total phenolic content (0.247 mg/100g) at sprout stage, and Tien Line had the highest phenolic content (4.034 mg/100g) at seedling stage.

Anthocyanin content values ranging from 0.045 to 1.471, 0.059 to 1.231 and 0.526 to 3.443 mg/100g in seeds, sprouts and seedlings, respectively, were observed among corn genotypes and rice genotypes. KKU-WX111031 had the highest anthocyanin content (1.471 mg/100g) at seed stage. Rice variety Khao Niew Dum Mong had the highest anthocyanin content (1.231 mg/100g) at sprout stage followed by KKU-WX111031 (1.051 mg/g). Khao Jaw Hawm Nin had the highest anthocyanin content (3.443 mg/100g) at seedling stage followed by sweet corn check 1 (2.219 mg/100g). Three rice varieties had high anthocyanin content at all stages compared to corn varieties.

Correlation coefficients among total anthocyanin content, carotenoid content, GABA content and total phenolic content were significant ($P \leq 0.01$), ranging from r=0.71 for total anthocyanin content and carotenoid content to r=0.871 for GABA content and total phenolic content (Table 4). Total anthocyanin was significantly correlated with GABA (r=0.741) and total phenolic content (r=0.771), whereas carotenoid was also significantly correlated with GABA (0.769) and total phenolic content (r=0.871).

Discussion

The problem of food security is increasingly important worldwide. Improvement of food quality and diversification of food utilization is an important means to increase food security when food is in shortage caused by natural disasters such as flooding and storms. In this situation, corn can be an important item in disaster rescue bags, and the victims can consume corn kernels immediately as grains and germinate corn kernels for sprouts or seedlings.

In this study, very low increases in carotenoid content, GABA content, total phenolic content and total anthocyanin content were found in sprouts of corn and rice. However, very high increases in these phytochemicals were observed in seedlings. Germination of corn at seedling stage is therefore very interesting for utilization than germination at sprout stage. Higher carotenoid content in seedlings than in seeds and sprouts indicated that carotenoid was newly synthesized in seedlings, and corn seedlings is the good source for this phytochemical.

In previous investigation in rice, the germination process significantly ($p<0.05$) increased GABA content, total phenolic content and antioxidant capacity, and there was little change in the early stage of germination and then a marked increase after 36 hours. For the GABA content after soaking, it gradually increased from 80 to 220 mg/100 g embryo fresh weight from 12 to 60 hours (Maisont and Narkrugsa, 2010). In another study, the highest GABA content was obtained when the rice was germinated for 36 hours and 48 hours, depending on rice varieties, and the GABA content in germinated brown rice increased 9.43-16.74 times compared to non=germinated brown rice (Banchuen *et al*., 2010). Similar increase in GABA content from germination process in rice were also reported in other studies (Saikusa *et al*., 1994a, 1994b; Varanyanond, 2005; Sasagawa *et al*., 2006; Watchraparpaiboon, 2007). Appropriate germination is the germination stages that provide the highest GABA content and temperature, moisture and oxygen are involved in the germination process (Duangpatra, 1986).

Khumkah *et al*. (2009) reported that GABA content at seedling stage was significantly lower than that at sprout stage. The results were similar to our results for Khao Niew Dum Mong and Khao Jao Hawm Nin, which slightly decreased GABA content, but different from Khao Maled Phai, which

increased in GABA content. For corn, however, most genotypes increased GABA content at seedling stage. GABA with antioxidant activity can be increased in corn and rice seeds during germination process and many enzymes are involved in synthesis of GABA (Lopez-Amoros *et al.*, 2006; Ngyuen and Ooraikul, 2008; Watchararparpaiboon *et al*., 2010).

For phenolic content, Khumkah *et al.* (2009) found in rice that germinated seeds had higher total phenolic content than non-germinated seeds, and the similar results were also reported in edible seeds of 13 species (Cevallos-Casals and Cisneros-Zevallos, 2009). Our results were in agreement with previous results and also added new information that corn seedlings had higher phenolic content than sprouts.

Anthocyanin content was similar to total phenolic content which increased remarkably at seedling stage. The anthocyanin content in grains is found in the area tissue and an outer layer of tissue in (Abdel-Aal *et al.*, 2006). However, the increase in anthocyanin content at seedling stage compared to seed stage and sprout stage indicated that anthocyanin was newly-synthesized in seedlings.

Differences among genotypes were low, but germination stage contributed to large variations for these phytochemicals. However, corn genotypes with yellow endosperm had the highest carotenoid content, and corn genotypes with purple kernels had the highest anthocyanin content, which were similar to black glutinous rice cultivars. When corn is consumed as vegetable, sweet corn and small ear waxy corn are very useful.

Although seedlings had the highest phytochemicals, whole corn seedling powder can be used as food additive to increase nutrition values in food, and grain maize is most suitable for these purposes. In this study, corn seedlings are a good source of bioactive compounds in our diet. The utilization of corn seedlings for food ingredient with health benefit is a means to increase value-added price in corn as production of corn seedlings is simple and not expensive. Corn seedling is a good source of diet fiber.

Conclusion

This research compared different types of corn and purple glutinous rice varieties at seed stage, sprout stage and seedling stage for carotenoid content, GABA content, total phenolic content and total anthocyanin content. Germination at sprout stage slightly increased these phytochemicals. However, very high increases in these phytochemicals were found at seedling stage in corn and rice. Therefore, corn and rice seedlings can be used as food additive to improve nutritional values in food. Grain maize is the most suitable for this purpose.

Acknowledgments

This work was supported by the national science and technology development agency, the plant breeding research center of sustainable agriculture, department of plant science and agricultural resources, faculty of agricultural, Khon Kaen University, Thailand, the department of biochemistry, faculty of science, Khon Kaen University, Thailand and Mahasarakham University, Thailand.

References

Abdel-Aal E-S, M., Young, J. C. and Rabalski, I. 2006. Anthocyanin composition in black, blue, pink, purple, and red cereal grains. Journal of Agricultural and Food Chemistry 54: 4696–4704.

Adom, K.K. and Liu, R.H. 2002. Antioxidant activity of grains. Journal of Agricultural and Food Chemistry 50: 6182–6187.

Banchuen, J., Thammarutwasik, P., Ooraikul, B., Wuttijumnong, P. and Sirivongpaisal, P. 2010. Increasing the bio-active compounds contents by optimizing the germination conditions of Southern Thai brown rice. Songklanakarin Journal of Science and Technology 32(3): 219–230.

Cevallos-Casals, B.A. and Cisneros-Zevallos, L. 2009. Impact of germination on phenolic content and antioxidant activity of 13 edible seed species. Food Chemistry 119: 1485–1490.

Chatsuwan, N. and Areekul, V. 2010. Color parameters, total phenolic and anthocyanin content in various rice cultivars. In Proceedings of the 48th Kasetsart University Annual Conference, p. 646.

Chavan, J.K. and Kadam, S.S. 1989. Nutritional improvement of cereals by fermentation. Critical Reviews in Food Science and Nutrition 28: 349–400.

Duangpatra, J. 1986. Seed testing and analysis. Agriculture Book Group, Bangkok. 194 p.

Hallauer, A.R. 2001. Specialty corn. Boca Raton London New York Washington, D.C. CRC Press LLC.

Hu, C., Zawistowski, J., Ling, W. and Kitts, D.D. 2003. Black rice (*Oryza sativa* L. indica) pigmented fraction suppresses both reactive oxygen species and nitric oxide in chemical and biological model systems. Journal of Agricultural and Food Chemistry 51: 5271–5277.

Hu, Q. and Xu, J. 2011. Profiles of Carotenoids, anthocyanins, phenolics, and antioxidant activity of selected color waxy corn grains during maturation. Journal of Agricultural and Food Chemistry 59: 2026–2033.

Jones, K. 2005. The potential health benefits of purple corn. Herbal Gram 65: 46–49.

Khalil, A.W., Zeb, A., Mahmood, F., Tariq, S., Khattak, A.B. and Shah, H. 2007. Comparison of sprout quality characteristics of desi and kabuli type chickpea cultivars (*Cicer arietinum* L.), Swiss Society of Food Science and Technology 40: 937–945.

Khampang, E., Kerdchoechuen, O. and Laohakunjit, N. 2009. Comparative study of phytochemical compounds from rice and 4 cereal grains. Agricultural Science Journal 40(Suppl.): 93–96.

Khumkah, O., Kerdchoechuen, O. and Laohakunjit, N. 2009. Change of vitamin b1, -amino–butyric acid (gaba) and phenolics of germinated brown rice and four kinds of cereal. Agricultural Science Journal 40 (Suppl.): 73–76.

Kitaoka, S. and Nakano, Y. 1969. Colorimetric determination of gamma amino acid. Journal of Biochemistry 66: 87–94.

Lopez-Amoros, M.L., Hernandez, T. and Estrella, I. 2006. Effect of germination on legume phenolic compounds and their antioxidant activity. Food Composition and Analysis 19: 277-283.

Lorenz, K. 1980. Cereal sprouts: composition, nutrition value, food application critical reviews. Food Science and Nutrition 13: 353–385.

Maisont, S. and Narkrugsa, W. 2010. The effect of germination on GABA content, chemical composition, total phenolics content and antioxidant capacity of Thai waxy paddy rice. Kasetsart J. (Nat. Sci.) 44: 912–923.

Ngyuen, J.S and Ooraikul, B. 2008. The physic-chemical, eating and sensorial properties of germinated brown rice. International Journal of Food Agricultural and Environment 6(2): 119-124.

Saikusa, T., Horino, T. and Mori, Y. 1994a. Distribution of free amino acids in the rice kernel and kernel fractions and the effect of water soaking on the distribution. Journal of Agricultural and Food Chemistry 42: 1122–1125.

Saikusa, T., Horino, T. and Mori, Y. 1994b. Accumulation of g-aminobutyric acid (GABA) in the rice germ during water soaking. Bioscience Biotechnology and Biochemistry 58: 2291–2292.

Sasagawa, A., Naiki, Y., Nagashima, S., Yakura, M., Yamazaki, A. and Yamada, A. 2006. Process for producing brown rice with increased accumulation of GABA using high pressure treatment and properties of GABA-increased brown rice. Journal of Applied Glycoscience 53: 27–33.

Schaub, P., Beyer, P., Islam, S. and Rocheford, T. 2004. Maize quick carotenoid extraction protocol. Downloaded from *http://www.cropsci.uiuc.edu/faculty/rocheford/quick_carotenoid_analysis_protocol*.pdf on 08/12/2011.

Tsuda, T., Horio, F., Uchida, K., Aoki, H. and Osawa, T. 2003. Dietary cyanidin 3-O-β-D-glucoside-rich purple corn color prevents obesity and ameliorates hyperglycemia in mice. The Journal of Nutrition 133: 2125–2130.

Varanyanond, W., Tungtrakul, P., Surojanametakul, V., Watanasiritham, L. and Luxiang, W. 2005. Effects of water soaking on gamma-aminobutyric acid (GABA) in germ of different Thai rice varieties. Kasetsart Journal 39: 411–415.

Vongsudin, W., Laohakunjit, N. and Kerdchoechuen, O. 2011. Phytochemical change and antioxidant activities of germinated cereals. Agricultural Science Journal 42 (Suppl.): 113–116.

Watchraparpaiboon, W., Laohakunjit, N., Kerdchoechuen, O. and Photchanachai, S. 2007. Effects of pH, temperature and soaking time on qualities of germinated brown rice. Agricultural Science Journal 38 (Suppl.): 169–172.

Watchraparpaiboon, W., Laohakunjit, N. and Kerdchoechuen, O. 2010. An improve process for high quality and nutrition of brown rice production. Food Science and Technology International 16: 147-158.

RESEARCH ARTICLE

SABRAO Journal
of Breeding and Genetics
49 (2) 144-154, 2017

GENOTYPIC VARIABILITY FOR INULIN CONTENT, TUBER YIELD AND TUBER WEIGHT OF JERUSALEM ARTICHOKE (*Helianthus tuberosus* L.) GERMPLASM

D. PUANGBUT[1]*, S. JOGLOY[2,3*] and W. VEERI YASUTHEE[2]

[1] Plant Production Technology, Faculty of Technology, UdonThani Rajabhat University, UdonThani, Thailand
[2] Department of Plant Science and Agricultural Resources, Faculty of Agriculture, Khon Kaen University, Khon Kaen, Thailand
[3] Peanut and Jerusalem Artichoke Improvement for Functional Food Research Group, Khon Kaen University, Khon Kaen, Thailand
*Corresponding author's email: sjogloy@gmail.com
Email addresses of co-authors: daruneepom@gmail.com; wanalai_v@hotmail.com

SUMMARY

Inulin content is a priority trait in Jerusalem artichoke breeding program. However, breeding for high inulin in Jerusalem has not been reported in the semi-arid tropics. The objective of this study was to evaluate the genotypic variation for inulin content and to the selection of parental line for useful in breeding for high inulin content under different seasons. Development of high inulin content genotypes with high yield and good agronomic traits is required, and it can be improved through breeding. Field experiments were conducted during the late-rainy season from September to December 2014 and early-rainy season from June to September in 2015 at the Field Crop Research Station of Khon Kaen University. A randomized complete block design (RCBD) with two replications was used. Ninety-six Jerusalem artichoke accessions were used in both seasons. Data were recorded on tuber number per plant, fresh tuber yield and inulin content at harvest. The results indicated that Jerusalem artichoke accessions were significantly different for inulin content, tuber number per plant and fresh tuber yield, and there were significant genotype × environment interactions for these traits. However, the interaction between genotype and environment for these traits was low compared to genotype effect. Therefore, the genotype with high inulin content could be identified in this study. HEL 278 had consistently high inulin content and fresh tuber yield across seasons. This genotype could be used to develop high inulin content coupled with high tuber yield in the breeding program. The information on genetic variation in inulin content is useful for selection of parental lines in Jerusalem artichoke breeding program for improvement of inulin content.

Keywords: Sunchoke, fructan, tuber yield, genotypic variation

Key findings: Significantly differences among Jerusalem artichoke accessions were observed for inulin content. HEL 272, HEL 278 and HEL 288 were identified as having high inulin content.

Manuscript received: December 5, 2016; Decision on manuscript: March 1, 2017; Manuscript accepted: March 20, 2017.

Communicating Editor: Naqib Ullah Khan

INTRODUCTION

Jerusalem artichoke (*Helianthus tuberosus* L.) is an inulin-containing tuber crop. Inulin is well recognized as a prebiotic food, and is also suitable for the patients with diabetes mellitus, high blood pressure and coronary artery disorders as it can reduce serum triglycerides, total cholesterol, LDL and VLDL (Davidson and Maki, 1999; Niness, 1999; Pool-Zobel, 2005; Gaafar *et al*., 2010; Byung-Sung, 2011). Moreover, inulin can increase immunity and reduce the risk for colorectal cancer (Farnworth, 1993; Watzl *et al*., 2005). Prebiotics are non-digestible complex carbohydrates that are fermented in the colon, yielding energy and short chain fatty acids.

Prebiotics are known to selectively promote the growth of Bifidobacteria and Lactobacillae in the gastro-intestinal tract. Inulin and oligofructose have been well-established as prebiotics (Roberfroid, 2007). Many vegetables, root and tuber crops as well as some fruit crops are well-known sources of prebiotic carbohydrates (Schaafsma and Slavin, 2015). Jerusalem artichoke is considered the most promising crop for functional food in the tropics (Puangbut *et al*., 2012). Therefore, a breeding program at Khon Kaen University is being carried out to improve Jerusalem artichoke varieties with high inulin content, high yield, and good agronomic traits.

The information on genetic diversity in Jerusalem artichoke is important and necessary for selection of suitable parental lines in Jerusalem artichoke breeding program for improvement of inulin content. However, the information on genotypic response to different seasons for inulin traits is rather limited and the extent to which the genotypic interact with the seasons has not been adequately researched. The previous study has been evaluated in 79 Jerusalem artichoke accessions and found a significant genetic variation for inulin content (Puttha *et al*., 2012). High interactions between genotype and environment (G × E) were observed for inulin content and multi-location trials are necessary to identify the best genotypes. Furthermore, the information on the variation in inulin content in a large number of Jerusalem artichoke accessions is rather limited researched. The objective of this study was to evaluate the genotypic variation for inulin content and to the selection of parental line for useful in breeding for high inulin content under different seasons.

MATERIALS AND METHODS

Plant materials and experimental design

Ninety-six Jerusalem artichoke accessions used in this study were donated from three institutions (Table 1). One accession from the North Central Regional Plant Introduction Station (NCRPIS), 71 accessions from the Plant Gene Resource of Canada (PGRC), 22 accessions from the Leibniz Institute of Plant Genetics and Crop Plant Research (IPK) of Germany and two accessions from Thailand (KT 50-4 is a hybrid clone).

Ninety-six accessions of Jerusalem artichoke were evaluated in field experiments during the late-rainy season from September to December 2014 and early-rainy season from June to September in 2015 at the Field Crop Research Station of Khon Kaen University. A randomized complete block design with two replications was used. Plot size was 1.6 × 5 m with a spacing of 50 cm between rows and 40 cm between hills in a row.

Crop management

The soil was ploughed once using a 3-disc tractor and twice using a 7-disc tractor and ridged at a distance of 2 m. Then, the ridges were leveled to make soil beds.

Seed tubers were cut into small pieces each of which had two or three buds. The tuber pieces were incubated in plastic bags containing moist coconut peat at the bottom and the top of the bags for 7 days under ambient conditions. The plastic bags were kept open for good aeration. The tuber pieces with active buds and roots were further transferred to germinating plug trays with mixed medium containing burnt rice husk and soil for 7 days for complete sprouting. The fourth leaf-sprouted (V4) seedlings were then suitable for transplanting in the plot (Puangbut *et al*., 2015a). One seedling was transplanted per hill. Fertilizer formula 15-

15-15 was applied at 30 days after transplanting (DAT) at a rate of 156 kg per ha^{-1}. Supplementary irrigation was applied to the crop with an overhead sprinkler system at two-day intervals.

Table 1. Jerusalem artichoke accessions, sources of origin and genetic resources.

Entry No.	Accession No.	Name of accession	Genetic resources*	Origin
1	JA 1	7305	PGRC	Canada
2	JA 2	7306	PGRC	Canada
3	JA 6	7310	PGRC	Canada
4	JA 7	7312	PGRC	Canada
5	JA 8	7512	PGRC	Canada
6	JA 9	7513	PGRC	Canada
7	JA 10	HM Hybrid A	PGRC	Canada
8	JA 12	HM Hybrid C	PGRC	Canada
9	JA 14	HM–3	PGRC	Canada
10	JA 15	HM–5	PGRC	Canada
11	JA 16	HM–7	PGRC	Canada
12	JA 18	HM–9	PGRC	Canada
13	JA 20	HM–11	PGRC	Canada
14	JA 23	DHM–3	PGRC	Canada
15	JA 35	W–97	PGRC	Canada
16	JA 36	W–106	PGRC	Canada
17	JA 46	DHM–14–3	PGRC	Canada
18	JA 47	DHM–14–6	PGRC	Canada
19	JA 58	Intress	PGRC	USSR
20	JA 59	Volzskij–2	PGRC	USSR
21	JA 60	Jamcovskijkrashyj	PGRC	USSR
22	JA 71	TUB–675 USD–ARS–SR	PGRC	USA
23	JA 72	TUB–676 USD–ARS–SR	PGRC	USA
24	JA76	#4	PGRC	Canada
25	JA 77	#5	PGRC	Canada
26	JA 93	Leningradskii (NC10–65)	PGRC	USSR
27	JA 108	83-001-3 (37 × 6)	PGRC	Canada
28	JA 109	83-001-4 (37 × 6)	PGRC	Canada
29	JA 114	83-001-9 (37 × 6)	PGRC	Canada
30	JA 122	83-004-2 (6 × 20)	PGRC	Canada
31	JA 132	83-007-2 (69 × 3)	PGRC	Canada
32	KKU Ac 001	Unknown	Unknown	Thailand
33	CN 52867	PGR–2367	PGRC	USSR
34	JA 37	Comber	PGRC	Canada
35	JA 38	B.C. #1	PGRC	Canada
36	JA 67	Oregon White	PGRC	USA
37	JA 89	Waldspindel	PGRC	France
38	JA 102	073–87	PGRC	Germany
39	HEL 53	–	IPK	Germany
40	HEL 61	TambovskijKrasnyi	IPK	Russian Federation
41	HEL 62	SachalinskijKrasnyi	IPK	Russian Federation
42	HEL 65	Sejanec 19	IPK	Russian Federation
43	HEL69	–	IPK	Unknown
44	HEL 231	–	IPK	Germany
45	HEL 335	–	IPK	Unknown
46	Ames 2729	TUB–49	NCRPIS	South Dakota
47	HEL 243	Bianka	IPK	Germany
48	HEL 246	–	IPK	Unknown

(cont'd)

Table 1. Jerusalem artichoke accessions, sources of origin and genetic resources.

Entry No.	Accession No.	Name of accession	Genetic resources*	Origin
49	HEL 248	Rote Zonenkugel	IPK	Germany
50	HEL 253	–	IPK	Unknown
51	HEL 256	–	IPK	Unknown
52	HEL 257	BT4	IPK	Unknown
53	HEL 265	D19–63–340	IPK	Hungry
54	HEL272	Voelkenroder	IPK	France
55	HEL278	Spindel	IPK	Unknown
56	HEL 280	RA1	IPK	Unknown
57	HEL288	RA9	IPK	Poland
58	HEL 293	–	IPK	Poland
59	HEL 308	–	IPK	Unknown
60	HEL 316	–	IPK	Unknown
61	HEL 317	–	IPK	Unknown
62	KT 50-4	[JA 102 × JA 89]-8	KKU	Thailand
63	JA 19	HM-10	PGRC	Canada
64	JA 22	HM-13	PGRC	Canada
65	JA 27	DHM-7	PGRC	Canada
66	JA 49	7513A	PGRC	Canada
67	JA 95	NACHODKA	PGRC	USSR
68	JA 98	242-62	PGRC	France
69	JA 99	29-65	PGRC	France
70	JA 107	83-001-2 (37 X 6)	PGRC	Canada
71	JA 111	83-001-6 (37 X 6)	PGRC	Canada
72	JA 113	83-001-8 (37 X 6)	PGRC	Canada
73	JA 116	83-001-11 (37 X 6)	PGRC	Canada
74	JA 119	83-002-1 (69 X 6)	PGRC	Canada
75	JA 125	83-005-1 (39 X 40)	PGRC	Canada
76	JA 127	83-005-2 (39 X 40)	PGRC	Canada
77	JA 129	83-006-1 (40 X 39)	PGRC	Canada
78	JA 130	83-006-4 (40 X 39)	PGRC	Canada
79	JA 133	83-001-11 (37 X 6)	PGRC	Canada
80	JA 134	83-002-1 (69 X 6)	PGRC	Canada
81	JA 135	83-005-1 (39 X 40)	PGRC	Canada
82	JA 21	HM-12 Canada PGRC	PGRC	Canada
83	JA 3	7307	PGRC	Canada
84	JA 123	–	PGRC	Canada
85	JA 86	–	PGRC	France
86	HEL 68	–	PGRC	Unknown
87	JA 55	–	PGRC	USA
88	JA 81		PGRC	France
89	JA 4	7308	PGRC	Canada
90	JA 5	7309	PGRC	Canada
91	JA 117	–	PGRC	Canada
92	JA 61	Vadim	PGRC	USSR
93	JA 11	HM Hybrid B	PGRC	Canada
94	JA 97	D19-63-340	PGRC	France
95	HEL 66	KievskijBelyj	PGRC	Ukraine
96	JA 120	83-003-1 (6 9 20)	PGRC	Canada

*NCRPIS = The North Central Regional Plant Introduction Station; IPK = The Leibniz Institute of Plant Genetics and Crop Plant Research; PGRC: Plant Gene Resources of Canada; KKU = Khon KaenUniversity

Data collection

Weather conditions

Weather data were recorded. The seasonal mean of maximum temperature in the late-rainy season was 32.0 ºC and minimum temperature was 21.0 ºC (Figure 1). The mean of maximum temperature in the early-rainy seasons was 35.2 ºC and minimum temperature was 25.0 ºC (Figure 2). The means of solar radiation in the late-rainy season were 17.9 MJ m^{-2} d^{-1} (Figure 1) and it was 17.8 MJ m^{-2} d^{-1} in the early-rainy season (Figure 2). Rainfalls in the late-rainy seasons were 211.7 mm (Figure 1) and it was 665 mm in the early-rainy season (Figure 2).

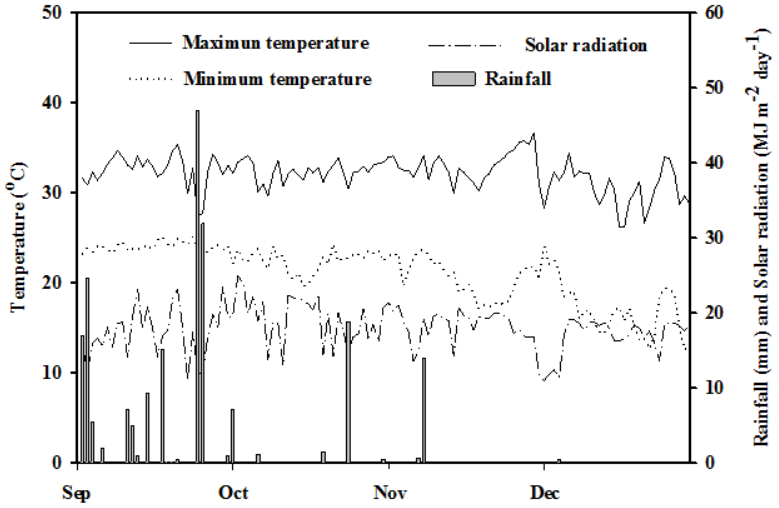

Figure 1. Daily maximum temperature, minimum temperature, solar radiation and rainfall during the late-rainy 2014 at Khon Kaen University, Khon Kaen, Thailand.

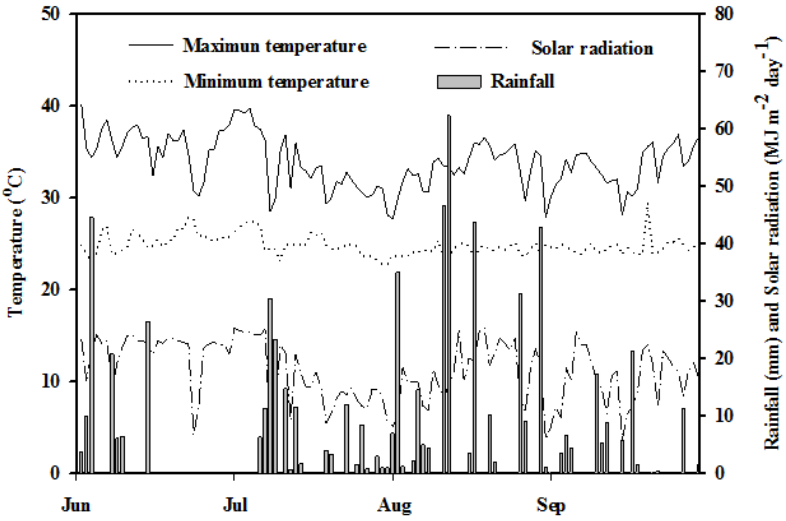

Figure 2. Daily maximum temperature, minimum temperature, solar radiation and rainfall during the early-rainy season 2015 at Khon Kaen University, Khon Kaen, Thailand.

The growing conditions were different between seasons and this could be due to the difference in temperatures. The results indicated that solar radiation is not a significant different between late-rainy and early-rainy seasons. Rainfall well distributed throughout the crop cycle in the early-rainy seasons. However, no water stress was observed during the growing season for late-rainy seasons.

Fresh tuber yield and number of tuber per plant

At harvest, plants at the end of the rows and border rows were discarded. Then, 16 plants in an area of 3.2 m^2were harvested. Plants were cut at the soil surface and separated into shoots and tubers. Tubers were washed in tap water to remove the potting medium and then tuber fresh weight was determined. Three plants in each plot were sampled randomly and used for determination of number of tubers per plant.

Inulin content

Inulin content was analyzed using the methods described by Saengkanuk *et al.* (2011). Briefly, the tubers were longitudinally sliced into thin pieces at the middle part of the tubers. Fifty grams of sliced tuber was soaked in absolute ethanol at 4 °C for 24 h then the samples were stored at -20 °C until analyzed. The samples were oven dried at 60 °C for 10 hours. To extract inulin, 2 g of dried sample was mixed with distilled water at 80 °C for 20 minutes. The solution was cooled to room temperature and filtered through a 0.45 µm membrane filter. The extracts (500 µl) were pipette into 25 ml volumetric flasks containing 3% HCl and diluted to 25 ml with water. The mixtures were then heated at 80 °C in a water-bath for 45 minutes. After cooling, the solutions were stored in plastic bottles before being analyzed by the spectrophotometer. Inulin analysis was shown as a percentage of inulin content on a dry weight basis.

Statistical analysis

Analysis of variance was performed for individual seasons and error variances were tested for homogeneity by Bartlett's test (Hoshmand, 2006). Because of, genotype × seasons interaction were significant for all characters (Table 2), data were reported for individual seasons. Duncan's multiple range tests (DMRT) was used to compare means within genotypes. Calculations procedures were done using MSTAT-C package (Bricker, 1989).

RESULTS

Genotypic variability and genotype x **environment interactions**

Significant differences between seasons (S) were observed for inulin content, tuber number and fresh tuber yield and significant differences among Jerusalem artichoke genotypes (G) were observed for all traits (Table 2).

Seasons contributed to a small portion of total variation for inulin content (21.2%), tuber number (0.68%) and fresh tuber yield (36.2%).Similar, the interactions between genotype and season contributed to medium portions of variations inulin content (34.1%), tuber number (25.6%) and fresh tuber yield (14.4%). The contribution of genotype was higher than that season for tuber number (60.2%) and fresh tuber yield (40.4%) and genotype contributed to medium for inulin content (35.2%).

Genotypic variations in inulin content, tuber number and fresh tuber yield

There were significant differences among Jerusalem artichoke accessions for inulin content, fresh tuber yield and tuber number in both seasons. The crop grown in the late-rainy season had higher inulin content and fresh tuber yield than did the crop grown in the early-rainy season (Table 3).

In the late-rainy season, the genotype with high or low inulin could be identified and the accessions were then divided into two extreme groups each of which has ten accessions (Table 4). JA 95, HEL 308, JA 98, HEL 278, HEL 293, HEL 272, HEL 288, JA 125, JA 10 and JA 36 were identified as having high inulin content ranged from 73.6-76.6% of dry weight.

Table 2. Mean squares from combined analysis of variance for inulin content, number of tuber per plant and fresh tuber yield of 96 Jerusalem artichoke accessions observed in the early-rainy season 2015 and late-rainy season 2014/15.

Source of variation	df	Inulin content	Number of tuber	Fresh tuber yield
Season (S)	1	5985.83(21.2)*	364.260 (0.68)*	1.700E+08(36.2)*
Rep. within S	2	30.73	341.354	5194217
Clone/genotype (G)	95	104.95(35.2)**	339.447(60.2)**	1996981(40.4)**
G × S	95	101.65(34.1)**	144.297(25.6)**	712130(14.4)**
Pooled error	190	13.80	34.623	166802
Total	383			

*, ** Significant at $P < 0.05$ and significant at $P < 0.01$
Numbers within the parentheses are percentages of sum squares to total sum of squares.

Table 3. Inulin content, number of tuber and fresh tuber yield for averaged over 96 Jerusalem artichoke accessions.

Seasons	Inulin content (% of dry wt)	Number of tuber (tuber plant^{-1})	Fresh tuber yield (kg ha^{-1})
Late-rainy season	61.5 ± 6.1 a	32.0 ± 8.4	2553 ± 230 a
Early-rainy season	54.0 ± 5.7 b	30.3 ± 5.6	1228 ± 280 b
F-test	**	ns	**

Data are presented as mean ± SD ($n = 2$)
Means in the same column with the different letters are significantly different by DMRT ($P < 0.05$).
ns; non-significant, ** Significant at $P < 0.01$

The low group comprised of HEL 243, HEL 253, HEL 53, HEL 69, HEL 248, JA 76, JA 97, HEL 231, JA 8 and HEL 335 with the range of 42.5-50.6%. The ranks in the two groups were not overlapped and statistically different, and, therefore, the genotypes with low and high inulin content were readily identified.

Tuber number of the high group ranged between 15.5-49.0 tubers per plant **(**Table 4**).** The ranges between high and low groups were overlapped. A wide range of fresh tuber yield was observed among Jerusalem artichoke accessions within the high group, ranging from 11,500 to 28,500 kg ha^{-1} (Table 4). However, the ranks of high and low groups were overlapped. HEL 278, HEL 272 and HEL 288 could be identified as inulin content combined with high fresh tuber yield.

In the early-rainy season, the genotype with high or low inulin could be identified and the accessions were then divided into two extreme groups (Table 5). JA 22, HEL 278, JA 61, HEL 288, HEL 62, HEL 272, HEL 256, Ames 2729, JA 19 and HEL 316 were identified as having high inulin content ranged from 61.3-75.0% of dry weight (Table 5). The low group comprised of HEL 69, JA 55, JA 117, JA 135, JA 49, JA 76, JA 111, HEL 68, JA 11 and JA 102 with the range of 39.3-47.1% of dry weight (Table 5). The ranks in the two groups were not overlapped and statistically different, and, therefore, the genotypes with low and high inulin content were readily identified.

Tuber number of high group ranged between 18.0-39.0 tubers per plant **(**Table 5**).** The ranges between high and low groups were overlapped. A wide range of tuber yield was observed among Jerusalem artichoke accessions within high group, ranging from 3,118 to 11,718 kg ha^{-1}(Table 5). However, the ranks of high and low groups were overlapped. However, the genotype with high inulin content coupled with high fresh tuber yield was observed in HEL 278, HEL 272, HEL 288 and JA 22.

Table 4. Inulin content tuber number and fresh tuber yield of 96 Jerusalem artichoke in late- rainy season 2014/15.

Groups	Entry no.	Genotypes	Inulin content (% of dry wt)	Tuber no. (tuber plant^{-1})	Fresh tuber yield (kg ha^{-1})
High	67	JA 95	76.6 ± 2.7 a	22.5 ± 5.7 f-z	1,800 ± 40 g-s
	59	HEL 308	76.3 ± 1.7 a	20.5 ± 0.5 w-z	17,250 ± 40 i-u
	68	JA 98	76.1 ± 0.2 a	31.5 ± 7.5 l-x	17,750 ± 40 h-s
	55	HEL 278	75.8 ± 1.2 ab	24.0 ± 1.2 s-z	28,500 ± 360 abc
	58	HEL 293	75.6 ± 0.8 ab	23.5 ± 5.5 s-z	11,500 ± 220 u-z
	54	HEL 272	74.9 ± 0.2 abc	31.5 ± 1.3 l-x	20,500 ± 280 e-m
	57	HEL 288	74.4 ± 4.1 a-d	34.0 ± 4.3 j-v	21,000 ± 260 e-k
	75	JA 125	74.3 ± 3.2 a-d	28.5 ± 3.3 n-z	15,500 ± 200 k-w
	7	JA 10	73.9 ± 6.7 a-e	15.5 ± 3.5 c-n	24,750 ± 200 a-e
	16	JA 36	73.6 ± 1.0 a-f	49.0 ± 4.0 c-k	12,750 ± 40 q-z
Low	47	HEL 243	50.6 ± 1.4 ab	24.0 ± 2.0 s-z	22,000 ± 120 d-j
	50	HEL 253	49.4 ± 2.6 abc	26.5 ± 1.7 p-z	14,250 ± 120 n-y
	43	HEL 53	48.7 ± 1.3 abc	26.5 ± 0.5 q-z	23,500 ± 120 e-m
	39	HEL 69	48.7 ± 0.1 abc	25.5 ± 1.5 p-z	20,250 ± 240 c-h
	49	HEL 248	48.5 ± 1.4 abc	21.0 ± 1.2 v-z	21,000 ± 240 e-l
	38	JA 76	48.3 ± 1.8 abc	24.5 ± 5.8 r-z	28,250 ± 120 abc
	94	JA 97	47.8 ± 0.9 abc	41.0 ± 5.3 d-o	18,000 ± 400 g-s
	44	HEL 231	47.7 ± 0.8 abc	19.5 ± 2.2 xyz	17,750 ± 280 h-s
	5	JA 8	46.5 ± 3.6 bc	54.0 ± 0.8 abc	9,250 ± 40 xyz
	45	HEL 335	42.5 ± 2.6 c	32.0 ± 4.0 k-x	15,250 ± 280 l-x
Max			76.6	60.5	29,750
Min			42.5	9.5	3,000
Mean			61.9 ± 6.1	32.0 ± 8.4	15,956 ± 732
F-test			**	**	**

Data are presented as mean ± SD (n = 2), minimum, maximum and mean values were calculated from 96 accessions
Means in the same column with the same letters are not significantly different by DMRT ($P < 0.05$).
** Significant at $P < 0.01$ probability level

DISCUSSION

The selection for high tuber yield and inulin content are priorities of Jerusalem artichoke breeding programs. Variation in genotype and environments can affect inulin content and tuber yield of Jerusalem artichoke. However, there is limited information on the variation in inulin content in a large number of Jerusalem artichoke accessions. Furthermore, information of genotypic response for inulin content to different environments is important for breeding programs. However, there was a few information on genotype, season and genotype × season interaction for inulin content.

This study revealed a significant genotypic variation for inulin content which could potentially be exploited in Jerusalem artichoke breeding programs. High genetic variation was found for inulin content and selection for this character is possible. The results also demonstrated that contribution of genotype was higher than that season for inulin content and fresh tuber yield. Similar to previous studies reported that genotypic contributed to a large portion of variation in fresh tuber yield and inulin content (Puangbut *et al*., 2011; Puttha *et al*., 2012; Puangbut *et al*., 2015c). A large estimate of genetic variance indicates that selection and breeding initiatives can proceed in this study.

Over all genotypes, inulin content in the late-rainy season was higher than that in the early-rainy season, while tuber number showed no significant differences between seasons. Contrast to previous studied reported that crop grown in the early-rainy season had higher inulin content than did the crop grown in the late-rainy season (Puangbut *et al*., 2015c).

Table 5. Inulin content tuber number and fresh tuber yield of 96 Jerusalem artichoke in early- rainy season 2015.

Groups	Entry no.	Genotypes	Inulin content	Tuber no. (tuber plant^{-1})	Fresh tuber yield (kg ha^{-1})
High	64	JA 22	75.0 ±8.3 a	39.0 ± 5.8 a-m	9,462 ± 220 b-t
	55	HEL 278	64.9 ± 6.1 b	20.0 ± 5.4 r-z	11,718 ± 200 a-k
	92	JA 61	64.4 ± 5.4 bc	36.0 ± 1.1 b-r	4,925 ± 7.3 i-x
	57	HEL 288	64.2 ± 1.3 bc	31.0 ± 3.2 f-x	8,818 ± 11 c-u
	41	HEL 62	64.0 ± 0.7 bcd	18.0 ± 4.2 u-z	6,365 ± 116 g-x
	54	HEL 272	64.0 ± 3.9 bcd	37.5 ± 0.9 b-0	9,138 ± 71 b-u
	51	HEL 256	62.7 ± 1.9 b-e	34.0 ± 3.9 c-u	6,594 ± 78 f-x
	46	Ames 2729	62.4 ± 4.3 b-f	32.0 ± 4.8 e-w	3,118 ± 178 p-x
	63	JA 19	61.8 ± 5.7 b-g	26.5 ± 1.6 i-z	5,906 ± 105 g-x
	60	HEL 316	61.3 ± 3.9 b-h	23.5 ± 0.8 m-z	5,644 ± 162 g-x
Low	43	HEL 69	47.1 ± 5.7 p-w	20.0 ± 1.3 r-z	6,144 ± 41 g-x
	87	JA 55	47.1 ± 2.8 p-w	30.5 ± 2.5 g-z	7,931 ± 53 c-x
	91	JA 117	46.9 ± 5.2 q-w	35.5 ± 4.5 b-s	4,494 ± 92 l-x
	81	JA 135	46.6 ± 0.7 r-w	34.0 ± 2.3 c-u	10,025 ± 60 b-p
	66	JA 49	46.1 ± 3.3 r-w	31.0 ± 4.4 f-x	2,793 ± 6.8 r-x
	24	JA 76	45.0 ± 2.7 t-w	13.0 ± 4.1 z	5,931 ± 144 g-x
	71	JA 111	44.9 ± 4.7 t-w	28.0 ± 6.3 i-z	6,981 ± 101 e-x
	86	HEL 68	43.1 ± 0.7 uvw	24.5 ± 0.7 k-z	8,406 ± 64 c-x
	93	JA 11	41.6 ± 0.8 vw	29.0 ± 6.5 h-z	8,700 ± 28 c-w
	38	JA 102	39.3 ± 3.6 w	24.5 ± 2.7 k-z	8,287 ± 233 c-w
Max			75.0	54.5	17,968
Min			39.3	11.5	1,487
Mean			54.0 ± 4.4	30.3 ± 6.1	7,675 ± 303
F-test			**	**	**

Data are presented as mean ± SD (n = 2), minimum, maximum and mean values were calculated from 96 accessions
Means in the same column with the same letters are not significantly different by DMRT ($P < 0.05$).
** Significant at $P < 0.01$ probability level

The differences in the results may be due to the differences in the plant materials and climatic factors such as temperature.

The results also indicated that the crop grown in the late-rainy season had higher fresh tuber yield than did the crop grown in the early-rainy. This study supported previous findings that Jerusalem artichoke grown in the late-rainy season produced higher tuber yield (Puangbut *et al*., 2012; Puangbut *et al*., 2015b, 2015c; Ruttanaprasert *et al*., 2013).This could be due to the vegetative growth was declined in the late-rainy season but induce high partitioning of assimilates from temporary sink to tuber and resulted in high tuber yield (Puangbut *et al*., 2015c; Rattanaprasert *et al*., 2013; Somda *et al*., 1999).

This result indicated that there was a possibility to select Jerusalem artichoke with high inulin content and high fresh tuber yield. The relationship between inulin content and fresh tuber yield were positive and significant. High correlation between inulin content and fresh tuber yield was found in the early-rainy season (r = 0.75*) and in the late-rainy season (r = 0.60*) (data not presented). Similar to the previous study indicated that inulin content was associated with fresh tuber yield (Puttha *et al*., 2012). HEL 278 showed consistently high inulin content and fresh tuber yield across seasons. This genotype could use as parental lines in Jerusalem artichoke breeding program for improvement of inulin content combined with high tuber yield, based on presented data on Tables 4-5.

CONCLUSION

Jerusalem artichoke accessions have high

variations in inulin content and fresh tuber yield and then selection for these characters is possible among these accessions. Genotype with high inulin content and fresh tuber yield could be identified among these accessions. Over both seasons, HEL 272, HEL 278 and HEL 288 had consistently high inulin content. These accessions can be used as sources of high inulin genotype for useful in the breeding program for high inulin content.

ACKNOWLEDGEMENTS

This work was supported by the Peanut and Jerusalem Artichoke Improvement for Functional Food Research Group and the research funding support of Khon Kaen University. We also thank the North Central Regional Plant Introduction Station, USA, the Leibniz Institute of Plant Genetics and Crop Plant Research, Germany and the Plant Gene Resource of Canada for the contribution of Jerusalem artichoke germplasm. Grateful acknowledgement is also made to Higher Education Research Promotion and National Research University Project of Thailand, Office of the Higher Education Commission, through the Food and Functional Food Research Cluster of Khon Kaen University, Thailand and to the Thailand Research Fund for providing financial supports to this research through the Senior Research Scholar Project of Professor Dr. Sanun Jogloy (Project no. RTA5880003). Acknowledgement is extended to the Thailand Research Fund (IRG 5780003), Khon Kaen University and Faculty of Agriculture, KKU for providing financial support for manuscript preparation activities.

REFERENCES

Bricker AA (1989). MSTAT-C User's Guide. Michigan State University, Michigan.

Byung-Sung P (2011). Effect of oral administration of Sunchoke inulin on reducing blood lipoid and glucose in STZ-induced diabetic rats. *J. Anim. Vet. Adv*. 10:2501-2507.

Davidson MH, Maki KC (1999). Effects of dietary inulin on serum lipids. *J. Nutr*. 129: 1474S-1477S.

Gaafar AM, Serag El-Din MF, Boudy EA, El-Gazar HH (2010). Extraction conditions of inulin from Sunchoke tubers and its effects on blood glucose and lipid profile in diabetic rats. *J. Am. Sci*. 6:36−43.

Farnworth ER (1993).Fructans in human and animal diets. In: M. Suzuki and N.J. Chatterton, eds, *Science and Technology of fructans*. CRC press, London. pp 257-272.

Hoshmand AR (2006). Design of Experiments for Agriculture and the Natural Sciences. Chapman & Hall, Florida.

Niness KR (1999). Inulin and oligofructose: What are they?. *J. Nutr*. 129:1402S−1406S.

Puangbut D, Jogloy S, Srijaranai S, Vorasoot N, Kesmala T, Patanothai A (2011). Rapid assessment of inulin content in *Helianthus tuberosus* L. tubers. *SABRAO J. Breed. Genet*. 43 (2):188−200.

Puangbut D, Jogloy S, Vorasoot N, Srijaranai S, Kesmala T, Patanothai A (2012). Influence of planting date and temperature on inulin content in Jerusalem artichoke (*Helianthus tuberosus* L.). *Aust. J. Crop Sci*. 6:1159−1165.

Paungbut D, Jogloy, S, Vorasoot N, Patanothai A (2015a). Growth and phenology of Jerusalem artichoke (*Helianthus tuberosus* L). *Pak J. Bot*. 47(6):2207−2214.

Paungbut D, Jogloy S, Vorasoot N, Patanothai A (2015b). Responses of growth,physiological traits and tuber yield in *Helianthus tuberosus* to seasonal variations under tropical area. *Sci. Hortic*. 195:108−115.

Paungbut D, Jogloy S, Vorasoot N, Holbrook CC, Patanothai A (2015c). Responses of inulin content and inulin yield of Jerusalem artichoke to seasonal environments. *Inter J. Plant Prod*. 9(4):599−608.

Pool-Zobel BL (2005). Inulin-type fructans and reduction in colon cancer risk: review of experimental and human data. *Br. J. Nutr*. 93:S73−S90.

Puttha R, Jogloy S, Wangsomnuk PP, Srijaranai S, Kesmala T, Patanothai A (2012). Genotypic variability and genotype by environment interactions for inulin content of Jerusalem artichoke germplasm. *Euphytica*. 183:119–131.

Roberfroid MB (2007). Prebiotics: the concept revisited. *J. Nutr*. 137:830S–837S.

Ruttanaprasert R, Jogloy S, Vorasoot N, Kesmala T, Kanwar RS, Holbrook CC, Patanothai A (2013). Photoperiod and growing degree days effect on dry matter partitioning in Jerusalem artichoke. *Int. J. Plant Prod*. 7:393-416.

Saengkanuk A, Nuchadomrong S, Jogloy S, Patanothai A, Srijaranai S (2011). A simplified spectrophotometric method for the determination of inulin in Jerusalem artichoke **(***Helianthus tuberosus* L.**)** tubers. *Eur. Food Res. Technol*. 233:609-616.

Schaafsma G, Slavin LJ (2015). Significance of inulin fructans in the human diet. Compr. *Rev. Food Sci. F*. 14:37−47.

Somda ZC, Mclaurin WJ, Kays SJ (1999). Jerusalem artichoke growth, development, and field storage. II. Carbon and nutrient element allocation and redistribution. *J. Plant Nutr*. 22:1315-1334.

Watzl B, Girrbach S, Roller M (2005). Inulin, oligofructose and immunomodulation. *Br. J. Nutr*. 93:S49–S55.